Rheological Properties, Loss of Workability and Strength Development of High-Strength Concrete

El–mahadi Ahmed

B.Eng (Hons.), MSc.

A Thesis submitted for the degree of Doctor of Philosophy
University of London

Department of Civil & Environmental Engineering
University College London

University of London

June
2002

Abstract

The successful production of high-strength concrete which meets the desired strength and durability is dependent on optimising its rheological (or flow) properties and reducing its loss of workability during the transportation, placing and compaction stages. The research presented in this thesis aimed to:

1. Determine whether mix stability and compactability can be adequately described by the two Bingham parameters of yield value and plastic viscosity.
2. Reduce the uncertainties in material selection with regards to the performance of superplasticizers and cement replacement materials.
3. Examine how the two Bingham parameters vary at different degrees of compaction by vibration.
4. Determine how these influence the strength development characteristics in the hardened state.
5. An additional aim was to carry out any modifications to the test apparatus and methods which experience makes necessary.

Measurements with Tattersall's MH two-point workability test apparatus indicated that mix stability correlates more closely with the yield value than with plastic viscosity, whilst the opposite is true with respect to compactability under self-weight.

The performance of conventional and new-generation superplasticizers (based on SMF, SNF, MLS, Vinyl and Acrylate polymers) was evaluated with different dosages, mixing procedures and cements. The SNF superplasticizer produced slightly lower initial workabilities than the Acrylate superplasticizer, but the longest workability retentions of the superplasticizers tested. Partial cement replacements by CSF in binary blends produced lower superplasticizer dosage demands, higher initial workabilities and longer workability retentions than those due to PFA and GGBS. When used in ternary blended cements, CSF enhanced the performance of mixes containing PFA or GGBS at w/b ratios of 0.30-0.22.

A novel method developed to assess the vibration response of fresh concretes has, for the first time, demonstrated that both the yield value and plastic viscosity decrease during compaction. The method has also demonstrated that the maximum compressive strengths and densities of concretes compacted for different vibration durations/amplitudes coincide with the attainment of zero yield value. Continuous reductions in plastic viscosity during vibration mainly reduced the homogeneity of concrete compacted in short columns.

Dedication

To my mother (Muram El-mahadi), father (Ahmed Abdallah) and brother (El-hadi).

To all those who persevere at personal expense and self-sacrifice in order to enlighten others.

Acknowledgements

The work presented in this thesis was undertaken under severe financial and health difficulties, and I therefore thank God for giving me the direction, foresight and strength to complete it.

I would also like to express my most sincere thanks to my family whose financial assistance and encouragement made this work possible.

The author would also like to extend his thanks to Dr P.L.J. Domone (supervisor) for reading the draft chapters of the thesis.

Mr J. Jackson is also acknowledged for organising college vans for me to pick-up the granite used from the relevant quarries. Mr O. Bourne is thanked for occasionally filling the aggregate storage bins, and cutting cube specimens from short-columns cast during the research. Much appreciation is extended to Mr S. Justin and Mr M. Saytch for their technical assistance in solving electronic/electrical problems experienced with the two-point test apparatus. Mr S. Mohammed is warmly thanked for his enthusiasm and support with pilot tests carried out to assess adsorption and Zeta-potential properties of superplasticizers.

Finally, I would also like to extend my sincere thanks to my colleagues, in particular to Dr V. Sheikh and P. Chai, for their cooperation during the research.

Contents

Notation

A, B, C, D, E	Constants representing variations in shear rate, inter-particle forces within the concrete, and surface friction
A	Aggregate
B_m	Bleeding mark
C	Cement
CRMs	Cement Replacement Materials
CSF	Condensed Silica Fume
D	Base diameter of slump cone (200 mm)
dH	Drop in height after vibration
FM	Fineness Modulus
g	Yield value, or Acceleration due to gravity
GGBS	Ground Granulated Blast Furnace Slag
h	plastic viscosity
HPC	High Performance Concrete
HSC	High Strength Concrete
LM	Medium-Low workability two-point test system
MH	Medium-High workability two-point test system
$MK_{I, II, III}$	Mark I, II, and III versions of Tattersall 's apparatus
MLS	Modified Lignosulphonate
mV	millivolts
n	Number of variables/molecules
N	Impeller speed (rps)
NG	New generation superplasticizer

NSC	Normal strength concrete
OPC	Ordinary Portland Cement
PC	Portland Cement
PFA	Pulverised Fuel Ash
r	Correlation coefficient
S	Slump value (or Sand)
SCC	Self-compacting Concrete
SC	Self-compactability (in kg/m^3)
Sf, sf	Final slump-flow spread, and slump-flow spread at time (t)
SI	Segregation index
sH	Up-lift measurement after two-point testing
$sH_{H, L, M}$	Up-lift measurements at High, Low and Medium slumps
SFS	Slump-flow spread (referred to as slump-spread)
ST	Slump-flow time (after complete collapse under self-weight)
SR	Slump-spread (or spread rate)
SMF	Sulphonated melamine formaldehyde
SNF	Sulphonated naphthalene formaldehyde
SP	Superplasticizer
SSD	Saturated Surface Dry (Aggregates)
s/w/b	Solids by weight of binder (%)
T	Torque (Nm)
T_c	Torque change
W	Water (or Energy transmitted to concrete during compaction)
$W_{A, W}$	Mass in air and mass in water
W_V	Total work done on concrete

$W_{1,2}$	Weights of aggregates (c.f. figure 4.6)
w/b	Water/Binder ratio
w/c	Water/Cement ratio
V	Voltage
$V_{A,R}$	Attractive & Repulsive energy between cement particles
Å	Angstrom
dW	Change in self-weight of concrete in time interval dt
dW/dt	Work done on concrete under its own self-weight
τ, τ_o	Shear stress, Yield stress
τ_o^R, τ_o^V	Yield stress at rest and during vibration
μ, η	Plastic viscosity
γ	Shear rate
λ	Surface friction of slump board
ξ_I	Inter-particle forces during slump collapse
ϕ	Frictional resistance due to form-work, reinforcement etc
ϕ_o, ϕ_S	Surface and Stern potentials

List of Figures

Chapter 1

Chapter 2

Chapter 4

Chapter 5

Chapter 6

Chapter 7

PFA/CSF on (a) spread and (b) V-flow time at 0.26 w/b (4 mins delayed add. of SNF).

Figure 7.9 : Mortar dosage-response tests for the effects of ternary blends of GGBS/CSF on (a) spread and (b) V-flow time at 0.26 w/b . (4 mins delayed add. of SNF).

Figure 7.10 : Effects of Ternary Blends of 10% CSF with 20-40% PFA and 40-60% GGBS on (a) slump loss and (b) loss of workability at 0.26 w/b. (All mixes tested at their respective sat. dosages, using 4 mins delayed add. of SNF).

Figure 7.11 : Effects of Ternary blends (of PFA/CSF and GGBS/CSF) and their equivalent binary mixes on (a) initial yield value and (b) plastic viscosity (at 0.26 w/b ratio).

Figure 7.12 : Mortar dosage-response tests for the effects of OPC, 10% CSF, and ternary mixes of 40%PFA + 10%CSF and 60%GGBS+ 10% CSF on (a) spread and (b) V-flow time at 0.30 w/b.

Figure 7.13 : Effects of OPC, 10%CSF, and Ternary blends of 40%PFA + 10%CSF and 60%GGBS+ 10% CSF on (a) slump loss and (b) loss of workability at 0.30 w/b ratio. (All mixes tested at their respective sat. dosages, using 4 mins delayed add. of SNF).

Figure 7.14 : Mortar dosage-response tests for the effects of 10% CSF, and trenary mixes of 40%PFA + 10%CSF and 60%GGBS + 10% CSF on (a) spread and (b) V-flow time at 0.22 w/b.

Figure 7.15 : Effects of 10% CSF, and Ternary mixes of 40%PFA + 10%CSF and 60%GGBS+ 10% CSF on (a) slump loss and (b) loss of workability at 0.22 w/b ratio. (All mixes tested at their respective sat. dosages, using 4 mins delayed add. of SNF).

Figure 7.16 : Effects of decreasing w/b ratios of 0.30, 0.26 and 0.22 on the saturation dosage demands of OPC, 10% CSF, 40%PFA+10%CSF and 60%GGBS+10%CSF mixes.

Figure 7.17 : Effects of decreasing w/b ratios of 0.30, 0.26 and 0.22 on the developments in yield value and plastic viscosity of (a) OPC and 10% CSF mixes.

and (b) ternary combinations of 40%PFA+10%CSF and 60%GGBS+10%CSF.

Chapter 8

Figure 8.1 : Relationships between the Bingham parameters and (a) final slump and (b) slump-spread under static conditions (details of mixes given in Tables B10 and C3, 5, 7, 10, 12 and 14 of Appendices B and C).

Figure 8.2 : Relationships between the final slump and slump-flow time with the final slump-spread.

Figure 8.3 : Schematic illustration of typical slumping behaviour of low and high workability HSC mixes having comparable final slump/spread. (a) Progressive collapse, (b) graphical variations in slump and slump-spread, under dynamic conditions.

Figure 8.4 : Relationships between the Bingham parameters and slump-spread measured at (a) 5, (b) 10, and (c) 20 secs of deformation.

Figure 8.5 : Relationships between the Bingham parameters and slump-spread measured at (a) 30 and (b) 60 secs of deformation, and (c) under static conditions. (Note: mixes which stopped flowing between e.g. 20-30 secs, appear only in figs. 8.4(a-c) and 8.5(c)).

Figure 8.6 : Illustration of slumping behaviour and changes in self-weight of concrete over the base area of the slump-cone. (These, and the accompanying variations in inter-particle forces with time, appear to be responsible for the observed differences in flow properties of HPCs).

Figure 8.7 : Schematic illustration of test set-up used to assess the vibration response of fresh concretes.

Figure 8.8 : Spread-time response curves for vibrated and non-vibrated 10% CSF mix at casting times of 120-130 mins (0.26 w/b ratio, SNF superplasticizer).

Figure 8.9 : Vibration response tests with (a) OPC and (b) 10% CSF mixes, at amplitudes of 0.1-0.7 mm and casting times of 60-130 mins (0.26 w/b ratio).

Figure 8.10 : Vibration response tests with ternary mixes of (a) 40/10 PFA/CSF

and (b) 60/10 GGBS/CSF, at amplitudes of 0.1-0.7 mm and a casting time of 60-130 mins (0.26 w/b ratio).

Figure 8.11 : Vibration response tests with (a) Acrylate superplasticizer and (b) superplasticized NSC, at amplitudes of 0.1-0.7 mm .

Chapter 9

Figure 9.1 : Effects of increasing vibration duration on 28-day compressive strength development of OPC and 10% CSF mixes (100 mm cubes, 0.26 w/b ratio, 0.70 mm vibration amplitude).

Figure 9.2 : Effects of increasing amplitude of vibration on 28-day compressive strength development of OPC and 10% CSF mixes (100 mm cubes, 0.26 w/b ratio, and varying vib. duration).

Figure 9.3 : Cube strength - density relationship for mixes in Tables 9.1-9.3.

Figure 9.4 : Cube strength - Bingham parameter relationships in terms of their (a) magnitudes (as shown in Tables 9.1-9.3) and (b) differences in magnitude (up to full-compaction).

Figure 9.5 : Relationship between cube strength and UPV (for granite based mixes).

Figure 9.6 : Variations in 28-day column strength with increasing vibration duration (10% CSF mix, 0.26 w/b, 0.70 mm vib. amplitude).

Figure 9.7 : Variations in 28-day column strength with increasing amplitude of vibration (10% CSF mix, 0.26 w/b, varying vib. duration).

List of Tables

Chapter 1

Chapter 2

Chapter 3

SCC.

Chapter 4

Chapter 5

Chapter 6

Chapter 8

Table 8.1 : Stiffening properties of OPC and 10% CSF mixes after 5 mins resting (at 0.26 w/b ratio).

Chapter 9

Table 9.1 : Summary of fresh and hardened concrete properties for increasing vibration durations (at 0.7 mm amplitude, 120-130 mins casting time).

Table 9.2 : Summary of fresh and hardened concrete properties of mixes compacted at increasing vibration amplitudes (120-130 mins casting time).

Table 9.3 : Influence of 60-70 mins casting time on the strength development characteristics of 10% CSF binary mixes (incorporating SNF and D2001 superplasticizers).

Table 9.4 : Summary of fresh properties and hardened concrete column measurements corresponding to increasing vibration durations (at 0.7 mm amplitude, and 120-130 mins casting time).

Table 9.5 : Summary of fresh properties and hardened concrete column measurements corresponding to increasing amplitudes of vibration (at 120-130 mins casting time).

Chapter 1
Introduction

1.1 Background

The development and interest in High Strength Concrete (HSC) have been gradual over many years and, as these continued, its definition has changed. In the 1950's concrete with a compressive strength of 35 Nmm^{-2} was considered as HSC. In the 1960's concrete with 40 to 50 Nmm^{-2} represented the upper limit, whilst by the early 1970's concrete with a ceiling strength of around 60 Nmm^{-2} was being commercially used[1]. In more recent years HSC has been defined as that having an average 28-day compressive strength in excess of 80 Nmm^{-2} [2-3].

The term High Performance Concrete (HPC) is sometimes used synonymously with HSC, but in reality high performance encompasses a much wider range of properties (such as high workability, enhanced durability)[4-6] than the attainment of high compressive strength alone. HSC is, therefore, just one of the possible types of HPCs.

HSC, like other concretes, has to comply with several criteria in both its fresh and hardened states. It must, for example, have sufficient workability to allow it to be mixed, transported, placed, and compacted in the forms; and be strong enough to carry the applied loads once it hardens. These criteria place conflicting demands on the concrete, since a reduction in water content or water/binder* (w/b) ratio increases strength but reduces the workability[4, 7-8]. This in turn increases handling difficulties and exerts greater demands on construction plant, meaning that conventional concreting processes cannot guarantee the required performance.

The earliest attempts to produce HSC differed considerably from today's HSCs, because they had no fluidity whatsoever, and therefore precluded the use of conventional construction techniques. For example, in 1930, Yoshida[9] produced

* A **binder** is a constituent which has cementitious value and contributes to strength (such as PFA, GGB and CSF).

concrete with a compressive strength of 104 Nmm^{-2} by pressing/moulding a concrete with a w/b ratio of 0.31 under a pressure of 10 N/mm^2. Around the same period, Menzel[10] produced concrete with a compressive strength of more than 100 Nmm^{-2} by steam curing.

Since then the use and acceptance of HSC as a viable construction material has been primarily driven by developments in materials technology, notably by the advent of fluidity-improving techniques provided by chemical admixtures such as superplasticizers. The inclusion of mineral admixtures as partial cement replacement materials (CRMs) to, for example, improve the workability properties[11], reduce problems of thermal cracking and/or enhance durability[12], has also promoted the use of HS and other HPCs (such as self-compacting and anti-wash-out concrete).

Despite much recent research into the properties of HSCs, many aspects regarding their rheological (or flow) properties in the fresh state, and their rapid losses in workability during the transportation, placing and compaction stages are still poorly understood. The lack of understanding of these properties has been a major drawback hindering the widespread use of HSC, and continues to present the main technical barrier in rationalizing the material in construction operations.

1.2 Production requirements and applications of HSC

1.2.1 Production requirements

The main features for achieving high strength in concrete are as follows:

- A **low w/b** (or w/c) **ratio** of 0.40-0.20[11, 13-14] to enhance the strength and densification of the hardened cement paste (hcp) matrix[5, 8, 11]. Achieving this by increasing the binder (or cementitious material) content will not in itself guarantee high strength[2].

- The use of **superplasticizers** to ensure that adequate workability is obtained at low w/b ratios. Without using superplasticizers, the water content of the mixture cannot be reduced very far as it would produce an unworkable (low or no-slump) mixture[11], and preclude the concrete from being placed and compacted in structures with conventional techniques[4]. Without a superplasticizer the w/b ratio cannot be reduced below 0.40[11, 13].

- The use of strong and uniform crushed rocks such as limestone and granite, with a maximum size of 10-12 mm[11], are normally preferred as **coarse aggregates**. **Fine aggregates** free from clay or silt, and with a fineness modulus of about 3.0 are often recommended[1, 3].

- Improving the strength of the **transition zone** between the aggregate and the hardened cement paste (hcp), which is typically 10 to 50 μm wide, is also considered a key factor in producing HSC. Cement replacement materials (**CRMs**), particularly condensed silica fume (CSF), are beneficial in this respect[2].

Optimizing the relative proportions of the various constituents in HSC is more complex than for conventional or normal-strength concretes[2] (NSCs). It requires careful selection of the materials, an understanding of their interactions (particularly with regards to superplasticizers and CRMs), and how these ultimately affect the fresh and hardened properties[5, 15].

The construction methods and equipment used in the production of HSC are essentially similar to those in conventional concreting[1]. The main difference being in accommodating for the rapid losses in workability[11 , 16-17] and higher energy demands imposed by the concrete during the mixing[1, 18], transportation, placement and compaction stages[11, 19-22].

1.2.2 Applications

Although many practical aspects regarding the fresh properties of HSCs during transportation, placement and compaction still need to be examined and understood, the material has nevertheless been successfully utilized in numerous civil engineering projects. The vast majority of these have been in **high-rise buildings**[11, 23-26], long span **bridges**[27-29], and **offshore structures**[30-32]. Some examples of the application of HSC in these areas are listed in **Table 1.1-1.3**.

The main exploitable attribute of HSC in high-rise buildings is the economic benefit of column cost optimisation. In this respect it has, for example, been reported that a tripling of the compressive strength of the concrete merely raises the material costs by 20-25%[33].

In long span bridges, the higher compressive strength per unit weight/volume of HSC allows increases in span capacity, reductions in girder depths, lighter and more slender piers, and thus reduces the load that has to be carried by the foundations. In offshore structures, the use of HSC has primarily been driven by its potentials for weight reduction and enhanced durability.

To overcome the problems associated with the rapid loss of workability of HSC, several methods have been adopted over the years to control its slump loss. (It is generally believed that the workability of fresh concrete increases with increasing slump level (section 2.2.2), and that a low slump loss is associated with a low rate of loss of workability). The main methods used are to :

- **add a higher than normal dosage** of superplasticizer at the mixing plant, and/or **use a retarder** in the formulation[30, 34]. These methods have, however, been reported to cause unacceptably low early strengths, or can in some cases even accentuate the slump loss problem[16, 19, 34].

- **redose the concrete** with additional superplasticizer on arrival at the job site[14, 30, 34]. Although the redosing method is the most widely used field method of reducing slump loss, it necessitates extra facilities, manpower, and greater control in the scheduling of trucks[25, 34]. Apart from strength penalties, it has been reported that the durability properties of the hardened concrete (abrasion resistance, etc.) may also be impaired by redosing[34-35].

- Employ more **efficient superplasticizers,** often referred to as High-performance or New-generation superplasticizers (section 2.5.1.2). These products generally enhance the productivity of concretes with very low w/b ratios (below 0.25), reduce the dosage requirement to obtain a given slump, and/or allow the slump to be retained during long transportation and placing periods of up to 150 mins[27-28, 30].

Many HSC applications have also successfully exploited the economic and technical benefits of using CRMs in binary blends (of OPC with PFA, GGBS or CSF), or Ternary blends (of OPC and CSF with either PFA or GGBS)[23-24, 26, 29-31]. Although the use of CRMs such as PFA and GGBS is normally considered to reduce the rate of slump loss (section 2.6), there is a lack of information on their workability/slump retention properties under field conditions.

Table 1.1 : Examples of some high-rise buildings utilizing HSC[11, 23-26].

Building	Location	Year	Strength (Nmm^{-2})	No. of Storeys
Water Tower PLace	Chicago	1975	65	79
La Lourentinenne Building	Montreal	1984	93	-
Scotia Plaza Building	Toronto	1987	70	68
Melbourne Central Building	Melbourne	1988	70	55
Pacific First center Building	Seattle	1989	96.5	46

Table 1.2 : Examples of some long-span bridges utilizing HSC[27-29].

Bridge	Location	Year	Max. Span (m)	Strength (Nmm^{-2})
Tower Road Bridge	Washington	1981	42	62
Joigny Bridge	France	1989	46	80
CNT Super Bridge	Japan	1992	-	100
Tsing Ma Bridge	Hong Kong	1995	>100	>/= 50

Table 1.3 : Examples of some off-shore structures utilizing HSC[30-32].

Platform	Location	Year	Strength (Nmm^{-2})	Concrete Vol. (m^3)
Ekofisk 1	Ekofisk	1973	45	80,000
Gullfaks C	Stavanger	1989	83	240,000
Heidrun	Heidrun	1995	60-70	* 65,000

All strengths are at 28 days

* Light weight concrete

1.3 Advantages and disadvantages of HSC

Although there are definite technical and economical advantages in using HSC, many of its proponents also recognize certain disadvantages in both its fresh and hardened states. Few of these are however considered to be insurmountable, but can, in some cases, negate the advantages of using HSC[36]. Some of the main advantages and disadvantages reported in the literature are summarized below.

1.3.1 Advantages

1. In the fresh state, flowing HSC produced by the use of high superplasticizer dosages and cement contents, although appearing viscous and sticky, has in some cases been reported to make **pumping and placing operations easier**[1, 12].
2. **Hardly any bleeding and segregation** are known to occur, particularly when silica fume is used or when the w/b ratio is very low[18].
3. The high early strength gains allow **earlier formwork removal**, implying important savings and simplifications[12].
4. In the hardened state, besides its **greater compressive strength**, HSC also has **enhanced tensile and shear strengths**[1, 3, 12]. These imply:
   - **reductions in** the size and/or number of **structural elements**
   - **greater resistance** of the elements **to** shear, point and impact **loads**.
5. The low water-binder ratio required to produce HSC also confers **enhanced durability** (i.e. improved resistance to abrasion, freezing and thawing, attack by aggressive chemicals)[1, 3] and, therefore, increased service life.

1.3.2 Disadvantages

1. In contrast with NSC applications, the use of **low slumps** is considered to be **impractical** in HSC applications. The minimum acceptable slump for site placing HSC is 65-75 mm[1, 37], below which special consolidation equipment and practices are considered necessary[1].
   - The necessity of **high slumps** (often in excess of 200 mm, particularly in

areas of congested reinforcement[18, 38-39]), **increases cost** in terms of superplasticizer dosage requirement, and requires **greater control** during batching.

- Despite their higher slumps, HSCs are generally considered to be **more sticky/cohesive**[1, 38, 40] (i.e. **less workable**)[17] than NSCs.

2. The **greatest draw back** in using HSCs is that they exhibit **rapid losses of workability**, making it practically impossible or uneconomical to recover the workability by adding more superplasticizer[39, 41]. Besides increasing handling difficulties, the reduced workability places greater demands on construction plant than NSCs[18, 21-22] and can cause cold joints, honey combing, and post holes in the hardened concrete[42].
3. The use of high cement contents (often in excess of 500 kg/m^3) can generate **high heat of hydration** temperature rises, and cause **thermal cracking** in massive sections[43].
4. The use of low water contents and CSF is believed to cause **self-desiccation** and, hence, **shrinkage** of the concrete[11-12, 44].
5. A major disadvantage of hardened HSC is that it exhibits increasing **brittleness** (i.e. **decreasing ductility**) with increasing strength[45-46]. The problem is of particular significance with regards to the energy absorption characteristics of structures in seismic areas[45], and is represented by sudden spalling of the concrete cover[47]. To obtain the same ductile behavior as NSC, a considerably larger amount of confinement/lateral reinforcement is required for HSC[46].

1.4 Workability issues

In general terms, the workability of fresh concrete is used to describe the ease with which the material can be mixed, transported, placed, compacted and finished[7, 48]. (The workability and rheological properties of fresh concretes are more fully defined in section 2.2). Although these properties are often considered to be only of transient interest in so far as they affect the hardened concrete, it is accepted that a concrete

mixture that can not be easily placed and fully compacted is not likely to produce its maximum strength and durability[11]. Representative evaluations of the workability properties and their evolutions with time are, therefore, crucial in assessing potential problems between the mixing and compaction stages, the suitability of construction plant and practices, and ultimately in determining how these influence the hardened properties.

In practice, the workability of fresh concrete is normally assessed by standard tests. such as the slump test (see section 2.2.2.1), which are known to be sensitive to, for example, changes in water content. It has however been widely established since the early 1970's (with the development of several two-point workability test devices (reviewed in section 2.2.2.2)), that the behaviour of fresh concrete under varying shear rates closely approximates to the **Bingham model** (**figure 1.1**). This requires measurements at two or more shear rates (or points), and gives a straight line relationship of the form:

$$\tau = \tau_o + \mu.\gamma \quad \text{or} \quad \mathbf{T = g + h.N} \qquad \mathbf{(1.1)}$$

where the intercept τ_o (or **g**) is known as the yield stress or (value), and the slope μ (or **h**) is called the plastic viscosity. The **yield value** is "a measure of the minimum force necessary to start movement" of the concrete, and is considered to influence its flow under self-weight[7]. The **plastic viscosity** is "the subsequent resistance to deformation" of the concrete at higher shear rates (or speeds), and is believed to influence its ability to be manipulated during pumping and compaction[7, 49-50].

According to Tattersall[7] all the standard workability tests are essentially single-point tests, which measure a single parameter reflecting either the yield (g) value of the concrete or its plastic viscosity (h). He argued that there are only two sets of circumstances where a single-point test may be useful:

1. When the effective shear rate in the test is the same that applied in practice.
2. When the Bingham flow-curves of concretes tested form non-crossing lines.

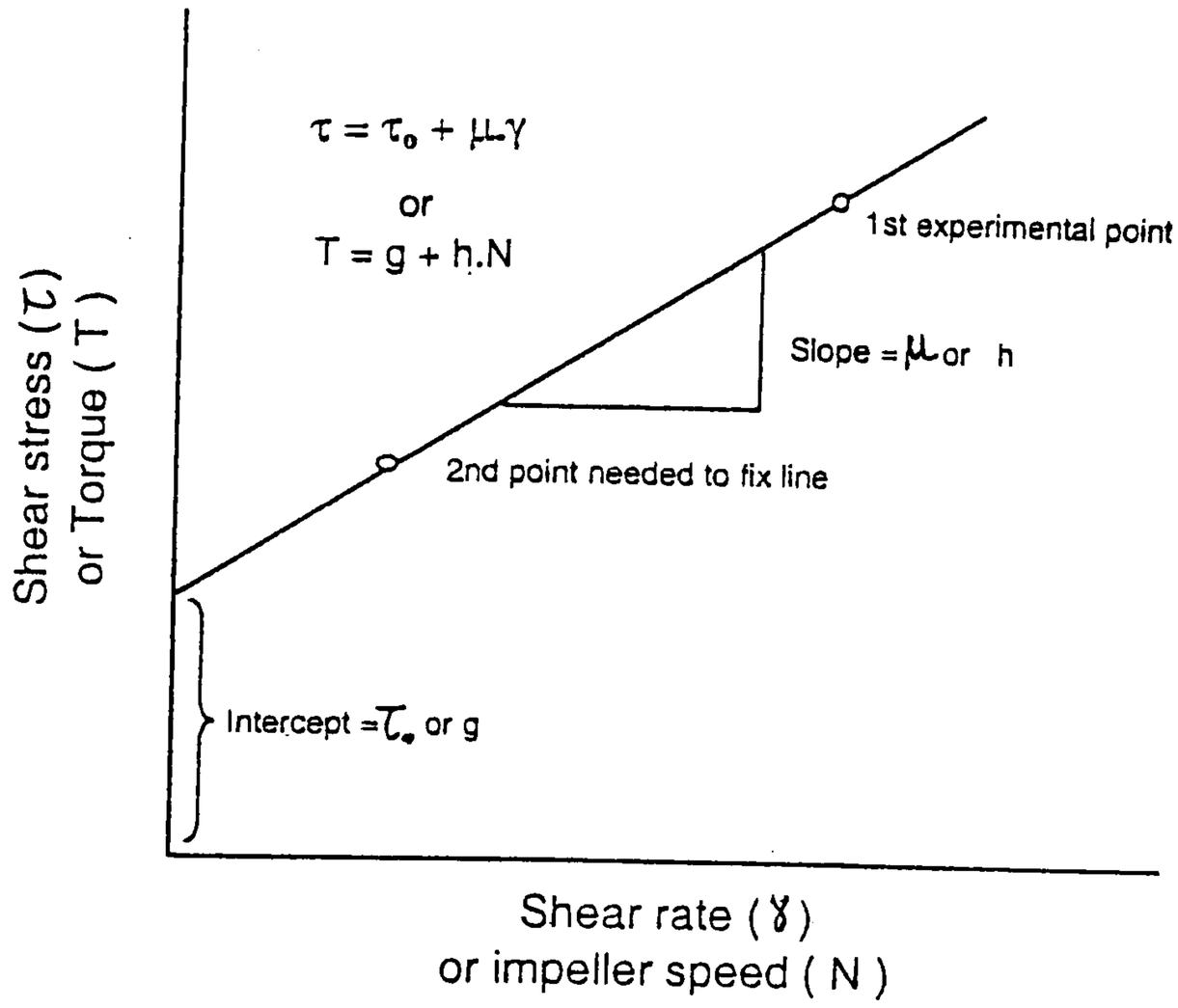

Figure 1.1 : Illustration of the Bingham model[7, 50]

Although it has been widely reported that the fresh properties of HSCs are distinctly different from those of NSCs[3, 5, 17, 30, 38], there is very little information on how they differ, particularly with regards to mix stability and compactability. Much of the information in the literature on the workability properties of both NS and HSCs has almost exclusively been confined to measurement with the slump and flow table tests, whose suitabilities has been even more widely questioned with regards to assessing the sticky/cohesive nature of HSCs[17, 51-54].

The lack of understanding of the workability, mix stability and compactability properties of HSC has led to considerable difficulties in the field. For example, it has been found on a number of sites that HSCs are extremely sticky and difficult to pump[40], and exhibit rapid losses of workability which can reduce the workability time to 15-20 minutes with some superplasticizer-binder combinations[16]. This is too short for rational concreting, even in precast element production, and can make full

compaction impossible. Indeed, maintaining satisfactory rheological properties (i.e. workability, mix stability and compactability) for a sufficient time of 60 to 90 minutes, to meet transportation and placement requirements, has been considered to present the greatest difficulty in producing HSC[11], and is one important reason why the material does not yet match its advantages[17, 40].

1.5 Research significance and thesis structure

Although HSC has been successfully used in many civil engineering structures, many practical aspects regarding its behaviour during construction still need to be examined and rationalized. The main concerns pertain to the:

- **assessment of** the **fresh properties** and their evolutions during the transportation, placing and compaction stages; and
- how these ultimately influence the **hardened properties**.

Following a summary of the main literature review (in chapter 2), a more comprehensive research Programme, detailing the aims and scope of the present research, is formulated in chapter 3. The materials used and the main experimental methods adopted in the research are described in chapter 4.

Chapter 5 presents the results of **preliminary rheological measurements** carried out with NS and HSCs. Chapters 6 and 7 respectively focus on the effects of **superplasticizers** and **CRMs** in reducing the rates of losses in workability prior to the placing and compaction stages. Chapter 8 introduces a novel method developed to assess the **placing characteristics** and **vibration response** of HS and other HPCs. The use of the method in optimising the **strength development** characteristics corresponding to different vibration inputs is explored in chapter 9. The thesis ends with conclusions and recommendations for further work (chapter 10).

Chapter 2
Literature Review : Workability, Material Selection, and Strength Development

2.1 Introduction

The previous chapter highlighted the production requirements, some important applications, advantages, disadvantages, and workability issues of HSC. Lack of attention to the selection of materials and evaluation of the workability properties of HSC is considered to be the origin of many of its technical problems in the fresh and hardened states.

Following many years of slow advances in HSC technology, much has been learned about its processing, fresh properties, testing, and strength development. The amount of information gained is reflected by the vast number of publications which have appeared over the last two decades, particularly with regards to the use of superplasticizers and CRMs. Most of the information in the literature is however fragmented, conflicting and thus confusing. This chapter reviews:

1. Important definitions and measurements of **workability/rheology** (section 2.2),
2. The effects of **material selection**, in terms of
   - water content and **w/b ratio**;
   - **aggregate characteristics** (particularly aggregate absorption);
   - **superplasticizers** (viz. type, mode of action, dosage, mixing procedure, and compatibility with cements), and
   - **CRMs** (in both binary and ternary blends).

   The effects of each of these mix design variables on the initial workability properties, workability retention and/or slump loss of NS, HS and/or HPCs are separately discussed in sections 2.3-2.6.
3. The effects of **mix stability** and **compactability** on the fresh properties (section 2.7).
4. How the **strength development** characteristics in the hardened state are influenced by different degrees of compaction/vibration (section 2.8).

2.2 Workability/Rheology

2.2.1 Definitions of workability and rheology

As mentioned previously in section 1.4, the term **workability** is generally used to describe the ease with which fresh concrete can be mixed, transported, placed, compacted and finished[7, 55]. There is however no single precise definition of workability in the literature, most definitions are qualitative in nature, and are more reflections of the personal viewpoint rather than having any scientific basis.

Despite his vast experience in testing fresh concrete, Tattersall[7] simply refers to the workability of fresh concrete as an intrinsic property governing the flow properties of the material (i.e. its ability to flow in a mould or formwork, be manipulated during pumping, compaction etc) which closely approximate to the **Bingham model** (c.f. figure 1.1). Although Tattersall has not given an unequivocal definition of workability, he suggests that the two Bingham parameters, together, provide a comprehensive description of the workability of fresh concrete. (Mechanistically, the yield value is believed to be related to inter-particle friction, whilst the plastic viscosity is considered to reflect the internal resistance to flow[56]).

In contrast, Mehta and Monteiro[57] consider workability as being composed of two components: **consistency*** (ease of flow) and **cohesiveness** (resistance to segregation) which they suggest can be related to the type of construction methods used. Many other workers[8, 19, 58] however ignore cohesiveness and use consistency synonymously with workability to refer to the stiffness or firmness of the mix, its slump, fluidity (or degree of wetness) etc.

The ASTM C 125-93[59] definition of workability is "that property determining the effort required to manipulate a freshly mixed quantity of concrete with minimal loss of homogenity". In contrast, Glanville et al[60] defined workability as "that property of fresh concrete which determines the amount of useful internal work required to produce full compaction".

* **Consistence** is the equivalent EC term.

Ritchie[61] considered such definitions too restrictive, and related the workability of fresh concrete to its rheological (or flow) properties. **Rheology** is the science which deals with the deformation and flow of materials, and includes the behaviour of freshly mixed and hardened concretes, as well as the behaviour of slurries and pastes under varying stress, strain and time [61, 65-67].

Ritchie[61] subdivided the rheology of fresh concrete into three main categories: stability, compactability, and mobility as shown in **figure 2.1**. Newman[62], Uzomaka[63] and Tassios[64] have similarly identified stability, compactability, and mobility as three separately distinguishable components of fresh concrete, but did not quantify them.

Although figure 2.1 points out these as distinct properties, Ritchie[61] did not show whether any relationships exist between them. In this respect ACI Committee 309[65] has, for example, stated that the mobility properties (i.e. the ease with which concrete can flow in a mould, around steel and be remoulded) may affect mix stability and compactability.

Although Tattersall[7, 68] and others[38, 61, 67] have used the terms workability and rheology synonymously, it should be noted that a high workability does not necessarily imply better rheology, since an increased workability has, particularly in NSC, been associated with reduced mix stability[18]. In this thesis :

- the **workability** of fresh concrete is used to refer to the ease with which the material can be used (i.e. manipulated or handled) and, in accordance with Tattersall[7], is expressed in terms of the Bingham model (figure 1.1).

- **Rheology** is, on the other hand, used to refer to the combination of the workability, mix stability and compactability properties in the fresh state as defined by Ritchie[61] (figure 2.1). (That is, workability is considered as only one component of the rheology of the fresh concrete).

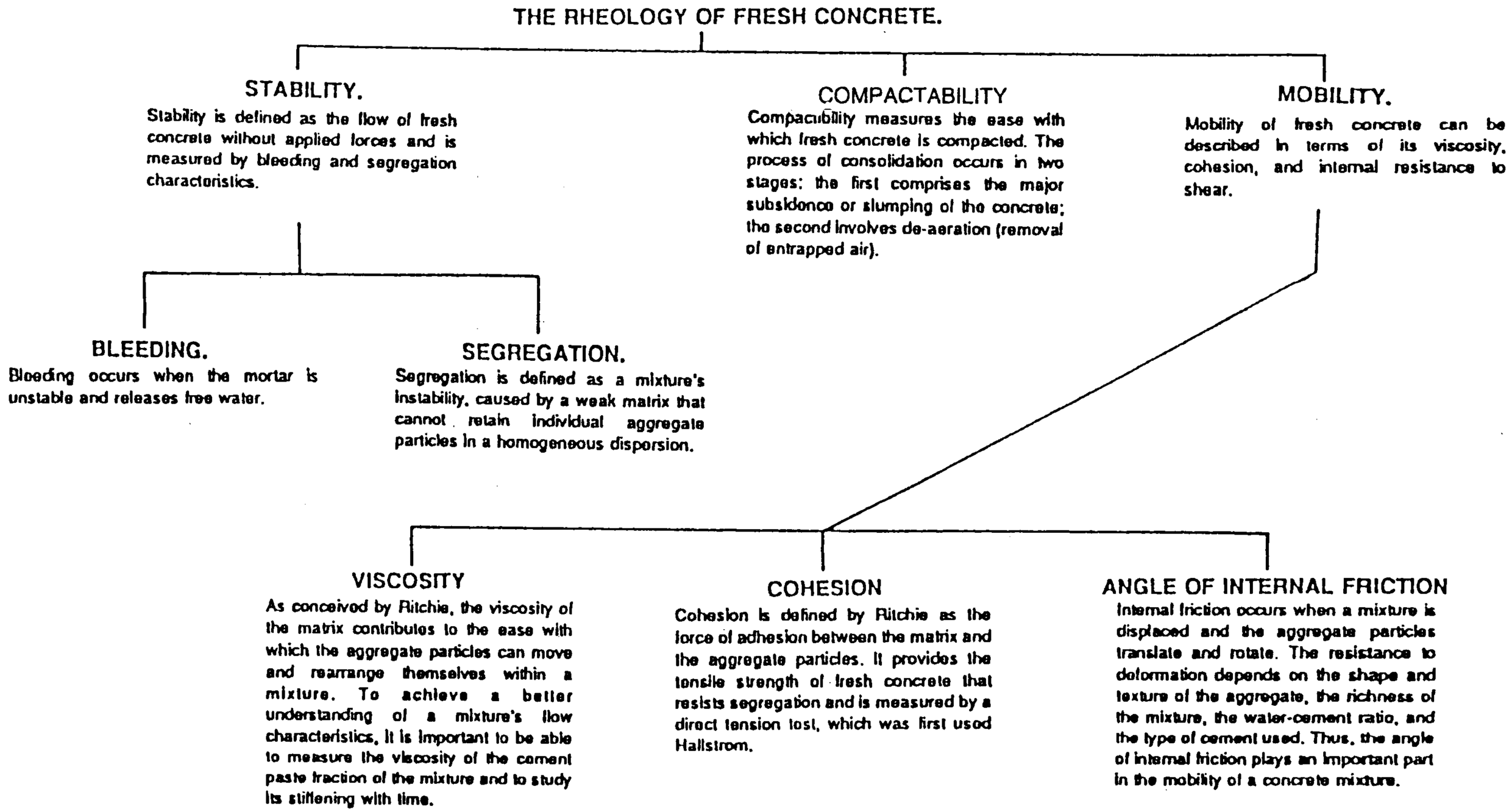

Figure 2.1 : Ritchie's sub-division of the rheology of fresh concrete[61].

Although many workers[7, 49, 67-70] refer to workability as a property dependant on both mix stability and compactability, most workability measurements have almost exclusively been confined to measuring the Bingham parameters, and/or using standard single-point tests.

2.2.2 Measurements of workability

2.2.2.1 Standard (or traditional) tests

As far back as 1968, Powers[71] identified nearly a hundred different empirical tests developed for the assessment of workability. Only a few of these tests have been incorporated into standards; the rest have received very limited use. Some of the more common standard (or single-point) tests are described below.

(I) The slump test

The slump test is by far the oldest and most widely used field test for the measurement of workability. It was introduced by Abram[72] in 1918, and is now described by BS EN 12350-2:2000[73] (**figure 2.2(a)**). The test consists of filling a steel mould with concrete in three layers of equal volume; each layer being rodded 25 times with a 16 mm diameter steel rod. The mould is then lifted away vertically, and the slump is measured by determining the difference in height of the mould and the collapsed concrete. (That is, the slump is a measure of the ability of the concrete to support its self-weight: a low slump implies a low workability, and vice versa).

Since the slump measurement is made on a stationary cone of concrete, it is assumed that the shear rate associated with the test is zero, or, in other words, that the slump test assesses the yield value of the concrete, but gives little or no information about its plastic viscosity[7, 40, 54]. Its success is primarily attributed to its sensitivity as a detector of small changes in water content between successive deliveries of the same concrete.

(II) Compacting factor test

The compacting factor test uses a double hopper arrangement to drop concrete into a standard cylinder mould (**figure 2.2(b)**). The test was developed in the UK by Glanville et al[60] to measure the compactability/workability after the application of

a standard amount of work, and is described by BS 1881: Part 103[74]. The upper hopper is filled with concrete, which is then dropped into the smaller hopper and into the bottom cylindrical mould. The excess concrete is struck off, and the compacting factor is determined as the density ratio of the concrete in the cylinder to the fully compacted concrete.

The test suffers from the disadvantage that the apparatus is not suitable for field use. It has also been reported that some cohesive mixes tend to stick to the sides of the hoppers, whilst mixes with low workabilities produce wide variations in results[7].

(III) Vebe test

The Vebe consistometer was developed in Sweden in 1940, and is described by BS 1881: Part 104[75]. A standard concrete slump cone is cast, the mould removed, and a transparent disk placed on top (**figure 2.2(c)**). This is then vibrated at a controlled frequency and amplitude until the lower surface of the disk is completely covered with grout. The time for this to occur is recorded as the Vebe time (in seconds). The main criticisms of the test are that the wetting of the disk with mortar is not uniform, and the end point of the test is often difficult to define.

(IV) Flow table test

The Flow table test is described by BS 1881: Part 105[76] and involves casting a sample of concrete in the form of a frustrum of a cone (200 mm ϕ at the base, 130 mm ϕ at the top, and 200 mm high). This is then dropped 15 times in 15 seconds through a height 40 mm in the centre of a drop table (**figure 2.2(d)**). The resulting flow diameter of the concrete is measured; a spread of 500 mm indicates high workability whilst 400 mm medium workability. Again, concretes with the same flow table spread value may have quite different workabilities in the field.

As mentioned previously, Tattersall[7] argued that all the standard tests are all single point tests (i.e. measure only one parameter) and, therefore, cannot be expected to provide intrinsic measurements of the workability of fresh concrete which approximates to the Bingham model. The tests essentially measure the

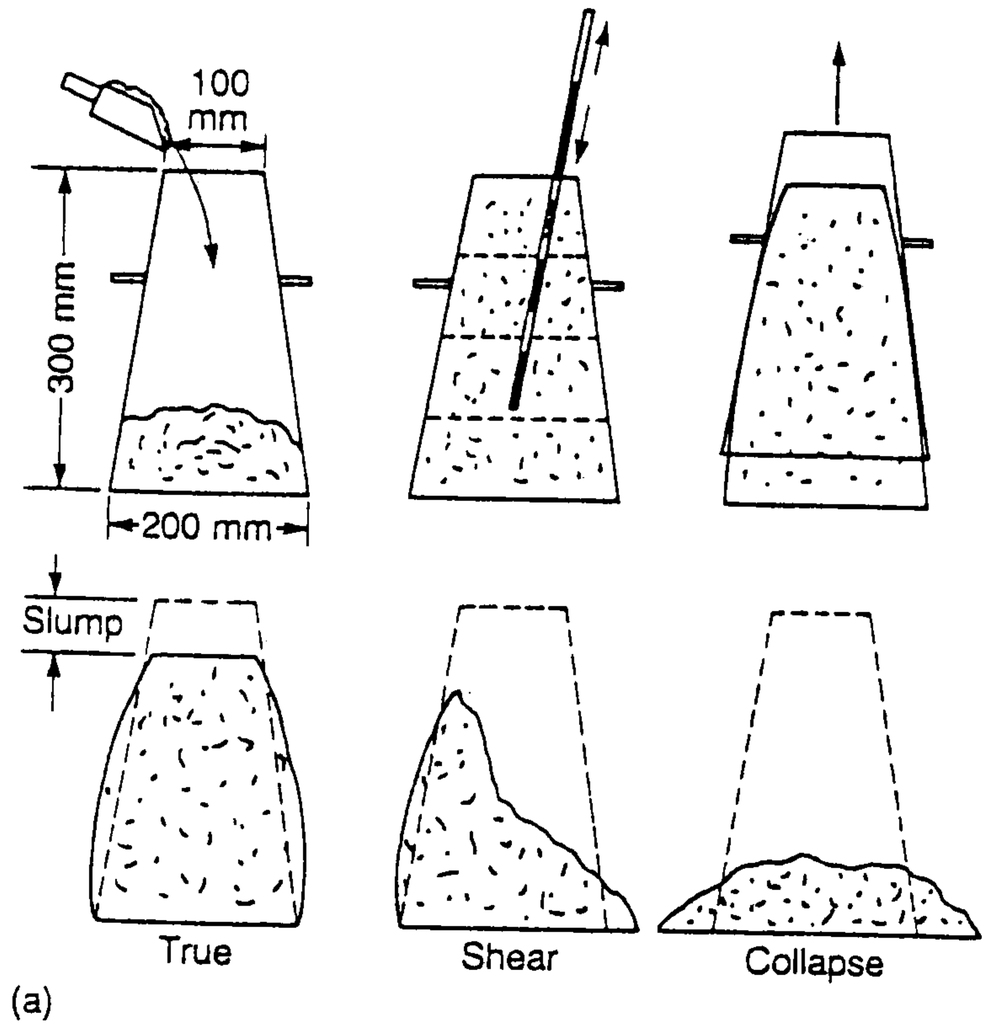

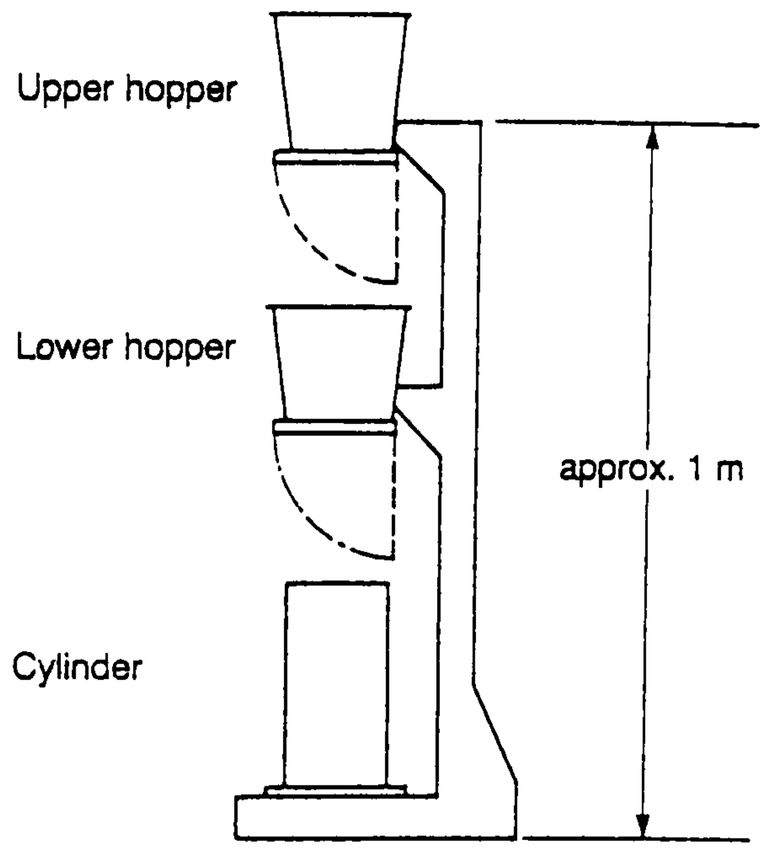

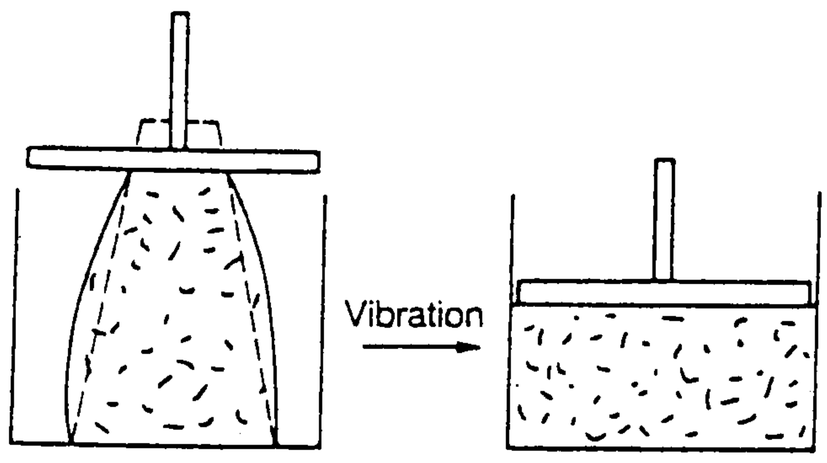

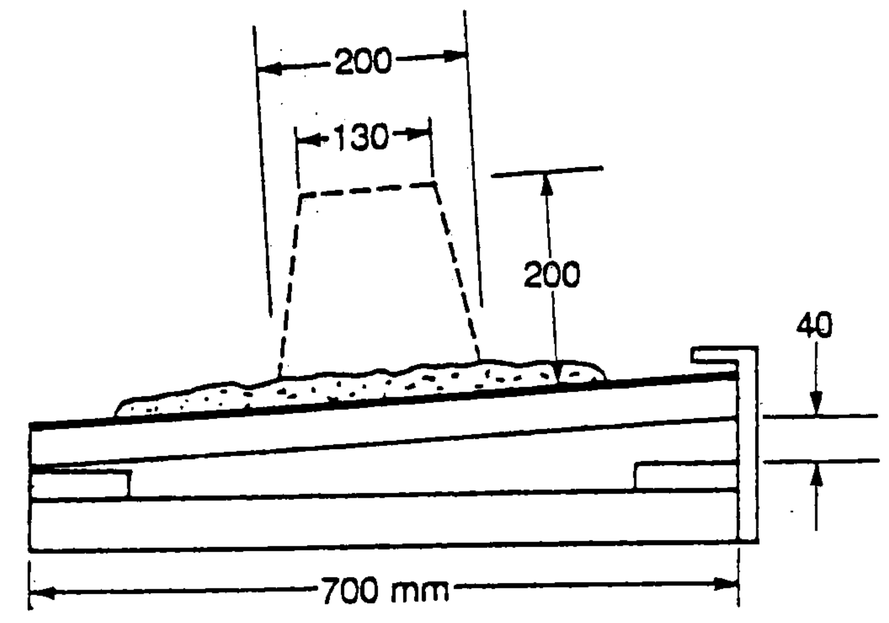

Figure 2.2 : Illustration of (a) the slump, (b) compacting factor, (c) Vebe, and (d) flow table single-point tests[263].

response of concrete under specific, but arbitrary test conditions, meaning they cannot be easily compared, and can therefore classify as identical two concretes that are subsequently found to behave differently on site. He stated that any two concretes which have the same Bingham (i.e. g and h) values as measured by his two-point workability test apparatus (section 2.2.2.2(I)) must behave in the same way in a given set of practical circumstances.

An important practical example highlighting the inadequacy of the standard slump test was reported by Helland[54], who compared the workability of three concrete mixes (1, 2 and 3) in terms of slump and the Bingham parameters with practical site experience. Despite having similar slumps and yield values (**figure 2.3**) mixes 1 and 2 behaved quite differently on site. Mix 1 responded well to a poker vibrator, whilst mix 2, which contained a high dosage of superplasticizer, did not. He attributed this to a greater internal resistance of mix 2 at higher rates of shear. The problem was resolved by adding an air-entraining agent (mix 3) which decreased the plastic viscosity. Helland concluded that the slump test reflects the situation when the rate of shear is near zero, and provides very little information on how fresh concretes behave in practice.

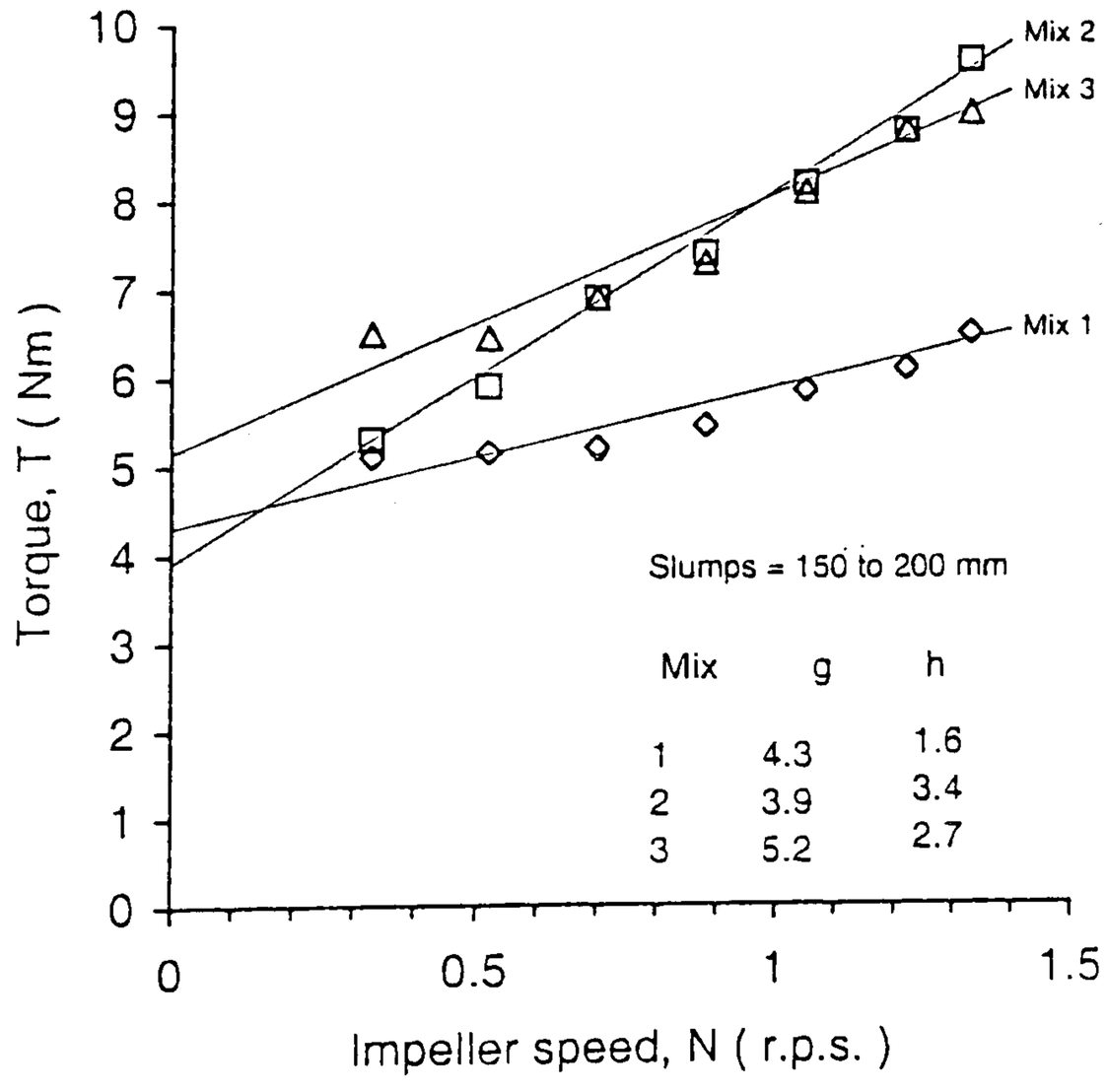

Figure 2.3 : Comparison of Bingham flow curves of concretes having comparable slumps of 150 to 200 mm (at w/b ratios of 0.65, 0.35, and 0.38 (mixes 1, 2, and 3))[54].

2.2.2.2 Two-point workability test measurements

Since the early 1970's there has been increasing awareness of the limitations of single-point tests and interest in rigorous testing of fresh concrete. This has been spurred by the development of several workability test devices, which characterize the behaviour of fresh concrete (usually in accordance with the Bingham model) - by determining the relationship between the torque (or shear stress) generated on an impeller, cylinder or plate rotating in/around fresh concrete at different speeds (or shear rates). In practice, absolute measurements of the Bingham parameters are difficult, since these do not only depend on the concrete properties, but also on equipment geometry and testing conditions. The main two-point workability test devices in the literature are reviewed below.

(I) Tattersall's two-point workability test apparatus

In all, Tattersall and his co-workers[68, 77-80] developed three versions of his two-point workability test apparatus. The first of these, the **MKI tester**, was introduced in 1973[68] and was based on an ordinary (Hobart) food mixer with a power requirement measuring device. During testing, an impeller in the shape of a hook, moved in planetary motion to ensure that it continuously came in contact with new concrete. Plots of the net torque (T, determined from the difference in power requirements with the bowl empty and when it contains concrete) at three available speeds (N) were shown to closely fit the linear Bingham relationship.

Work by Scullion[77] and Bloomer[80] had, however, indicated several inadequacies with the MKI arrangement. Notably the restricted number of speeds, the inconsistency of its electrical characteristics, and the insensitivity of the equipment at high workabilities. To overcome these deficiencies, Tattersall and Bloomer[78, 80] developed a new (**MKII**) two-point test apparatus during the late 1970's (as shown in **figure 2.4**). The concrete under test is contained in a cylindrical bowl, and is sheared by an interrupted helical impeller rotating uniaxially. This is driven by an electric motor operating through an infinitely

variable hydraulic transmission system and a right-angled reduction gear box.

The torque at each of a range of speeds is determined by reading the pressure of the oil in the hydraulic transmission (via a pressure gauge). The apparatus in this form was considered suitable for testing **high-medium workability** concretes, and is more commonly referred to as the **MH system**. At lower workabilities, the helical impeller tends to move concrete to the side of the bowl and proceeds to rotate in the resulting hole, that is, the concrete sheared during testing fails to fall back to the centre of the test bucket[7].

This limitation led to the development of the **MKIII** apparatus[79]. This is a simple modification of the MKII system, in which satisfactory movement of the concrete at **low-medium workabilities** is achieved by replacing the helical impeller with a H-shaped impeller rotating in planetary motion (**figure 2.5**). To prevent the impeller from returning to the same position and making a continuous channel during shearing, a 20:1 gear box and a planetary drive (with a 2.25 gear ratio) are used. The apparatus in this form is commonly referred to as the **LM** (low-medium workability) **system**. According to Tattersall[7, 81] the MH system and its complementary LM system can together cover almost the whole range of practical workabilities, and are useful in assessing a wider range of mix design variables.

Several workers have made minor modifications to Tattersall's two-point test apparatus while preserving its essential principles[82-85]. Cabrera and Hopkins[82] incorporated strain gauges and slip rings to record the torque directly on a chart recorder. Wimpenny et al[83] and Wallevik et al[84] used an electronic tachometer and pressure transducer to relay the test output to a computer or recorder. More recently, Domone et al[85] have produced a more compact machine with a single gearbox to obviate the need for changing from the MH to LM modes. The relevant theory for calibrating Tattersall's two-point test apparatus and expressing the Bingham parameters in fundamental units (Pa and Pa.s, to enable comparison of instruments) has been fully described elsewhere[7, 66, 78].

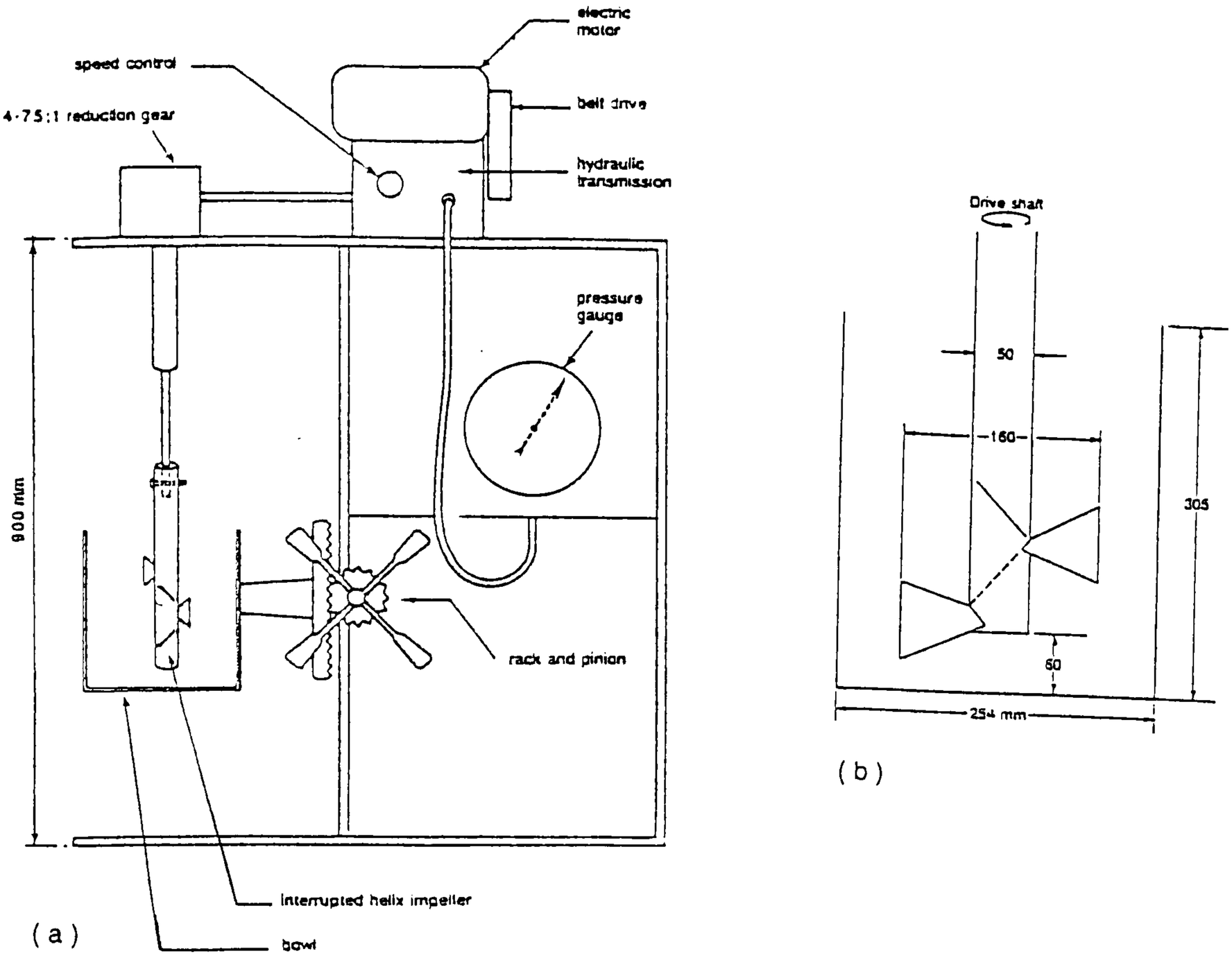

Figure 2.4 : Tattersall's two-point workability test apparatus in the (a) MH mode, together with (b) dimensions of test bucket and helical impeller[7].

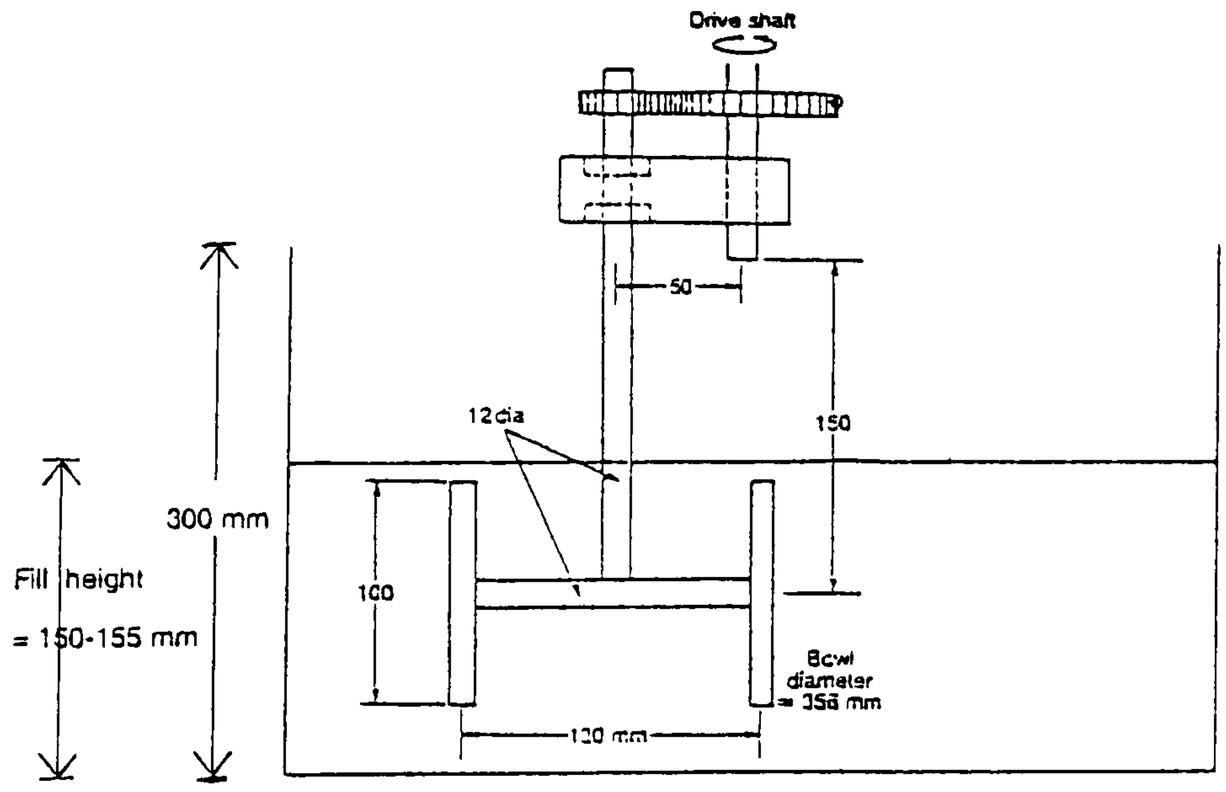

Figure 2.5 : Dimensions of H-shaped impeller and test bucket used for the LM mode[7].

(II) BML viscometer

The BML viscometer is a coaxial cylinder system developed in Norway in the late 1980's[86]. **Figure 2.6** shows a schematic cross section of the viscometer. The inner and outer cylinders (with respective radii of 100 and 200mm) are ribbed to prevent concrete slippage, whilst the rigid cone avoids any end effects. The inner cylinder which is 200 mm high, registers the torque via a load cell. The apparatus is fully computer controlled.

By measuring the torque (or the shear stress) produced on the stationary inner cylinder, while the outer cylinder is rotating at different speeds, the values of yield stress (τ_o) and plastic viscosity (μ) are determined[87] by analysing the behaviour of the concrete with and without plug flow in the 50mm annular gap[40]. (Plug flow is when the shear stress is low, and the flow occurs only in the region between the inner cylinder and a certain radius, while the rest of the material rotates as a solid plug at the same angular speed as the outer cylinder).

There is some uncertainty regarding the lower workability range of the BML viscometer. Mork[88] claims that reliable Bingham measurements can be obtained with slumps as low as 50 mm; whereas Hu et al[40] stated that the equipment is not very suitable for testing concrete mixes having slumps less than about 100 mm. It should be noted that conventional coaxial cylinders viscometers have been widely criticised as being far too small to accommodate for the coarse aggregate particles in concrete[66, 80, 89].

(III) BT Rheometer

The BT rheometer (also called the BT Rheom) is a torsional rheometer developed in France in the early 1990's[89-90]. **Figure 2.7(a-b)** shows the apparatus. The rotating and fixed parts of the container (i.e. top and bottom plates) are both spoked and symmetrical about the horizontal mid-plane (figure

2.5(b)). During testing a 7 litre sample of concrete is sheared between the two horizontal spoked plates which minimise slippage. The apparatus is computer controlled and, has the added facility that vibration can be applied to the concrete through the top plate.

The BT Rheom is reported to be suitable for testing soft-to-fluid mixes with slumps in excess of 100 mm[49, 91-92]. A single concrete sample, sheared from time to time, is used for assessing loss of workability[49, 92]. Values of yield stress and plastic viscosity are obtained from the torque/speed relationship - by assuming laminar flow[49].

The main uncertainty with measurements from the BT rheometer concerns the influence of concrete wall friction. Hu et al[91] suggested that this does not have a significant influence on the shear yield stress, but the plastic viscosity could be improved by applying a constant 10% reduction to the measured value. Another uncertainty relates to the capability of the apparatus in generating different amplitudes of vibration. Banfill[93] recently expressed some reservations about the choice of test geometry, whereas Tattersall[93] criticised some of the claims made for the device (particularly in relation to it presenting any advance on the MH and LM systems).

All the two-point test devices reviewed above provide a measure of the Bingham parameters only, and, therefore, the workability of fresh concretes. Based on the distinctions made between workability and rheology on page 14, additional tests to quantify mix stability and compactability would therefore be needed for a more comprehensive assessment of the rheological (or flow) properties of the concrete.

Some of the main test methods proposed in the literature for evaluating the mix stability and compactability of fresh concretes are reviewed in section 2.7.

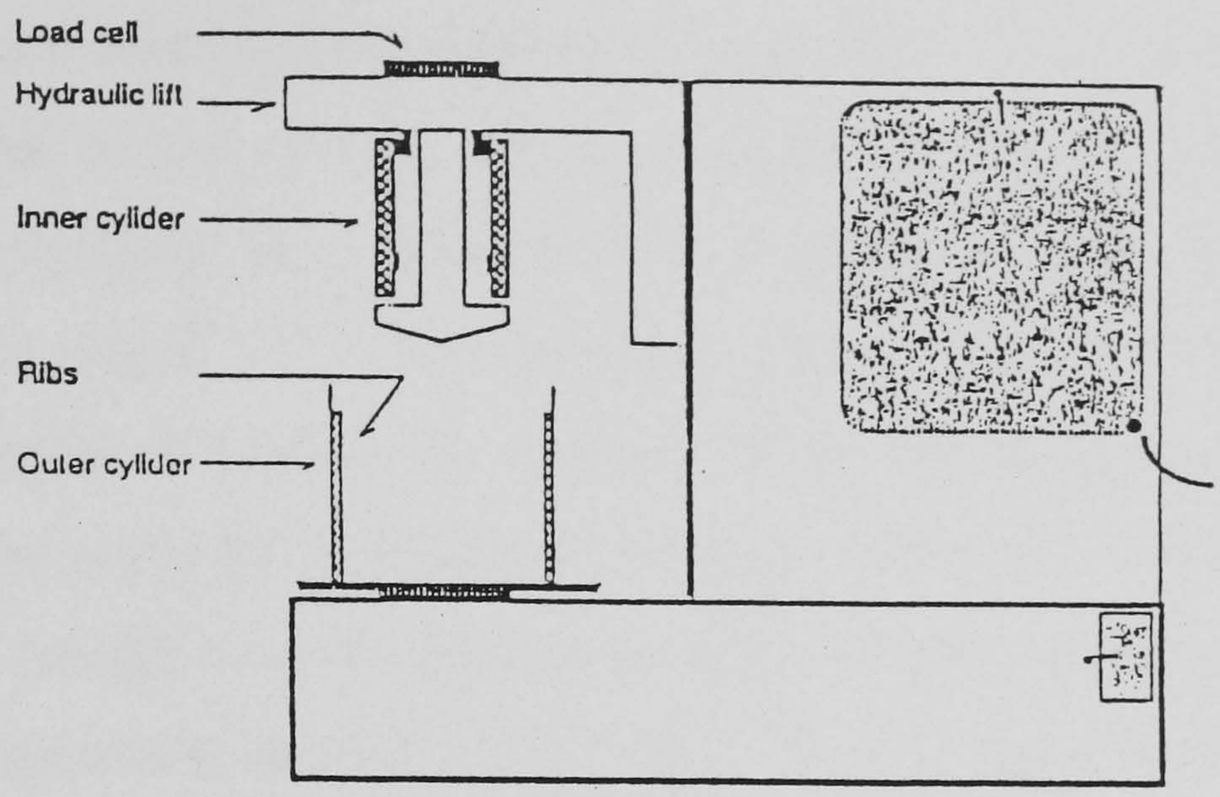

Figure 2.6 : Schematic illustration of the BML-Viscometer[86].

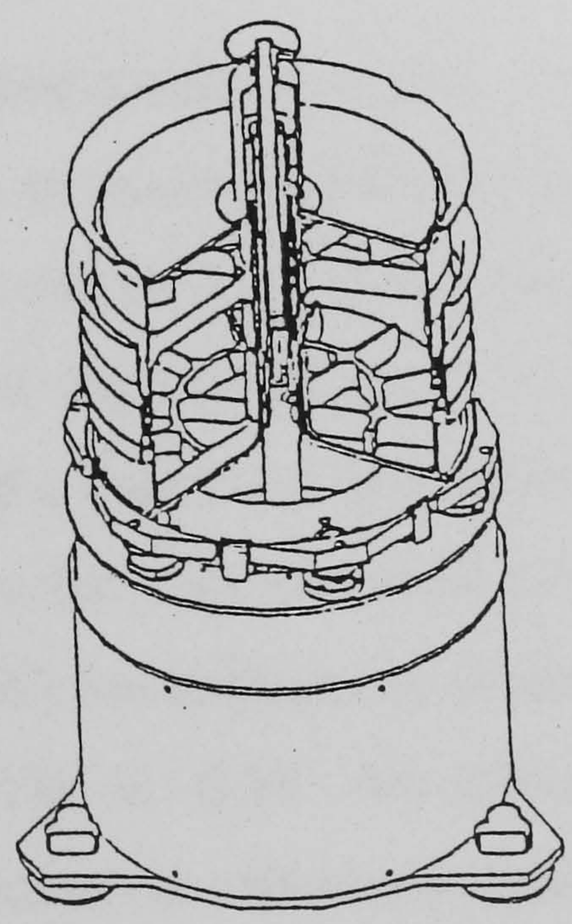

(a) 3-D diagram of the apparatus
(Body dimensions : H 30 × ϕ 30 cm
container dimensions : H 24 × ϕ 27 cm)

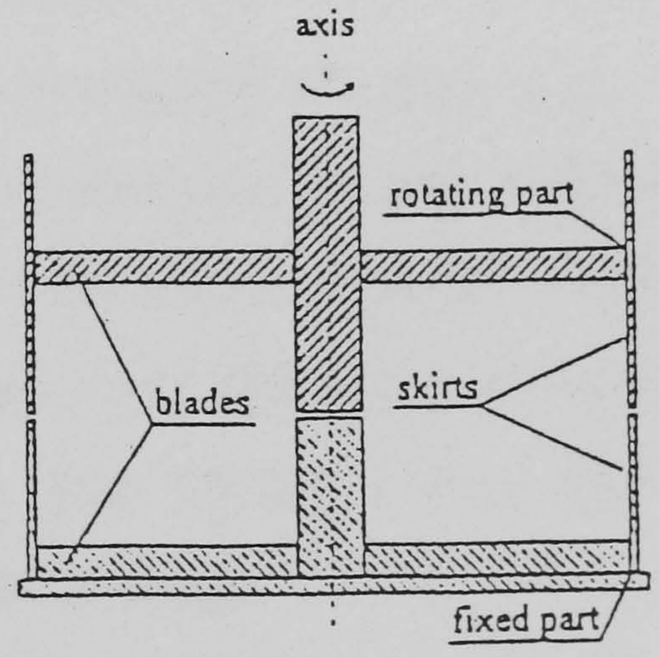

(b) 2-D diagram of the container

Figure 2.7 : Schematic illustration of (a) the BT Rheometer, and (b) testing container[91].

2.3 Water content and water/binder (w/b) ratio

The quantity of water added during concrete mixing plays two essential roles: in ensuring **hydration** of the cement, and in participating actively towards the **workability** by providing the necessary flow properties needed for ease of placement and compaction[12, 94]. The water/binder ratio is widely accepted as the most important factor influencing the strength of the hardened concrete - the higher the w/b, the lower the compressive strength. Although concrete should ideally have only enough water to develop the full and final hydraulic potential of the cement (theoretically about 22 to 17.5%)[11, 95], an excess amount of water is necessary in order to obtain a workable mixture.

A typical relationship between water content and slump is illustrated in **figure 2.8**. According to Owens[95] the quantity of water needed generally increases by 5 to 15 litres/m^3 for every 25 mm increase in slump.

As mentioned earlier in section 1.2.1, the limiting w/b ratio with respect to the production of non-superplasticized concrete is about 0.40[11, 13]. At lower w/b ratios, the constraint in workability arises, in broad terms, from an increasing tendency of the cement grains to flocculate (or cluster) and trap water. The presence of a superplasticizer deflocculates the cement particles and fluidises the mixture, so that very low water contents of 120-135 l/m^3 (compared to 150-220 l/m^3 in NSC) are sufficient to obtain high slumps of 180-200 mm at w/b ratios as low as 0.30 to 0.20. According to Aitcin and Neville[11] 5-15 L/m^3 of superplasticizer can effectively replace 45-75 L/m^3 of water.

Although many workers have investigated the effects of varying w/b ratios on the workability properties of fresh concretes, their work has been limited to individual two-point test measurements taken after the initial mixing sequence, and/or to assessing slump loss. With the MH two-point test system, Tattersall[7, 96] demonstrated that a reduction in the w/b ratio from 0.70 to 0.40 decreases the workability, in that both the Bingham parameters increase, giving a fan-shaped set

of flow curves as shown in **figure 2.9**.

More recently, Ellis[97] examined the effects of decreasing the w/b ratio from 0.50 to 0.30 (i.e. down to the domain of HSC) using Tattersall's LM two-point test system. In agreement with Tattersall's findings[7, 96], his results in **Table 2.1**, show progressive increases in both the Bingham parameters (i.e. reductions in workability) with decreasing w/b ratio. Similar results, involving individual two-point test measurements carried out immediately after mixing or at constant slump, have also been reported by Soutsos[53] with the MH system at w/b ratios 0.38-0.26, and by Hu et al[40] with the BML viscometer at w/b ratios of 0.45-0.29. Such measurements are however of limited practical significance since they do not reflect the rapid losses in workability with time and, therefore, the state in which HSC is used.

In terms of slump loss, it has been widely documented that the rate of slump loss increases with decreasing w/b ratio[14, 16, 19, 30, 34, 39]. In non-superplasticized NSC, Dewar[98] stated that mixes of lower water content or initial slump lose workability at a faster rate, because a given water loss by evaporation or hydration will have a proportionately higher effect. Collepardi[34] and Baoju et al[99] provided a similar explanation for superplasticized concretes. They suggested that the closer proximity of the cement particles at low w/b ratios (**figure 2.10**) significantly increases the rate of slump loss when the same quantity of water is lost through evaporation or by cement hydration.

In HSC, Tachibana et al[18] compared the slump loss characteristics at three water contents (of 150, 135, and 120 kg/m^3) in mixes of 0.25 w/b ratio and 10 % CSF. They found that the slump loss at the lowest water content (120 kg/m^3) was significantly higher (decreasing down to 80 mm after 90 mins) compared with only about a 20 mm reduction at the higher water contents (**figure 2.11**). From an extensive study on NSC, Pollet et al[100] have reported that there is a single rule governing slump loss: "the lower the water content, the greater the slump loss" (**figure 2.12**). They however claim that the free (or effective) water content seems to be the only relevant parameter influencing slump loss - and the effects of other

mix design variables (such as cement content, and the presence of superplasticizers or CRMs) are relatively insignificant.

Other researchers[7, 39, 101] have broadly related the rate of slump or workability loss to the quantity of water consumed during cement hydration or the formation of ettringite, and to the amount of superplasticizer molecules trapped by newly formed ettringite crystals. (These are hydrates produced by the reaction of C_3A and gypsum). According to Mehta and Aitcin[101] the rate of loss of workability in non-superplasticized concretes depends mainly on the rate of crystallization of ettringite. They suggested that precipitating ettringite crystals entrap or immobilise large volumes of water leading to consequent losses in workability with time.

In superplasticized concrete, Dejellouli et al[39] believe that it is the subtraction of the two fluidizing agents, trapped water and superplasticizer, which lead to the critical workability problem. They suggest that three possible ways of rectifying the rapid losses of workability at low w/b ratios are by:

1. using a **less reactive cement**;
2. using a **superplasticizer that is less adsorbed**; and
3. substituting part of the cement by a **less** initially **reactive CRM**.

The effects of superplasticizers and CRMs on loss of workability are discussed in sections 2.5 and 2.6.

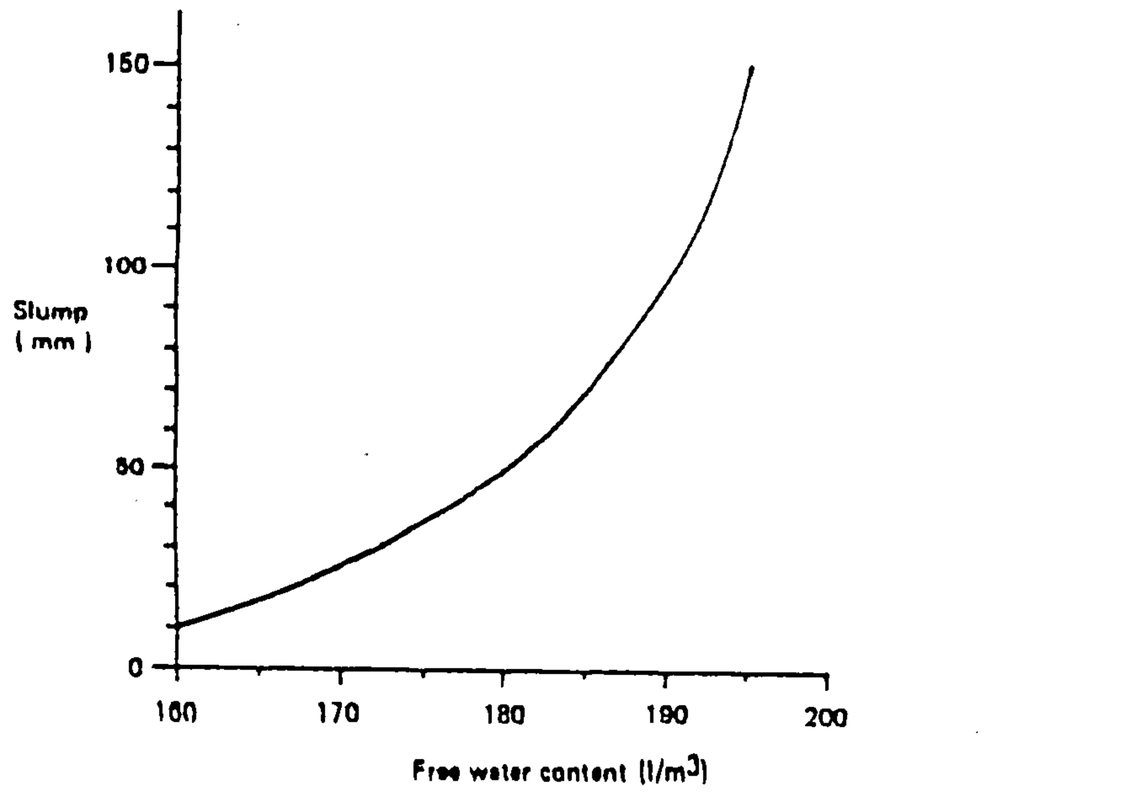

Figure 2.8 : Relationship between slump and water content[98].

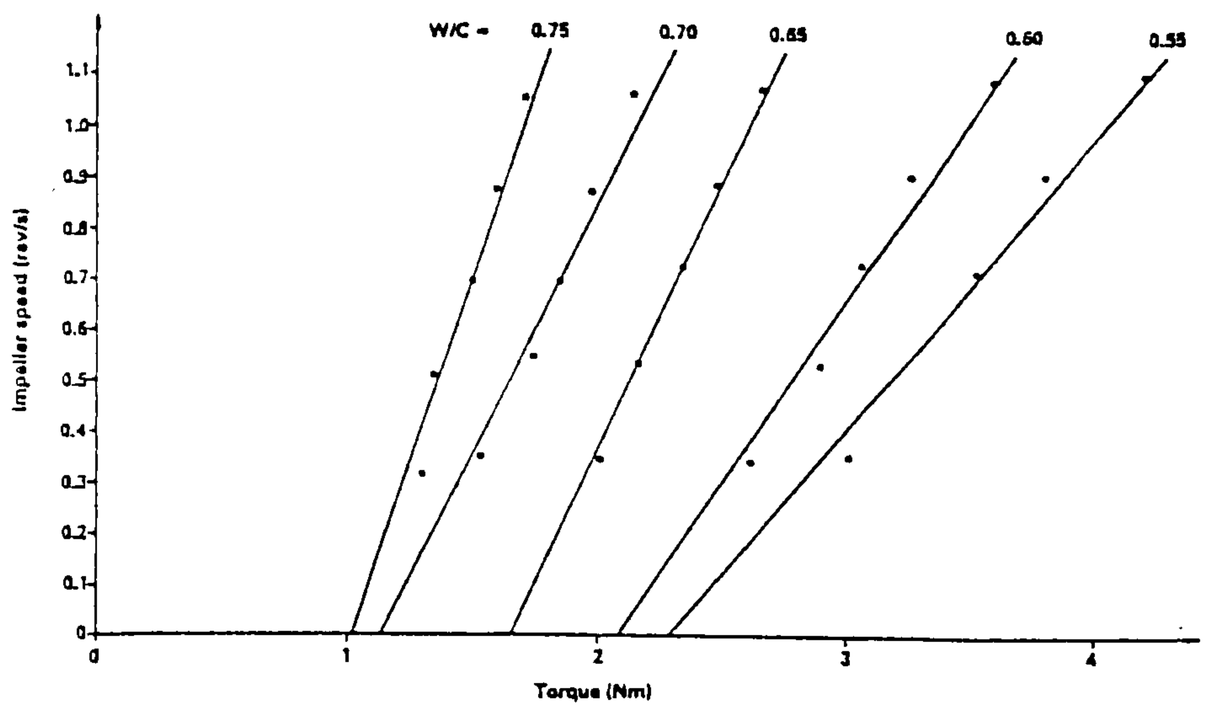

Figure 2.9 : Bingham flow curves showing effect of increasing water/cement ratio on the workability properties of fresh concrete (plastic viscosity = reciprocal slope)[7].

Table 2.1 : Workability test measurements showing the effect of decreasing w/b ratio (using the LM system, at comparable slumps and flow table values)(97).

Mix	1	2	3	4	5
w/b ratio	0.50	0.40	0.36	0.33	0.30
SP dosage % (s/w/b)	0.00	0.42	0.83	1.65	2.41
Slump (mm)	70	65	70	65	80
Flow table value (mm)	460	400	410	370	380
Yield value **g** (Nm)	3.83	10.47	11.27	13.82	13.65
Plastic viscosity **h** (Nms)	0.73	1.56	3.05	3.42	4.89
r	0.88	0.99	0.99	0.99	0.99

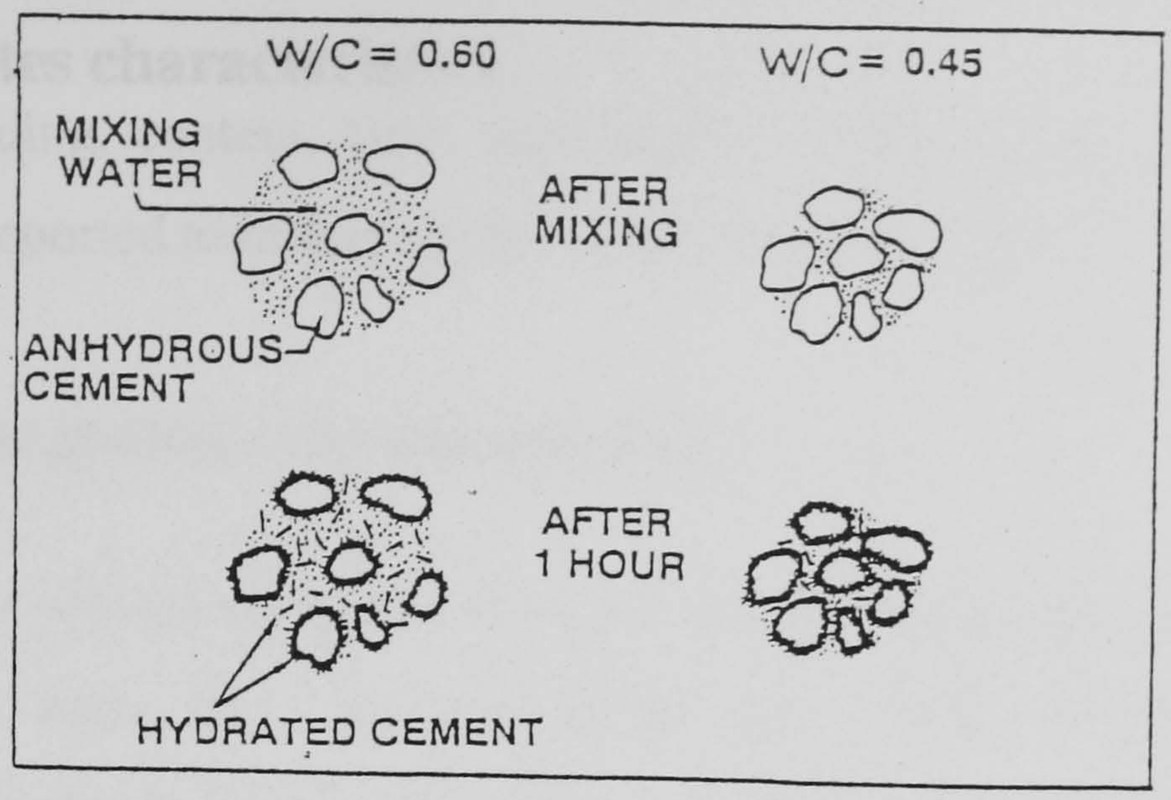

Figure 2.10 : Schematic illustration of effect of w/b ratio on loss of workability[34].

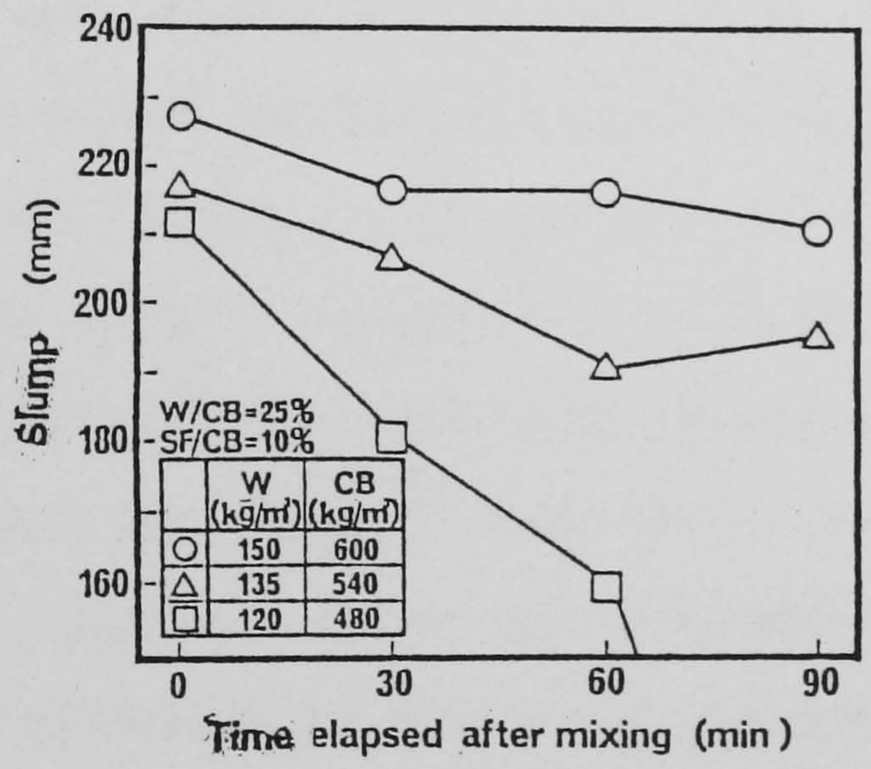

Figure 2.11 : Relationship between slump loss and water content (at 0.25 w/b ratio, using 10% CSF)[18].

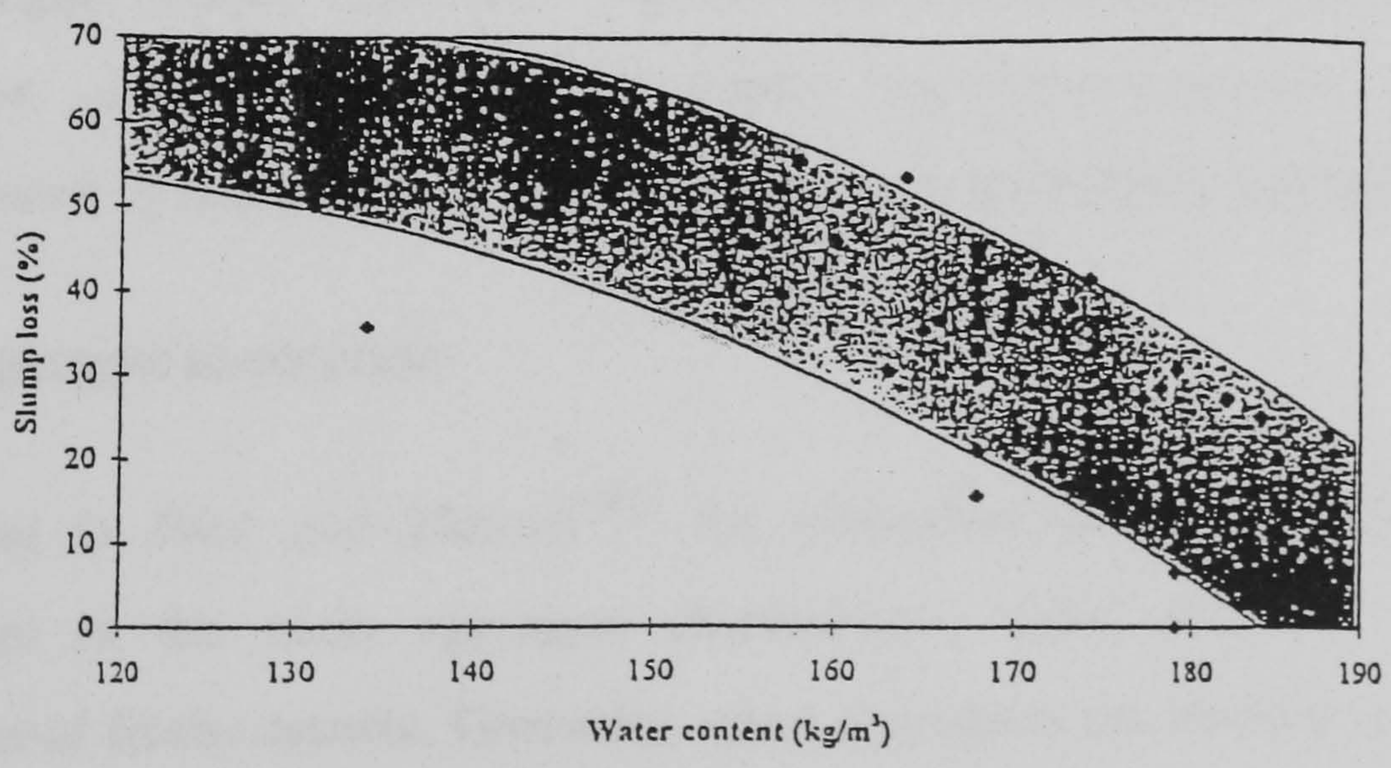

Figure 2.12 : Relationship between slump loss (%) and water content (using a wide range of NSC mixes - having different cements contents, superplasticizers and CRMs. The time interval for the slump measurements was not reported)[100].

2.4 Aggregates characteristics

Aggregate grading, content, type, size, shape, surface texture, and absorption have all been reported to influence the workability properties of fresh concrete.

2.4.1 Aggregate grading, type, size and shape

It is difficult to provide comprehensive and unequivocal generalisations for these characteristics, since they are inter-linked and change simultaneously. For example, a variation in the content of either the fine or coarse aggregate alters the grading, whilst a change in the type or shape of aggregate may alter the surface texture. With regards to:

- **grading**, it has been reported that the yield value increases systematically with increasing fines content, particularly at lower w/b ratios. The corresponding effect on the plastic viscosity is considered to be more complicated[87, 102].
- **aggregate type**, Gjorv[87] reported that the plastic viscosity is distinctly reduced by replacing a crushed coarse aggregate with gravel.
- **coarse aggregate size**, Saeed[102] found that an increase in the maximum aggregate size from 10 to 20 mm generally reduces workability (i.e. gives higher g and h values) and decreases slump, particularly in rich mixes (having a high cement content). According to Soutsos[53] **sand** with a **fineness** modulus (FM) of 2.73 produces only slightly lower yield values and almost identical plastic viscosities compared to fine sand mixes of 2.1 FM.
- **aggregate shape**, Tattersall[7] reported that rounded gravel aggregates give similar yield values, but lower plastic viscosities compared to crushed limestone. (i.e. the effect is similar to that due to a change in aggregate type).

2.4.2 Aggregate absorption

According to Pilar and Manuel[103] the absorption of mixing water by dry aggregates is the main aggregate characteristic influencing the workability properties of fresh concrete. Generally, when aggregates are batched in a dry state it is assumed that sufficient water will be absorbed from the mix to bring them to a saturated state. The amount absorbed is broadly related to the porosity of the

aggregates and is included with the net or free mixing water[104]. Many workers have qualitatively addressed the effects of aggregate absorption on fresh concrete properties, but very little quantitative information is available.

Neville[104] stated that the absorption of free water by the aggregates inevitably causes some loss of workability with time, but beyond about 15 minutes the loss becomes small. He suggested that since absorption of water by dry aggregates slows down or is stopped due to coating of the particles with cement paste, it is more useful to determine the quantity of water absorbed in 10-30 minutes instead of the total water absorbed, which may never be achieved in practice. Murdock[105] concurs with this, and showed, using the compacting factor test, that most of the absorption in gravel and limestone aggregates occurs in the first 10 minutes (**figure 2.13**). Tuthill[106] similarly reported that aggregate absorption is not a significant factor with most natural aggregates, and that more than 90% of the absorption capacity is fulfilled in the first few minutes of mixing.

Several workers have however expressed opposite views[49, 103, 107]. Davis[107] described an exceptionally absorptive sand which caused significant slump loss problems with time. From a study involving six different aggregates at a w/c ratio of 0.33, Pilar and Manuel[103] stated that, for similar absorption capacities, other aggregate characteristics (shape, size, gradation etc) are only of secondary importance, but did not provide supporting data to substantiate this.

Using a single mix and the BT Rheometer, de Larrard et al[49] examined the effects of dry aggregates on loss of workability. They suggested that some 10-30 litres of water migrate from the paste into the aggregates during the first hour, and that both the yield stress and plastic viscosity increase with time (**figure 2.14**). They also stated that the effect of pre-saturating the aggregates (by pre-mixing them with water) reduces the loss of workability, and that no significant increase in plastic viscosity occurs. Further work is however needed to confirm this, by comparing the effects of both dry and saturated aggregates on the evolution of the Bingham parameters with time.

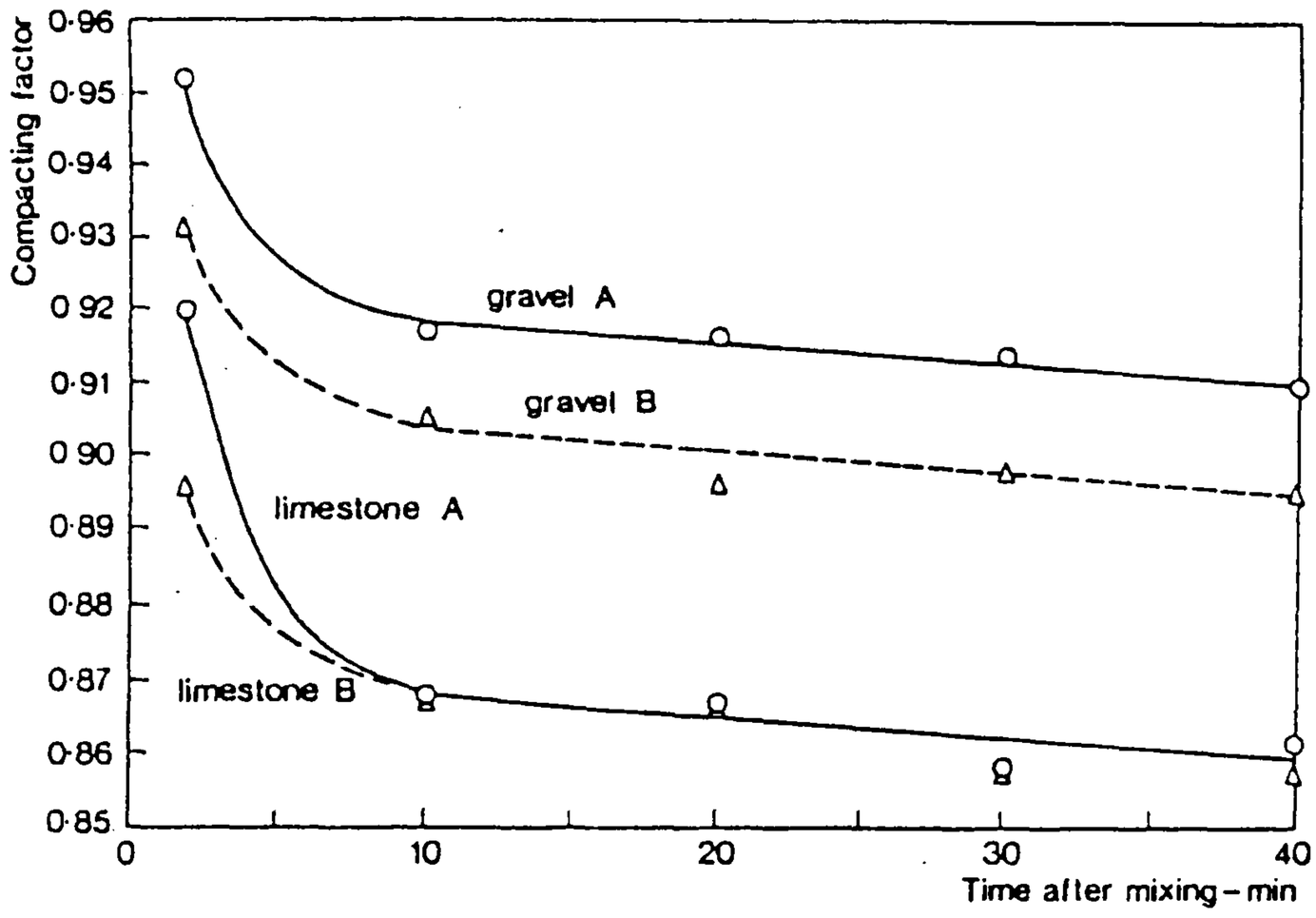

Figure 2.13 : Effect of aggregate absorption on loss of workability as assessed by the compacting factor test[7].

___ dry aggregates

- - - soaked aggregates

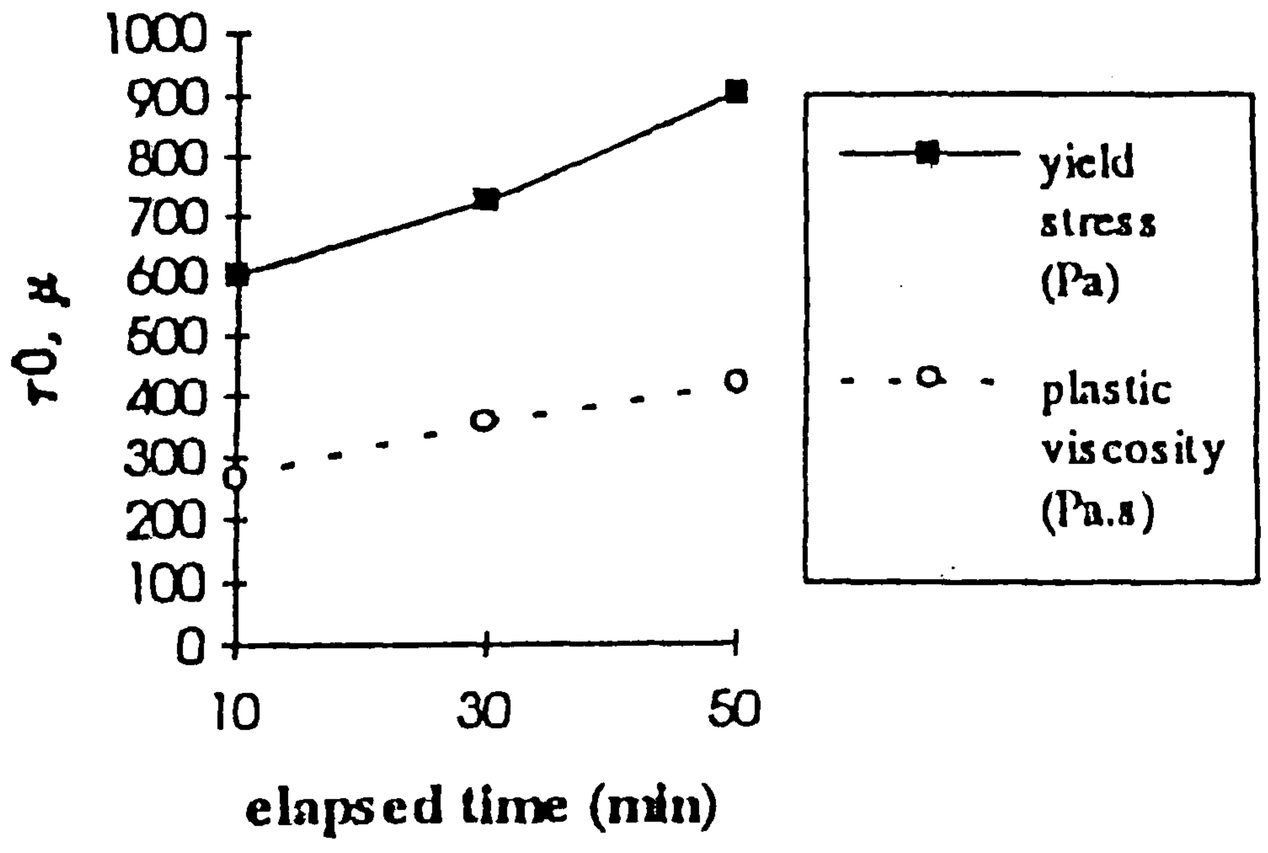

Figure 2.14 : Effect of water absorption by dry aggregate on the evolution of Bingham parameters[49].

2.5 Superplasticizers (and other chemical admixtures)

The number of commercially available chemical admixtures, their uses, and basic compositions have been steadily increasing since they were first developed in the early 1930's[108]. Today, chemical admixtures are used world wide for a variety of purposes in concrete, including: retardation and acceleration of the setting processes, waterproofing, and air entrainment. Plasticizers and superplasticizers (or water-reducing and high-range water reducing agents) have been developed specifically to[34]:

1. **increase** the **workability** without changing the mix composition (i.e. to enhance the placing and compacting characteristics of concrete);
2. **reduce** the **w/b ratio** (or mixing water), in order to increase strength and improve durability at a given workability;
3. **reduce** both the **water and cement contents** (in order to minimise creep, shrinkage and thermal strains caused by heat of cement hydration).

The use of superplasticizers has today become an integral part of all HPCs[109], and is considered to be the most essential feature in producing HSC[33]. The following sub-sections describe the characteristics of the main **types** of chemical admixtures; and review some of the advances made in understanding their **modes** of action, **dosage effects**, **mixing procedures**, and their **compatibilities with** portland **cements**.

2.5.1 Types

The various types of chemical admixtures are commonly classified by their composition, and/or function in concrete. The classification according to ASTM C 494-92[110] is shown in **Table 2.2**. In contrast, Tattersall and Banfill[66] divided chemical admixtures into two groups according to their effects on the rheology/workability of fresh concrete :

- **plasticizers** and **superplasticizers** which predominantly affect the yield value;
- **air-entraining agents** which principally affect the plastic viscosity.

Kreijger[111] has, on the other hand, differentiated between water reducing admixtures and air-entraining agents in terms of their effects on the solid-liquid and air-liquid interfaces, and by the orientation of their molecules on cement surfaces (c.f. pages 48 and 51, figures 2.24 and 2.29(a)). It is however interesting to note that the ASTM classification[110] of admixture type takes no account of air-entraining agents, but BS 5075: Part 3 does[112].

2.5.1.1 Plasticizers (or water reducers)

Plasticizers are organic products, principally composed of lignosulphonates which are produced from the waste liquor in paper pulp production. Their purity and compositions depend on several factors, such as the neutralizing alkali and the pulping process used, the degree of fermentation and even the type and age of wood used as pulp feedstock[113].

The lignosulphonate molecule is a substitute phenyl propane unit containing hydroxyl, carboxyl, methoxy and sulphonic acid groups. Although the exact structure is not known, a possible representation is a polymer having the repeating unit shown in **figure 2.15(a)**. It exhibits much cross-linking and has an average molecular weight ranging from a few hundred to 50,000[55, 66], depending on the degree of polymer refinement used[113]. The lignosulphonate polymer is believed to exist in solution in the form of spherical microgels (**figure 2.15(b)**), where only the carboxyl and sulphonate (–COOH and $-SO_3H$) groups on the outer surface are ionized[66, 113].

With the MKI two-point workability test system, Scullion[77] cited by Tattersall[7] showed that a lignosulphonate plasticizer has a greater effect on the yield value than on plastic viscosity. With the LM system, Tattersall and Banfill[66] reported

that the use of a lignosulphonate plasticizer gives an immediate increase in yield value, which continues to increase with time compared to a plain mix. They stated that field testing of the plasticizer produced rapid slump loss – decreasing from about 180 mm to 100 mm in 10 minutes.

Apart from variations in compositions, the main difference between plasticizers and superplasticizers (described in section 2.5.1.2) has been attributed to the extent rather than type of performance. According to Collepardi[34] the slump increase for a given mix is about 50-70 mm for plasticizers, and about 150-200 mm with superplasticizers. Moreover, superplasticizers are capable of reducing the water demand at a given slump by about 20-30%, whereas plasticizers usually reduce it by only 5-12%[34, 66, 114] - typically at optimum dosages of 0.2-0.4%, compared to 1-2%[57]. Superplasticizers are also capable of allowing reductions in w/b ratio down to 0.16[115], but attempts to use plasticizers at w/b ratios less than or equal to 0.30 have proven to be unsuccessful in providing sufficient fluidity[111].

Another major drawback of plasticizers is their very brief action. They are only efficient for 15 to 30 minutes in the better cases[116], and are therefore normally added to the concrete at construction sites.

Retarders and accelerators (ASTM Types B and C) only have secondary water reducing capabilities, but are considered to belong to the plasticizers group[113]. In practice, they are usually blended with other plasticizers or superplasticizers. **Retarders** are essentially used to extend the workability time during which concrete can be transported, placed and finally compacted. **Accelerators** are, on the other hand, used to increase the rate of cement hydration and early strength development. These specific functions can not in practice be obtained through mix design considerations only.

Table 2.2 : ASTM classification of chemical admixtures[110].

Type A	Water-reducing (or plasticizing)
Type B	Retarding
Type C	Accelerating
Type D	Water-reducing and retarding
Type E	Water-reducing and accelerating
Type F	High-range water-reducing (or superplasticizing)
Type G	High-range water-reducing and retarding (or superplasticizing and retarding)

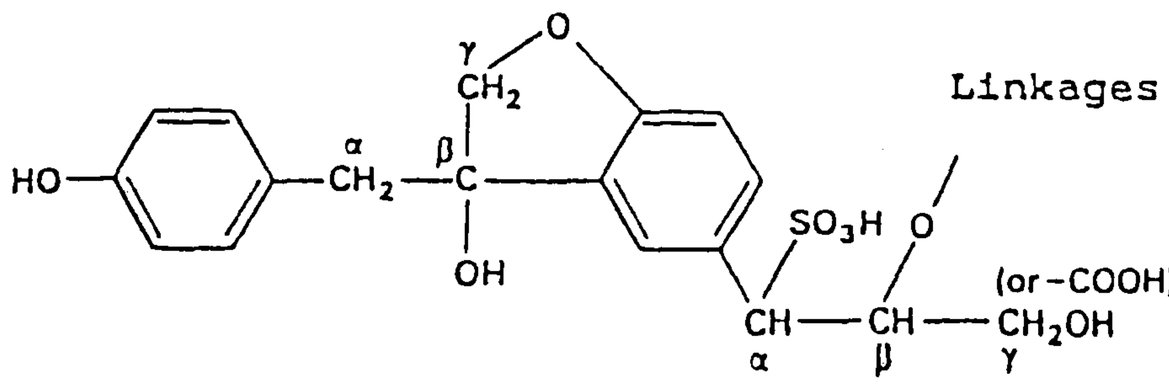

Figure 2.15 : Schematic representation of (a) a possible lignosulphonate unit, and (b) lignosulphonate microgel[55, 66, 113]

2.5.1.2 Superplasticizers

These high-range water-reducing admixtures (also known as super water-reducers and super-fluidizers)[117] mainly consist of water-soluble linear organic polymers. They are usually synthesized using complex polymerization processes, to produce long-chained molecules of high molecular mass, and are relatively more expensive than plasticizers. Superplasticizers can be classified according to their chemical composition into the following four types:

1. sulphonated **melamine**-formaldehyde condensate (**SMF**)
2. sulphonated **naphthalene**-formaldehyde condensate (**SNF**)
3. **modified lignosulphonates** (**MLS**)
4. **other formulations** based on various polymers (such as sulphonic-acid esters, salts of carboxylic or polyhydroxcarboxylic acids, hydroxylated polymers, and some sulphonated substances) [34, 117-119].

The first three types comprise the first generation (or conventional) superplasticizers which first entered into commercial use in the 1960's and 1970's. The polymers in the fourth category represent the second generation of superplasticizers, and are often referred to as high-performance or new generation (**NG**) superplasticizers. The miscellaneous products in this category include vinyl and various acrylic-based co-polymers[34, 118], as well as a family of products known as comb polymers[119]. The latter comprise polycarboxylates containing various types of pendant groups (or side chains) based on oxyethylene/oxypropylene polymers.

Although significant variations exist in each category, all four types of superplasticizers are capable of reducing the water requirements of concretes by as much as 30%, and simultaneously increasing the slump in the range of 200 mm or more. The characteristics of each type of superplasticizer are described below.

(I) Conventional (first-generation) superplasticizers

(a) Melamine

Sulphonated melamine formaldehyde condensates (SMF) are synthesized from melamine by treatment with formaldehyde ($3CH_2O$), and sulphonated by addition of calcium or sodium bi-sulphonate ($NaHSO_3$), before polymerization (**figure 2.16(a)**). During the sulphonation process, the sulphonate (SO3-) group is introduced into the organic molecule, and the process converts it into a soluble compound. The polymerization process produces long-linear polymers of high molecular mass, but requires careful regulation in achieving optimum characteristics with regards to molecular length and reducing cross-linking. Unlike lignosulphonate-based plasticizers, SMF condensates have low contents of impurities and, therefore, do not exhibit harmful side-effects, even at high dosages.

They typically have molecular weights up to 30,000[113, 120] , and the number of molecules in the chain (n) is about 150.

(b) Naphthalene

Sulphonated naphthalene formaldehyde condensates (SNF) are broadly produced in a similar way as the melamine-based superplasticizers, but the process involves successive treatments of naphthalene with sulphuric acid (H_2SO_4), formaldehyde and sodium hydroxide (as shown in **Figure 2.16(b)**). The reaction with formaldehyde leads to polymerization and the sulphonic acid is normally neutralized with sodium hydroxide. In comparison with SMF, the SNF superplasticizers are less highly polymerized[55], the number of repeating units is low (typically n is 2)[120], and a dimer is predominantly formed.

Such a structure is able to reduce the surface tension of water in the mix and entrain air. This can be prevented by using a high molecular weight polymer, typically one having a value of n=10[55, 120]. Ferrari et al[121] found that SNF-based superplasticizers exerted their best fluidizing effects in the molecular weight range 6000-8000.

(c) Modified lignosulphonates

Because of the relatively low price of lignosulphonates there has been continued interest in developing superplasticizers based on them. Modified lignosulphonates (**figure 2.16(c)**) are lignosulphonates from which sugars, which cause excessive retardation and reductions in early strength development, are removed[113-114, 120]. Although they contain fewer impurities than conventional lignosulphonate-based plasticizers, large dosages of purified lignosulphonates are rarely used, because they can severely delay setting. When used, they are usually accompanied by a large dosage of a set accelerating admixture[122]. This is probably one reason why most published data on conventional superplasticizers is with SMF and SNF-based superplasticizers.

There is limited comparative information in the literature on the performance of MLS with other superplasticizers. Tattersall and Banfill[66] stated that purified lignosulphonates appear slightly more efficient than SMF and SNF superplasticizers. Ramachandran[120] has however presented data showing that the slump performance of MLS (at 0.40 and 0.38 w/b) is comparable to that obtained with SMF and SNF superplasticizers.

In contrast, many investigations have compared the efficiencies of SMF and SNF[16, 53, 123-125]; the majority showing superior performance with SNF-based superplasticizers. In flowing NSC, Banfill[124] has, for example, found that the SNF superplasticizer exhibits greater fluidizing effects and experiences lower loss of workability compared to the SMF type (**figure 2.17**). He concluded that the rate of increase in the g and h values with the SNF superplasticizer is: about two to three times lower than with the SMF type, but is comparable to that of non-superplasticized flowing concrete. In HSC, Soutsos[53] observed consistently lower workabilities (higher g and h values) with a SMF superplasticizer compared to a SNF polymer at 0.38-0.26 w/b ratios. His work was however limited to individual two-point test measurements taken with the MH system immediately after mixing.

With the exception of Banfill 's time-dependent results[124] with the SNF-based

superplasticizer, many researchers[99, 126-128] have reported more rapid slump (or workability) losses in superplasticized concrete. Malhotra[126] stated that the high initial slump obtained with superplasticizers is only maintained for about 30 minutes, and is therefore a serious problem for ready-mixed concrete producers. Early studies by Perenchio et al[127] with a SMF superplasticizer showed that the slump loss in both ordinary and high-strength superplasticized concretes is significantly increased, particularly at lower w/c ratios (**figure 2.18**).

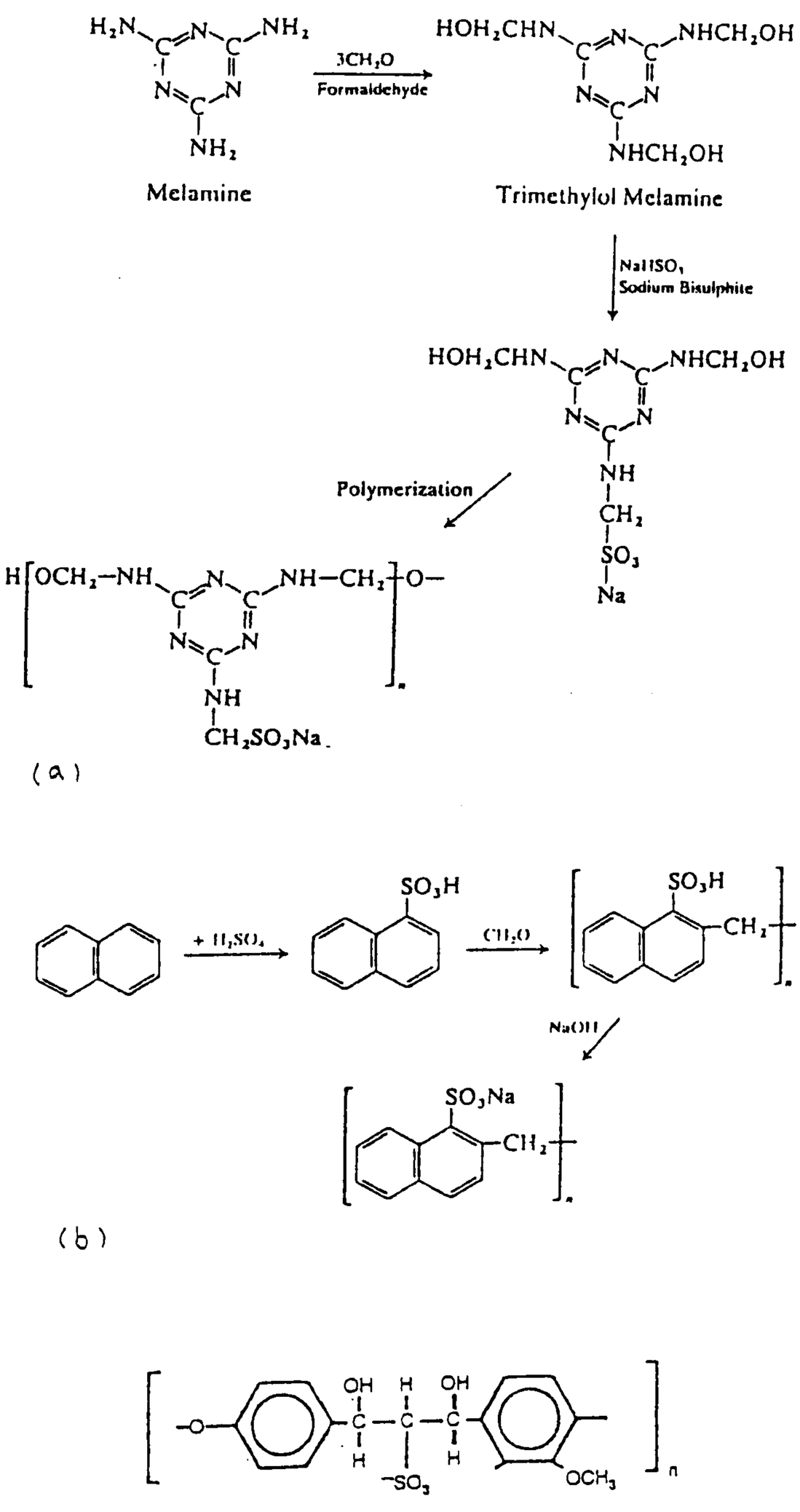

Figure 2.16 : Synthesis and chemical structures of (a) sulphonated Melamine formaldehyde, and (b) sulphonated Naphthalene formaldehyde[55, 113]. (c) shows the chemical structure of a MLS superplasticizer[117].

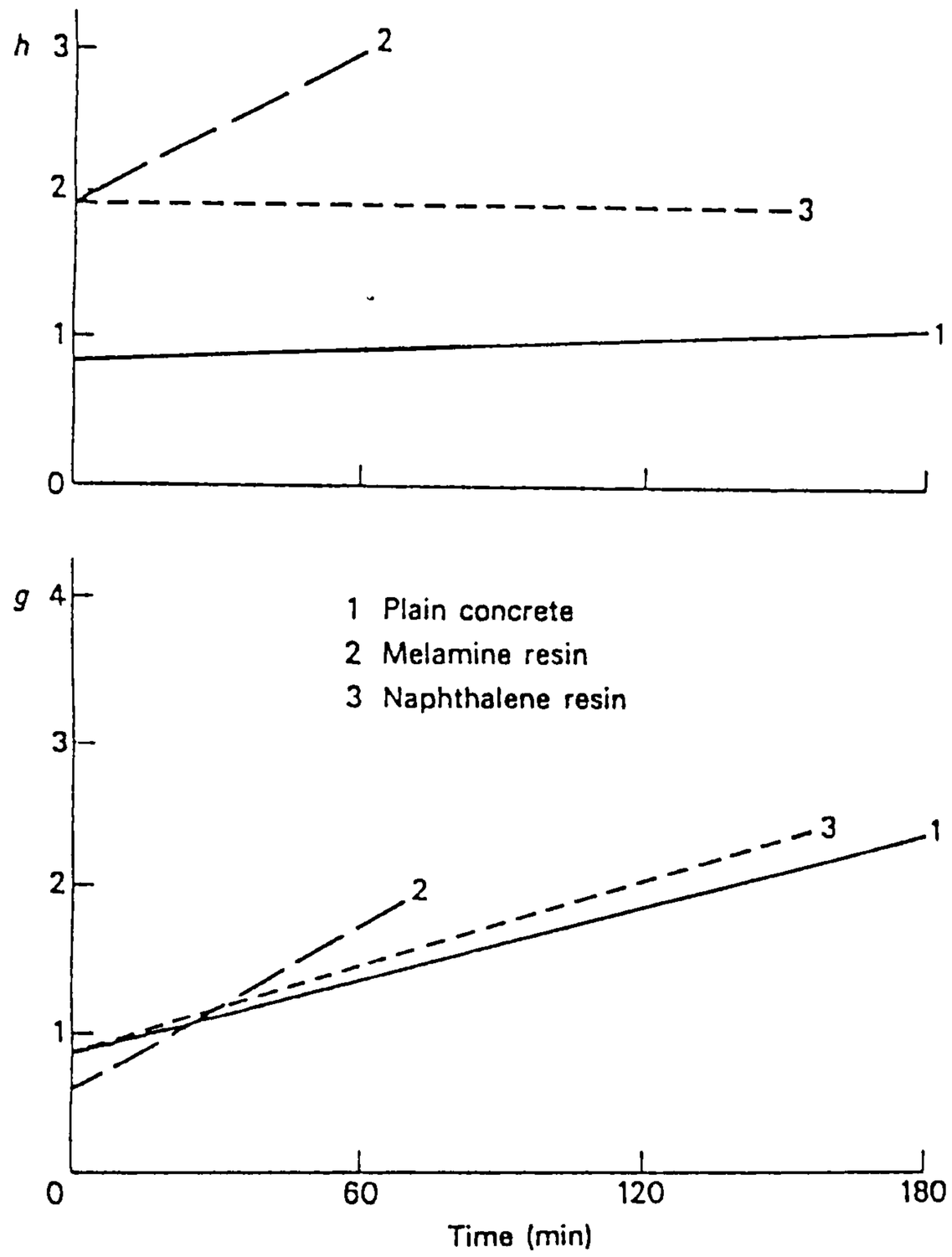

Figure 2.17 : Effects of time on Bingham values of superplasticized NSC mixes (MH system, 0.78 w/c. Details of slump range and/or slump loss were not reported)[66, 124].

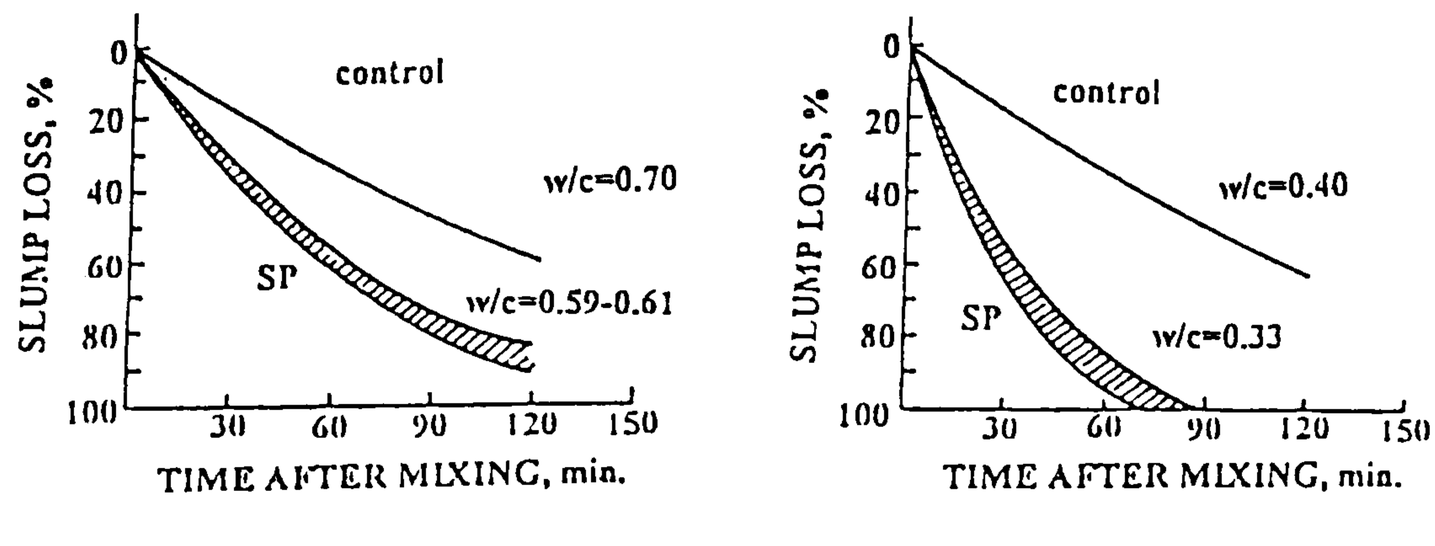

Figure 2.18 : Slump loss of (a) NS and (b) HSCs with and without superplasticizers[127].

(II) New-generation superplasticizers

The drawbacks associated with the first generation (or conventional) superplasticizers have since the 1980's led to continued interest and development of various types of higher performance superplasticizers - to extend workability retention (long-life), and others which are more efficient at very low w/b ratios of 0.25 or less (super-superplasticizers). These high performance (or second generation) superplasticizers mainly differ from conventional superplasticizers in their chemical compositions and/or the side-chains in their molecules. As mentioned previously, the term "New generation superplasticizers" has in some cases been coined as a generic description of all the various new formulations or types of polymers mentioned on page 38[6, 118, 129]. Chemical structures for some of the main types of new-generation (NG) superplasticizers reported in the literature are shown in **figure 2.19**.

The first NG superplasticizers appeared in the mid-late 1980's. They included a **polymeric dispersant** (with functional groups of esters, amides and acid anhydrides)[130], a **bi-component superplasticizer** (comprising a SNF polymer and a copolymer with sulfonic/carboxylic functional groups)[131], and a **bi-component superplasticizer** (with a SNF polymer and a reactive polymer)[132]. These NG superplasticizers were all found to be more effective in reducing the rate of slump loss compared to conventional superplasticizers at w/b ratios ranging from 0.60-0.25.

In the early 1990's, Collepardi et al[133] investigated the effects of a water soluble mono-component copolymer of **carboxylic acrylic acid with acrylic ester** (CAE), containing carboxylic (COO^-) instead of sulphonic (SO_3^-) groups. His results showed that, at a constant dosage of 1% (by mass of cement), the CAE-based superplasticizer is more effective compared to SNF for water-reducing capability, and has considerably better slump retention (**figure 2.20**). Similar slump loss characteristics were reported by Tazawa et al[134] with a **methacrylic-based polymer** at w/b ratios of 0.50 and 0.30.

More recently, Jeknavorian et al[119] found that concrete treated with a **polycarboxylate comb polymer** (ADVSP) exhibits much lower slump loss than a SNF (NSFC) and a formulation of SNF with a retarding agent (NSFCR) at 0.542 w/c (**figure 2.21**). Apart from better slump retention, they reported that the comb polymer requires as much as 65-80% lower dosages (s/w/c) than the SNF type superplasticizer.

In another study, Mitsui et al[28] compared the performance of an **acrylic graft copolymer super-superplasticizer** (SSP) and a SNF superplasticizer on the slump and viscosity properties of HSC at a very low w/b ratio of 0.20. They claimed that the viscosity properties can be measured by the flow speed of concrete in an L-shaped flow test. From their results (**figure 2.22**), they concluded that the SSP reduces the viscosity (at a lower dosage) and maintains sufficient workability for two hours compared to conventional superplasticizers. The excellent dispersion capability and workability retention of the acrylic graft copolymer (SSP) has also been confirmed by Kinoshita et al[135] on cement pastes at 0.20 w/c ratio.

Very few comparative two-point test measurements with different NG and conventional superplasticizers have been reported in the literature. In one study with the BML viscometer, Billberg et al[118] compared the Bingham properties and slump loss characteristics of a **modified acrylic polymer** (P1) and a **vinyl-based superplasticizer** (MC-1) with conventional superplasticizers based on SMF and SNF condensates. They concluded that the two NG superplasticizers exhibit noticeably lower slump losses (**figure 2.23(a)**), lower yield values and plastic viscosities, and better workability retention than the conventional superplasticizers (**figure 2.23(b-c)**). As can be seen, the improvements in the workability properties are particularly pronounced with the acrylic-based polymer.

In another study involving a coaxial cylinder viscometer, Wallevik and Simmerman[125] compared the performance of nine superplasticizers (comprising 2 SNF, 3 SMF, 2 MLS, and 2 NG) in cement pastes at 0.30 w/c. With the

conventional superplasticizers, they concluded that SNF has greater fluidizing effects, whilst SMF has the lowest. Of all the superplasticizers tested, the most effective was one of the two NG superplasticizers (referred to as Mapeifluid), but no information pertaining to its composition and/or workability retention was presented.

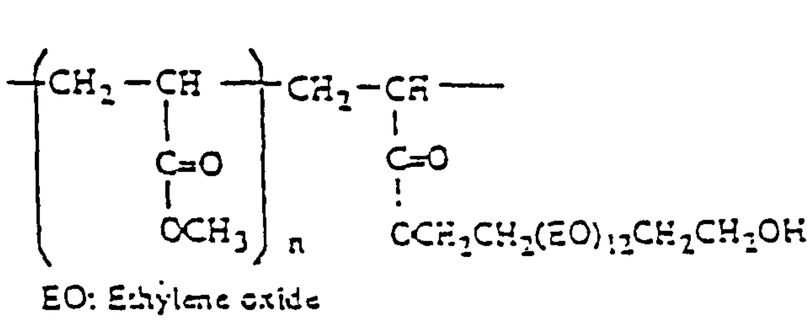

PC
(Polycarboxylate ester)

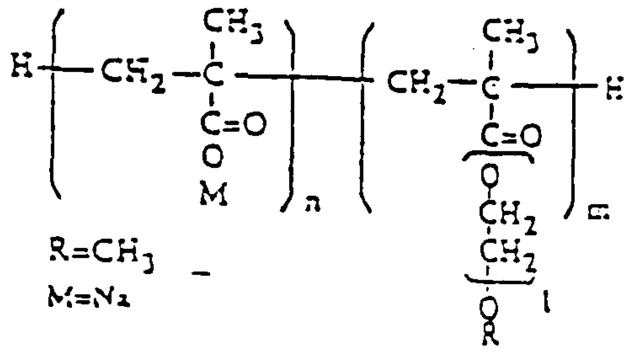

CAE
(Copolymer of carboxylic acrylic acid with acrylic ester)

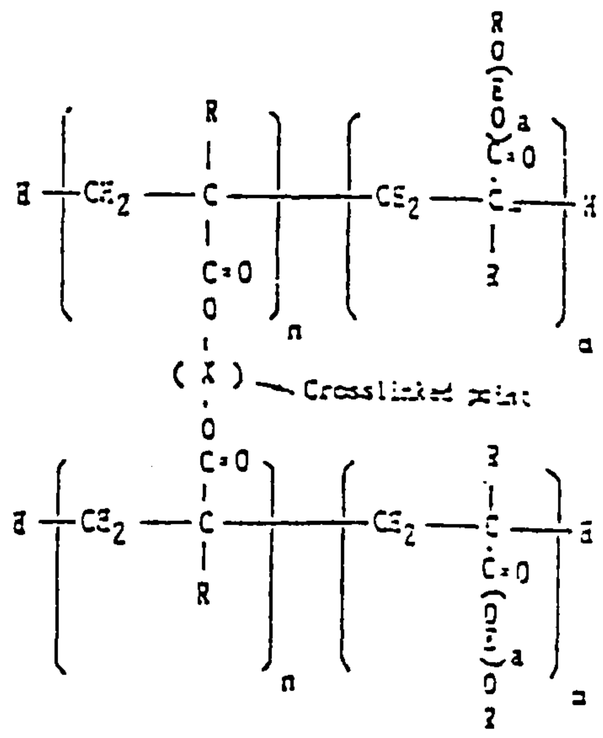

CLAP
(Cross-linked acrylic polymer)

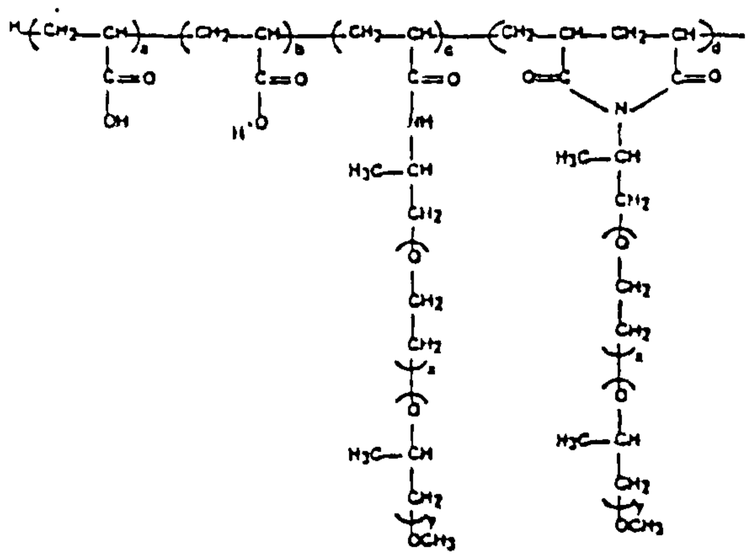

polymer dispersant in ADVSP

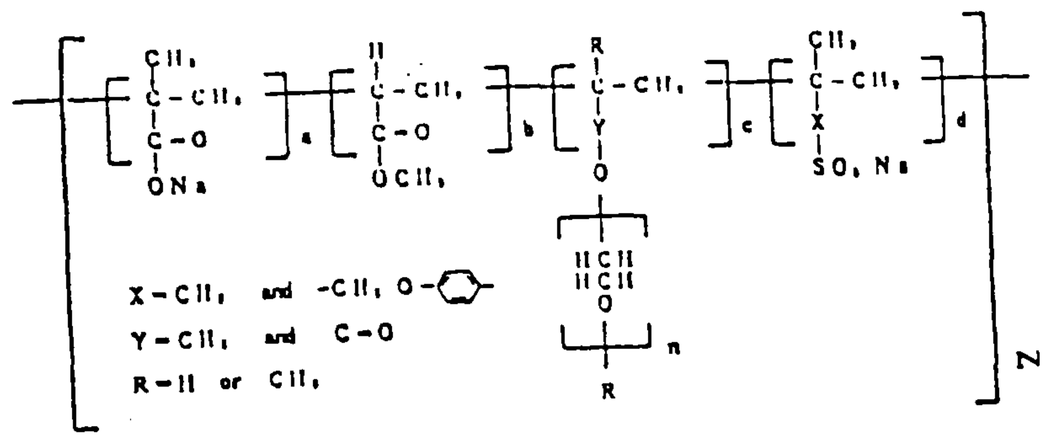

acrylic graft copolymer based new superplasticizer (SSP)

Figure 2.19 : Chemical structures of some new generation superplasticizers[28, 34, 119].

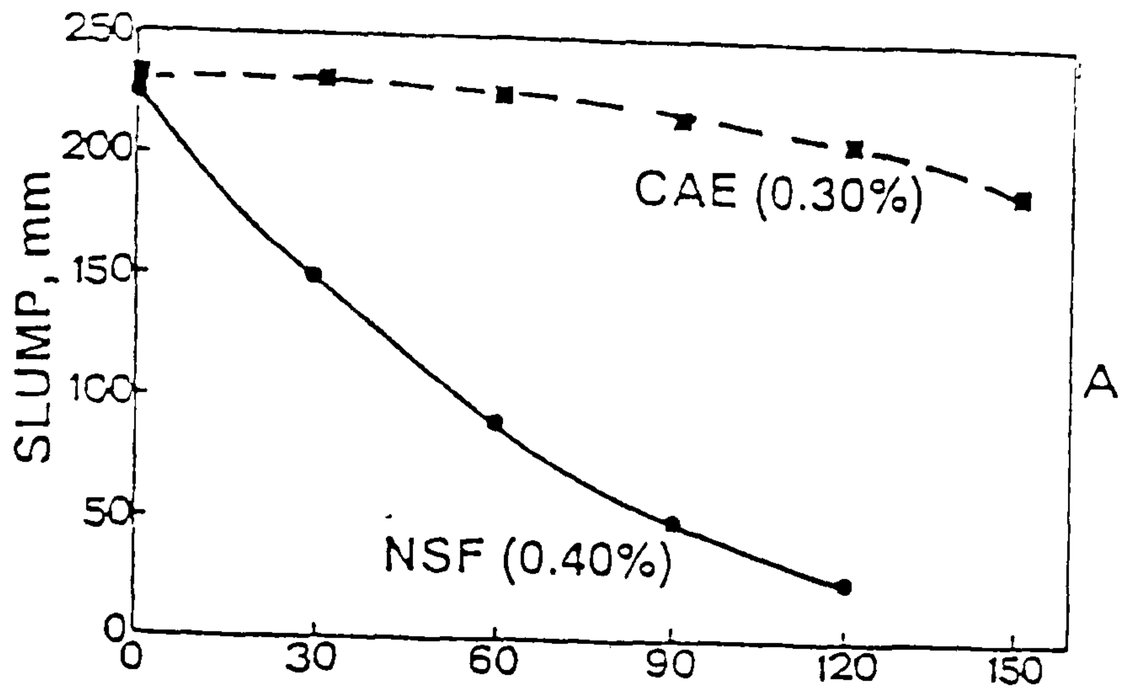

Figure 2.20 : Slump loss characteristics of carboxylic acrylic acid ester (CAE) compared to a naphthalene (SNF) superplasticizer (% represents solids content)[133].

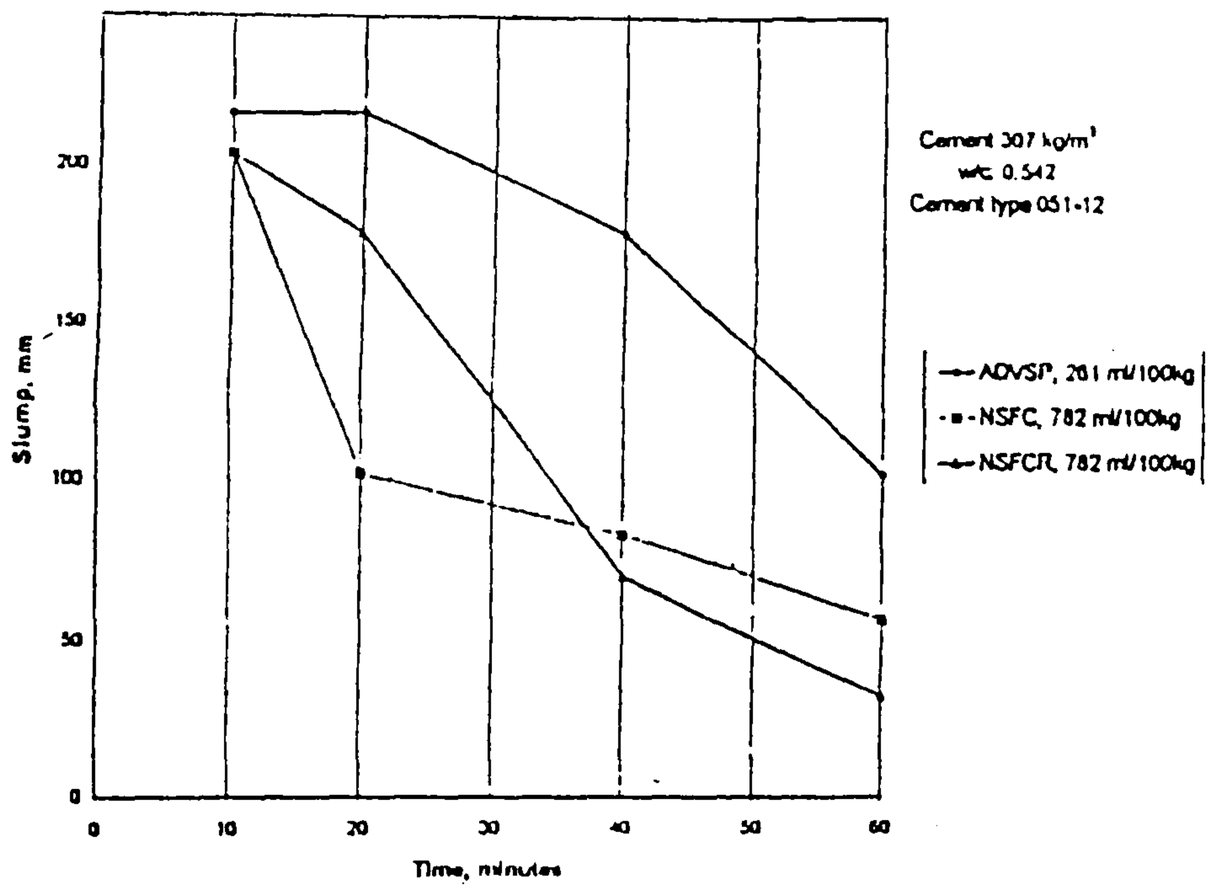

Figure 2.21 : Slump loss characteristics of a polycarboxylate comb polymer (ADVSP) compared to a naphthelene (NSFC) superplasticizer, and a mixture/blend of naphthalene superplasticizer and retarder (NSFCR)[119].

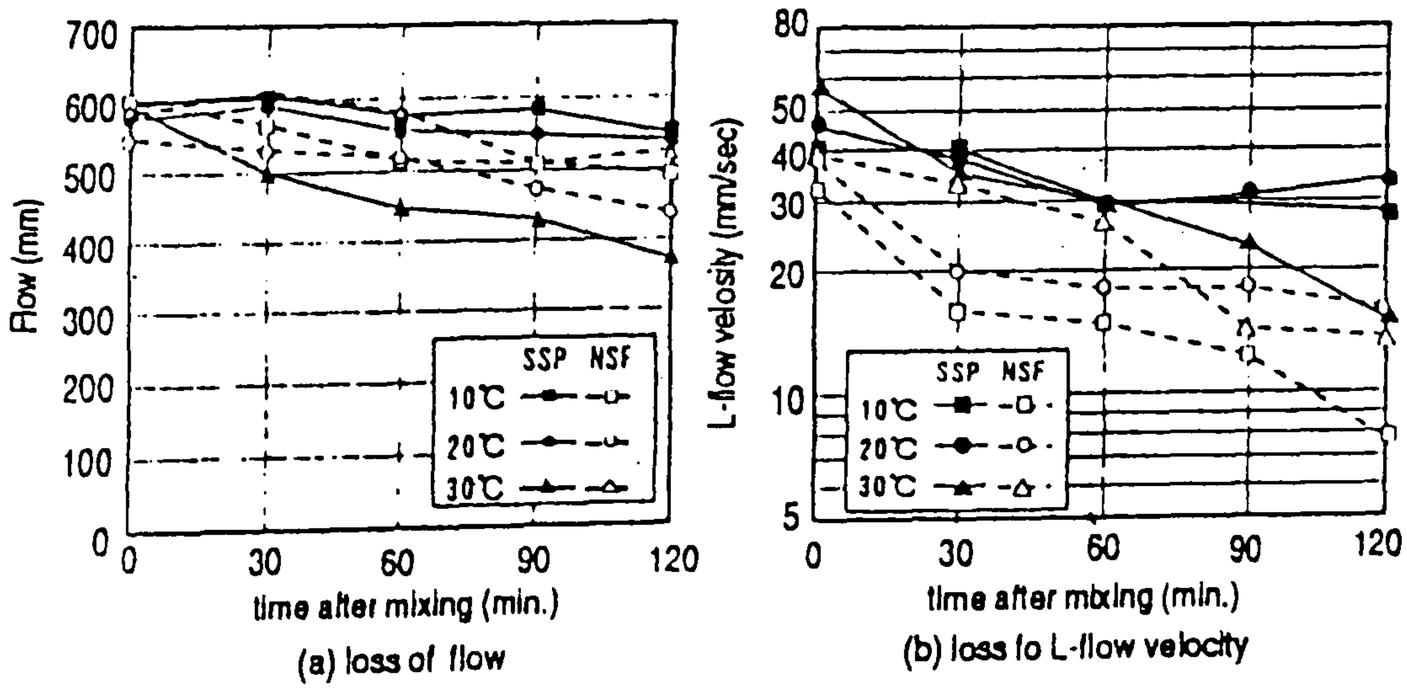

Figure 2.22 : Variations in (a) slump flow spread (mm) and (b) L-flow velocity (mm/s) of an acrylic graft copolymer Super-superplasticizer (SSP) compared to a SNF superplasticizer (at 0.20 w/b ratio and different temperatures)[28].

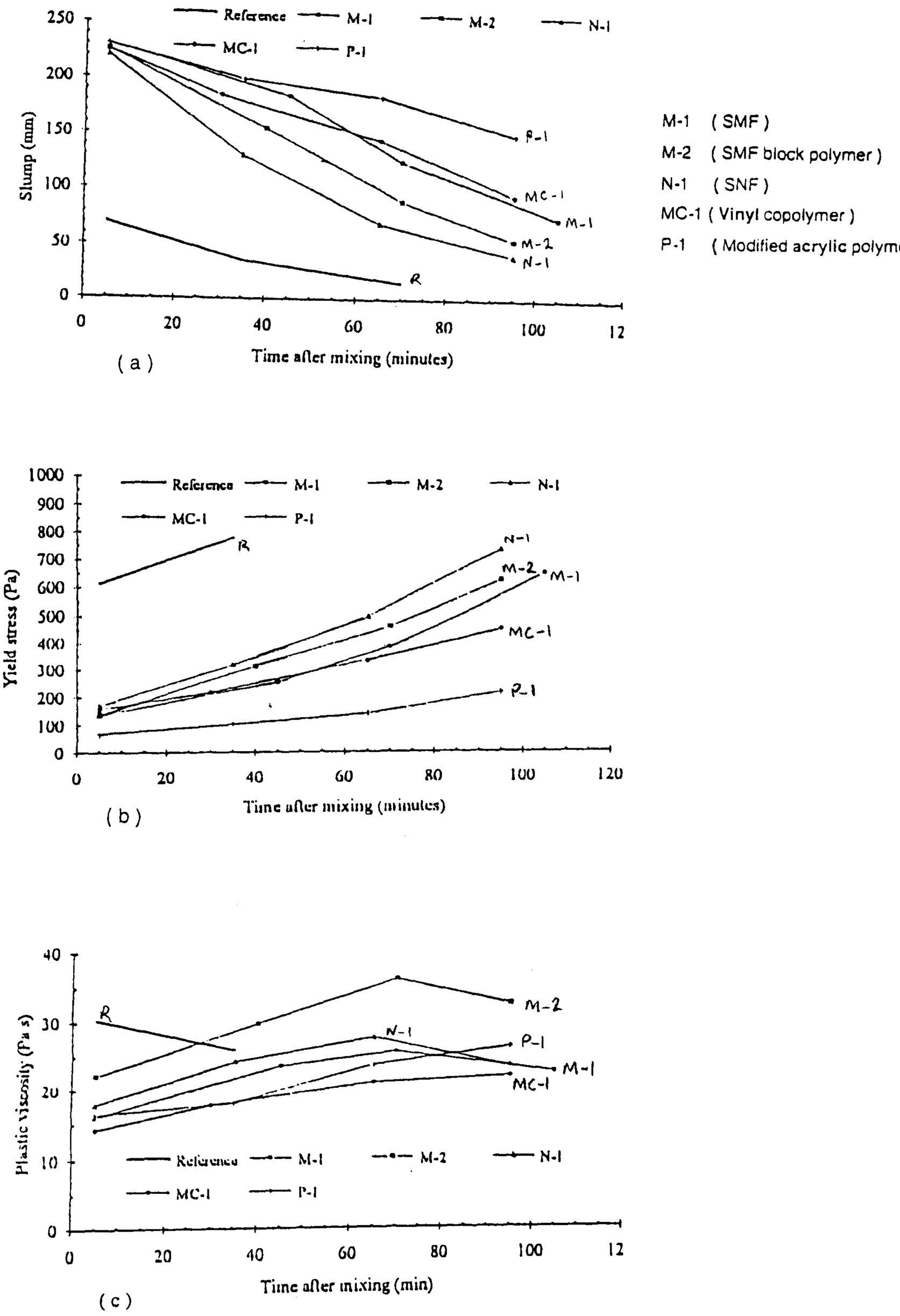

Figure 2.23 : Comparison of conventional and NG superplasticizers on (a) slump loss, and variations in (b) yield stress and (c) plastic viscosity with time(BML viscometer, 0.60 w/b ratio)[118].

2.5.1.3 Air-entraining agents

Air-entraining agents tend to modify the surface tension of the liquid phase of the mix, and lead to the formation of uniformly distributed microscopic air-bubbles (ranging from 10 to 250 μm in diameter). In the hardened concrete, these microscopic air-bibbles (at entrained air volumes of 4-7 %) provide a discontinuous reservoir for water to expand into when it freezes, and hence effective protection against successive freeze-thaw cycles. Typical air-entraining agents include wood resins, lignosulphonates, synthetic detergents, and salts of petroleum acids.

According to Kreijger's[111] classification of chemical admixtures (page 35), air-entraining agents are mainly active at the air-water interfaces, whereas water-reducing admixtures are mainly active at the solid-liquid interface (section 2.5.2). He suggests that air-entraining agents align themselves in such a way that their non polar chains/tails are directed towards the water, whilst their negatively charged heads are adsorbed onto the cement surfaces (**figure 2.24**). The negatively charged air bubbles adhering to the cement particles are able to form bridges between them, giving an increased yield value. Once flow occurs, Kreijger suggested that the spherical bubbles act as ball-bearings, move easily past each other and reduce the plastic viscosity. The proposed effects are consistent with Helland's findings[54] (c.f. figure 2.3).

Results indicating that air entrainment can also decrease the yield value have however been reported[66, 87]. Gjorv[87] summarised the effects of air-entraining agents by providing a comparative illustration of the changes in the initial Bingham parameters due to increasing quantities of water and water-reducing admixtures (**figure 2.25**). Information pertaining to the effects of air entraining agents on loss of workability is however lacking.

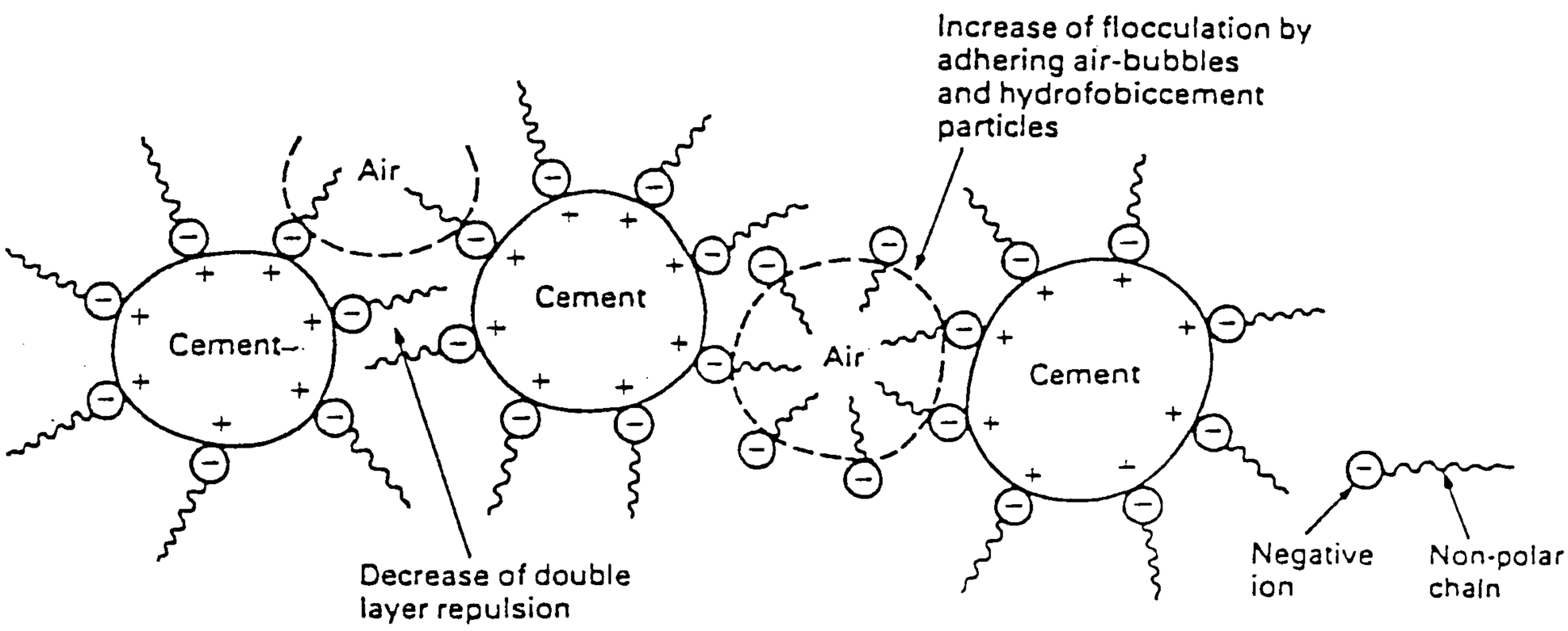

Figure 2.24 : Mode of action of air-entraining agents in cement paste (Note: the negatively charged heads are hydrophilic (i.e. water-attracting), and tails are hydrophobic (water repelling))[111].

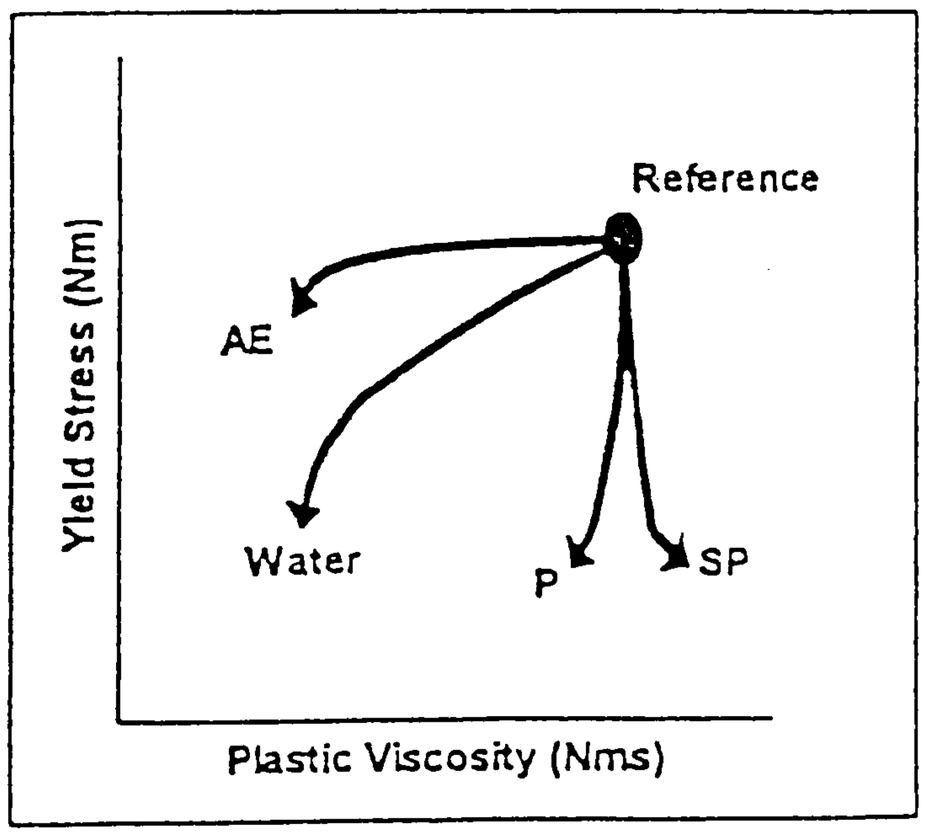

Figure 2.25 : Comparative illustration of the effects of increasing quantities of air-entraining agent (AE), water, and water-reducing admixtures (P and SP)[87].

2.5.2 Mode of action of superplasticizers and plasticizers

The strong tendency of cement particles to flocculate (or coagulate) when mixed with water[113] is the result of three types of interactions: van der Waals forces between the particles; electrostatic attractive forces from sites bearing opposite charges; and bridging with time to build rigid agglomerates[58, 136]. These lead to the formation of an open network of particles (**fig. 2.26(a)**), which traps a considerable amount of the mixing water, and consequently decreases the workability. A lower w/c ratio reduces the distance between the cement particles and increases the attractive forces between them[111, 137].

2.5.2.1 With conventional superplasticizers and plasticizers

The presence of water reducing admixtures is effective in: breaking the cement agglomerates/networks, dispersing them into primary particles[34, 55, 58, 111] (**fig. 2.26(b)**), and preventing premature linkage[118] by altering their interparticle forces (**figure 2.27**). These release water trapped within the flocs, and hence further improve the workability.

Early studies by Ernsberger and France[138-139] on water-cement suspensions indicated that cement particles do not migrate in an electrical field, but in the presence of a calcium lignosulphonate solution they move towards the anode, demonstrating that a negative charge is induced. They attributed this to adsorption of lignosulphonate anions, and concluded that dispersion and viscosity reduction took place due to mutual electrostatic repulsion between the cement particles.

Diamon and Roy[136, 140] observed that with increasing dosages of SMF and SNF condensates the charges on the cement grains (i.e. zeta-potential) became increasingly negative, and reached ceiling values of –35 to –45 mV. The increases in zeta-potential, amount adsorbed (in cement suspensions), and improvements in paste fluidity with increasing dosages were all positively correlated (**figures 2.28(a-c)**). Diamon and Roy concluded that the increase in

zeta potential was the major cause for the improved dispersion. Similar results, were reported by Hattori and Kenichi[141].

Such studies led to broad acceptance that induced electrostatic repulsion was the principal mechanism responsible for the fluidizing action of conventional superplasticizers. In contrast with air-entraining agents, the superplasticizer chains are adsorbed by the cement particles "alongside" (**figure 2.29(a)**) instead of "end like" (c.f. figure 2.24)[111]. Upon adsorption, the sulphonate (SO_3^-) groups present in commercial superplasticizers are believed to project out from the polymer chains[117, 142], and deflocculate the cement particles[119] by conveying strong negative surface charges (i.e. increasing zeta-potential). These are generated in the electric double layer extending outside the adsorption layer of the admixture (c.f. figure 2.27(b)).

With lapsed time, the magnitude of the electrostatic repulsive forces decreases as successive layers of hydration products are deposited on the cement surface[119]. The adsorbed molecules become built in a watery ettringite-shell which grows in thickness and time[111] (**figure 2.29(b)**) – leading to consequent loss of dispersion retention[119].

Several other mechanisms have also been proposed to explain the dispersion/fluidizing effects of superplasticizers. These have been collated by Collepardi[143] as follows:

(a) reduction of the surface tension of water;

(b) protective adherent sheath of water molecules;

(c) release of water trapped within cement flocs;

(d) inhibition of surface hydration, leaving more water to fluidize the mix;

(e) change in the morphology of hydration products; and

(f) induced steric hinderance, preventing particle – to – particle contact.

Although many of these mechanisms may contribute concurrently to the fluidizing effects of superplasticizers, some are currently better documented and, more likely than others. For example, the lowering of the surface tension of water (mechanism

(a)) has been considered to be of little or no importance in the fluidizing action of superplasticizers[58], but may play a greater role with air-entraining agents.

In the steric hindrance mechanism (f), it is believed that the adsorption of superplasticizers in overlapping layers can form an effective non-ionic barrier which prevents close approach and hinder the flocculation of the cement particles into large irregular agglomerates[34, 133, 136-137, 144]. Banfill[144] argued that multilayer adsorption can occur with an average of 40 layers and sheath thickness of $400A^0$ around the cement particles. He believes that a layer of this thickness would give steric stabilization a role at least as important for dispersing action, as for instance, the change in zeta potential resulting from long-range electrostatic forces.

Kreijger[111] and Penttala[33, 142] have also argued that it is highly unlikely that the action of superplasticizers is controlled by a single mechanism, and stated that the actual mechanism is probably a combination of both electrostatic repulsive forces and steric hinderance effects. Tattersall and Banfill[66] agree with this, and used it to differentiate between the performance of water-reducing admixtures and air-entraining agents (page 34). With regards to plasticizers, Taylor[55] stated that their mode of action is similar to that of superplasticizers. The essential difference is that the properties which limit the dosages with which plasticizers can be used are weaker or absent in conventional superplasticizers.

2.5.2.2 With new-generation superplasticizers

In addition to the aforementioned, several other mechanisms have been proposed for the modes of action of NG superplasticizers. These rely on the chemical composition of the polymers, their ability to compensate for the amount of dispersant consumed by the cement hydrates[130-132], their effects on the electrokinetic properties[34, 119, 133-134, 145], and/or on the orientation of their molecules upon adsorption on the cement particles[146-147].

With acrylic-based polymers (CAE), work by Collepardi et al[133] on cement suspensions (at 2.0 w/c) showed that the adsorption of the CAE copolymer after

5 mins (85%) is higher than with SNF (75%), but the zeta potential was much lower (-5 mV compared to -35 mV respectively), even though the corresponding mortar mix was considerably more fluid (**figures 2.30**). According to Collepardi[34] these findings indicate that polymer adsorption and steric hindrance, rather than electrostatic repulsion associated with higher zeta potentials, is responsible for the enhanced dispersion and remarkable increase in fluidity with CAE copolymers. He also stated that this mechanism is in agreement with the relatively smaller number of negative anionic groups (COO^-) in the CAE copolymer compared with those present as SO_3^- in conventional superplasticizers (c.f. figure 2.19).

With ADVSP comb polymers, several researchers[119, 145] have shown that although these polymers experience significant adsorption (> 70 %), similar to SMF and SNF, they appear to be electrically neutral. It was concluded that a significant steric hindrance effect accounts for the dispersion stability, along with only a minor contribution from electrical repulsive forces due to negatively charged carboxylate ions.

With an acrylic graft copolymer super-superplasticizer (SSP), Kinoshita et al[135] found that its adsorption and zeta potentials at different dosages were (about 4 mg/g and –20 mV) lower than with SNF, despite having higher paste fluidity. They concluded that the adsorption of the graft copolymer is spatially more extensive, and has greater surface coverage on the cement particles compared to that of the linear SNF polymer.

Mitsui et al[28] stated that steric hinderance of the SSP's graft chains is effective in preventing physical agglomeration of the binder particles, and therefore in reducing slump loss at very low w/b ratios. **Figure 2.31** shows proposed adsorption and steric effects of a typical graft copolymer. Unlike SNF superplasticizers, which adhere to the surface two-dimensionally, its steric structure is considered to reduce its consumption by the cement hydrates[146].

The validity of relating electrokinetic measurements to paste/mortar flow properties is however questionable, since the former are normally performed on suspensions or dilute pastes having w/b ratios outside the practical range (typically in excess of 1.0).

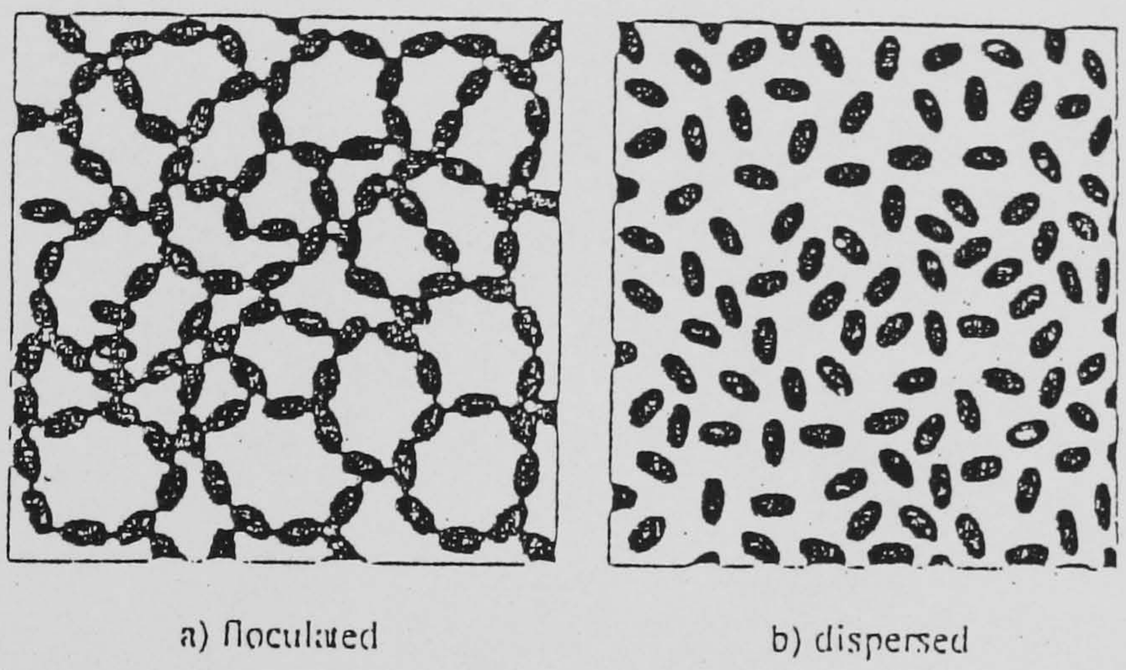

Figure 2.26 : Schematic illustration of cement paste in (a) flocculated and (b) dispersed states[58].

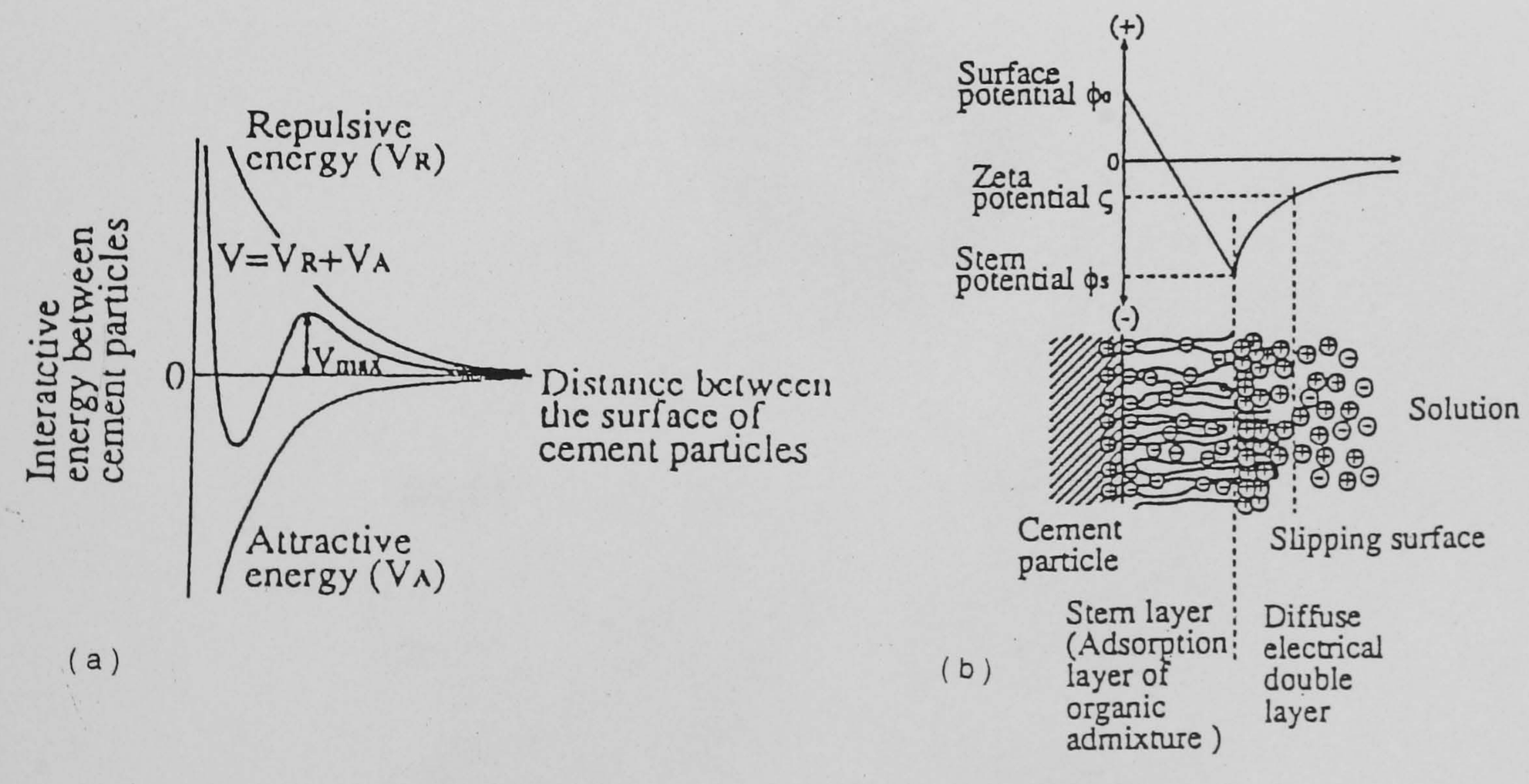

Figure 2.27 : Representation of (a) changes in repulsive and attractive interparticle forces, and (b) variations in surface potential with distance from a cement particle surface[137].

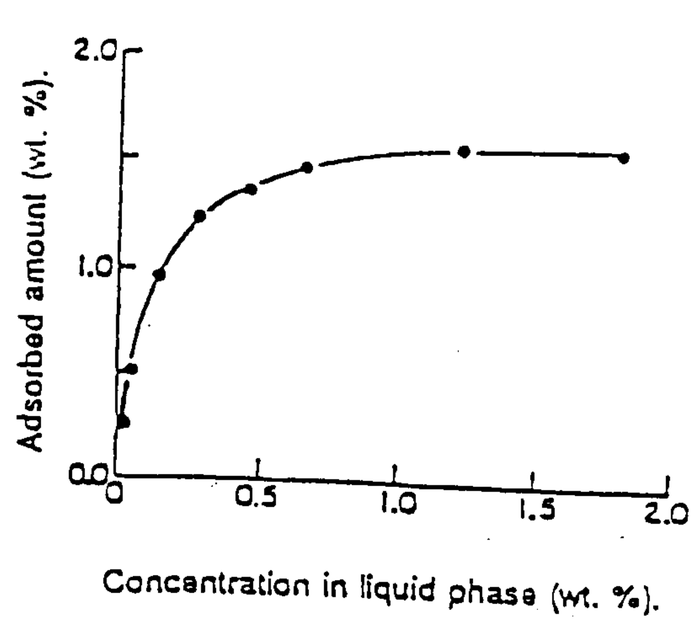

Figure 2.28 : Effects of increasing dosages of organic admixtures on the changes in (a) adsorption, (b) zeta potential of cement suspensions, and (c) flow spread properties of cement pastes[136, 140]. (Spa No. 1 & No. 2 respectively represent SNF and SMF SPs).

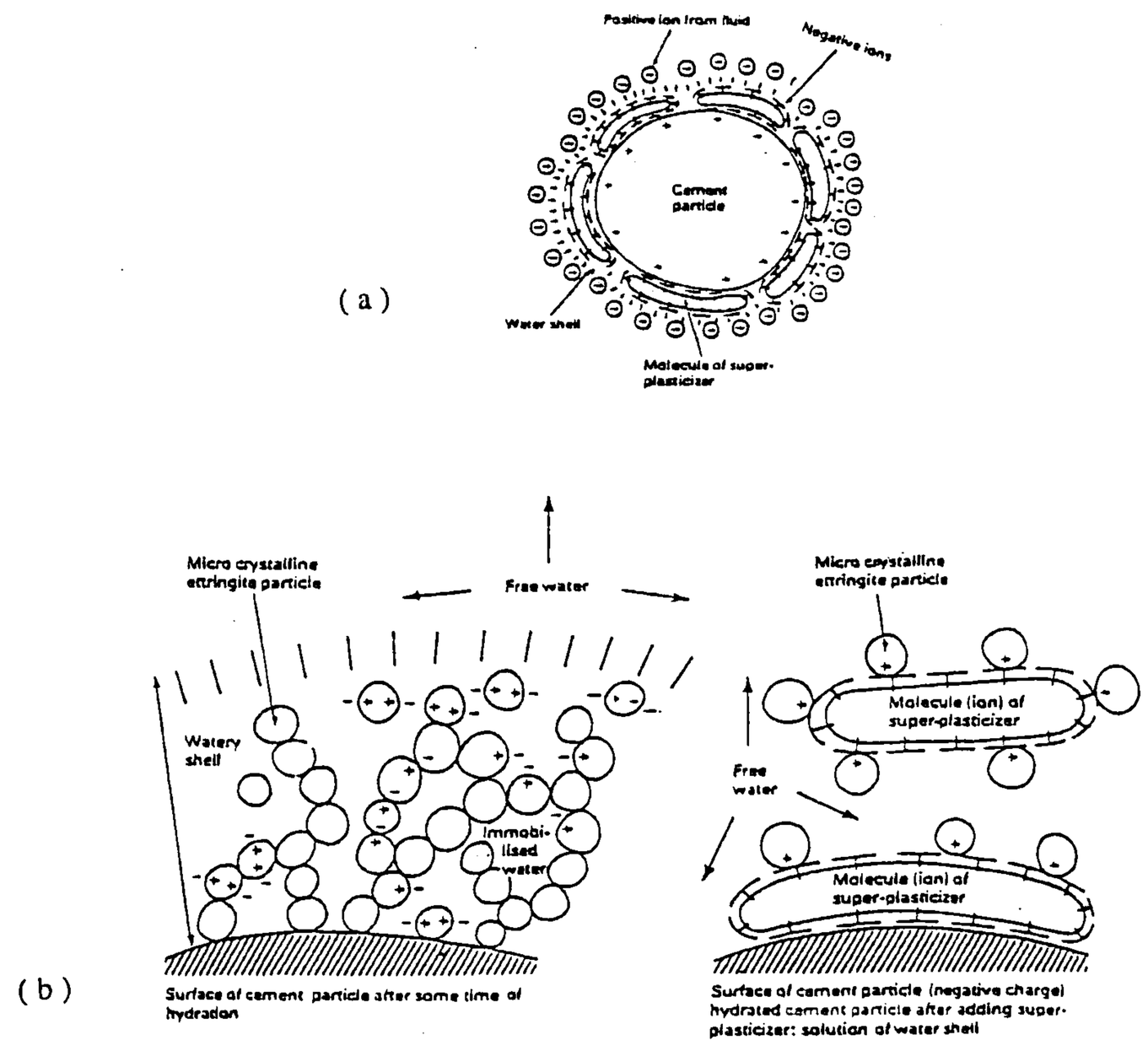

Figure 2.29 : Illustration of (a) mode of action of superplasticizers and, (b) time-dependency of superplasticizer action in partially hydrated cement particles[111].

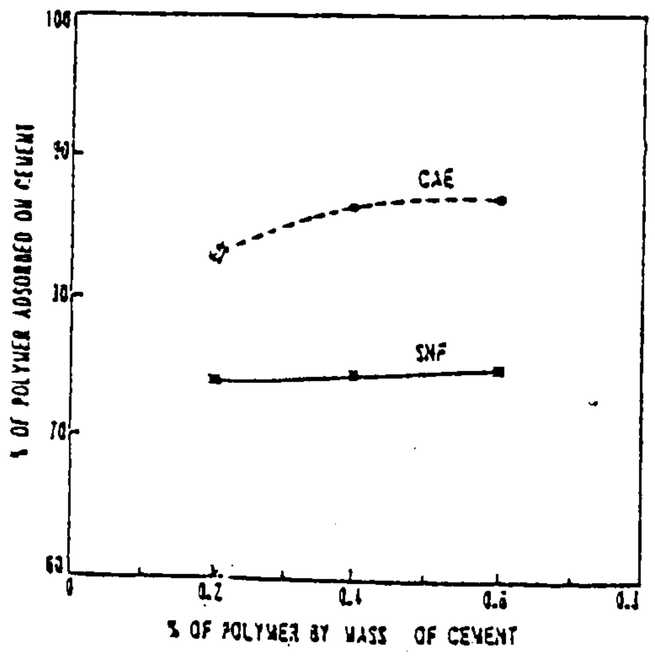

(a)

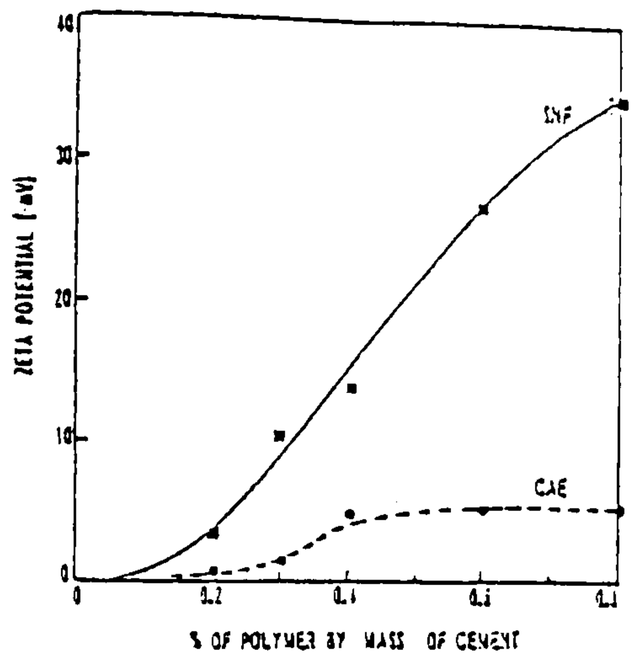

(b)

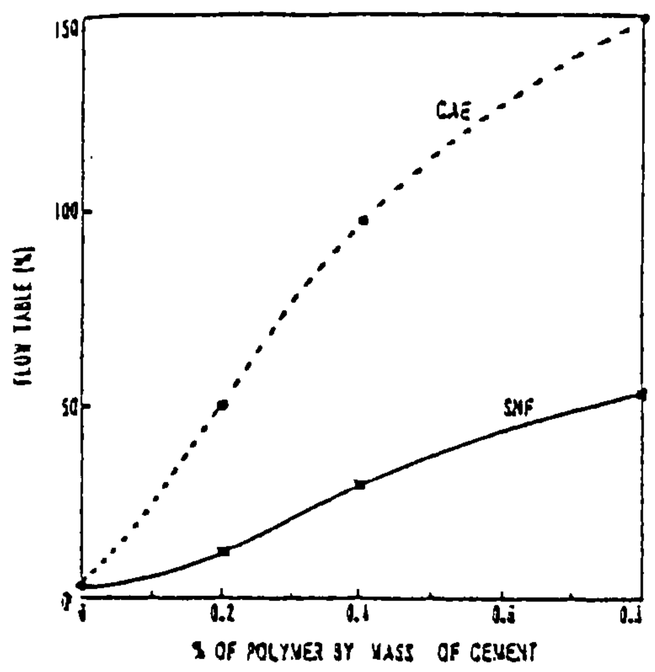

(c)

Figure 2.30 : Changes in (a) adsorption, (b) zeta potentials, and (c) mortar flow properties of Acrylic (CAE) and SNF based superplasticizers as a function of polymer dosage[133].

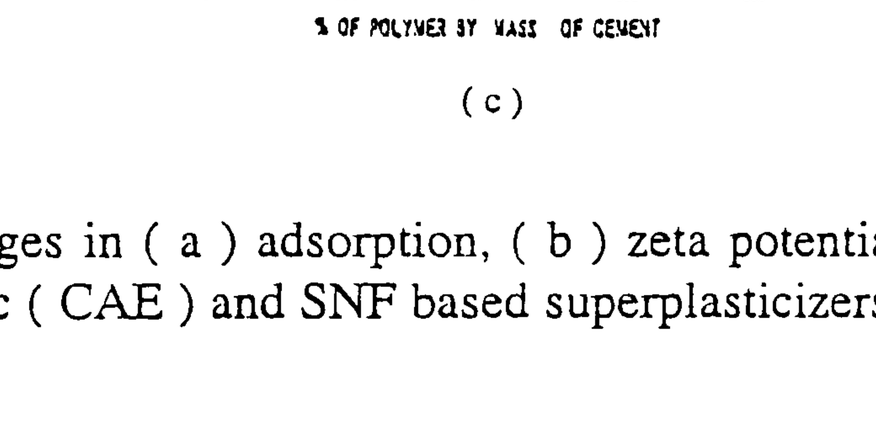

Figure 2.31 : Model for adsorption of a typical Carboxylic graft copolymer, showing its steric structure on cement surfaces[146].

2.5.3 Superplasticizer dosage effects

It is widely accepted that the workability of HS and other HPCs increases with increasing dosage of superplasticizer, up to a certain **saturation dosage** (or point), beyond which no further increases are possible[17, 38, 148]. When the dosage is less than the saturation value, the dispersion induced is considered to be less effective, and the slump rapidly decreases to that of a non-superplasticized concrete of the same water content[114, 149]. Dosages higher than the saturation value, are believed to provide little or no benefit in reducing the rate of loss of workability[17], but instead cause undesirable side-effects, such as air-entrainment, segregation and retardation of early strength development[14, 17, 19].

To assess the dosage requirements for a given slump, and/or the effectiveness of a given superplasticizer and cement, several workers[13, 58, 148, 150] have developed small scale tests based on measuring the flow time of pastes or mortar through a standard orifice, known as the Marsh cone. This gives reductions in flow time with increases in superplasticizer dosage, up to the saturation point. Loss of workability is typically assessed by comparing the increase in flow time occurring between 5 and 60 minutes[13]. A similar orifice in the shape of a V-funnel has also been developed in Japan for both mortar and concrete[151].

Other workers[152-153] have used a mini-slump test which, like the slump test in concrete, is considered to reflect the flowability or yield property. In contrast, the Marsh cone (or V-funnel) is believed to provide an indication of viscosity[58]. The choice between orifice or mini-slump test however appears to be made on a preference basis[8]. (Typical results are presented in sections 2.5.4 and 2.5.5).

In concrete, Tattersall[7] demonstrated that increasing dosages of a plasticizer produce a set of parallel flow curves, represented by decreasing yield value and constant plastic viscosity (**figure 2.32**). Similar results have been reported by Banfill[154] in mortar. Banfill's results[124] in concrete, with SMF and SNF superplasticizers and different cements, however showed some evidence of

significant increases in plastic viscosity (h), followed by continuous reductions once the minimum yield (g) value is reached (**figure 2.33**). The increases in plastic viscosity at low dosages are however in contradiction with the first use of superplasticizers (page 34), that they increase the workability of concrete (i.e. reduce both the g and h values). In this respect, Banfill argued that the increases in plastic viscosity are outweighed by the larger reductions in yield value.

In another study, Wallevik and Gjorv[50] investigated the effects of increasing superplasticizer dosages on loss of workability. Their results with Tattersall's MH system showed that the initial yield (g) value slightly decreases whilst the plastic viscosity (h) is significantly increased with increasing dosages (**figure 2.34**). The time effect of the superplasticizer is demonstrated by continuous increases in yield value, but reductions in plastic viscosity, particularly at high dosages. Wallevik and Gjorv[86] suggested that such results may be influenced by segregation in Tattersall's apparatus, but have surprisingly stated that their BML viscometer is capable of assessing segregation resistance and gives good correlations with the MH system.

More recently, Punkki et al[17] examined the effects of three SNF superplasticizer dosages (of 1.9, 2.5 and 3.1%) on the slump loss and workability retention of HSC using the BML viscometer. The higher dosages of 2.5 and 3.1% were found to give similar slump reductions (of 70-90 mm, from 210 to 140 and 120 mm over a period of 60 mins), whilst the 1.9% dosage gave a larger slump loss of about 160 mm (**figure 2.35(a)**). The effect of the 3.1% dosage on the initial Bingham parameters is represented by approximately a two-fold increase in plastic viscosity, but similar yield stress compared to the 1.9% dosage (**figure 2.35(b)**). After a lapse of 60 minutes, they concluded that the lowest dosage (1.9%) mainly increases the yield stress, whilst the highest dosage mainly increases the plastic viscosity.

Although their results are consistent with the expected increases in the Bingham parameters with decreasing workability, Punkki et al appear not to have fixed the

water contents of their mixes with changes in superplasticizer dosage. They report varying w/b ratios of 0.39, 0.37 and 0.36 for the 1.9, 2.5 and 3.1% dosages respectively. Moreover, their results do not clearly demonstrate whether saturation was reached.

In comparison with conventional superplasticizers, several workers[28, 119, 133] have shown marked differences in the dosage efficiency of NG superplasticizers, particularly with comb and acrylic based polymers. In one study, Jeknavorian et al[119] found that the dosage requirement to obtain a comparable mortar flow spread at 0.47 w/b ratio was up four times lower with the ADVSP comb polymer than with SNF or lignosulphonate-based superplasticizers. With an acrylic based super-superplasticizer (SSP), Mitsui et al[28] observed that when the w/b ratio is reduced to 0.20, the demands for SNF and polycarboxylic-based superplasticizers (NSF, SP) are approximately three and five times higher (**figure 2.36**). Similar results have been reported by Kinoshita et al[135] in pastes at w/b ratios of 0.30 and 0.20.

The author is unaware of any published work which has unequivocally demonstrated the effects of superplasticizer saturation dosage on workability retention. Although this is generally considered to reduce the rate of workability or slump loss[14, 149, 155], conflicting information has been reported by several researchers[19, 156-158]. For example, Previte[157] and West[158] stated that the problem of slump loss in superplasticized concrete is largely a function of the initial slump: the higher the initial slump, the greater the slump loss. Mindess and Young[156] concur with this, and suggested that it may be a general rule. In HSC, Detwiler[19] stated that the rapid slump loss may primarily be due to the high dosage of superplasticizer added to the concrete at the batching plant.

Further work is therefore clearly needed to ascertain the effects of saturation dosages on the workability retention of HSC.

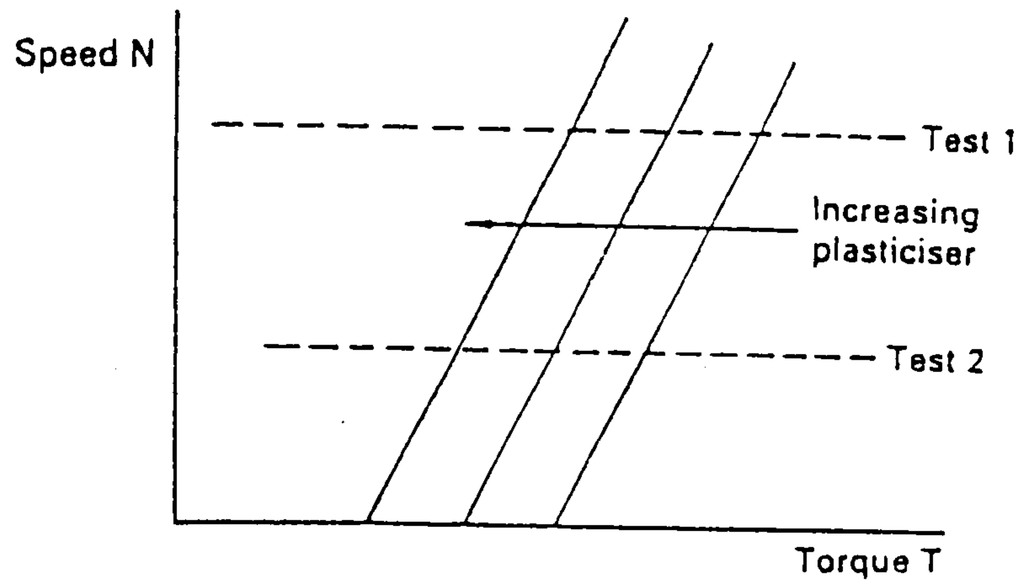

Figure 2.32 : Bingham flow curves showing effect of increasing plasticizer dosages (MH system, "the reciprocal slope" is a measure of plastic viscosity)[7].

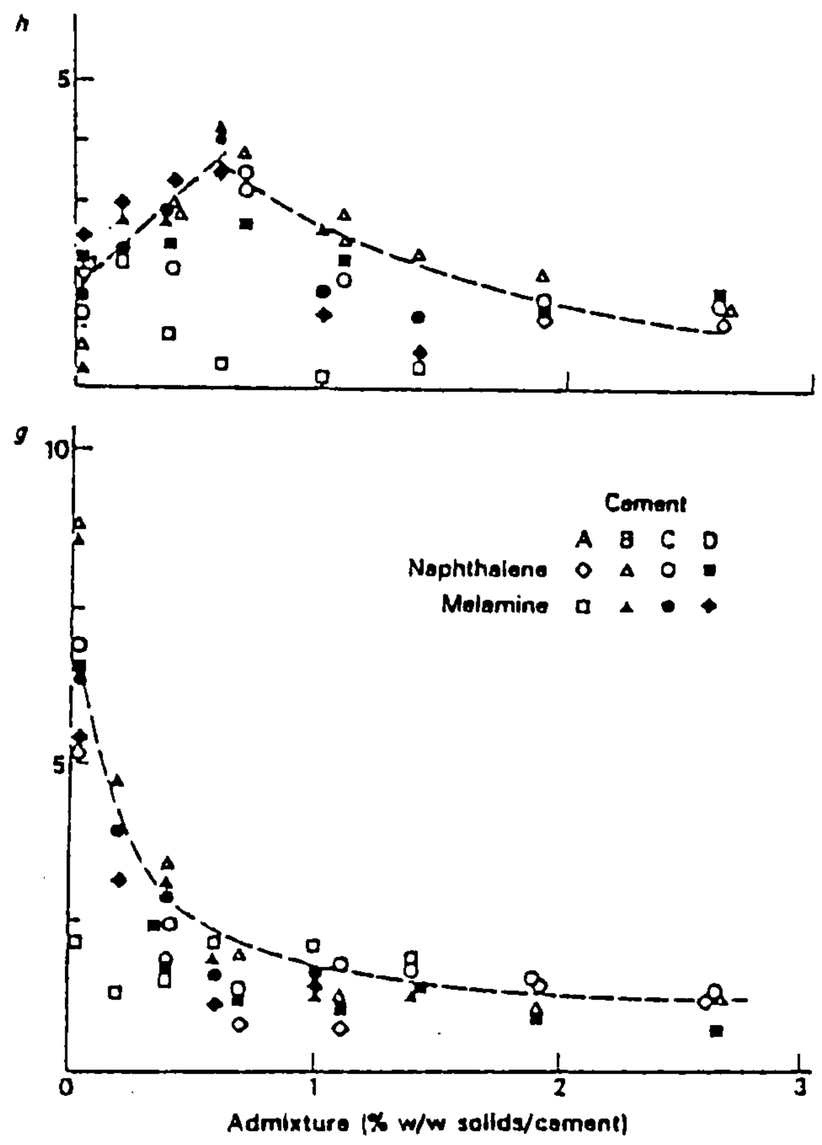

Figure 2.33 : Variations in g and h values with superplasticizer concentartion (MH system, 0.70 w/c)[124].

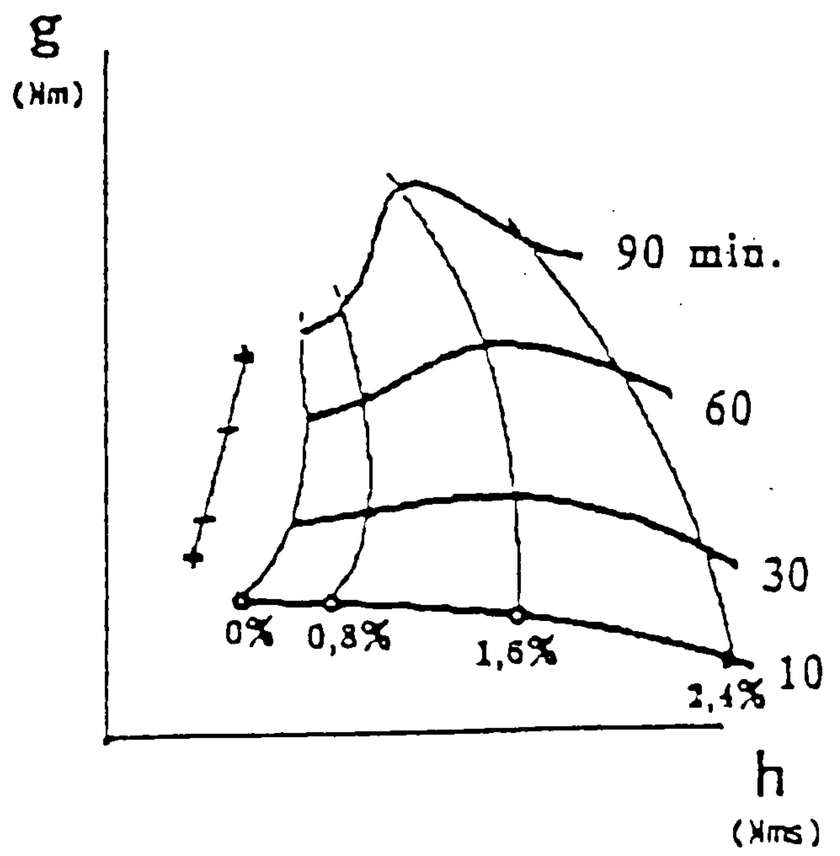

Figure 2.34 : Effect of increasing superplasticizer dosages on the Bingham properties of fresh concrete as a function of time (MH system)[50].

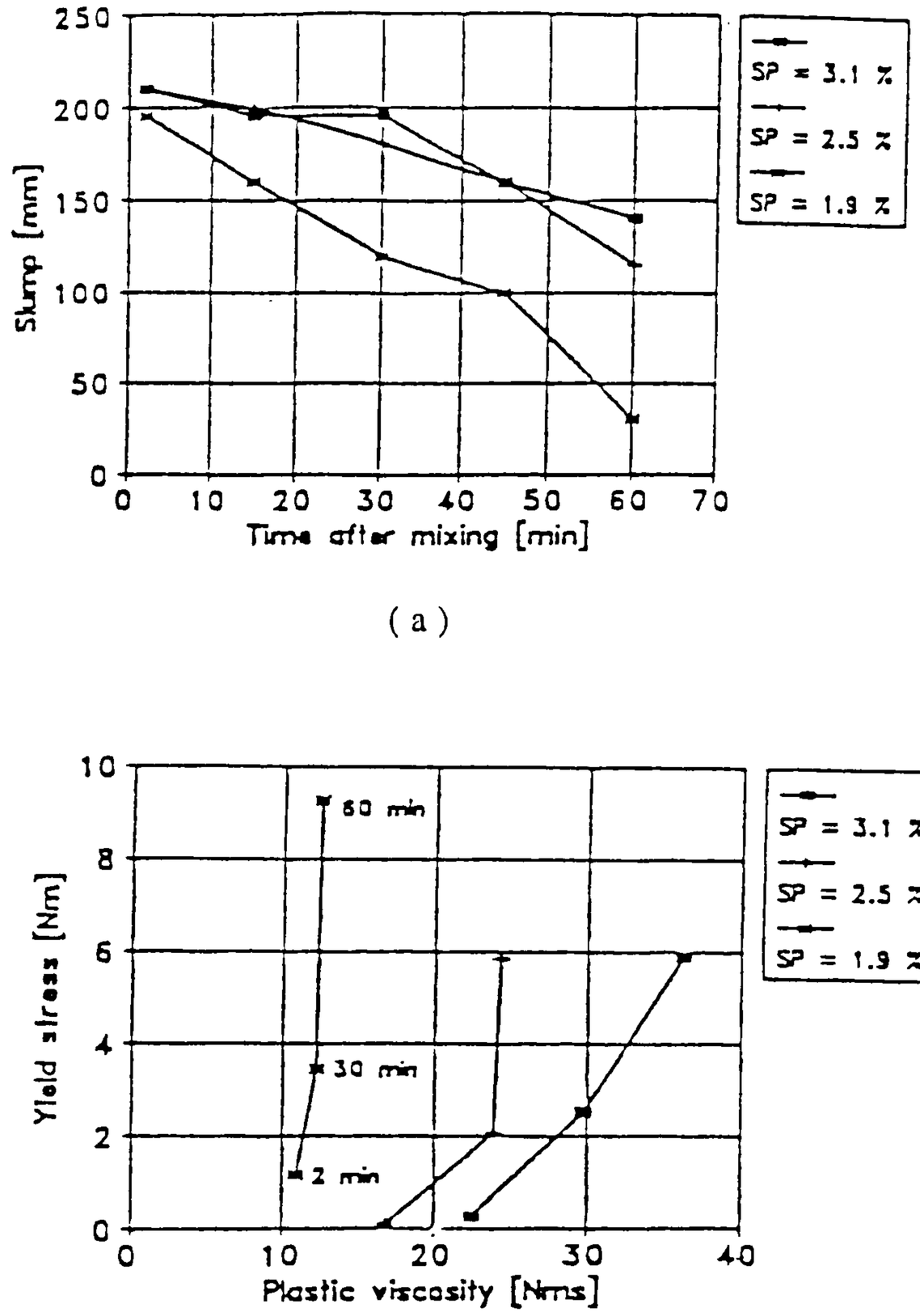

Figure 2.35 : Effect of SNF superplasticizer dosage on (a) slump loss, and (b) Bingham properties of HSC - at 2, 30 and 60 mins (BML viscometer)[17].

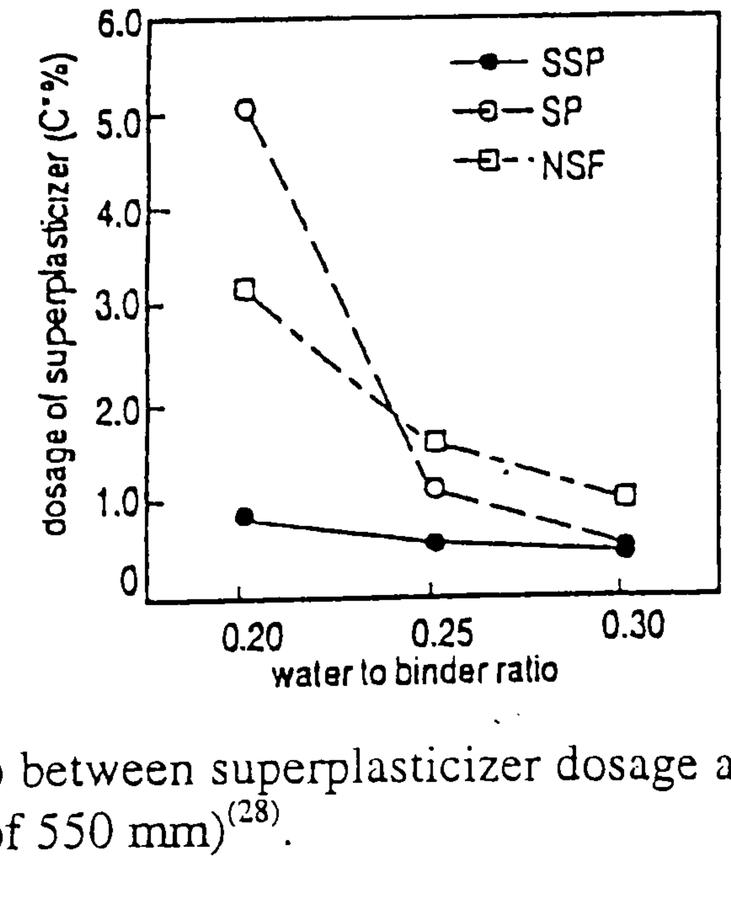

Figure 2.36 : Relationship between superplasticizer dosage and w/b ratio (obtained at a target slump-flow spread of 550 mm)[28].

2.5.4 Superplasticizer mixing procedures

Three superplasticizer mixing procedures or methods used to minimise the problem of rapid loss of workability are[34, 66]:

1. **redosing** with superplasticizers;
2. **blending** superplasticizers with retarders (or other chemical admixtures);
3. **delayed superplasticizer addition**.

(I) Redosing methods

Several redosing methods, based on single or multiple additions of superplasticizer, have been used in the field. One method is to add part of the superplasticizer at the mixing plant, and the remainder at the point of discharge. The premise of this method is that only enough of the superplasticizer is needed to ensure adequate dispersion of cement particles during mixing and transportation, so the original slump at arrival in the field need only be between 50 to 100 mm[8, 41].

From work with the BML viscometer, Hu et al[40] reported that sequential addition of a SMF-based superplasticizer in HPCs typically reduces the initial shear yield stress (τ_o) and increases the plastic viscosity (μ). They attributed the measured increases in plastic viscosity to significant increases in the amounts of superplasticizer molecules remaining in solution (instead of being adsorbed at the liquid-solid interface), which consequently increases the viscosity of the liquid phase relative to pure water. In contradiction to this, Domone et al[85] reported that the plastic viscosity as measured with the MH system (at 0.40 w/c ratio) remains approximately constant upon addition of a SNF superplasticizer. Their results are consistent with Tattersall' s findings (c.f. figure 2.32).

With the MH system, Banfill[124] compared the effects of single redoses of SMF and SNF-based superplasticizers on the Bingham properties at 0.78 w/c. From

his results (**figure 2.37**), he concluded that the original workability of flowing concrete (in terms of the initial g and h values) can be regained by adding a second dose of SMF superplasticizer after 60 minutes or up to 160 minutes with SNF.

In HSC, Chan et al[14] showed that multiple additions of a SNF superplasticizer can be successfully used to maintain an initial slump of 200mm during the first two hours. Dodson[122] suggested that with lapsed time, the dispersant becomes engulfed with hydration products which are sheared off during mixing, and the redosed superplasticizer is adsorbed by the freshly exposed cement surfaces to produce a sudden surge in dispersion and hence a marked increase in slump.

Chan et al[14] pointed out that one important practical limitation of the redosing method is during pumping, where it is impossible to recover the workability of concrete in the pipe line by manual redosing from the outside. (Other disadvantages of the redosing method were mentioned in page 5).

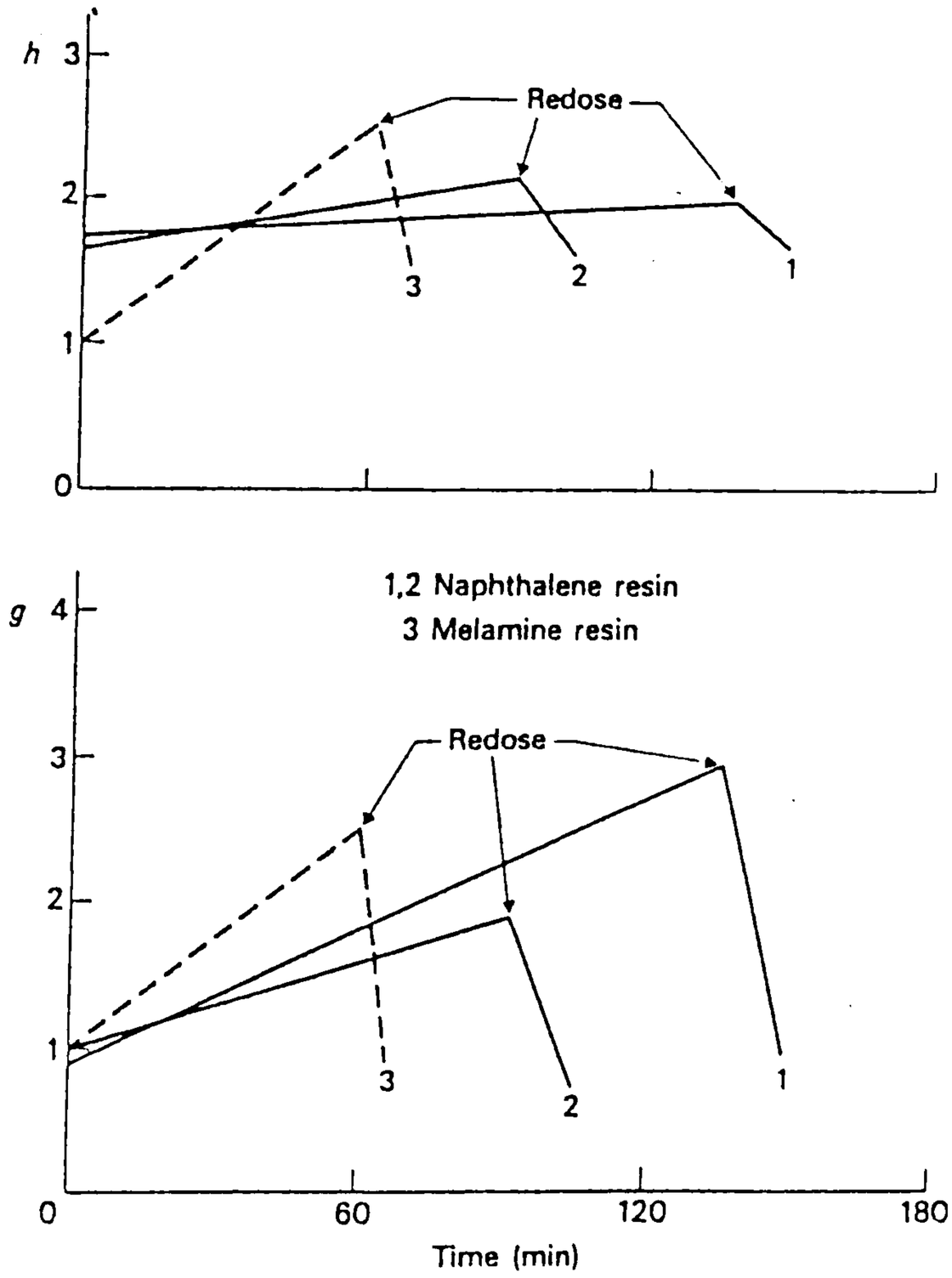

Figure 2.37 : Effect of redosing on g and h values of superplasticized NSC mixes (0.70 w/c)[66, 124].

(II) Blending of chemical admixtures

The simultaneous use of various combinations of water reducers, retarders, accelerators and air entraining agents with superplasticizers have all been reported to be compatible in extending slump retention and/or modifying the workability properties[7, 120]. Most reported studies have mainly focused on the technical benefits of blending retarders with superplasticizers to reduce slump loss during long transportation and/or in hot weather concreting[14, 19, 41, 58, 122, 159]. Retarders are believed to delay cement hydration by slowing down the growth of gel-like ettringite layers[111] and $Ca(OH)_2$ nuclei[8].

In HPCs, Aitcin[41] stated that the use of a 5-10% retarding agent (s/w/b) during mixing can solve the slump loss problem without unduly retarding the setting characteristics. In contrast, Larrard[160] suggested that the addition of a retarder may not reduce slump loss in cases where water is lost by aggregate absorption. Penttala[16] has however reported that the blending of superplasticizers with retarders has insignificant effects on the workability retention of HSCs.

According to Aitcin et al[58] the blending of SMF or SNF-based superplasticizers with lignosulphonate plasticizers presents two advantages when used at low dosages. The first advantage is economical: since lignosulphonates are less costly than SNF and SMF. The second is chemical: the sugars present in lignosulphonates in most cases slightly retard setting, so that concrete keeps its workability longer. In HPCs, they stated that with blends of SMF and SNF condensates: the SNF could be used at the mixing plant, while the SMF would be added at the job site to produce the desired workability and reduce retardation.

None of the above studies[14, 19, 41, 58, 122, 159] have provided qnatitative information on how the blending of chemical admixtures influences the Bingham properties and, hence, the workability retention of HSCs.

(III) Delayed additions of superplasticizers

The time at which a superplasticizer is added to a mix is widely known to influence its effectiveness. As early as 1973, Blick[161] stated that for optimum efficiency, the addition of superplasticizers in HSC should be delayed until all the cement has come into contact with the mixing water. Rixom and Mailvaganam[113] stated that if the admixture is added just at the end of the initial mixing sequence of aggregates, cement and total gauging water, greater adsorption of the admixture on to the initial hydrates is obtained resulting in a higher workability.

Most researchers and concrete producers however provide no details of their superplasticizer mixing procedure, giving the impression that the admixture is added directly with the mixing water. In HSC, Soutsos[53] has even argued that the lumps of concrete formed during the mixing sequence without the superplasticizer, will eventually deter uniform dispersion once the superplasticizer is added.

In an investigation with the slump test, Collepardi[162] found that a one minute delayed addition of a SNF superplasticizer at 0.45 w/c, when compared with direct addition, produces a more workable mix (A), or requires less mixing water (B) or dosage (C) for the same slump (**figure 2.38**). Similar results have been reported by Penttala[16] and Baoju et al[99], showing that a 1 min delayed addition of SNF superplasticizer produces significantly less slump loss compared to direct addition in HSC mixes.

Collepardi's results[162] with the carboxylated acrylic ester (CAE) copolymer however showed that its performance is independent of mixing procedure (**Table 2.3**). As mentioned earlier, the performance of the CAE polymer is considered to be related to steric hindrance effects rather than to the presence of negatively charged anionic (COO^-) groups[34] (c.f. figure 2.19).

In cement pastes at 0.30 w/b ratio, Chiocchio and Paolini[152] compared the effects of five delayed additions (at 0, 1, 2, 4, and 10 minutes) using SMF and SNF

superplasticizers. They observed that the optimum addition time, which gives the maximum workability as measured by a mini-slump test, is obtained when the superplasticizer is added after 2 minutes (**figure 2.39**). As can be seen, the effect is independent of admixture type. Longer delayed additions reduce the initial workability, but slightly extend workability retention. Chiocchio and Paolini concluded that the maximum workability is obtained when the addition time of the superplasticizer corresponds to the beginning of the dormant period of cement hydration without admixture.

In HPCs, Penttala[142] stated that delayed addition of a superplasticizer by 0.5 to 3.0 minutes significantly increases its efficiency, and extends workability retention. In contrast, Hsu et al[6] have more recently found that the slump (at 0.30 w/b ratio) decreases substantially with delayed addition times beyond about 15 mins, particularly at low SNF dosages. They concluded that the optimum addition time for a SNF superplasticizer occurs at approximately 10-15 mins. Although this also corresponds to the beginning of the dormant period, it is much longer than that reported by Chiocchio and Paolini[152] in cement pastes.

In a study with the BML viscometer, Punkki et al[17] investigated the effects of five superplasticizer mixing procedures on the slump loss and Bingham properties of HSC at 0.37 w/b ratio and a constant superplasticizer dosage of 2.5%. Their mixing procedures, comprising three single additions and two split additions of superplasticizer are summarised in **figure 2.40(a)**.

The slump test results showed that delayed additions of the superplasticizer significantly reduce the rate of slump loss, but revealed no clear tendency between the various delayed and split additions (**figure 2. 40(b)**). In contrast, their results with the BML viscometer indicated more distinct effects of mixing procedure on both the initial workability properties and workability retention (**figure 2. 40(c)**). They concluded that direct addition gives relatively higher initial g and h values, and pronounced increases in the yield stress with time; whereas the 1 and 2 minute delayed additions (procedures B and C) reduce the initial yield value and, give gradual increases in both the yield stress and the

plastic viscosity with time. The split additions of the superplasticizer/plasticizer during initial mixing (procedures D and E) exhibit significantly lower initial plastic viscosities, which increase considerably during the first 30 minutes. (No explanation was provided for this).

The effects of addition time on the performance of conventional superplasticizers has generally been attributed to adsorption of their molecules onto the tricalcium aluminate, which occurs in substantial amounts, even in a few seconds[8, 16, 143]. According to Collepardi[143] when added directly with the mixing water, the superplasticizer is rigidly attached in substantial quantities to the C_3A-gypsum system leaving only small amounts for dispersion of the silicate phases (**figure 2.41**). When the addition of the superplasticizer is delayed, the C_3A has time to develop a protective layer of ettringite so adsorption is reduced, and more superplasticizer molecules are available to promote dispersion of the silicate phases and thus increase workability.

Neville[8] stated that with lapsed-time, the supply of dispersant diminishes as some of the superplasticizer molecules become entrapped by the hydration products, and the workability of the mix is rapidly lost. Edmeades et al[163] suggests that rapid loss of workability may be due to super-saturation of the mixing water with gypsum followed by competition for active C_3A and C_4AF sites between calcium sulfate and the chemical admixture. They stated that delayed addition of the admixture by several minutes allows the hydration reactions to become established before the admixture molecules are available to block reactive sites where ettringite can form.

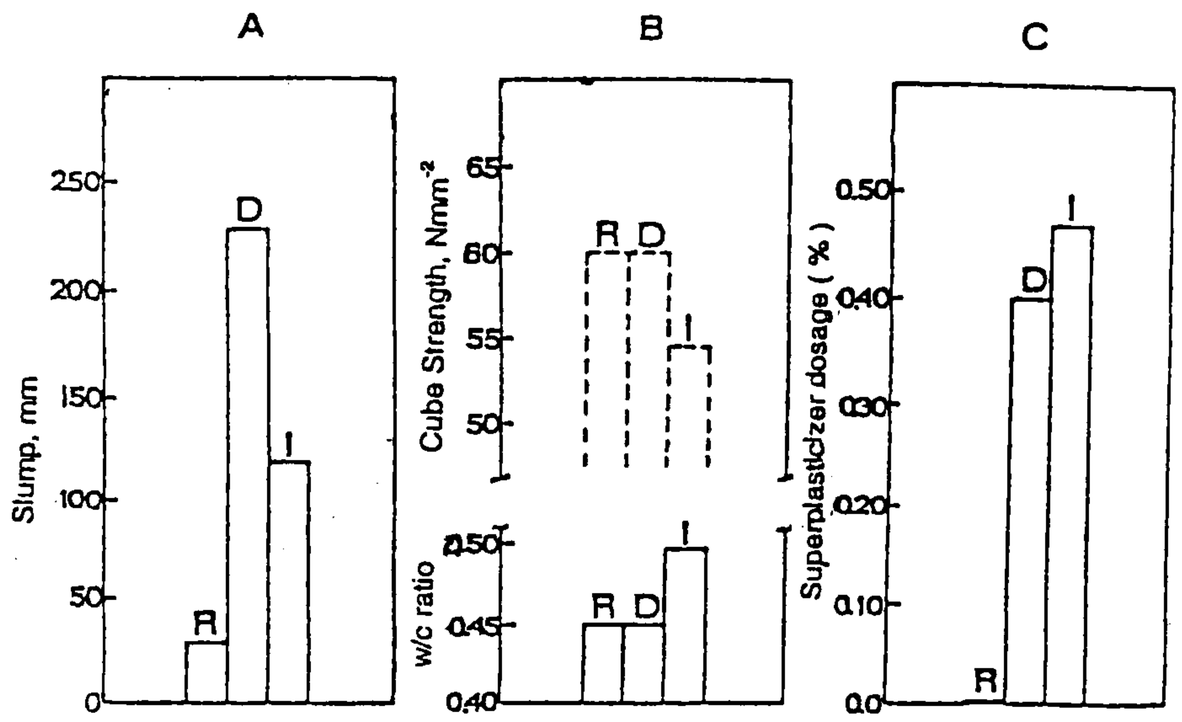

Figure 2.38 : Comparison of direct and 1 min delayed additions of a SNF superplasticizer on (A) slump, (B) w/c reduction and (C) dosage requirement. (Note: R=reference mix (without SP), D=1 min SP addition, I=immediate/direct SP addition)[162].

Table 2.3 : Comparison of direct and 1 minute delayed addition on the slump properties of mixes prepared with SNF and CAE superplasticizers[162].

TYPE	ADMIXTURE DOSAGE* (%)	ADMIXTURE METHOD OF ADDITION**	W/C RATIO	SLUMP (mm)
NSF	0.48	IMMEDIATE	0.40	100
NSF	0.48	DELAYED	0.40	230
CAE	0.30	IMMEDIATE	0.39	230
CAE	0.30	DELAYED	0.39	235

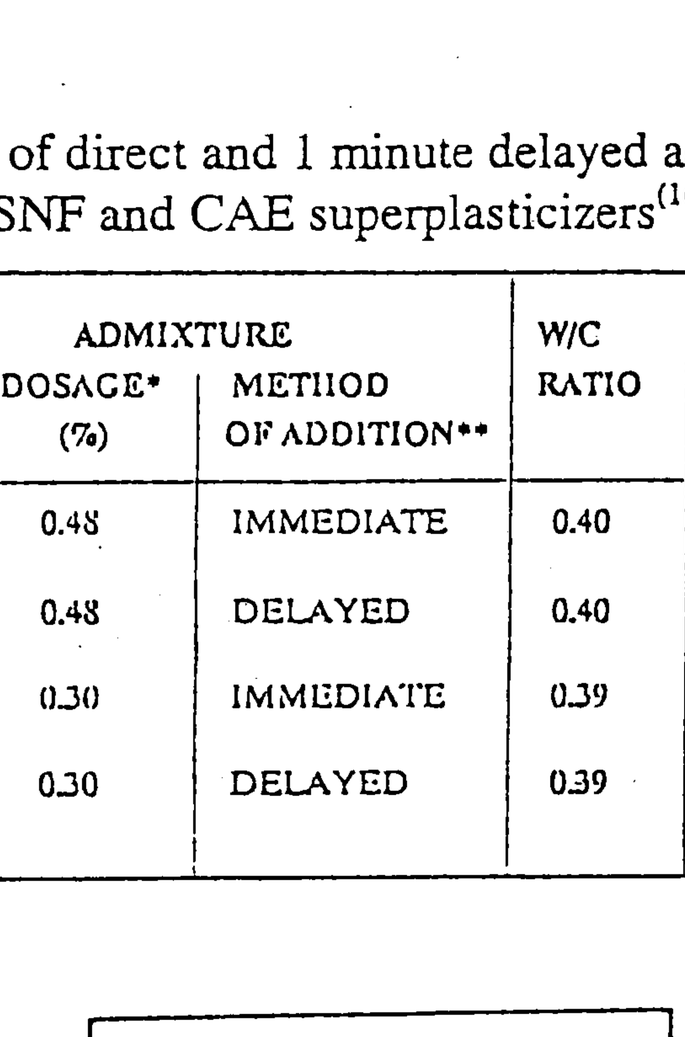

Figure 2.39 : Variations in the workability of cement pastes using 0-10 minutes delayed additions of SNF and SMF superplasticizers (at constant dosage of 1% s/w/b, 0.30 w/c)[152].

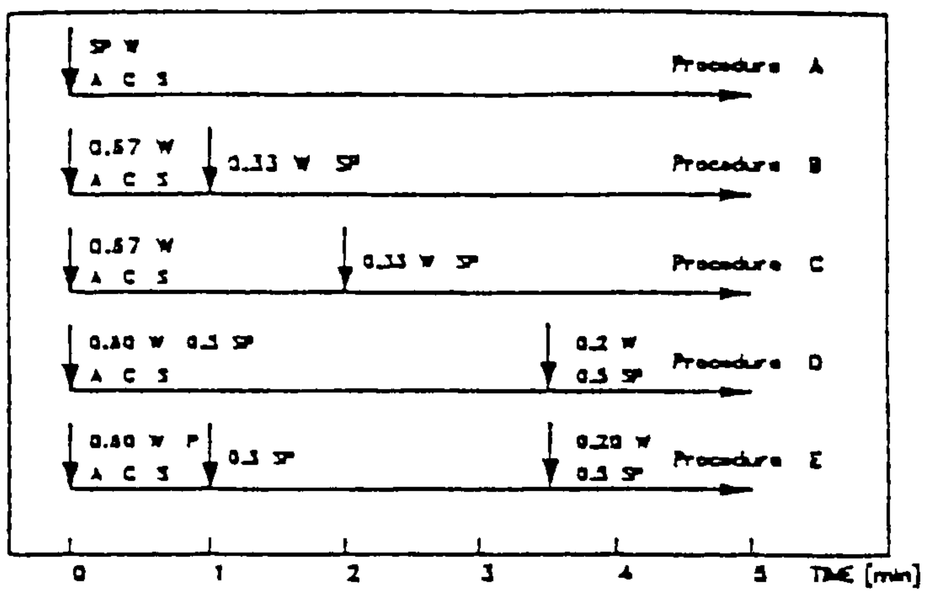

(a) A = Aggregates, C = Cement, S = Sand, W = Water, SP = Superplasticizer and P = Plasticizer.

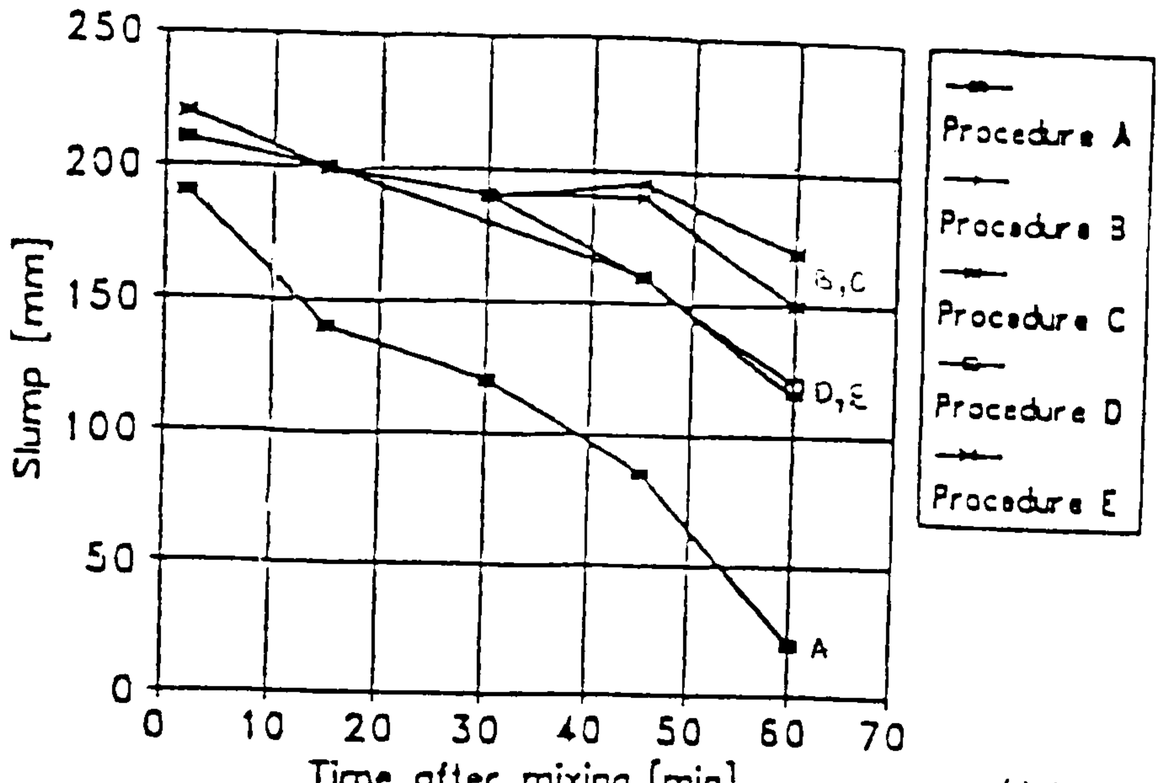

(b)

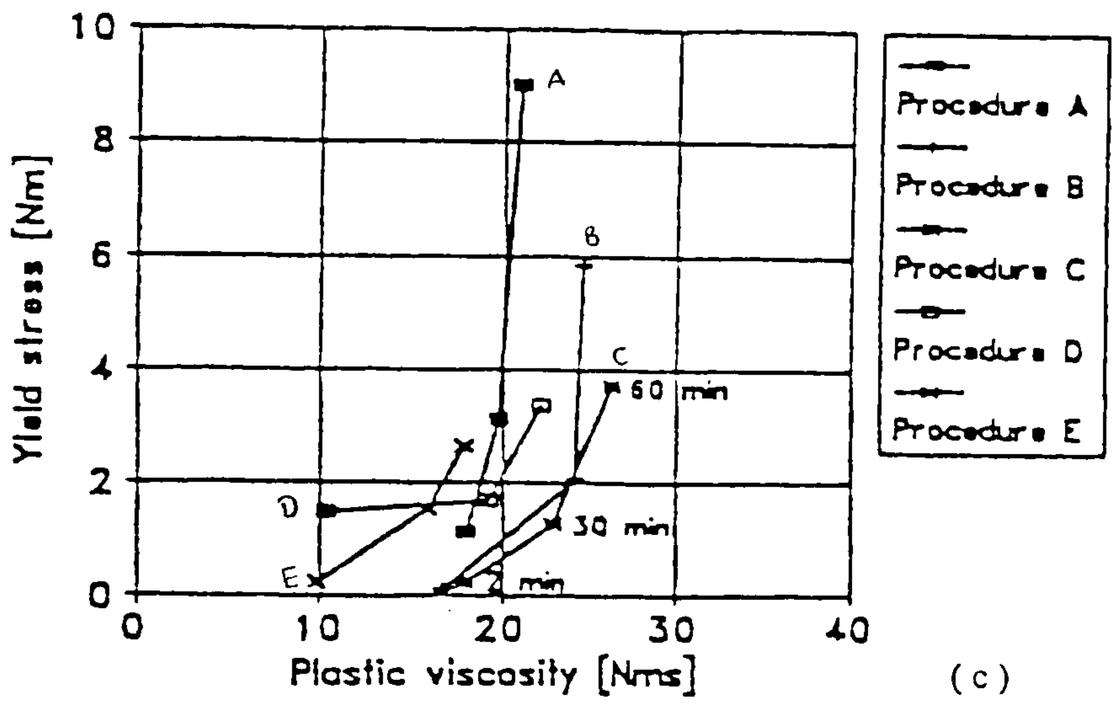

(c)

Figure 2.40 : Effect of (a) superplasticizer mixing procedure on (b) slump loss, (c) variations in yield stress and plastic viscosity at 2, 30 and 60 mins after mixing (at a constant dosage of 2.5% s/w/b, 0.37 w/b ratio)[17].

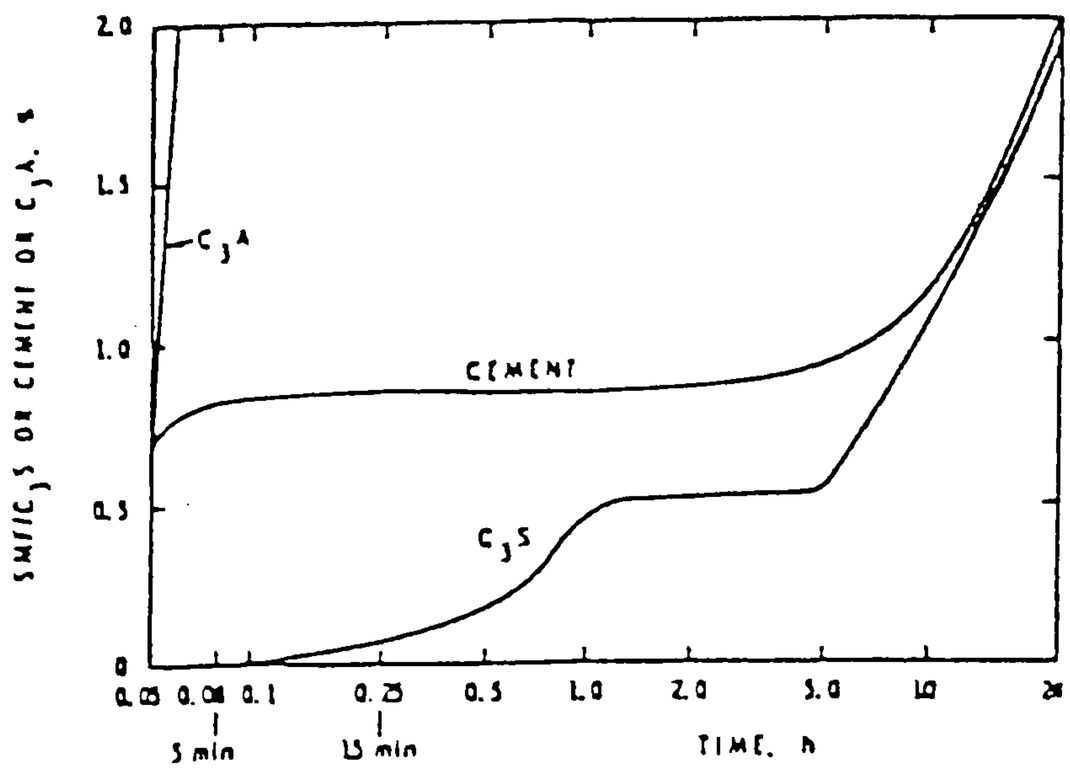

Figure 2.41 : Adsorption of SMF on cement compounds during hydration[143].

2.5.5 Cement-superplasticizer compatibility

It has been widely documented that it is not always possible to produce HPCs that are still workable one hour after mixing by simply choosing any random combination of portland cement and superplasticizer. According to Aitcin[41], the performance of superplasticizers depends critically on both: the reactivity of the cement, and on the compatibility of the superplasticizer with the cement. The former refers to the rate at which the cement consumes water during mixing, whilst the latter refers to the rate at which some of the superplasticizer molecules are trapped within the hydrates formed.

Cement-superplasticizer incompatibility is generally believed to cause poor dispersion, higher superplasticizer dosage requirements and/or rapid slump/workability losses - leading to placing and consolidation problems, together with reduced strength and durability[42]. The commonest of these in HSC is slump loss, which can reduce the workability time to 15-20 minutes with some superplasticizer-binder combinations[16].

In the past, few cases of poor compatibility between cements and water reducers were reported[161, 164-165]. More recently, with the increasing popularity of HS and other HPCs, these have become more frequent, and have led to numerous studies to determine the causes of cement-superplasticizer incompatibility[13, 33, 58, 109, 166-167]. As rigorous testing on concrete is difficult, most studies have been confined to assessing/optimizing the performance of a limited number of cements or superplasticizers. The tests have often been carried out on cement pastes or mortar, using either the Marsh cone[13, 167] or mini-slump[153] tests (described in section 2.5.3).

In one study, Aitcin and Baalbaki[13] reported four typical situations to illustrate the effects of cement-superplasticizer compatibilities as shown in **figure 2.42(a-d)**. Figure 2.42(a) represents a perfectly compatible cement/superplasticizer combination, where the saturation dosage of the superplasticizer is low and the

Marsh cone flow times at 5 and 60 minutes are similar. Figure 2.42(b) on the other hand shows a case of incompatibility, the superplasticizer dosage at the saturation point is quite high and the flow time after 60 minutes is much larger than that at 5 minutes. Figures 2.42(c-d) represent intermediate cases.

From a literature review, Aitcin and Neville[11] attempted to identify the main factors responsible for cement-superplasticizer incompatibility. For the cement, they suggest these are: the C_3A and C_4AF contents, the reactivity of the C_3A, the calcium sulfate content, and the final form of the calcium sulfate in the ground cement (namely gypsum ($CaSO_4.2H_2O$), hemihydrate ($CaSO_4.½H2O$), or anhydrite ($CaSO_4$)). For the superplasticizer, the important factors are the molecular chain length, the position of the sulphonate group in the chain, the counter-ion type, and the presence of residual sulfates, which all affect the cement deflocculation properties.

For HPCs, they postulated that from the rheological point of view:

- "**An ideal cement**" is one which is not too fine, with a very low C_3A content, and with an interstitial phase whose reactivity is easily controlled by the sulfate ions derived from the solution of the sulfates present in the cement.
- "**An ideal superplasticizer**" should consisted of rather long molecular chains in which, for example, the sulphonate groups occupy the β-position in salts of SNF condensates.

When superplasticizers are used in NSC, Aitcin and Neville[11] stated that these requirements are probably not applicable, primarily because the relatively large amount of mixing water plays a dominant role in determining their rheological properties. At low w/b ratios, the incompatibility problem is believed to be acute for two main reasons[13, 168]:

1. In HPCs, the low w/b ratio implies that there is less water available to accept the sulfate (SO_4^{2-}) ions from the calcium bearing minerals.
2. Because of the very high cement content, there is more C_3A present per unit volume whose reactivity must be controlled to ensure the desired workability.

According to Neville and Aitcin[168], a given cement and superplasticizer become incompatible when the solubility of the gypsum is low, and it does not release sulfate ions fast enough to react with and, therefore, neutralize the C_3A which is the first component of the cement to hydrate. If there is too little soluble sulfate available, the sulphonate ends of the superplasticizers become fixed by the C_3A, and the superplasticizer therefore can not provide the required workability.

According to Dodson[122] all cements exhibiting cement-superplasticizer incompatibility contain natural anhydrite ($CaSO_4$) in relatively large amounts. This differs from gypsum in its rate of solution in water and in the amount of water bound in its crystal structures. He states that when the weight ratio of gypsum to natural anhydrite ($CaSO_4.2H_2O/CaSO_4$) in the cement is less than 2, poor response to dispersion (water reduction) and rapid stiffening (i.e. loss of workability) will occur in the presence of water-reducing admixtures.

From a study with a SNF superplasticizer and 5 cements at 0.35 w/c ratio, Jiang et al[166] reported that an adequate soluble alkali content during the first few minutes after mixing cement pastes is of primary importance in ensuring cement-superplasticizer compatibility. They concluded that at an optimum soluble alkali content (of 0.4 - 0.5 % Na_2O equivalent) the initial workability is maximum, loss of workability is minimum and is independent of C_3A content.

In agreement, Kim et al[153] have recently concluded (from a study on four cements at 0.35 w/b ratio) that for a given cement there exists an optimal soluble alkalies content for both SNF and SMF-based superplasticizers. Their results in **figure 2.43** showed that cements E and F (with Na_2O soluble equ. of 0.57 and 0.72) are compatible with a SNF superplasticizer by maintaining the fluidity of cement pastes for up to 90 mins; whilst cements L and N (having Na_2O soluble equ. of 0.07 and 0.06) are incompatible – due to poor mini-slump retention. According to them the soluble alkalies inhibit the adsorption of SNF or SMF molecules on the aluminate phases by providing the necessary sulfate (SO_4^{2-}) ions to neutralize active sites on the C_3A and C_4AF. In the absence of soluble alkalies, they reported that up to 70% of the superplasticizer can be adsorbed by the C_3A in the first 2

mins.

Very few investigations have however assessed the performance of different cements and superplasticizers on the slump or Bingham properties of fresh concrete mixes. In one study, Jeknavorian et al[119] compared the cement-superplasticizer compatibility of a polycarboxylate comb polymer (ADVSP) and a conventional SNF superplasticizer (NSFC) with four cements at 0.53 w/c ratio. They found significantly lower sensitivity to cement composition and better slump performance with the ADVSP polymers (**figure 2.44**), which they attributed to a lower dependence on electrostatic repulsion.

In another study, involving tests with the BT rheometer, de Larrard et al[49] presented the limited results shown in **figure 2.45** as an illustrative example of cement-superplasticizer incompatibility. These indicate considerable increases in yield value but little or no change in plastic viscosity with mixing time. de Larrard et al concluded that the effect on the workability properties is the same as that observed when the initial amount of superplasticizer decreases: i.e. the yield stress increases whilst the plastic viscosity is relatively unaffected. Surprisingly, they did not provide any details of the type of superplasticizer, cement composition, or mix proportions used in their study.

Further work is clearly needed to determine the effects of: individual cement components (such as C_3A and calcium sulfate contents), cement fineness, gypsum/(natural anhydrite ratios) etc, on the dosage requirements and workability properties of HSCs incorporating conventional and NG superplasticizers.

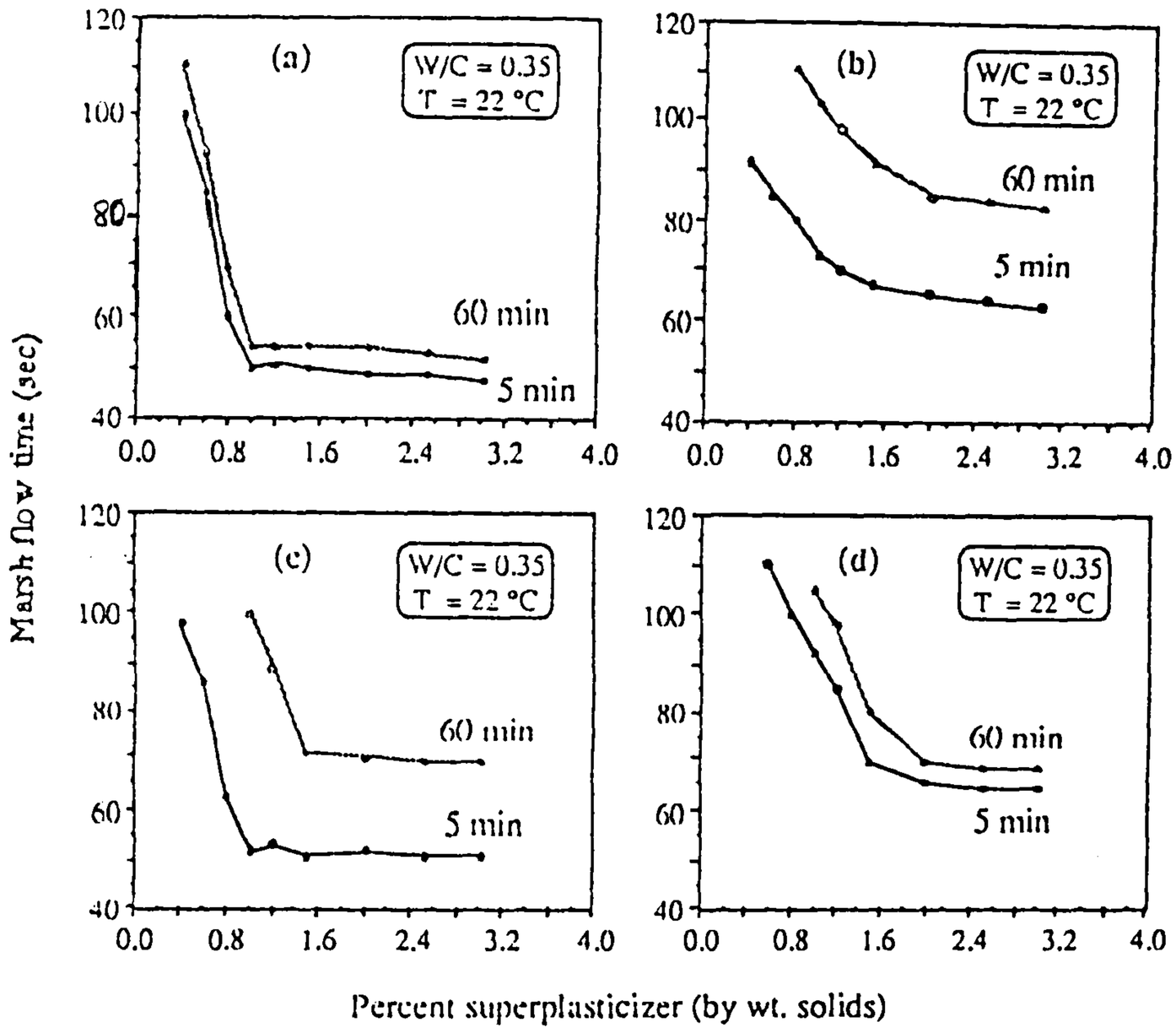

Figure 2.42 : Four examples to illustrate the effects of cement-superplasticizer compatibility as assessed with the Marsh cone test (details of the type(s) of superplasticizer(s) and/or cement(s) used were not reported)[13].

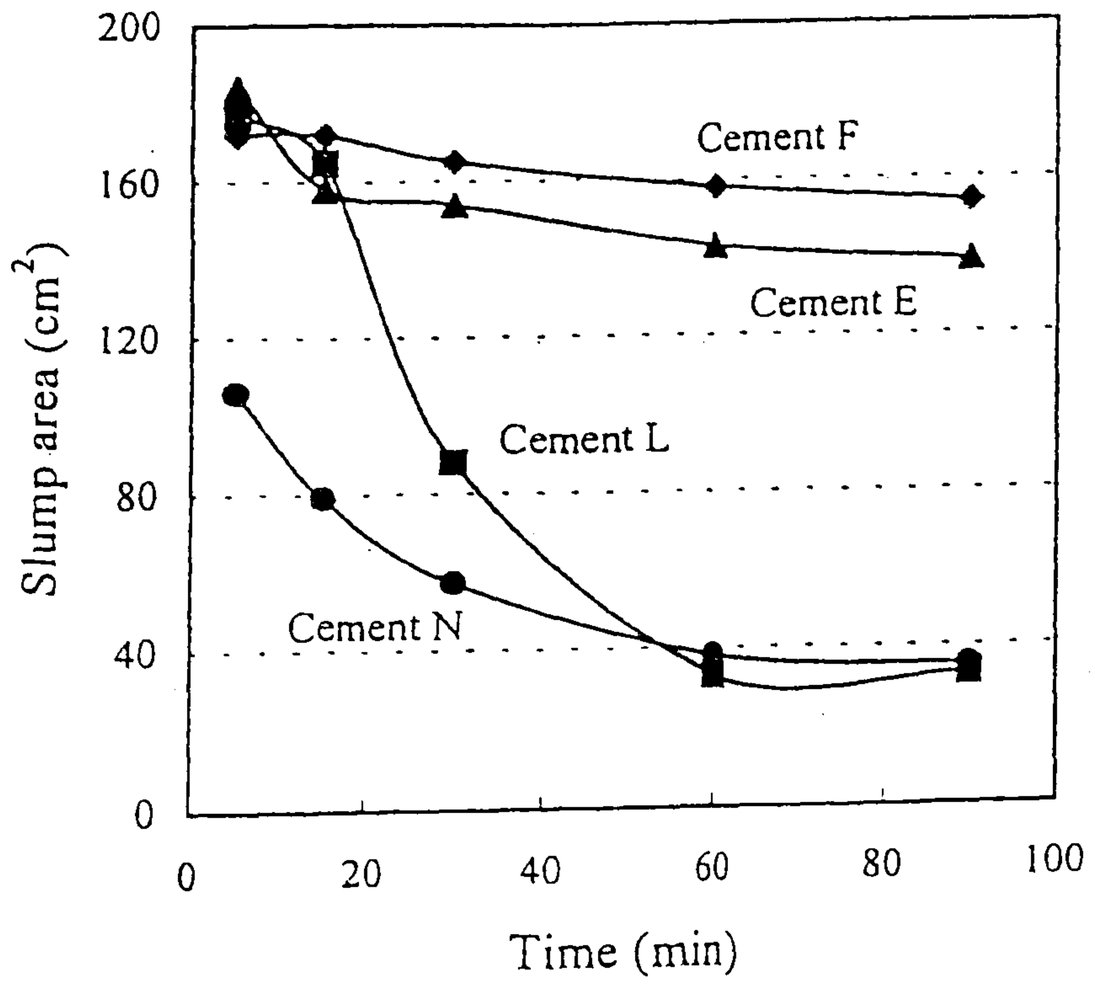

	E	F	L	N
C_3A	10	6	7	11
C_4AF	7	9	10	6
SO_3	2.90	3.40	2.67	2.95
Alkali as Na_2O	0.92	0.74	0.35	0.31
Soluble Na_2O eq.	0.57	0.72	0.07	0.06
Fineness (m^2/kg)	370	410	380	380

Figure 2.43 : Effect of four cements on the mini-slump performance of cement pastes (using SNF superplasticizer, at 0.35 w/b ratio)[153].

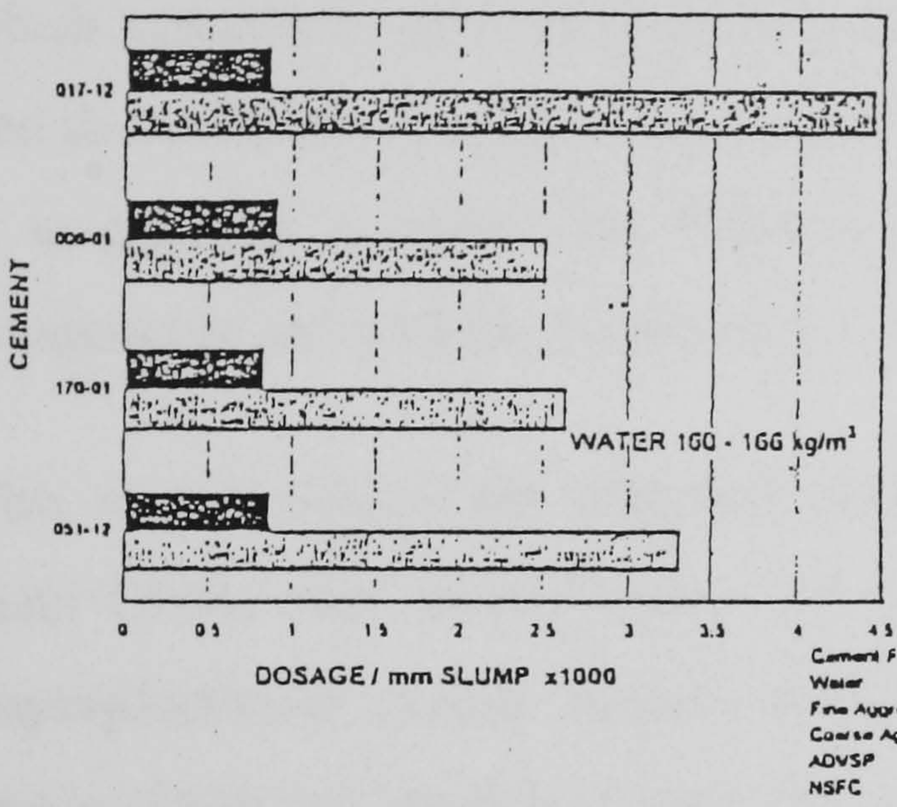

	017-12	006-01	170-01	051-12
C_3A	6	11	7	7
C_4AF	10	8	10	9
SO_3	2.65	4.21	2.32	2.91
Alkali as Na_2O	0.61	0.98	0.45	0.58
Fineness (m^2/kg)	459	334	368	394

Figure 2.44 : Slump-dosage response of ADVSP and SNF superplasticizers with four cements (percentages of soluble alkalis (as $Na_2O_{equ.}$) not reported)[119].

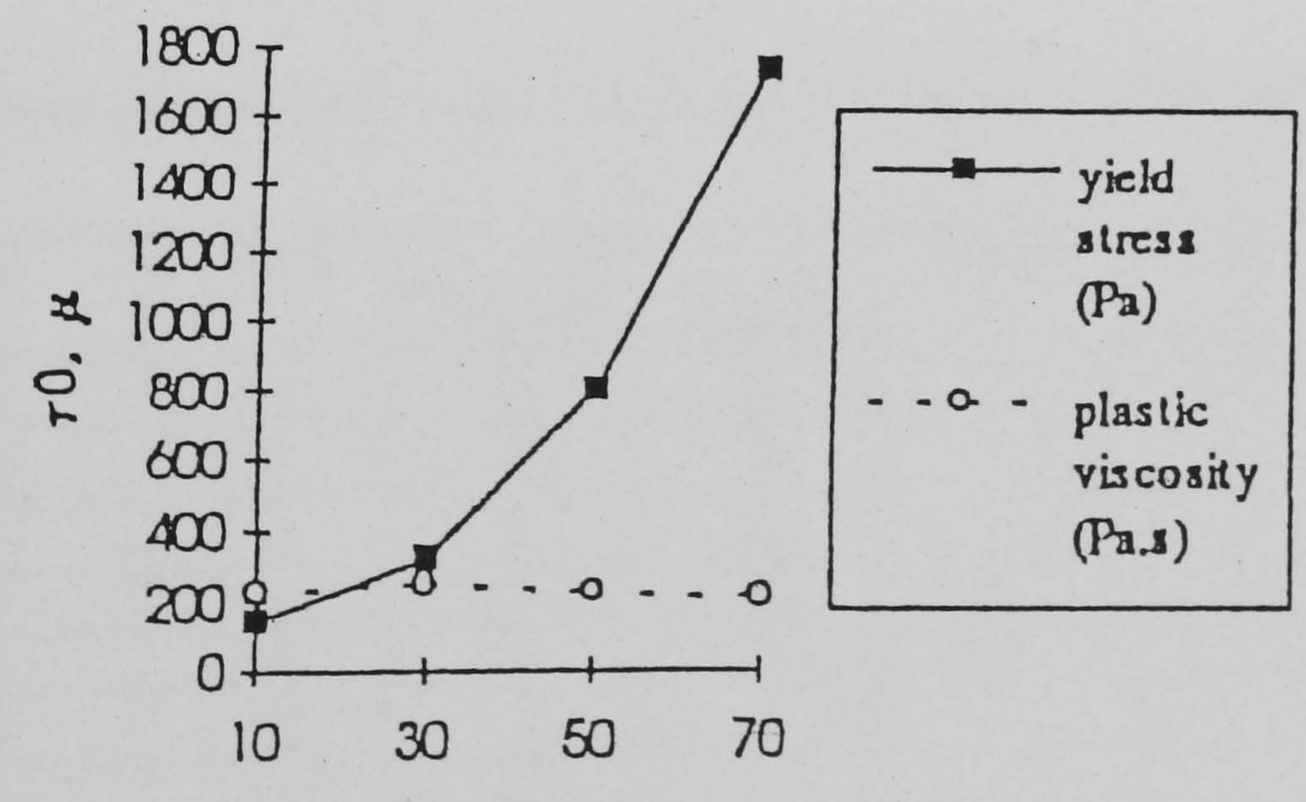

Figure 2.45 : Evolution of Bingham parameters for cement/superplasticizer incompatibility - (results based on a single mix as tested with the BT Rheometer)[49].

2.6 Cement and cement replacement materials (CRMs)

CRMs (also known as mineral admixtures and supplementary cementing materials) can be broadly classified according to their reactivity as: those from which hydraulicity and cementitious properties can be expected (such as GGBS), and those which exhibit pozzolanic activity (such as PFA, CSF, volcanic ash)[169]. It is generally accepted that these properties are dependant on mineralogical composition and particle characteristics (**Table 2.4**).

This section reviews the **material characteristics** of portland cements and the main CRMs used in HSC (viz. PFA, GGBS, and CSF). Their effects on the **superplasticizer dosage requirement** (or water demand), **loss of workability** and/or slump loss are in each case discussed. The section also includes a review of published work on ternary blends of cement and CSF with PFA or GGBS. The effects of metakaolin which has recently gained some acceptance[260-262] as a viable cement replacement material which enhances the early strength and durability of HSC were considered to be beyond the scope of this research. Metakaolin is manufactured by calcining Kaolin, and is a highly reactive pozzolan that increases the water demand and reduces the workability of concrete[262].

Table 2.4 : Typical chemical and physical properties of Ordinary portland cement (OPC) and CRMs[263].

Oxide	OPC	PFA		GGBS	CSF
		Class F	Class C		
SiO_2	20	48	40	36	97
Al_2O_3	5	27	18	9	2
Fe_2O_3	4	9	8	1	0.1
MgO	1	2	4	11	0.1
CaO	64	3	20	40	
Na_2O	0.2	1	-	-	
K_2O	0.5	4	-	-	
Oxide compositions (% by weight)					
Specific gravity	3.15	2.4		2.9	2.2
Particle size range (microns)	0.5-100	10 - 150		3-100	0.01-0.5
Specific surface area (m^2/kg)	350	350		400	20,000

2.6.1 Portland cement

Portland cements are produced by burning chalk (or limestone) with clay (or shale) in a rotary kiln at 1500 ^{0}C to form a clinker rich in calcium and aluminium silicates. The clinker is ground to a fine powder with a small proportion of gypsum (calcium sulphate dihydrate, $CaSO_4.2H_2O$), or a mixture of gypsum and natural anhydrite ($CaSO_4$), to control the hydration of the aluminate phases and regulate the setting of the cement. When the temperature during the grinding process is excessively high, the gypsum is reduced to other forms of calcium sulfates, notably to: hemihydrate ($CaSO4.½H_2O$) at 128 ^{0}C and/or to soluble anhydrite ($CaSO_4$) at 163 ^{0}C. The solubility of these compounds is approximately three times higher than gypsum, and an uncontrolled variation in their proportions can therefore affect the chemical reactivity of the cement and hence its workability.

ASTM C 150-94[(170)] divides portland cements into five main types: Type I (ordinary), Type II (modified), Type III (rapid hardening), Type IV (low heat), and Type V (sulphate resisting). The ranges in compound composition for each cement type are shown in **Table 2.5**. Although most portland cements comprise the same active compounds, their proportions are different. They typically have specific gravities between 3.12 and 3.16, and their particle size (or fineness) can range between 0.5 and 100 microns.

Although the current European standard (BS EN 197-1:2000)[(170)] also divides cements into five main types, it uses complicated terminology and as many as 25 sub-types. All the portland cements are grouped into one type (CEM I, with up to 5% minor constituents). The other four main types (CEM II-V) refer to blended cements containing 6-95% active/inert materials such as microsilica, PFA, GGBS, or limestone. Although BS EN 197-1:2000 accounts for the strength performance of each cement type (viz. 32.5, 42.5 N (or R), 52.5N and 62.5N), it does not classify some commercially available cements such as sulfate resisting portland cement (SRPC).

As mentioned in section 2.5.5, an ideal cement for HPC is considered to be one which is not too fine, has a low C_3A content, and whose reactivity is easily controlled by the sulfate in the cement. Most research studies have however been confined to assessing the effects of a limited number of cements of varying C_3A and SO_3 contents, cement fineness and/or content, at high w/c ratios. With regards to:

- the **C_3A** (tricalcium aluminate) content, it is widely accepted that cements containing large quantities of C_3A exhibit more rapid slump loss[16, 127, 171]. However, Mailvaganam[128] found that concretes made with type V cements (with 2.6% C_3A) and 0.53 w/c ratio have only slightly lower rates of slump loss than those made with type I cements (with C_3A contents varying from 6.9 to 12.6%).

- the **SO_3** (sulfate) content, Khalil and Ward[172] showed that there is an optimum range of SO_3 content for which slump loss is minimised. In cement pastes (at 0.58 w/c) they observed that the optimum SO_3 content with a SNF superplasticizer is 3.15% at 25 ^{0}C, and 5.65% at 40 ^{0}C. In concrete, they found cements with these SO_3 contents exhibit approximately 20 mins longer slump retention.

- **cement fineness**, it is widely known that the more finely ground the cement the faster is its rate of reaction and slump loss[7, 15, 173]. According to Pilar and Manuel[103] finer cements require higher dosages of superplasticizer to cover the excess surface and properly separate the cement particles.

- **cement content**, there is broad agreement that mixes with higher cement contents lose workability at a faster rate, because the rate of temperature rise is greater and a larger proportion of water is used in the hydration process at a given time[128, 156-157]. The superplasticizer dosage requirement is generally believed to decrease with increasing cement content[8, 122, 156].

According to Dodson[122] the water demand decreases linearly with increasing C_3A, alkali and cement contents as shown in **figure 2.46 (a-c)**. As a general rule, he stated that for maximum performance of chemical admixtures (irrespective of their type) the percentage ratio of the C_3A to SO_3 must be less than 2.5, and preferably close to 2.0.

In a study with the MH system, Wallevik and Gjorv[50] compared the Bingham properties of ASTM Type I and Type III cements together with a modified portland cement containing 20% PFA, at three cement contents of 200, 300 and 400 kg/m^3. Their results (**Figure 2.47**) showed that higher cement contents mainly increase the yield stress, the Type III cement (which has a greater fineness) gives much lower plastic viscosities and larger yield stresses, whilst the blended cement (MP) produces comparatively lower yield values but higher plastic viscosities. (They however provided no information on loss of workability or details of the w/b ratio, type and dosage of superplasticizer used).

With the BML viscometer, Mork and Gjorv[174] more recently found that a reduction in the gypsum-hemihydrate ratio with a reactive cement (having a high C_3A and alkali content) increases the initial yield stress and its development with time, but hardly affects the plastic viscosity (**figure 2.48**). They also reported that in non-superplasticized concrete at 0.61 w/c, an increased fineness (from 300-400 m^2/kg) produces an increased yield stress, but lower plastic viscosity.

According to Aitcin[41] with some very reactive cements it is difficult to produce very low w/c ratio HPC which still has a 50 mm slump 30 minutes after mixing, even when the initial slump is 200 mm. In such cases, he recommends adding a small amount of water to recover the slump practically instantaneously, but states that the recovered slump is rapidly lost once the additional water has reacted. According to Meyer and Perenchio[116] as long as there is sulfate available to react with the C_3A and form ettringite, the rate of reaction is low, but when the sulfate is depleted, C_3A hydration accelerates and leads to faster losses of workability.

Indeed, when selecting materials for HPC, cements are more often eliminated because of their rheological behaviour than because of their ability to achieve the required compressive strength[11]. As mentioned in section 2.3, Dejellouli et al[39] suggested that replacing in some cases up 20% of the cement by a less reactive cementitious material like PFA, or up to 50% by GGBS, can solve the slump loss problem observed with some very reactive cements at low w/b ratios.

Table 2.5 : Typical compound compositions of different types of portland cements[170].

Cement	Value	Compound composition, per cent							
		C_3S	C_2S	C_3A	C_4AF	$CaSO_4$	Free CaO	MgO	Ignition Loss
Type I	Max.	67	31	14	12	3.4	1.5	3.8	2.3
	Min.	42	8	5	6	2.6	0.0	0.7	0.6
	Mean	49	25	12	8	2.9	0.8	2.4	1.2
Type II	Max.	55	39	8	16	3.4	1.8	4.4	2.0
	Min.	37	19	4	6	2.1	0.1	1.5	0.5
	Mean	46	29	6	12	2.8	0.6	3.0	1.0
Type III	Max.	70	38	17	10	4.6	4.2	4.8	2.7
	Min.	34	0	7	6	2.2	0.1	1.0	1.1
	Mean	56	15	12	8	3.9	1.3	2.6	1.9
Type IV	Max.	44	57	7	18	3.5	0.9	4.1	1.9
	Min.	21	34	3	6	2.6	0.0	1.0	0.6
	Mean	30	46	5	13	2.9	0.3	2.7	1.0
Type V	Max.	54	49	5	15	3.9	0.6	2.3	1.2
	Min.	35	24	1	6	2.4	0.1	0.7	0.8
	Mean	43	36	4	12	2.7	0.4	1.6	1.0

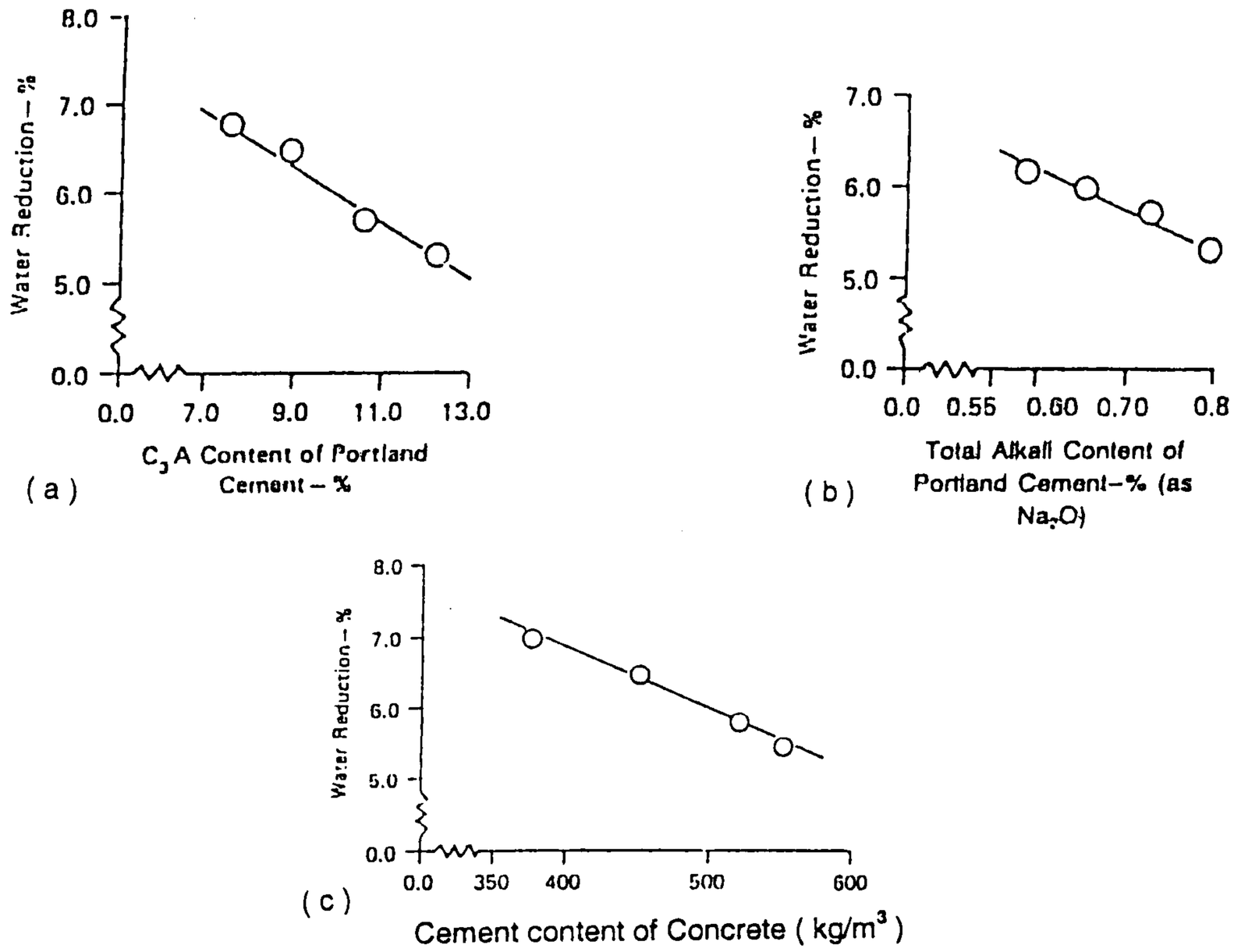

Figure 2.46 : Effects of (a) C_3A, (b) alkali, and (c) cement contents on water reduction[122].

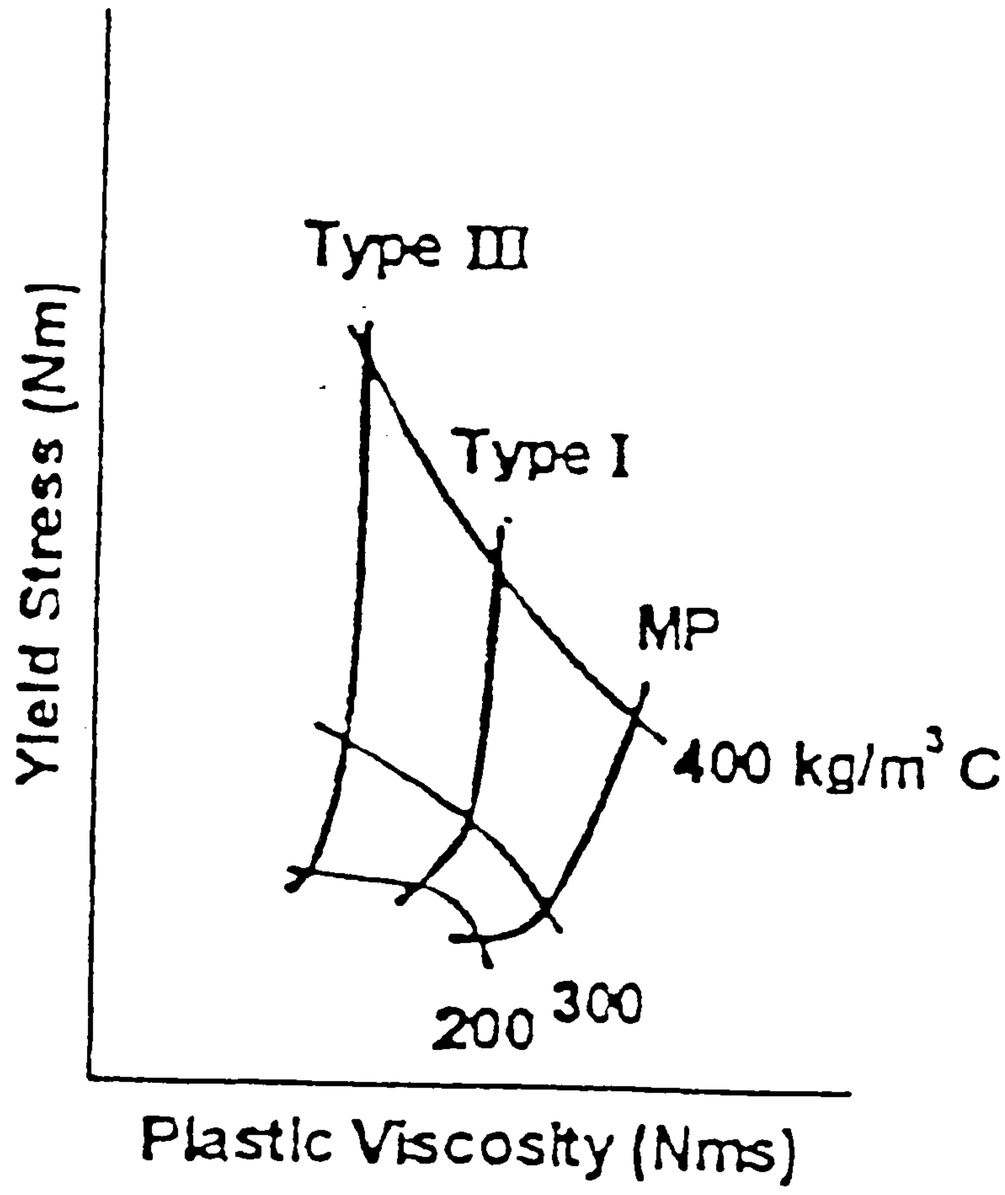

Figure 2.47 : Effects of different contents of ASTM types I and III cements, and a modified portland cement (MP) on the Bingham properties of concrete[50].

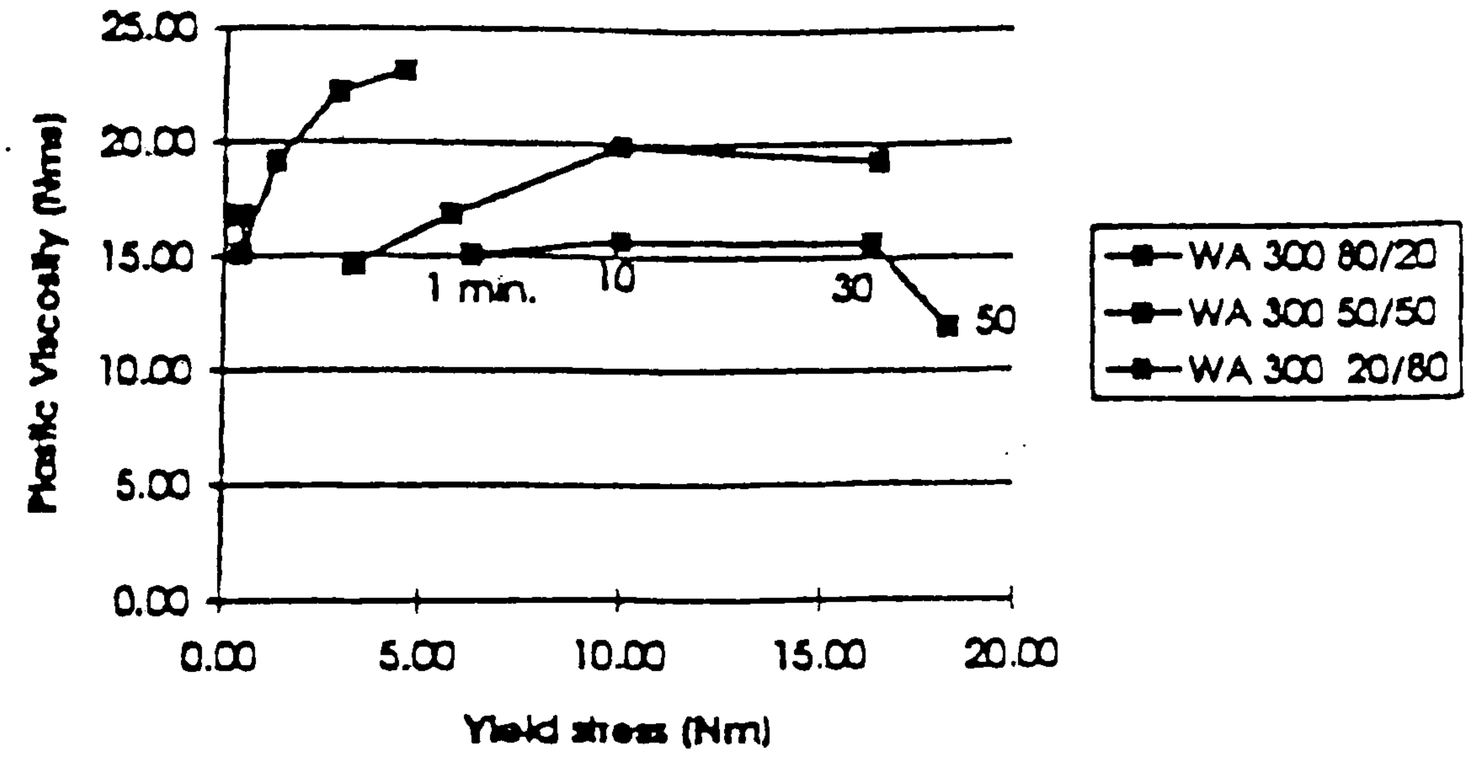

Figure 2.48 : Effect of three gypsum-hemihydrate ratios on the variation in yield stress and plastic viscosity of a reactive cement (with 10% C_3A and 0.13% alkali content)[174].

2.6.2 Pulverised Fuel Ash (PFA)

PFA is a by-product of the combustion of pulverised coal in thermal power plants. It is extracted by the dust collection system as a fine particulate residue from the combustion gases before they are discharged into the atmosphere.

PFA is broadly classified into two classes as shown in Table 2.4. Class F PFA usually contains less than 5% calcium oxide, and exhibits pozzolanic properties only (i.e. no cementitious value). Class C PFA can have a lime content in excess of 10 %, has cementitious properties (i.e. a capacity for self hardening in the absence of cement), and tends to be finer than low calcium PFA[169]. Most of the PFA that is used by the concrete industry is class F. Class C is mainly produced in the U.S.A. and Canada. BS EN 179-2000[170] sub-divides blends of low and high lime PFA into four sub-types, containing either 65-79% or 80-94% Portland cement.

The PFA particles mainly exist in the form of hollow glassy spheres, ranging from less than 10 to more than 150 μm in diameter, with the majority being less than 45 μm. Their particle size distribution is determined by the type of dust collection equipment used, whilst their chemical composition is determined by the types and relative amounts of incombustible materials in the coal. More than 85% of PFAs comprise chemical compounds and glasses composed of the elements silicon, aluminium, iron, calcium, and magnesium (c.f. Table 2.4). The specific gravity of PFA varies in the range 2.1-2.6.

Nagataki[175] found that the beneficial effects of PFA in reducing the water demand are directly related to the percentage of spherical particles. Only when these exceed 70-80% does a partial cement replacement by PFA produce a reduced water demand (**figure 2.49**). However according to Owens[176], the main factor influencing the water demand and workability properties of PFA concretes is the proportion of coarse material (> 45 μm). He found that a 50% replacement of the cement by mass with fine particulate PFA reduces the water demand by 25%, whilst an equivalent substitution using PFA with 50% of the material greater than 45 μm had no effect on water demand.

In HSC, Soutsos[53] found that increasing cement replacement by PFA reduces the superplasticizer dosage requirement needed to obtain a target slump of 150 mm compared to the equivalent portland cement mix (**figure 2.50**). Accompanying improvements in workability due to increasing levels of cement replacements by PFA have also been widely documented by several researchers[99, 177-179]. Bayasi[177] showed that increasing cement replacements by 20-80% PFA produce essentially linear increases in workability as measured by the slump test. Besari et al[178] attributed the improvements in slump to the combined effects of an increased paste volume resulting from the lower specific gravity of PFA compared to that of portland cement, and to a lubricating (or ball bearing) effect due to the spherical shape of PFA particles.

Hansen[180] stated that the observed reductions in water demand and workability improvements result from the fly ash acting as a water-reducing agent, much like an air-entraining agent or plasticizer. In contrast Helmuth[181] stated that very small PFA particles become adsorbed on the surface of electrically charged cement grains, causing dispersion of the system in a manner similar to conventional water-reducing chemical admixtures.

The effects of partial cement replacements by PFA on the initial workability (or Bingham) properties of concrete, mortar, and cement pastes have been investigated by numerous researchers[50, 53, 154, 182-183]. The results mainly differ with regards to the effects of PFA on the plastic viscosity.

In a study with the LM system, Ellis[182] showed that increasing cement replacement by PFA (on mass and volume basis) reduces both the yield (g) value and plastic viscosity (h) (**figure 2.51**). From a study on cement pastes at 0.35 w/b ratio, Banfill[183] however found the yield value is reduced whilst the plastic viscosity remains unchanged with replacement levels of 10-60% PFA.

With the MH system, Soutsos[53] found that partial cement replacements by 20, 30 and 40% PFA reduce the yield value, but noticeably increase the plastic viscosity at

a w/b ratio of 0.26 (**figure 2.52**). His results, which are in agreement with those reported by Wallevik and Gjorv[50] with the 20% PFA mix (c.f. figure 2.47, (MP)), are however at variance with the widely accepted view that PFA increases workability[99, 177-179] (i.e. reduces both the g and h values). Several other researchers[85, 184] have also concluded that PFA increases the initial plastic viscosity, but they have provided no explanations for this.

In terms of slump loss, Ryan and Munn[185] found that partial cement replacements by PFA have insignificant effects on the rate of slump loss in NSC mixes having initial slumps of 180-200 mm. Their results indicated that the rate of slump loss is noticeably reduced (by about 70 mm after three hours) only when a complete replacement of the cement is made by PFA.

In contrast, Ravina[186] found that after prolonged mixing of 180 minutes, the slump of concretes containing up to 40% PFA was greater by 40-80 mm compared to the control portland cement concretes. He suggested that PFA agglomerates may break down during prolonged mixing, and release very fine particles into the mix. According to him these may be absorbed on the cement particle surfaces, create repulsive forces between them and prevent the build up of a skeleton structure which would otherwise increase the rate of slump loss and stiffen the mix.

More recently Baoju et al[99] found that the use of ultra-fine PFA (with a Blain surface area of 740 m^2/kg) significantly reduces the rate of slump loss after 3 hours by about 36% and 12-19% at the 50 and 35% cement replacements levels and 0.28 w/b ratio. They attributed the lower slump loss to an extended setting time, and the high specific surface area of the PFA particles which they suggested allows better interaction with the superplasticizer.

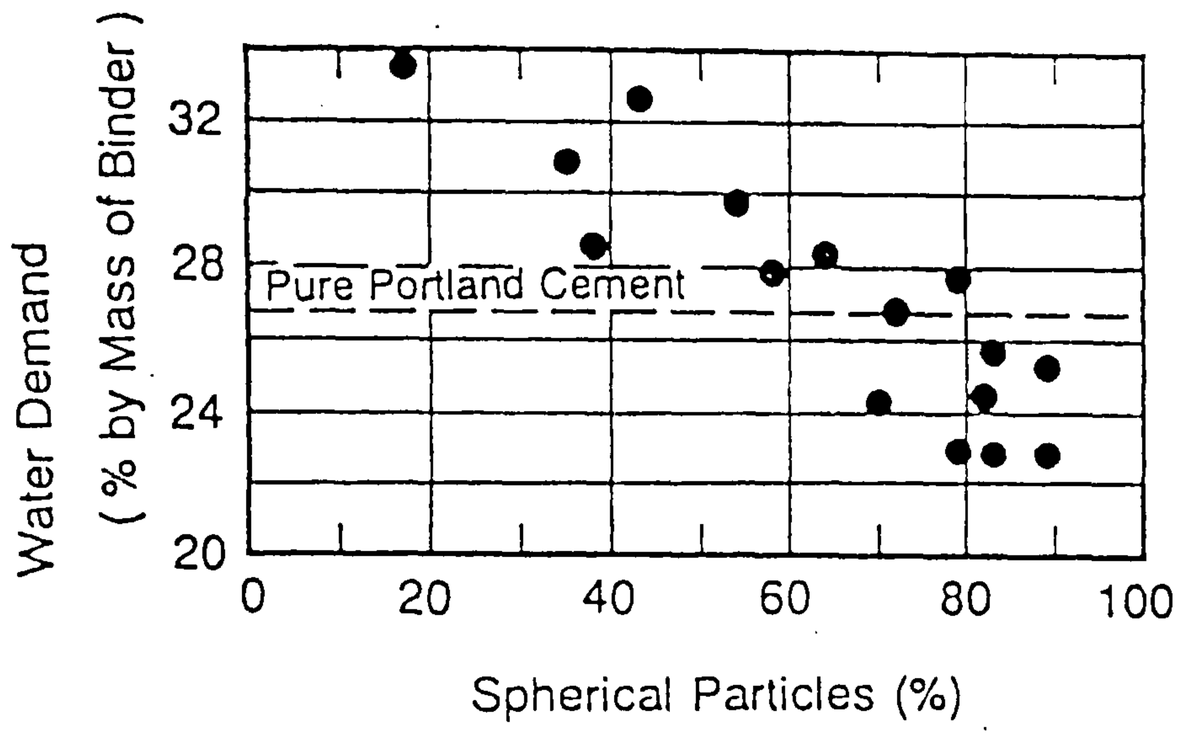

Figure 2.49 : Influence of spherical particles of PFA on the water demand (30% PFA paste)[175].

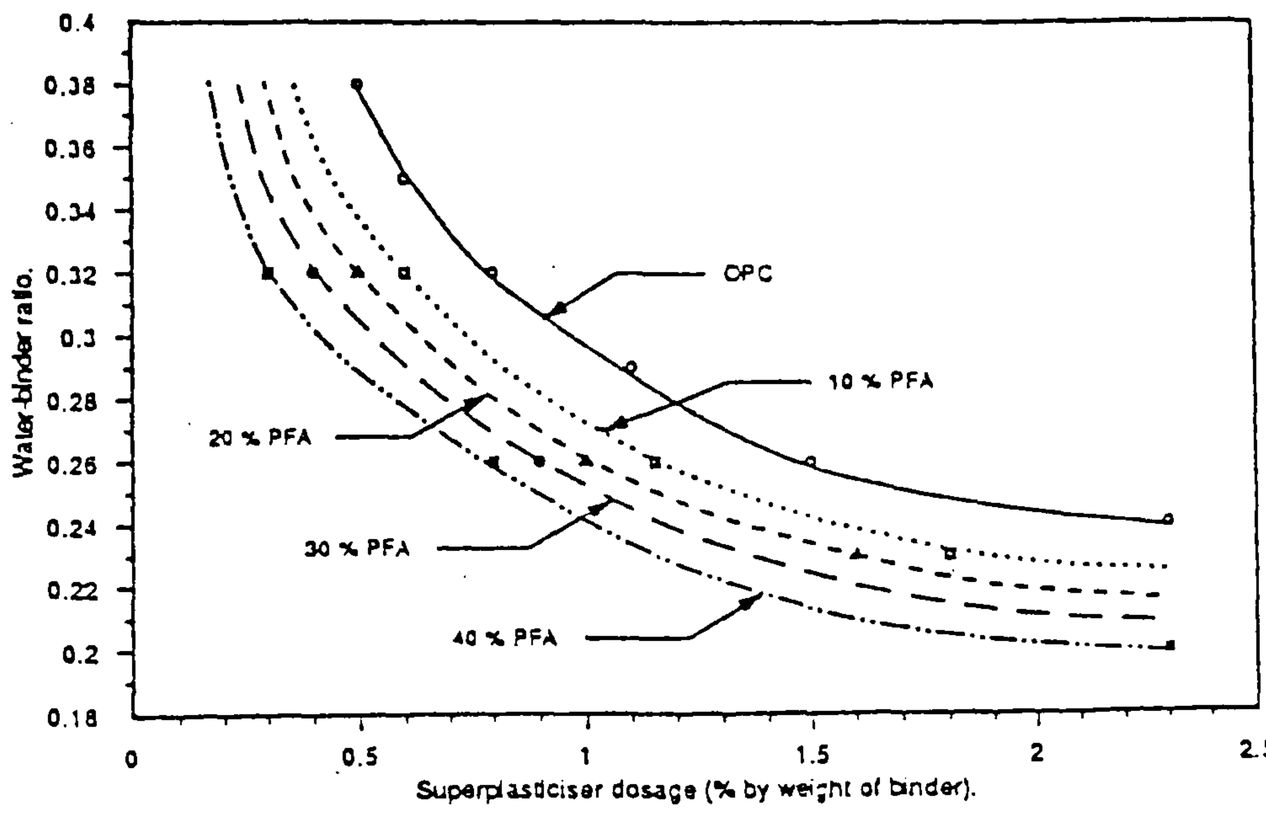

Figure 2.50 : Effect of partial cement replacement by PFA on the superplasticizer dosage required for HSC mixes with a slump of 150 mm[53].

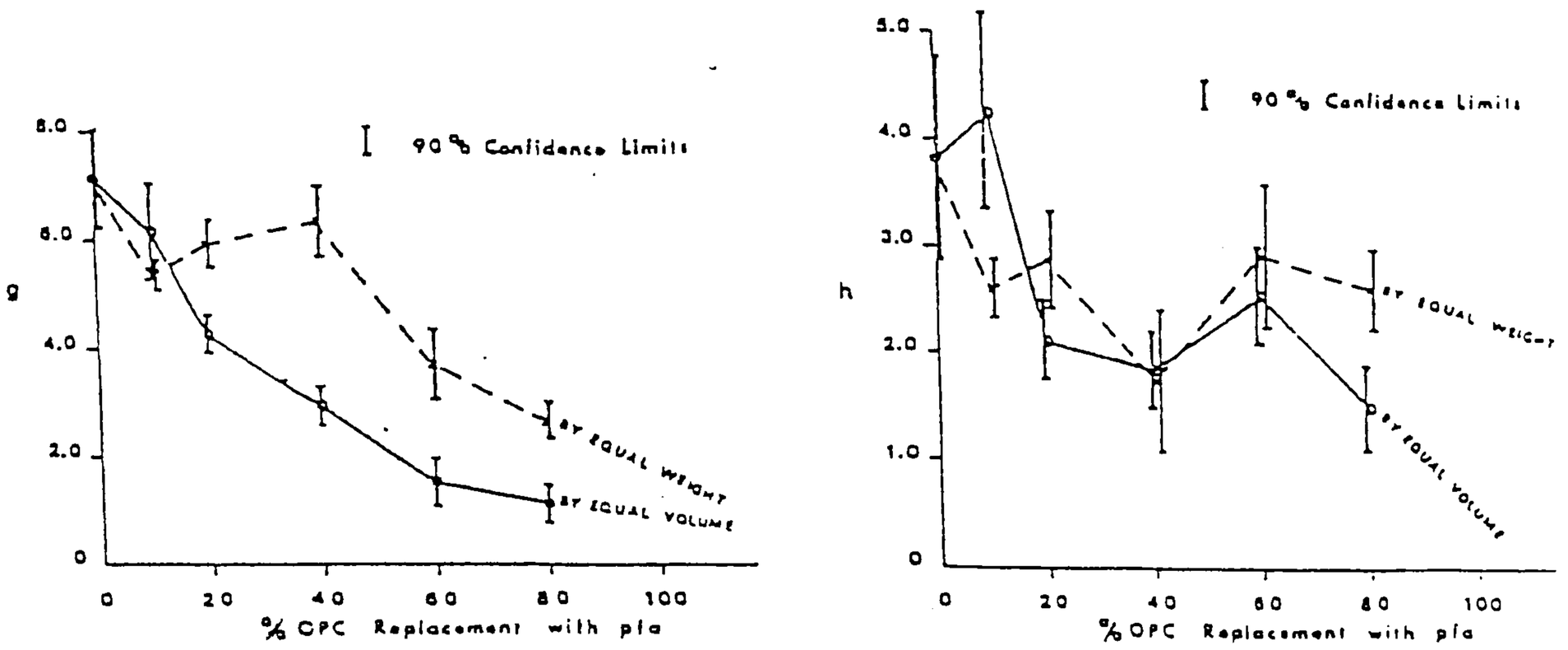

Figure 2.51 : Relationships between yield value and plastic viscosity with percentage cement replacement by PFA at 0.45 w/b ratio[182].

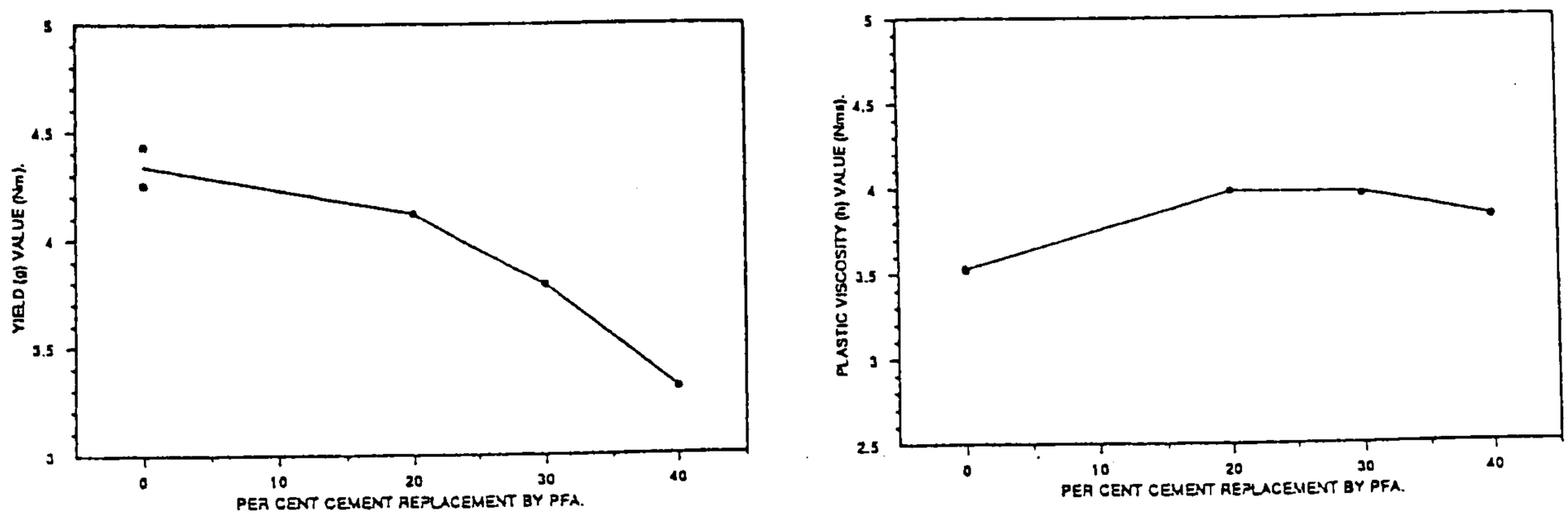

(a) Yield (g) value.

(b) Plastic viscosity (h) value.

Figure 2.52 : Effect of level of cement replacement by PFA on the yield value and plastic viscosity of HSC at a w/b ratio of 0.26 and 150 mm slump[53].

2.6.3 Ground Granulated Blast-furnace Slag (GGBS)

GGBS is a by-product of the manufacture of pig iron in a blast furnace. It is tapped from the liquid slag floating on the molten iron that collects at the bottom of the furnace at 1350-1500 ^{0}C. The slag primarily consists of silica and alumina (originating from the iron ores), calcium and magnesium oxides (from the fluxing stone), combined with impurities from the coke charged into the furnace.

The cementitious characteristics of the slag are mainly dependent on its rate of cooling and on its glass content. Slow cooling of the slag leaving the furnace gives a product that is predominately crystalline and possesses minimal cementitious value. Rapid quenching or chilling by spraying with high-pressure water jets minimises crystallization and converts the molten slag into a sandy material, which is predominately glassy. When the material is dried and finely ground it is called GGBS. The major constituents are SiO_2 (30-40%), Al_2O_3 (9-15%), CaO (40-43%), and MgO (5-15%) which typically comprise more than 95% of the total oxides (Table 2.4).

Compared to PFA and CSF, the GGBS particles are more angular, and their particle size resembles that of coarse cement particles. The fineness of GGBS is typically 300-400 m^2/kg (Blaine), and its specific gravity is approximately 2.9, which is slightly lower than that of cement but higher than that of PFA and CSF.

The effects of partial cement replacements by GGBS on the water demand and/or superplasticizer dosage requirement for a given slump have been investigated by several researchers[53, 187-189]. In non-superplasticized concrete, Meusel and Rose[188] reported that when the GGBS content is increased there is an accompanying increase in slump.

In plasticized concretes having 0.43-0.46 w/b ratios, Nishibayashi et al[187] found that the water demand needed to obtain a given slump decreases with increasing GGBS content, and is typically reduced by 11 kg/m^3 at the 85% replacement level. They concluded that GGBS in concrete appears to act as a superplasticizing agent.

Similar results were reported by Swamy et al[189], who observed that a 70% replacement of the cement by GGBS reduces the superplasticizer dosage by about 10-12% compared to concrete without GGBS at 0.45-0.35 w/b ratios. In HSC, Soutsos[53] found that the higher the cement replacement by GGBS, and the lower the w/b ratio, the larger is the reduction in the superplasticizer dosage needed to obtain a target slump of 150 mm (**figure 2.53**).

Read et al[190] stated that the rheology of fresh concrete is very favourably affected by the inclusion of GGBS in the binder, but provided no supporting experimental data. Tachibana et al[18] similarly stated that the use of GGBS in HSC can lead to significant improvements in workability. However, from measurements with the MH system, Soutsos[53] reported that the effects of GGBS on the workability properties of HSC (at 0.26 w/b ratio) are inconclusive as to whether the Bingham parameters are increased or reduced (**figure 2.54**). He suggested that the results may depend on small variations in slump, and concluded that GGBS content has only a small effect on the workability properties of HSC.

In another study, Wimpenny et al[191] investigated the effects of two sources of GGBS, three cementitious contents, at three GGBS levels (40, 70 and 100%) and a fixed water content of 165 l/m^3. From their results (**figure 2.55**) they merely concluded that the GGBS level, type (or source), and cementitious content all have significant effects on the workability of fresh concrete. As can be seen their results however reveal no systematic effects of, for example, GGBS content on the Bingham parameters.

More recently, Domone et al[85] reported that the incorporation of GGBS at 0.40 w/b ratio gives lower slumps, and higher plastic viscosities (as measured by the MH system). However, like Soutsos[53] and Wimpenny et al[191], they have not presented any time-dependent measurements for the effects of GGBS on loss of workability.

In terms of slump loss, Dejellouli et al[39] stated that replacing a certain fraction of the cement by GGBS, which is less reactive and reduces the amount of

ettringite formed during early hydration, provides better control of the slump loss problem in HSC. In contrast, Tazawa et al[134] reported that the slump losses are only marginally reduced by using 50% GGBS at w/b ratios of 0.50 and 0.30. Nishibayashi et al[187] similarly found the slump losses in GGBS mixes tend to be high (decreasing from about 120 mm to 75 mm in 60 minutes), and are not significantly different from those of the control mix without GGBS.

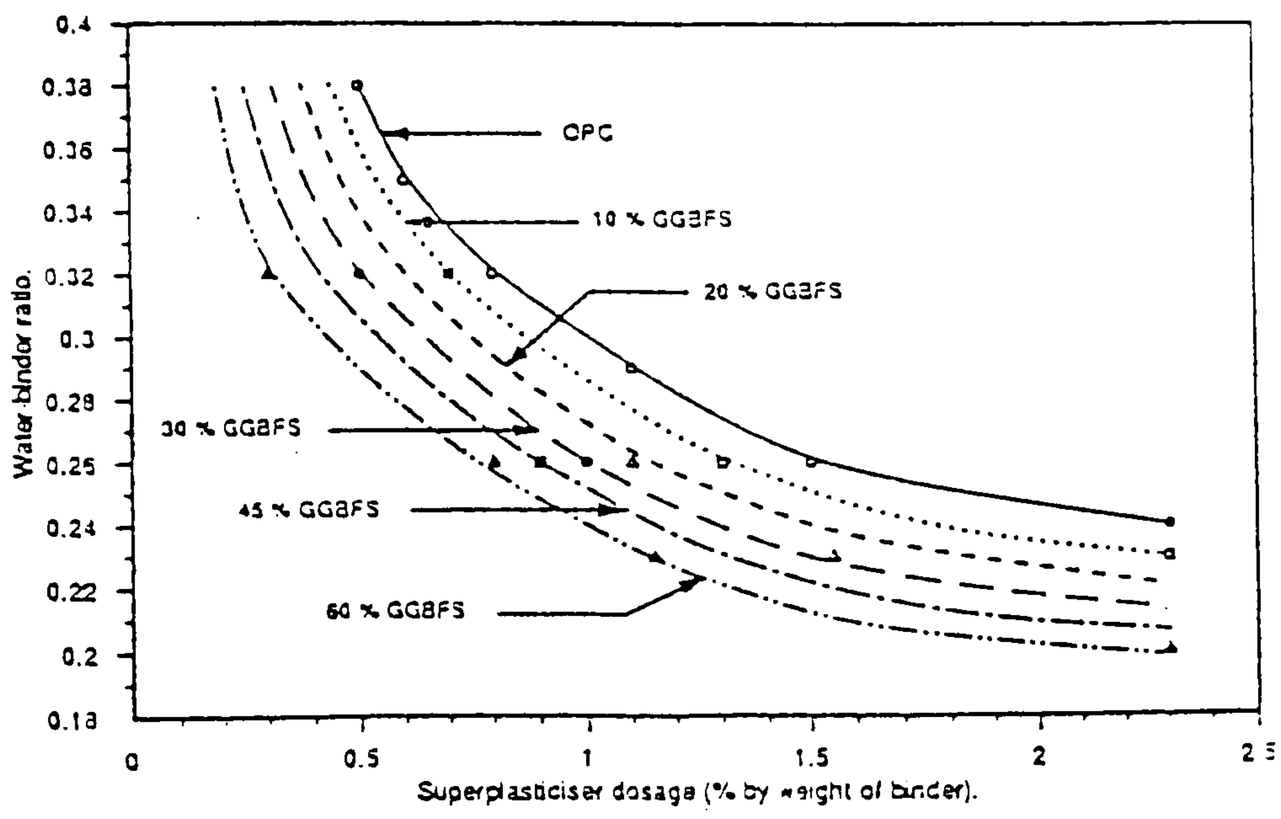

Figure 2.53 : Effect of partial cement replacement by GGBS on the superplasticizer dosage required for HSC mixes with 150 mm slump[53].

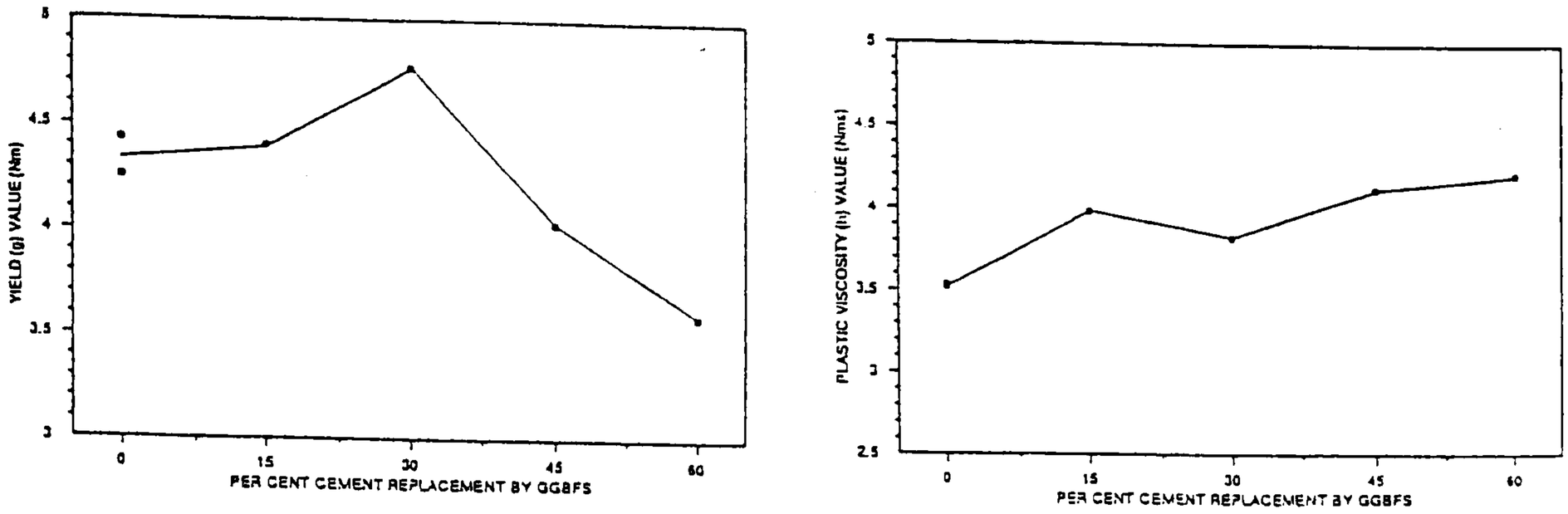

(a) Yield (g) value.

(b) Plastic viscosity (h) value.

Figure 2.54 : Effect of level of cement replacement by GGBS (a) yield value and (b) plastic viscosity of HSC at 0.26 w/b ratio and 150 mm slump[53].

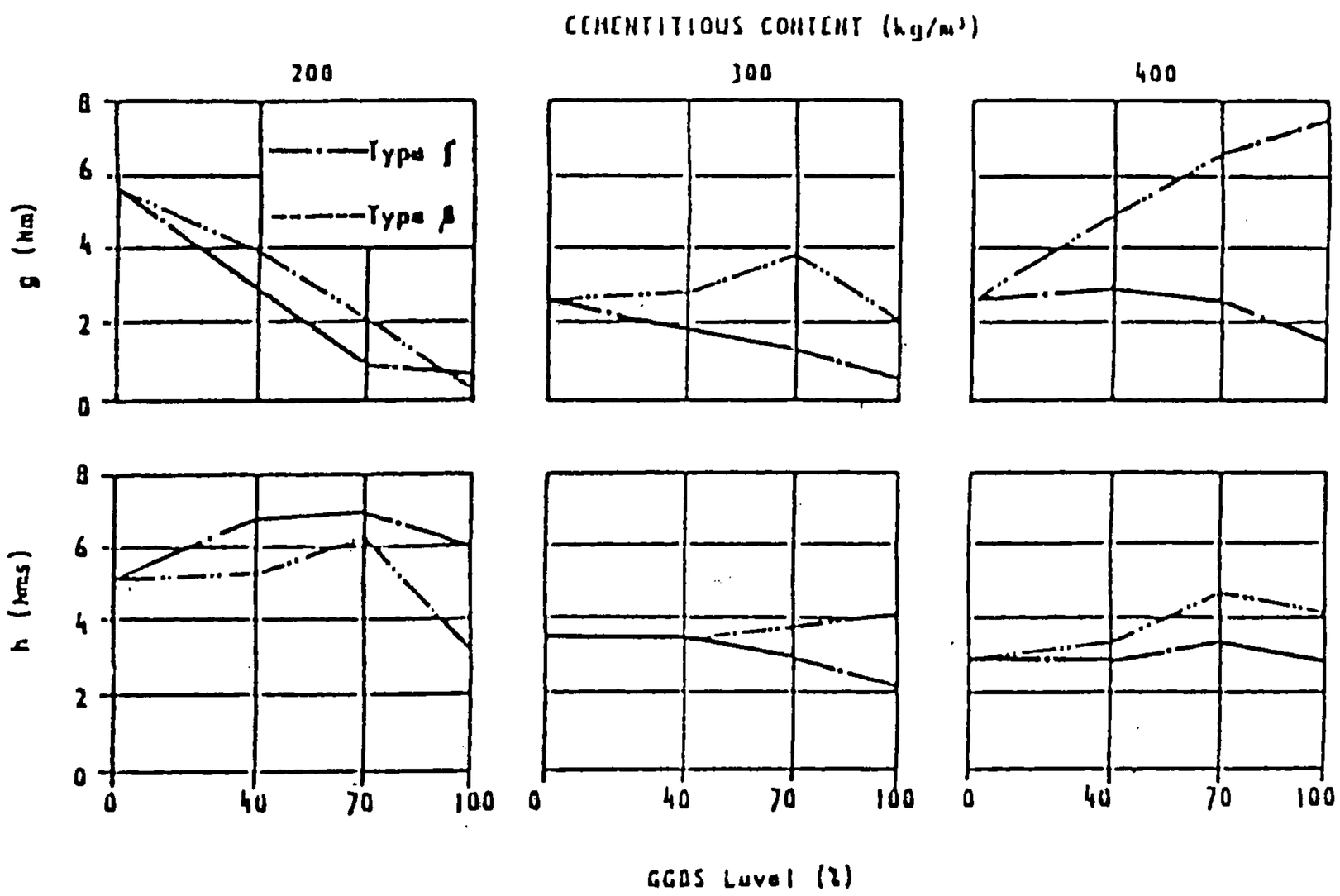

Figure 2.55 : Effect of GGBS content and type on the Bingham parameters at different cementitious contents and slumps of 70-80 mm (LM system, GGBS types "S" and "P" respectively have finenesses of 406 and 452 m^2/kg, and particle sizes of 13 and 90 microns and similar chemical compositions)[191].

2.6.4 Condensed Silica Fume (CSF)

CSF is a by-product of the production of silicon metal or ferro-silicon alloys by reducing high-purity quartz in electric arc furnaces. It is collected from the escaping gases and consists of extremely fine spherical glassy particles containing more than 90% silicon dioxide (SiO_2). The SiO_2 content of CSF generally varies between 85 to 98%, depending on the type of alloy produced.

Most of the CSF particles are smaller than one micrometer (1 μm) and have an average diameter of about 0.1 μm, which is approximately 100 times smaller than that of portland cement (10 μm). CSF has a specific gravity of 2.2, compared to 3.1 for portland cement, and its specific surface area is approximately 20,000 m^2/kg which is 50-60 times larger than that of portland cement (330-400 m^2/kg).

When compared with other CRMs, the main characteristics which make CSF a highly reactive pozzolanic material are its high SiO_2 content and extreme fineness (Table 2.4). CSF is not available in as large amounts as PFA and GGBS, and is therefore more expensive. It has also been widely reported that the use of CSF in HSC reduces the workability as a result of increased water demand, and therefore requires more superplasticizer to compensate[14, 19, 148, 160, 192-196]. This has mainly been attributed to its very fine particle size and high specific surface[160, 195-196].

Chan et al[14] reported that the water (or superplasticizer dosage) demand increases significantly with increasing CSF content. Detwiler[19] reached a similar conclusion, and added that each pound of CSF used in the mix increases the water demand of HSC by an equivalent amount.

In one study, Yogendran et al[193] investigated the dosage response of CSF mixes at constant slump and w/b ratios of 0.34 and 0.28. Their results showed that at the 0.28 w/b ratio the dosage of superplasticizer needed to maintain the slump is comparable to that of the control mix; whilst at the 0.34 w/b ratio the dosage increases linearly above the 10% replacement level. Using the Marsh cone, de

Larrard[160, 195] found that the saturation dosage demand increases with increasing CSF content (**figure 2.56**). As can be seen, the saturation dosage is about 1.3, 2.0 and 2.5% s/w/b at the 0, 10 and 20% CSF replacement levels. Similar Marsh cone test results have been reported by Agullo et al[148] with cement pastes incorporating 5-15% CSF at 0.33 w/b ratio.

In contradiction to these findings, several researchers[18, 30, 39, 197-198] have reported an increased workability and reduced water demand (or superplasticizer dosage) in CSF mixes. Dejellouli et al[39] found that the superplasticizer dosage of HSC is reduced by 18% compared with a control portland cement mix at 0.27 w/b ratio. They suggested that the reduced superplasticizer dosage is due to a reduction in the quantity of C_3A, thereby reducing the formation of ettringite. Austin and Robins[197] provided an alternative explanation, suggesting that the small particle size and spherical shape of the CSF particles produce more efficient filling of the void space between the much larger cement grains, which would otherwise trap free water and reduce the workability.

According to Soutsos[53] more superplasticizer is required as the CSF content increases, but above a certain dosage (depending on the w/b ratio and replacement level) CSF has a water reducing effect (**figure 2.57**). He attributed this behaviour to the ultrafine spherical CSF particles being sufficiently dispersed to act as a workability aid at high superplasticizer dosages.

Similar findings were reported by Tachibana et al[18] at w/b ratios of 0.31-0.22. They found that when the w/b ratio is below 0.25, concrete without CSF required more mixing time and 38-46% higher cumulative electric energy to mix it uniformly than concrete incorporating CSF. In contrast with the foregoing explanations, they suggested that in HSC, CSF acts as if it were water, dispersing between the cement particles, and produces high flowability. However, Yonezawa[30] attributed the workability improvements to both a ball bearing effect of the CSF particles, and to electrostatic repulsion by the superplasticizer or CSF.

With the MH system, Wallevik and Gjorv[50] reported that increasing cement replacements by CSF significantly reduce the plastic viscosity (by as much as 50%) down to certain threshold values at which the yield value is relatively unaffected (**figure 2.58**). The threshold values are approximately 2, 3 and 6% for cement contents of 200, 300 and 400 kg/m^3 respectively. At CSF contents above the threshold values, substantial increases in both yield stress and plastic viscosity occur. Similar results were reported by Beaupre et al[199] with a modified version of the LM system and 0.43 w/b ratio. They found that CSF at low contents produces modest reductions in both the Bingham parameters but intense increases at higher contents (between 7.5 and 15%).

Using the BML viscometer and w/b ratios of 0.44-0.29, Hu et al[40] however concluded the addition of 10% CSF increases the yield stress (τ_o) but reduces the plastic viscosity (μ). In contrast, Juvas[200] reported that addition of CSF in high-slump concrete has a reducing effect on plastic viscosity (μ) but the yield value (g) remains essentially unaltered.

In contradiction to these findings, Soutsos[53] observed that both the g and h values of HSC incorporating 5-15% CSF are lower than the control portland cement concrete (**figure 2.59**). Similar results were reported by Smeplass[201] with the MH system for HSC mixes at 0.36 w/b and constant slump of about 200 mm.

There is limited information in the literature on the effects of CSF on the rate of loss of workability[17, 202]. In a study with the BML viscometer, Osterberg[202] examined the effects of silica fume (in compacted, non-compacted and slurry forms) on the rate of slump and workability loss at 0.27 w/b ratio. He found that the slurry increases the initial slump and slump retention, but observed no clear trends with regards to the effect of CSF on the evolution of the Bingham parameters with time. He attributed these to formation of plug flow and a separation of the concrete at the inner cylinder of the BML viscometer.

In another study involving the slump test and BML viscometer, Punkki et al[17] found that the rate of slump loss increases with increasing silica fume content (**figure 2.60(a)**). Their results with the BML viscometer showed that an increasing CSF content reduces the initial plastic viscosity but slightly increases the initial yield value (**figure 2.60(b)**). With regards to loss of workability, they concluded that after of 60 minutes from mixing, the presence of silica fume reduces the change in plastic viscosity and distinctly increases the change in yield stress. In contradiction to Osterberg[202], their results show that the workability properties are relatively unaffected by whether the CSF is used in powder or slurry form.

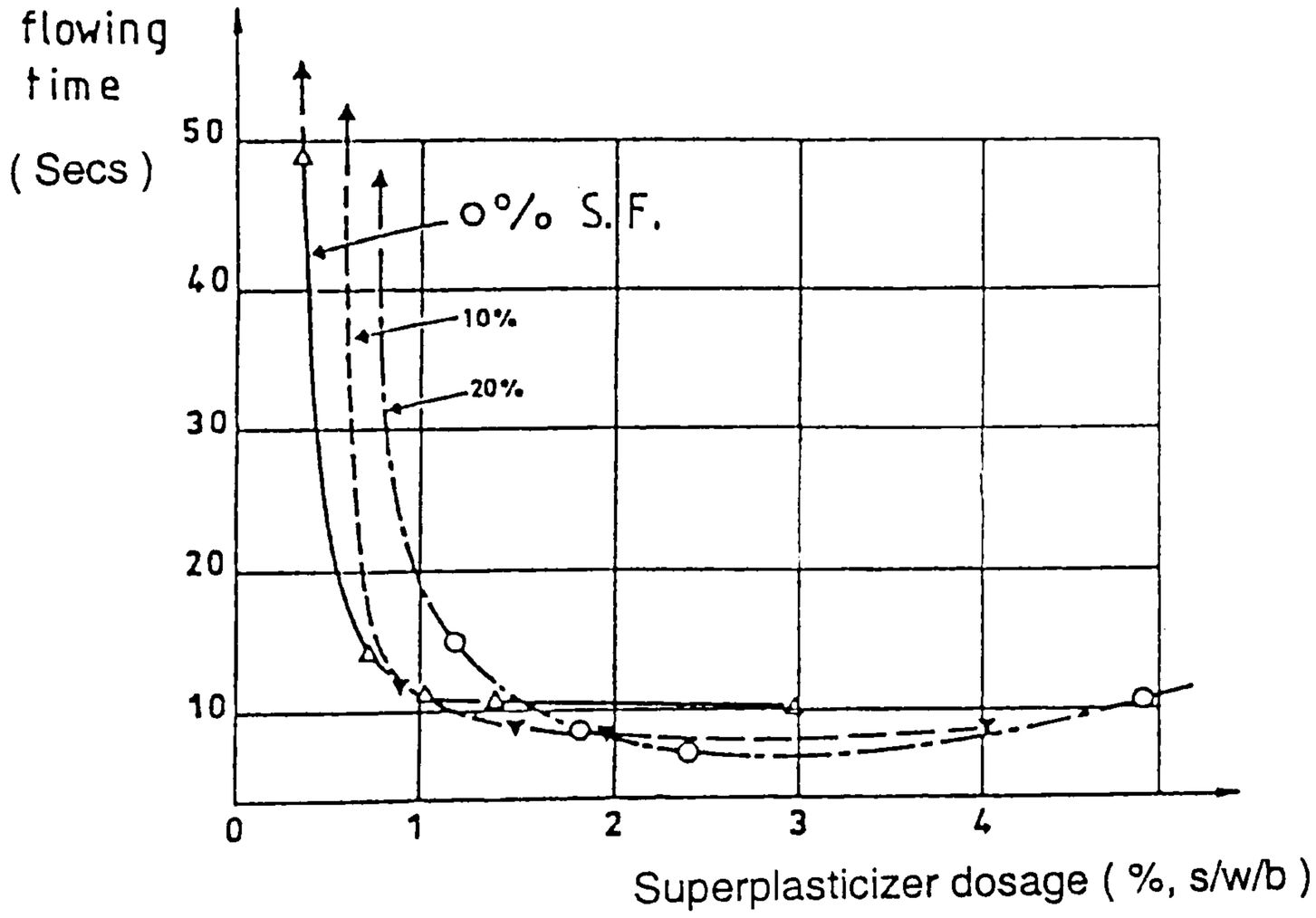

Figure 2.56 : Effects of increasing silica fume (i.e. CSF) content on the saturation dosage requirement as assessed by the marsh cone test in cement pastes (0.35 w/b)[195].

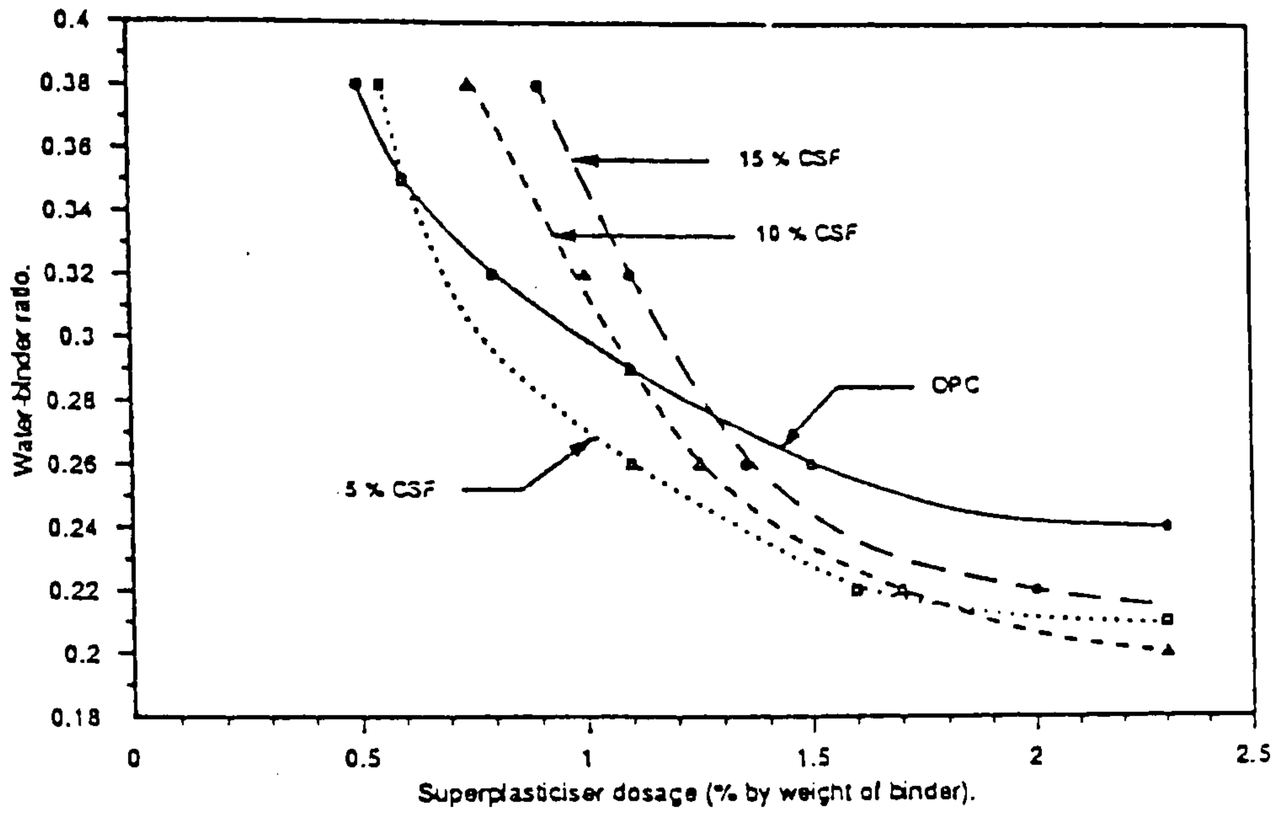

Figure 2.57 : Effect of partial cement replacement by CSF on the superplasticizer dosage required for HSC*s* at 150 mm slump[53].

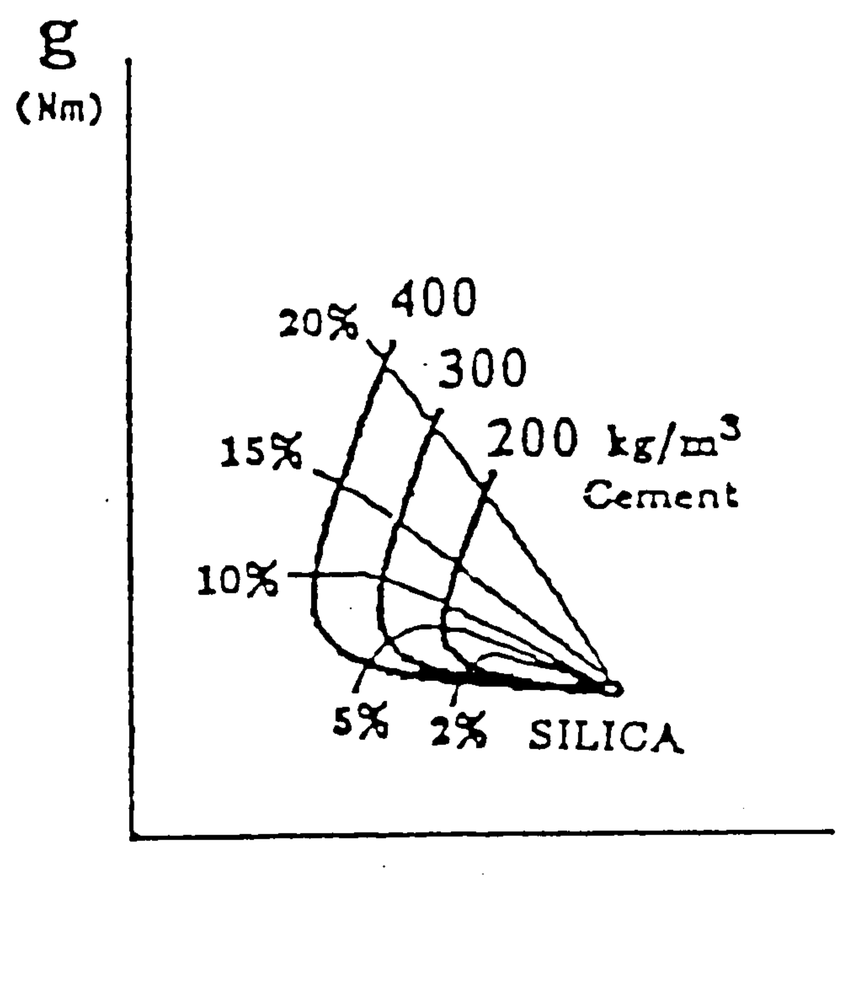

Figure 2.58 : Effect of partial cement replacement by CSF on the Bingham properties of fresh concrete at different cement contents (MH system, mix details not reported)[50].

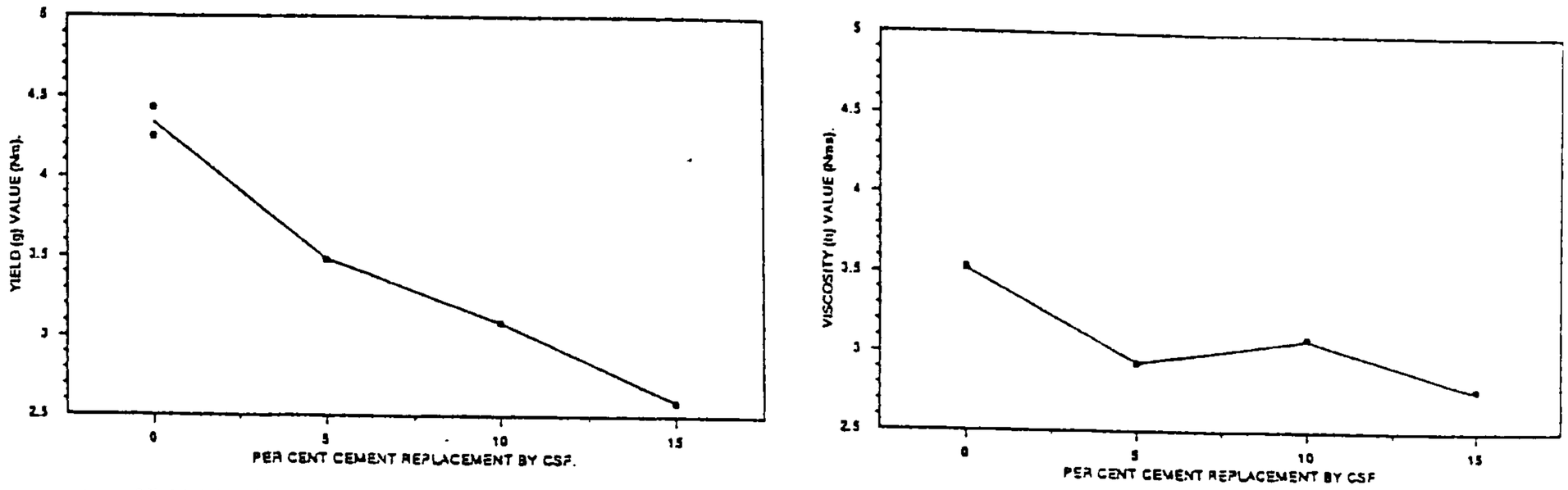

(a) Yield (g) value.

(b) Plastic viscosity (h) value.

Figure 2.59 : Effect of level of cement replacement by CSF on the g and h values of HSC at 0.26 w/b ratio and 150 mm slump (MH system)[53].

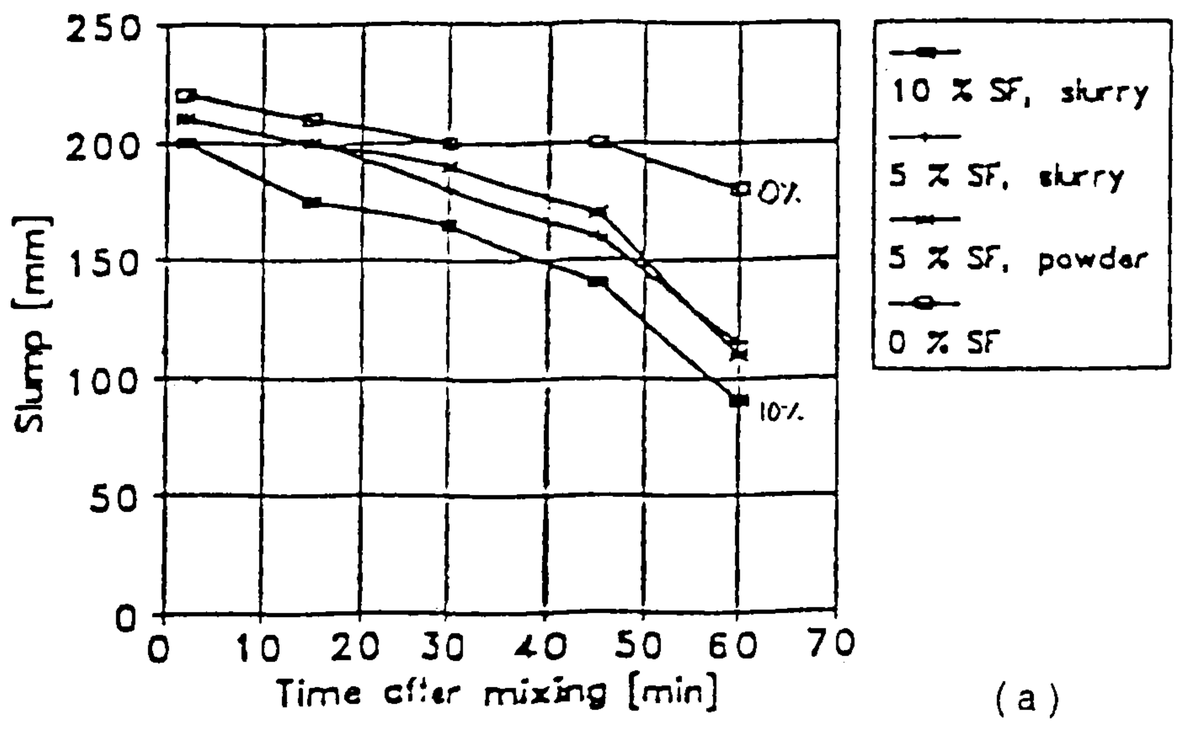

Figure 2.60 : Effect of CSF content on (a) slump loss and (b) variations in yield stress and plastic viscosity at 2, 30 and 60 minutes after mixing (BML viscometer, 0.37 w/b, and constant dosage of 2.5% s/w/b)[17].

2.6.5 Ternary blends

There is very little information in the literature on the effects of ternary blends of OPC and CSF with PFA or GGBS on the workability properties of HS and other HPCs.

Using ternary blended cements incorporating PFA and CSF, Bayasi[177] investigated the slump response of mixes comprising 20% PFA with 10-20% CSF at a w/b ratio of 0.41 and a constant superplasticizer dosage of 1.0 %. He concluded that the inclusion of PFA in the binder increases the slump and workability of CSF-concrete by approximately 25-100 mm. In mortar mixes at 0.31 w/b ratio, Sone et al[203] also found that mini-slump of a 50% PFA and 10% CSF mix was about five-times (or 80 mm) higher than a control portland cement mix at a constant superplasticizer dosage of 2.5% s/w/b.

With ternary blended cements incorporating GGBS, Read et al[190] stated that the use of GGBS in combination with CSF contributes to increased workability at low w/b ratios, and therefore in reducing the water content or superplasticizer dosage requirement. At 0.27 w/b ratio, Dejellouli et al[39] found that the amount of superplasticizer needed to produce a 200 mm slump was reduced by 36% in a ternary mixture of 30% GGBS + 10% CF compared to a reference OPC mix. As with their CSF binary mixes (section 2.6.4), they attributed the enhanced dosage performance to a reduction in the quantity of C_3A and to lower ettringite formation.

Soutsos[53] found that a ternary blended cement containing 50% GGBS + 10% CSF gives continual reductions in the quantity of superplasticizer required to produce a 150 mm slump compared to the reference OPC mix at w/b ratios lower than 0.36 (**figure 2.61**). He pointed out that at a w/b ratio of 0.20 the ternary GGBS/CSF mix requires a superplasticizer dosage of 1.3% compared to 2.3% with the 10% CSF or 60% GGBS binary mixes. His work with the MH system showed that both the Bingham parameters increase as the w/b ratio decreases (**figure 2.62**), but are significantly lower when compared to the reference OPC mix.

At any given w/b ratio the workability improvements with the ternary mixture are reflected by larger reductions in yield value than in plastic viscosity, but are essentially similar to those imparted by the CSF binary mix. The author is unaware of any other published work on the effects of ternary blends on the workability properties of HSC.

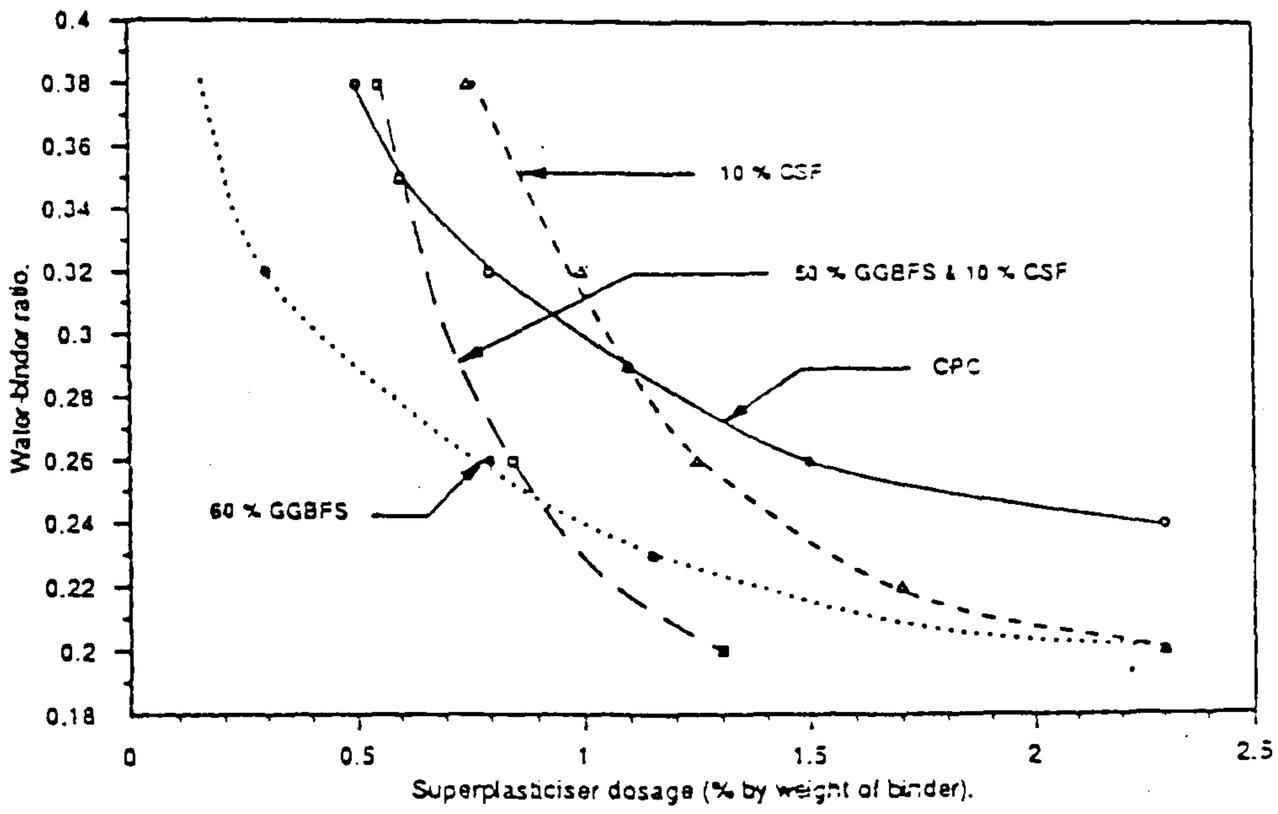

Figure 2.61 : Effect of partial cement replacement by a ternary blend of 50% GGBS and 10% CSF on the superplasticizer dosage required to produce HSC with a slump of 150 mm[53].

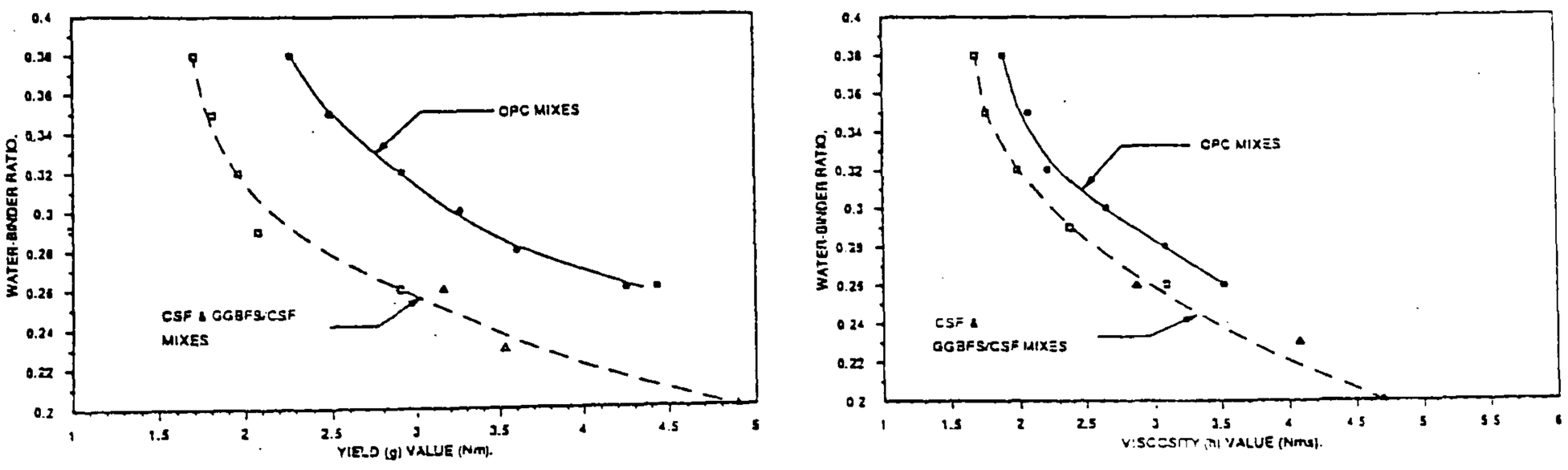

(a) Yield (g) value.

(b) Plastic viscosity (h) value.

Figure 2.62 : Effect of a 50% GGBS and 10% CSF ternary blend on the g and h values compared to portland cement reference mixes, and 10% CSF-concretes at different w/b ratios[53].

2.7 Mix stability and compactability of fresh concrete

Ritchie's[61] sub-division of the rheology of fresh concrete into: mobility, mix stability, and compactability (c.f. figure 2.1) has surprisingly received limited attention in the literature. The vast majority of the work on NS and HPCs has been confined to measuring the mobility (or workability) properties, presumably to minimise handling and placing difficulties, and/or because of the lack of rational tests to assess mix stability and compactability.

2.7.1 Mix stability (bleeding and segregation tendencies)

Although some bleeding is considered to be necessary for good finishing, a high quantity of bleed water can delay slab finishing, increase labour costs, and lead to blemishes and blistering of surfaces[204]. Almeida and Goncalves[205] stated that the use of superplasticizers, alone or together with CRMs, eliminates bleeding in HSC. When compared with NSCs, Mailvaganam[128] reported that superplasticized flowing concrete at low w/c ratios possesses good cohesion and slurry like consistency to self level without segregation; and can therefore be readily placed and compacted with minimal vibration.

According to Collepardi[34] the segregation resistance of superplasticized concrete is primarily caused by a coagulation effect of higher molecular weight polymers – from hundreds of thousands to millions – to bridge different cement particles. He states that this could explain why acrylic-based polymers have higher segregation resistance compared to SMF and SNF superplasticizers with lower molecular weights. Aitcin et al[58] stated that the segregation phenomenon in superplasticized concrete may be primarily related to exceptionally high dosages, beyond the saturation value (i.e. to overdosing).

Dodson[122] suggested that CRMs also improve the mix stability of fresh concrete (i.e. reduce bleeding and segregation) and at the same time increase workability. Mehta[169] attributed the enhanced mix stability to the finer particle size and

dense particle packing of CRMs between the larger portland cement and fine aggregate particles. However, Tachibana et al[18] states that segregation between coarse aggregate and mortar occurring when ultra-high slump is applied to HSC might become a serious issue. This can cause in delays by blocking pump lines, and lead to honeycombing of formed surfaces[204]. Several test methods proposed for quantifying the segregation resistance of fresh concrete are reviewed below.

In one study, Tachibana et al[18] compacted NS and HSC mixes in cylindrical moulds (ϕ150x300 mm) using a vibrating table (set at 50 Hz and 1.1 mm amplitude) for 10, 30, 60 and 120 seconds. From the differences in coarse aggregate contents in the upper and lower parts of the moulds (**figure 2.63**), they concluded that the segregation resistance of HSC mixes with slumps of 230 mm or more is comparable to that of NSC mixes with 85 mm slump. This was attributed to the lower w/b ratio, and a higher viscosity imparted by the inclusion of CSF.

In another study, Miura et al[206] reported that the flow-out time through a large funnel (**figure 2.64**) provides a useful measure of the segregation resistance of high slump HPCs, and is independent of flowability. The higher the flow rate, the lower the segregation resistance. They however reported that mixes with very low segregation resistance could cause partial blocking of the funnel and, give unstable concrete flow and large fluctuations in results.

With the LM system, Wimpenny and Ellis[83] suggested that the change in the shape of the pressure traces during two-point testing can be used as a possible guide to assess the proneness of mixes to segregation. Wallevik and Gjorv[84] similarly reported that the difference between the repeat torque at the end of the two-point test with that at the start can provide a measure of segregation resistance in the MH system.

Wimpenny et al[191] used the change in shearing resistance (or torque change, T_c) before and after two-point testing as a measure of segregation resistance, and subjectively assessed the bleeding tendencies (by awarding bleeding marks on a scale of 0 to 10). A further measure of mix stability was provided by the variation

in transit times of ultrasonic pulse velocity (UPV) taken through the hardened concrete. Both the bleeding mark and transit time range increased linearly with torque change (**figure 2.65**). They concluded that the change in impeller torque after two-point testing provides an objective measure of mix stability, but did not draw any correlation's with their measured Bingham parameters (c.f. figure 2.55), or directly quantify the segregation occurring in the two-point test bucket.

2.7.2 Compactability/Vibration of fresh concrete

The compaction of fresh concrete has been recognized for a long time as a pre-requisite to achieving optimum hardened properties, and has been subject to numerous investigations. Many of the early studies into the mechanisms, and general fluidizing effects of different vibration parameters (such as variable amplitude, frequency and acceleration) on fresh concretes have been reviewed by ACI Committee 309[(65)]. These studies have however not focused on the influence of vibration on the workability properties as expressed by the Bingham model.

As early as 1948, L'Hermite and Tournon[(207)] identified that the friction between the individual particles is the most important factor preventing consolidation (densification) of fresh concretes, and reported that it is practically eliminated when NSC is subjected to vibration. Kolek[(208)] divided the behaviour of fresh concrete during the vibration process into two main stages: the first comprising **rapid subsidence** or slumping of the uncompacted concrete, followed by a **de-aeration** stage – involving removal of entrapped air.

Glanville et al[(60)] reported that the total work done during placing and compaction is composed of that lost in shock; and the useful work expended in overcoming the internal friction of the concrete itself and the friction from the mould and reinforcement. Kirkham[(209)] postulated that the energy (W, in Joules) transmitted to the concrete during compaction is given by :

$$W = c_1 . m . s^2 . f . t$$

where c_1 is a constant (depending on the stiffness and damping of the concrete), m is the mass of the concrete (in kg), s is the vibration amplitude, f is the frequency (in Hz), and t is the vibration duration (in secs).

Although the compactability (or vibration response) of fresh concretes has been subject to several more recent investigations[49, 89-92, 210-216], none of these have sufficiently characterized how the Bingham parameters vary during vibration, and how they can ultimately be used in optimizing the hardened properties.

In one study, Tattersall and Baker[210] mounted the test-bucket of the MH system on an electromagnetic vibrating table and compared the vibration response flow-curves of NSC mixes to those without vibration. It was found that the application of vibration alters the speed-torque flow curve, and that the yield value is essentially eliminated (**figure 2.66**). They concluded that the flow curve approximates to a power law model passing through the origin, and that fresh concrete behaves as a Newtonian fluid (i.e. having zero yield value) under vibration.

In another study, Kakuta and Kojima[212] used a modified version of Tattersall's LM system with a table-vibrator attached to the test-bucket, to investigate the effects of vibration on four NSC mixes with and without chemical admixtures at 0.50 w/b ratio. They also found that the flow curves of mixes without vibration are of the Bingham type, whereas during vibration they tend towards Newtonian behaviour (**figure 2.67**). It is however worth noting that although the yield value appears to reduce to zero, the non-linearity of the flow curve makes it difficult to determine the magnitude of the plastic viscosity during vibration.

The increases in slope of the flow curve, like those obtained by Tattersall and Baker[210] (figure 2.66), nonetheless indicate progressive increases in plastic viscosity during vibration, which they did not comment on. They have however stated that inhomogeneity of the concrete under vibration induces convection

currents (or re-circulation of flow), and that some interference occurs from the impeller - leading to collisions and interlocking of the aggregates particles.

Surprisingly very little work has been published on the vibration response of NS or HPCs as assessed by the BT rheometer, which has been designed with the added facility of measuring the changes in the Bingham parameters during vibration. de Larrard and his co-workers[49, 89-92] merely reported that when fresh concrete is subjected to vibration, its flow properties are changed; and the yield stress is mainly affected (**figure 2.68**). In agreement with the findings by Tattersall and Baker[210] and Kakuta and Kojima[212], it is interesting to note that de Larrard et al's results[49] also show noticeable increases in the plastic viscosity during vibration, particularly at low shear rates.

More recently, Banfill et al[215] used a vertical pipe apparatus to examine the fluidity (viz. flow velocity or efflux rates) of 10 vibrated concrete mixes (at 0.44-0.30 w/b ratios), and compared these with the Bingham parameters of the non-vibrated concretes as measured with a modified version of the LM system. They concluded that the application of vibration appears to reduce the yield value, and that there is a strong indication that the maximum fluidity achieved at peak vibrational velocities corresponds to a Newtonian viscosity numerically equal to the plastic viscosity of the unvibrated concrete.

None of the foregoing investigations have examined how the presence of superplasticizers and/or CRMs influences the vibration response characteristics of fresh HS and other HPCs. The next section deals with the effects of compaction by vibration on the strength development of hardened concretes.

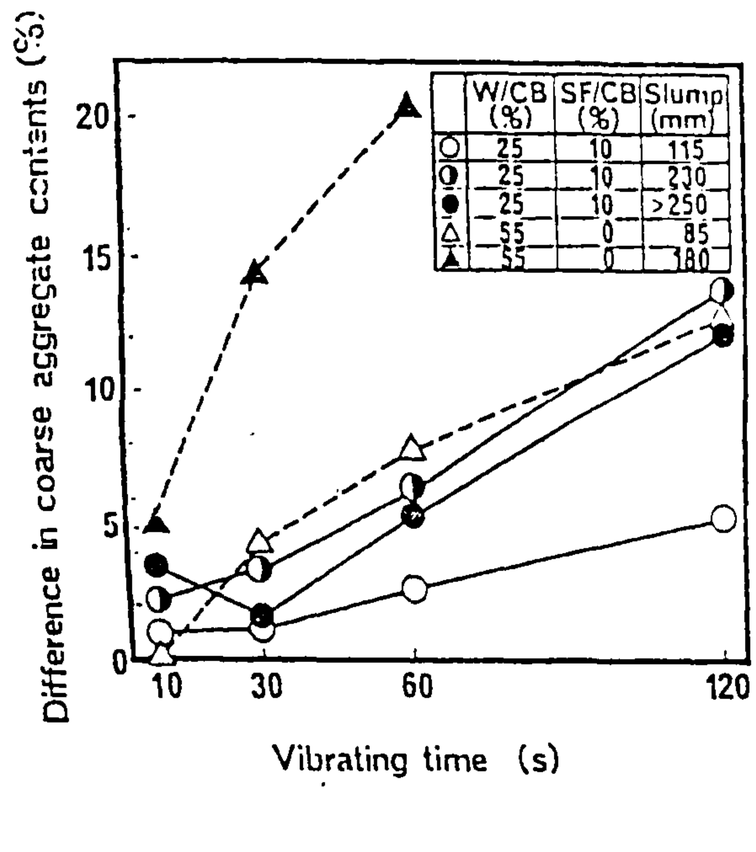

Figure 2.63 : Segregation resistance of NS and HSC mixes as assessed by the differences in coarse aggregate contents at different vibration durations[18].

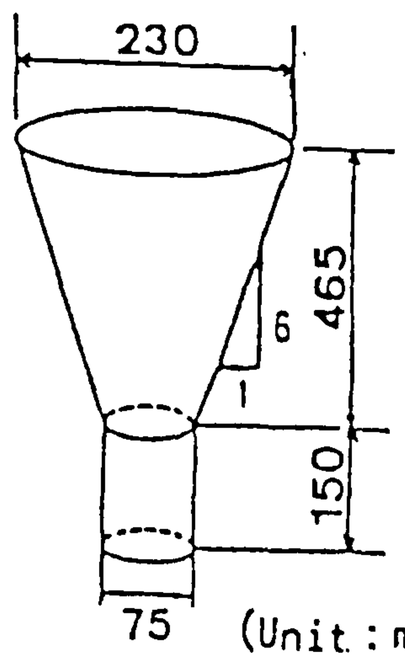

Figure 2.64 : Test apparatus for measuring segregation resistance of flowing HPC mixes in terms of flow-out time or rate[206].

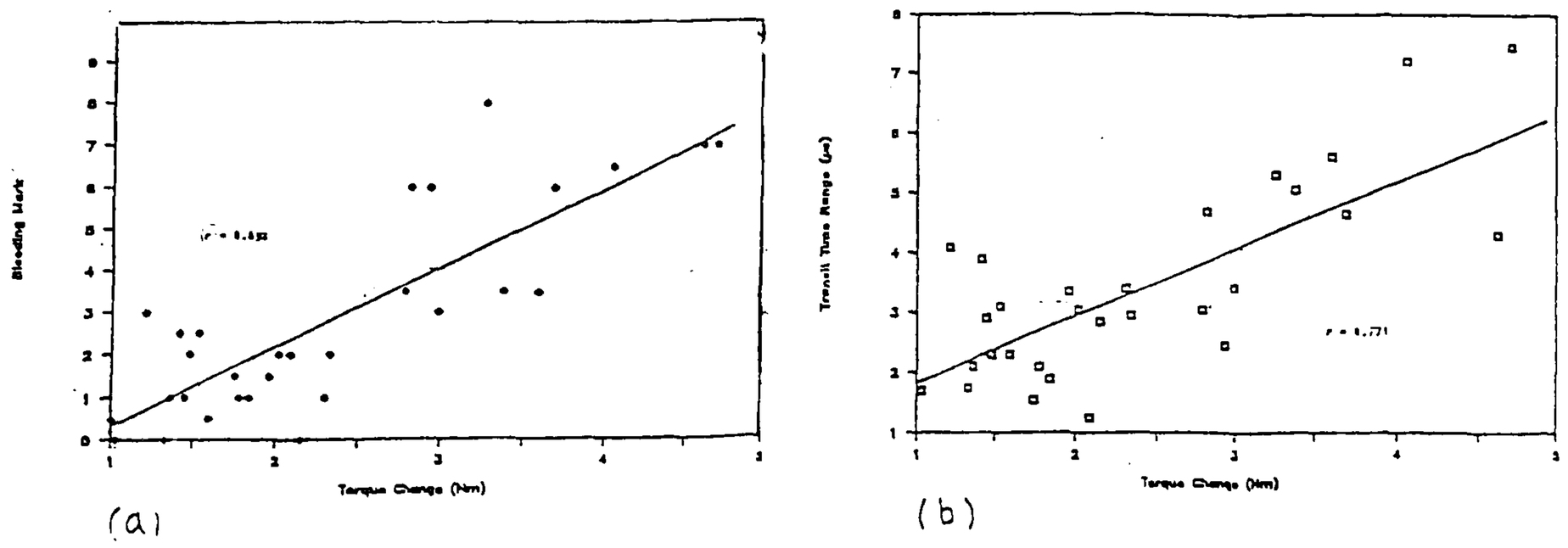

Figure 2.65 : Relationship between impeller torque change with (a) subjective bleeding marks, and (b) hardened concrete homogeneity (as assessed by the range in ultrasonic pulse velocity)[191].

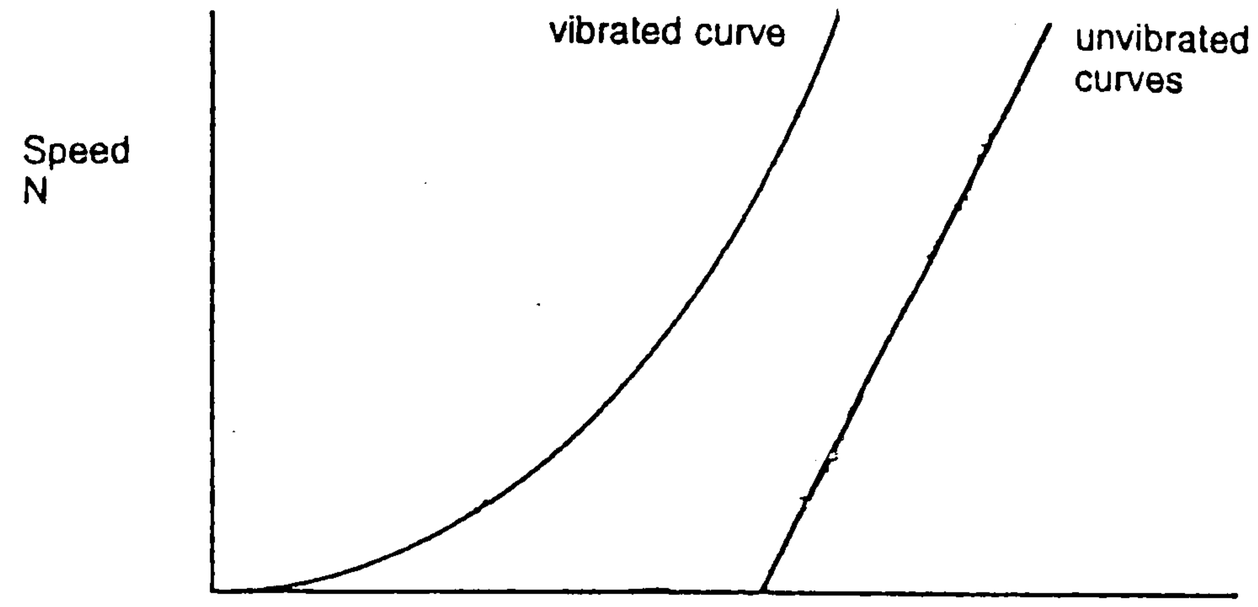

Figure 2.66 : Speed-Torque flow curves for unvibrated and vibrated NSC (obtained by mounting the MH test bucket on a vibrating table)[210].

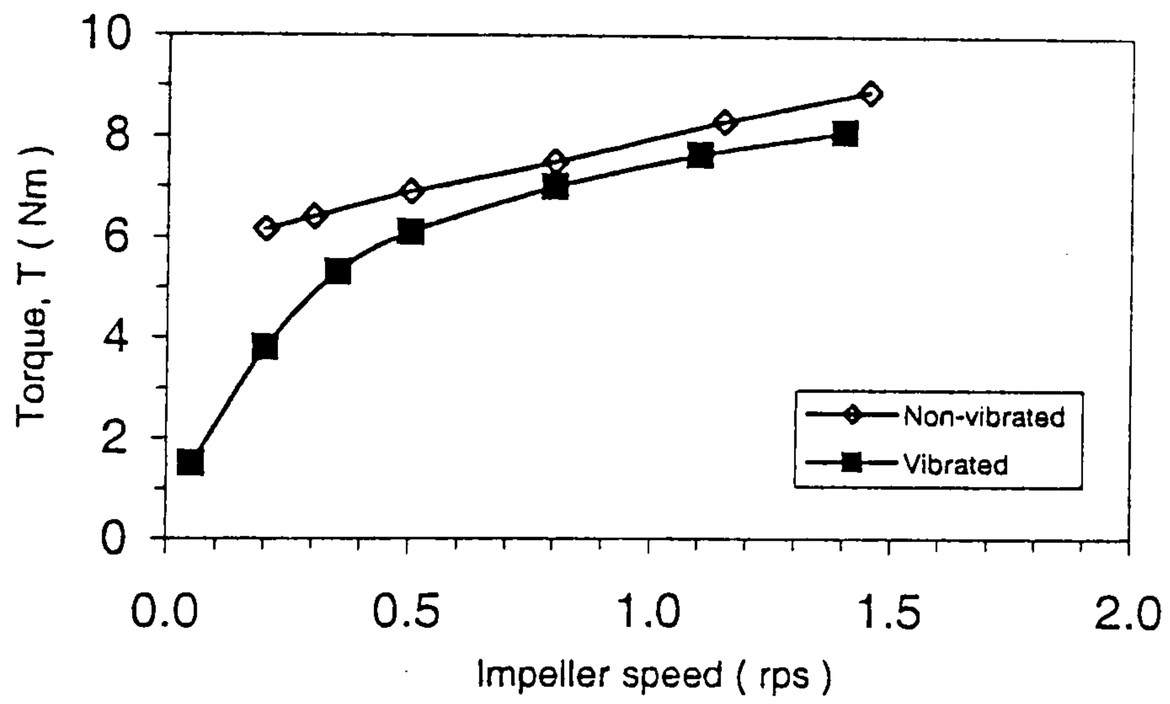

Figure 2.67 : Typical Torque-Speed flow curves for superplasticized NSC (obtained by mounting the LM test bucket on a vibrating table, at 0.50 w/b) [212].

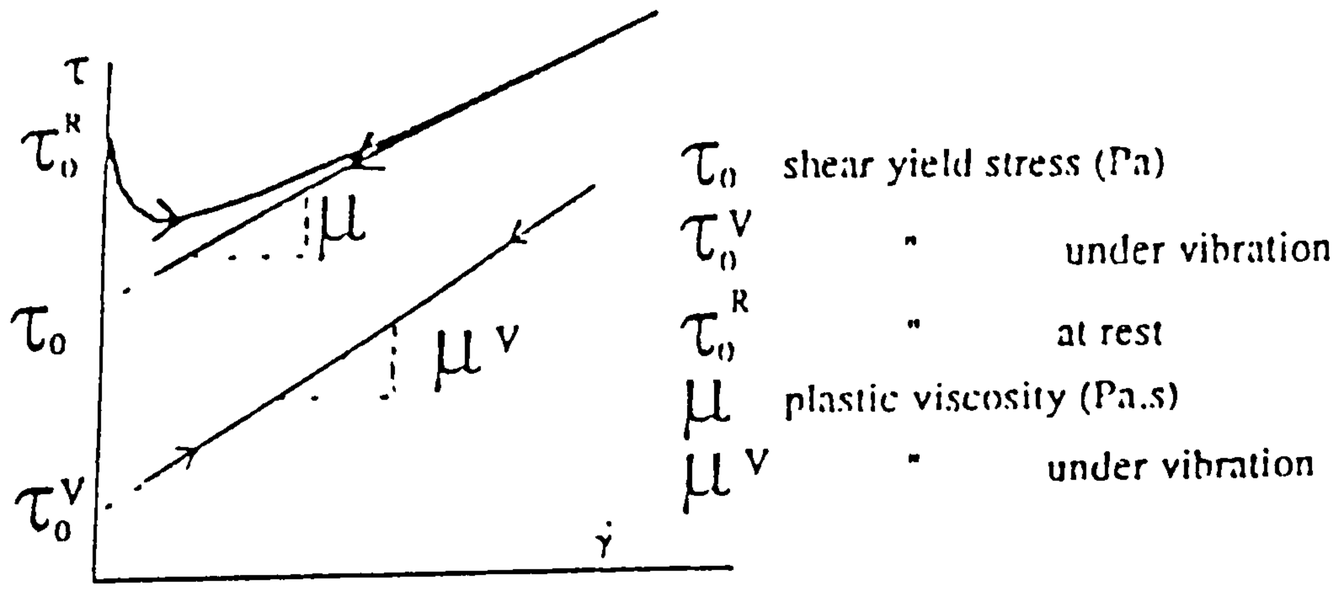

Figure 2.68 : Variations in the Bingham properties of fresh concrete under vibration - as measured with the BT Rheometer (mix design and vibration details not reported)[49].

2.8 Compressive strength development

The compressive strength of concrete is normally considered to be its most important property since it is directly related to the structure of the hydrated cement paste (hcp)[8] matrix. It is thus believed to be an indicator of the overall quality of the concrete, and is often assessed at 28 days.

Several workers[8, 22, 217] have reported that the compressive strength of concrete at a given age primarily depends on: the **water/binder ratio** and the **degree of compaction** applied. At very low w/b ratios, the inverse relationship between compressive strength and w/b ratio (as shown in **figure 2.69**) however ceases to be followed as full-compaction is no longer possible. According to Neville[8] the actual position of departure in the curve depends on the means of compaction used. Bresson[22] reported that a reduction in w/b ratio from 0.40 to 0.30 essentially doubles the vibration energy requirement and increases the compressive strength by about 12 Nmm^{-2}.

According to Welton[218] the application of vibration has **five main roles** in increasing the strength and density of the concrete, by:

(1) eliminating **mechanical voids** in the mass,

(2) unintentional **air voids**,

(3) removing unnecessary **water**,

(4) shaking the particles into their **closest nesting**, and

(5) **attacking** the **micro-pores** and micro-**capillaries**.

The current guidelines in BS 1881: part 108[219] and ASTM C192-98[220] for compacting fresh concrete merely advocate that the concrete should be compacted in such a way as to release as many entrapped air bubbles as possible. They suggest that full-compaction is achieved when the surface of the concrete becomes relatively smooth, but provide no provisions for relating the workability properties with for example the minimum energy requirements to achieved full-compaction.

Very few researchers have in fact investigated the effects of different vibration inputs on the strength development characteristics and/or other mechanical properties of hardened concretes.

In one study on NSC, Al-khalaf and Yousif[217] investigated the optimum vibration duration required to reach full compaction (revibration period), and the effects of casting time (which they referred to as the time between initial vibration and revibration). They found that the optimum degree of compaction necessary to produce maximum compressive strength (i.e. full compaction) corresponds to a vibration duration of 10 seconds per layer (**figure 2.70(a)**). Their results indicated that the dangers of over-compaction (which they ascribed to instability caused by prolonged vibration) are lower than those due to under-compaction (resulting from the presence of internal voids).

They also found that there are continual increases in compressive strength with casting time up to a period of 3 hours (**figure 2.70(b)**), which they attributed to the elimination of: plastic shrinkage, settlement cracks, and internal defects caused by bleeding. Beyond the optimum 3 hours casting time, they suggested that the compressive strength decreases due to disturbance of the setting processes by vibration, which causes some damage to the bonds formed by the hydration products.

In another study, Forssblad and Sallstrom[221] investigated the degree of vibration required for full compaction of moderate-strength concretes having slumps of 75-240 mm under field conditions. The degree of vibration required was referred to as the "vibration effort", which they suggested is a measure of the transmitted compaction energy and is equal to the effective time of vibration (expressed in seconds per cubic meter (S/m^3)).

In concrete having an uncompacted air content of 2.5% (**figure 2.71**) they found that both the compressive strength and density increase to optimum values with increasing vibration effort, and that a prolonged vibration effort from 250 to 600 s/m^3 has insignificant effects on the hardened properties. In concrete with an

uncompacted air content of 5-6% (**figure 2.72**), they reported that a prolonged vibration effort of 1200 s/m^3 produces a maximum density increase of approximately 3% (from about 2300 kgm^{-3} to 2400 kgm^{-3}) and a 12% increase in strength (from 43 Nmm^{-2} to 50 Nmm^{-2}). As can be seen the improvements appear to be largely due to a reduction in total pore volume.

Although it is widely accepted that the low workability of HSCs leads to greater shearing resistance and compaction problems than NSCs[11, 22, 48, 223], there is very little quantitative information pertaining to the effects of vibration on the strength development characteristics of HSCs. Based on experience gained from trial HSC mixes, Wild et al[222] stated that CSF can result in incomplete compaction and long-term strength reductions brought about by its high water demand and rapid loss of workability. They however suggest that it is possible using high superplasticizer dosages of as much as 3.4% (s/w/b) to produce workable CSF concretes having high degrees of compaction under vibration with a w/b ratio of 0.35.

Similar suggestions have also been made by Chan et al[14], who stated that at a constant superplasticizer dosage, the low workability of HSC mixes containing CSF contents exceeding 10% causes a reduction in the compressive strength due to poor compaction. Although Kwan[223] recently reported that CSF and high superplasticizer dosages can be used to produce self-compacting HSCs having slumps > 200mm and 28-day compressive strength ≥ 80Nmm^{-2}, they did not show how these relate to different degrees of compaction. (The effects of superplasticizers and CRMs on the strength development characteristics of HSCs compacted in accordance with BS 1881: part 108[219] and/or ASTM C192-98[220] are briefly discussed in chapter 9).

The author is unaware of any work which has managed to establish how the changes in the Bingham parameters, slump or other rheological properties of fresh concretes during vibration influence the strength development characteristics, density or other mechanical properties of hardened concretes.

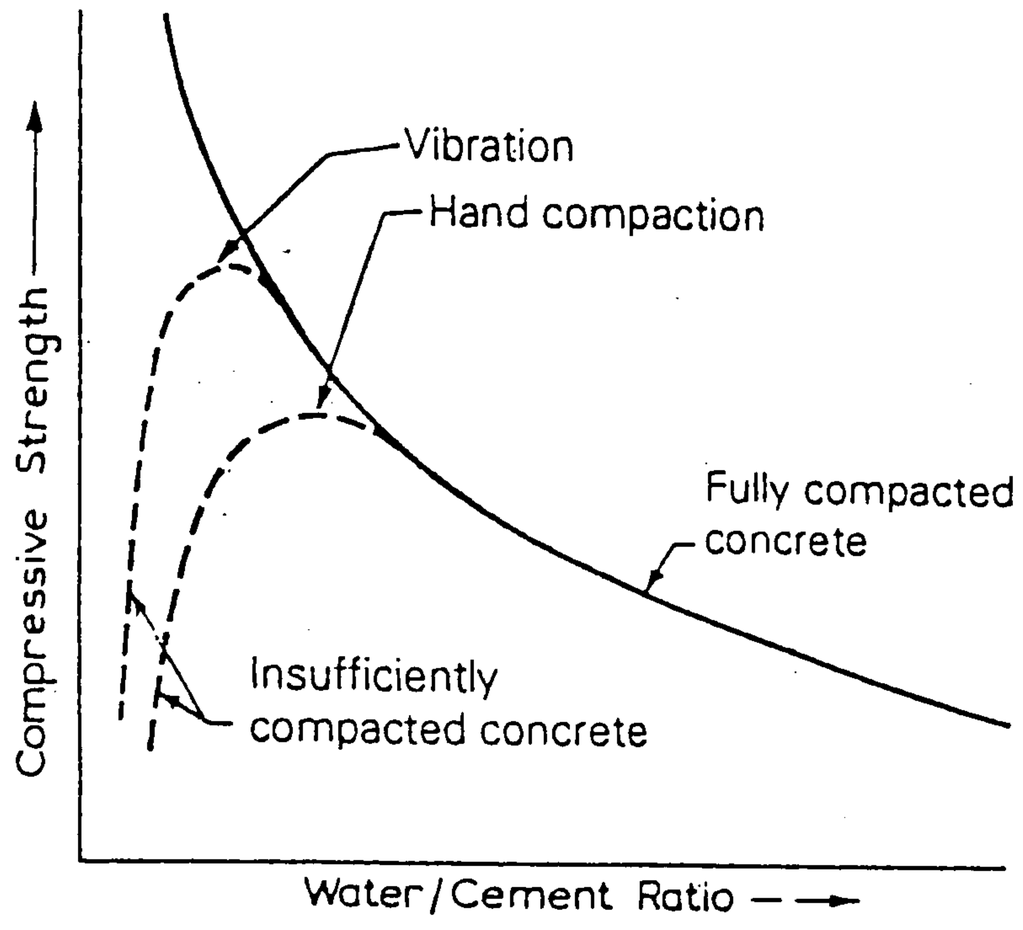

Figure 2.69: Relationships between strength, water/cement ratio and degree of compaction[8].

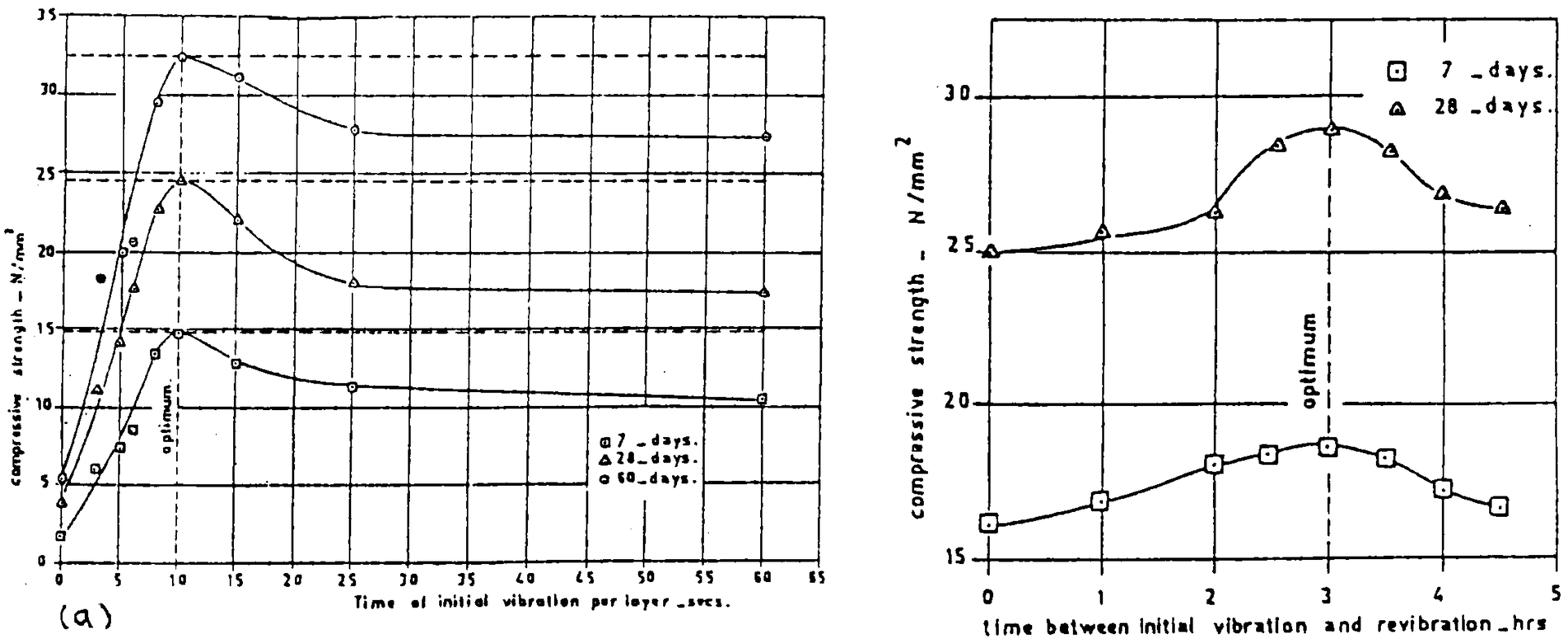

Figure 2.70: Relationships between (a) vibration time/duration per layer, and (b) casting time (expressed as the time between initial vibration and revibration) with the compressive strength of 150 mm cubes[217].

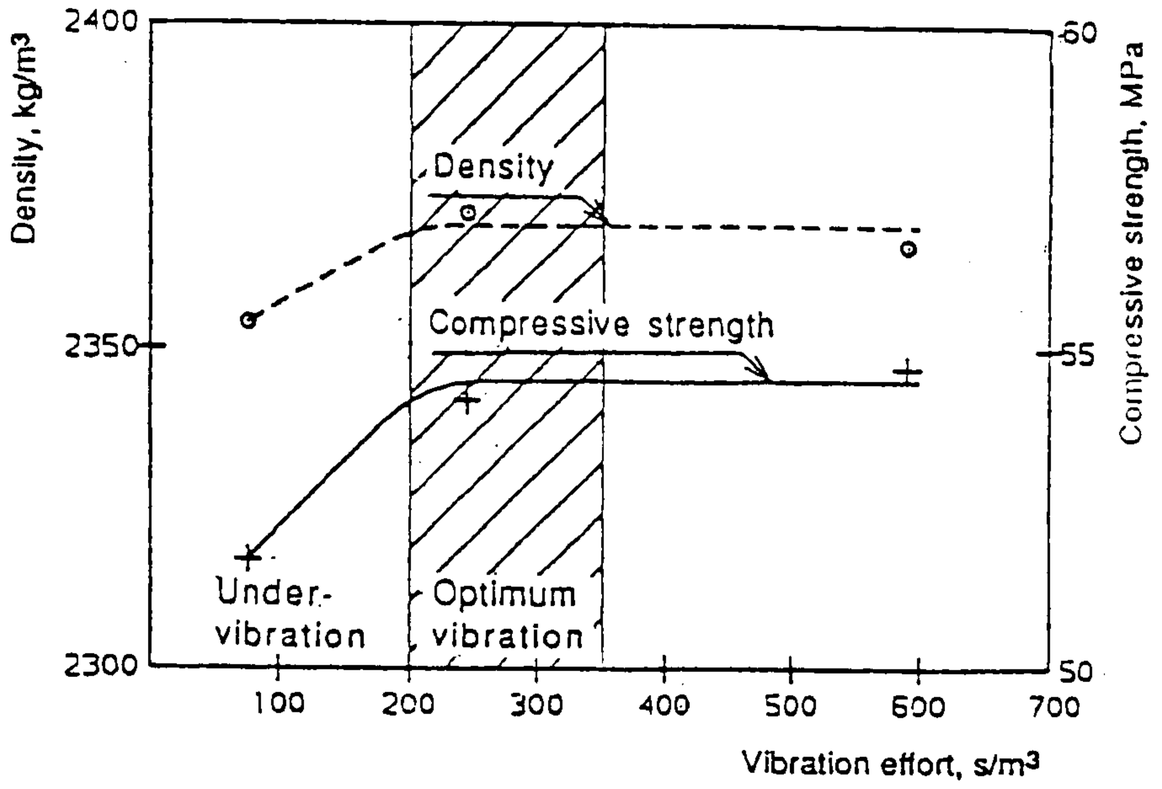

Figure 2.71: Relationship between internal vibration effort/duration, density and 28-day compressive strength of concrete having an uncompacted air content of 2.5% (using 125mm ϕ cores, w/b ratio not reported)[221].

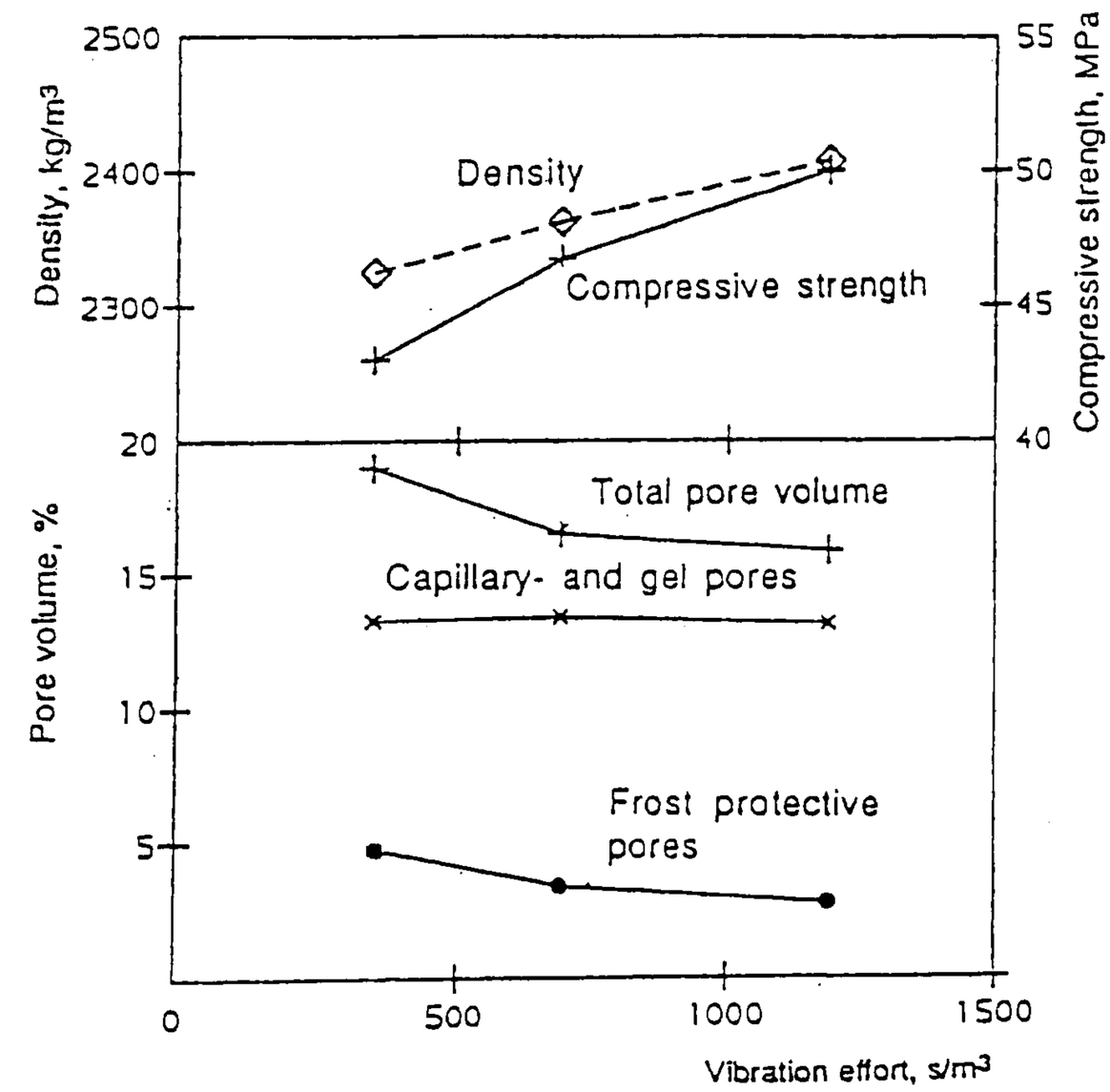

Figure 2.72: Relationship between vibration effort/duration, density, pore volume, and 28-day compressive strength of concrete having an uncompacted air content of 5-6% (using 125mm ϕ cores, w/b ratio not reported)[221].

2.9 Conclusions

Despite the vast amount of work reported in the literature on the performance of HS and other HPCs, the review indicates that there are several key questions that need to be addressed :

1. Do **mix stability and compactability** represent distinct rheological components of fresh concretes as defined by Ritchie[61] (c.f. figure 2.1), or can they be adequately described by the Bingham parameters from the two-point workability test ?

2. In terms of **materials selection**:
   - How does the rate of loss of workability (when expressed in terms of the Bingham parameters) vary with **decreasing w/b ratio** ?
   - How effective are different types of **superplasticizers** in enhancing the initial workability properties and reducing the rate of loss of workability?
   - How do **binary and ternary blended cements** influence the superplasticizer dosage requirements and rates of loss of workability ?

3. How do the Bingham parameters vary during the **placing** and **compaction stages** ?

4. How could the changes in the Bingham parameters during compaction by vibration be used in **optimizing the compressive strength**, density and other mechanical properties in the hardened state ?

These and other more specific research needs are outlined in the next chapter.

Chapter 3
Aims and Scope of Research

3.1 Introduction

The previous two chapters showed that despite the vast amount of research that has been performed on HS and other HPCs, there are still many areas where further research is needed to ensure their efficient and economical application. Some of the major concerns relate to the: assessment of the workability/rheological properties, uncertainties in material selection; the behaviour of HSCs during placing/compaction, and how these influence the hardened properties. This chapter highlights the main research deficiencies existing in these areas, and outlines the aims and scope of the present research.

3.2 Aims

The main aims of the research presented in this thesis are to:

1. Assess the **workability** properties and their evolutions with time prior to placing and compaction in terms of the two Bingham parameters; and determine whether these can provide sufficient descriptions of the variations in **mix stability** and **compactability**.
2. Reduce the uncertainties in **material selection** with regards to the:
   - effects of **aggregate absorption** and decreasing **w/b ratio**,
   - performance of **superplasticizers** and **CRMs**.
3. Determine how the Bingham parameters vary during the **placing** and **compaction** stages.
4. Examine how the **strength development** characteristics are influenced by changes in the Bingham parameters and different degrees of compaction.
5. An additional aim was to carry out any modifications to the test apparatus and methods which experience makes necessary.

The overall objective of these is to provide data to help users optimise HSC. This section summarizes the main uncertainties existing in the literature and identifies key research needs for each of the main aims in (1)-(4). More specific aims and the scope of the research is outlined in **Tables 3.1-3.5** (section 3.3). The basic mix proportions used in the investigation are given in **Tables 3.6-3.7** (section 3.4).

3.2.1 Assessment of workability/rheological properties

It has been widely documented[2, 30, 40, 201] that the use of single point (or traditional) tests such as the slump test (section 2.2.2.1) can give the wrong impression of the workability of HS and other HPCs, which should instead be expressed according to the Bingham model (c.f. figure 1.1).

The literature review has however shown some erroneous workability measurements with the various two-point test devices described in section 2.2.2.2. Two major deficiencies relate to measurements of representative:

- **losses of workability** (i.e. higher Bingham values) with time, and
- **improvements in workability** due to, for example, the use of **superplasticizers** (discussed in page 115) and the effects of **redosing** with increasing amounts of superplasticizers (i.e. lower Bingham values).

Although some explanations have been proposed for these, they are in some cases confusing. For example, although Wallevik and Gjorv[50, 86] stated that Tattersall's MH system suffers from segregation during two-point testing and may be incapable of measuring loss of workability, they have surprisingly reported that it gives good correlations with their BML viscometer[86], which is considered suitable for assessing soft-fluid concretes (page 58).

On the other hand, the re-dosing results reported by Hu et al[40] (c.f. Page 62) conflict with the effects due to increasing water contents (c.f. figure 2.9) and the first use of superplasticizers (page 34). The combined effects of these two fluidizing agents, which occurs when successive re-doses/additions of superplasticizers are used, would intuitively be expected to reduce both the Bingham parameters.

Although Ritchie 's[61] insight (c.f. figure 2.1) indicated that a full description of the rheological (or flow) properties of fresh concrete must take into account the mobility, mix stability and compactability properties, he did not point-out whether any relationships exist between them. *The present research therefore aims to:*

- *establish a greater understanding of the factors influencing representative two-point test (i.e. Bingham) measurements, and*
- *determine whether any relationships exist between the Bingham parameters, mix stability and compactability.*

3.2.2 Material selection

The selection of efficient materials and their proportions, particularly in terms of superplasticizers and CRMs, is considered essential in overcoming the poor initial workability properties and rapid losses of workability in HSC[11, 39, 49]. The main points from the literature on how the various mix design variables (in sections 2.3-2.6) influence the workability properties and dosage requirements are summarised below.

3.2.2.1 Water content and w/b ratio

Section 2.3 showed that there are significant reductions in initial workability (i.e. higher Bingham values), increases in slump loss and superplasticizer dosage requirements with decreasing w/b ratio[7, 18, 40, 53, 97, 100]. Information on how the rate of loss of workability (when expressed in terms of the Bingham parameters) varies with decreasing w/b ratio is however lacking.

The present research therefore aims to examine how reductions in the w/b ratio influence the rate of loss of workability when expressed by time-dependent measurement of the Bingham parameters.

3.2.2.2 Aggregate characteristics

The absorption of mixing water by dry aggregates was reported to be the most significant aggregate characteristic influencing the workability[103] properties of fresh concretes (section 2.5.4). Although de Larrard et al's measurements[49] were confined to dry aggregates (c.f. figure 2.14), they stated that the effect of pre-saturating the aggregates prior to mixing reduces the rate of loss of workability in that no significant increase in plastic viscosity occurs.

The present work aims to clarify this through comparative tests using both dry and pre-saturated aggregates.

3.2.2.3 Superplasticizers

The review in section 2.5 indicated that the effectiveness of superplasticizers and other water-reducing admixtures in enhancing the workability properties depends significantly on their **type**, **dosage**, **mixing procedure** and **compatibility** with different cements.

(I) Types

Many researchers[7, 17, 30, 49-50, 201] reported that the presence of conventional superplasticizers and other water-reducing admixtures significantly reduces the yield value, but can increase (or have little effect on) the plastic viscosity. This however conflicts with the first use of superplasticizers (page 34), that they increase the workability (i.e. reduce both the Bingham parameters) – and may be related to deficiencies associated with the two-point test devices used.

Although the use of new-generation (NG) superplasticizers has been widely reported to reduce the rate of loss of workability[28, 50, 119, 130-135], this has largely been based on slump loss measurements (pages 43-47).
The present research therefore aims to assess the initial workability properties and workability retentions of both conventional and NG superplasticizers through comparative two-point test measurements.

(II) Dosage effects

The investigations by Wallevik and Gjorv[50] and Punkki et al[17] showed that although increasing dosages of superplasticizers generally produce lower initial yield values, they increase the initial plastic viscosity (c.f. figure 2.34-2.35). With regards to loss of workability, Punkki et al 's measurements[17] showed that a low superplasticizer dosage mainly increases the development of the yield stress with time[17, 50], whereas high dosages give smaller variations in yield stress but distinct increases in plastic viscosity (c.f. figure 2.35). Their work has however not demonstrated the existence/effects of the saturation (or optimum) dosage, which is believed to give maximum initial workability[17, 38, 148] (i.e. lowest Bingham values)

and longest workability retention[14, 149, 155].

The research therefore aims to examine the beneficial effects of increasing superplasticizer dosages (up to and beyond the saturation value) on the initial workability properties and workability retention of HSC.

(III) Mixing procedure

The review in section 2.5.4(I-III) showed that the reported effects of superplasticizer mixing procedures have largely been confined to slump testing and/or examining a limited number of variables. In particular, the review revealed a lack of quantitative information on the blending of superplasticizers with other water-reducers (page 64); and how different delayed/split additions of superplasticizers could be used to optimise the workability properties of HSCs (c.f. pages 65-67, figure 2.40). *The present research therefore aims to:*

- *compare the efficiencies of a range of delayed and split superplasticizer mixing procedures, and*
- *examine the beneficial effects of blending conventional and NG superplasticizers with air-entraining agents and retarders in controlling the workability properties of HSC.*

(IV) Cement-superplasticizer compatibility

Section 2.5.5 showed that the compatibility between cements and superplasticizers is significantly influenced by: the C_3A and calcium sulfate contents, the form of the calcium sulfate and fineness of the cement[11], the gypsum/(natural anhydrite) ratio[122], the soluble alkali contents[153, 166], and the type of superplasticizer used[119]. de Larrard et al's[49] limited work (c.f. figure 2.45) suggested that the effect of cement-superplasticizer incompatibility is represented by considerable increases in yield value but little or no change in plastic viscosity with time. Their work, like that reported by other researchers[119, 153] (c.f. figures 2.42-44), has however not demonstrated how the dosage requirements and/or Bingham parameters are influenced by the interactions of different cements and superplasticizers.

The present research therefore aims to determine whether the use of different

cement compositions and superplasticizers has any distinct effects on the dosage requirements and Bingham properties of HSCs.

3.2.2.4 Cement replacement materials (CRMs)

(I) Binary blends

Section 2.6 showed that partial cement replacements by PFA or GGBS cause reductions in the superplasticizer dosage requirement, and increases in the slump (or workability) compared to the equivalent portland cement mixes[18, 99, 175-181, 187-189, 190]. The benefits claimed for the use of PFA and GGBS in reducing the rate of loss of workability[11, 39], have however not been confirmed through time-dependent two-point test measurements by previous researchers.

The review also highlighted some controversy regarding the effects that CSF has on water demand and workability. Although many researchers reported that the use of CSF reduces the workability and requires a compensating addition of superplasticizer[14, 19, 148, 160, 192-196], several other researchers[18, 30, 39, 197-198] have reported results to the contrary; and that above a certain superplasticizer dosage CSF has a water reducing effect[53]. With regards to loss of workability, Punkki et al's work[17] (c.f. figure 2.60) showed that CSF increases the rate of slump loss, reduces the development in plastic viscosity but distinctly increases the development in yield stress at 0.37 w/b ratio.

The present research therefore aims to examine the effects that partial cement replacements by binary blends of PFA, GGBS and CSF have on the superplasticizer dosage requirements and workability properties at low w/b ratios.

(II) Ternary Blends

Although the use of ternary combinations of OPC and CSF with PFA or GGBS is considered to be very promising in meeting the stringent construction requirements of HSC[18, 39], very little work has been published in this area (section 2.6.5). Soutsos's work[53] showed that partial cement replacements by a single ternary blend of 10% CSF and 50% GGBS requires less superplasticizer dosage, and

reduces both the Bingham parameters compared to the equivalent OPC mix (c.f. figures 2.61-2.62).

The present research aims to compare the effects that ternary blends of both PFA/CSF and GGBS/CSF have on the superplasticizer dosage requirements and workability retentions of HSCs.

3.2.3 Vibration response

Despite the importance of achieving full-compaction in any given concrete mixture, the review in section 2.7.2 indicated a lack of basic understanding of how the Bingham parameters vary during compaction/vibration. de Larrard et al[49] and others[89-92, 210-216] essentially showed that the application of vibration reduces the yield value, but did not sufficiently comment on how the plastic viscosity is affected, or how the use of, for example, different vibration inputs and mix compositions influence the vibration response of fresh concretes.

The present research therefore aims to examine how the Bingham parameters are affected by the use of different vibration durations/inputs, and determine how they differ in NS and HSCs.

3.2.4 Strength development

It has been widely documented[8, 11, 22, 218, 223] that insufficient compaction of a fresh concrete mixture can preclude it from attaining its maximum strength and durability. The investigations by Al-kalaf and Yousif[217] and by Forssblad and Sallstrom[221] (c.f. figures 2.70-2.72) showed that both the compressive strength and density increase up to maximum levels depending on the vibration durations/inputs used, but did not demonstrate how they are influenced by changes in the fresh properties during compaction.

The research therefore aims to examine how the changes in the Bingham parameters during compaction by vibration influence the compressive strength and density of hardened concretes.

3.3 Scope of research

The research presented in this thesis comprised five key areas:

1. **Preliminary rheological measurements** (carried out to primarily determine the effects of aggregate absorption, decreasing w/b ratios, and whether any relationships exist between the Bingham parameters, mix stability and compactability).

Assessments to reduce the uncertainties associated with the performance of:

2. different types of **superplasticizers**, and
3. **CRMs** (in both binary and ternary blends).
4. An examination of the **flow properties**, **placing characteristics** and **vibration response** of HSCs.
5. An examination of the **strength development** characteristics of NS and HSCs at different vibration durations and amplitudes.

The scope of the research performed in each of these areas is summarised in Tables 3.1-3.5.

3.3.1 Preliminary rheological measurements

These comprised four main series of tests as shown in **Table 3.1**. The third series of these were carried out to compare the suitability of: different two-point testing methods (viz. Shear duration and direction) and various modifications of the MH and LM systems (in terms of bucket size, impeller blade orientation and size) in giving representative measurements of loss of workability. (That is, higher Bingham values with time). The work also included comparative tests to assess the capabilities of Tattersall 's MH and LM systems in measuring the fluidizing effects due to successive redoses of superplasticizer (i.e. reductions in the Bingham parameters, as discussed in page 113).

The fourth series of tests were introduced to assess the validity of using small-scale mortar tests (based on mortar spread and V-funnel flow time (described in section 4.3.2)) in predicting the workability properties of concrete. Mortar repeatability

tests were also performed to assess the statistical significance of the measurements and variability in the results using dry and moist sand.

3.3.2 Assessment of superplasticizers

The assessment of superplasticizers comprised four series of tests summarized in **Table 3.2**. The first series compared the performance of different types and brands of conventional and new generation superplasticizers with an air-entraing agent and retarder at a constant dosage of 2.00% (s/w/b). To reduce the number of concrete tests much of the work was performed on the mortar fraction of the concrete mixes. Eight repeat mixes prepared with a SNF superplasticizer, and two mixes with SMF and Acrylate-based superplasticizers were used to assess the variability of superplasticizers and two-point test measurements in concrete.

The assessments of superplasticizer dosages, mixing procedures, and cement-superplasticizer compatibility (series 3.2.2-3.2.4) involved comparative tests using five superplasticizers (comprising: SMF, SNF, MLS, and two new-generation superplasticizers (based on Acrylate and Vinyl polymers)). (Details of theses are given in chapter 4). In each case mortar tests were used to establish the dosage response and/or workability retention of the superplasticizers before concrete testing.

3.3.3 Assessment of CRMs

Five series of tests were carried out to investigate the effects of binary and ternary blends on the saturation dosage requirements and workability properties of HSC. The test variables used for each type of blend at 0.26 w/b ratio are summarised in **Table 3.3** (series 3.3.1-3.3.4). In series 3.3.5, the effects of 100% OPC, 10% CSF, and two ternary (PFA/CSF and GGBS/CSF) blended mixes at the optimum replacement levels (from series 3.3.4) were investigated at w/b ratios of 0.30 and 0.22, and compared with the equivalent mixes at 0.26 w/b ratio. In each series, mortar dosage-response tests were performed to fix the saturation dosages to be used for the concrete mixes.

3.3.4 Flow properties, placing characteristics and vibration response

A novel method, based on measuring the flow properties during slump-collapse, was developed to assess the placing characteristics and vibration response of HS and other HPCs. The method (described in chapter 8) allowed the workability properties (in terms of the yield value and plastic viscosity) to be determined following 5mins resting of the concrete, and at different vibration durations/amplitudes. The variables investigated are outlined in **Table 3.4**.

3.3.5 Strength development

Table 3.5 shows the variables used to examine how the 28-day strength development of duplicate mixes (tested in series 3.4.3) are influenced by different vibration durations (corresponding to 0, ½, 1 and 2 times those needed to obtain zero yield value) and amplitudes (of 0-0.7 mm). The work involved tests on both 100 mm cubes and short columns (500x100x100mm). The former included a study to assess the influence of 60-70 mins and 120-130 mins casting times. The column tests were primarily used to examine the effects of segregation caused by different degrees of compaction in the fresh state on the homogeneity (or uniformity) of the hardened concrete.

The strength development characteristics from the cube and column tests were in each case complimented by density measurements.

3.4 Mix proportions used

(I) For HSC (and mortar) mixes

The basic mix proportions used in the investigations on the HSC and corresponding mortar mixes in series 3.1-3.5 are shown in **Table 3.6**. These were based on mixes designed by Soutsos[53] using a Modified Maximum Density Theory (MMDT). According to him, this does not only require that the aggregates occupy as large a relative volume as possible (to produce minimum void content

and hence volume of cement paste), but also accounts for the influence that aggregate surface area has on the requirement of excess paste needed for lubrication. In the present research, Soutsos's mix proportions were modified to accommodate for different types and dosages/levels of superplasticizers and CRMs.

Portland cement mixes 1-4 (at 0.42, 0.40, 0.38 and 0.34 w/b ratios) were used in the assessment of decreasing w/b (or more precisely w/c) ratios in series 3.1.2. Mixes 5, 6 and 7 (at 0.30, 0.26 and 0.22 w/b ratios) were used in both the preliminary rheological measurements and the assessment of CRMs in series 3.1.2 and 3.3.5. Mix 6 (0.26 w/b) was used in all five research areas in Tables 3.1-3.5. The mortar fractions of the mixes were in each case produced by eliminating the coarse aggregates.

(II) For NS and HP-SCCs

The mix proportions used in the investigations on NSC in series 3.1.1, 3.4.3 and 3.5.1 are shown in **Table 3.7(a)**. The control NSC mix (1) was based on a trial mix, and was subsequently modified by pre-saturating the aggregates (mix 2), replacing all the cement with PFA and reducing its water content (mixes 3-6). Mix 7 (used in series 3.4.3 and 3.5.1) was designed in accordance with the DOE guidelines[237] and subsequently modified by using a superplasticizer to obtain a high initial slump of 220 mm. The two high-performance self-compacting concrete (SCC) mixes shown in **Table 3.7(b)** were designed by a fellow researcher at UCL[224], and were used to compare their flow properties under self-weight with those of the HSC mixes in series 3.4.1.

The next chapter (4) gives details of the materials and experimental methods used in the research. Chapters 5, 6, 7, 8 and 9 respectively discuss the results of the five key research areas listed in section 3.3 (Tables 3.1-3.5).

Table 3.1: Aims and scope for **preliminary rheological measurements.**

Series	Aims	Scope	Experimental details
3.1.1	Examine the effects of **aggregate absorption** & a SNF **superplasticizer** in NSC	Use of : dry and pre-saturated aggregates (with 100% OPC and PFA mixes) & a SNF SP at 0.48, 0.45, & 0.42 w/b ratios.	Use of slump test & MH system to assess workability.
3.1.2	Assess the effects of **decreasing w/b ratio** on the loss of workability in HSC. Examine possible **relationships** between the Bingham (workability) properties, mix stability & compactability.	Decreasing w/b ratios of : 0.42, 0.40, 0.38, 0.34, 0.30, 0.26 and 0.22. Mixes tested at a constant initial slump of 220+/-10 mm.	Use of slump test & MH system to assess workability. Assessment of : Bleeding tendencies (subjectively[191]); Segregation resistance (by Tc method[191] & % of coarse agg.s after 2-pt. testing); Compactability (by a density method[224], the compacting factor test[60], & subsidence after vibration[7]).
3.1.3	Compare different **two-point testing** methods.	Effects of : shear duration & direction; bucket size; impeller type, size & orientation. Comparision of redosing tests with the MH & LM systems.	Tests involving various modifications of the MH and LM systems (at 0.26 w/b ratio).
3.1.4	Assess the **validity of** small-scale **mortar tests**.	Effects of decreasing w/b ratios of : 0.42, 0.38, 0.30, 0.26, & 0.22. Re-dosing tests at 0.26 w/b. Repeatability tests using dry & moist sand at 0.26 w/b ratio.	Mortar spread & V-funnel tests of concrete mixes in series 3.1.2.

All the HSC mixes in Table 3.1 were produced using a SNF (Conplast SP 435) superplasticizer and OPC.

Table 3.2: Aims and scope for assessment of **superplasticizers.**

3.2.1	Comparision of different **types /brands** of superplasticizers and **water-reducers** (at a constant dosage of 2.00% s/w/b).	Mortar tests with : 7 conventional SPs/brands (based on SMF, SNF & MLS); 2 NG SPs (based on Acrylate & Vinyl polymers); an air-entraining agent (A.E.A.) & retarder (R). Concrete tests with : 5 SPs based on SMF, SNF, MLS & the 2 NG SPs (referred to as " **SPs*** "). Repeatability tests involving: 8 concrete mixes using SNF, 2 concrete mixes with the SMF and acrylate polymer.	Mortar spread and V-funnel tests . Slump test & LM system to assess workability. Segregation resistance assessed using % difference in coarse aggregates after 2-pt. testing.
3.2.2	Assessment of **dosage effects.**	Mortar-dosage response tests with the 5 SPs in series 3.2.1 (" **SPs*** "). 5 concrete mixes dosed with SNF at 1.50, 2.00, 2.50, 3.00, and 4.00% s/w/b..	Selected compactability tests in terms of subsidence after vibration.
3.2.3	Influence of superplasticizer **mixing procedure.**	Mortar-dosage response tests involving: delayed adds. at 0, 1, 2, 3, 4, 6, & 8 mins with the 5 SPs in series 3.2.1 (" **SPs*** "); 50/50% Split adds. at 0/4 & 1/4 mins (SNF); 50/50% Blends of SNF & acrylate SPs with SMF, MLS, A.E.A & R. Concrete mixes involving : 0, 1, 2, 4 mins delayed SNF additions; 0/4 min SNF split add.; blends of 90/10 SNF/R & 90/10 acrylate/R.	
3.2.4	cement-superplasticizer **compatibility.**	Mortar-dosage tests using: 5 cement compositions & the 5 SPs in 3.2.1 (" **SPs*** "). Concrete tests with 5 cements and SNF.	

All the mixes in Table 3.2 were produced using 10% CSF (at 0.26 w/b ratio).

Table 3.3: Aims and scope for assessment of **CRMs.**

Series	Aims	Scope	Experimental details
3.3.1	Cement replacements by **CSF** (at 0.26 w/b)	CSF Additions at: 0, 15, 30, 45 & 60 secs. Mortar-dosage response tests at: 0, 2.5, 5, 10, & 15% CSF. Concrete tests at: 0, 2.5, 5, 10, & 15% CSF.	Mortar spread and V-funnel tests. Slump test & LM system to assess workability.
3.3.2	Cement replacements by **PFA** (at 0.26 w/b)	Mortar-dosage response tests at: 0, 10, 20, 40 & 60% PFA. Concrete tests at: 0, 10, 20, and 40 % PFA.	Segregation resistance assessed using % difference in coarse aggregates after 2-pt. testing.
3.3.2	Cement replacements by **GGBS** (at 0.26 w/b)	Mortar-dosage response tests at: 0, 20, 40, 60 & 80% GGBS. Concrete tests at: 0, 20, 40 & 60% GGBS.	Selected compactability tests in terms of subsidence after vibration.
3.3.4	Cement replacements by **ternary blends** of OPC/CSF/PFA and OPC/CSF/GGBS (at 0.26 w/b)	Mortar-dosage response tests for: 10% CSF wih 10, 20, 40 & 60% PFA. Concrete tests for cement replacements by: 10% CSF wih 20 and 40 % PFA. Mortar-dosage response tests for: 10% CSF wih 20, 40, 60 & 80% GGBS. Concrete tests for cement replacements by: 10% CSF wih 40 and 60 % GGBS.	
3.3.5	Effects of **w/b ratios** of 0.30 and 0.22	Mortar-dosage response and concrete tests with: 100% OPC, 10% CSF and two Ternary mixes of 40/10% PFA/CSF and 60/10% GGBS/CSF.	

All the above % 's are of Portland cement replacement by weight, for mixes using a SNF superplasticizer (added 4 mins delayed).

Table 3.4: Flow properties, placing characteristics and **vibration response**

3.4.1	Examine the **flow properties** under self-weight.	Static & dynamic flow properties under self-weight (using mixes in Table 3.3 & 2 SCCs).	Slump-spread at 5, 10, 20, 30 & 60 secs.
3.4.2	**Placing characteristics.**	Workability reductions following 5 mins resting of 100% OPC & 10% CSF mixes.	
3.4.3	**Vibration response.**	Vibration amplitudes of 0.1, 0.4 & 0.7 mm. 6 mixes tested, comprising 5 HSCs (of 100% OPC, 10% CSF, 40/10 PFA/CSF, 60/10 GGBS/CSF with SNF, & 10% CSF with acrylate SP) and 1 NSC mix (at 0.50 w/b ratio).	Vibrating table operating at 0.1-0.7 mm amplitude & fixed frequency of 50 HZ.

Table 3.5: Strength development characteristics (under different vibration durations and amplitudes).

3.5.1	Effects of different vibration **durations**, **amplitudes** & **casting times** on cube strength.	Vibration durations corresponding to: 0, $^1/_2$, 1 & 2 times those required to obtain zero yield value. Amplitudes of 0, 0.1, 0.4, & 0.7mm. Casting times of 60-70 & 120-130 mins (Using mixes in series 3.4.3).	Two 100 mm cubes casted for each test variable in series 3.5.1 (to account for damping effects).
3.5.2	Effects of different vibration **durations** & **amplitudes** on column strength.	In accordance with variables in series 3.5.1 (using 100% OPC & 10% CSF mixes, & 120-130 mins casting time).	One short column (500x100x100 mm) casted for each test variable in series 3.5.2 (to account for damping effects).

Table 3.6 : Basic mix proportions (in kg/m^3) used for **HSC**.

Mix	Binder	Sand	Granite	Free water	w/b ratio	SP* dosage
1	400	670	1115	168	**0.42**	Variable
2	411	670	1115	164	**0.40**	Variable
3	421	670	1115	160	**0.38**	Variable
4	447	670	1115	152	**0.34**	Variable
5	480	670	1115	144	**0.30**	Variable
6	510	670	1115	133	**0.26**	Variable
7	546	670	1115	120	**0.22**	Variable

The cement and water contents for the 0.42, 0.40, 0.34, and 0.30 w/b ratio mixes were modified from proportions reported by soutsos[53] at similar w/b ratios. All other mix proportions were obtained directly from soutsos's work[53].

The **Superplasticizer dosage** (**SP***) is expressed as % of solids by weight of total binder (s/w/b).
Substitution by **CRMs** was on a one to one basis by weight.

The paste volume is approximately 29.7% for all the equivalent OPC mixes.

The mortar fractions of the mixes were produced by excluding the granite content.

Table 3.7 (a) : Mix proportions (in kg/m^3) used to investigate the effects of aggregate absorption, a SNF superplasticizer, and vibration in **NSC**.

Mix	Variables investigated	Binder		Sand	Gravel		Water		Free w/b ratio	SNF SP (%)
		Cement	PFA		20-10	10-5	Total	Free		
1*	Dry aggregates	370	-	725	600	490	208	179	0.48	None
2	Pre-saturated Aggs.	370	-	725	600	490	208	*179	0.48	None
3	Dry aggregates	-	370	725	600	490	183	154	0.42	None
4	Pre-saturated Aggs.	-	370	725	600	490	183	*154	0.42	None
5	Non-superplast-icized mix	370	-	725	600	490	195	167	0.45	None
6	Superplasticized mix	370	-	725	600	490	195	167	0.45	0.14
7	Vibration response	390	-	618	765	382	214	195	0.50	0.15

* control mix.
Pre-saturation of the aggregates in mixes 2, 4-6 was achieved by pre-soaking the coarse aggregates, and pre-wetting the sand (in the mixer) for ~ 2 hrs with 117.6 l/m^3 of the total mixing water.

Table 3.7 (b) : Mix proportions (in kg/m^3) used to assess the flow properties of **SCC**.

1	Flow properties	585	-	815	556	249	-	175	0.3	0.85
2	Under self-weight	351	234	815	556	249	-	175	0.3	0.85

Chapter 4

Materials and Experimental Methods

4.1 Introduction

This chapter provides details of all the materials and the main experimental methods used in the research. These include descriptions of the mixing and testing methods for fresh concrete and mortar; casting, curing and testing of the hardened concrete. A general description of the novel method developed to assess the vibration response of the mixes in series 3.4.3 (Table 3.4) is also provided. The premise of the method is more conveniently discussed in chapter 8.

4.2 Materials

4.2.1 Portland cement

In total nine batches of Portland cement (PC, class 42.5 N), complying with BS EN 197-1: 2000[225] (Type CEM1) and ASTM C 150-95[170] (Type I), were obtained from Rugby Cement plc and used in the research. (Other strength classes of Portland cement (viz. 52.5 and 62.5N) were not available during the investigation). The large number of batches were used because other students/researchers working on concrete related projects were also using the same cements. Two 50 kg consignments of rapid hardening (RHPC, ASTM Type III) and sulfate resisting (SRPC, ASTM Type V) cement were also obtained from Rugby Cement to compare their cement-superplasticizer compatibilities with three of the Type I cements. The chemical and physical characteristics of all eleven cements used in the research are shown in **Table 4.1**.

4.2.2 Cement replacement materials

The following CRMs were used:

- Condensed silica fume (**CSF**) obtained as a 50/50 slurry in water, from Elkem Chemicals.
- Pulverised fuel ash (**PFA**), complying with BS 3892 : Part 1:1992[226], was

supplied in powder form by Ash Resources Ltd.

- Ground granulated blast furnace slag (**GGBS**), complying with BS 6699:1992[227], was supplied in powder form by Civil and Marine Ltd.

Partial cement replacements by CSF, PFA and GGBS were, as mentioned in section 3.4 (Table 3.6), on a one to one basis by weight. The chemical and physical characteristics of the three CRMs used are shown in **Table 4.2**.

4.2.3 Water

Ordinary tap water was used in all the mixes. Its temperature varied between 17 ^{0}C in winter to 23 ^{0}C in the summer.

4.2.4 Superplasticizers (and other chemical admixtures)

Eleven commercially available chemical admixtures from three suppliers (Fosroc Expandite Ltd, Sika Ltd, and Grace Construction Products) were used to examine their efficiencies in producing HSC. These comprised nine superplasticizers and two plasticizers, supplied as liquids complying with BS 5075: part 103[112] and ASTM C-494[110]. Their effects on the fresh and hardened properties as reported by the manufacturers, their specific gravities and measured active solids contents are summarized in **Table 4.3**. Information regarding their molecular weights, chain-lengths and/or chemical structures was however not provided by the suppliers.

The nine superplasticizers comprised :

- Two sulphonated melamine formaldehyde, **SMF**, based admixtures (conplast M1 and Sika FF),
- two based on sulphonated naphthalene formaldehyde, **SNF** (Conplast SP 435 and Sika N),
- one modified lignosulphonate, **MLS** (Darcem SP 4),
- two **new generation** (or high-performance) superplasticizers based on **Vinyl** and **Acrylate** co-polymers (Sika 10 and Darcem 2001), and
- two **pre-blended superplasticizers** (Darcem SP 6 and Conplast SP 450).

The two plasticizers (an air-entrainer : Conplast PA21, and a retarder - Conplast R) were used for comparison, and blending with the superplasticizers (in series 3.2.1 and 3.2.3). Both plasticizers were obtained from Frosroc Ltd.

4.2.5 Fine and coarse aggregates

Four samples of Thames Valley sand with fineness moduli (FM) ranging from 2.20 to 2.60 were used in the research.

To produce the HSC mixes, five batches of 10 mm granite were obtained (in deliveries of 0.75-1.00 tonnes) from Tarmac Road Stone, Hayes, Middlessex. These had aggregate crushing (ACV) values of 11.3 to 13.1, which are typical of granite. Two samples of 20-10 and 10-5 mm Thames Valley gravel were used to produce the NSC and two high-performance self-compacting concrete (SCC) mixes (in Table 3.7(a-b)). Granite was not used in these mixes since they are typically produced with gravel aggregates.

The coarse and fine aggregate gradings together with physical properties determined in accordance with BS 812 : 1985[228] are shown in **Table 4.4**.

Table 4.1 : Portland cement compositions and physical properties

Sample No.	C_3S (%)	C_2S (%)	C_3A (%)	C_4AF (%)	SO_3 (%)	Alkalis (%) $Na_2O_{(eq)}$	SSA (m^2/kg)	Strength* (Nmm^{-2})
PC-1	59	12	9.6	9.0	2.57	0.61	376	62.5
PC-2	55	14	10.6	9.1	2.95	0.63	355	59.4
PC-3	56	15	9.9	8.9	2.81	0.64	335	58.3
PC-4	50	18	11.0	9.0	2.75	0.63	380	55.0
PC-5	57	13	9.5	9.2	2.69	0.62	395	60.5
PC-6	59	10	9.6	9.2	2.50	0.62	370	59.4
PC-7	53	15	9.8	9.9	2.75	0.69	380	53.2
PC-8	54	15	9.0	9.3	2.73	0.71	345	55.1
PC-9	57	14	10.1	8.6	2.51	0.62	330	60.0
SRPC	63	12	0.1	15.2	2.14	0.49	440	-
RHPC	60	11	9.2	7.2	2.90	0.78	375	-

* 28 day mortar compressive strength (by suppliers).

Cement PC-1 was used to produce the mixes in series 3.1.1; cements PC-2, PC-3 and PC-4 were used in series 3.1.2-3.1.3; whereas cements PC-5-PC-6 were used in series 3.1.3 - 3.1.4.

Cements PC-7, PC-8 and PC-9 were respectively used in series 3.2, 3.3 and 3.4. Cement PC-9 was also used to produce the mixes in series 3.5.

The cement-superplasticizer compatability of the SRPC and RHPC cements was compared with that of cements PC-7, PC-8 and PC-9 in series 3.2.4.

Table 4.2 : Compositions and physical properties of CRMs

CRM type	CaO	SiO_2	Al_2O3	Fe_2O3	MgO	LOI	SSA (m^2/kg)	Specific gravity
CSF	0.3	92	1.0	1.0	0.6	-	15000 - 20000	~ 2.20*
PFA	1.4	51.4	25.0	9.4	1.4	4.80	< 45 um	2.40
GGBS	41.3	33.7	11.5	1.8	9.0	-	400 - 440	2.90

Table 4.3 : Summary of different **types/brands of chemical admixtures** used

Brand	Supplier	Type/Formulation	Manufacturers Claimed Properties			Standards Compliance		Solids content (%)	Specific gravity	Recommended dosages (%, s/w/b)
			Workability	Workability Retention	Strength Development	BS 5075[112]	ASTM C-494[110]			
I. Conventional superplasticizers										
Conplast **M1**	Fosroc	Sulphonated **melamine** formaldehyde Polymers (**SMF**)	can produce flowing concrete	of short duration	increased at all ages	Part 3	Types A, F	20	1.10	1.0 - 4.0
Sikament **FF**	Sika	Sulphonated **melamine** formaldehyde (**SMF**)	can impart extremely high workability	-	early & ultimate strength gains	Part 3	Type F	40	1.25	0.7 - 3.0
Conplast **SP 435**	Fosroc	Sulphonated **naphthalene** formaldehyde (**SNF**)	produces high work-ability & flowing conc.	Longer than SMF SPs	suitable for producing HSC	Part 3	Types A, F	40	1.19	0.7 - 2.0
Sikament **N**	Sika	Sulphonated **naphthalene** formaldehyde (**SNF**)	produces high work-ability & flowing conc.	extened during first 60 mins	can produce HSC	Part 3	Type F	40	1.20	0.7 - 3.0
Darcem **SP 4**	Darcem	**Modified Lignosulphonate (MLS)**	produces SCC & flowing concrete	excellent	-	Parts 1,3	Types A,D,G	33	1:15	0.28 - 1.0
II. New-generation (NG) superplasticizers (Vinyl and Acrylate)										
Sikament **Sika 10**	Sika	**Vinyl** co-polymer	can produce Flowing concrete	extended for up to 2 hrs	can produce HSC	Part 3	Types A, F	20	1.11	0.6 - 1.2
D 2001	Darcem	**Acrylate-methacrylate** co-polymer	imparts high Workability	excellent	good early age strengths	Part 3	Type G	35	1.18	0.4 - 1.0
III. Pre-blended superplasticizers										
Darcem **SP 6**	Darcem	blended **polymeric sulphonate materials**	high workability particularly with CSF	excellent	early & ultimate strength gains	Parts 1,3	Types A,D,G	40	1.19	0.4 - 3.0
Conplast **SP 450**	Fosroc	blend of **melamine** polymers & selected **Lignosulphates**	produces flowing concrete	excellent	early & ultimate strength gains	Part 3	Types A, F	30	1.18	1.3 - 2.5
IV. Plasticizers (Air-entraining agent & retarder)										
Conplast **PA21**	Fosroc	Selected sugars & reduced **Ligno-sulphonates** (Air entraining agent)	improved	-	better than other Air ent. agents	Part 2	Type A	35	1.18	0.25 - 0.60
Conplast **R**	Fosroc	**Hydrocarboxlic materials** (Retarder)	improved	extended	no adverse effect	Part 1	Types B, D	42	1.13	0.25 - 0.60

Table 4.4 : Properties of fine and coarse aggregates

Sieve Analysis

Sieve size	Percentage retained by weight												
	Sand				Gravel				Granite				
	S-1	S-2	S-3	S-4	20-10 mm		10-5 mm		G-1	G-2	G-3	G-4	G-5
					G20-1	G20-2	G10-1	G10-2					
25.4 mm	100	100	100	100	100	100	100	100	100	100	100	100	100.0
19.1 mm	100	100	100	100	75.2	84.16	100	100	100	100	100	100	100.0
10.0 mm	100	100	100	100	0.5	8.8	91.47	93.84	82.0	86.0	91.0	90.0	91.0
5.0 mm	99.1	99	98.0	97.73	0.0	2.0	16.17	16.48	5.0	2.7	3.8	3.9	4.1
2.36 mm	88.03	87	87.0	86.97	0.0	0.0	3.1	0.0	2.0	0.0	0.1	0.0	0.0
1.18 mm	78.5	77	75.0	77.07	0.0	0.0	0.0	0.0	0.0	0.0	0.0	0.0	0.0
600 um	69.9	69	55.0	63.36	0.0	0.0	0.0	0.0	0.0	0.0	0.0	0.0	0.0
300 um	28.71	41	19.0	25.74	0.0	0.0	0.0	0.0	0.0	0.0	0.0	0.0	0.0
150 um	4.91	8	4.0	2.53	0.0	0.0	0.0	0.0	0.0	0.0	0.0	0.0	0.0
F.M.	2.31	2.2	2.6	2.5	-	-	-	-	-	-	-	-	-

Other properties

S.G.	2.64	2.64	2.64	2.64	2.60	2.60	2.60 2.567	2.60	2.70	2.70	2.70	2.70	2.70
Absorption at SSD	1.5%	1.2%	1.2%	1.2%	1.0%	1.0%	2.5%	1.1%	0.7%	0.7%	0.7%	0.7%	0.7%
Bulk density (kg/m^3)	-	-	1756	1760	1566	1590	-	1560	-	1595	1578	1584	1592
ACV										11.31	11.72	12.85	11.95

4.3 Mixing and testing of fresh concrete and mortar

4.3.1 Mixing methods

(I) For concrete

Two mixers (a Soroto type 60 L-33 and a Liner laboratory pan mixer) were used in the research. The Soroto mixer (with a capacity of 30 litres and 30 rpm) was used to produce the NSC mixes, whilst all the HSC (and two SCC) mixes were produced using the pan mixer (capacity of 113 litres and 18 rpm). To minimise wastage of materials, 35 or 45 litre batches of concrete were usually prepared with the pan mixer.

Some of the NSC mixes tested in series 3.1.1 (Tables 3.1 and 3.7(a)) used oven dry aggregates, and therefore the mixing water included the absorption (or SSD) water of the aggregates. All the constituents (including any superplasticizer) were placed in the mixer before mixing commenced.

To produce the HSC mixes four main superplasticizer mixing procedures were used as shown in **figure 4.1**. Procedure 1, involving a 30 secs delayed addition of the superplasticizer was used throughout the preliminary rheological tests (series 3.1.2-3.1.3), and is in accordance with the minimum addition time recommended by Penttala[142] for HPCs (page 66). Procedures 2-4 were used for the assessment of delayed and split superplasticizer additions (in series 3.2.3).

To examine the effects of the 4, 6 and 8 mins delayed superplasticizer additions in series 3.2.3, the initial mixing duration (in procedure 2) was extended to 5½, 7½ and 9½ mins respectively. This is in accordance with a minimum superplasticizer mixing duration of 90 secs cited by Neville[8].

The aggregates used for the HSC mixes were pre-saturated and placed in storage bins for 2-3 days before mixing. Their moisture contents were then measured (using a microwave powered at 80-90% of full capacity), and their batch weights together with the remaining amount of mixing water were determined.

To ensure uniform and reproducible mixing, the amount of surface water on the aggregates (which typically varied between 17-25% of the free mixing water content) was increased to approximately 32% (at 0mins) in procedures 2-4. The remaining constituents were added to the mixer in the following sequence :

- cement (together with any PFA or GGBS),
- CSF (when used, the slurry was introduced after 30 secs), and finally
- all the superplasticizer (premixed with the rest of the mixing water) was added and mixing continued for up to 5 or 5 ½ minutes.

(II) For Mortar

To produce the mortar mixes a Hobart food mixer (with 2.5 litres capacity, planetary motion of the blades, and operating at 62 rpm) was used. The mortar mixing procedures used were consistent with those used for the concrete mixes. However, for reasons of quality control (discussed in section 5.6.2) most of the mortar mixes were prepared with dry sand (using small batch volumes of 1.5 litres).

4.3.2 Testing of fresh mortar

The mortar tests were introduced following the preliminary tests with the NS and HSC mixes in series 3.1.1-3.1.3 :

- to reduce the number of variables to be investigated in concrete, and
- in fixing suitable dosages for the assessment of superplasticizers and CRMs (Tables 3.2-3.3).

The mortar tests were performed using both the spread and V-funnel tests. Although these tests are believed to provide measurements of fluidity[58] and viscosity[151] respectively (page 57), previous researchers have generally used either the spread or the V-funnel test (or their counterparts: the mini-slump and Marsh cone tests). According to Neville[8], the choice between these tests has usually been taken on a preference basis. In the present research, the spread and V-funnel tests were used concurrently in an attempt to provide a more comprehensive description

of the workability properties of mortar – i.e. give parameters which may be equivalent to the yield value and plastic viscosity.

(I) Mortar spread test

In the mortar spread test, a mould in the form of a frustum of a cone (60 mm high, with upper and base diameters of 70 mm and 100 mm – **figure 4.2(a)**) is placed on the center of a glass plate, and filled with mortar. (For very low workability mortars having spreads lower than about 200 mm, the cone was filled in two layers, each layer being compacted with 15 strokes of a steel rod). Immediately after filling, the cone was lifted and the average mortar spread diameter after complete collapse under self-weight was measured (to the nearest 5 mm) in two perpendicular directions. Time-dependent measurements of mortar spread were usually performed at 8, 30, 60, and 90 minutes. With the exception of the first measurement (at 8 mins), all subsequent spread tests were preceded by 60 seconds of re-mixing.

In contrast to the spread test, the mini-slump test (consisting of a mould 57 mm high, with top and bottom diameters of 19 and 38 mm) has been used by previous researchers[152-153] to assess the workability (or flowability) of cement pastes in terms of the average spread area (in cm^2) (c.f. figures 2.39 and 2.43).

(II) V-funnel test

The V-funnel test (**figure 4.2(b)**) is similar in principal to the Marsh cone test in that both tests essentially measure the flow time through an orifice.

In the V-funnel test, the funnel is filled with approximately 1.1 liters of mortar, the gate is then opened, and a stop-watch is simultaneously started to measure the flow-out time through the funnel. The watch is stopped when light is seen through the outlet when viewed from above. The flow-out time, representing the rate of deformation of the mortar under self-weight, is then recorded as the V-flow time.

All the V-funnel measurements were preceded by 60 seconds re-mixing, and were usually completed 2-4 minutes after the spread measurements.

In contrast with the V-funnel test, the Marsh cone test (350 mm high, with top and nozzle diameters of 155 and 8 mm) has been used by previous researchers to measure the time taken for a certain volume of paste[13, 58, 148] or mortar (excluding sand sizes > 2mm)[150] to flow. In the present research the 8 mm nozzle opening was considered restrictive for testing the mortar fractions of HSC mixes, which are normally produced with coarse sand (page 3).

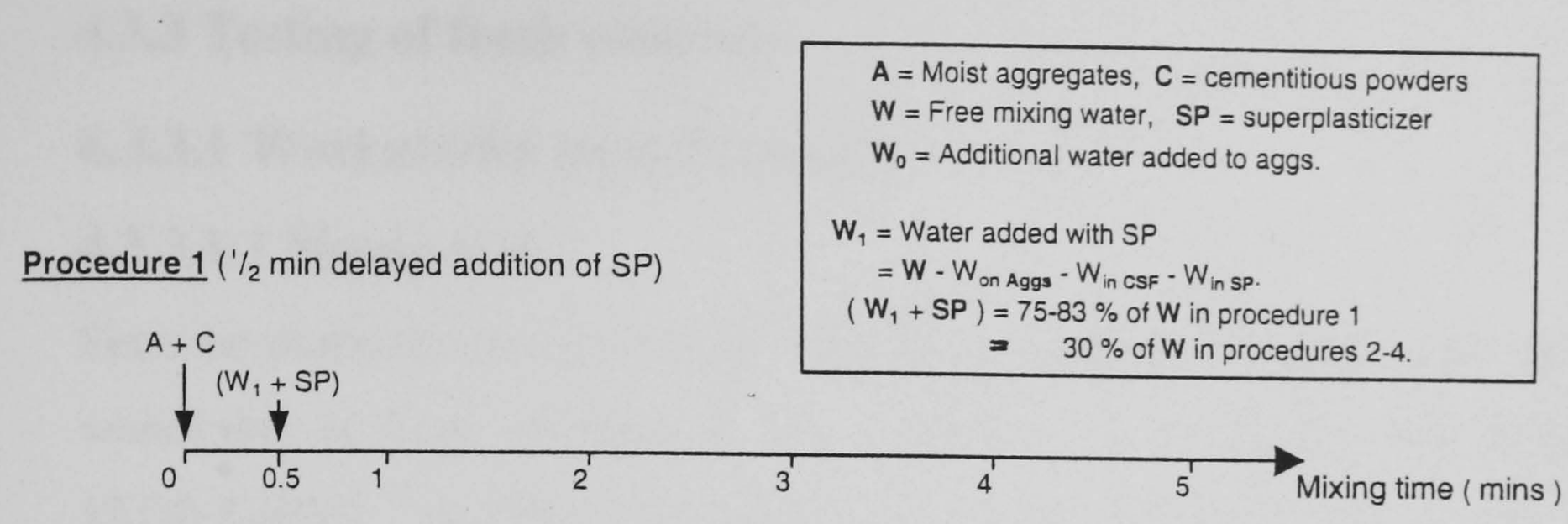

Figure 4.1 : Main superplasticizer mixing procedures used (the liquid phases (W, CSF slurry, and SP) were in each case poured gradually into the mixer over about 10 secs).

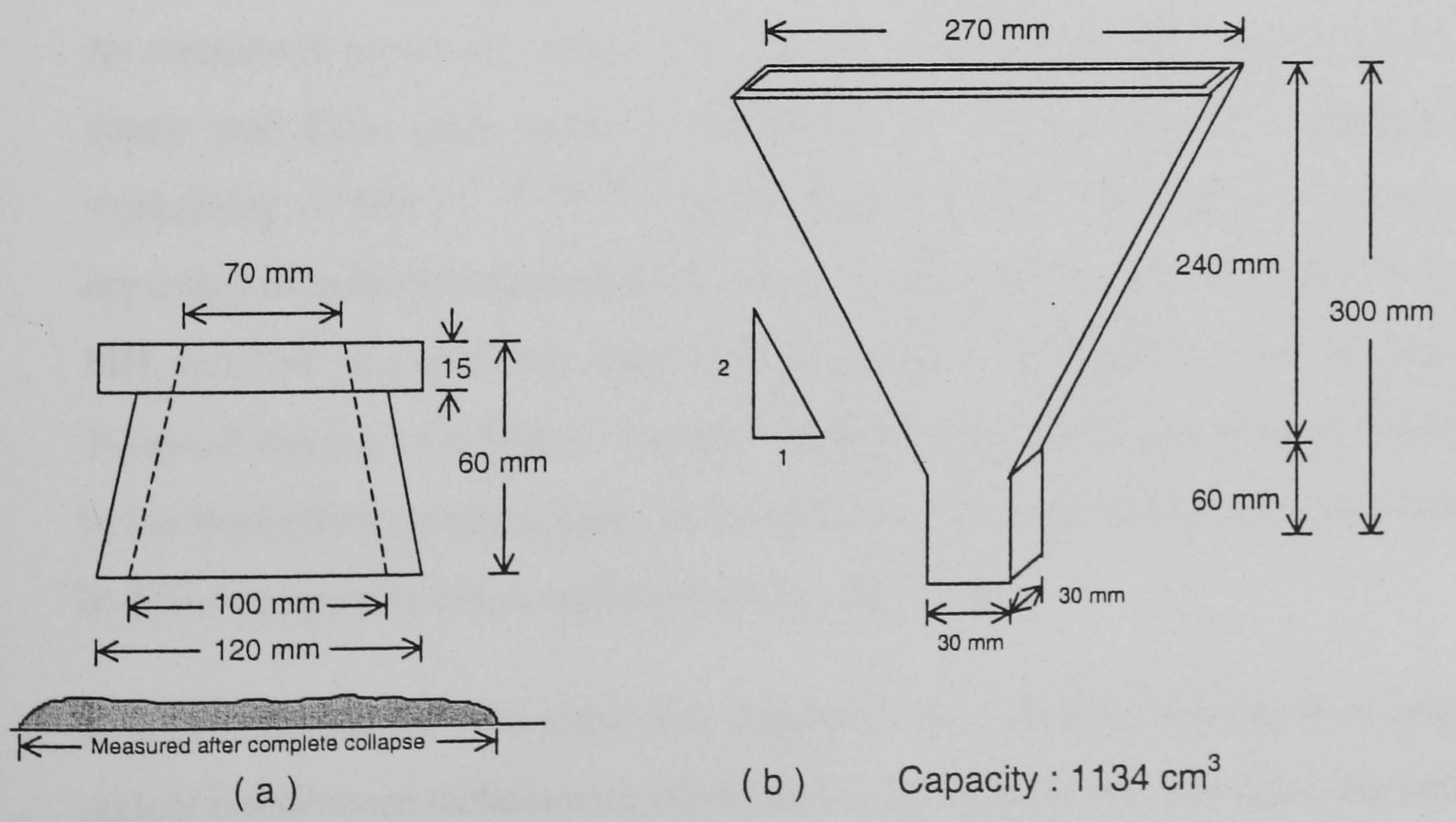

Figure 4.2 : Dimensions of (a) the mortar-spread[229] and (b) V-funnel[230] tests.

4.3.3 Testing of fresh concrete

4.3.3.1 Workability measurements

4.3.3.1.1 Slump tests

Since the slump test (section 2.2.2.1 (I)) is the current field method of assessing the workability of fresh concretes, it was performed (in accordance with BS EN 12350-2:2000)[73] in all the concrete mixes. However, in contrast with the 180 mm limit set by BS EN 12350[73], slumps up to 260 mm were measured, as these were found to reflect real and quantifiable differences in workability. The first slump measurement was started immediately after the 5-5½ mins initial mixing sequence, and was completed approximately 2-3 mins later. All subsequent slump measurements were preceded by 60 seconds re-mixing, and were usually completed at 35, 65, 95 and 125 mins. The slump measurements were in each case complemented by measurements of average slump-spread (determined across two perpendicular diameters) after the concrete collapses under self-weight.

The flow table test (section 2.2.2.1(IV)) which is sometimes used to assess the workability of high-slump (≥ 150 mm) field mixes was not used in this research, partly to restrict the overall number of tests, and because of limited published data for comparison.

4.3.3.1.2 Two-point tests

As mentioned previously (page 113), the use of all single-point tests (such as the slump and flow table tests) is thought to be inapplicable in assessing the workability of HSCs[2, 30, 40, 201]. In the present study, Tattersall's two-point test apparatus in both the Medium-High and Low-Medium workability modes (i.e. the MH and LM systems) was used. The apparatus in its original form, as used by Tattersall and his co-workers, involved reading average pressures from fluctuations in the Budenberg pressure gauge to determine the torques developed during testing at different speed settings, and hence the g and h values.

In this research, the two-point test apparatus was modified by incorporating an optical interference tacheometer (fitted to the drive shaft) and a pressure transducer in the hydraulic line - to record the two-point test data in the form of flywheel

speed and pressure transducer voltages on a multi-channel Windograf digital recorder. These voltages relate respectively to the speed settings used and the corresponding pressures developed in the Budenberg pressure gauge. The test data was recorded on floppy discs, and in the form of chart-outputs to provide an opportunity for reference and/or re-analysis. The LM version of the two-point test apparatus and the Windograf recorder are shown below in **figure 4.3**.

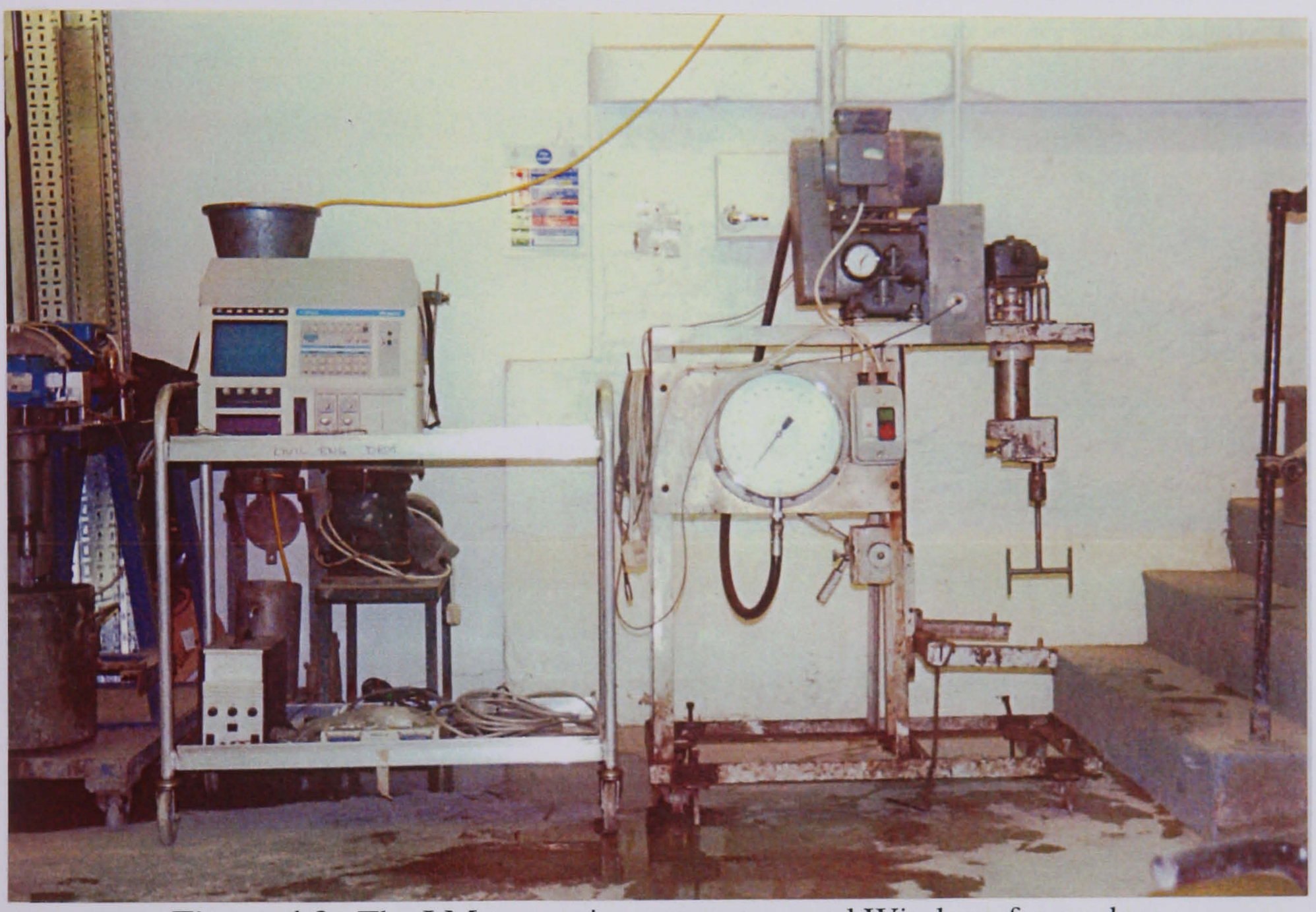

Figure 4.3 : The LM two-point test system and Windograf recorder.

(I) Testing procedure

The two-point testing procedure was as follows :

1. The apparatus was initially warmed-up for one hour at the highest speed setting used during testing (4 in the case of the MH system, and 6 for the LM system)[(231)].
2. The Windograf recorder was then connected to the flywheel and pressure transducer outputs of the two-point test apparatus.
3. Using the real time visual display facility of the recorder, the voltage traces for the flywheel and pressure transducer were zeroed, recording set on Glitch mode and chart speed on 2.5 mm/s.

4. With the test-bucket in the raised position, the impeller speed was reduced to the lowest speed setting of ½ (approximately 0.2 rps), and concrete was then gradually loaded to about 75 mm (MH system) or 140 mm (LM system) from the rim of the respective bucket.
5. The impeller speed was then increased to the highest speed setting, and maintained for either 2-4 secs (in series 3.1.2) or 12-15 seconds to allow for pressure stabilisation. At the same time disc and chart-output records were started.
6. Continuous sweeps (involving gradual reductions of the testing speed to setting ½) over approximately 30 seconds were used to record the two-point test data. (To assess segregation resistance by the Torque change (Tc) method[191] and difference in coarse aggregate contents (sections 2.7.1 and 4.3.3.2(II)), the speed was subsequently raised back to setting 4 or 6, maintained for about 2-4 secs or 12-15 secs (as in steps 1 and 5), and then sharply reduced to setting ½).
7. The test-bucket was finally emptied, and steps (5)-(6) repeated to record the machine idling pressure without concrete.

Typical chart-outputs for the two-point and idling tests are shown in **Figures 4.4** (**a**-**b**). As can be seen, the pressure voltage trace (T P_v) from the two-point test exhibits erratic fluctuations, ascribed mainly to aggregate trapping between the impeller and the test-bucket. The two-point test measurements were usually completed at 10, 30, 60, 90, and 120 minutes (workability permitting), each test being preceded by 60 seconds of re-mixing.

(II) Data analysis

The disc data from the two-point tests was initially converted to ASCII coding using appropriate software (Dasa Utilities and View to ASCII) supplied with the Windograf recorder. Although the ASCII text files can be conveniently analyzed on a spread sheet, in the research FORTRAN 77 programs were used – primarily to reduce processing time. These were written by Chai[224] (a fellow researcher at UCL) and comprised two programmes (given in Appendix A) to analyze the two-point and idling test data from the MH and LM systems (mc.exe and mct20.exe).

The algorithms used for the programs are as follows :

1. For each 0.15 drop in flywheel speed voltage, an arithmetic mean is determined.
2. The corresponding pressure voltages in each voltage interval are sorted in order of increasing magnitude and their median pressure voltage is determined. (The median was used since it is not highly influenced by large fluctuations in the pressure signal, such as those due to aggregate trapping).
3. The test data is analysed in this way until a lower limit of 0.4 volts in the flywheel speed signal (equivalent to speed settings of about ½) is reached.
4. Using the relevant calibration relationships for the two-point test apparatus (appendix A), the impeller speed (rps) and pressure (psi) for each 0.15 voltage interval is determined :

   MH impeller speed (rps) = fly wheel voltage / 0.50 / 4.6815 (gear ratio) (**4.1**)

   LM impeller speed (rps) = flywheel voltage x5/ 0.50 / 2.25 x 20 (gear ratio) (**4.2**)

   Total pressure (psi) = 176.4 x two-point test pressure voltage - 155.5 (**4.3**)

   Idling pressure (psi) = 176.4 x idling pressure voltage - 155.5 (**4.4**)

5. The net pressure and torque for each voltage interval is calculated as :

   Net pressure (psi) = Total pressure (with concrete) – Idling pressure (without)

   = 176.4 x { (total pressure – idling pressure) voltage } (**4.5**)

   Torque, T (Nm) = 0.0215 x { Net pressure (psi) } (**4.6**)

6. The two Bingham parameters (g and h) from the best fit flow curve

   $$\mathbf{T}\ (\mathrm{Nm}) = \mathbf{g} + \mathbf{h}.\ \mathbf{N}\ (\mathrm{rps}) \qquad (\mathbf{4.7})$$

and the correlation coefficient are finally computed by linear regression. A typical output for the LM system (using programme mct20.exe) is shown in **figure 4.5**.

Comparisons of the Bingham values from the digital analysis with subjective readings from the chart-output traces and fluctuations in the Budenberg pressure gauge showed good agreement, typically within ±0.20 Nm and ±0.25 Nms.

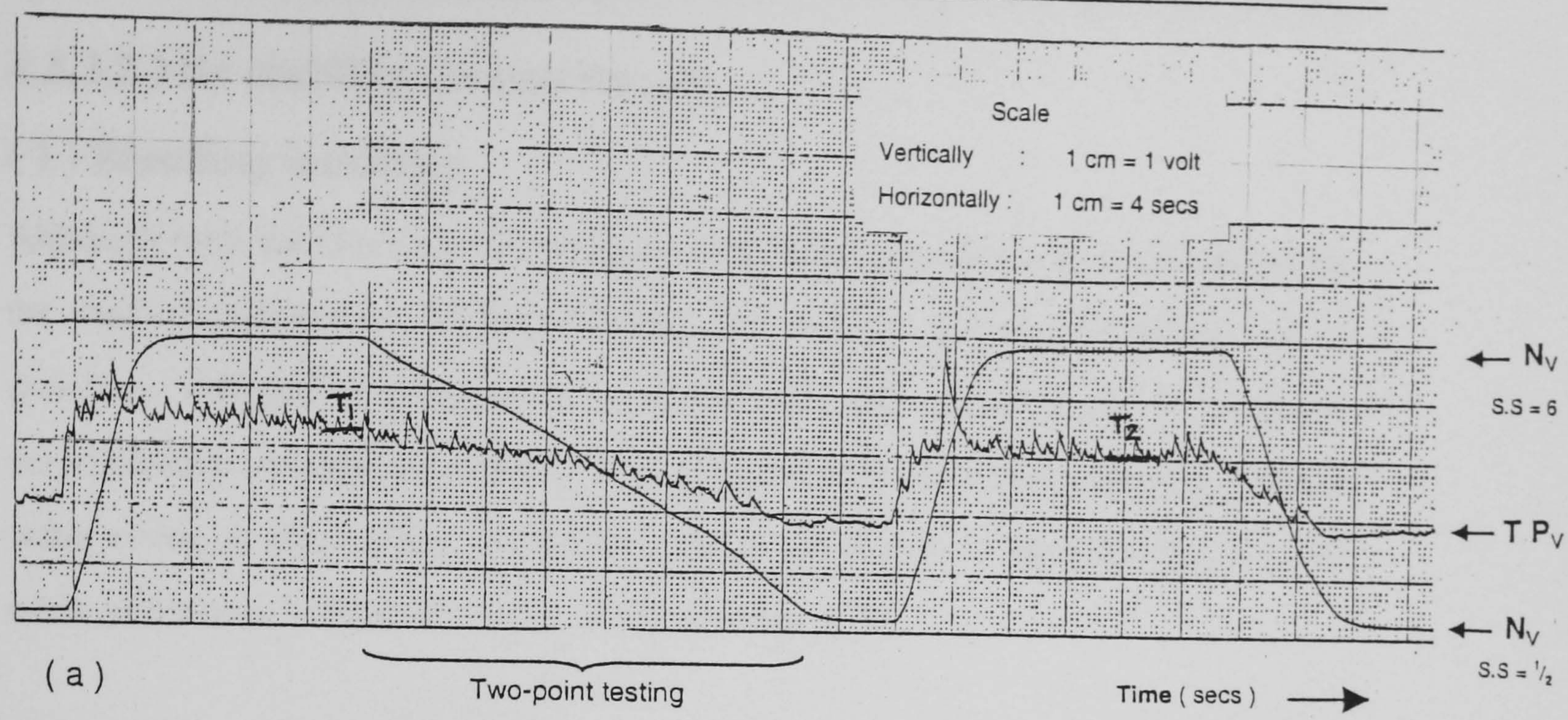

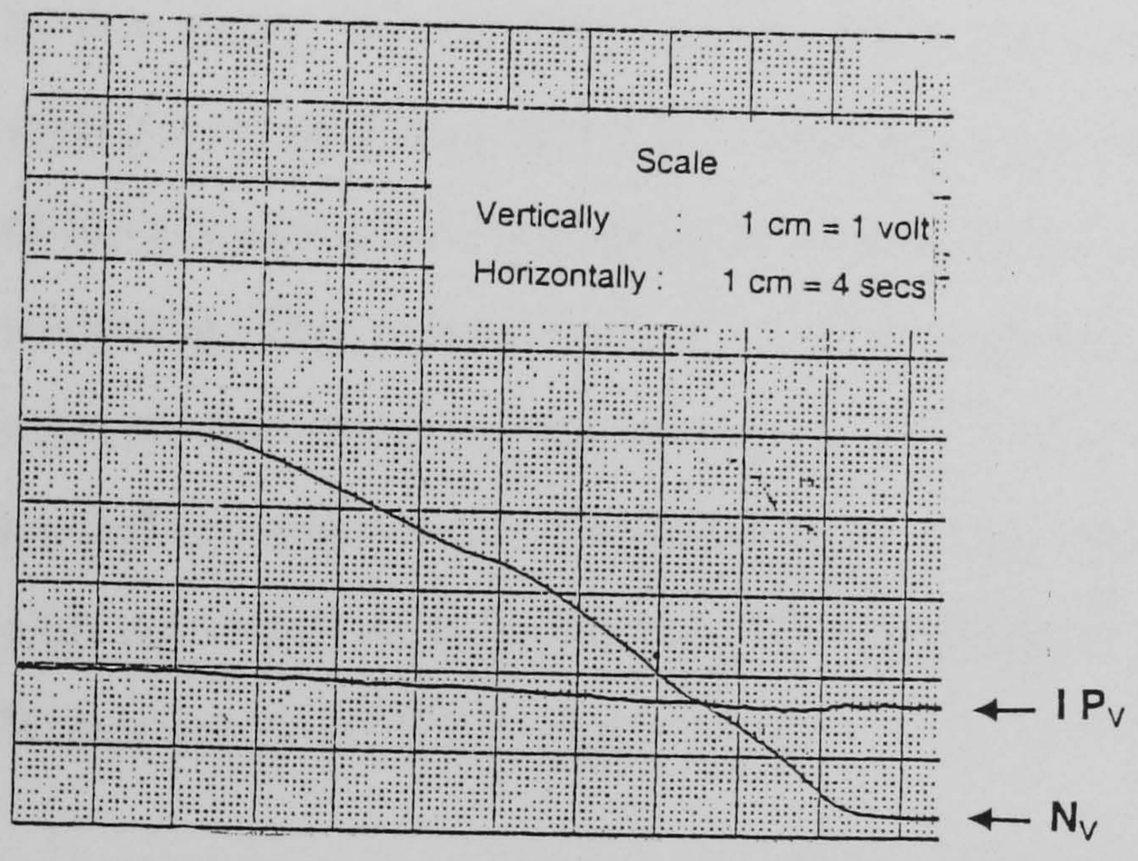

Figure 4.4 : Typical chart-outputs for (a) two-point and (b) idling tests (using the LM system).

Note : **S.S** = Speed setting (6 to 1/2).
T P_V = Total pressure voltage trace
I P_V = Idling pressure voltage trace
N_V = Flywheel speed voltage trace

Torque change, $T_C = T_1 - T_2$ (in Nm)

```
Run mct20.exe under DOS system(<0.15,k1=100,<0.40 out  T=0.0215P,use median,
May/97, gear 20, 2.25 LM)   W/C = 0.26 : 10 % CSF ((Control))
Test:   M1MAR26        M1 Trigger Date:          03/26/1998      03/26ime:
    Test:       IP1MAR2     Trigger Date:        03/26/1998      03/26Time:
Idling pressure n and correlation coefficient r==>          108
Idling pressure ai bi==>        1.51970          .07459
 n    flywheel speed voltage  pressure voltage        idling pressure voltag
 800            4.823                  3.260                  1.879
 400            4.474                  3.153                  1.853
 500            4.146                  3.045                  1.829
 500            3.826                  2.957                  1.805
 400            3.482                  2.862                  1.779
 400            3.126                  2.799                  1.753
 300            2.738                  2.635                  1.724
 400            2.419                  2.591                  1.700
 400            2.048                  2.474                  1.672
 400            1.708                  2.332                  1.647
 300            1.345                  2.200                  1.620
 300             .969                  1.946                  1.592
 300             .584                  1.824                  1.563
-------------------------------------------------
Torque(Nm)      Shaft speed(rps)
  5.237                 1.085
  4.928                 1.007
  4.614                  .933
  4.371                  .861
  4.107                  .783
  3.967                  .703
  3.456                  .616
  3.380                  .544
  3.040                  .461
  2.598                  .384
  2.201                  .303
  1.344                  .218
   .990                  .131
-------------------------------------------------
n=13
Two point test constant g(Nm)=   .78
Two point test constant h(Nm s)= 4.25
Linear regression correlation coefficient r= .9862
90% confidence limits on g(%)= 33.99
90% confidence limits on h(%)=  9.11
```

Figure 4.5 : Digital analysis corresponding to the two-point test and idling data shown in figure 4.4 (using programme mct20.exe).

4.3.3.2 Mix stability measurements

(I) Bleeding tendency

Although both the bleeding rate and total bleeding capacity can be measured using the method outlined in ASTM C232-92, the method is time consuming and is therefore difficult to carry out concurrently with other tests. It involves consolidating a sample of concrete in a container, from which the amount of bleed water rising to the surface is carefully drawn off every 10 mins for the first 40 mins, and every 30 mins thereafter until bleeding stops.

In this study, the bleeding tendencies of the mixes were visually assessed by subjectively awarding bleeding marks (B_{MS}), on a **scale of 10 to 0**, for the quantity of bleed water accumulating on the surface of the concrete after about 30 secs from re-mixing. This assessment was usually made during sampling and loading of the concrete for two-point testing. A mark of " 10 " was used for very high bleeding tendencies, with extensive channeled bleeding, whilst " 0 " was used for dry mixes with no visible surface bleeding. The method is consistent with that adopted by Wimpenny et al[191] (c.f. figure 2.65).

(II) Segregation resistance

Although segregation is difficult to assess quantitatively, it is often easily observed during handling, testing and placing of fresh concrete. One example where segregation is often noticed during testing is in the flow table test. The jolting action applied during this test encourages segregation of the aggregates from the mortar, and if the mix is not stable, the larger aggregate particles will separate out and move toward the edge of the table[8]. The suitability of the funnel test (c.f. figure 2.64) proposed by Miura et al[206] in assessing segregation resistance has not been appropriately validated, and the test (like the vibration test method used by Tachibana et al[18] (c.f. figure 2.63)) may involve unique shearing conditions and, therefore conceal any possible relations with the Bingham parameters.

In the present research, it was noticed that after shearing the concrete in the MH

two-point test apparatus, some segregation was apparent in the upper and lower parts of the test-bucket. With the LM system, two distinct forms of segregation were observed. Either a sedimentation of the coarse aggregates from the top to the bottom of the test bucket (as in the MH system), or a dislodgement of the coarse aggregates from the centre to the sides of the bucket. The former was apparent in high slump mixes, whereas the latter was more noticeable in mixes with slumps less than or equal to about 150 mm.

The differences in coarse aggregate contents after two-point testing (as shown in **figures 4.6(a-b)**) were, therefore, used as indices to quantify the segregation resistance of fresh concrete mixes. In both cases, samples of approximately 2 kg of concrete were taken from the locations shown, placed on a 5 mm sieve, and then washed to remove their mortar fractions. After air-drying of the coarse aggregates, the segregation index (SI) was determined as :

$$\mathbf{SI}\ (\%) = \frac{(\mathbf{W_1} - \mathbf{W_2})_{\text{at SSD}}}{\text{Total weight of sample}} \times 100 \qquad (\mathbf{4.8})$$

where W_1 and W_2 are the weights of the aggregates at locations 1 and 2 in figure 4.6. For each mix, two measurements of segregation resistance (corresponding to the first and last two-point tests) were usually made using the SI, or both the SI and Tc methods (discussed in chapter 5).

4.3.3.3 Compactability (and vibration response) measurements

There is currently no accepted test for measuring the compactability of fresh concrete. The vibration response tests by de Larrard et al[49] and others[89-92, 210-216], as mentioned previously in section 3.2.3, have not managed to sufficiently describe how the Bingham parameters vary during compaction by vibration. In the present research four test methods (three in the preliminary tests (series 3.1.2), and one in series 3.4) were used to assess the compactability of fresh concretes.

(I) Preliminary compactability tests

The first three methods comprised :

1. A **cube** (or bulk density) **method** (**figure 4.7(a)**), involving casting fresh concretes (under self-weight only) in 150 mm steel cubes/moulds and measuring their bulk density in the hardened state. (A similar method was used by Chai[224] to assess the self-compacting properties of SCC mixes).
2. The **compacting factor test** (c.f. figure 2.2(b)), which is the most widely used field test for assessing the compactability of fresh concretes. The test was originally developed by Glanville et al[60] to measure compactability in accordance with their definition of workability (pages 13, 16).
3. A **cylinder-vibration method** (**figure 4.7(b)**), involving filling a 300x150 mm steal cylinder with fresh concrete and then subjecting it to vibration (at 50 HZ and an amplitude of 0.7 mm). The amount of subsidence (or drop in height) undergone by the concrete after vibration was used as a measure of compactability. (A similar method was described by Tattersall[7], and has recently been incorporated in BS EN 12350-4:2000[233] for measuring the compactability of fresh concretes).

In both the cube and cylinder-vibration methods care was taken during filling (by tilting the moulds to about 45^0) to minimize any work being done on the concrete. When filled, the top surface of the concrete was in each case gently struck flush. (The cube and compacting factor tests in series 3.1.2 were carried out with the assistance of a fellow researcher).

(II) Spread-time (vibration response) method

This method (developed in chapter 8) was used to assess the flow properties under self-weight and during compaction by vibration. The method (**figure 4.8**) involves using a hand-held tape-measure to determine the slump-spread at 5, 10, 20, 30, and 60 secs after removal of the slump cone - with or without vibration. The spread-time measurements were aided by marking 10 mm - spaced circles from the centre of the slump board. Additional details of the test procedure used to determine the vibration response of the mixes tested are given in chapter 8 (figure 8.7).

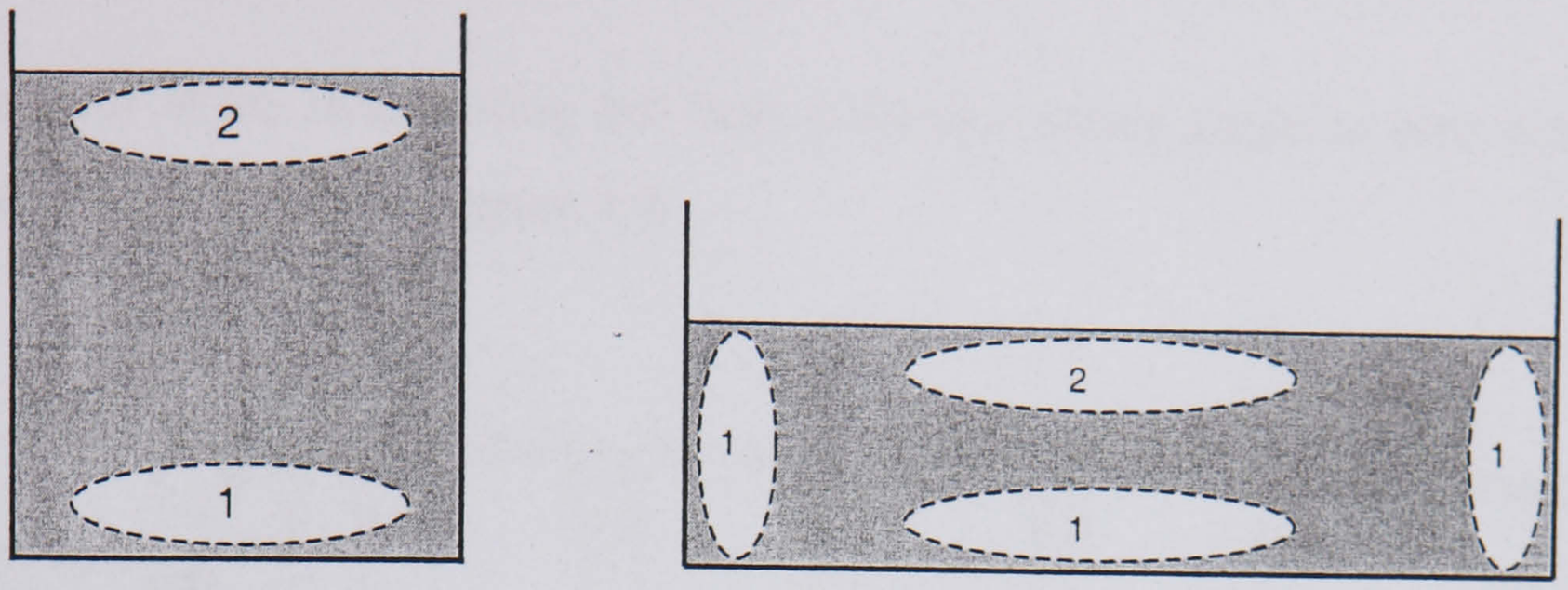

Figure 4.6 : Sampling locations for assessment of segregation resistance with the MH and LM two-point test systems.

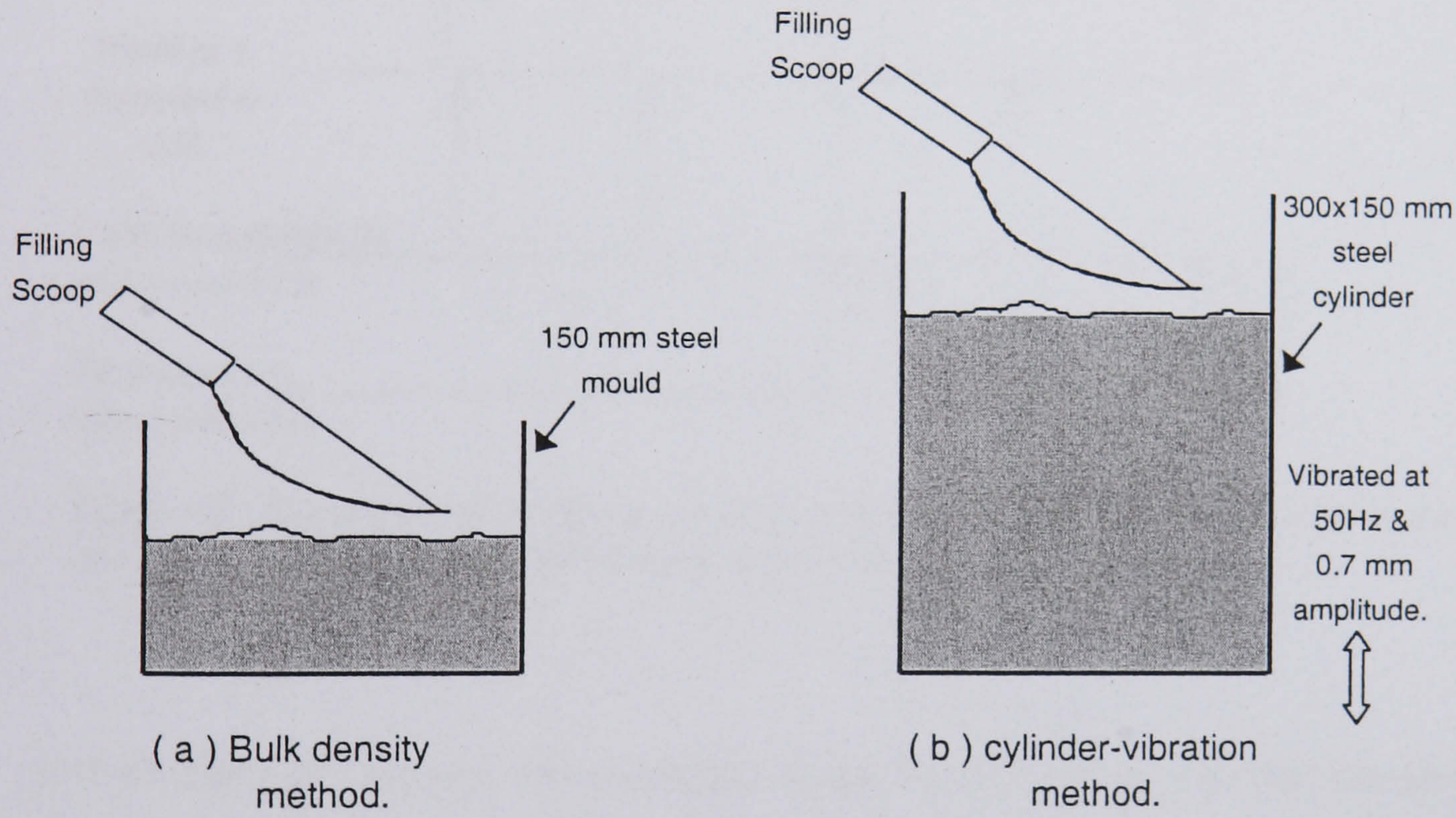

Figure 4.7 : Test methods used for assessing compactability under (a) self-weight and (b) vibration.

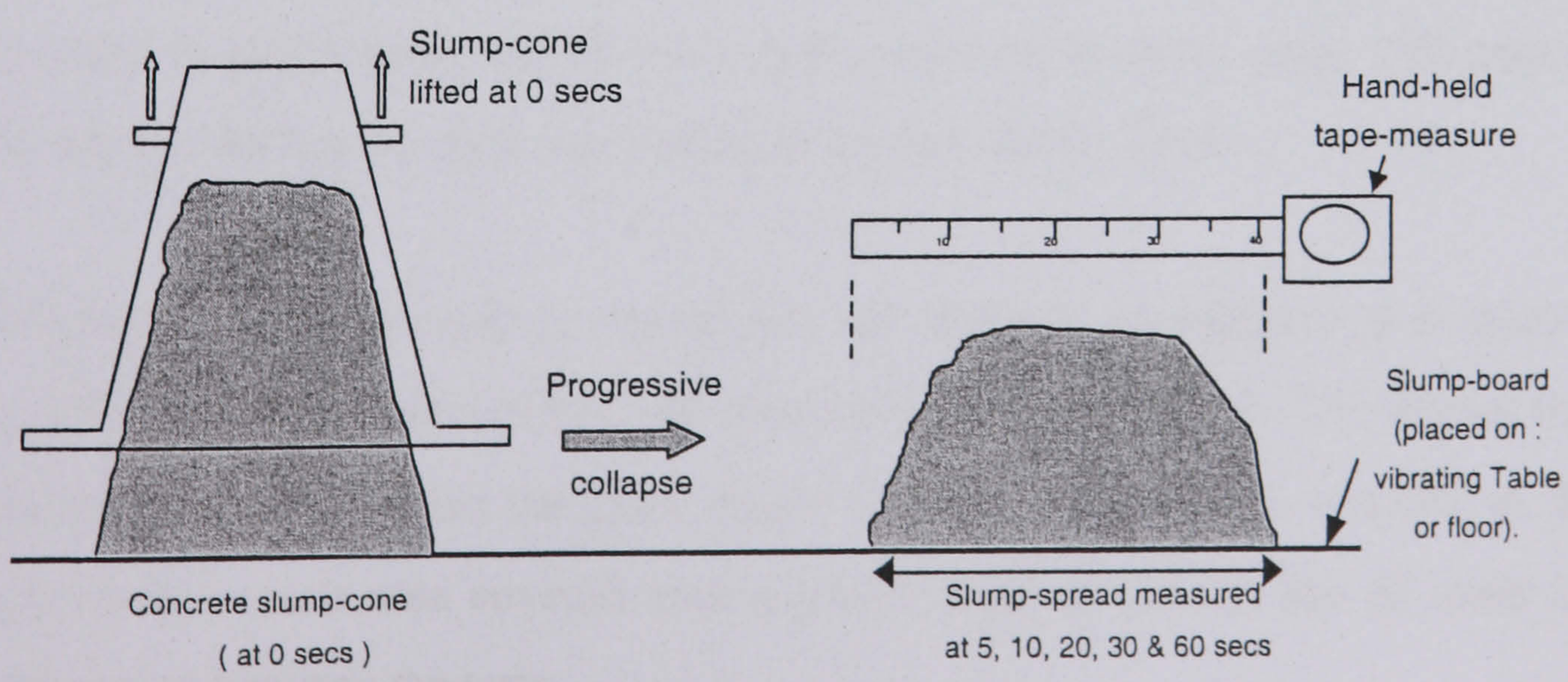

Figure 4.8 : Spread-time method used to assess the vibration response (and flow properties under self-weight) in terms of the slump-spread at 5, 10, 20, 30 & 60 secs of deformation.

4.3.3.4 Summary of mixing and fresh property testing sequence

A summary of the main mixing and fresh properties testing sequence used in the research is given below in **figure 4.9**.

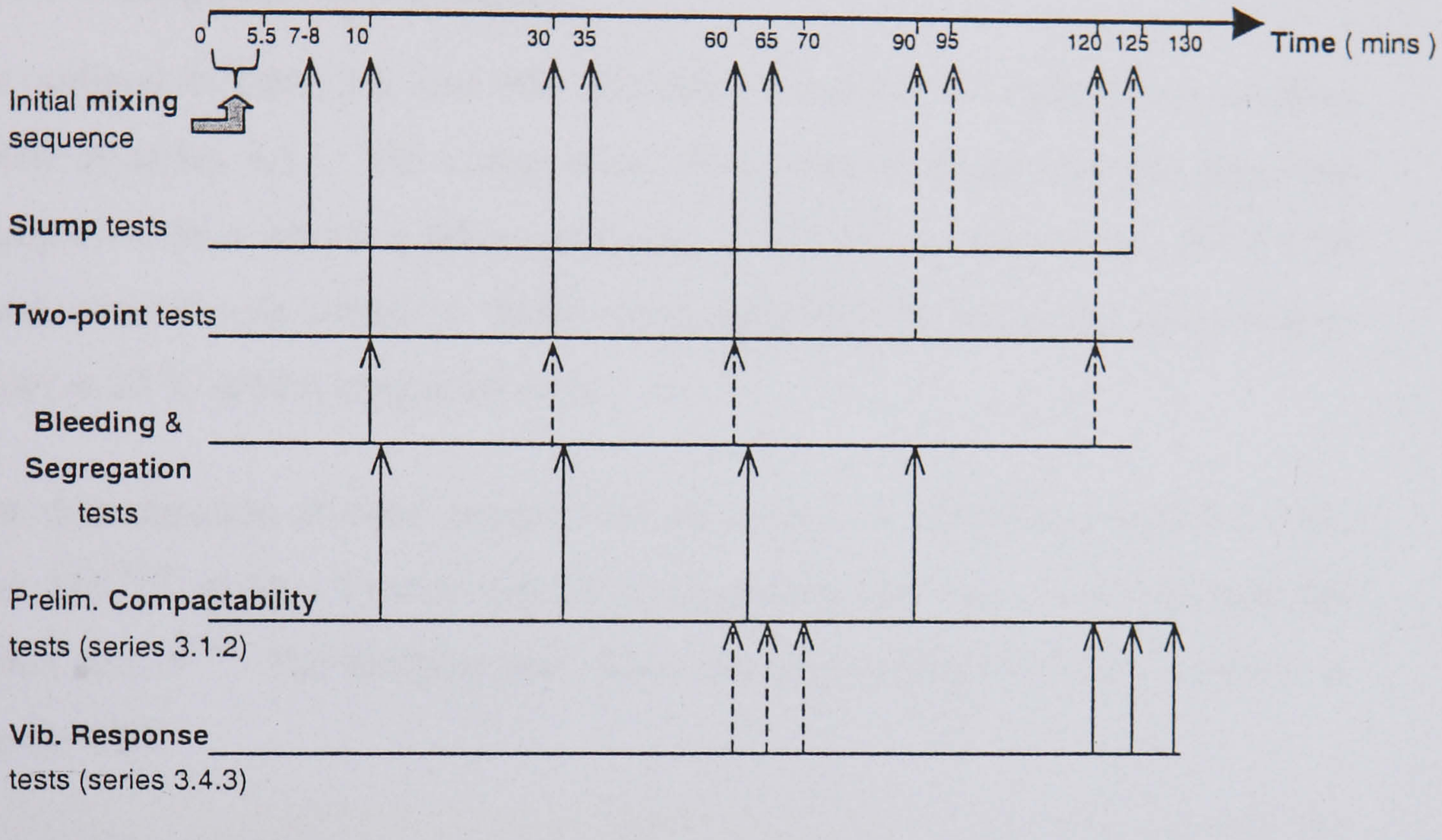

Figure 4.9 : Summary of main mixing and fresh property testing sequence used (variations in testing time, represented by dashed arrows, are outlined in subsequent chapters).

In each case strict control was exercised to ensure uniform/reproducible sampling and testing times. For the slump and other single-point tests, the time lapsed between re-mixing and completion of the tests was kept within 90-120 secs. For the two-point tests, the loading time of the concrete into the test bucket also typically varied between 90-120 secs, and as described earlier (page 139, step 6) the actual shearing duration was limited to approximately 30 secs.

To ensure consistent testing conditions, the ambient temperature and relative humidity were monitored before and after the fresh property tests. The former was generally 20±2 ^{0}C, whilst the latter ranged between 55-75%. The concrete in the mixer was in each case covered with a plastic sheet to prevent loss of water by evaporation between the tests.

4.4 Tests on hardened concrete

After completion of the vibration response tests in series 3.4.3, duplicate mixes were produced to examine the effects of different degrees of compaction on the 28-day compressive strength, homogeneity and density of the hardened concrete.

4.4.1 Compressive strength

As outlined in Table 3.5, two 100 mm cubes were cast for each of the variables listed in series 3.5.1. The cubes were filled using a single concrete pour and compacted on a vibrating table (operating at 50 HZ and amplitudes of 0.1-0.70 mm), covered with polythene sheets, demoulded after 24 hours, and then cured in water at 20 ^{0}C until testing at 28 days.

The determination of cube strength was carried out in accordance with BS 1881: part 116[234], using a Contest GD10A compression machine complying with BS 1881: part 4[235]. The machine used has a capacity of 2500 KN and is shown in **figure 4.10**.

Figure 4.10 : Contest GD10A compression machine used to measure 100 mm cube strengths.

4.4.2 Column (homogeneity) tests

Nine short columns (500x100x100 mm) were cast to assess the effects of segregation during compaction on the homogeneity (uniformity) of the hardened concrete. As with the 100 mm cubes, the columns were in each case filled using a single concrete pour, placed on the vibrating table and compacted at the different vibration durations/amplitudes listed in Table 3.5.

The variations in concrete homogeneity or quality after vibration were assessed in two ways: by determining the changes in column strength and column density with height. Due to geometric and surface irregularities of specimens cut from the columns, the strengths were predicted non-destructively by comparing ultrasonic pulse velocity (UPV) measurements (using a Pundit device) at heights of 50, 150, 250, 350, and 450 mm from the base of the columns. In each case, the UPV through the concrete was carried out in accordance with BS 1881: Part 206[236], and determined from the time taken for the pulse to travel between transmitting and receiving transducers held on opposite sides of the columns. The variations in column strengths with height were determined from a relationship obtained between the changes in UPV and compressive strength measured on 100 mm cubes (details given in section 9.5, and Appendix E).

4.4.3 Density measurements

In accordance with BS 1881 : part 114[264], the densities of the cube and column specimens in sections 4.4.1-4.4.2 were measured by weighing them in air and then in water. The density (ρ) in kg/m^3 was then determined as :

$$\rho = \frac{W_A}{(W_A - W_W)} \cdot \rho_W \qquad (4.9)$$

where, W_A is the mass in air (in kg),

W_W is the mass in water (in kg), and

ρ_W is the density of water (i.e. 1000 kg/m^3).

Chapter 5

Preliminary Rheological Measurements

5.1 Introduction

The literature review in chapter 2 showed a lack of universally accepted test methods to assess the workability, mix stability and compactability properties; and uncertainties as to whether these constitute distinct components of the rheology (or flow properties) of fresh concrete. When the workability properties are expressed in terms of the Bingham model, from measurements with any of the existing two-point test devices, they depend on both the concrete properties and apparatus geometry, but provided that the latter is kept constant then different concretes can be compared. Lower Bingham (g and h) values indicate a more fluid/workable mix, whilst the rates at which they increase with time is indicative of the rate of loss of workability.

This chapter presents the results of the preliminary rheological measurements used to:

- Examine the **effects of aggregate absorption** and a **SNF superplasticizer** on the rate of loss of workability **in NSC**.
- Assess the **effects of** decreasing **w/b ratios** of 0.42-0.22 **on** the:
  - rate of **loss of workability**,
  - variations in **mix stability** (i.e. bleeding and segregation tendencies),
  - variations in **compactability** (under: self-weight, a standard amount of work, and vibration).
- Examine the existence of possible **relationships between** the three **rheological sub-divisions** (viz. mobility, mix stability and compactability) as defined by Ritchie[61].
- **Compare** the capabilities of Tattersall 's **MH and LM** two-point test **systems** to measure representative variations in workability (for different shearing conditions, equipment geometries, and successive redoses of superplasticizer).
- Assess the **validity of mortar tests** in fixing the superplasticizer dosages needed for a given slump, and in predicting the workability properties of concrete.

5.2 Effects of aggregate absorption and superplasticizing in NSC

As mentioned in section 2.4.2, the absorption of mixing water by dry aggregates is considered to be the most significant aggregate characteristic influencing the workability properties[103], and it has been suggested that up to 30 litres of water could migrate from the cement paste to fill the aggregate pore spaces during the first hour[49]. The removal of such large amounts of mixing water would be particularly critical at low w/b ratios, and can increase the rate of slump loss (c.f. figures 2.11 and 2.18). It has also been reported that the presence of superplasticizers increases the rate of slump/workability loss primarily as a consequence of:

- the closer proximity of the cement particles at low w/b ratios[34, 99] (figure 2.10),
- a greater exposure of the cement particle surfaces to increased hydration[8, 22, 136],
- the amount of superplasticizer molecules trapped by newly formed ettringite crystals[7, 39, 101, 111, 119] (c.f. figure 2.29(b)).

This section examines the effects of aggregate absorption and a SNF (Conplast SP 435) superplasticizer on the loss of workability in NSC by comparing the use of dry and pre-saturated aggregates (at 0.48 w/b ratio), and mixes with and without the SNF superplasticizer (at 0.45 w/b ratio). Since the effects of aggregate absorption can be masked by those of the hydrating cement, the work includes studies on both neat portland cement and PFA mixes. The mix proportions used in the investigation were given in Table 3.7(a). The loss of workability of the mixes was in each case assessed by the slump test and the MH two-point test apparatus, with measurements taken after the initial mixing sequence, and then at 15-25 minute intervals. The results obtained are presented in **figure 5.1(a-c)**.

5.2.1 Effects of aggregate absorption

A comparison of the slump curves with the dry and pre-saturated aggregates in **figure 5.1(a)** shows that the dry aggregates (in both the portland cement and PFA mixes) give similar initial slumps, but more rapid slump losses. The results therefore mean that the capacity of the dry aggregates to absorb mixing water is not fulfilled during the first 5 minutes mixing sequence, and that the aggregates continue to absorb water with time. The 150mm slump difference between the PFA mixes in the

first two hours, and the slump vs water content relationship in figure 2.8, suggest that the quantity of free water absorbed by the dry aggregates during mixing is approximately 35 l/m^3. This is comparable to the full capacity of the aggregates (29.1 l/m^3, determined from the SSD values in Table 4.4) and the 30 litres reported by de Larrard[49] during the first hour (page 32).

As with the slump test results, the two-point test results in **figure 5.1(b-c)** also show that the dry aggregates (in both the portland cement and PFA mixes) give similar initial workabilities, and much higher rates of loss of workability compared to the pre-saturated aggregates. The higher rates of loss of workability are reflected by much larger time-dependent increases in yield value with the dry aggregates (consistent with their higher slump losses in figure 5.1(a)), but no systematic or overall pattern for the development of plastic viscosity. From these results, it can therefore be concluded that as soon as the dry aggregates come into contact with the mixing water they start to absorb water, and continue to do so for at least two hours after the initial mixing sequence.

This contradicts the suggestions by Neville[104] and others[105-106] that the effects of aggregate absorption are insignificant, and become negligible after the first 15-20 minutes of mixing due to coating of the aggregates by cement paste. The fact that the pre-saturated aggregate PFA mix gives similar time-dependent increases in both the Bingham parameters, also contradicts de Larrard et al's suggestion[49] that pre-saturated aggregates primarily reduce loss of workability by minimising the rate of increase in plastic viscosity (c.f. page 32, figure 2.14). The small but systematic increases in both the Bingham parameters of this mix (where the effects of the hydrating cement and aggregate absorption are eliminated) may be due to losses of free water by evaporation between successive tests.

5.2.2 Effects of SNF superplasticizer

A comparison of the slump loss curves for the superplasticized and plain mixes in figure 5.1 shows that the fluidizing action of the SNF superplasticizer is of short-duration, and significantly increases the rate of slump loss (from about 70 mm/hr to

140 mm/hr). This is consistent with the observations by Perenchio et al[127] and others[99, 126, 128] (page 41), but contradicts Pollet et al's conclusion[100] that only the water content influences the rate of slump loss (c.f. figure 2.12).

In agreement with Banfill's observations[124] in flowing NSC (c.f. figure 2.17), the two-point test results in **figure 5.1(b-c)** show that although the fluidizing action of the superplasticizer reduces the initial yield value, it increases the initial plastic viscosity (by approximately 0.4 Nms (or 25%)). This however disagrees with the first use of superplasticizers[34] (page 34) that they increase the workability (i.e. reduce both the Bingham parameters). The sharp reductions in plastic viscosity with time also disagree with the expected losses in workability (i.e. increases in the Bingham parameters) and, Banfill's results[124] which show no time-dependent reductions in plastic viscosity as measured with the MH system. The sharp reductions in plastic viscosity would in practice imply that the superplasticized and non-superplasticized mixes become increasingly more workable with time and decreasing slump.

However, at slumps lower than 100 mm the helical impeller displaced increasing amounts of concrete away from the centre of the test bucket, and caused noticeable holing of the concrete around the central shaft after two-point testing at very low slumps of about 50 mm. That is, the concrete displaced by the impeller at the beginning of the two-point test failed to return to the centre of the test bucket, and was partially sheared at low impeller speeds. (The effect is further discussed in section 5.5.3).

According to Tattersall[7] for low-medium workability concretes (having slumps between 25 and 75 mm), the apparatus should be used in its LM mode, with planetary motion of the H-shaped impeller and larger test bucket (c.f. page 21). He has however not provided any supporting data to substantiate this, and/or commented on the capabilities of the two versions of his apparatus to measure time-dependent losses of workability. The capability of the MH system to measure loss of workability in high-medium slump HSCs is examined in the next section.

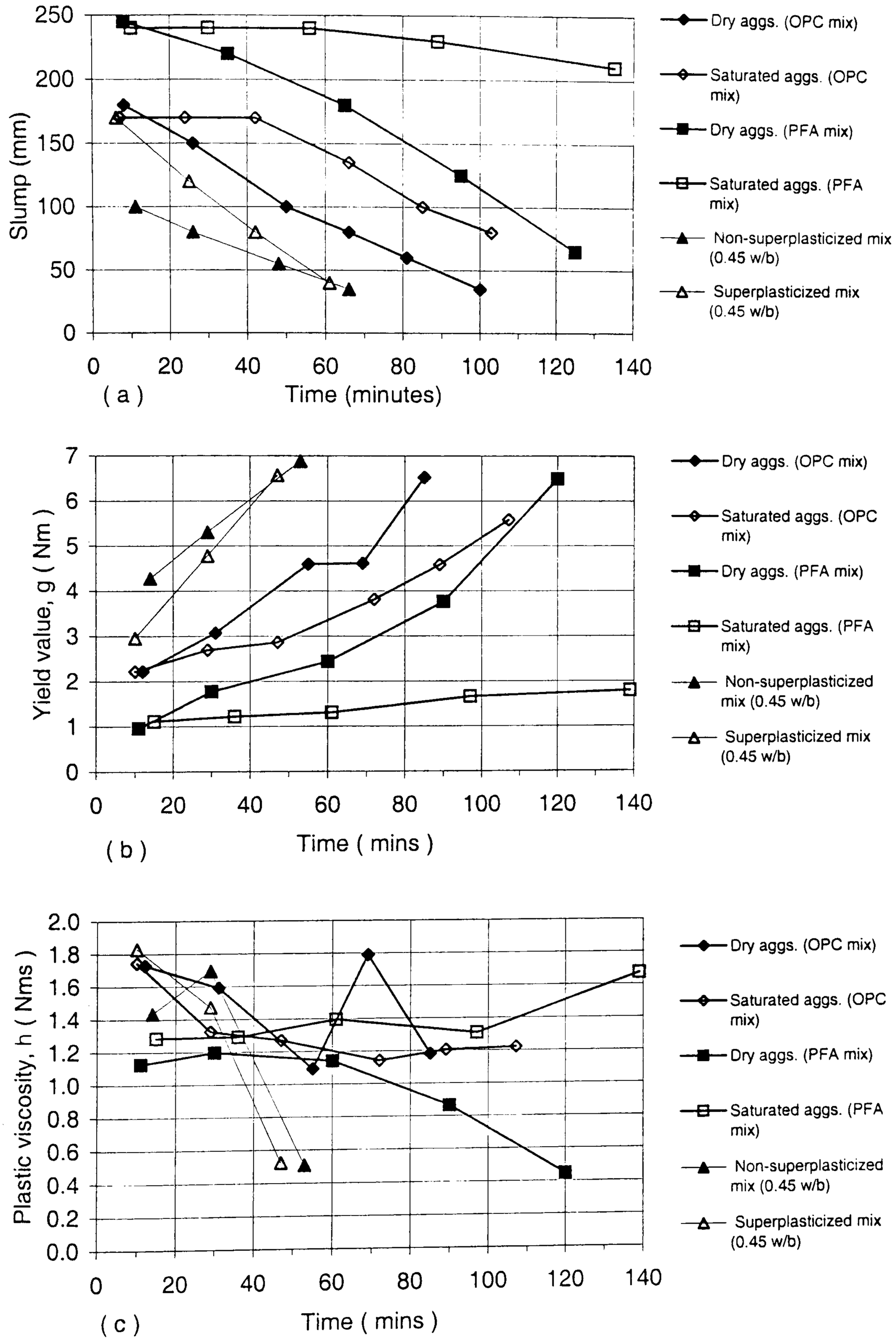

Figure 5.1: Effects of dry and pre-saturated aggregates, superplasticized and plain NSC mixes on (a) slump loss, and variations in (b) yield value and (c) plastic viscosity with time (mix details given in Table 3.7(a)).

5.3 Effects of decreasing w/b ratio on the rheological properties of HSC

In addition to measurements of loss of workability, the tests in HSC also included other rheological measurements to account for the variations in mix stability and compactability with decreasing w/b ratios of 0.42-0.22 and time. The measurements are therefore in accordance with Ritchie's[61] sub-division of rheology of fresh concrete into mobility/workability, mix stability and compactability as shown in figure 2.1. The loss of workability measurements involved slump tests at 7 to 90 minutes; and two-point tests at 10, 30, and 60 minutes after mixing. To minimise the effects of segregation during two-point testing as reported by Wallevik and Gjorv[84], the initial testing speed (at setting 4) was maintained for a short duration of 2-4 seconds, and the 30 seconds continuous sweep (described in chapter 4) was used.

As described in section 4.3.3.2, the bleeding tendencies were assessed subjectively, whilst the segregation resistance was quantified in terms of the differences in coarse aggregate contents in the MH test bucket (c.f. figure 4.6(a)) and, the torque changes (T_C) occurring during the two-point tests[84, 191]. The T_C values were determined from differences in the initial and repeat torques at speed setting 4.

The variations in compactability were assessed by the cube-density method, the compacting factor test, and cylinder vibration method (described in section 4.3.3.3). As mentioned previously, the cylinder-vibration method assesses the compactability in terms of the drop in height (or amount of subsidence) of the concrete after vibration. In contrast, the cube-density method assesses the changes in self-compacting properties (in terms of hardened concrete bulk density), whereas the compacting factor test determines the degree of compaction due to the application of a standard amount of work. This was performed concurrently with the two-point tests, whilst the cube and cylinder-vibration methods were generally completed 2 minutes after.

The mix proportions used in the investigation were given in Table 3.6. SNF (Conplast SP 435) superplasticizer dosages of 0.45, 0.55, 0.70, 0.90, 1.30, 2.15 and

5.00% (s/w/b) were respectively used to obtain an initial target slump of 220±5 mm in mixes 1-7 (i.e. at w/b ratios of 0.42, 0.40, 0.38, 0.34, 0.30, 0.26 and 0.22). The HSCs tested in this chapter were all produced using neat OPC mixes and the ½ min delayed addition of superplasticizer shown in figure 4.1 (procedure 1).

5.3.1 Effects on loss of workability

Figure 5.2(a) shows that the reduction in w/b ratio from 0.42 to 0.26 produces continuous slump losses of 120-140 mm/hr, but reveals no systematic pattern with decreasing w/b ratio. These results therefore contradict the widely accepted view that the rate of slump loss increases with reduced w/b ratio[14, 16, 19, 30, 34, 39] (c.f. section 2.3, figure 2.18), and would in practice imply similar initial workabilities and rates of loss of workability at both low and high w/b ratios.

In agreement with the observations by Tattersall[7, 96] and others[40, 53, 97] (c.f. figure 2.9, Table 2.1), the two-point test results in **figure 5.2(b-c)** however show that, despite their constant initial slumps, the 0.42-0.26 w/b ratio mixes exhibit considerable reductions in initial workability (i.e. higher Bingham parameters) with decreasing w/b ratio. As can be seen, the increases in the initial yield values are particularly pronounced at the 0.26 w/b ratio, and are about three times larger than those at the 0.30 w/b, and about ten-twenty times larger than at the 0.38-0.42 w/b ratios. The corresponding increases in initial plastic viscosity are more noticeable below the 0.34 w/b, and are nearly twice as large at the 0.26-0.30 w/b ratios compared to those at 0.38-0.42 w/b ratios.

In terms of loss of workability, the two-point test measurements (with one exception at 0.26 w/b and 30 mins) show continuous increases in yield value, but reductions in plastic viscosity with time. These are particularly pronounced at the 0.30 and 0.26 w/b ratios, and are therefore in contradiction with the reasonable expectation that the plastic viscosity (like the yield value) increases with time and more rapidly with reduced w/b ratio.

In contrast with the 0.42-0.26 w/b ratio mixes, the 0.22 w/b ratio mix was more

difficult to produce and, even the very high superplasticizer dosage used (5.00%), did not give the target slump of 220 mm. The workability of the mix was so low that the concrete seemed to actively resist rodding with the tamping-rod during slump testing, was more difficult to remove from the mixer, and generated very high pressures (up to 400 psi) during loading for two-point testing. These handling difficulties meant that the two-point testing speed could not be raised above setting 2 (or about 0.6 rps) without damaging the pressure transducer.

Observations of the slumping behaviour of the mixes, after removal of the slump cone, indicated that the slump-flow time (i.e. the period for the concrete to stop deforming under self-weight) varies considerably with the reduction in w/b ratio. Mixes at high w/b ratios collapsed rapidly, whilst those at lower w/b ratios slumped at increasingly slower rates.

The initial slump-flow time at the 0.22 w/b ratio was more than 120 seconds, compared to about 90 and 30 seconds at the 0.26 and 0.30 w/b ratios, and 20-10 seconds at the 0.34-0.42 w/b ratios. These reductions in slump-flow time are in contrast with instantaneous slumps observed with the NSC mixes in section 5.2, and are therefore consistent with the higher workabilities (i.e. lower Bingham values) from the two-point test measurements.

The relationships in **figure 5.3**, which include NSC data reported by Tattersall and Banfill[66] (under both laboratory and field conditions), suggest that the apparent success of the slump test in adequately evaluating the workability properties of NSCs, may rely on the fact that the plastic viscosities at high w/b ratios vary within a narrow range of 1-2 Nms. That is, the workability of NSCs is mainly governed by changes in the yield value which can range between 1-8 Nm; and the lower the plastic viscosity, the more representative the slump will be of the workability of the concrete. The fact that the plastic viscosities in HSCs vary over a wider range (4-15 Nms) and show no overall correlation with the yield value demonstrates the importance of the two-point test in measuring the workability of low w/b ratio mixes. (Relationships between the slump-flow time and the Bingham parameters of HSCs are examined in chapter 6).

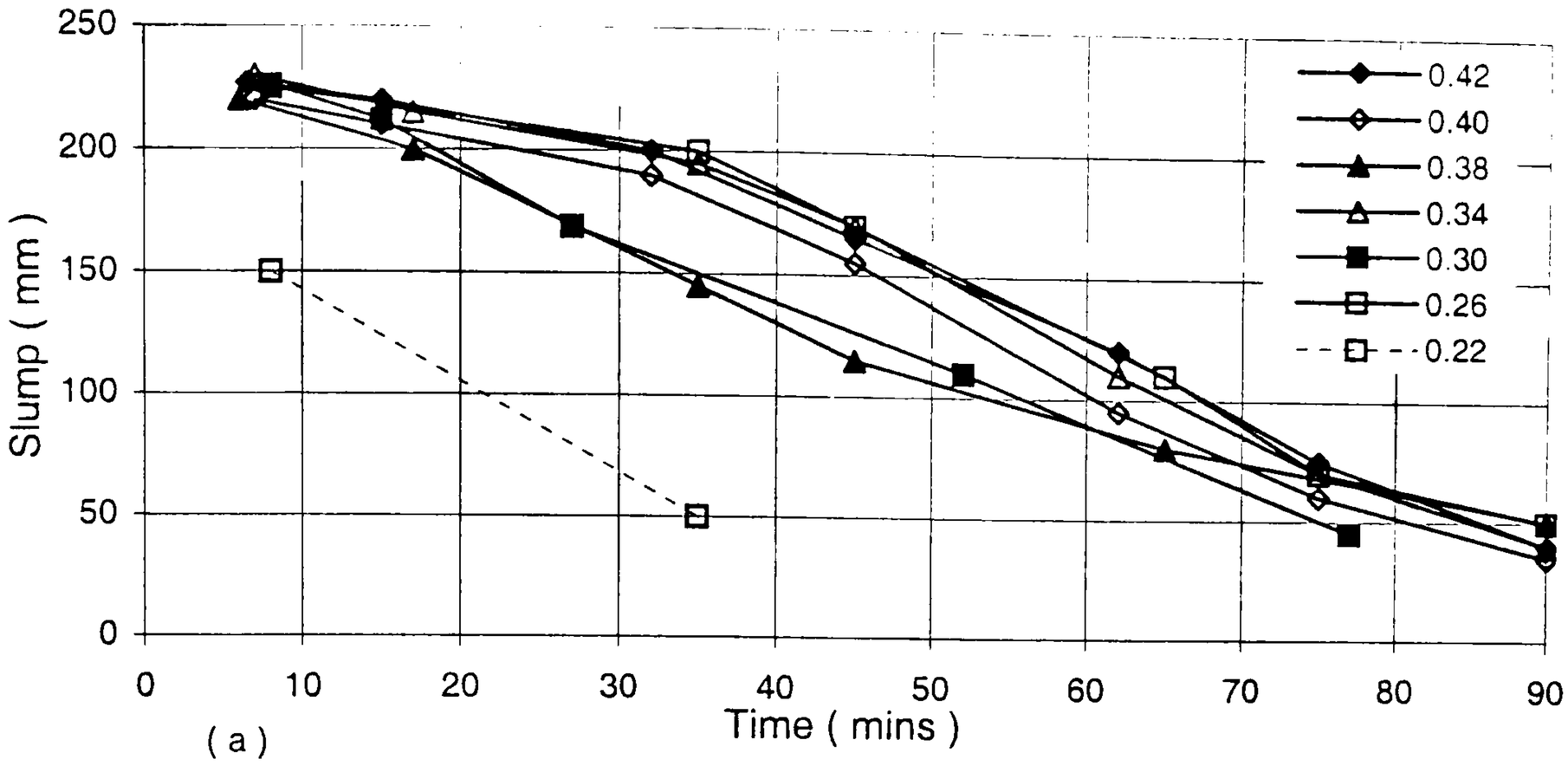

(a)

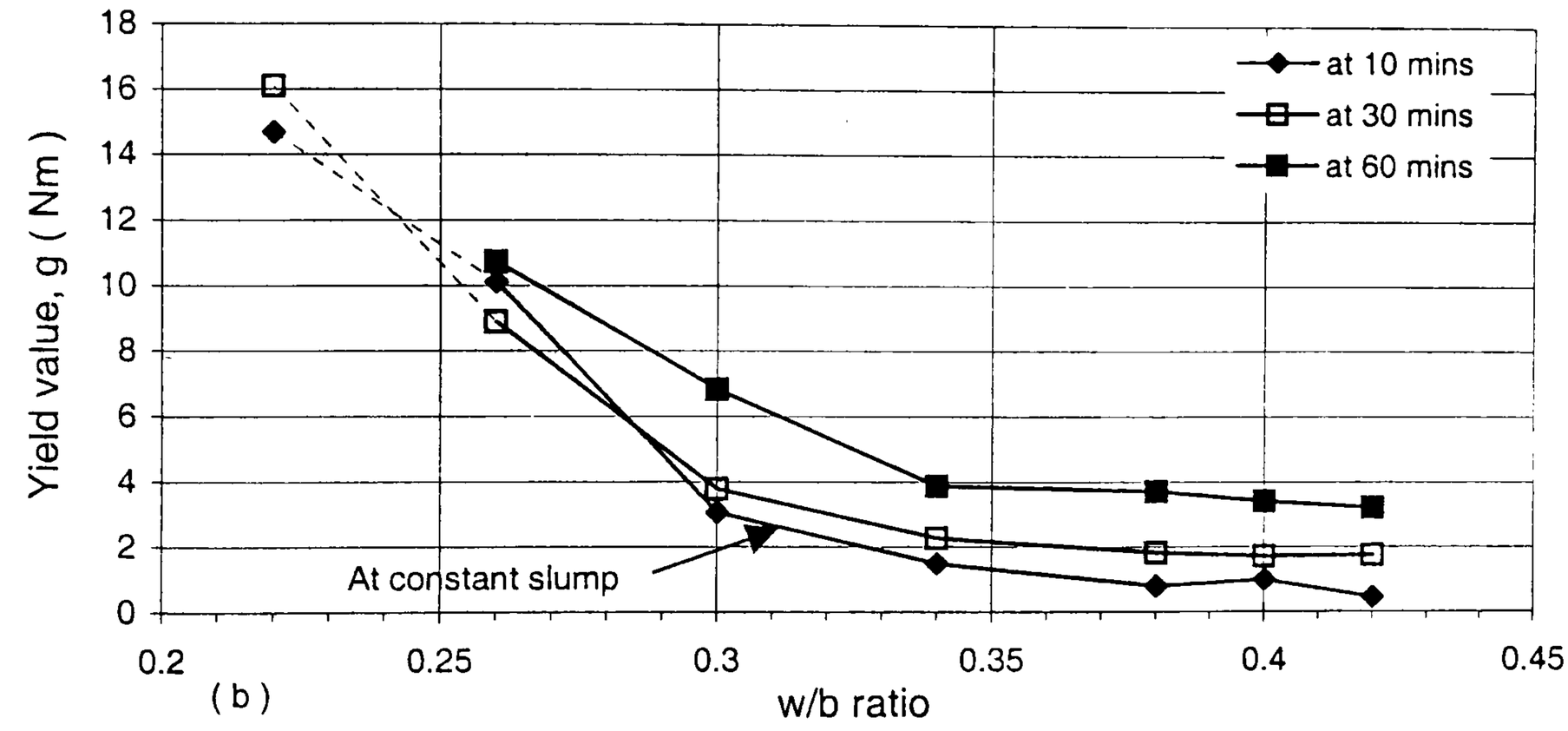

(b)

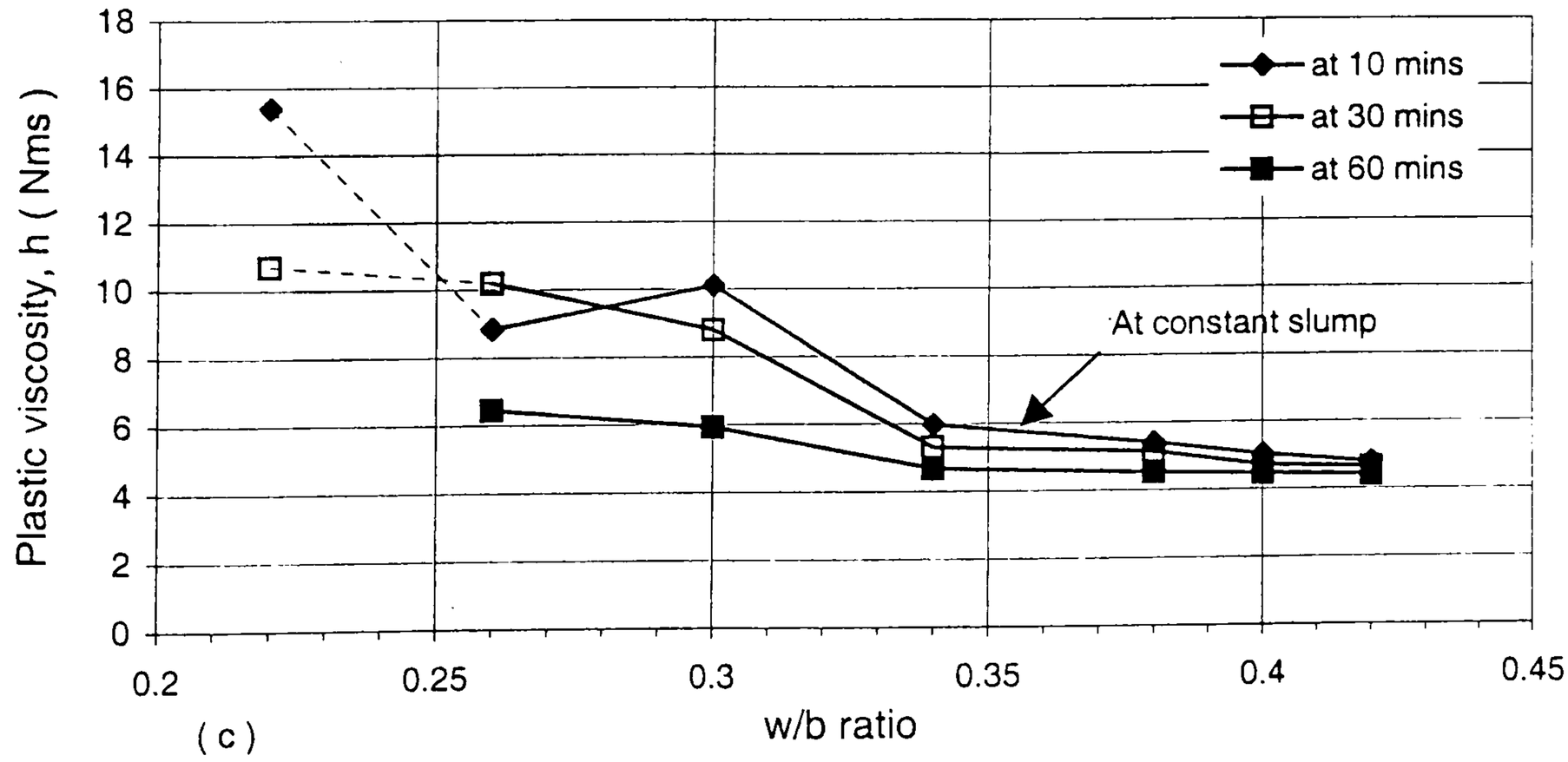

(c)

Figure 5.2 : Effects of decreasing w/b ratios of 0.42-0.22 on (a) slump loss, and variations of (b) yield value and (c) plastic viscosity with time.

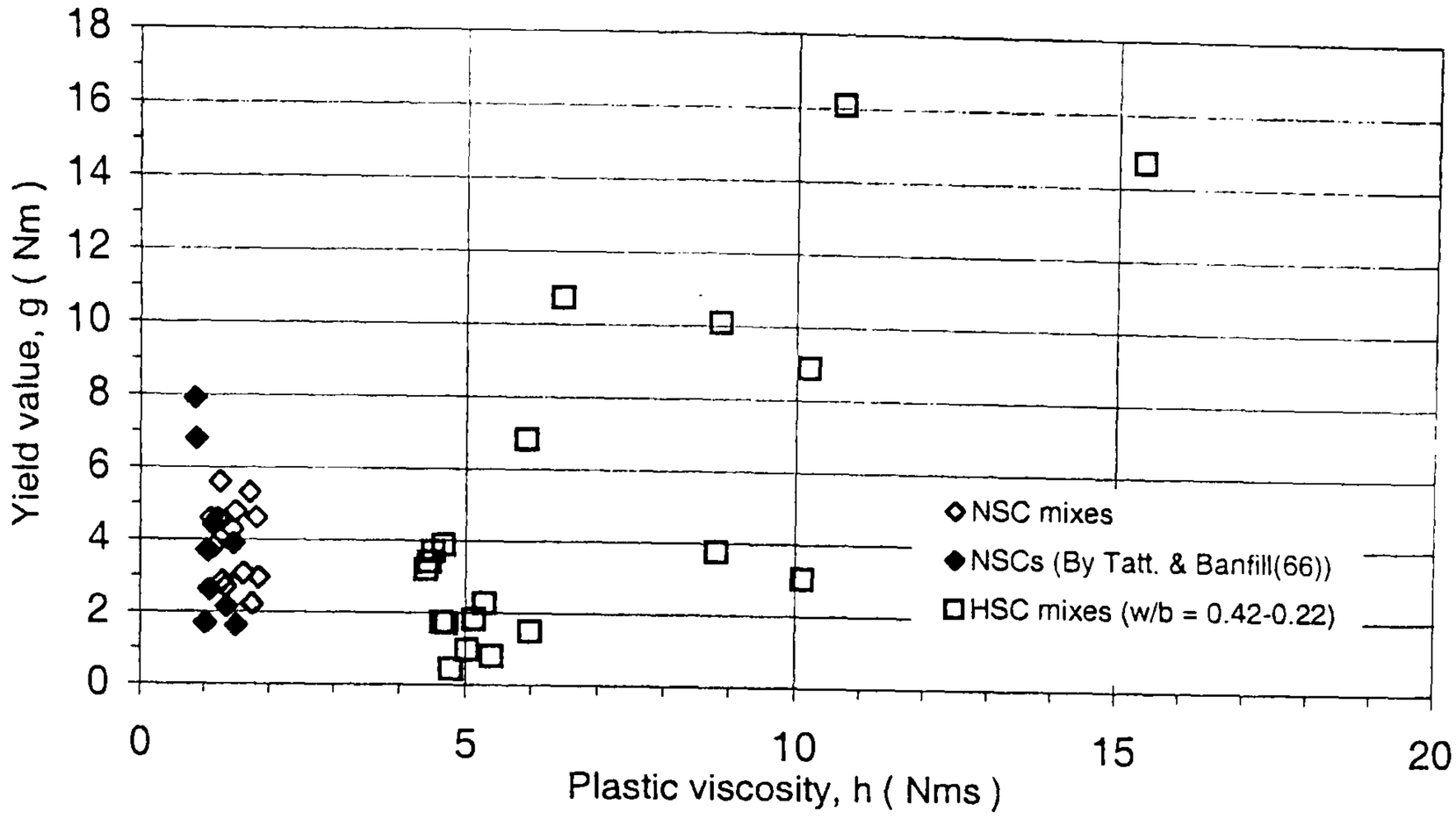

Figure 5.3: Comparison of yield values and plastic vicosities of NSC and HSC mixes (at slumps greater than 70 mm).

5.3.2 Variations in mix stability

(I) Bleeding tendency

As mentioned in chapter 4, a subjective bleeding mark of " **10** " was chosen to describe very high surface bleeding, whist a bleeding mark of " **0** " was used to describe dry mixes. From **figure 5.4(a)** it can be seen that the 0.42-0.26 mixes all exhibited high initial bleeding tendencies represented by bleeding marks (B_{Ms}) of 7-8. These decrease with mixing time, giving little or no surface bleeding at 60 minutes (B_{Ms} of 2-0), and show no trend with decreasing w/b ratio. That is, the bleeding tendency appears to vary with slump level – the higher the slump, the greater the bleeding tendency.

(II) Segregation resistance

In contrast, the reductions in both the torque change (Tc) and the segregation index (SI) values in **figure 5.4(b-c)** show systematic increases in segregation resistance with decreasing w/b ratio and time after mixing (particularly at w/b ratios greater than 0.30). The segregation index values, for example, show that: the reduction in w/b ratio from 0.42 to 0.26 more than doubles the initial resistance to segregation; and that at high w/b ratios of 0.42-0.38 the resistance to

segregation is improved by about a third during the first 60 mins.

From these results it can therefore be concluded that HSCs of very low w/b ratios:

- can exhibit similar bleeding tendencies to those at higher w/b ratios, but
- their ability to resist segregation and hold the solid constituents in a homogeneous mass during shearing is much greater.

5.3.3 Variations in compactability

The variations in the compactability of the mixes as assessed by the changes in self-compacting properties under self-weight, the compacting factor test, and after vibration are presented in **figure 5.5(a-c)**. Both the density and vibration methods (**figure 5.5(a** and **c)**) indicate gradual reductions in compactability during the first 60 minutes, followed by slightly sharper reductions at 90 minutes.

Although the Compacting factor test was specifically designed to measure the compactability[60] of fresh concretes, it does not necessarily reflect these tendencies during the first 60 minutes (**figure 5.5(b)**). In agreement with other workers[7, 8, 65, 238], cohesive mixes, particularly at 0.30 w/b ratio, were found to stick to the hoppers and had to be rodded through, even at high slumps. This implies that the assumption that the work done against surface friction (i.e. wasted work) represents a constant proportion of the total work done regardless of the properties of the mix is not justified. It is however worth noting that all three methods show no systematic relationship with decreasing w/b ratio.

In practice, the total work done during compaction is essentially composed of three main components, namely :

- that done by the concrete as it flows under its self-weight,
- by the application of an external (mechanical) vibration input, and
- that lost in friction around the reinforcement and formwork.

In this respect, the cube density method reflects the variations in compactability under self-weight only (i.e. near zero shearing conditions); whereas according to

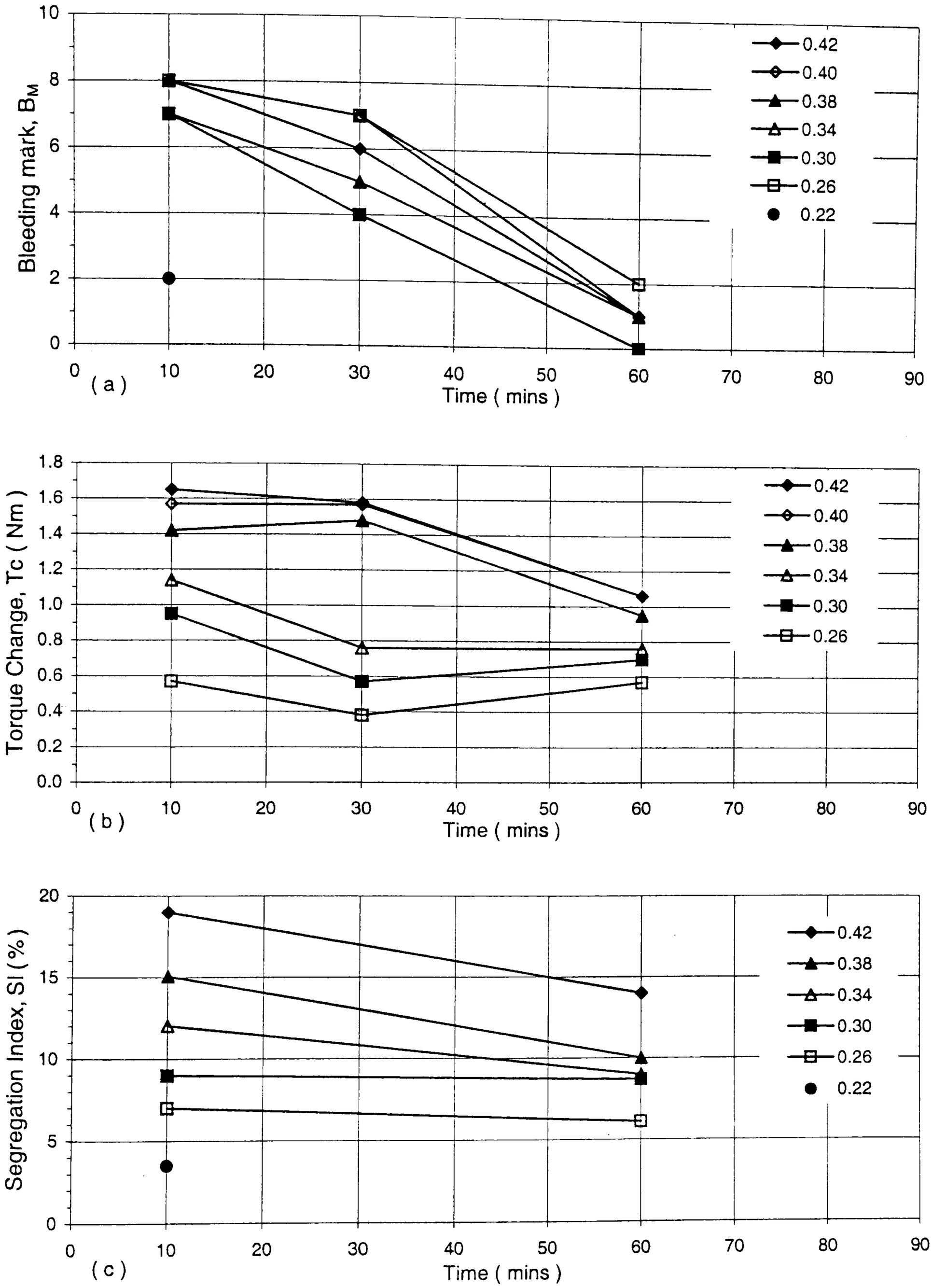

Figure 5.4 : Effects of decreasing w/b ratio on time-dependent variations in (a) subjective bleeding tendency, and segregation resistance as assessed by (b) the Torque change and (c) the difference in coarse aggregate contents during 2-pt. testing

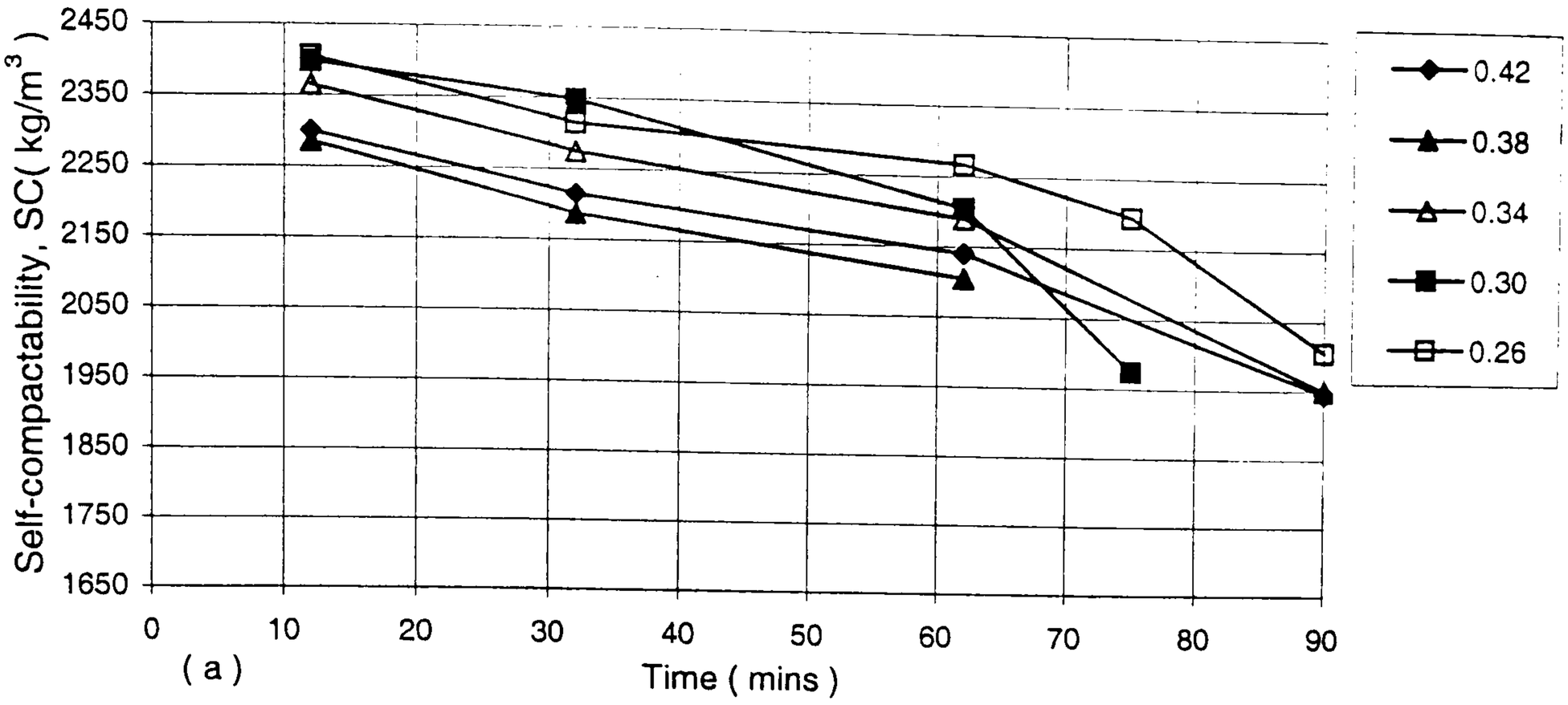

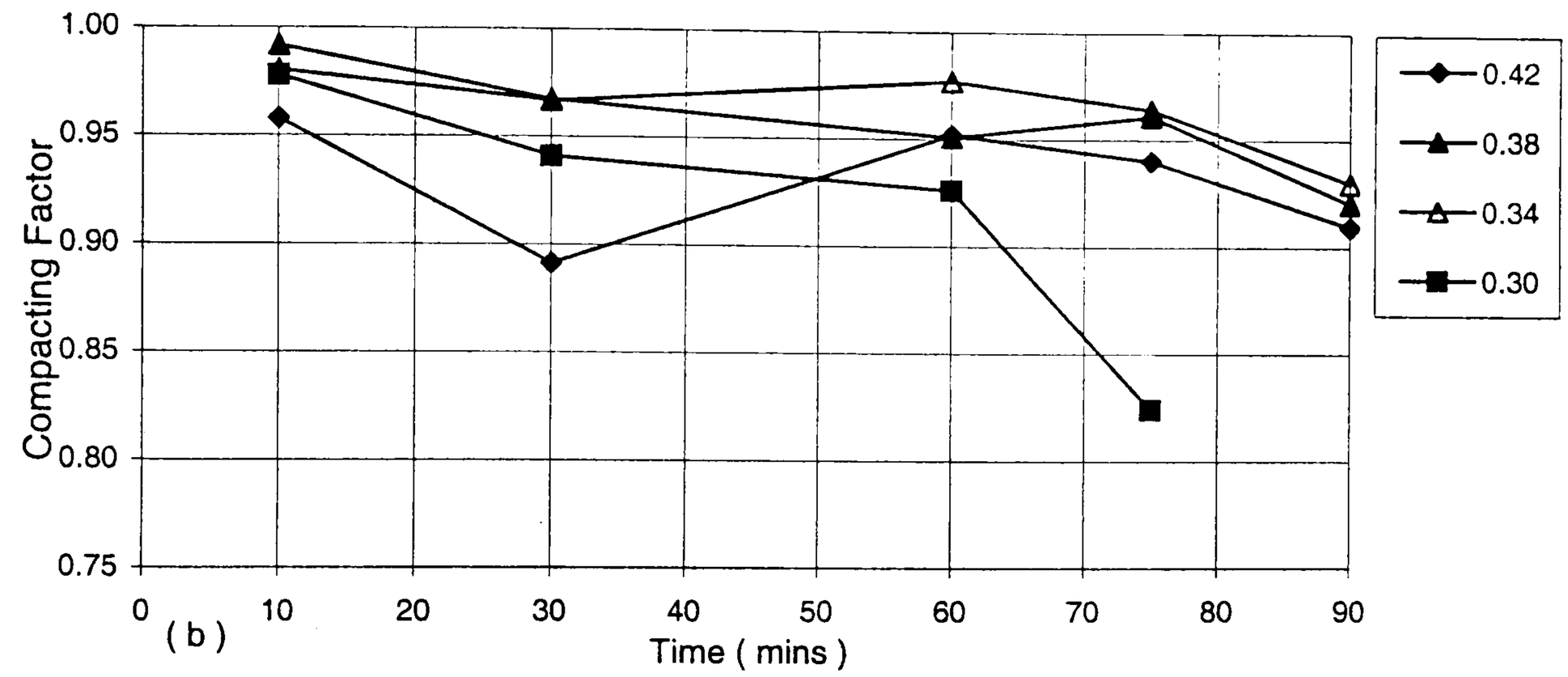

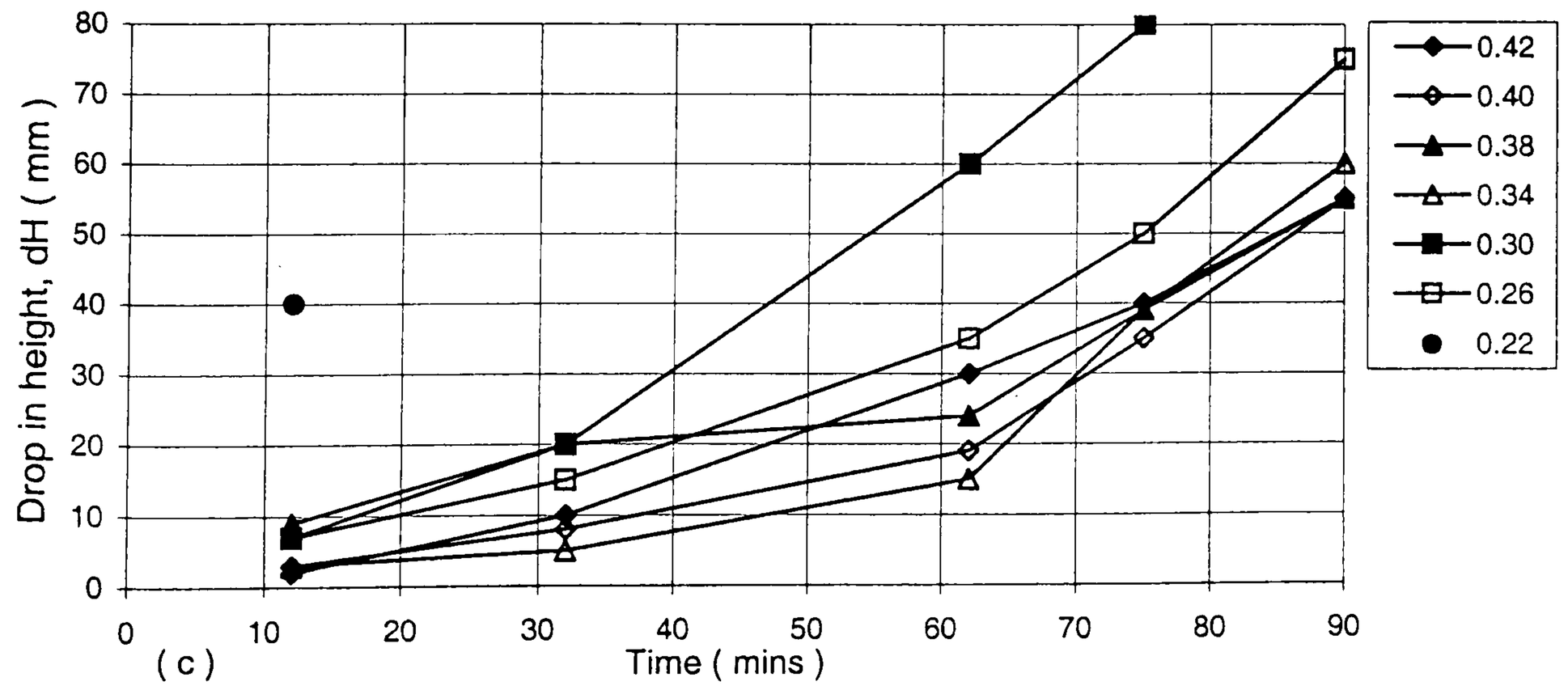

Figure 5.5 : Effects of decreasing w/b ratio on compactability as assessed by the (a) losses in self-compactability (using the cube density method), (b) Compacting Factor test, and (c) drop in height after vibration (at 50 Hz and 0.7 mm amplitude).

Cusens[238] the amount of work done on the concrete in falling into the compacting factor cylinder is much less than that used in practice. Several tests with the cylinder-vibration method had however shown little or no difference in the compactability imparted by low vibration amplitudes of 0.1 and 0.4 mm compared to the 0.7 mm amplitude. In each case, the final subsidence (in mm) and the time taken for the concrete to stop subsiding during vibration was similar. (The latter was typically less than 5 secs). The suitability of the method to assess the compactability of high and low workability concretes containing different superplasticizers and CRMs, is further discussed in chapters 6, 7, and 8.

5.4 Relationships between Ritchie's rheological sub-divisions

As mentioned in sections 2.2.1 and 3.2.1, Ritchie's insight[61] into the rheological properties of fresh concrete did not reveal whether any relationships exist between the various sub-divisions shown in figure 2.1. Relationships between the two-point test, compactability, segregation resistance and the slump measurements obtained in sections 5.3.1-5.3.3 are presented in **figures 5.6(a-c)**.

Figures 5.6(a) indicates that a linear relationship exists between the self-compacting properties and plastic viscosity (giving a correlation coefficient, r, of 0.7750) but not with yield value (r = 0.1876). That is, the results suggest that the apparent reductions in plastic viscosity with time (figure 5.2(c)) are closely related to the losses in self-compacting properties (figure 5.5(a)). The lower the self-compactability (or mass per unit volume) of concrete, the lower is its shearing resistance during two-point testing and, hence, the lower is its measured plastic viscosity. It is however worth noting that relationships drawn between the cylinder-vibration test results and the Bingham parameters gave very low correlation coefficients (0.5711 for g value, and 0.2284 for h), which surprisingly suggest that the vibration response of HSC is not necessarily dependent of its non-vibrated properties (c.f. appendix A, figure A4).

With regards to segregation resistance, the results in **figures 5.6(b)** show that the segregation of the coarse aggregates during two-point testing is more closely

related to the yield value (r = 0.9420) than plastic viscosity (r = 0.6779). Similar non-linear relationships were obtained between the torque change (T_c) and yield value (r = 0.8717), and T_c with plastic viscosity (r = 0.6224). In this respect, it should however be noted that, the determination of the T_c values is particularly sensitive to fluctuations in the pressure voltages at the start of the two-point tests (c.f. figure 4.4). A subjective reading error of only 1 mm (or 0.1 volt) in the chart-output traces can, for example, reduce the initial T_c value at 0.42 w/b from 1.65 to 1.27 Nm (i.e. by almost a quarter).

Figures 5.6(c) shows that the widely accepted relationship[7, 49, 91] between yield value and slump appears to be valid only at w/b ratios higher than 0.30. That is, in high workability concretes having yield values lower than about 7 Nm. This is despite the fact that both the slump and yield value are associated with zero shear rate[7, 40, 54]. The bleeding tendencies were found to correlate strongly with slump (r = 0.9604), to a lesser extent with yield value (r = 0.9261, at high w/b ratios > 0.30) and self-compactability (r = 0.7417), but not with plastic viscosity (r = 0.6735) or segregation resistance (r = 0.4034). (The relevant graphs are given in Appendix A).

The validity of the relationships drawn from the present two-point test results is, however, questionable, because of the erroneous time-dependent measurements obtained with the MH system (c.f. figure 5.2). In relation to Ritchie's sub-division of the rheology of fresh concrete into three distinct components[61], the results nevertheless show that in HSC the:

- mix stability depends more on the yield value (i.e. the initial resistance to deformation) than on plastic viscosity, whereas the
- self-compactability at or near zero shear rates depends more on the plastic viscosity (i.e. the subsequent resistance to deformation).

The existence of more definitive relationships between the Bingham parameters, segregation resistance, and compactability are further examined in chapters 6, 7 and 8. The next section compares the capabilities of Tattersall's MH and LM systems to measure representative variations in workability as discussed in section 3.2.1.

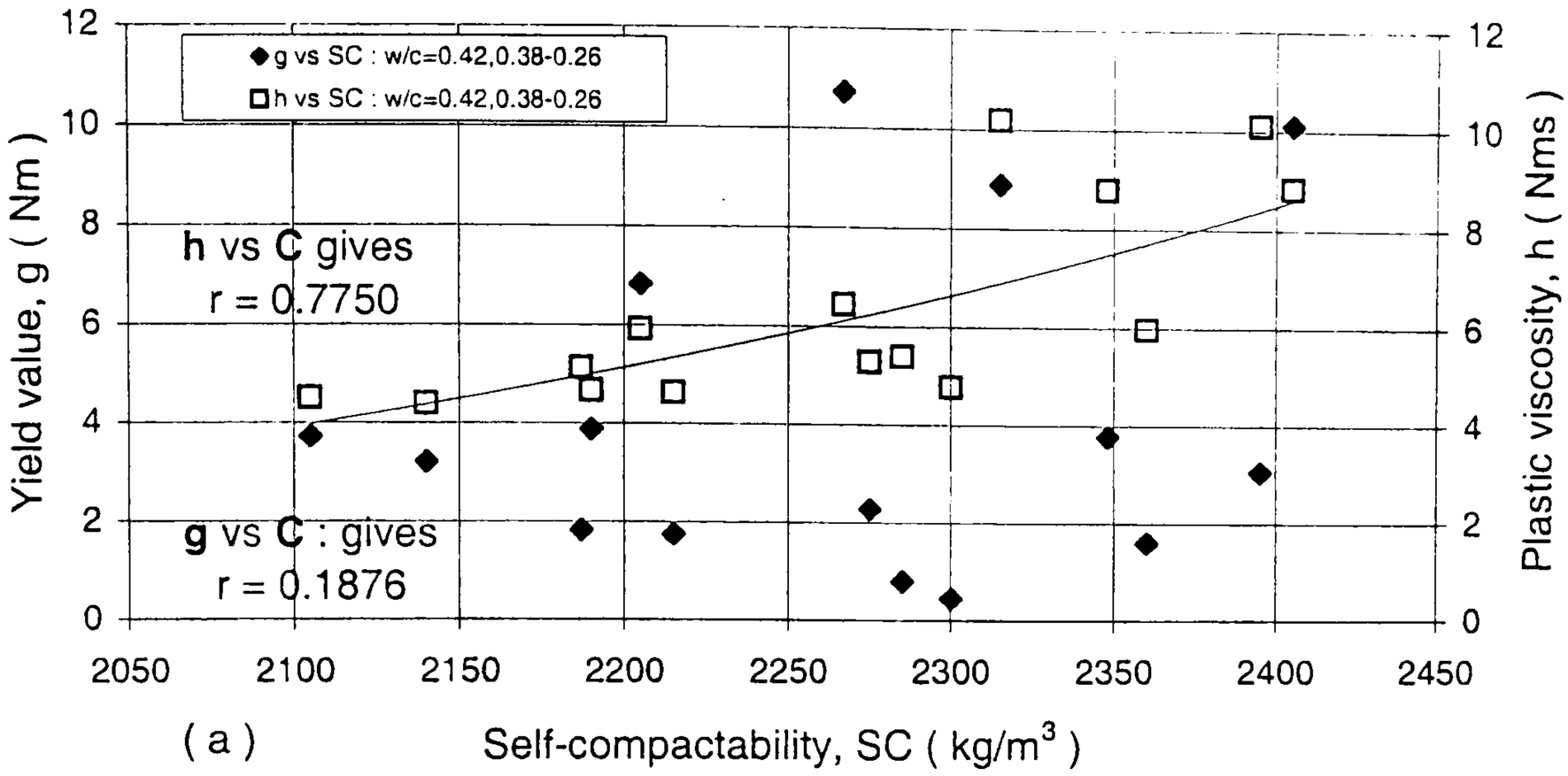

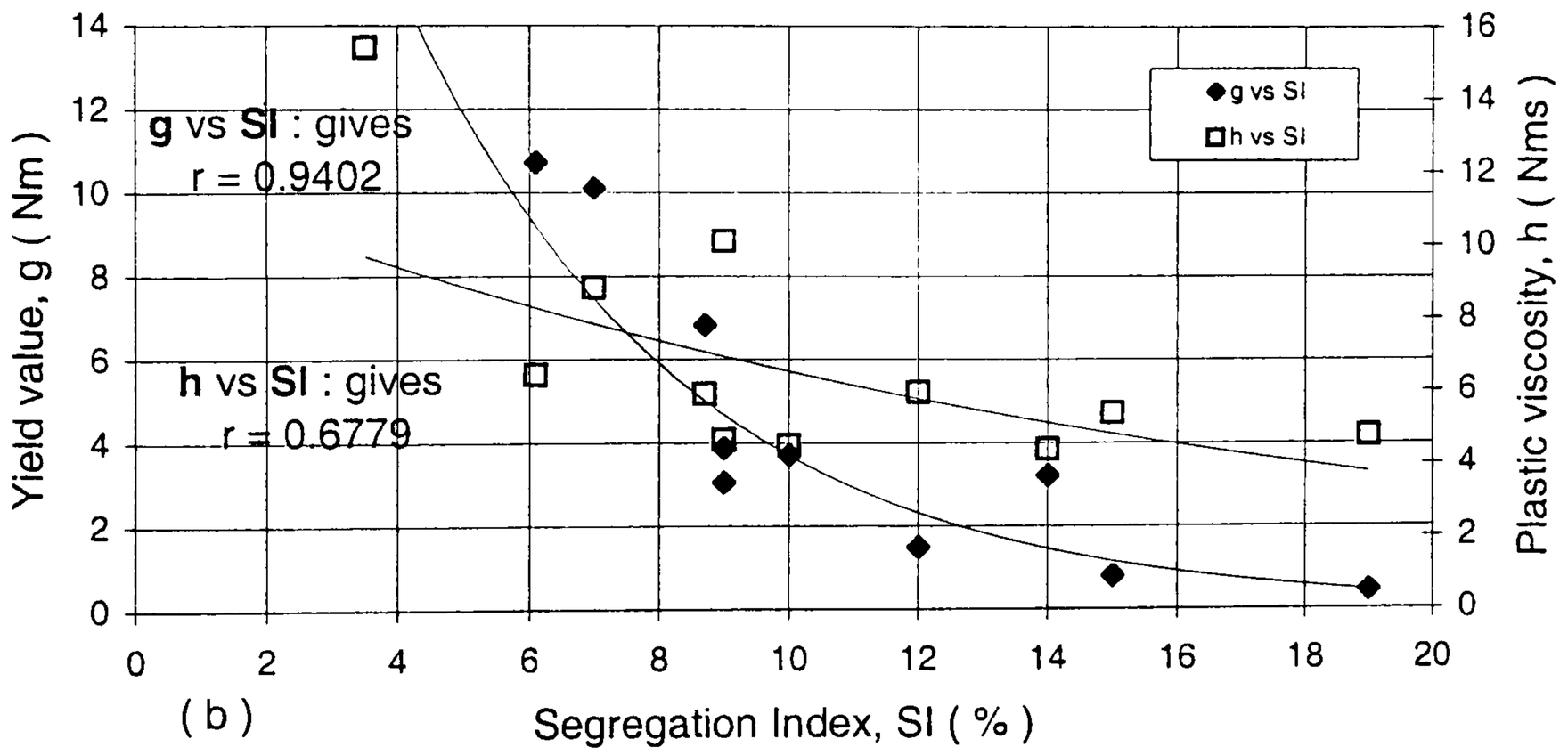

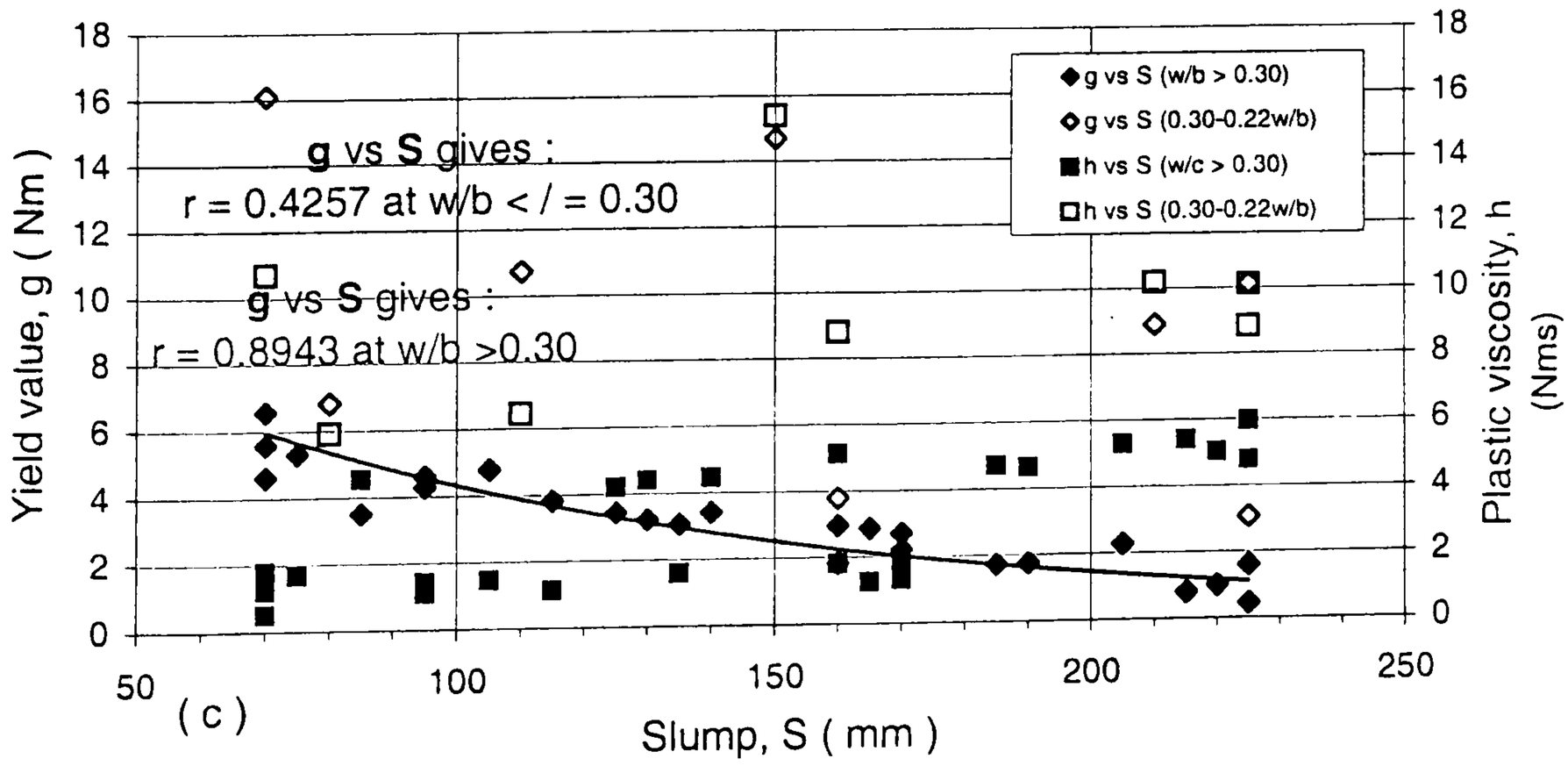

Figure 5.6 : Relationships between the Bingham parameters and (a) self-compactability, (b) segregation resistance, and (c) slump

5.5 Comparison of the MH and LM two-point test systems

Previous researchers have attributed erroneous workability measurements (particularly in terms of time-dependent reductions in plastic viscosity) with Tattersall's MH system[86] (c.f. figures 2.34) and the BT Rheometer[49] mainly to segregation during testing, and to increasing stiffening and/or slippage of the concrete round the inner cylinder of the BLM viscometer[118] (c.f. figure 2.23). In this respect it has been reported that in any given two-point test device :

- the **shear rates** applied during testing should be within the practical handling conditions of the concrete[66, 86], and that
- the **characteristics of** the **apparatus** used (specifically, the design and dimensions of the impeller and bowl) should not exaggerate the measured workability properties and/or cause segregation[7].

The work in this section was carried out to examine and better understand the effects of different two-testing procedures (namely shear duration and shear direction) and various modifications of the MH and LM systems (in terms of bucket size, impeller blade orientation and size) on measurements of loss of workability and segregation resistance. To minimize the effects of batch-to-batch variabilities, parallel measurements on the same sample of concrete were performed. The variables investigated and the results obtained are summarized in **Table 5.1**. As mentioned in section 3.3.1, the work also includes tests to assess the capabilities of the MH and LM systems to measure the fluidizing action due to successive redoses of superplasticizer (**Table 5.2**).

5.5.1 Effects of shear duration and shear direction

Several studies[55, 154, 199, 239] have shown that the shear duration and shear direction during testing can both significantly influence the workability properties of cement pastes, mortar and concrete, but have not demonstrated their effects on measurements of loss of workability.

Table 5.1: Summary of test variables and results obtained with the MH and LM two-point test systems.

Factor investigated	Test variables	Slump testing		Two-point testing				SI	Up-lift Measurements	
		Time (mins)	Slump (mm)	Time (mins)	g (Nm)	h (Nms)	r	(%)	sH (mm)	% AV
Decreasing **Shear duration** (MH system)	*** 60 secs** and **30 secs** shearing durations	10	220	*12	8.81	8.03	0.9824	8.43		
				20	7.51	8.96	0.9643	7.88		
		25	215	*34	8.95	6.99	0.9831			
		65	105	39	7.9	7.34	0.9639			
				55	8.84	6.2	0.9418	7.11		
		75	70	*61	12.35	3.14	0.9511	6.52		
	30 secs and *** 15 secs** shearing durations	7.5	220	10	8.11	8.84	0.9468	6.93		
				*19	6.92	10.2	0.9828	5.87		
		38	200	44	8.02	7.91	0.9546			
				*49	7.95	8.24	0.9865			
				65	10.73	5.97	0.967	5.91		
		75	85	*71	9.47	6.64	0.9287	5.33		
Shear direction (MH system)	**low-high** and *** high-low** impeller speeds (settings $^1/_2$-4)	7	225	10	Non-linear flow curves			-		
				*11	9.10	9.81	0.9831	-		
		35	185	30	Non-linear flow curves					
				*31	10.31	7.56	0.9766			
		65	110	60	Non-linear flow curves			-		
				*61	11.37	5.49	0.9679	-		
Bucket size (MH system, helical impeller)	**MH** and ***LM** test buckets	7	225	10	9.1	9.8	0.9892	7.07		
				*15	8.5	8.8	0.9934	11.22		
		37	190	30	9.15	8.7	0.9703			
				*35	9.02	7.3	0.9959			
				*50	9.4	5.8	0.9522	9.79		
		65	100	60	10.2	7.01	0.9234	5.41		
Impeller Blade Orientation (MH system)	**Helical** and *** Vertical** (I.e. 45° and 90°) blades	7	230	10	7.36	10.27	0.9768	5.21	40	17.4
				*15	8.02	14.88	0.9675	*4.09	*15	6.5
		20	220	30	7.87	9.98	0.9805		45	19.6
		38	200	*35	9.31	14.11	0.9641		*15	6.5
				60	8.94	7.31	0.9881		55	23.9
		68	145	*65	10.43	13.37	0.9543		*25	10.9
				90	10.05	6.19	0.9711	4.89	70	30.4
		98	70	*95	10.99	12.93	0.9487	*2.22	*30	13.0
	Helical and *** Vertical** (I.e. 45° and 90°) blades * (at speed Settings 2 - $^1/_2$)	8	235	10	7.11	12.05	0.9907	4.6	30	13.0
				*15	9.16	13.47	0.9631	*3.83	*20	8.7
				30	8.11	10.73	0.9861		35	15.2
		38	205	*35	9.76	13.22	0.955		*20	8.7
				60	8.52	8.96	0.9868		40	17.4
		68	150	*65	11.02	12.51	0.9443		*25	10.9
				90	9.93	7.54	0.9714	4.73	55	23.9
		98	80	*95	11.47	11.31	0.9131	*3.20	*30	13.0
Impeller size (LM system)	**Standard** and *** broader** H-impellers	7.5	235	10	6.25	8.31	0.9897	5.77	No noticeable effects	
				*15	9.77	14.01	0.9411	2.98		
		25	210	30	6.91	8.8	0.9872			
				*35	10.14	12.31	0.9253			
		55	150	60	8.75	9.71	0.9783			
				*65	11.71	17.89	0.9015			
		98	70	90	9.42	10.55	0.9537			
				*95	15.15	15.5	0.8891	-		
		125	45	120	11.57	9.33	0.9578	3.44		

Note : All tests were carried out at 0.26 w/b (using the mix proportions for mix 6 in Table 3.6, and cements PC 4-6 of Table 4.1).

* Represent parallel measurements (on the same concrete sample). + Represent supplementary tests.

r is the correlation coefficient, and is a measure of the strength of the T / N relationship.

The uplift measurements (sH, mm) were determined from the differences in the average heights/levels of the concrete at the beginning and end of the 2-pt. tests (I.e. at speed settings 4 and $^1/_2$).

The volume expansions (AV, %) were determined from the increases in height of the concrete sample during 2-pt. testing (sH) relative to that before testing (I.e. sH*100/230 mm)

5.5.1.1 Effects of shear duration

The results in **Table 5.1** show that reductions in the shear duration (i.e. two-point testing time) from 60 to 30 seconds and 30 to 15 seconds consistently decrease the yield value, increase the plastic viscosity, reduce segregation, but more importantly do not significantly influence the variations in the plastic viscosity with time. That is, the shear duration has no substantial effect on measurements of loss of workability. Similar trends were also obtained with the 0.42 w/b ratio mix, but the numerical differences in the results were much lower.

In these tests, the initial speed of the impeller (as described in chapter 4) was maintained for approximately 12-15 seconds at setting 4 in order to achieve full stabilization of the initial pressure voltages and, therefore, reduce the difficulties associated with determining the torque change (T_c) values (page 163). Although the segregation index (%) and Bingham values were similar to those obtained previously, it was noticed that the T_c values were much lower, and showed marginal variations with w/b ratio and time. For example, at 0.42 w/b, the T_c values at 10 and 60 minutes were respectively reduced from the 1.65 Nm and 1.06 Nm (as in section 5.3.2) to 0.50 Nm. These results therefore demonstrate that the Torque change method used by Wimpenny et al[191] and others[83-84] (section 2.7.1) is highly dependent on the initial shearing conditions, and not necessarily on the segregation of coarse aggregates occurring during two-point testing.

5.5.1.2 Effects of shear direction

Figure 5.7 compares the up and down flow curves obtained by incrementally increasing the speed of the impeller from setting ½ to 4 (in 4-5 secs steps), and when it is then incrementally reduced back to setting ½ (also in 4-5 secs steps). As can be seen, the torque-speed relationships for the up-curves are all non-linear; giving higher torques than the down-curves but, more importantly, show no discernible pattern for the variations in workability with time. The fact that the up-curves bend away from the torque axis (i.e. show progressive reductions in torque with increasing impeller speed) implies shear thinning of the concrete during testing, and that the Bingham model (which assumes a simple straight line relationship) is not

applicable under these shearing conditions.

Similar results from individual measurements with the LM system and concrete mixes of 0.43-0.38 w/b ratios have been reported by Beaupre et al[199] who, in agreement with other workers in cement paste[55, 66], attributed the non-linearity of the flow curves to thixotropic effects. (That is, to reductions in apparent viscosity (defined as the ratio of shear stress divided by shear rate) during testing, followed by a gradual recovery when the stress is removed[66]). These effects have however not been unequivocally demonstrated, and previous work cited by Banfill and Saunders[239] had in fact shown that two suspensions of quite different thixotropic properties could give similar up and down flow curves. More recently, Banfill[154] reported that the non-linearity of the flow curves in cement pastes and mortar does not denote thixotropic behaviour, but is instead the result of irreversible breakdown of structure due to shearing in the test. (The effects of thixotropic/stiffening properties on the placing characteristics of HSCs are briefly discussed in chapter 8).

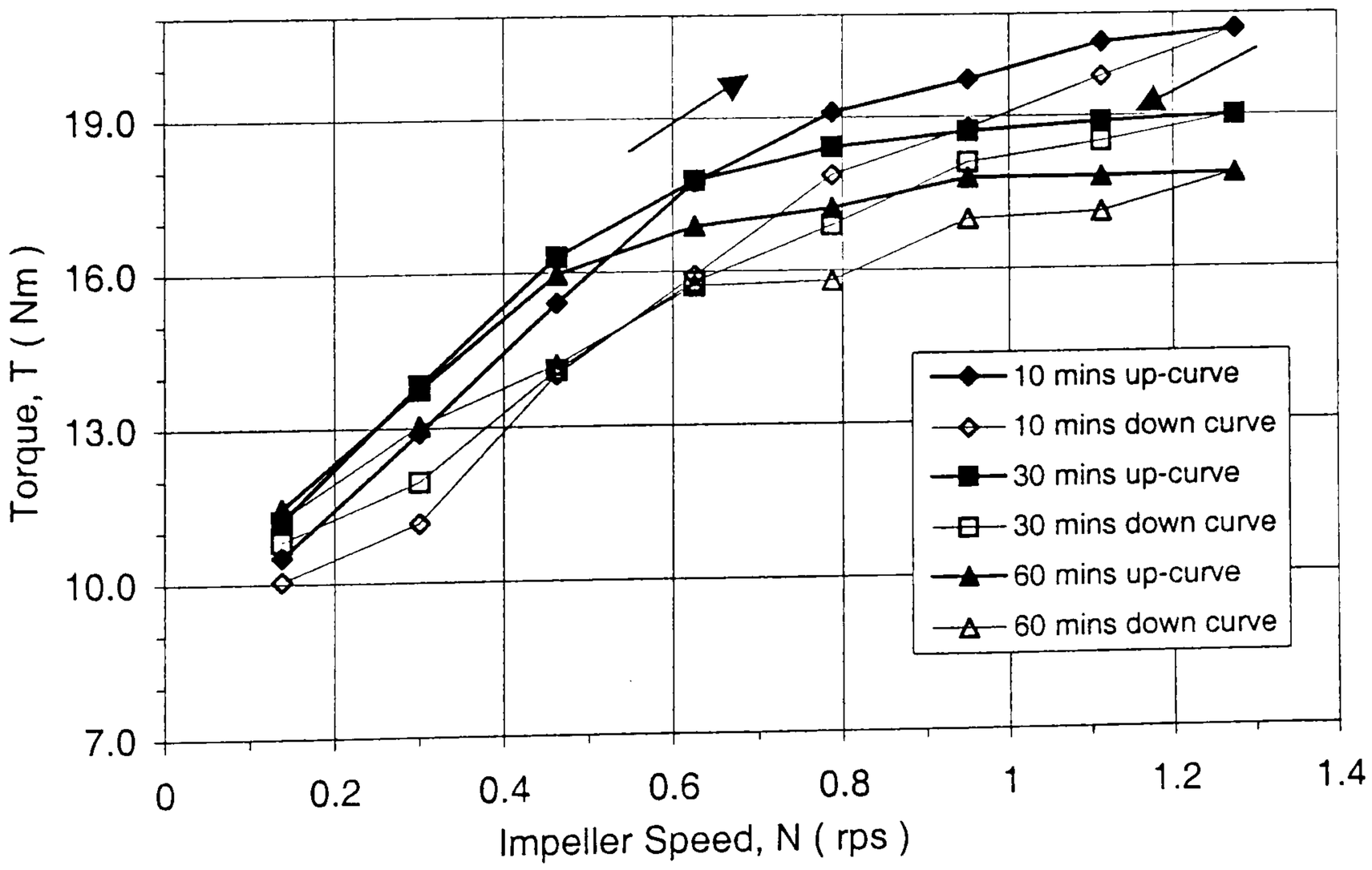

Figure 5.7: Effects of shear direction, showing up and down-flow curves at 10, 30 and 60 mins (all values determined by reading of chart-output traces).

5.5.2 Effects of bucket size

Although several researchers[40, 102, 240-241] have investigated the effects that different bucket sizes (or impeller-bucket gap widths) have on the Bingham parameters, they have not provided information on their effects on measurements of loss of workability.

A comparison of the results obtained with the MH and larger LM bucket (in **Table 5.1**) shows that the increase in bucket size (or gap width) reduces the Bingham values by about 0.2-0.6 Nm and 0.7-1.7 Nms, but has no significant influence on the development of either the yield value or plastic viscosity with time. The higher workability and segregation tendency obtained with the larger LM test bucket (Table 5.1) appeared to be due to localised shearing represented by higher paste contents in its centre. An attempt to more fully shear the concrete in the MH bucket with a larger helical impeller (which reduced the impeller-bucket gap width to about 5 mm (Appendix A)), resulted in very high pressures (possibly due to excessive aggregate trapping) during loading of the concrete and, no two-point test measurements were possible.

From the results shown in Table 5.1 it can be concluded that bucket size has no substantial influence on the ability of the MH system to measure loss of workability.

5.5.3 Effects of impeller blade orientation and impeller size

In the preceding tests with the MH system, it was noticed that the helical impeller causes the level of the concrete to rise up towards the rim of the test bucket when its speed is initially increased to setting 4, and subsequently fall to almost its original level when the speed is reduced to setting ½ at the end of the test. At very low slumps of 75-50 mm, the concrete in the centre of the test bucket was however observed to fall more rapidly (i.e. produce concave surfaces) with decreasing impeller speed, and is partially sheared due to eventual holing of the material at the end of the test. The effect is illustrated in **figure 5.8**.

Although Tattersall[7] stated that for low-medium workability concretes (having slumps $\leq$ 75 mm) the apparatus should be used in its LM mode, he has not provided

any supporting data to substantiate this, and/or commented on the capabilities of the standard versions of his apparatus to measure loss of workability. Tests were therefore carried out to:

- examine the effects of changing the orientation of the helical blades in the MH system from 45^0 to 90^0 to the direction of rotation, and
- compare the performance of a broader H-shaped impeller with the standard H-impeller in the LM system.

The change in helical blade orientation was used to reduce the observed uplift effects (in figure 5.8), whilst the broader H-shaped impeller was used to assess any possible insensitivity of the standard LM system at slumps greater than 75 mm. The dimensions of the impellers used in the investigation and the results obtained are shown in **figures 5.9** and **5.10**. Measurements of up-lift effects determined from the differences in the level of the concrete at the start and end of the MH two-point tests (i.e. at speed settings 4 and ½) are included in Table 5.1.

5.5.3.1 Helical impeller blade orientation

The measurements with the MH system in **figure 5.10** show that the vertical blades increase both the Bingham parameters (by about 0.5-1.5 Nm and 4-6.5 Nms), but significantly reduce the rate of drop in plastic viscosity (from approximately 3.1 Nms/hr to 1.5 Nms/hr) compared to the helical blades. The uplift measurements in Table 5.1 also show that the vertical blades typically reduce the uplift effects (i.e. % volume expansion) of the helical blades from 40 to 15 mm (i.e. by 10.9%) at high slumps of 230 mm, and from much as 70 mm to 30 mm (i.e. by 17.4%) at low slumps of about 70 mm.

Although the shearing area of the impellers was the same, the vertical blades generated higher pressures and larger fluctuations in the pressure voltage-time traces, which meant that the initial testing speed could not be raised beyond setting 2. The supplementary tests with both impellers operating at initial speed setting 2 (Table 5.1) also show that the helical impeller produces larger volume expansions and a higher rate of drop in plastic viscosity (3.3 Nms/hr instead of 1.6 Nms/hr)

compared to the vertical blades.

From these results it can therefore be concluded that the continuous reductions in plastic viscosity with time in the MH system are a direct consequence of increasing up-lift effects exerted by the helical shape of the impeller, and are not necessarily dependent on the initial testing speed. The up-lift effects increase with decreasing slump, reduce the intrinsic shearing resistance of the concrete during testing, and therefore mean that the plastic viscosity measurements with the MH system become increasingly less representative as the material losses its ability to self-level in the test bucket. The smaller volume expansions obtained with the vertical blades may be due to secondary effects caused by dislodged concrete being forced upwards along the sides of the bucket by the higher pressures generated.

The fact that the volume of concrete displaced by the helical impeller decreases with decreasing impeller speed, and is negligible before and after two-point testing at high-medium slumps, suggests that the uplift effects do not significantly influence the measured yield values and their evolutions with time. Exceptions to this are however likely if the concrete undergoes partial shearing at/near the end of the two-point tests (slumps $\leq$ 70 mm), as some reductions in the torques generated at low impeller speeds would be expected, and the yield values would accordingly be reduced.

5.5.3.2 Effects of H-shaped impeller size

Contrary to Tattersall's suggestions[7], the results with the standard H-impeller in **figure 5.10** show that the LM system is in fact sufficiently sensitive for measuring loss of workability (i.e. gives progressive increases in both the Bingham parameters with time) in the high-medium slump range. As can be seen from Table 5.1, in the first 90 minutes where the slump decreases from about 235 to 70 mm, the yield value is increased by approximately 50% (from 6.25 Nm to 9.42 Nm) and the plastic viscosity is increased by about 25% (from 8.31 Nms 10.55 Nms).

At slumps lower than 70 mm, the H-impeller was however observed to dislodge and densely compact substantial amounts of concrete on the sides of the test bucket, and then rotate in the channel/cavity formed (i.e. it partially shears the concrete). This characteristic may be the main reason for the reduction in plastic viscosity after the first 90 minutes, and could be associated with significant losses in the self-compacting properties of the concrete (as shown in figure 5.5(a)).

In comparison with the standard H-impeller, the results with the broader H-impeller (figure 5.10) show that it increases the Bingham parameters (by as much as 3-6 Nm and 3.5-8 Nms), but gives erratic variations in plastic viscosity. These characteristics may be attributed to greater aggregate collisions and higher pressures produced by the smaller impeller-bucket clearance, which meant that the two-point testing speed could not be raised beyond setting 3.

When compared to the results with the standard MH system, it can be seen that the standard LM system reduces the initial Bingham parameters by about 1.0 Nm and 2.0 Nms (i.e. by 15 and 20 %). The fact that the plastic viscosities from the MH and LM systems vary in opposite directions, and their numerical differences increase with lapsed time, however, suggests that the time-dependent measurements from the two systems can not be easily reconciled.

This contradicts conclusions by Tattersall and his co-workers[7, 66, 102] that the results from the standard MH and LM systems give good experimental and theoretical correlations represented by positive straight-line relationships. The experimental comparisons were based on individual measurements in NSC, presumably taken immediately after initial mixing and at constant slump; whilst the theoretical relationships were determined after detailed calibration of the apparatus with fluids of known properties. In this respect it should however be noted that although the use of calibration fluids is believed to account for geometric differences in impeller and bucket sizes, it is unlikely to accommodate for the contrasting shearing performance observed with the MH and LM systems.

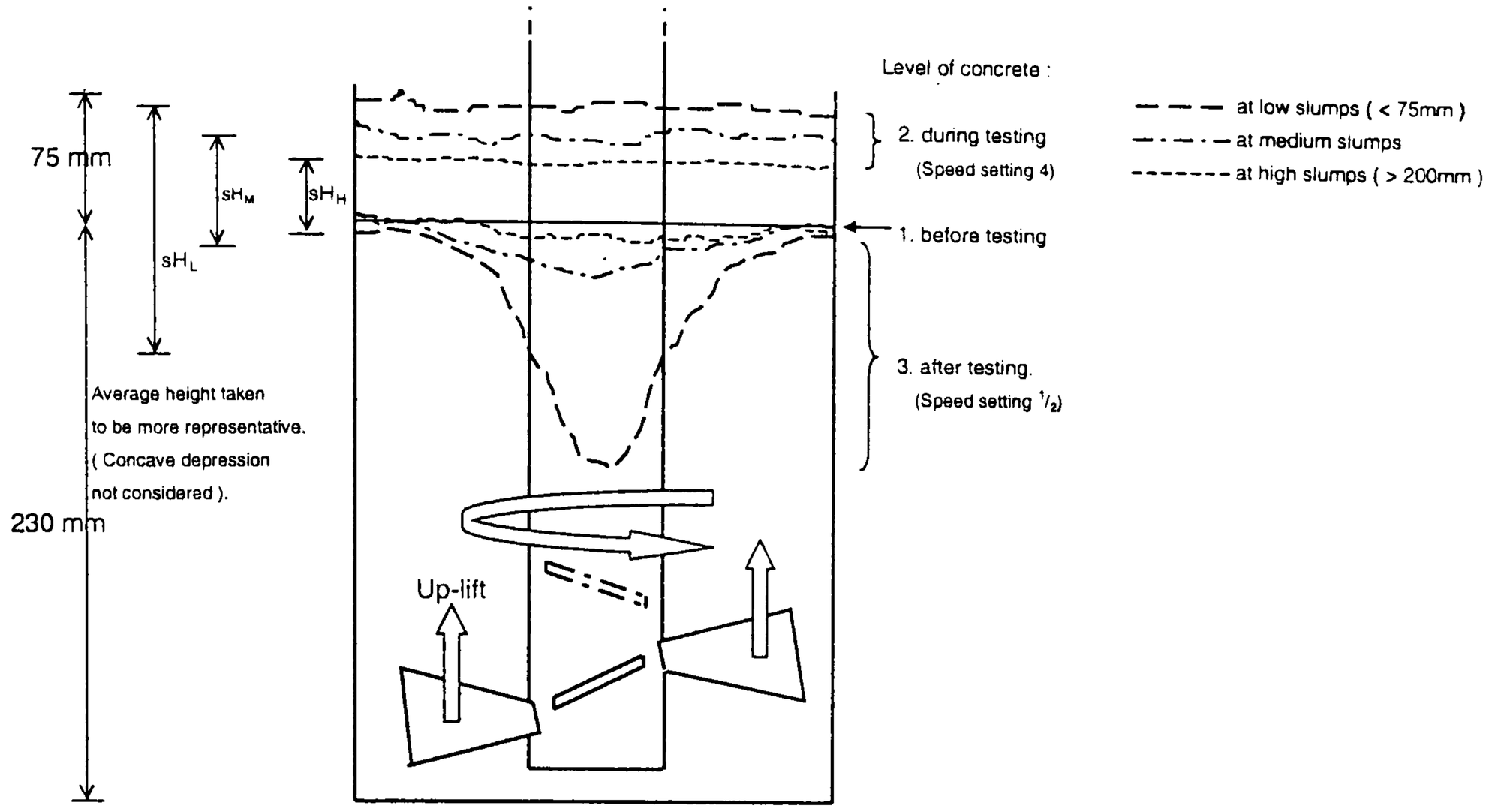

Figure 5.8 : Schematic illustration of up-lift effects exerted by the helical impeller during two-point testing with the MH system (sH_H, sH_M and sH_L represent up-lift measurements at high, medium and low slumps).

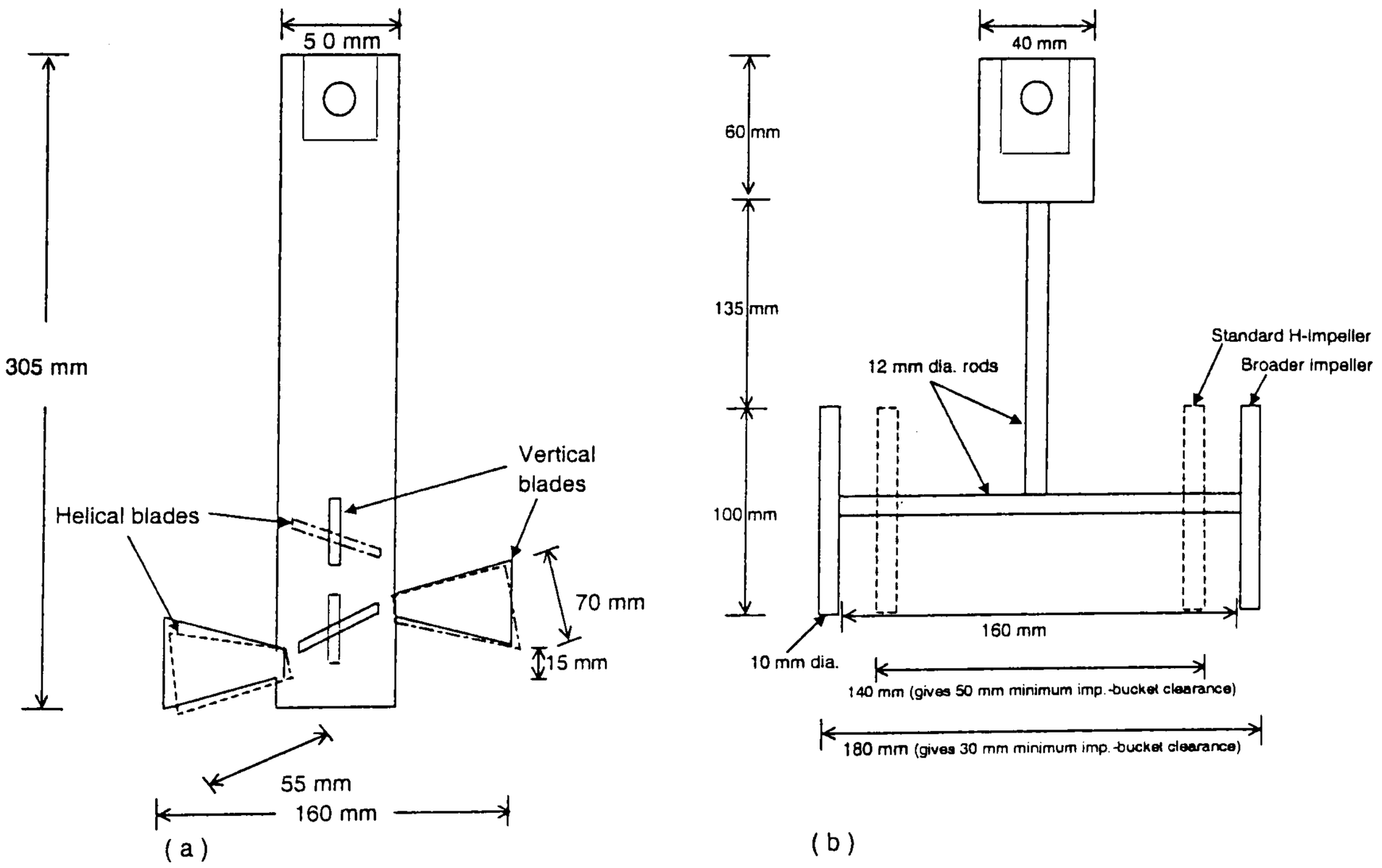

Figure 5.9 : Dimensions of (a) impeller with helical and vertical blades used for the MH system, and (b) the standard and broader H-impeller used for the LM system.

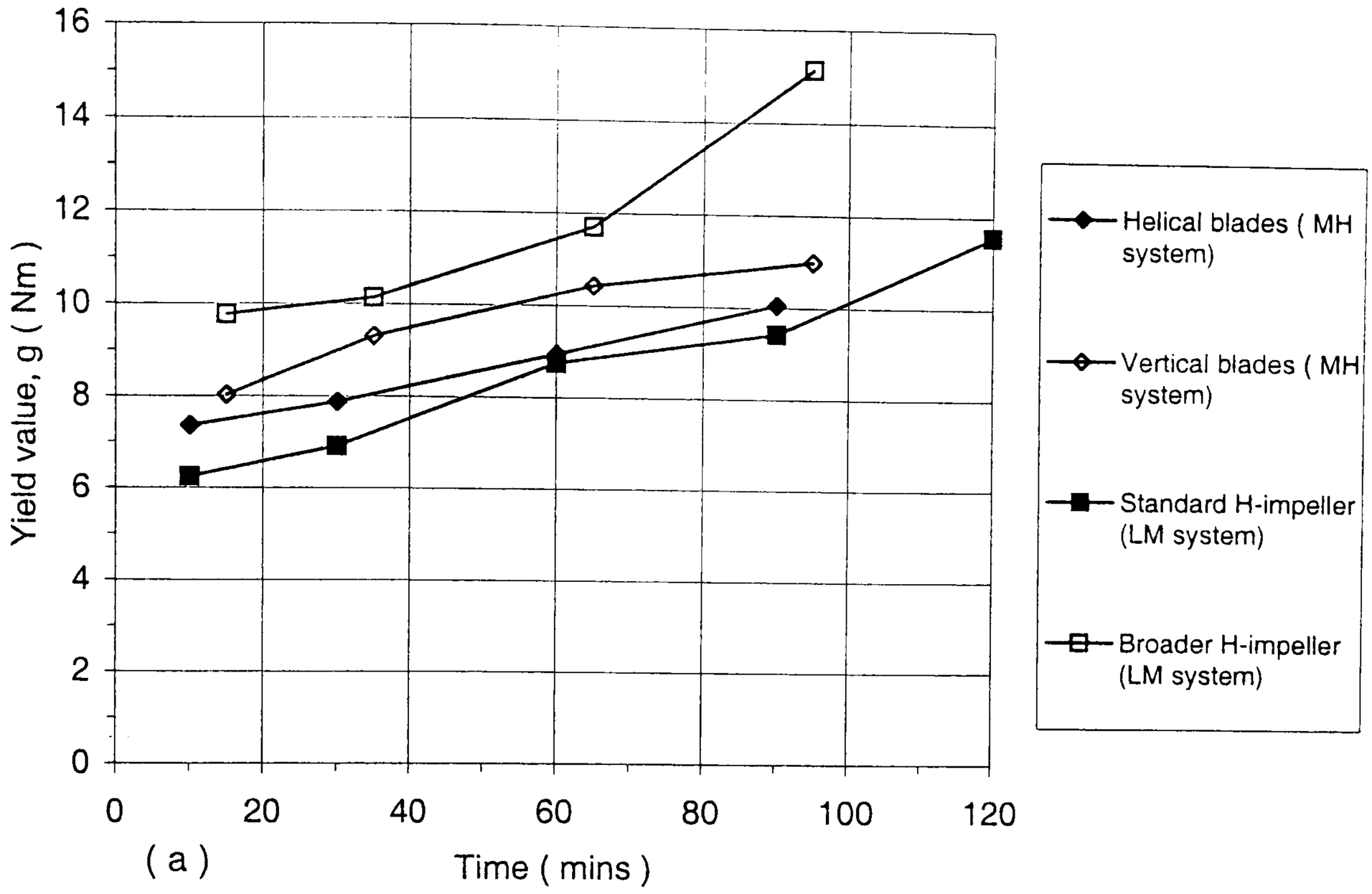

Figure 5.10 : Effects of impeller blade orientation and impeller size on variations of (a) yield value and (b) plastic viscosity with time.

In the LM system, the planetary motion of the H-impeller essentially stirs/mixes the concrete, and has no noticeable influence on its volume during testing; whereas in the MH system, the concrete sheared around the central shaft experiences increasing up-lift effects with decreasing slump. These contrasting shearing effects are not likely to be observed, and hence reconciled by the use of calibration fluids of stable/uniform self-levelling properties. There is currently no standard granular material to calibrate the instruments.

5.5.4 Redosing tests with the MH and LM systems

As mentioned in section 3.2.1, the fluidizing action resulting from the combined effects of increasing water contents and active superplasticizer solids (which occurs during successive redoses of superplasticizers), would intuitively be expected to increase the workability of a given concrete mixture (i.e. reduce both its Bingham parameters) following each redose. This is in accordance with the first use of superplasticizers (page 34) and the effects of increasing water contents (c.f. figure 2.9), but it has however not been demonstrated by previous researchers. The slump and two-point test results obtained by successive redoses with 0.25-0.50% SNF superplasticizer, at 10-15 minute intervals, are shown in **Table 5.2** and **figure 5.11(a-b)**.

The slump test results in Table 5.2 show that successive additions of superplasticizer (from 1.5 to 3.0%) increase both the slump and slump-spread from approximately 100 mm and 200 mm to about 260 mm and 605 mm respectively. With further additions of superplasticizer (beyond 3.0%), there is little or no change in slump, but the slump-spread continues to increase at a decreasing rate. This is in agreement with the expected improvements in workability, and may be due to the continual increases in water content at dosages exceeding the saturation value of the superplasticizer.

(I) With the MH system

The results with the MH system show that successive redoses of the superplasticizer, from 1.50 to 3.0%, considerably reduce the yield value of the mix (from 10.88 Nm

to zero), but increase its plastic viscosity (from 8.61 to 14.02 Nms). This is in contradiction with what would be expected, and implies that the concrete undergoes progressive reductions in inter-particle friction but increasing internal resistance to flow[56] (c.f. page 13). Although it can be argued that the increases in plastic viscosity are outweighed by the larger reductions in yield value[124], it is difficult to conclusively say whether the overall workability is actually increased or reduced in this dosage range.

With further redosing of the mix, the yield value remains relatively unaffected, whilst the plastic viscosity reaches a plateau at approximately 14 Nms, and then starts to decrease with increasing dosage (i.e. the mix exhibits Newtonian behaviour). These results, and the time-dependent increases in the Bingham parameters after the last redosing test (Table 5.2), are in agreement with Banfill's workability measurements[124] in flowing NSC (c.f. figures 2.17, 2.33 and 2.37).

The uplift measurements in figure 5.11(b) however show that the increases in plastic viscosity are consistent with decreasing volume expansions of the concrete in the MH system. In the 1.5-3.0% dosage range, where the plastic viscosity is increased by 5.4 Nms, the up-lift effects exerted by the helical impeller decrease from 75 mm (32.6%) to 25 mm (10.9%); and thereafter reach a minimum value of 20 mm (or 8.7%) before the plastic viscosity starts to decrease at higher dosages.

From these results, it can therefore be concluded that the ability of the MH system to measure representative variations in workability is directly related to whether the measurements are made at or below the 20 mm minimum (or threshold) value with regards to concrete uplifting.

- Below the threshold value, the variations in plastic viscosity are influenced by increasing volume expansions of the concrete with decreasing fluidity.
- At the threshold value, the helical impeller exerts a small but constant uplift on the concrete, and the MH system can detect the relative increases in fluidity or losses of workability resulting from increased or reduced dispersion of the cement particles.

(II) With the LM system

In contrast, the redosing measurements with the standard LM system show that increasing additions of superplasticizer (from 1.5 to 3.0%) give progressive reductions in both the Bingham parameters and are, therefore, in agreement with what would be expected. The workability improvements in this dosage range are more pronounced with regards to yield value which is completely eliminated (i.e. reduced to zero), whereas the plastic viscosity is reduced by about a half (from 7.79 to 4.01 Nms). With further redosing of the concrete, the yield value, as in the MH measurements, remains essentially unchanged (at zero Nm), whilst the plastic viscosity continues to decrease with increasing dosage. This is consistent with the observed increases in slump-spread in Table 5.2.

Although the redosing measurements with the broader H-impeller (Table 5.2) show similar variations in the Bingham parameters to those with the standard H-impeller, they indicate that the lowest measurable yield value is about 2.0 Nm. This would therefore represent a limitation in assessing high workability concretes having no initial resistance to deformation, and may, as mentioned in page 172, be associated with greater aggregate interference (or collisions) with the sides of the test bucket.

Contrary to suggestions by de Larrard et al[49] and Wallevik and Gjorv[86], the segregation results in Table 5.2 show that capabilities of both the MH and LM systems to measure loss of workability are independent of segregation tendency during testing. That is, both versions of the apparatus are capable of measuring the stability of mixes to resist segregation and loss of workability.

Table 5.2 : Summary of **redosing test results** with the MH and LM systems (at 0.26 w/b).

Test	Property	Successive redoses with SNF superplasticizer (%, s/w/b)										Loss of workability after	
		1.50	1.75	2.00	2.25	2.50	3.00	3.50	4.00	4.50	5.00	15 mins	30 mins
Slump	Slump (mm)	95	170	230	245	255	260	260	255	255	260	255	245
	Spread (mm)	200	320	490	550	590	605	615	620	630	635	615	580
Standard MH system	g value (Nm)	10.88	8.4	4.92	1.49	0.43	**0.10**	**0.08**	**0.11**	**0.05**	**0.15**	0.36	0.91
	h value (Nms)	8.61	9.2	10.8	12.4	13.8	14.02	14.14	11.9	9.1	7.11	7.52	8.31
	r	0.9667	0.9711	0.9801	0.9781	0.9824	0.9948	0.9942	0.9984	0.9982	0.9991	0.9973	0.9979
	SI value (%)	3.2	-	-	-	17.5	-	-	-	-	30	24	28
	Up-lift, AH (mm)	75	55	40	35	30	25	20	20	20	20	20	25
Slump	Slump (mm)	105	180	235	240	250	255	255	250	255	250	250	240
	Spread (mm)	200	315	505	555	595	615	625	630	635	640	605	585
Standard LM system	g value (Nm)	9.4	7.01	3.5	1.01	0.31	**0.05**	**0.11**	**-0.03**	**-0.09**	**0.02**	0.29	0.79
	h value (Nms)	7.79	7.17	6.44	5.89	4.91	4.01	3.42	3.02	2.51	2.02	2.43	3.71
	r	0.9720	0.9789	0.9801	0.9872	0.9885	0.9985	0.9987	0.9979	0.9992	0.9993	0.9989	0.9984
	SI value (%)	5.19	-	-	-	-	-	-	-	-	35	30.1	29.5
Slump	Slump (mm)	90	-	230	-	250	250	255	250	255	255	-	235
	Spread (mm)	200	-	485	-	585	610	620	625	630	630	-	570
LM system (**Broader impeller**)	g value (Nm)	13.15	-	8.91	-	4.01	-	1.75	1.88	-	1.79	-	2.91
	h value (Nms)	14.18	-	10.89	-	8.37	-	7.09	6.41	-	5.78	-	6.44
	r	0.9221	-	0.9413	-	0.9523	-	0.9704	0.9817	-	0.9839	-	0.9771
	SI value (%)	2.85	-	-	-	-	-	-	-	-	-	-	17.7

Note : All yield values in **Bold** are taken as zero.

The successive redoses from 1.50 to 5.00% increase the water content of the mix from 133 to 163 l/m^3 (I.e. from 0.26 to 0.32 w/b ratio).

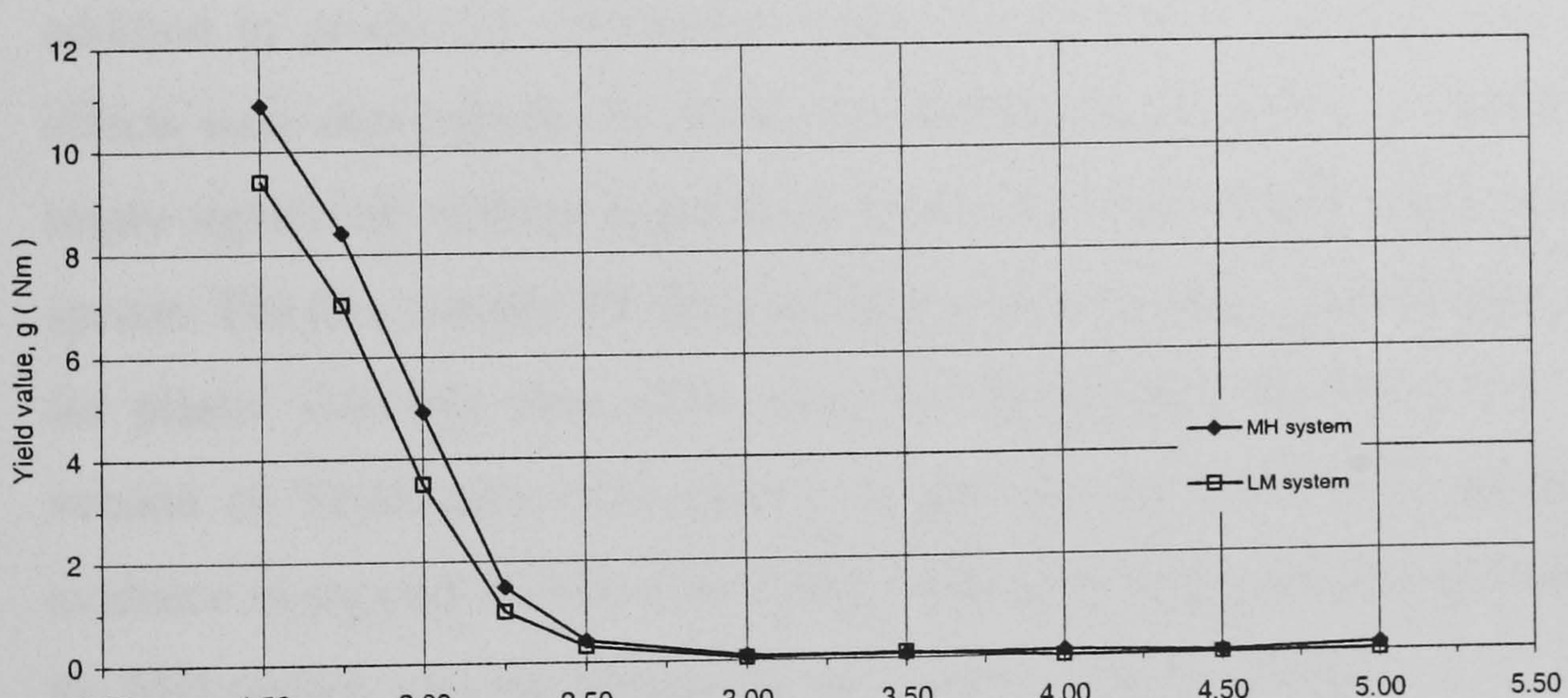

Figure 5.11 : Effects of successive doses of SNF superplasticizer on (a) yield value and (b) plastic viscosity as measured by the MH and LM systems. ((b) also shows up-lift effects in MH system).

5.5.5 Summary and further discussion

The results in this section have shown that, apart from **time-dependent** measurements of loss of workability, the **up-lift** and **redosing measurements** can provide additional and invaluable diagnostics tests to assess the shearing efficiency of different two-point test instruments. With the MH system, the tests showed that, at slumps lower than 230 mm, the deficiency of the apparatus to measure representative variations in workability is a direct consequence of the helical shape of its impeller and the volume expansions this exerts on the concrete during testing.

These findings indicate that similar problems may exist with the BT Rheometer, whose bottom spoked plate (like the helical impeller in the MH system) was reported by de Larrard et al[49] to cause the concrete in the container (figure 2.7) to expand, and the coarse aggregates to rise to the surface of the sample during testing (particularly in mixes having high aggregate contents or low paste viscosities). In addition to producing continuous reductions in plastic viscosity with time, these effects were also reported to cause time-dependent reductions in yield value, which imply significant volume expansions of the concrete at both low and high testing speeds. The fact that the BT Rheometer has been found to give stronger correlations for plastic viscosity than yield value (0.99 compared to 0.81) with a modified version of Tattersall's MH system (known as the LAFARGE rheometer[91]), is evidence in support of this. (The LAFARGE rheometer uses helical blades and, like the MH system, was reported to lift the concrete during testing).

The redosing measurements with the MH system also indicate that Hu et al's suggestion[40] (page 62) that the increases in plastic viscosity (μ) as measured by the BML viscometer with sequential additions of superplasticizer, are due to increases in the viscosity of the liquid phase (relative to pure water), is incorrect, or less significant. Their results instead indicate similar deficiencies with the BML viscometer in measuring representative variations in workability as those observed with the MH system. The fact that the BML viscometer has been found to give good correlations (0.99 for plastic viscosity and 0.94 for yield value) with the MH

system[86], is evidence in support of this, and suggests that the viscometer may also suffer from some uplift effects, possibly due to upward movement (or slippage) of the concrete between the inner and outer cylinders.

In contrast, the present observations with the LM system have shown that its shearing performance is unaffected by any noticeable up-lift effects from the H-impeller, and the apparatus gives results consistent with the expected variations in workability. Its time-dependent and redosing measurements (respectively showing progressive increases and reductions in both the Bingham parameters) imply that the results from the LM system are mainly governed by :

- the build-up of inter-particle forces with time, and
- the dispersion induced by superplasticizers and/or increasing water contents.

It is however reasonable to assume some secondary effects in the measurements with the LM system, due to, for example, bucket wall friction and aggregate interference, particularly at low slumps.

In a recent investigation to compare measurements from the BML viscometer, BT rheometer, MH system, and two other rheometers (based on modifications of the BML viscometer and LM system) at slumps of 90-235 mm, Ferraris et al[242] concluded that:

- the slump test (contrary to the results in figure 5.6(c)) correlates well with the measured yield stress from all five instruments, and
- the instruments give different values of the Bingham parameters of yield stress and plastic viscosity, even when these are expressed in fundamental units.

Ferraris et al[242] stated that the latter may be attributed to several causes, such as slippage at the concrete/wall interface, or confinement of the concrete between the moving parts of the rheometers, but did not identify the uplift effects (i.e. volume expansion) of concrete during testing as a primary cause.

The validity of measurements reported with the BML viscometer, BT Rheometer and MH system are further discussed in subsequent chapters.

5.6 Validity of mortar tests

As mentioned previously in sections 2.5.3 and 4.3.2, the spread test in mortar (like the slump test in concrete) is believed to provide a measure of the flowability[58] or yield property, whilst the flow time through an orifice (such as the Marsh cone or V-funnel) is considered to provide an indication of viscosity[8, 58, 151]. In this section the spread and V-funnel tests (described in chapter 4) were used to determine whether the mortar fractions of the concrete mixes tested in sections 5.3 and 5.5 could be used for:

- fixing the superplasticizer dosages needed for a given slump in concrete; and
- predicting the workability properties of concrete.

The tests were also used to assess the variability/repeatability of mortar mixing procedure, and to broadly compare loss of workability in mortar and concrete. These aspects have not been adequately investigated by previous researchers.

5.6.1 Comparison of mortar and concrete workability properties

The spread and V-funnel measurement for the mortar fractions of the concrete mixes tested in sections 5.3 (at 0.42, 0.40, 0.30, 0.26, and 0.22 w/b) and 5.5 (for successive redoses of superplasticizer) are shown in figure 5.12 and Table 5.3.

As with the concrete mixes, the mortar spreads of the mixes (in **figure 5.12**) varied with the superplasticizer dosages used and slumps measured in section 5.3. Comparable spreads of 320-330 mm were obtained for the mortar fractions of the concrete mixes having w/b ratios of 0.42-0.26 and initial slumps of 220± 5 mm, whilst a lower spread of 280 mm was obtained for the 150 mm slump of the 0.22 w/b ratio mix (before redosing).

When compared to the two-point test measurements in figure 5.2, the results in figure 5.12 also indicate broad agreement between the increases in the Bingham parameters in concrete and the V-flow times in mortar for decreasing w/b ratio. The results however do not clearly show whether the V-funnel flow times explicitly represent measurements of viscosity, or are dependent on both viscosity and yield value.

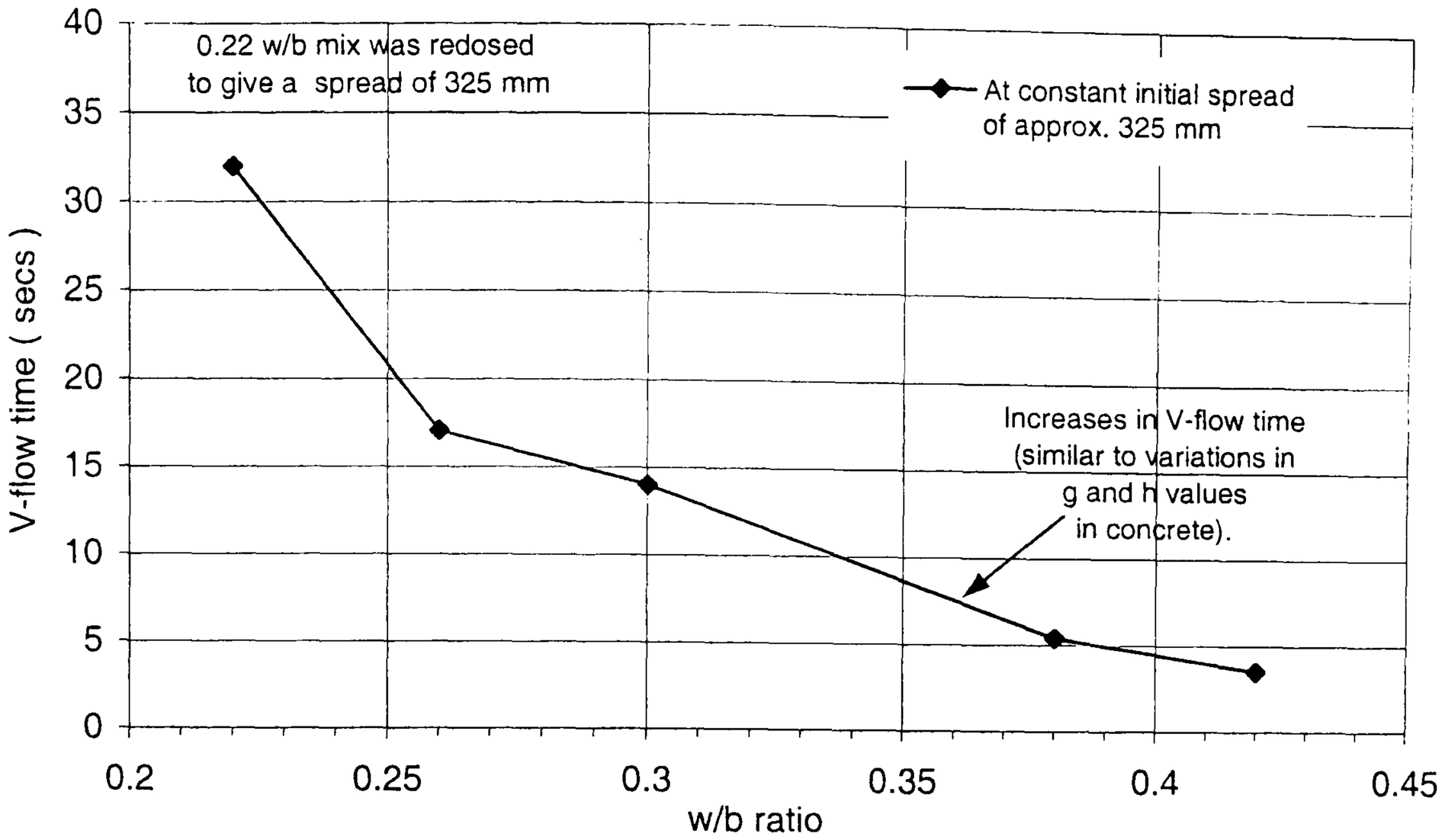

Figure 5.12 : Variations in mortar V-flow time with w/b ratio (using moist sand).

The fact that the V-flow time from the redosing tests (in **Table 5.3**) systematically decreases with dosages higher than 3.0%, does however provide some indication of a greater dependence on plastic viscosity than on yield value (c.f. Table 5.2), at least at high spreads/workabilities. From these results it can therefore be concluded that:

- the mortar spread varies in accordance with concrete slump and superplasticizer dosage, whilst
- the mortar V-flow time appears to correlate with variations in both the Bingham parameters.

5.6.2 Assessment of repeatability

A major source of variability experienced during preparation of the mortar mixes was that the time taken in ensuring that all the moist sand comes into contact with the cement (before introducing the superplasticizer), was long and difficult to consistently control. In contrast with the ½ min. delayed addition of the superplasticizer used to produce the concrete mixes (in sections 5.3-5.5), the preparation of the mortar fractions required 2½-3½ minutes manual mixing with a

palette knife to sufficiently blend the moist sand and cement. This was followed by 1 minute mixing in the Hobart food mixer, before adding the superplasticizer and the rest of the mixing water.

To assess the variability/repeatability of mortar mixing procedure, the mortar fraction of mix 6 (in Table 3.6) was replicated and tested seven times with both dry and moist sand. A statistical analysis showing the mean, range, standard deviation, and 95% confidence limits of the results obtained is given in **Table 5.4**(**a** and **b**). For each statistical parameter it can be clearly seen that the variability in the results increases with time after mixing, and is much higher with the moist sand. For example, the range in the spread and V-funnel results is respectively reduced from 15 mm and 4.50 secs with the moist sand to 7.5 mm and 1.60 secs with the dry sand at 8-12 minutes; and from as much as 55 mm and 8.04 secs to 27.5 mm and 2.3 secs at 90-95 minutes.

These results therefore clearly show that the degree of control and confidence in making comparative mortar measurements is significantly higher with dry sand. This eliminates the problems experienced in premixing the sand and cement. The high variability with the moist sand can be attributed to varying superplasticizer performance resulting from differences in its addition time[152] (c.f. figure 2.39), and the small capacity of the Hobart mixer.

In terms of loss of workability, it is however worth noting that, although the time-dependent increases in the mean V-flow times (in Table 5.4) are consistent with the increases in the Bingham parameters from the LM system (c.f. figure 5.10), the mean mortar spread losses during the first 90 mins are about four-to-seven times lower than the observed slump losses. That is, the rate of loss of workability in concrete appears to be much faster than in its mortar fraction. More direct relationships between the workability properties of mortar and concrete are presented in chapter 6.

Table 5.3 : Redosing tests with mortar at 0.26 w/b (using moist sand)

Measured property	**% redose** of SNF superplasticizer									
	1.50	1.75	2.00	2.25	2.50	3.00	3.50	4.00	4.50	5.00
Spread (mm)	270	-	320	-	335	345	350	360	355	365
V-flow time (secs)	26.4	-	12.7	-	8.8	7.4	6.5	5.3	4.53	4.11

Table 5.4 : Repeatability of mortar test results **with moist and dry sand** (at 0.26 w/b)

(a) With moist sand

Measured Property	Time (mins)	Replication Numbers							Statistical Analysis of results (R1-R7) Mean	Range	Standard Deviation	95% confidence Limits (+/-)
		R1	R2	R3	R4	R5	R6	R7				
Mortar	8-9	325.0	327.5	315.0	312.5	327.5	325.0	315.0	321.1	15.0	6.59	4.88
spread	30	300.0	312.0	285.0	280.0	295.0	310.0	310.0	298.9	32.0	12.81	9.49
	60	265.0	300.0	270.0	255.0	290.0	290.0	305.0	282.1	50.0	18.90	14.00
(mm)	90	255.0	292.5	255.0	240.0	265.0	285.0	295.0	269.6	55.0	21.33	15.80
V-flow	11-12	16.1	12.8	17.2	16.9	15.5	13.9	12.7	15.0	4.50	1.88	1.39
time	35	15.4	15.7	19.1	18.9	16.4	16.7	13.9	16.6	5.20	1.88	1.39
	65	20.7	16.8	21.0	21.0	17.5	18.8	15.4	18.7	5.60	2.26	1.67
(secs)	95	23.7	20.4	24.7	25.2	19.4	21.7	16.8	21.7	8.40	3.07	2.27

(b) With dry sand

Measured Property	Time (mins)	Replication Numbers							Statistical Analysis of results (r1-r7) Mean	Range	Standard Deviation	95% confidence Limits (+/-)
		r1	r2	r3	r4	r5	r6	r7				
Mortar	8-9	317.0	312.5	315.0	315.0	320.0	317.5	315.0	316.0	7.5	2.40	1.78
spread	30	307.5	305.0	310.0	307.5	310.0	312.5	310.0	308.9	7.5	2.44	1.81
	60	300.0	290.0	300.0	285.0	295.0	295.0	300.0	295.0	15.0	5.77	4.28
(mm)	90	287.5	267.5	285.0	275.0	285.0	285.0	295.0	282.9	27.5	8.95	6.63
V-flow	11-12	14.1	14.0	13.0	12.5	13.2	13.6	13.6	13.4	1.60	0.57	0.42
time	35	15.5	16.0	14.5	14.1	15.0	14.5	14.2	14.8	1.90	0.71	0.52
	65	16.3	17.4	15.7	16.0	16.7	16.7	15.4	16.3	2.00	0.68	0.51
(secs)	95	17.4	19.4	19.1	18.7	17.9	17.9	17.1	18.2	2.30	0.87	0.64

Note The **mean** is the average of the results.

The **range** is the difference between the max. and min. measured values.

The **standard deviation** is a measure of how widely the results are dispersed from the mean. (It is equal to the " root, mean, square, deviation from the mean ").

The **confidence limits** indicate the range on either side of the sample mean.

BS 5497 : Part 1[243] defines **Repeatability** as " the value below which the absolute difference between two single test rsults obtained by the same operator, materials, apparatus etc may be expected to lie within a specified probability ".

BS 5497 : Part 1[243] defines **Reproducibility** in a similar way, except it refers to different conditions (I.e. results obtained by different operators, using different facilities or at different times).

5.7 Conclusions

- The absorption of water by dry aggregates is continuous with time, and significantly reduces the workability of NSC in the first two hours. The use of 0.15% (s/w/b) SNF superplasticizer at 0.45 w/b ratio reduces the initial yield value by 1.32 Nm (or 31%), increases the initial plastic viscosity by 0.4 Nms (or 28%), but gives continuous reductions in plastic viscosity with time as measured by the MH system.

- A reduction in w/b ratio from 0.42 to 0.26 reduces the initial workability by as much as 9.66 Nm (or more than 20 fold) and 4.1 Nms (or 85%), but gives no conclusive trend with respect to loss of workability when assessed by the MH system at a constant initial slump of 220±5 mm.

- The bleeding tendency of HSCs decreases with decreasing slump level, but does not appear to be influenced by decreasing w/b ratios from 0.42 to 0.26. In contrast, the segregation resistance of coarse aggregates during two-point testing in the first 60 mins increases by two-three times with a reduction in the w/b ratio from 0.42 to 0.26.

- The compactability of HSC mixes as assessed by the amount of subsidence (or drop in height) after vibration decreases by more than 50mm (or 8 fold) in the first 60 mins, but does not appear to vary with decreasing w/b ratio.

- Two-point test measurements with the MH system indicate that:
  - the mix stability of HSCs is influenced more by the yield value than the plastic viscosity; whereas
  - the compactability under self-weight is more influenced by the plastic viscosity. (A more sensitive method is however needed to assess the vibration response of HSCs at different amplitudes of vibration).

- Tattersall's assertions[7] that the MH and LM versions of his two-point test apparatus respectively measure medium-to-high and low-to-medium workabilities are misleading and incorrect.
  - The MH system suffers from significant up-lift effects exerted by the helical shape of the impeller. These increase the volume of the concrete during testing by as much as 30%, reduce its shearing resistance with decreasing slump, and lead to continuous reductions in plastic viscosity with time.
  - In contrast, the LM system does not cause any noticeable volume expansions of the concrete and, is capable of measuring representative variations of workability in the high-medium slump range.

- Mortar spread and V-funnel flow time measurements appear to be closely related to variations in the slump and Bingham properties of concrete. (Further work is however needed to determine whether the mortar spread and V-funnel measurements can be explicitly related to measurements of yield value and plastic viscosity, and assess their suitability in predicting loss of workability in concrete).

These aspects are addressed in the next chapter which focuses on the effects of superplasticizers on dosage response and loss of workability in HSCs.

Chapter 6
Assessment of Superplasticizers

6.1 Introduction

The selection of an efficient superplasticizer, which is capable of providing the desired initial workability and maintaining sufficient workability retention during the placing and compaction stages, is considered to be the most important feature in the production of HSC[33]. That is, the superplasticizer must be capable of: efficiently dispersing the cement particles at low w/b ratios, and providing sufficient dispersion stability to overcome the strong tendency for the particles to flocculate with time. The literature review in section 2.5 showed that the fluidizing action of superplasticizers depends critically on their type (or brand), dosage amount, mixing procedure and compatibility with different cements. The information available on each of these areas is however fragmented, and is generally based on studies involving a narrow range of superplasticizers and/or test variables.

This chapter presents the results of tests used to assess the workability properties of conventional and new-generation superplasticizers with regards to their:

- **type or brand** at constant dosage (including repeatability tests)
- **dosage** performance (up to and beyond the saturation value)
- **mixing procedure** (viz. delayed and split additions, and blending)
- **compatibility** with different cements.

The chapter also discusses the **role** of superplasticizers **on mix stability** and **compactability**, and examines possible **relationships between** the **Bingham parameters** with slump-flow time **and** the **workability properties of mortar**. The workability enhancing properties of the superplasticizers were in each case assessed by the spread and V-funnel tests in mortar, and subsequently by the slump and LM two-point test system in concrete. The assessments in the concrete and mortar fractions were carried out at 0.26 w/b ratio, using mix 6 (proportions given in Table 3.6) and a 10% replacement of the cement by CSF.

6.2 Comparison of chemical admixtures (at constant dosage)

The performance of different types of superplasticizers and other water reducers, as highlighted in section 2.5, is usually determined by comparing their workabilities at either a constant dosage (i.e. active solids content)[8], or in terms of their dosage requirements to obtain a given slump[53, 118-119, 133]. The performance of superplasticizers can in practice also be based on economic efficiency to obtain a given level of workability[41].

In this section the performance of the nine superplasticizers and two plasticizers shown in Table 4.3 is compared in mortar at a constant dosage of 2.00% (s/w/b) and, using the one minute delayed addition of superplasticizer shown in figure 4.1 (procedure 2). The dosage used was based on a trial concrete mix with the control SNF (Conplast SP 435) superplasticizer to achieve a slump of 220 mm. The performance of five of the nine superplasticizers, comprising three conventional (a SMF, MLS, SNF) and the two new-generation superplasticizers, is subsequently compared for slump loss and workability retention in concrete.

The loss of workability measurements from the LM two-point tests are presented on a " **g vs h plot** " (c.f. figure 6.2(b)) to provide more direct comparisons of the overall changes in workability with time. The first point (nearest the origin) represents the overall workability at 10 mins, the second point represents it at 30 mins, ..., whilst the fifth and last point (when determined) represents it at 120 mins. This graphical illustration of the two-point test results is used in the rest of the thesis.

6.2.1 Comparison of chemical admixtures in mortar

The mortar test results in **figure 6.1(a-b)** show that the various types of admixtures have significant effects on both the initial workability properties and workability retention. The initial mortar spread values and V-flow times differ by as much as 210 mm and 28 secs respectively, and although the spread-time reductions are relatively small and follow the same pattern, the admixtures exhibit noticeable differences in workability retention in terms of their V-flow time increases.

As can be seen, the lowest initial workability (i.e. lowest spread and highest V-flow time) is produced by the retarding admixture (Conplast R), whilst the highest initial workability is obtained with the NG Acrylate-based (D 2001) co-polymer. Contrary to previous suggestions[118-119, 133], the longest workability retention is obtained with the two SNF superplasticizers (equivalent to about 21 mm/hr spread loss, and 2.4 secs/hr increase in V-flow time) and not the two new-generation superplasticizers based on Vinyl (33 mm/hr and 4.6 secs/hr) and Acrylate (35 mm/hr and 3.5 secs/hr) co-polymers.

The contrasting workabilities of the two **SMF superplasticizers** (Conplast M1 and Sika FF) suggest that factors other than generic type can significantly influence performance. The mortar spread with Sika FF is as much as 50% higher, and its V-flow time is up to 60% lower compared to Conplast M1 in the first 60 mins. The lower dispersion efficiency of Conplast M1 may be associated with a lower molecular weight and/or shorter chain length compared to Sika FF. According to Ramachandran[120] and others[55, 113, 147], superplasticizers with higher molecular weights and/or longer chain lengths exhibit more effective water reductions, and hence produce higher workabilities.

In contrast, the two **SNF superplasticizers**, Conplast SP 435 and Sika N, produce comparable initial mortar spreads and V-flow times (310-315 mm and 5.5-6 secs) which are only marginally lower than those obtained with the Acrylate-based co-polymer (D 2001), but, as mentioned above, exhibit longer workability retention. The performance of the single **MLS superplasticizer** tested (Darcem SP 4), is intermediate to those of the SMF and SNF superplasticizers.

In relation to the two **pre-blended superplasticizers**, Darcem SP 6 (based on blended sulphonate materials) produces a 70-75 mm (i.e. 20-25 %) higher spread, and as much as 12-34 sec (i.e. a three-five-fold) lower V-flow time during the first 90-95 mins compared to Conplast SP 450 (comprising a blend of melamine and lignosulphonates). However, despite its comparable workability properties to the

two SNF superplasticizers, Darcem SP 6, like the **Acrylate**-based **co-polymer** (D 2001), obtained from the same suppliers), was found to produce strong pungent smells which meant breathing masks were necessary during testing.

Contrary to Billberg et al's observations[118] (figure 2.23), the **Vinyl**-based **superplasticizer** (Sika 10) did not impart the relatively high initial workability and long workability retention expected with new-generation superplasticizers. Its workability properties are instead comparable to those of the MLS superplasticizer (Darcem SP 4).

Although the dosage used is more than three-times higher than the suppliers maximum recommended value for the two **plasticizers** (Conplast R and PA21), it is interesting to note that both of these products produced measurable workabilities at the 0.26 w/b ratio. This is in contrast with previous attempts by Kreijger[111] which indicated that plasticizers are ineffective at w/b ratios less than or equal to 0.30.

In fact the air-entraining admixture (Conplast PA21) imparts a higher workability than the SMF superplasticizer (Conplast M1), and its V-flow time is lower than all the other products. Its contrasting effects in reducing the mortar spread and the V-flow time below that of, for example, the mixes with the SNF superplasticizers, lends support to Kreijger's suggestion[111] that air-entraining agents increase the yield value but reduce the plastic viscosity. (As mentioned previously, the spread and V-flow time measurements are respectively believed to reflect the yield value and plastic viscosity properties[8, 58, 151] (further discussed in section 6.7.2)). These characteristics, and the excellent spread retention obtained with the retarding admixture (Conplast R) suggest that these plasticizers may offer significant workability benefits when blended with superplasticizers (examined in section 6.4.2).

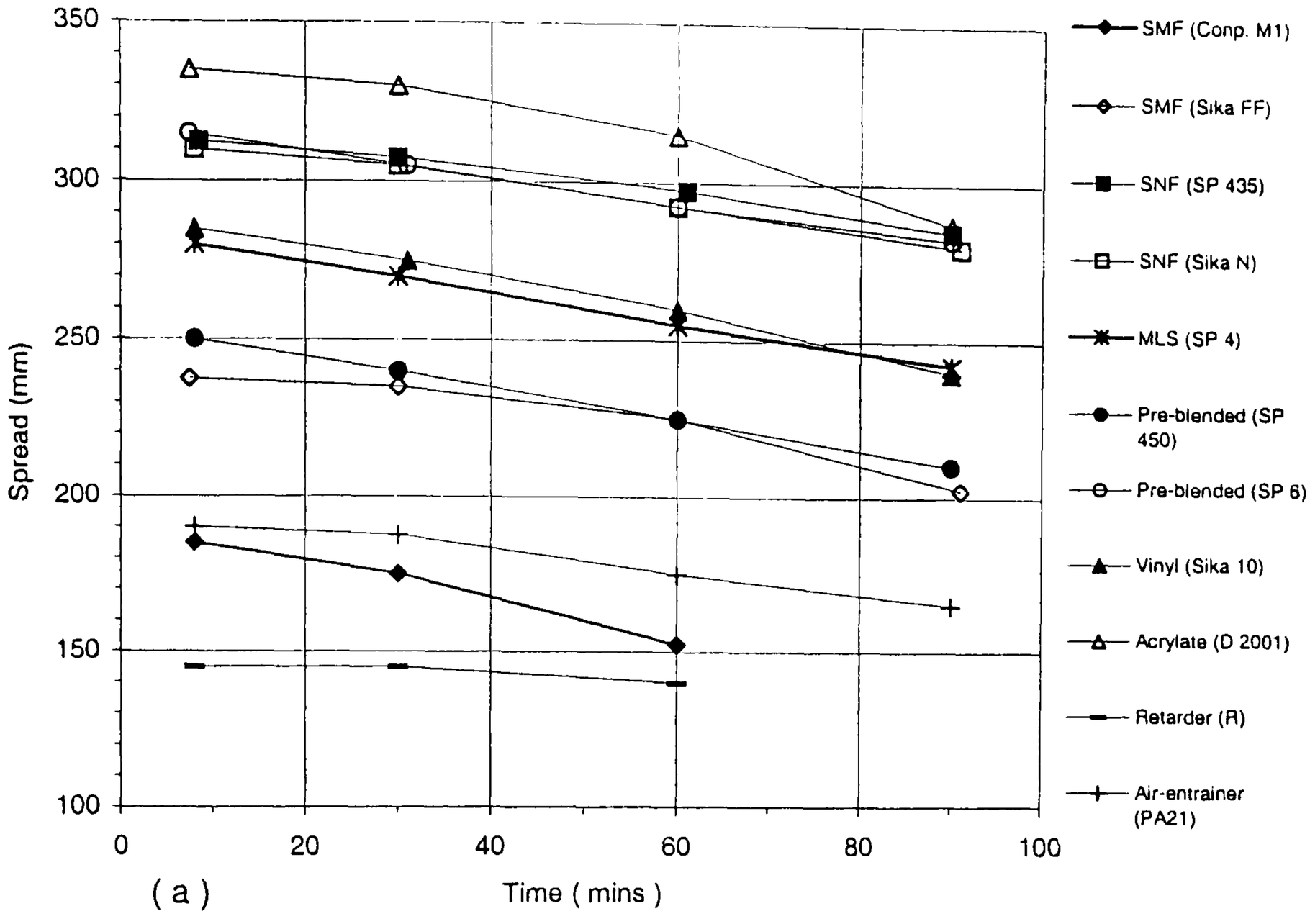

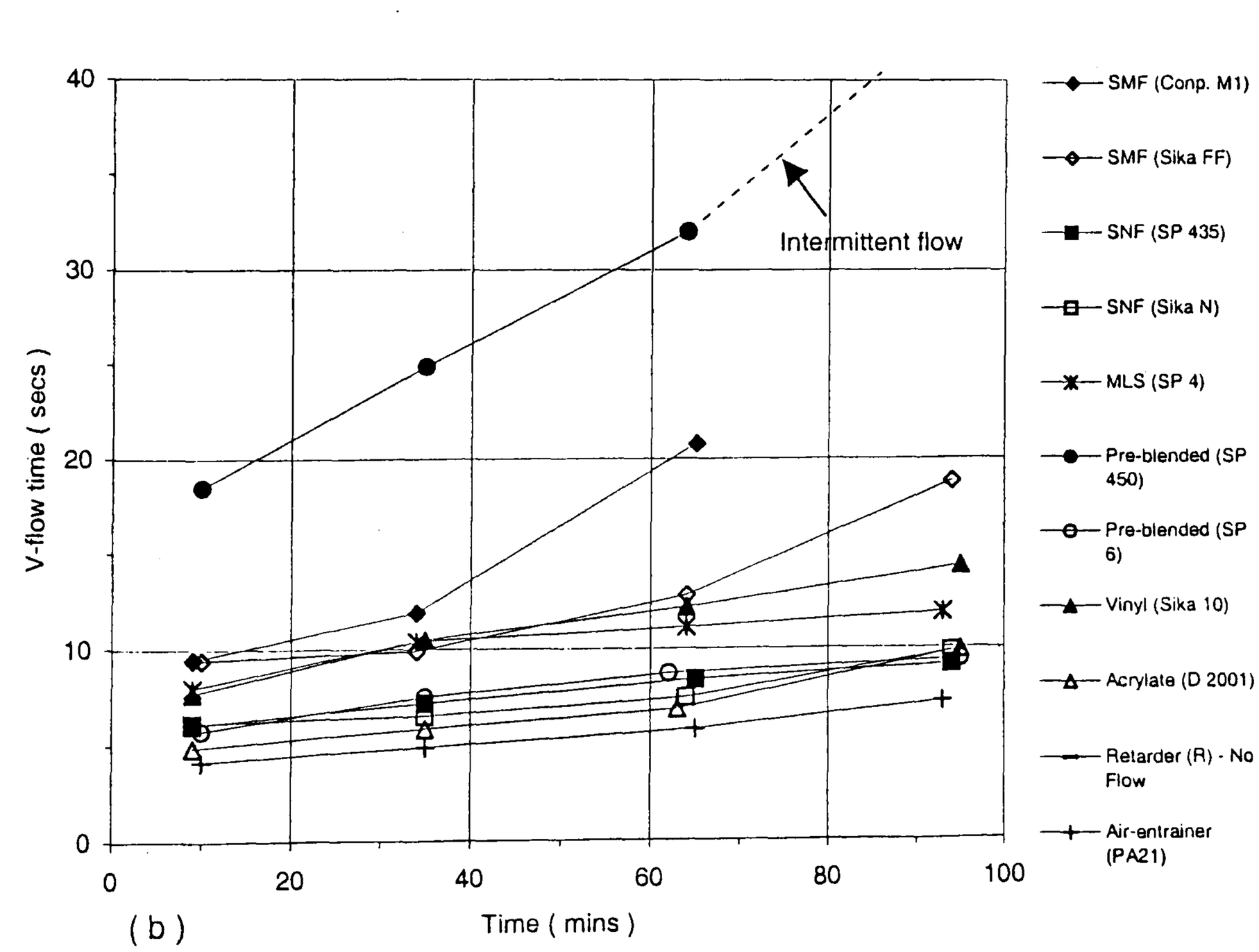

Figure 6.1 : Effects of different types/brands of chemical admixtures on mortar (a) spread and (b) V-flow time at a constant dosage of 2.00% s/w/b. (Using 1 min delayed Addition, 10 % CSF, 0.26 w/b).

6.2.2 Comparison of superplasticizers in concrete

The slump losses and workability retentions of the three conventional superplasticizers (Sika FF, SP 4 and SP 435) and the two new-generation superplasticizers (Sika 10 and D 2001) in concrete are presented in figure 6.2(a-b). The slump loss characteristics of the superplasticizers in **figure 6.2(a)** show more pronounced reductions in fluidity compared to the mortar spread losses in figure 6.1(a).

In particular, the slump reduction with the D2001 superplasticizer (of 210 mm or 87%, in the first 95 mins) is much larger than the corresponding spread reduction observed in its mortar fraction (of 50 mm or 14%), and the 80 mm (35 %) slump reduction reported by Billberg et al[118] with their acrylic-based copolymer at 0.60 w/b ratio (c.f. figure 2.23). The slump reductions with Sika 10, however closely agree with Billberg et al's results[118] with their Vinyl-based co-polymer (also shown in figure 2.23).

The two-point test results in **figure 6.2(b)** show that the five types of superplasticizers produce distinct effects on both the initial Bingham parameters and their evolution with time. The results therefore contradict the conventional view presented by Tattersall[7, 81] and others[30, 40, 49, 201], that superplasticizers essentially reduce the yield value but have little or no effect on the plastic viscosity.

As can be seen, the highest initial workability (i.e. lowest g and h values) is obtained with the Acrylate-based (D 2001) copolymer, the lowest with the SMF superplasticizer, whilst the intermediate initial workabilities of the SNF, Vinyl, and MLS superplasticizers mainly differ in the yield values. These results are consistent with the overall workability ranking order shown by the slump and mortar measurements, that is: **SMF << MLS < Vinyl < SNF < D 2001**. The comparatively low initial workability obtained with the SMF superplasticizer is represented by nearly a ten-fold increase in yield value and a doubling of the plastic viscosity compared to the D 2001 co-polymer.

In terms of loss of workability, it can be seen that both the SMF and MLS superplasticizers produce relatively larger increases in plastic viscosity during the first 30 minutes; whilst the Vinyl and Acrylic-based new-generation superplasticizers exhibit more pronounced increases in yield value than in plastic viscosity with time. In contrast, the SNF superplasticizer gives smaller and more comparable increases in both the Bingham parameters with time.

The higher rate of loss of workability produced by the D 2001 superplasticizer in the first 90 minutes nearly doubles the initial plastic viscosity (compared to only a 20% increase with the SNF), and increases the initial yield value by more than fifteen fold (compared to a two-fold increase with the SNF). These results, and the similarly large increases in the Bingham parameters with the Vinyl-based superplasticizer contradict Billberg et al's conclusions[118] that NG superplasticizers produce longer workability retention than, for example, SNF (page 44).

The fact that the rates of loss of workability of the superplasticizers in concrete (particularly with the D 2001 polymer) are much larger than those in the mortar fractions (figure 6.1), can however suggest some variability in superplasticizer performance, and/or differences in behaviour in concrete and mortar. Information regarding the variability of the various types of superplasticizers used was unfortunately not provided by the admixture suppliers, and there is generally very little published work pertaining to the repeatability of their performance in HS and other HPCs.

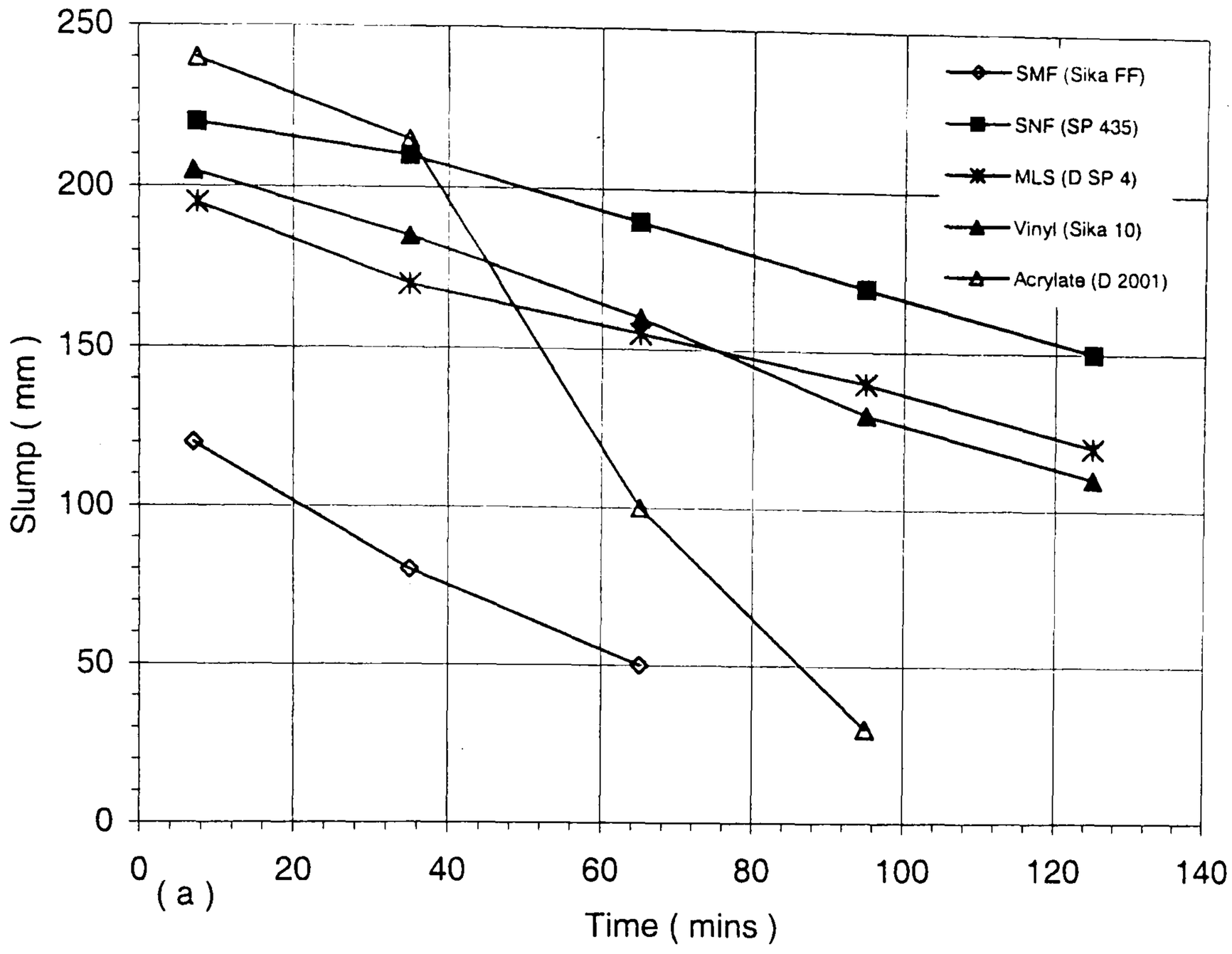

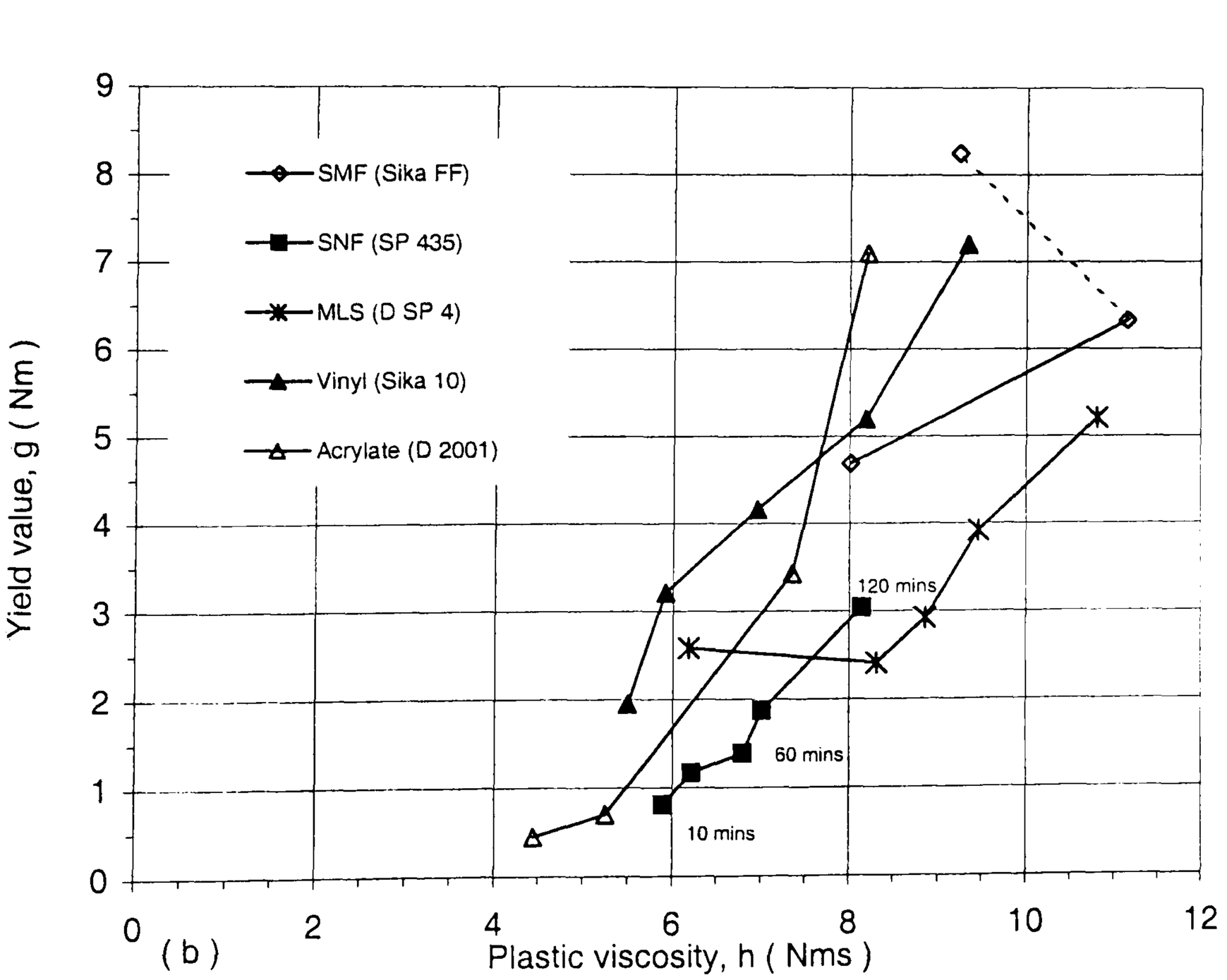

Figure 6.2 : Effects of SMF, SNF, MLS, Vinyl and Acrylate-based superplasticizers on (a) slump Loss and (b) loss of workability at constant dosage of 2.00 % s/w/b. (1 mins delayed addition, 0.26 w/b concrete)

6.2.3 Assessment of repeatability

In the present investigation seven mixes were repeated to statistically assess the repeatability of the results with the LM system and the control SNF (Conplast SP 435) superplasticizer (**Table 6.1**). The results of an eighth mix (R8), in which the CSF slurry was accidentally added to the dry cement (rather than after 30 secs as described in section 4.3.1), are included to account for a change in mixing/batching procedure. Two repeat tests were also carried out to confirm the losses in workability observed with the D2001 and SMF superplasticizers (**Table 6.2**).

(I) Repeatability with SNF superplasticizer

The statistical analysis of the results of the first seven repeat mixes (R1-R7) in **Table 6.1(a)** shows, in contrast with the mortar test results in Table 5.4(b), no systematic or significant increases in variability during the first two hours. The individual and mean g and h values of the mixes are essentially similar during the first 120 mins, and give standard deviations of 0.15-0.40 Nm and 0.57-1.03 Nms, and 95% confidence limits of ±0.11-0.30 Nm and ±0.43-0.76 Nms respectively. Similar results were reported by Banfill[124], who stated (from work involving eight repeat NSC mixes with a SNF superplasticizer) that the MH system is sufficiently sensitive in detecting small differences in concrete properties, and gives standard errors for the g and h values of 0.20 and 0.40 respectively, with 95% confidence limits of ±0.4 and ±0.8.

The 25 mm maximum slump range in Table 6.1(a) is also within acceptance limits (of ±25 mm) set by BS 5497[243] and used in several HPC field applications[244-246]. The 95% confidence limits for the slump (± 3.96-6.67 mm) and slump-spread measurements (±7.36-12.04 mm) are also consistent with values reported by Khayat et al[232] (±10 mm for slump, and ±25 mm for spread) at 0.46 w/b ratio. The results therefore mean that it is possible to produce HSC having average slumps of 221 ± 3.96 mm to 154 ± 6.21 mm, with standard deviations of less than 10 mm, at 10 to 120 mins after mixing.

The repeatability of the slump and two-point test results is however considerably reduced by including the results of mix R8 in the statistical analysis (**Table 6.1(b)**). As can be seen, the confidence in the slump and Bingham measurements at the 95% significance level are, for example, reduced from 174 ± 6.67 mm, 2.10 ± 0.18 Nm and 7.04 ± 0.60 Nms at 90 mins, to 159 ± 29.62 mm, 2.4 ± 0.69 Nm and 6.9 ± 0.63 Nms. That is, a slight change in mixing/batching procedure of even a single mix constituent, can significantly affect the repeatability, and hence quality control of HSC. (The effects of different CSF addition times are discussed in section 7.2).

On the other hand, an exclusion of the results of both mixes R7 and R8 from the analysis significantly reduces the variability in the results as shown in **Table 6.1(c)**. (The high initial workability of repeat mix R7 suggests inaccurate determination of aggregate moisture contents, and there appear to be some sampling errors in the two-point tests at 30-60 mins). As can be seen, the range and standard deviations for the plastic viscosity measurements are, for example, reduced from 3.21 and 1.03 Nms at 60 mins to 0.79 and 0.30 Nms respectively.

From the results of mixes R1-R7 in Table 6.1(a) it can nevertheless be concluded that (providing a consistent mixing, batching and testing procedure is used) it is possible to produce HSC with satisfactory repeatability of workability (of ±6.67 mm, ± 0.30 Nm and ± 0.76 Nms) up to 120 mins after mixing.

It is possible that the systematic reductions in repeatability with time observed in the mortar tests (Table 5.4(a-b)) are related to the small sample size used (1.5 litres compared to 35 litres in concrete), and consequently, to larger losses of paste and/or water to the testing equipment and by evaporation.

(II) Influence of superplasticizer type

The slump and two-point test results of the SMF and D 2001 superplasticizers, like those of the SNF superplasticizer, agree closely with the previous measurements (**Table 6.2**) and show no apparent reductions in repeatability with

Table 6.1 : Statistical assessment of repeatability with SNF superplasticizer (2.00% dosage, 1 min addition, 0.26 w/b ratio)

Workability Measurements	Time (mins)	Repeat mix numbers R1	R2	R3	R4	R5	R6	R7+	R8 *	(a) Statistical analysis of results R1-R7 Mean	Range	Standard Deviation	95% confidence Limits (+/-)	(b) Statistical analysis of R1-R8 Mean	Range	Standard Deviation	95% confidence Limits (+/-)	(c) Statistical analysis of R1-R6 Mean	Range	Standard Deviation	95% confidence Limits (+/-)
	8	220	215	220	215	225	220	230	130	221	15	5.35	3.96	209	100	32.45	22.49	219	10	3.76	3.01
Slump	35	210	200	210	205	210	205	220	100	209	20	6.27	4.64	195	120	38.82	26.90	207	10	4.08	3.27
(mm)	65	190	190	190	185	180	195	200	80	190	20	6.45	4.78	176	120	39.35	27.27	188	15	5.16	4.13
	95	170	165	165	170	175	180	190	55	174	25	9.00	6.67	159	135	42.74	29.62	171	15	5.85	4.68
	125	150	155	145	150	160	150	170	35	154	25	8.38	6.21	139	135	42.88	29.71	152	15	5.16	4.13
	8	475	480	460	455	480	480	490	245	474	35	12.39	9.18	446	245	81.87	56.73	472	25	11.25	9.01
Slump-	35	410	390	405	400	380	400	395	215	397	30	9.94	7.36	374	195	65.05	45.08	398	30	10.84	8.67
Spread	65	365	335	350	365	335	370	350	205	353	35	14.39	10.66	334	165	53.95	37.38	353	35	15.71	12.57
	95	310	290	290	305	300	325	330	200	307	40	15.77	11.69	294	130	40.60	28.13	303	35	13.29	10.64
(mm)	125	245	270	245	250	270	245	285	200	259	40	16.26	12.04	251	85	25.60	17.74	254	25	12.42	9.93
Yield (g)	10	0.81	0.72	1.00	0.95	0.89	0.85	0.54	2.50	0.82	0.46	0.15	0.11	1.03	1.96	0.61	0.42	0.87	0.28	0.10	0.08
value	30	1.17	1.29	1.50	1.11	0.95	1.21	1.10	4.22	1.19	0.55	0.17	0.13	1.57	3.27	1.08	0.75	1.21	0.55	0.18	0.15
	60	1.39	1.37	1.77	1.71	1.62	1.40	1.27	7.08	1.50	0.50	0.19	0.14	2.20	5.81	1.98	1.37	1.54	0.40	0.18	0.14
	90	1.87	2.09	2.37	2.41	1.98	2.20	1.78	4.84	2.10	0.63	0.24	0.18	2.44	3.06	0.99	0.69	2.15	0.54	0.21	0.17
(Nm)	120	3.04	2.83	3.35	3.49	3.22	3.37	2.33	-	3.09	1.16	0.40	0.30	3.09	1.16	0.40	0.30	3.22	0.66	0.24	0.19
Plastic	10	5.89	5.72	5.30	6.04	6.03	5.80	4.28	7.15	5.58	1.76	0.63	0.46	5.78	2.87	0.80	0.56	5.80	0.74	0.27	0.22
viscosity	30	6.21	4.89	6.52	6.41	6.04	6.42	5.70	7.92	6.03	1.63	0.57	0.43	6.26	3.03	0.85	0.59	6.08	1.63	0.61	0.49
(h)	60	6.79	6.72	7.51	6.85	6.92	6.73	4.30	8.66	6.55	3.21	1.03	0.76	6.81	4.36	1.21	0.84	6.92	0.79	0.30	0.24
	90	7.01	7.90	7.70	7.15	7.04	7.10	5.40	5.58	7.04	2.50	0.80	0.60	6.86	2.50	0.91	0.63	7.32	0.89	0.38	0.31
(Nms)	120	8.14	7.75	7.59	8.71	7.17	7.90	6.85	-	7.73	1.86	0.61	0.46	7.73	1.86	0.61	0.46	7.88	1.54	0.52	0.42
SI	10	11.8	11.6	10.2	11.4	10.8	10.4	12.8	3.8	11.29	2.59	0.90	0.66	10.4	8.99	2.77	1.92	11.04	1.59	0.66	0.52
(%)	120	4.9	4.9	5.8	5.8	6.14	5.4	7.7	-	5.80	2.82	0.96	0.71	5.8	2.82	0.96	0.71	5.48	1.26	0.51	0.41

Note : The order of the mixes was randomised over a two months period to account for possible variations in the materials and testing conditions.

Two samples of Conplast SP 435 (delivered over a 6 months period) and aggregates G4, G5 were used. Cement PC-7 was used for all the mixes.

Mix R7+ is suspected to involve some sampling and batching errors. Mix R8 * involved a change in CSF mixing procedure.

The mean, range, standard deviation and confidence limits were previously defined in Table 5.4.

time. The maximum statistical ranges for the slump and Bingham parameters with the SMF and D2001 superplasticizers are similar to those with the SNF superplasticizer and, therefore, suggest that the variability/repeatability of HSC mixes is not significantly affected by a change of superplasticizer type or decreasing level of workability.

Table 6.2 : Repeatability tests with SMF and D2001 superplasticizers

Super-plasticizer type	**Previous** results (from figure 6.2)					**Repeat** results					**Difference** in		
	Time (min)	Slump (mm)	Time (min)	Yield value (Nm)	Plastic viscosity (Nms)	Time (min)	Slump (mm)	Time (min)	Yield value (Nm)	Plastic viscosity (Nms)	Slump (mm)	Yield value (Nm)	Plastic viscosity (Nms)
SMF	7	120	10	4.69	8.01	7	90	10	5.06	7.66	30	0.37	0.35
	35	80	30	6.33	11.15	35	75	30	6.28	9.45	5	0.05	1.70
	65	50	60	8.25	9.23	65	55	60	7.13	8.30	5	1.12	0.93
D2001 (Acrylate)	8	240	10	0.35	4.44	8	240	10	0.47	4.85	0	0.12	0.41
	35	215	30	0.7	5.25	35	190	30	0.69	5.95	25	0.01	0.70
	65	100	60	3.43	7.35	65	95	60	4.07	8.21	5	0.64	0.86
	95	30	90	7.1	8.2	95	20	90	8.38	8.89	10	1.28	0.69

In contrast with its use in mortar, the D2001 superplasticizer was however found to exhibit increasing exothermic effects and release more pungent odours at slumps lower than 200 mm. The loss of workability with the D 2001 superplasticizer in concrete was in fact so fast, that it resulted in considerable difficulties in removing the concrete from the two-point test bucket after the first 90 mins. (A repeat mortar test with the D 2001 superplasticizer confirmed the previous results in figure 6.1 (to within ±15 mm and ±0.5 secs) and indicated no noticeable exothermic effects). The reason(s) for the contrasting performance of the D 2001 co-polymer in concrete and mortar is not clear, but may be related to small variations in, for example, ambient temperature and/or the amounts of bleeding water during testing.

(III) Other factors influencing repeatability

The main sources of variability in fresh concrete can be grouped into three main categories :

- **Material variability** (viz. aggregate moisture contents and grading, w/b ratio, cement composition, superplasticizer dosage and type).

  The need for strict control of aggregate moisture content and w/b ratio has been discussed elsewhere[3, 102, 244], and may be partly demonstrated by the results of mix R7. With regards to cement composition, it has been suggested that the variability associated with superplasticizers is less than that with cements, primarily because superplasticizers are fabricated from a limited variety of raw materials in a highly controlled process[41]. (The variability resulting from small variations in cement composition is briefly discussed in section 6.5).

- Variabilities associated with the **mixing**, **batching**, **sampling and testing procedures** used.

  These can be quite significant as demonstrated by the results of the mortar tests in Table 5.4(a-b), as well as those of mix R8 and to a lesser extent mix R7 (Table 6.1(a-c)).

- The variability associated with the **operator and testing equipment**.

  The two-point test apparatus, unlike the slump and other single-point tests, is essentially operator insensitive[7, 66] and, when connected to a computer or chart-recorder (as in this study) eliminates subjective reading errors. In HSC mixes, strict control would however be needed in limiting the time lapsed between re-mixing, sampling and loading of the concrete in the two-point test bucket. In this study, these typically varied from 90-120 secs as described in section 4.3.3.4.

A more comprehensive understanding of the repeatability/variability of both laboratory and field based HSC mixes would require rigorous assessments of all the factors listed above; and would ultimately need to cater for different placing and compaction practices and equipment in ensuring satisfactory quality control of the hardened concrete.

6.3 Superplasticizer dosage performance

Although it is widely accepted that an optimum (or saturation) dosage exists for superplasticizers which gives the highest initial workability and longest workability retention[17, 114, 149], this has not been demonstrated by previous researchers (c.f. section 2.5.3).

6.3.1 Mortar-dosage response tests

The performance of the five different types of superplasticizers tested in section 6.2.2 is shown as a function of dosage in **figure 6.3**(**a**-**b**). The dosage-response curves all follow a similar pattern, in which the initial workability increases at a decreasing rate, up to the saturation dosage, where the highest spread and lowest V-flow time coincide. At higher dosages, the workability appears to remain essentially constant with the SNF and two NG superplasticizers, but noticeably decreases with the SMF and MLS superplasticizers (possibly due to increased amount of solids in the liquid phase). These results are in contrast with those from the redosing tests (in Table 5.3) which showed no clearly defined end point(s) and, therefore, no saturation value(s), particularly with respect to V-flow time.

As can be seen, the saturation dosage is lowest with the SMF and MLS superplasticizers (1.75%) albeit at a reduced maximum workability, and highest with the SNF superplasticizer (2.50%). The two new-generation superplasticizers give intermediate saturation dosages of 2.25%. These dosages are typically 0.50-1.25% (s/w/b) higher than the suppliers maximum recommended dosages in Table 4.3 (which place no specific emphasis on w/b ratio or cement type).

In agreement with the ranking order established in section 6.2, the highest and lowest initial workabilities (or dispersion efficiencies) are respectively produced by the Acrylate and SMF-based superplasticizers. The other superplasticizers exhibit spread ceilings and minimum V-flow times in between those of the Acrylate and SMF polymers. These results are in broad agreement with those by

Daimon and Roy[136, 140] showing lower paste fluidities with SMF compared to SNF (c.f. figure 2.28(c)), as well as those by Collepardi et al[133] which showed higher paste fluidities with their acrylic-based polymer than with SNF (c.f. figure 2.30(c)).

According to Daimon and Roy[136, 140] the increases in fluidity are due to increasing zeta-potentials (i.e. negative charges) up to the maximum dosage, above which no further adsorption takes place (c.f. figure 2.28(a-b)). The increased fluidity of the acrylic-based polymer, according to Collepardi et al[34] is however associated with higher adsorption but lower zeta potential compared to the SNF superplasticizer (c.f. figure 2.30(a-b)). The observations by Collepardi et al[133] and those by Daimon and Roy[136, 140] respectively illustrate the effects of steric hindrance and electrostatic repulsion as described in section 2.5.2.

Mortar tests to assess loss of workability with the SNF superplasticizer showed that the saturation dosage (2.50%) gives better workability retention when compared to higher and lower dosages shown in figure 6.3. Mortar tests with the other superplasticizers at their respective saturation dosages showed, as before, slightly lower workability retention with the Acrylate (D 2001) superplasticizer, and relatively higher V-flow times with the SMF, MLS and Vinyl polymers compared to the SNF superplasticizer (Appendix B). The differences in the workability of the superplasticizers were however less pronounced than those obtained with the constant dosage of 2.00% in section 6.2.1.

6.3.2 Loss of workability in concrete

The effects of increasing dosages of the SNF superplasticizer on slump and workability retention in concrete are shown in figure 6.4(a-b). **Figure 6.4(a)** shows systematic increases in initial slump and longer slump retention with increasing dosages from 1.50% up to the saturation value of 2.50% as determined from the mortar tests. Dosages higher than the saturation value show slightly lower initial slumps, and no improvement in slump retention. These results are therefore in contradiction with the suggestions by West[158] and

others[19, 156-157] (page 59) that the rate of slump loss increases with increasing initial slump and/or dosage.

The two-point test results in **figure 6.4(b)** also show that increasing dosages up to the saturation value of the superplasticizer, produce systematic increases in the initial workability and reductions in the rate of loss of workability. The higher dosages (of 3.00 and 4.00%) show slightly lower initial workabilities, but, unlike the slump test results, much larger rates of loss of workability.

The initial workability improvements obtained with the increase in dosage from 1.50% to 2.50% (saturation value) are represented by nearly a seven-fold reduction in yield value (from 4.06 to 0.56 Nm) and a 40% reduction in plastic viscosity (from 6.33 to 3.79 Nms). It is interesting to note that the small increases in initial plastic viscosity obtained with the over-dosed mixes (of 3.00 and 4.00%) are much lower than those observed in the redosing tests with the MH system in figure 5.11 (0.12-0.82 Nms compared to 5.53 Nms), and may be due to increases in the viscosity of the liquid phase as suggested by Hu et al[40].

In terms of loss of workability, the results show gradual changes in the pattern of loss of workability: from relatively large increases in yield value at the lowest dosage of 1.50%, to comparatively larger increases in plastic viscosity at the highest dosages of 3.00 and 4.00%. In contrast, the saturation dosage (2.50%) shows smaller and more gradual increases in both the Bingham parameters compared to those at higher and lower dosages.

The higher losses in workability with, for example, the 2.00% and 3.00% dosages increase the yield value at 120 mins from 1.46 Nm to 3.09-3.24 Nm (i.e. by more than two fold) and increase the plastic viscosity from 6.71 Nms to 7.73-9.39 Nms (i.e. by 15-40%) compared to the saturation dosage. These increases in the Bingham parameters are outside the statistical repeatability ranges shown in Table 6.1(a), and, therefore, demonstrate for the first time that the saturation dosage not only gives the highest initial workability, but also the longest workability retention.

These results, and the mortar dosage-response tests in figure 6.3, also suggest that the contrasting losses in workability in figure 6.2(b) do not necessarily represent distinct characteristics of the various superplasticizers tested, but are in fact directly related to the dosages used. That is, the relatively large increases in plastic viscosity obtained with the SMF and MLS superplasticizers are likely to be due to 0.25% over-doses, whilst the pronounced increases in yield value with the new-generation superplasticizers may be due to 0.25% under-doses compared to their respective saturation values in figure 6.3. These results consequently mean that the use of arbitrary dosages (and/or slumps), in isolation of the dosage response behaviour of superplasticizers, does not necessarily provide a valid approach for comparing superplasticizer performance.

In contrast with the present observations, Wallevik and Gjorv[50] found that increasing dosages of superplasticizer (from 0 to 2.4%) produce slight reductions in initial yield value, and higher initial plastic viscosities which progressively decrease with time as measured with the MH system (c.f. figure 2.34). The continuous and significant increases in initial plastic viscosity observed by Punkki et al[17] with increasing dosage (figure 2.35) provide further evidence that the BML viscometer, like the MH system, suffers from increasing up-lift effects at lower slumps. The fact that the BML viscometer gives similar losses in workability to those shown in figure 6.3, does however suggest that its up-lift effects, as discussed in section 5.5.5, are not as large as those observed with the MH system.

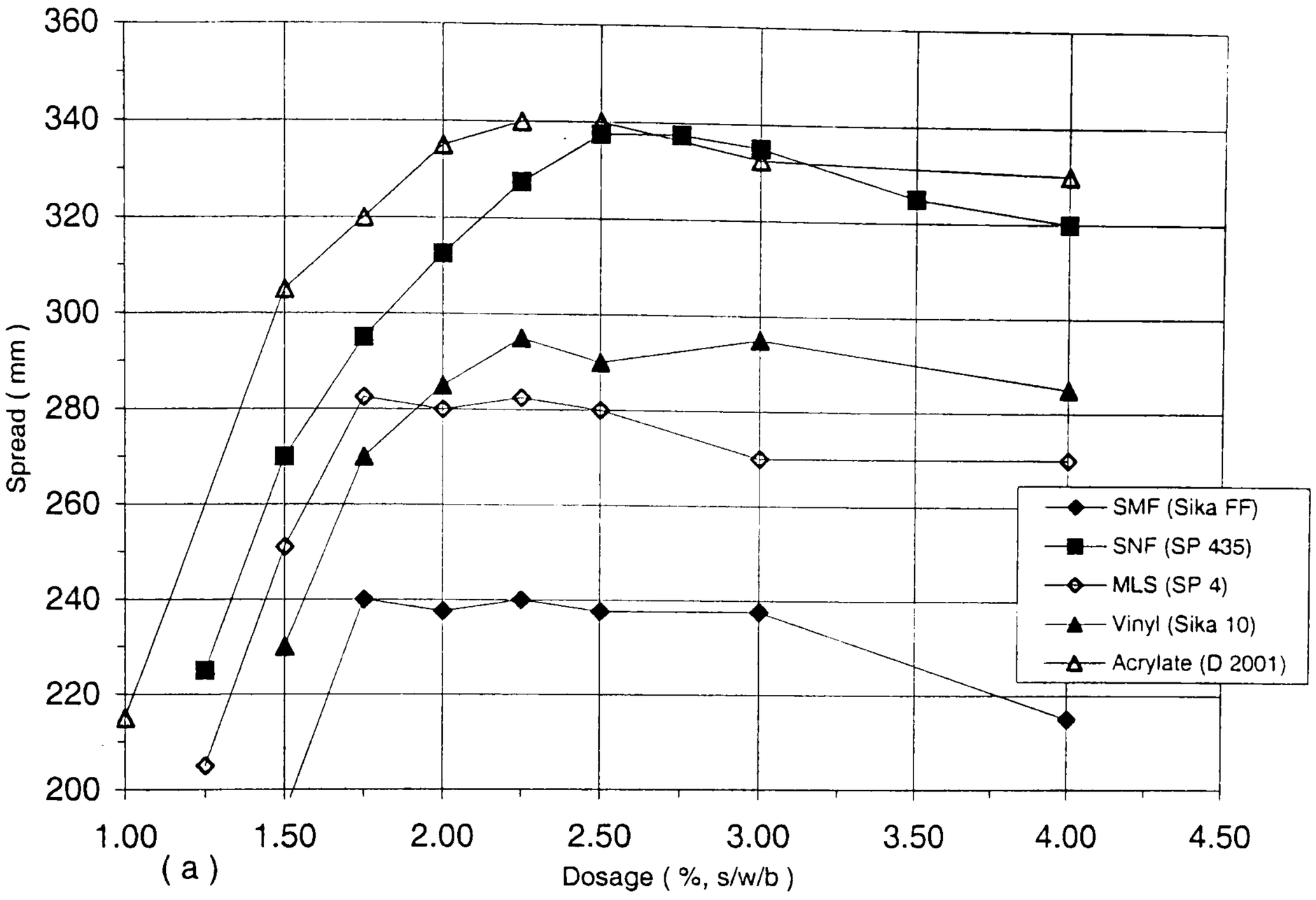

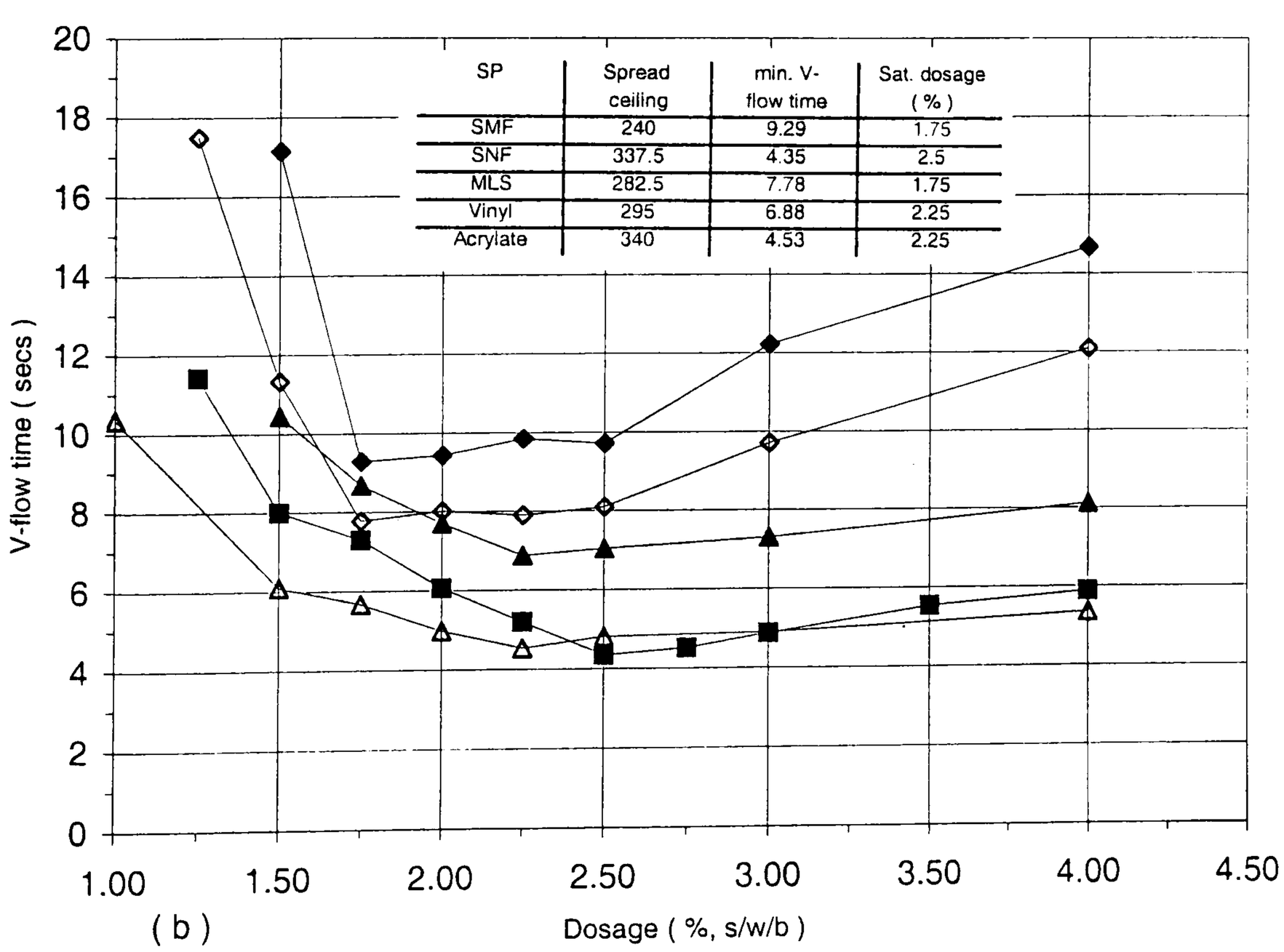

SP	Spread ceiling	min. V-flow time	Sat. dosage (%)
SMF	240	9.29	1.75
SNF	337.5	4.35	2.5
MLS	282.5	7.78	1.75
Vinyl	295	6.88	2.25
Acrylate	340	4.53	2.25

Figure 6.3 : Mortar dosage-response tests with SMF, SNF, MLS, Vinyl and Acrylate superplasticizers, showing variations in (a) initial spread and (b) V-flow time. (1 min delayed addition, 0.26 w/b)

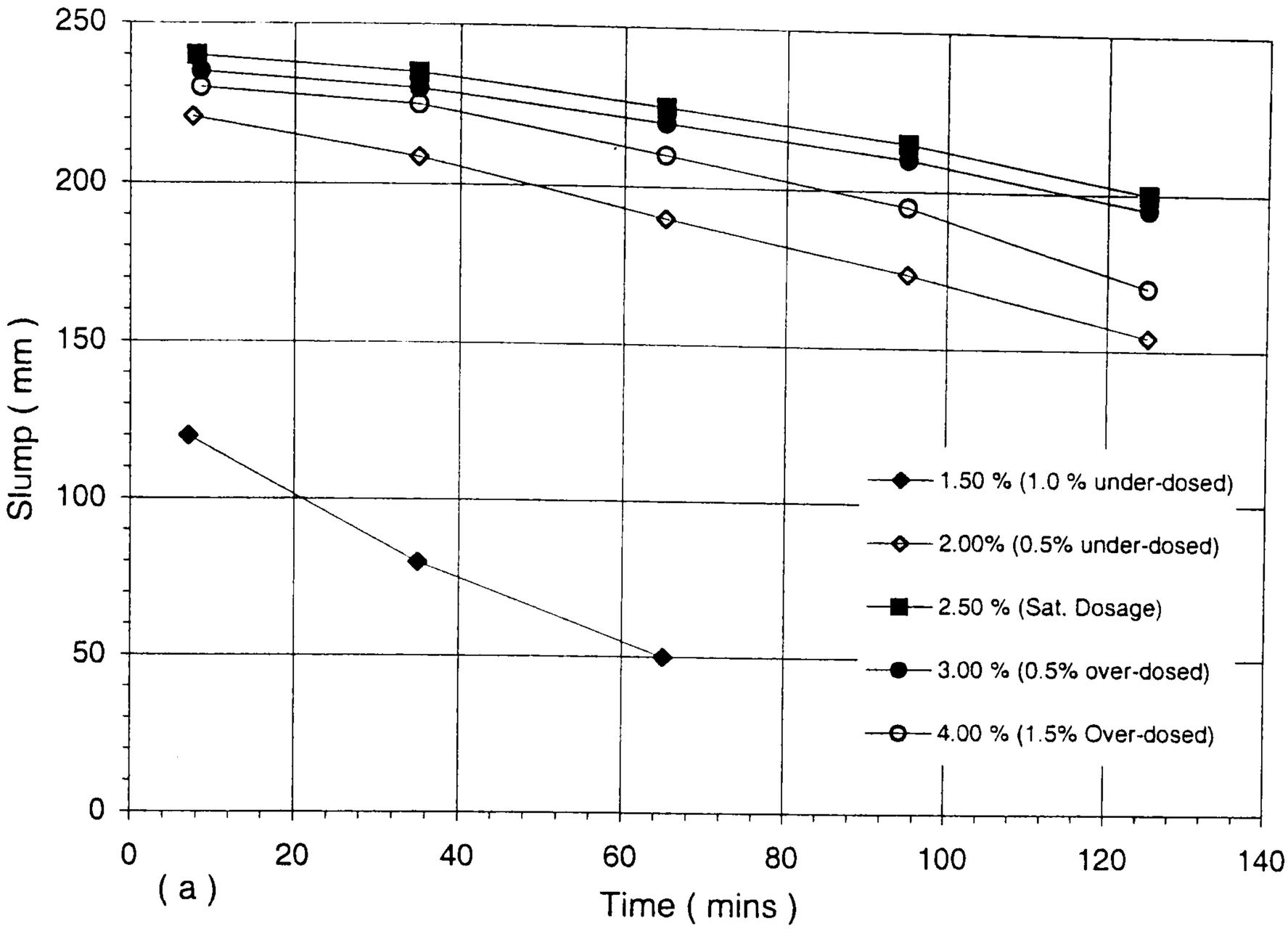

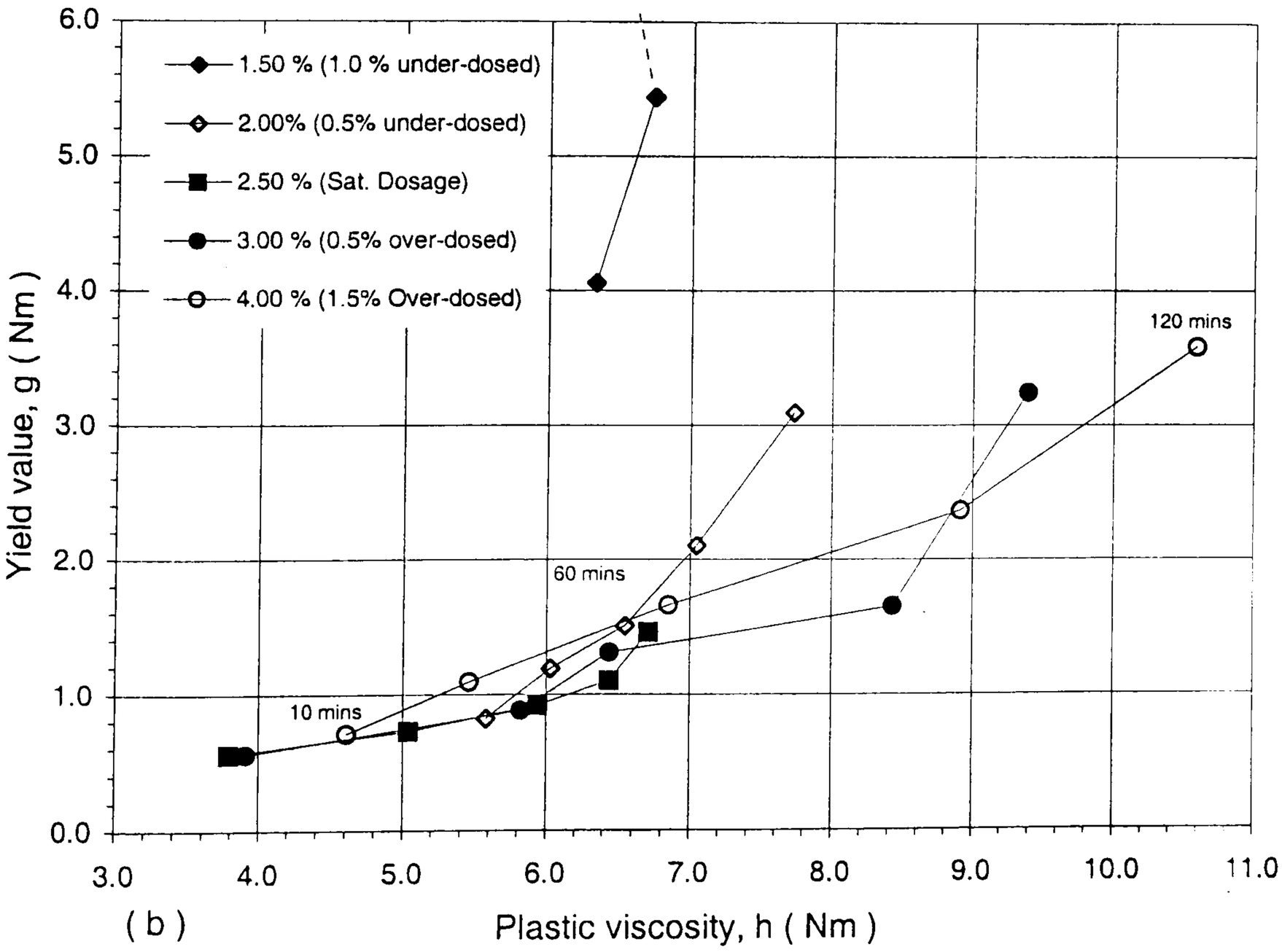

Figure 6.4 : Effects of increasing SNF superplasticizer dosages on (a) slump loss and (b) workability retention . (Saturation point determined to the nearest 0.25% in mortar, 1 min. delayed addition, 0.26 w/b ratio)

6.4 Superplasticizer mixing procedure

As mentioned previously in section 2.5.4, the effectiveness of superplasticizers is considered to be highly influenced by the rate of dissolution of the sulfates and their reactivity with the C_3A to form a protective layer of ettringite during the initial mixing sequence. When the sulfate (SO_4^{2-}) ions are released too slowly (page 72) the sulphonate SO_3^- ends of conventional superplasticizers (c.f. figure 2.16) are believed to become fixed by adsorption onto the C_3A, and are therefore not available to disperse the cement particles[13, 168]. The ability of superplasticizers to provide the desired initial workability and maintain sufficient dispersion stability is believed to last as long as enough of their molecules are available at the cement-liquid interface[8, 58].

This section examines the effects of delayed and split superplasticizer additions, and several superplasticizer blends on the workability properties of HSC. The mixing procedures used were illustrated in figure 4.1 (procedures 2, 3 and 4).

6.4.1 Delayed additions of superplasticizers

6.4.1.1 Mortar dosage-response tests

Figure 6.5(a-b) shows the mortar dosage-response of the SNF as a function of delayed additions of 0, 1, 2, 3, 4, 6 and 8 minutes. The corresponding results with the other four superplasticizers (excluding the 3 and 6 mins delayed addition times) are shown in **Table 6.3(a-d)**. The ranking order of the five superplasticizers in terms of highest spread ceiling and lowest V-flow time is consistent with that in sections 6.2-6.3, that is: **SMF < MLS < Vinyl < SNF < D 2001**. In each case there are systematic reductions in saturation dosage and improvements in maximum workability (particularly in terms of V-flow time) with delayed additions from 0 to 4 mins. Longer delayed additions of up to 8 mins show little or no effect on dosage demand, but slightly reduce the maximum workability with respect to spread ceiling as shown in figure 6.5.

The 4 min optimum addition time of the superplasticizers obtained in mortar is intermediate to the 2 and 10-15 mins addition times reported by Chiocchio and Paolini[152] in cement paste and by Hsu et al[6] in concrete (c.f. page 66). According to Hsu et al[6] differences in the optimum addition time in paste and concrete may be attributed to aggregate dilution effects. Other possible causes may relate to differences in the type of cements/binders, amounts of pre-mixing water, dosages, and/or differences in the molecular weights and chain lengths of the superplasticizers used. With regards to the latter, it has been reported that lower molecular weight and shorter superplasticizer molecules have a greater affinity to react with the C_3A phase during the first few minutes of cement hydration, and are, therefore, less efficient dispersants[13].

The apparent sensitivity of both the Vinyl (Sika 10) and Acrylate (D 2001) based NG polymers to delayed addition (in Table 6.3(c-d)) contradicts the observations by Collepardi et al[162], who found that their NG acrylic-based (CAE) copolymer was insensitive to mixing procedure (c.f. Table 2.3). As mentioned previously, Collepardi[34] attributed the performance of the CAE copolymer to steric hinderance rather than electrostatic repulsion resulting from the presence of negatively charged anionic (COO^-) groups (c.f. figures 2.19 and 2.30). He has however not commented on whether the steric effects of the polymer are in any way influenced by, for example, the rate of dissolution of the sulphates and their reactivity with the C_3A phases.

6.4.1.2 Loss of workability in concrete

Figure 6.6(a-b) shows the slump and two-point test results of the SNF superplasticizer as a function of increasing delayed addition times of 0, 1, 2, and 4 mins. **Figure 6.6(a)** shows that both the initial slump and slump retention increase with delayed addition of the superplasticizer. In agreement with Punkki et al's slump measurements[17] (c.f. figure 2.40(a)), the improvements in slump performance are particularly pronounced between the 0 and 1 min delayed additions.

The two-point test results in **figure 6.6(b)** show systematic and significant improvements in initial workability and longer workability retention with increasing delayed additions from 0 mins up to the 4 mins optimum delayed addition time found in mortar. The workability improvements with the 4 mins addition time are mainly represented by :

- consistently lower plastic viscosities (of 0.84 to 1.58 Nms) compared to the 2 mins delayed addition, and by
- much lower time-dependent increases in yield value (of 1.15-2.25 Nm) compared to the 0 and 1 mins delayed additions.

It is interesting to note that the differences between the initial workabilities and workability retentions of the 4 and 1 min delayed additions are similar to those resulting from the increase in dosage from 2.00 to 2.50% as shown in figure 6.4(b) (0.46-1.15 Nm and 0.36-2.06 Nms compared to 0.26-1.37 Nm and 0.60-0.77 Nms). These results therefore mean that adequate attention to superplasticizer mixing procedure can in practice provide significant technical and economic benefits in reducing handling difficulties and cost.

When compared with the 1 min delayed addition at its higher saturation dosage of 2.50% (figure 6.4(b)), the results of the 4 mins optimum addition also show consistently lower Bingham values of up to 0.42 Nm and 1.25 Nms. These may be due to a smaller influence of unreacted C_3A on the adsorption characteristics of the superplasticizer.

Although Punkki et al's measurements[17] show comparable slump losses to those in figure 6.6, their results with the BML viscometer (c.f. figure 2.40(c)) indicate significantly higher plastic viscosities with the 1 and 2 mins delayed additions than the direct addition of superplasticizer (at 0 mins). Their measured increases in plastic viscosity at higher slumps further highlight the volume expansions of the concrete occurring in the BML viscometer (as discussed in section 5.5.5).

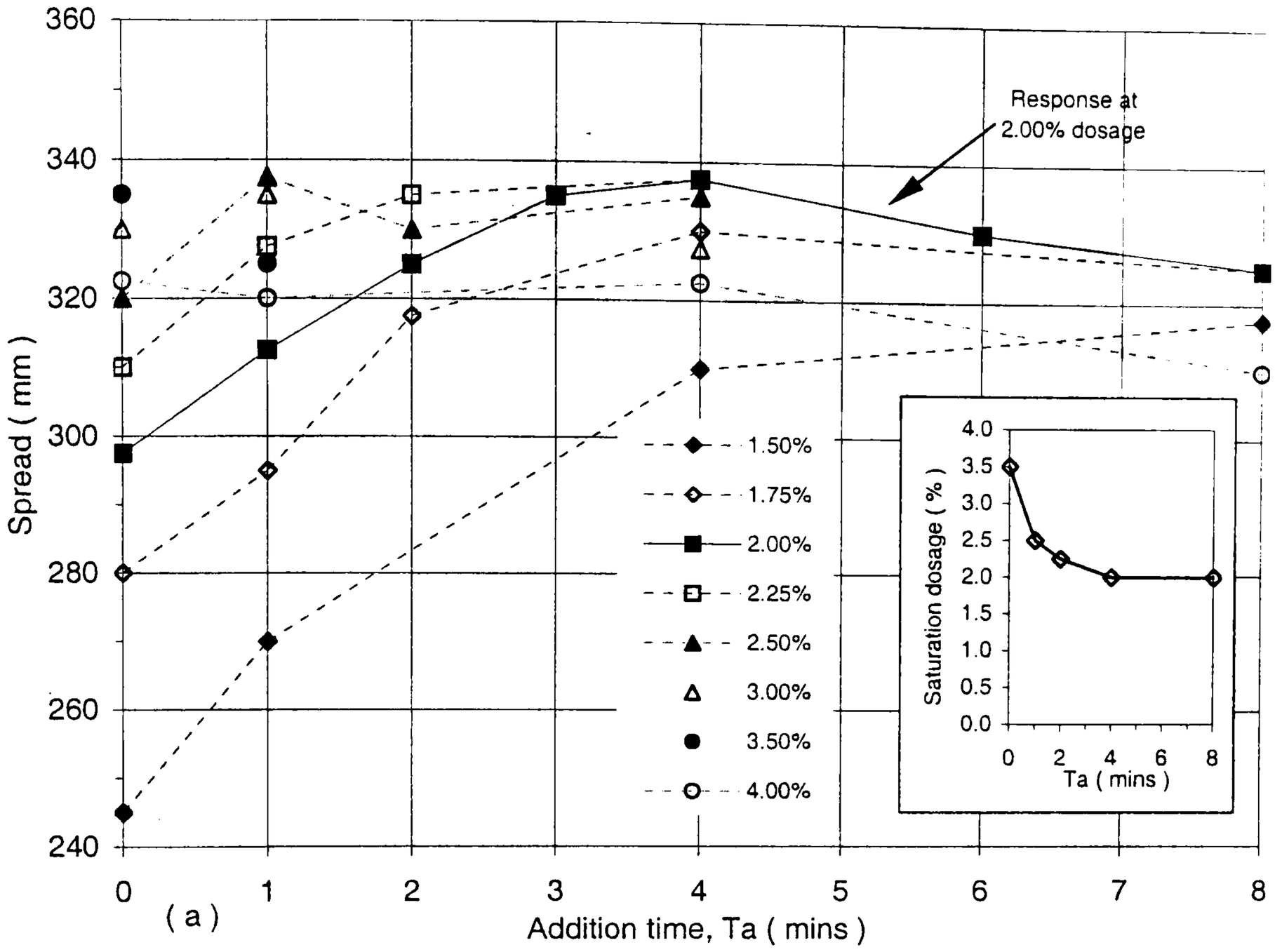

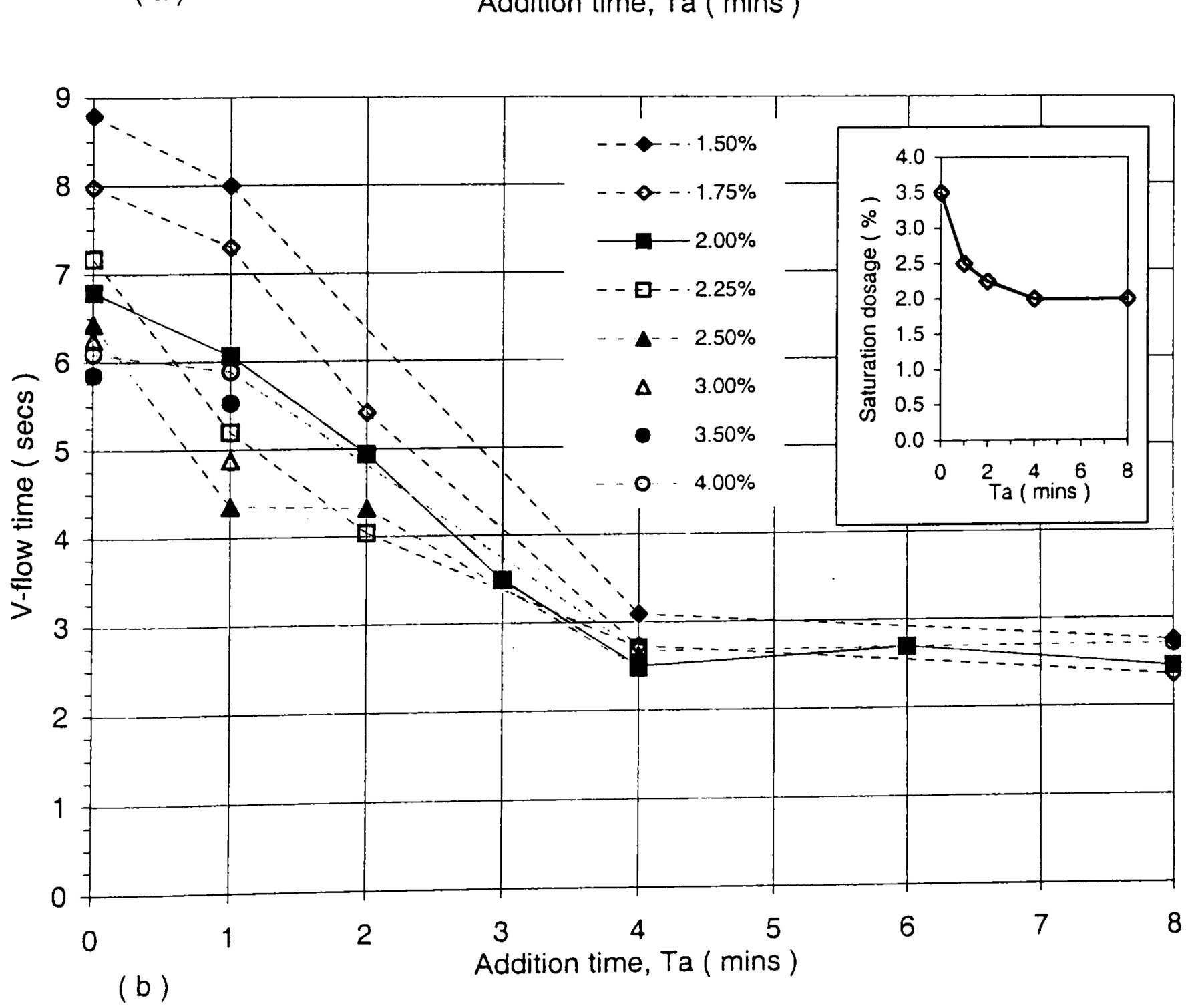

Figure 6.5 : Effects of delayed additions of SNF superplasticizer on initial (a) mortar spread and (b) V-flow time. (0.26 w/b).

Table 6.3 : Effects of delayed addition on mortar dosage-response of (a) SMF, (b) MLS, (C) Vinyl and (d) Acrylate-based superplasticizers

Type	Ta (mins)	Dosage (%)	Spread (mm)	v-time (secs)
(a) **SMF**	0	1.50	150	No flow
	1	1.50	195	17.4
		*1.75	240	9.29
		2.00	237.5	9.43
	2	1.50	220	8.71
		1.75	240	8.05
		2.00	240	8.08
	4	1.25	170	9.78
		*1.5	242.5	6.71
		1.75	240	7.04
	8	1.50	225	7.11
(b) **MLS**	0	1.50	190	15.5
	1	1.50	250	11.32
		*1.75	282.5	7.78
		2.00	280	8.01
	2	1.50	270	8.17
		1.75	280	7.89
		2.00	282.5	8.04
	4	1.25	260	9.01
		*1.5	285	7.04
		1.75	285	7.44
	8	1.50	277.5	7.18

Type	Ta (mins)	Dosage (%)	Spread (mm)	V-time (secs)
(c) **Vinyl**	0	1.75	255	9.23
	1	2.00	285	7.7
		*2.25	295	6.88
		2.50	290	7.05
	2	1.75	295	6.77
		*2.00	305	6.19
		2.25	300	6.14
	4	1.50	290	5.85
		*1.75	305	5.36
		2.00	305	5.32
	8	1.75	295	5.03
(d) **Acry-late**	0	1.75	295	7.11
	1	2.00	335	4.98
		*2.25	340	4.53
		2.50	340	4.81
	2	1.75	327.5	3.89
		*2.00	340	3.27
		2.25	340	3.41
	4	1.50	325	3.17
		*1.75	342.5	2.14
		2.00	340	2.69
	8	1.75	325	2.27

Ta represents the addition time of superplasticizer.

* represents the saturation dosage determined to the nearest 0.25% s/w/b.

Table 6.4 : Split addition and blending tests in mortar

Mixing procedure	Variable	Dosage % (s/w/b)	Spread (mm) Time (mins)			V-flow time (secs) Time (mins)		
			8	60	120	9	62	122
(**a**) Split addition	0/4 mins	2.00	295	240	200	1.90	3.01	8.31
	1/4 mins		320	305	290	4.11	6.41	8.19
	* 4 mins		340	335	320	2.44	3.21	4.15
(**b**) blends with SMF	0.5SMF + 0.5SNF	1.50	265	255	235	4.01	6.21	11.79
	0.5SMF + 0.5D 2001		275	260	230	4.29	7.8	No flow
	* SMF		240	235	215	6.95	8.95	14.04
(**c**) blends with MLS	0.5MLS + 0.5SNF	1.50	310	305	295	6.44	7.05	10.31
	0.5MLS + 0.5D 2001		315	305	285	6.16	6.93	11.22
	* MLS		290	280	270	6.88	7.89	11.73
(**d**) blends with PA21	0.5SMF + 0.5PA21	1.50	210	205	180	5.18	6.88	10.43
	0.5MLS + 0.5PA21		255	250	230	4.91	5.23	7.89
(**e**) retarded blends	0.9SNF + 0.1R	2.00	310	315	310	3.43	4.04	4.27
	* SNF		340	335	320	2.44	3.21	4.15
	0.9D 2001 + 0.1R	1.75	325	320	315	3.34	3.75	4.99
	* D 2001		340	325	285	2.38	5.41	8.97

* Represents control mix. The admixtures in (a)-(e) were added using 4 mins delayed addition.

All dosages used correspond to the saturation values of control mixes (figure 6.5 and Table 6.3).

All mixes were prepared with cement PC-7 (Table 4.1), and sand S-3 (Table 4.4).

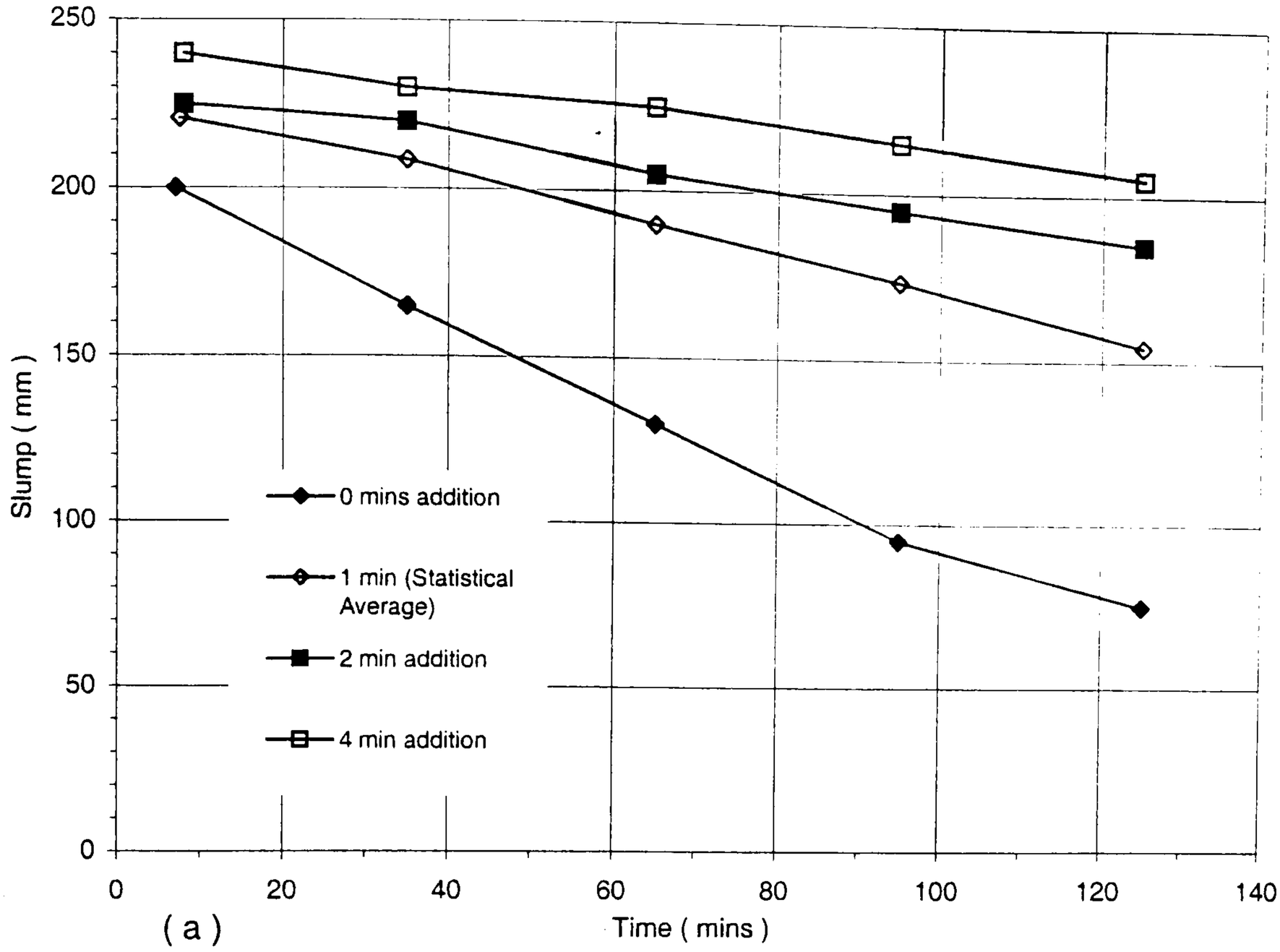

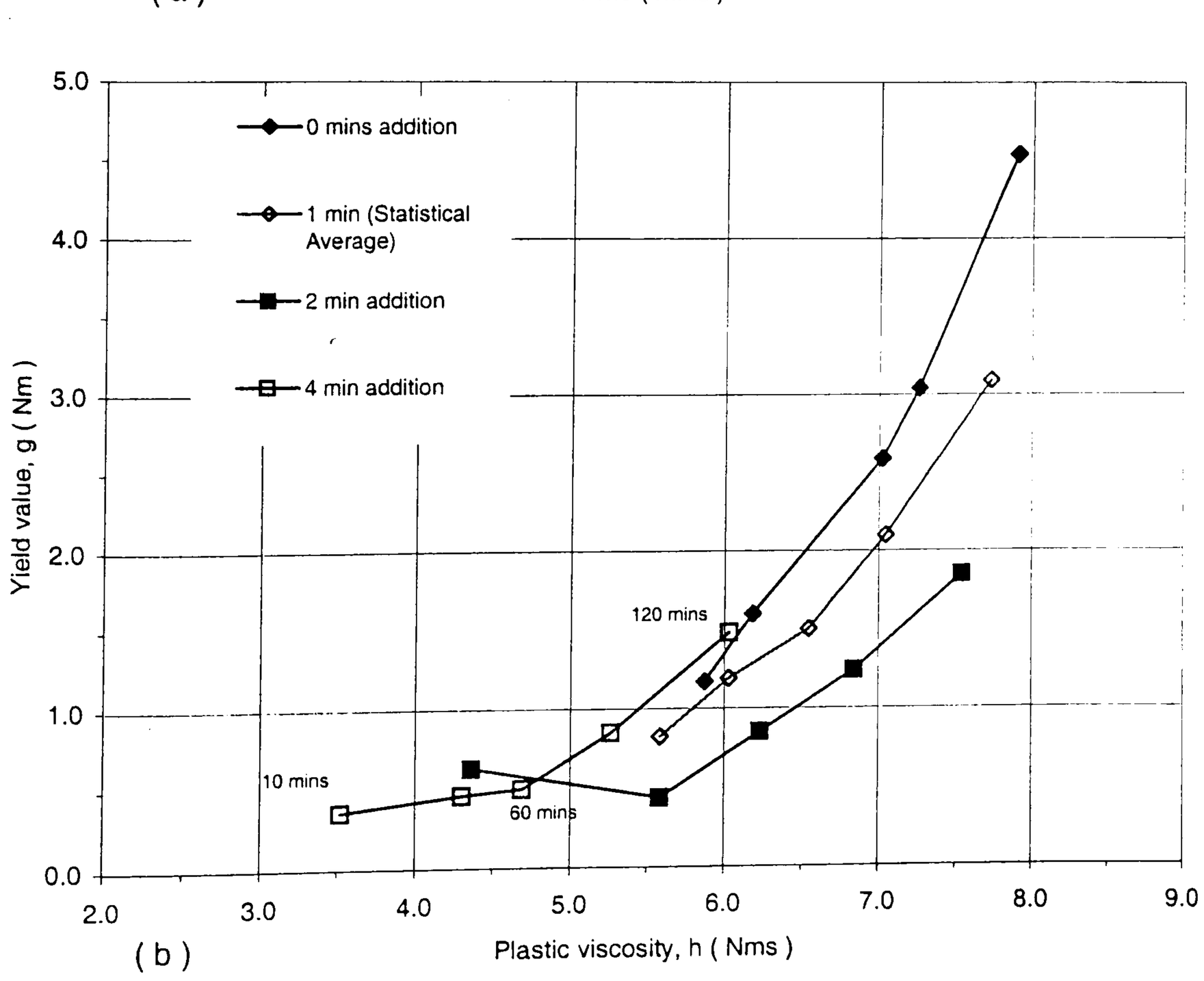

Figure 6.6 : Effects delayed additions of SNF superplasticizer on (a) Slump loss and (b) loss of workability. (At constant dosage of 2.00%, 0.26 w/b ratio)

6.4.2 Split additions and blending of superplasticizers

6.4.2.1 Tests in mortar

The review in section 2.5.4 highlighted a lack of sufficient information in the literature on the effects of split additions of superplasticizers, as well as on the blending of superplasticizers and/or superplasticizers with plasticizers. In this section, two 50/50% split additions of the SNF superplasticizer (at 0/4 mins and 1/4 mins); and four series of binary blends with the SMF, MLS, SNF, Acrylate (D 2001) superplasticizer, air-entraining agent (Conplast PA21) and the retarder (Conplast R) were tested as shown in Table 6.4(a-e), page 210.

The results in **Table 6.4(a)** show lower spread values with both the 0/4 and 1/4 mins split additions, but improved V-flow times with the 0/4 mins split addition compared to the control 4 mins delayed addition of the superplasticizer during the first 60 mins. The results with the 0/4 mins split addition in the first hour are similar to those obtained with the air-entraining agent (PA21) in section 6.2.1, and suggest that the introduction of part of the superplasticizer at 0 mins produces distinct interactions with the early hydration products in aerating the mix.

The 50/50 binary blends of the SMF with the SNF and D 2001 superplasticizers in **Table 6.4(b)** typically show 15-30 mm higher spreads and 2-3 secs reductions in V-flow time compared to the unblended SMF control mix. The corresponding tests with the MLS superplasticizer (**Table 6.4(c)**) show similar improvements in spread (of 15-25 mm) but less pronounced improvements in V-flow time (of 0.5-1.5 secs).

When blended with the air-entraining admixture (PA21), the mortar spread values and V-flow times for both the SMF and MLS mixes are typically reduced by 30-45 mm and 1.5-4 secs respectively (**Table 6.4(d)**). The 90/10 blends of the SNF and Acrylate (D 2001) superplasticizers with the retarding admixture (Conplast R) show reduced initial workabilities (represented by slightly lower spreads (of 15-30 mm) and higher V-flow times (of about 1 sec)), but enhanced

workability retention compared to the control mixes (**Table 6.4**(**e**)). Tests with other binary and/or ternary blends of the admixtures were considered to be outside the scope of this research.

6.4.2.2 Tests in concrete

The slump and two-point test results for the 0/4 mins SNF split addition, and the two retarded blends with the SNF and Acrylate-based (D 2001) superplasticizers are shown together with the results of the control mixes in figure 6.7(a-b).

Figure 6.7(**a**) shows that the 0/4 mins split addition reduces the initial slump by approximately 35 mm (or 15%) and increases the rate of slump loss from 40 mm to 100 mm in the first two hours compared to the control mix. The two-point test results in **figure 6.7**(**b**) show that the 0/4 mins split addition of the SNF superplasticizer increases the initial yield value by nearly three times, but reduces the initial plastic viscosity by approximately 30%. These results, like those with the mortar fraction in Table 6.4(a), lend support to Kreijger's suggestion[111] that air-entrainment increases the yield value but reduces the plastic viscosity (page 48).

In terms of loss of workability, the 0/4 mins split addition gives higher plastic viscosities after the first 30 mins, and pronounced increases in yield value after 90 mins. The procedure may therefore be advantageous only in placing and/or handling situations where a low early plastic viscosity is considered more important than a low yield value. In contrast, Punkki et al's measurements[17] with the BML viscometer in figure 2.40(c) showed consistently lower plastic viscosities with their 0/3.5 mins split addition (procedure D) compared to their higher slump mixes (procedures B and C, i.e. the 1 and 2 mins delayed additions).

The slump and two-point test results with the retarded SNF and D 2001 mixes in figure 6.7(a-b) show lower initial workabilities, but contrary to the suggestions by Penttala[16] (page 64), longer workability retention compared to the control mixes. The retarded SNF mix exhibits lower workability in the first 30 mins, but

essentially constant workability during the first two hours. The small variations in its slump and Bingham values with time are within the statistical repeatability range shown in Table 6.1(a), and may therefore be due to sampling errors. As mentioned in section 2.5.4(II), retarders are believed to delay cement hydration, and hence reduce loss of workability, by slowing down the growth of gel-like ettringite layers[111] and $Ca(OH)_2$ nuclei[8].

The results however show that the present retarder (based on hydrocarboxylic materials) is not as effective when blended with the Acrylate-based (D 2001) superplasticizer. It gives much larger increases in the Bingham parameters with time compared to its blend with the SNF superplasticizer, but better workability retention after the first 60 mins than the non-retarded D 2001 control mix.

Information regarding the chemical structure, mode of action, or compatibility of the Acrylate-based (D 2001) co-polymer was not provided by the suppliers. As shown in figure 2.19, other NG superplasticizers, such as acrylic-based polymers, have complex and varying chemical structures compared to SNF superplasticizers (c.f. figure 2.16(b)), and may therefore exhibit greater compatibility problems with other chemical admixtures.

Further work should therefore compare the efficiencies of the Acrylate-based (D 2001) and other NG superplasticizers with different retarder formulations, and determine how these are, for example, influenced by the presence of different side chains on their polymers.

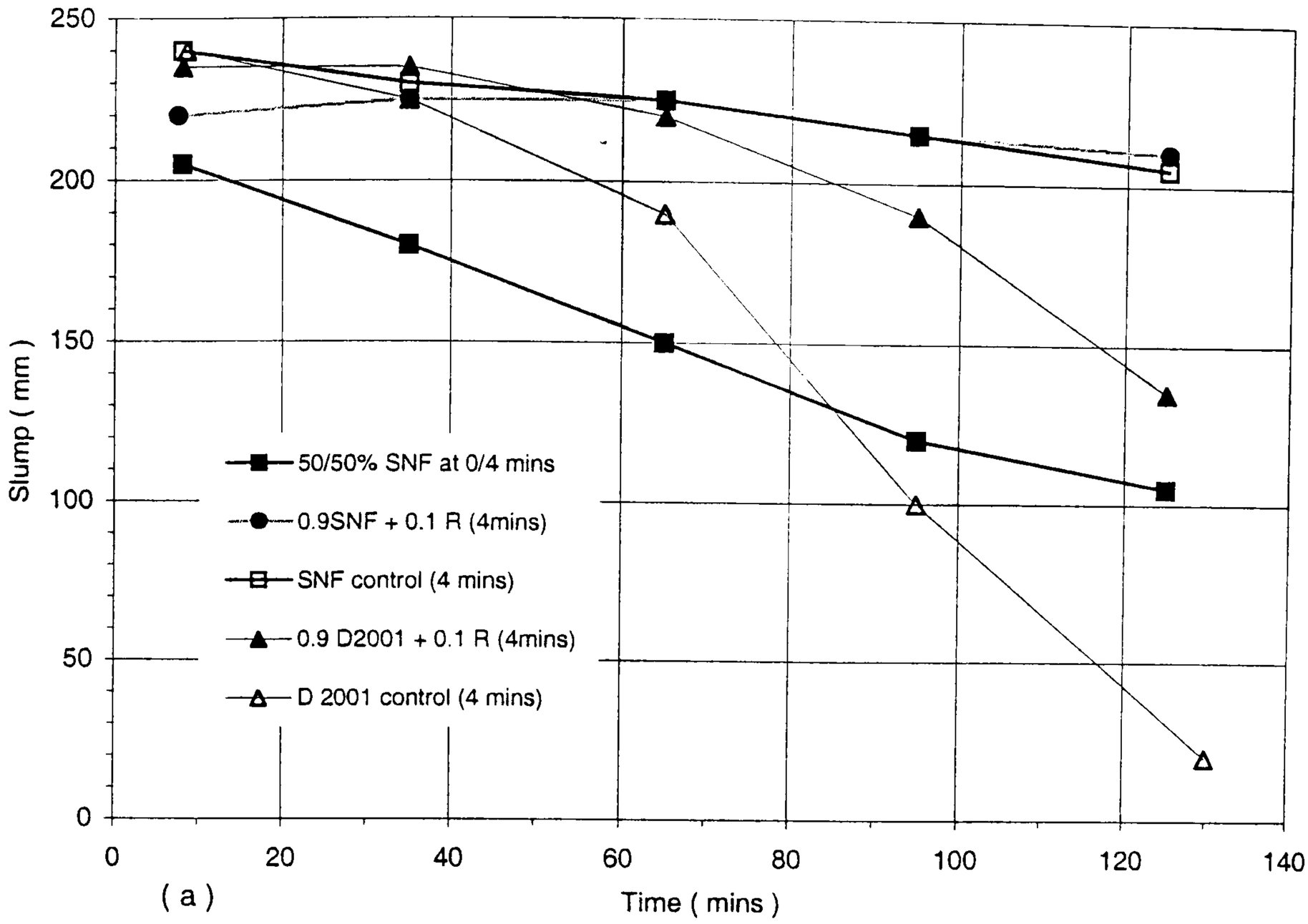

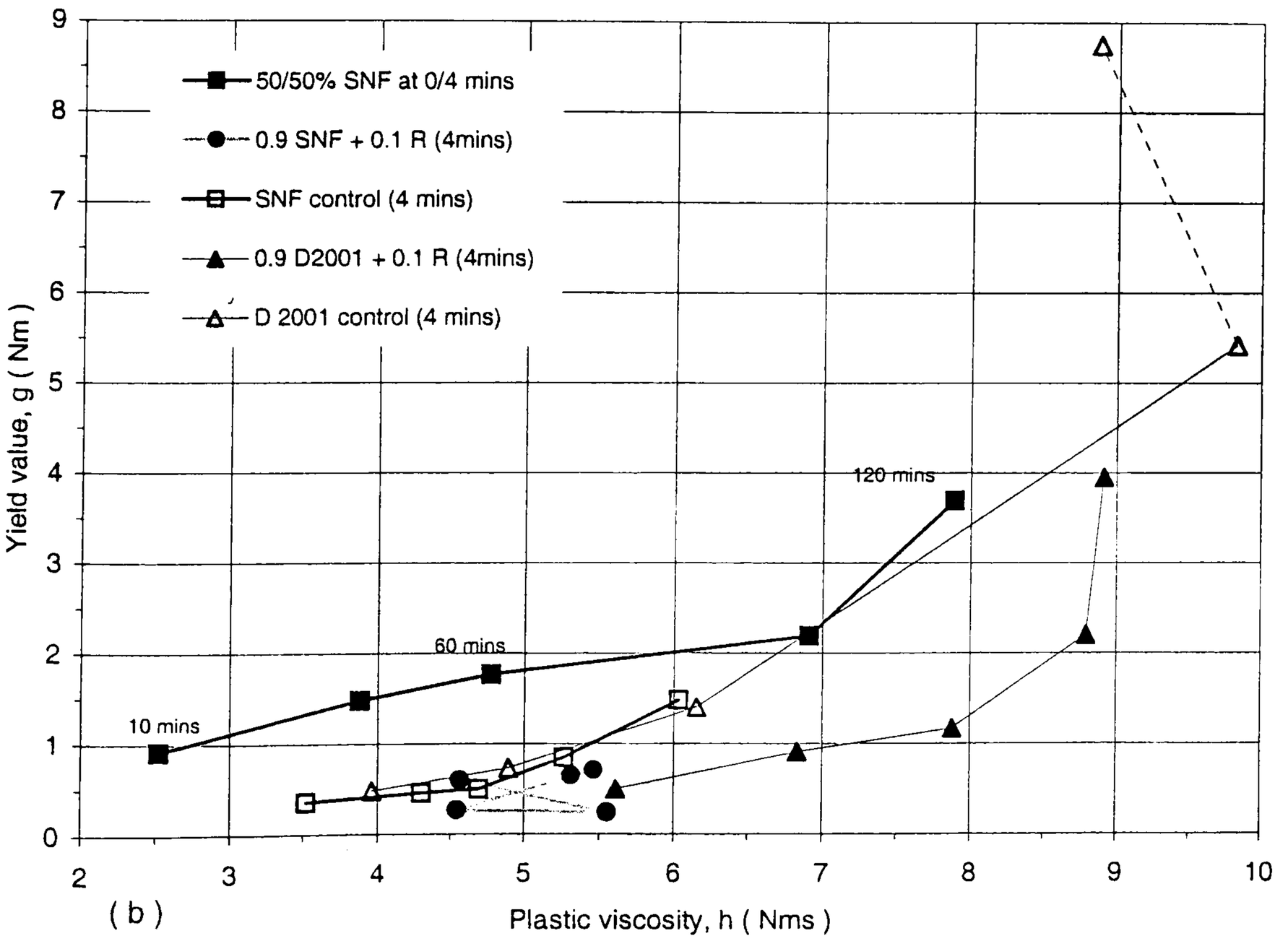

Figure 6.7 : Effects of split addition and retarded blends on (a) slump loss and (b) loss of workability. (using 2.00% SNF, and 1.75% D 2001 at 0.26 w/b).

6.5 Cement-superplasticizer compatibility

The compatibility of cements and superplasticizers is considered to be one of the most important aspects influencing the performance of HSCs, and is affected by many factors related to the type of cement and superplasticizer (as outlined in section 2.5.5). Although it has been cited as being the main cause of many anomalous results and field problems[11, 53, 58, 161, 165], it has not been adequately investigated. Most of the work reported on the effects of cement-superplasticizer compatibility is either qualitative in nature, or based on a few single-point tests on paste, mortar or concrete – often involving only one cement or superplasticizer.

This section examines the performance of the SMF, SNF, MLS, Vinyl and Acrylate-based superplasticizers with the Type I control cement (PC-7) used in sections 6.2-6.4, the rapid-hardening (RH) and the sulphate resisting (SR) (i.e. ASTM Types III and V) cements shown in Table 4.1. In order to assess the variability between nominally identical cements, the tests with the SNF superplasticizer include comparative measurements with two additional Type I cements, PC-8 and PC-9 (also shown in Table 4.1). These cements have similar chemical compositions to the control cement PC-7 (i.e. comparable C_3A (9.0-10.1), SO_3 (2.51-2.75) contents etc), but differ mainly in their fineness which ranges from 330 to 380 m^2/kg.

The sulphate resisting cement has a low C_3A content of 0.1% and a specific surface area of 440 m^2/kg. Although the compound compositions of the rapid hardening cement provided by the suppliers agree with the requirements of Type III cements (c.f. Table 2.5), the cement has an unusually low fineness of 375 m^2/kg (compared to the typical range of 450-600 m^2/kg).

Section 6.5.1 discusses the effects resulting from the changes in cement and superplasticizer type, whilst the existence of possible relationships between the characteristics of the cements and the Bingham parameters are discussed in section 6.5.2.

6.5.1 Effects of cement and superplasticizer type

6.5.1.1 Mortar dosage-response tests

(I) With the SNF superplasticizer

The mortar dosage-response tests with the SNF superplasticizer in **figure 6.8(a-b)** show that the change in cement type has significant effects on both the saturation dosage requirements and maximum workability properties of the superplasticizer. As can be seen, the SR cement gives the lowest saturation dosage and highest workability, whilst the RH cement gives the lowest workability and highest saturation dosage. The Type I cements (PC-7, PC-8 and PC-9) exhibit intermediate dosage demands and workabilities to those of the SR and RH cements.

Although the Type I cements exhibit noticeable performance differences at low dosages, their saturation dosages are equal (2.00%), and their differences in spread ceilings (5 mm) and minimum V-flow times (0.5 secs) are within the initial repeatability range shown in Table 5.4(b). That is, the results imply that small variations in cement composition have negligible effects on the initial workability properties at high superplasticizer dosages.

The results with the RH cement conform to the accepted view that it increases the water demand and reduces workability[8, 81, 156], but indicate that these effects are not due to the high fineness typical of these cements. The results with the SR cement, which has a 60 m^2/kg higher fineness than the control cement PC-7, in fact show a 15-20 mm increase in spread ceiling and, more importantly, a 0.25% s/w/b (or one-eight) reduction in saturation dosage. This therefore contradicts Pillar and Manuel 's suggestion[103] that higher dosages are required with increased cement fineness to cover the excess surface area and separate the cement particles (page 78).

(II) With the SMF, MLS, Vinyl and Acrylate superplasticizers

Figure 6.9 shows that the SMF, MLS, Vinyl and Acrylate superplasticizers essentially produce similar mortar dosage-responses with each of the three cement types. However, although the overall workability ranking of the cements is consistent with that of the SNF superplasticizer (i.e. **Type III < Type I < Type V**), the relative effects of the superplasticizers on the saturation dosages and/or maximum workabilities are not necessarily the same. For example, the SMF superplasticizer shows no noticeable differences in the saturation dosages with the control and the SR cement; but when used with the RH cement, it gives no-flow through the V-funnel, and more than a two-fold reduction in spread ceiling compared to cement PC-7. On the other hand, the Acrylate-based (D2001) superplasticizer shows significant differences in the saturation dosages with all three cement types, but less pronounced differences in the maximum workabilities with the control and RH cement.

Despite the contrasting differences in dosage demands and workabilities of the various cement-superplasticizer combinations, the ranking order of the three cements, as mentioned above, is essentially the same with each of the five superplasticizers. That is, none of the cements show increased workability with one superplasticizer, but reduced with the others.

This observation suggests that the five superplasticizers tested have similar mode(s) of action and interactions with the various cement components. As most conventional superplasticizers are mainly believed to operate through a combination of electrostatic and steric repulsive forces[33, 66, 111, 142], it is therefore possible that the relative differences observed in dosage demand and workability may be associated with variations in the relative magnitude of these forces.

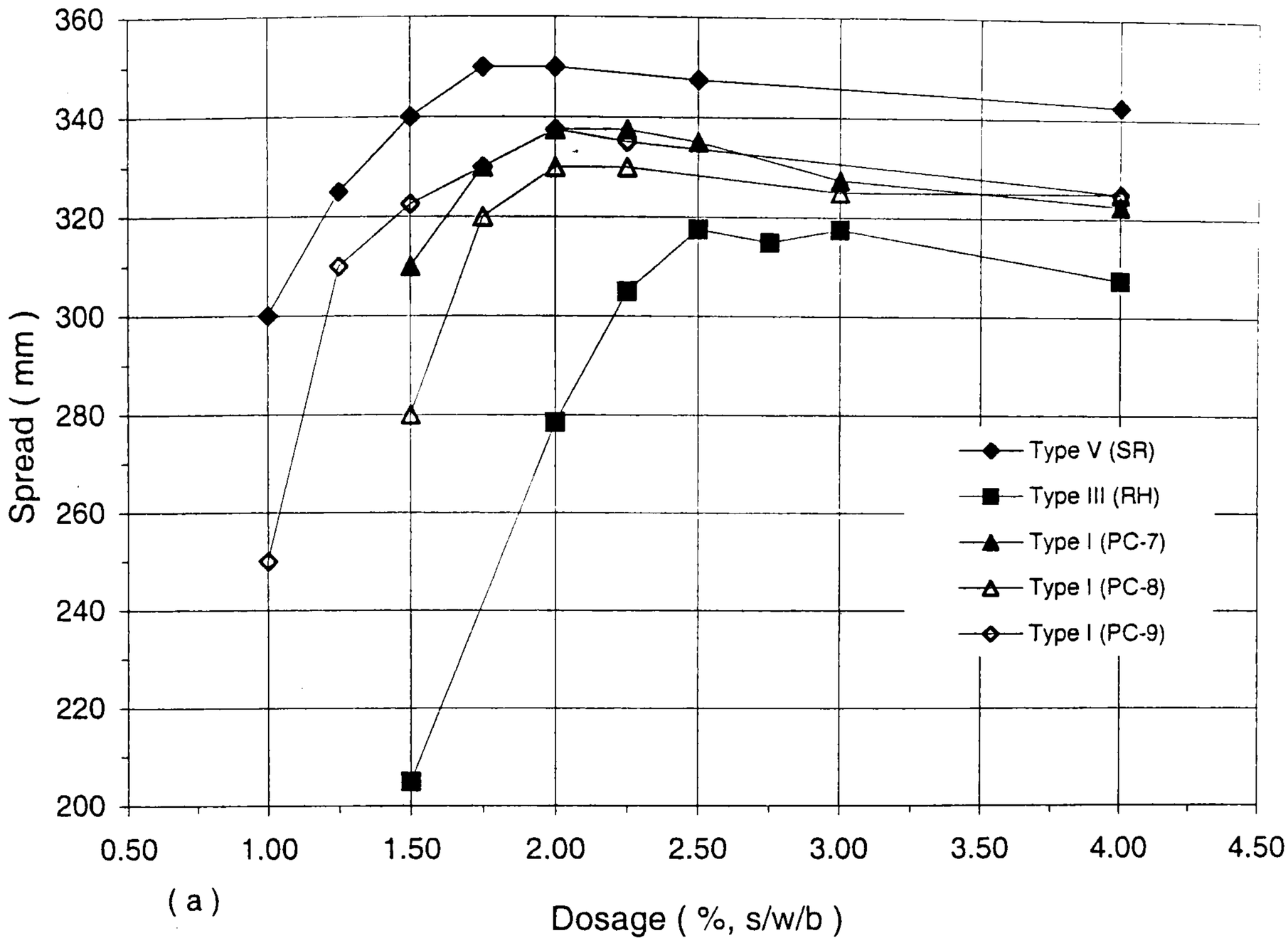

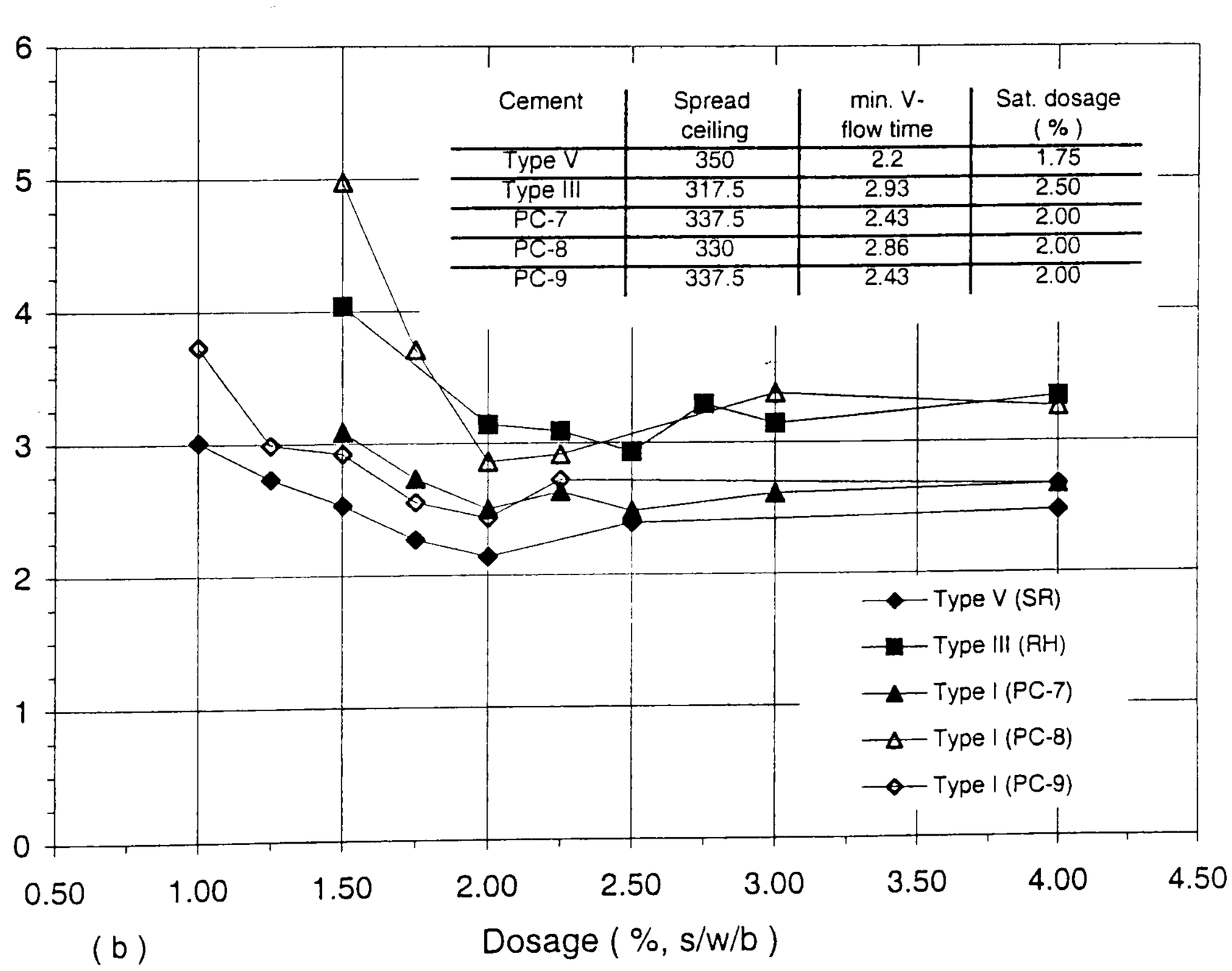

Cement	Spread ceiling	min. V-flow time	Sat. dosage (%)
Type V	350	2.2	1.75
Type III	317.5	2.93	2.50
PC-7	337.5	2.43	2.00
PC-8	330	2.86	2.00
PC-9	337.5	2.43	2.00

Figure 6.8 : Mortar dosage-response tests for the compatibility of the SNF superplasticizer with cement types I, III, and V. (4 mins delayed add., 0.26 w/b)

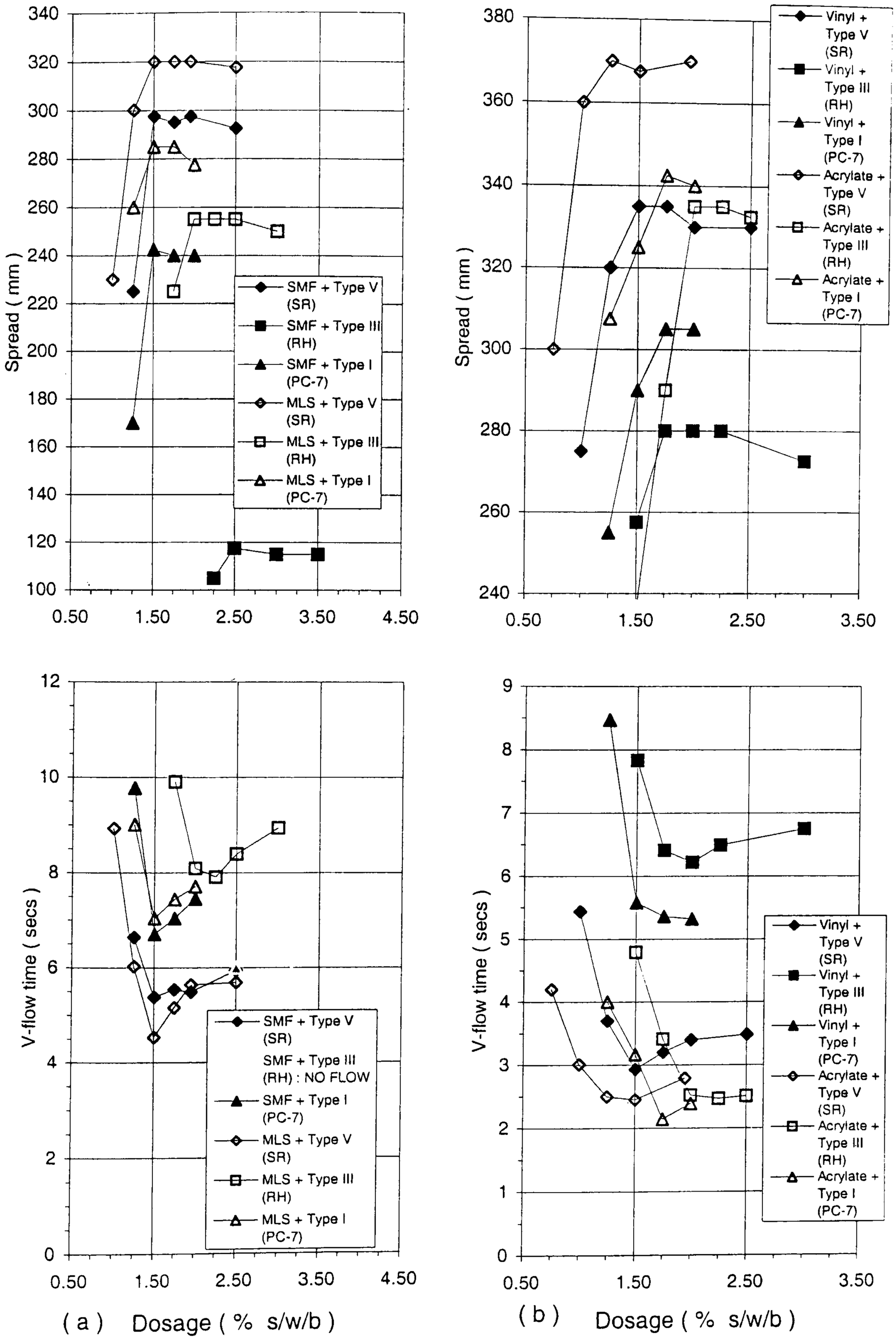

Figure 6.9 : Mortar dosage-response tests showing the compatibilities of (a) the SMF, MLS and (b) Vinyl, Acrylate-based superplasticizers with cement Types I, III, and V. (4 mins addition, 0.26 w/b).

6.5.1.2 Loss of workability in concrete

Figure 6.10(a-b) shows the slump and two-point test results for the performance of the SNF superplasticizer with the five cements (PC 7-9, the RH and SR cements) at their respective saturation dosages. The figure also shows results obtained with the SMF superplasticizer and SR cement.

In agreement with the mortar spread results (figure 6.8), the slump test results in **figure 6.10(a)** show that the highest initial slump is obtained with the SR cement, the lowest with the RH cement, whilst the Type I cements (PC 7-9) give intermediate and comparable slumps. The similarity of the slump losses with the SNF superplasticizer indicate that, with the optimum dosages and mixing procedure used, it is possible to produce high-slump HSC having a slump of 125 mm or more up to 120 mins after mixing with any of the three cement types. The faster slump loss with the SMF superplasticizer indicates a higher reactivity and/or lower dispersion stability compared to the SNF superplasticizer.

In contrast to the slump test results, the two-point test results with the SNF superplasticizer in **figure 6.10(b)** show that the cements produce pronounced differences in both the initial workabilities and the rates of loss of workability. When compared with the 55 mm (or 21%) initial slump difference observed between the SR and RH cements, the initial Bingham parameters with the SR cement show a considerable reduction in yield value (from 0.77 to 0.13 Nm) and a 36% reduction in plastic viscosity (from 3.75 to 2.40 Nms) due to the change in cement type. The 40-90 mm slump reductions occurring during the first two hours are, on the other hand, reflected by a substantial increase in the initial yield value with cement PC-9 (from 0.36-4.3 Nm), and a four-fold increase in the initial plastic viscosity with the SR cement (from 2.4-8.91 Nms).

It is interesting to note that although the Type I cements produce similar initial Bingham values, and have workabilities which lie in between those of the RH and SR cements, they exhibit significant differences in loss of workability. In

particular, the differences in the losses of workability of cement PC-9 and the other type I cements after the first 60 mins lie well outside the repeatability range shown in Table 6.1(a), and do not appear to be explained by the differences in fineness of the cements. (15 m^2/kg between cements PC-9 and PC-8, and 50 m^2/kg between PC-9 and PC-7). These findings therefore mean that the losses of workability resulting from slight variations in cement compositions of nominally identical cements can not necessarily be reproduced in HSC.

The results with the RH cement, when compared to those of the control cement PC-7 (which has a similar fineness), suggest that 7-2.7% differences in, for example, C_3S and C_4AF contents (Table 4.1) may be sufficient to account for a noticeably lower initial workability and a faster loss of workability. The observed workability differences are in contrast to those reported by Wallevik and Gjorv[50] (figure 2.47), which show consistently higher yield values and lower plastic viscosities with the MH system when Type III cement replaces Type I. The differences in the results of the RH and control cement are however less pronounced than, for example, those between cements PC-7 and PC-9, or those obtained between the direct and 4 mins delayed additions in figure 6.6(b).

The results obtained with the SR cement confirm the higher initial workability and longer workability retention of the SNF compared to the SMF superplasticizer (in figure 6.2(b)). The results also suggest that the relative increases in the Bingham parameters at the saturation dosage are closely related to the magnitude of the initial yield value.

- When the initial yield value is near zero, the overall loss of workability appears to be reflected by more pronounced increases in plastic viscosity than in yield value (as observed with the SNF and SR combination).
- When the initial yield value is ≥ 0.36 Nm, the relative increases in the Bingham parameters at the saturation dosage appear to be more comparable (as observed with the other cement-superplasticizer combinations).

These results are in contrast with those reported by de Larrard et al[49] (c.f. figure

2.45), which suggest that the incompatibility between cements and superplasticizers causes considerable increases in yield value, but little or no change in plastic viscosity with time. Although de Larrard et al have not reported their mix details (i.e. the type of cement, superplasticizer or mixing procedure used), their results are more typical of those due to direct addition of superplasticizer (c.f. figures 2.40 and 6.6), rather than due to a change in cement and/or superplasticizer type. In this respect, it is worth noting that the volume expansions of the concrete in the BT Rheometer (as discussed in section 5.5.5), can conceal the changes in plastic viscosity with time and decreasing workability.

It is however not possible to generalize that the lack of unusual behaviour (or incompatibility) shown by the present cement-superplasticizer combinations (in figures 6.8-6.10) would apply to all types of commercial cements and superplasticizers. The observations by Jeknavorian et al[119], for example, showed that the slump performance of their polycarboxylate comb polymer (ADVSP) is much less sensitive to a change in cement composition than that of a SNF superplasticizer (c.f. figure 2.44). Their results, like those reported by Collepardi et al[162] with the acrylic-based polymer (as discussed in section 6.4.1), suggest that the availability of the ADVSP superplasticizer, which is also believed to operate through steric hinderance[119, 162], is unaffected by, for example, fixation on the C_3A phases during the initial mixing sequence.

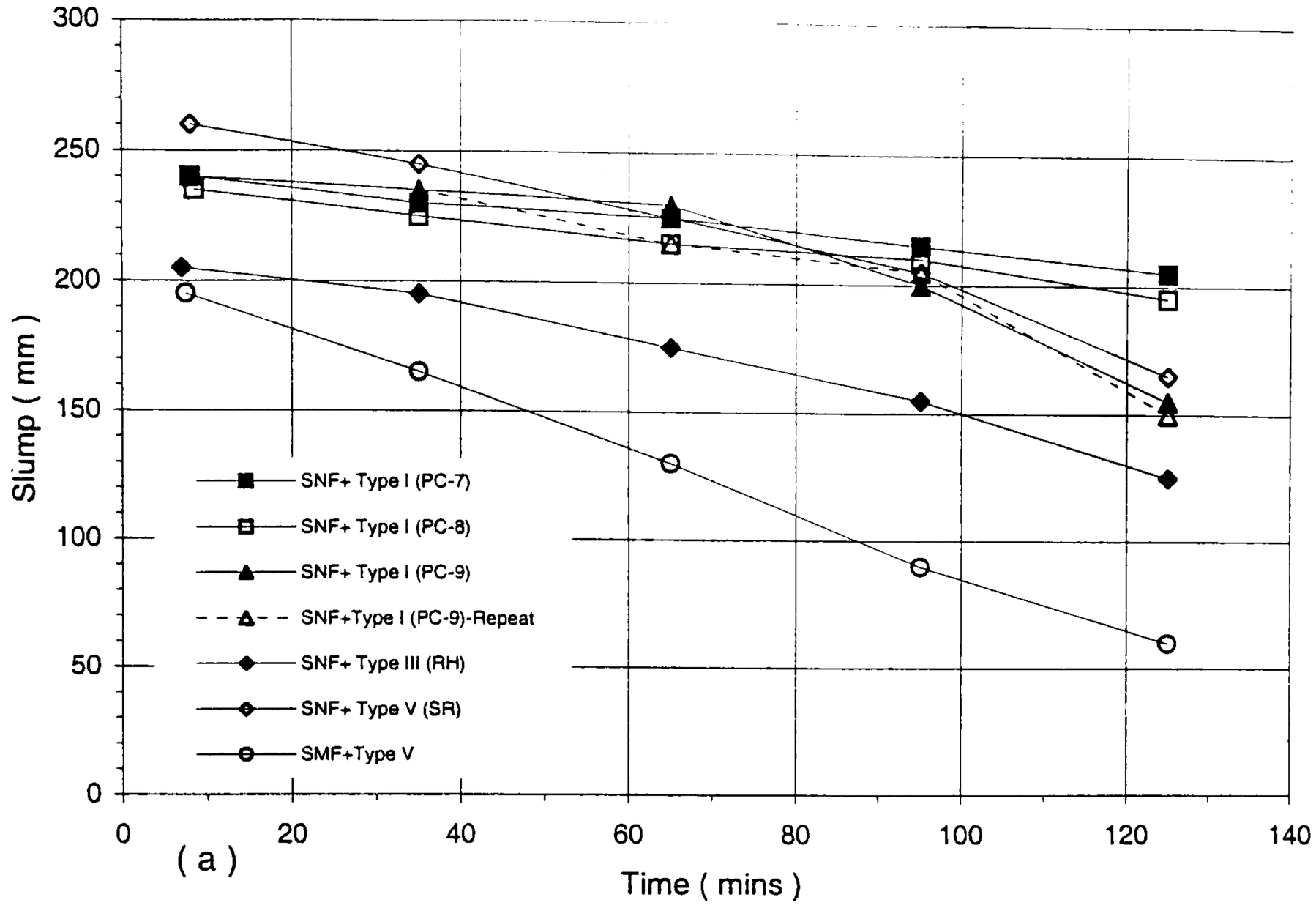

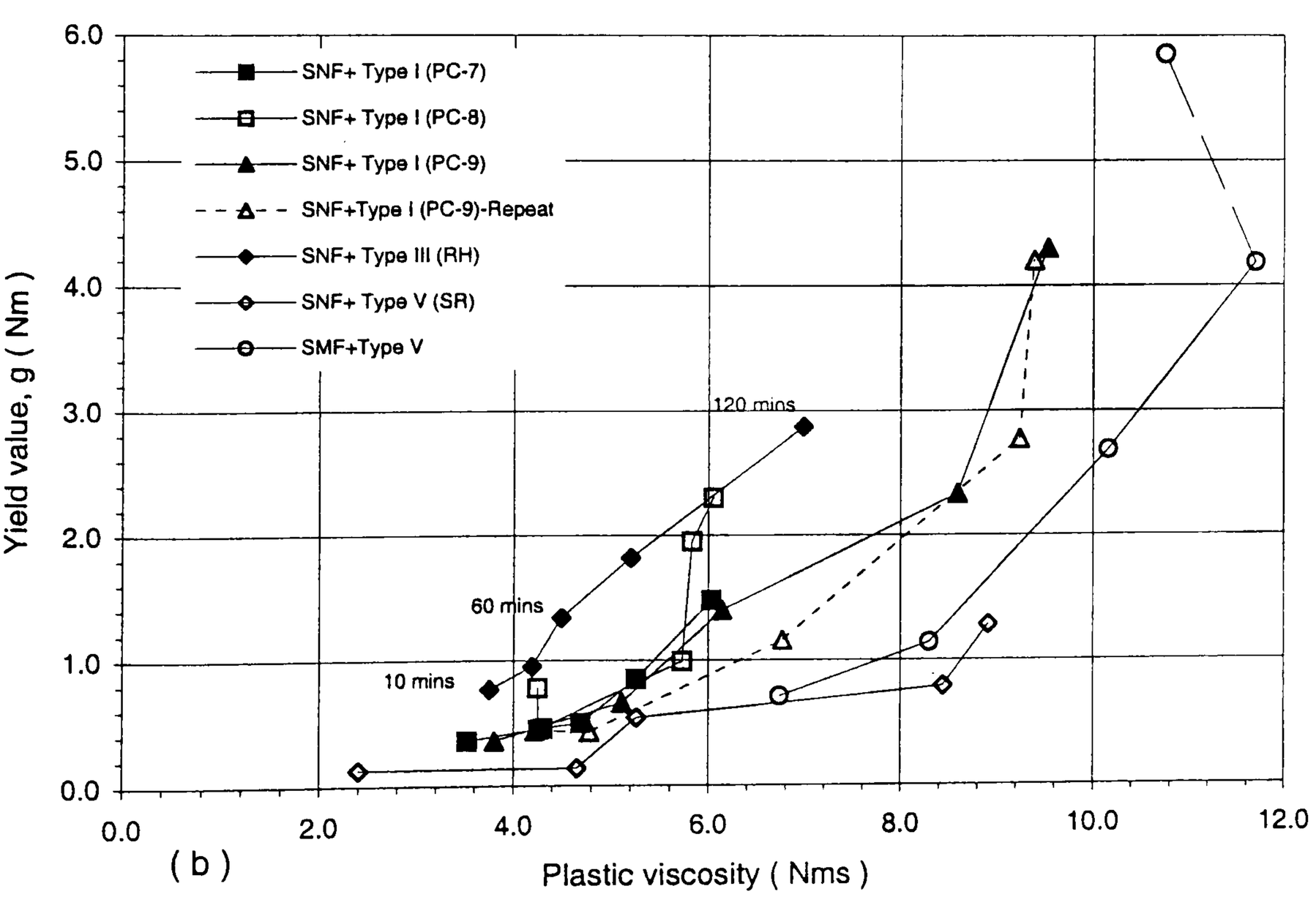

Figure 6.10 : Effects of cement Types I, III and V on (a) slump loss and (b) loss of workability of mixes with SNF superplasticizer. Includes compatibility of cement Type V and SMF (mixes tested at their respective sat. dosages 4mins add., 0.26 w/b).

6.5.2. Cement characteristics - Bingham parameter relationships

Figure 6.11(a-c) illustrates the effects of individual cement compositions (Viz. C_3A and SO_3 contents) and cement fineness on the Bingham parameters obtained with the five cements and SNF superplasticizer in figure 6.10(b). Although the results in **figure 6.11(a)** suggest possible linear tendencies of decreasing initial workability, better retention of plastic viscosity and larger time-dependent increases in yield value with increasing C_3A content from 0.1 to 9.0%, the relationships are discontinuous at higher C_3A contents. The relationships in **figure 6.11(b-c)** show that it is similarly difficult to draw any definite conclusions for the effects of total SO_3 content and cement fineness on the initial Bingham parameters and their evolution over the first two hours.

The results in figure 6.11(c) do however provide some indications of possible drawbacks associated with extreme cement fineness. Cements with a fineness of 330 m^2/kg and 440 m^2/kg appear to increase the rate of loss of workability, particularly in terms of plastic viscosity. The results with the highest cement fineness of 440 m^2/kg lend support to Aitcin and Neville's suggestion[11] that an ideal cement for HPCs should not be too fine (page 71).

In relation to the absence of any clear tendencies between the SO_3 contents and Bingham parameters (figure 6.11(b)), it should be noted that: two cements can have the same total sulfate content, but depending on their form and origin, more or less sulfate will be available to neutralise the C_3A by converting it to ettringite[168]. As mentioned earlier, this is considered to be the main factor influencing the availability of superplasticizer molecules to disperse the cement particles, and hence contribute to workability[13, 168]. Information regarding the relative proportions of the types of calcium sulfates in the cements (i.e. the amounts of gypsum, hemihydrate and/or soluble anhydrite – which have different solubilities in water) was not provided by the cement suppliers.

Although none of the five cements produced extremely high initial g and h values at their respective saturation dosages, the mortar dosage-response results (figure

6.8) suggest that the trends shown in figure 6.11(a-c) would not significantly alter at lower dosages and/or workabilities. That is, the contrasting effects observed in figure 6.10(b) are likely to be due to complex interactions between the various cement components and superplasticizer molecules, which make it difficult to isolate the effects of individual cement components.

In this respect, although the Type I and III cements used in this investigation have much higher C_3A/SO_3 ratios (3.17 to 4.00) than the maximum (of 2.0-2.5) recommended by Dodson[122] for optimum workability (page 78), they nevertheless produce satisfactory slump retentions and less significant increases in plastic viscosity with time compared to the SR cement which has a very low C_3A/SO_3 ratio of 0.046. Moreover, with the exception of the SR cement (which has a total alkali, Na_2O equ. content of 0.49%), all the other cements have Na_2O contents of 0.6% or more (Table 4.1), and are therefore at variance with the optimum value of 0.4 to 0.5% reported by Jiang et al[166] for increasing the initial workability and reducing the rate of loss of workability (page 72).

Further work is needed to clarify the roles played by the soluble alkalis and form of the calcium sulfates on the Bingham properties of HSC mixes.

6.5.3 Summary

Although the results in sections 6.5.1-6.5.2 have shown a consistent ranking order for the cements and superplasticizers used, i.e. no incompatibility (or unusual behaviour), it is not possible to generalise that these observations would be applicable in all cases. The results suggest that many of the problems associated with cement-superplasticizer incompatibility may be complicated by, for example, inadequate attention to superplasticizer mixing procedure, and the varying sensitivity of different cement-superplasticizer combinations at low dosages and w/b ratios. Further work is however needed to determine the role of steric hinderance on the workability properties of HSCs having different cements, CRMs and w/b ratios.

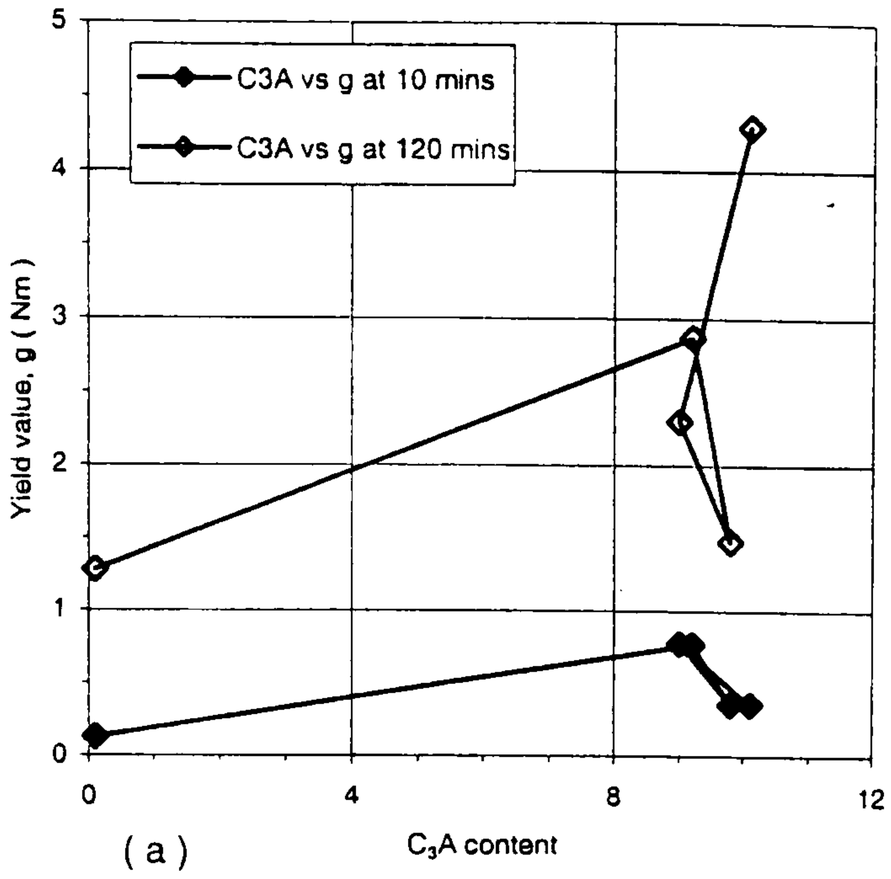

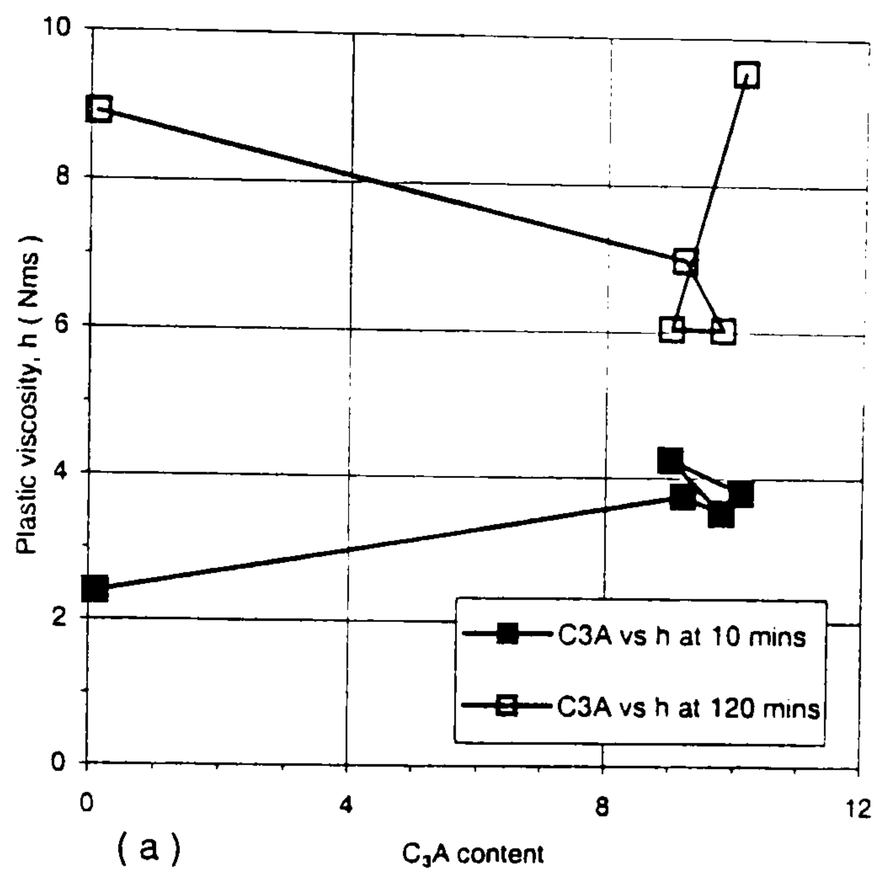

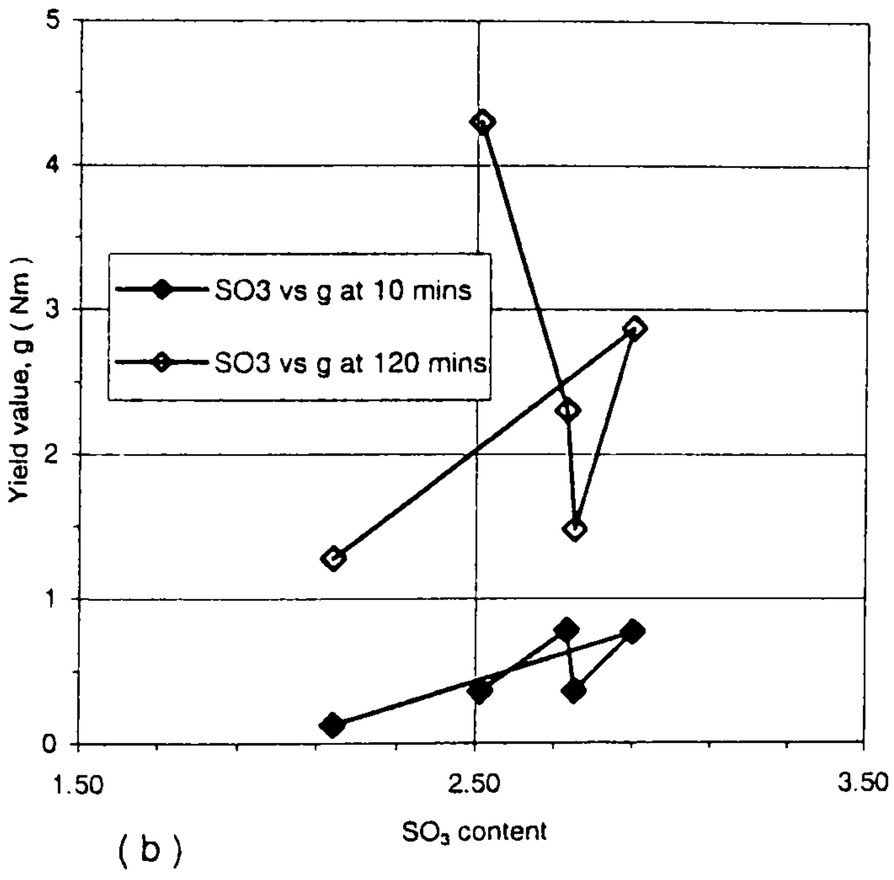

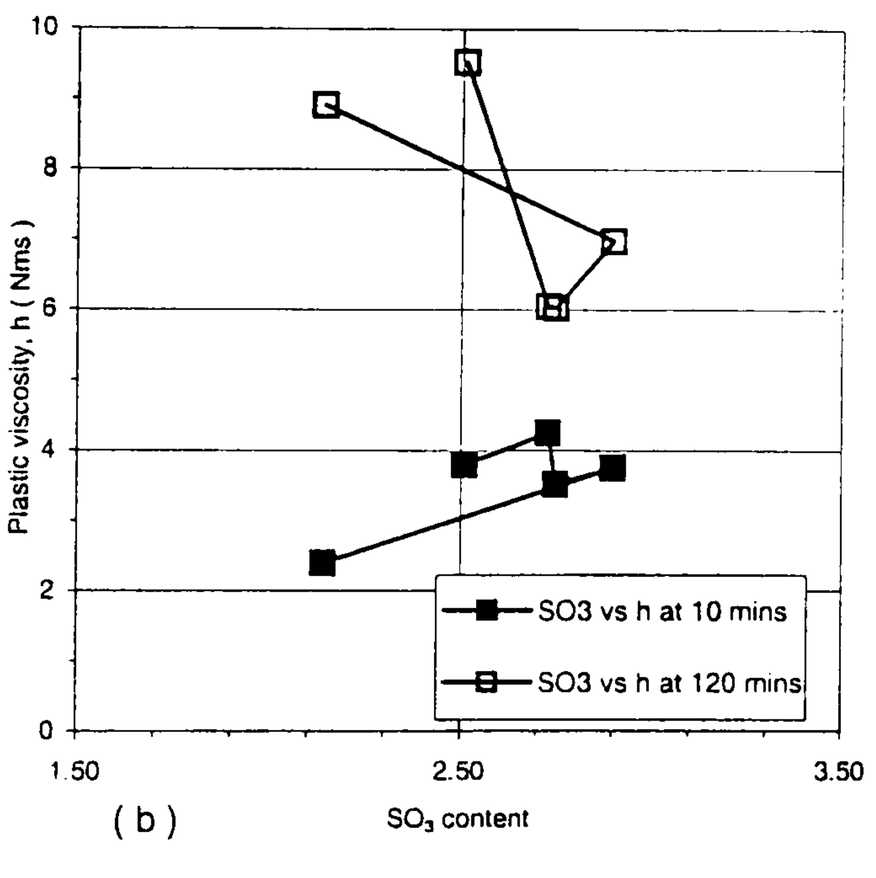

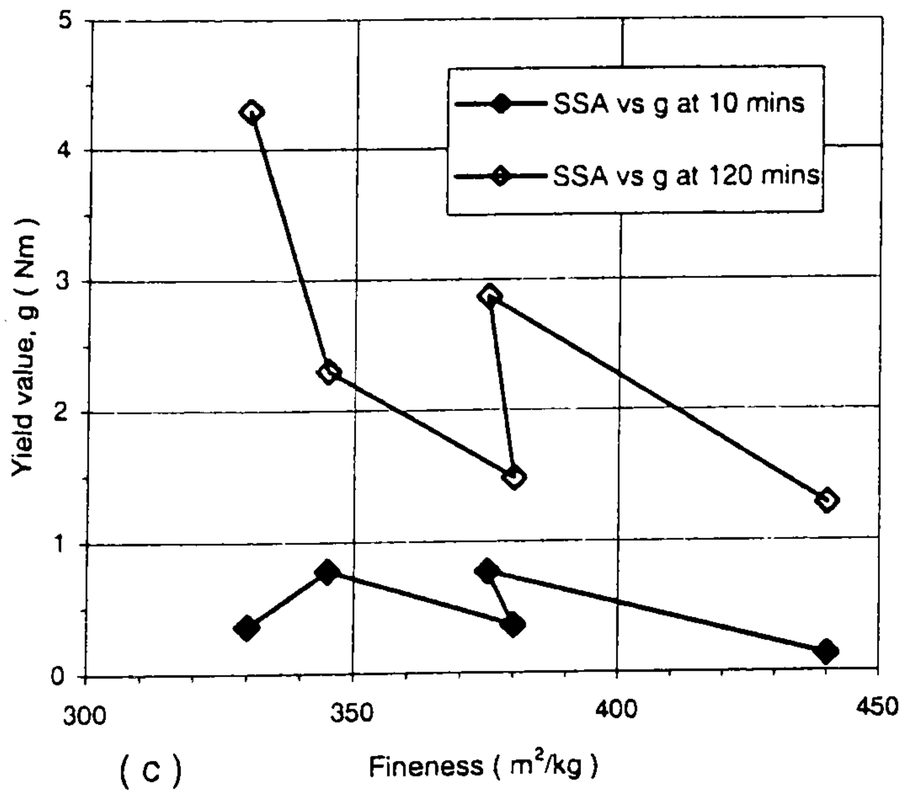

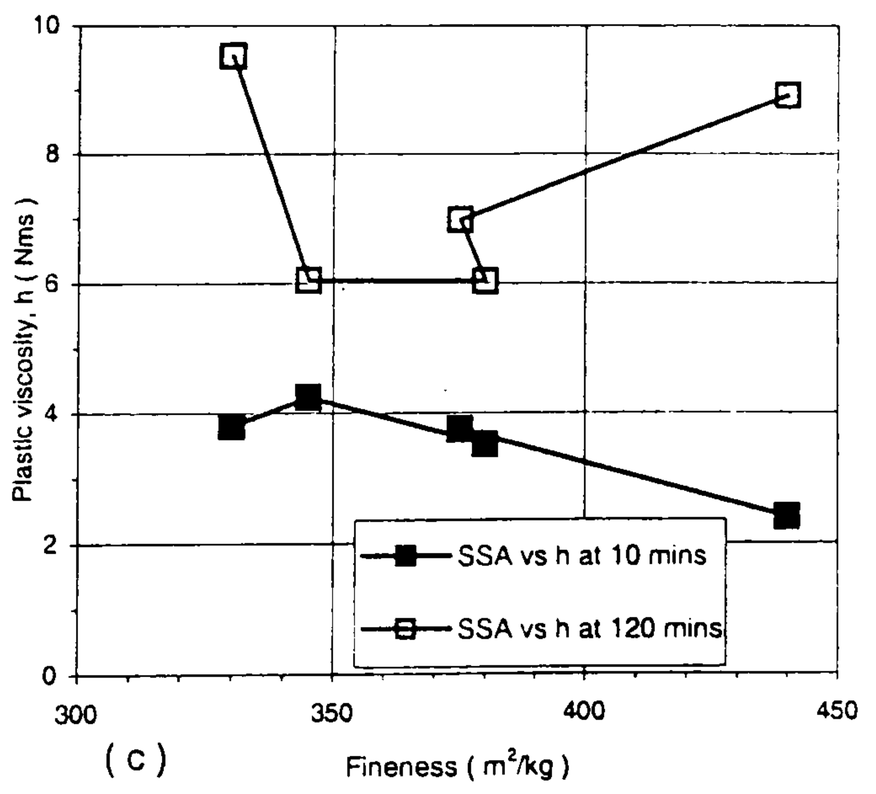

Figure 6.11 : Effects of (a) C_3A content, (b) SO_3 content and (c) cement fineness on the Bingham parameters. (SNF superplasticizer, 0.26 w/b)

6.6 Effects of superplasticizers on mix stability and compactability

Increases in the workability of the superplasticized mortar and concrete mixes in sections 6.2-6.5 were accompanied by noticeably higher bleeding and segregation tendencies. As in section 5.3.2, the bleeding tendencies of the concrete mixes varied with slump. In mixes with slumps $\geq$ 230 mm, the surface bleed water (often 1-5 mm in thickness) exhibited intense bubbling, particularly after re-mixing and two-point testing. As described in chapter 4, mixes with slumps $\geq$ 150 mm showed increasing tendencies towards sedimentation of the coarse aggregates during two-point testing; whilst in lower slump mixes the coarse aggregates primarily packed around the sides of the LM test bucket.

The relationship between segregation resistance and the Bingham parameters of the concrete mixes tested in sections 6.2-6.5 is shown in **figure 6.12**. In contrast with the results obtained with the MH system (figure 5.6(b)), the results in figure 6.12 show that the segregation resistance (SI) is highly influenced by both the Bingham parameters.

- At low-medium workabilities, the resistance to segregation appears to depend equally on both the yield value and plastic viscosity.
- At high workabilities, when the yield value is near zero, the results however indicate that the resistance to segregation is mainly governed by changes in the plastic viscosity.

The small scatter in the results at both high and low workabilities is essentially within the statistical variability range shown in Table 6.1(a), and suggests no distinct effects of superplasticizer type, dosage, mixing procedure or compatibility with different cements.

These results contrast with Collepardi 's suggestion[34] that the low segregation tendency associated with the high fluidizing action of their NG acrylic-based superplasticizer is caused by coagulation or bridging effects of higher molecular weight polymers compared with SMF and SNF superplasticizers. The results also contrast with the suggestion by Aitcin et al[58], that the segregation of superplasticized concrete may be primarily related to overdosing (page 99). In fact, the overdosed 3.00% and 4.00% mixes in figure 6.4 gave slightly higher

segregation resistance, consistent with their higher Bingham parameters, but more pronounced bleeding tendencies, compared to the 2.50% mix at the saturation dosage.

Several compactability tests with the cylinder-vibration method used in section 5.3.3. indicated very little influence of superplasticizer type or level of workability on the vibration response of HSCs having slumps greater than or equal to 200 mm. Tests carried out with, for example, the 2.50% and 4.00% mixes, despite their contrasting workabilities as shown in figure 6.4, gave almost identical compactabilities under vibration. The values in the first 120 mins typically fluctuated between 5-10 mm as show in **Table 6.5**. The vibration response of the SNF and Acrylate-based (D 2001) superplasticizers, together with mixes containing CRMs, are further explored with a novel vibration method in chapter 8.

6.7 Bingham parameter relationships with slump-flow time, and the workability properties of mortar

6.7.1 Relationships between the Bingham parameters and slump-flow time

The previous observations in section 5.3.1 showed that the final slump-flow time, for the concrete to stop collapsing under its self-weight, may provide a more useful index of the workability properties of HSCs than the actual slump value. The relationship between slump-flow time and the Bingham parameters of the concrete mixes tested in sections 6.2-6.5 is shown in **figure 6.13**. In contrast with the previous indications, this shows no correlation between the slump-flow time (ST) with either the yield value or plastic viscosity. The large scatter in the results does not even show a broad trend of increasing slump-flow time with decreasing workability.

Observations of the mixes during slump collapse had instead indicated significant differences in the rates at which mixes with different workabilities deform. At a given time after removal of the slump-cone, high workability mixes typically exhibited larger collapse spreads than lower workability flowing concrete mixes

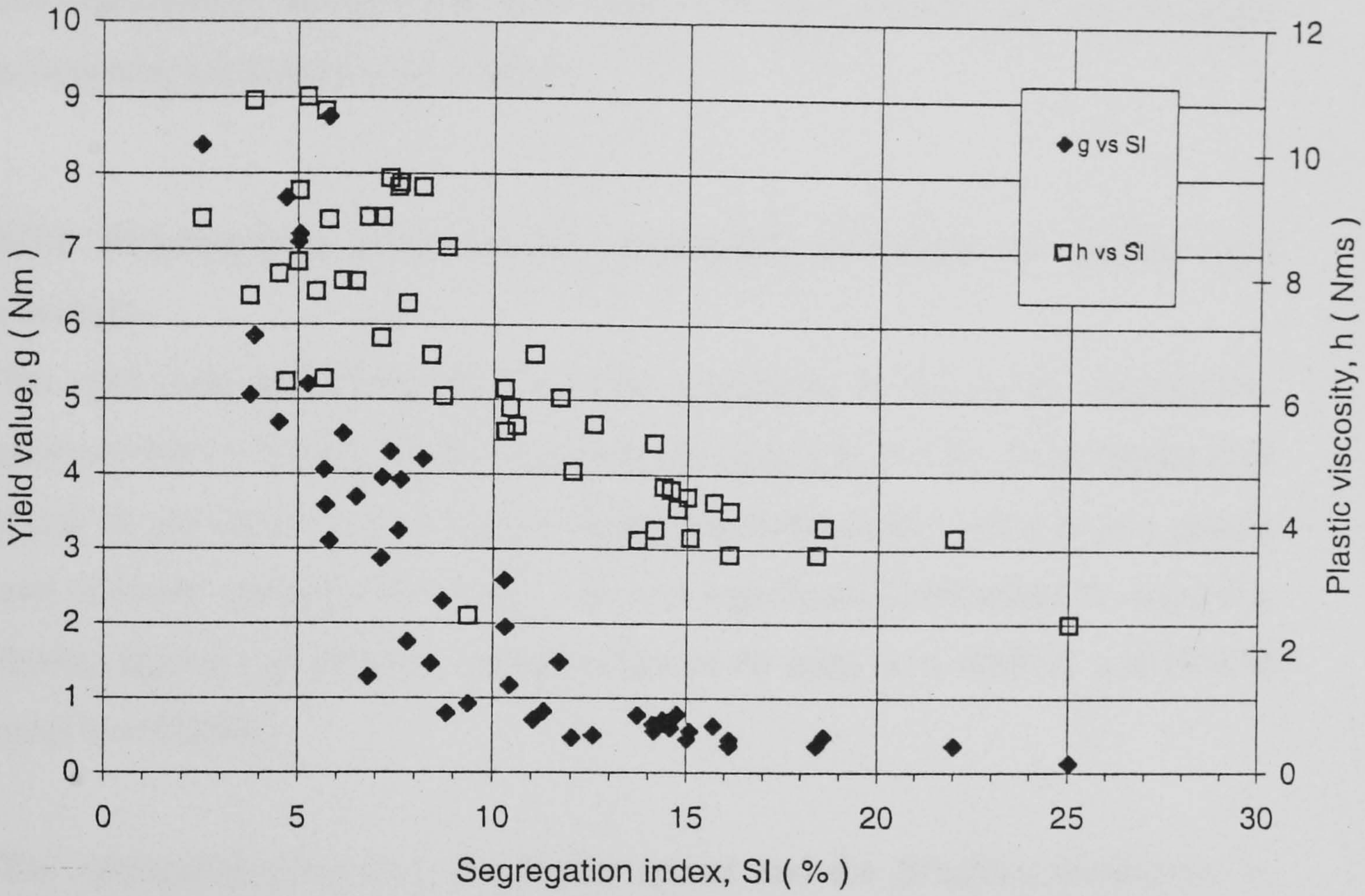

Figure 6.12 : Relationship between the Bingham parameters and Segregation Index.

Table 6.5 : Some typical compactability measurements with the cylinder-vibration method

Superplasticizer Type (and dosage)	Time (mins)	Slump (mm)	Time (mins)	Yiled value, g (Nm)	Plastic viscosity, h (Nms)	Time (mins)	Compactability dH (mm)
SNF (at 2.00%)	7.5	220	10	0.81	5.89	12	5
	65	190	60	1.39	6.79	62	10
	125	150	120	3.04	8.14	122	20
Acrylate (at 2.00%)	7.5	240	10	0.45	4.44	12	5
	65	100	60	3.43	7.35	63	35
	-	-	-	-	-	-	-
SNF (at 2.50%)	8	240	10	0.56	3.79	12	10
	65	225	60	0.92	5.94	63	5
	125	200	120	1.46	6.71	122	5
SNF (at 4.00%)	8.5	230	10	0.71	4.61	12	5
	65	210	60	1.66	6.85	62	10
	125	170	120	3.58	10.59	122	5

with comparable final slump-spreads. The dependence of slump-spread value (at 5-60 secs after removal of the slump cone) on the Bingham properties of HSCs is investigated with mixes containing CRMs in the next chapter. The results of these, and relationships between the final slump and slump-spread with the Bingham parameters, are discussed in chapter 8.

6.7.2 Relationships between the workability properties of mortar and concrete

The relationships between the workability properties of the mortar and concrete mixes tested in sections 6.2-6.5 are shown in figures 6.14-6.16. From **figure 6.14** it can be seen that there is a good correlation between the initial mortar spread and concrete slump ($r = 0.9252$), but less significant correlations between the mortar spread and concrete slump values at 60 mins ($r = 0.6842$) and 90-120 mins ($r = 0.3491$).

The relationships between the mortar spread and the Bingham parameters in **figure 6.15(a-b)** show similarly poorer correlations between the workability properties of mortar and concrete with lapsed time, but indicate a noticeably higher dependence of initial mortar spread on yield value ($r = 0.8987$) than on plastic viscosity ($r = 0.7600$). Although the relationships in **figure 6.16** show a slightly higher dependence of initial mortar V-flow time on plastic viscosity ($r = 0.8408$) than on yield value ($r = 0.8170$), the non-linearity of the curves in **figure 6.16(a)** indicates that there is an increasing influence of yield value at V-flow times higher than 5-6 secs. (The correlation coefficients in figure 6.16, like those in figures 6.14-6.15, also decrease systematically with time).

From these results it can therefore be concluded that:

1. The mortar spread and V-flow time
   - respectively have slightly greater dependencies on the yield value and plastic viscosity, but
   - can not be explicitly related to either of the Bingham parameters.

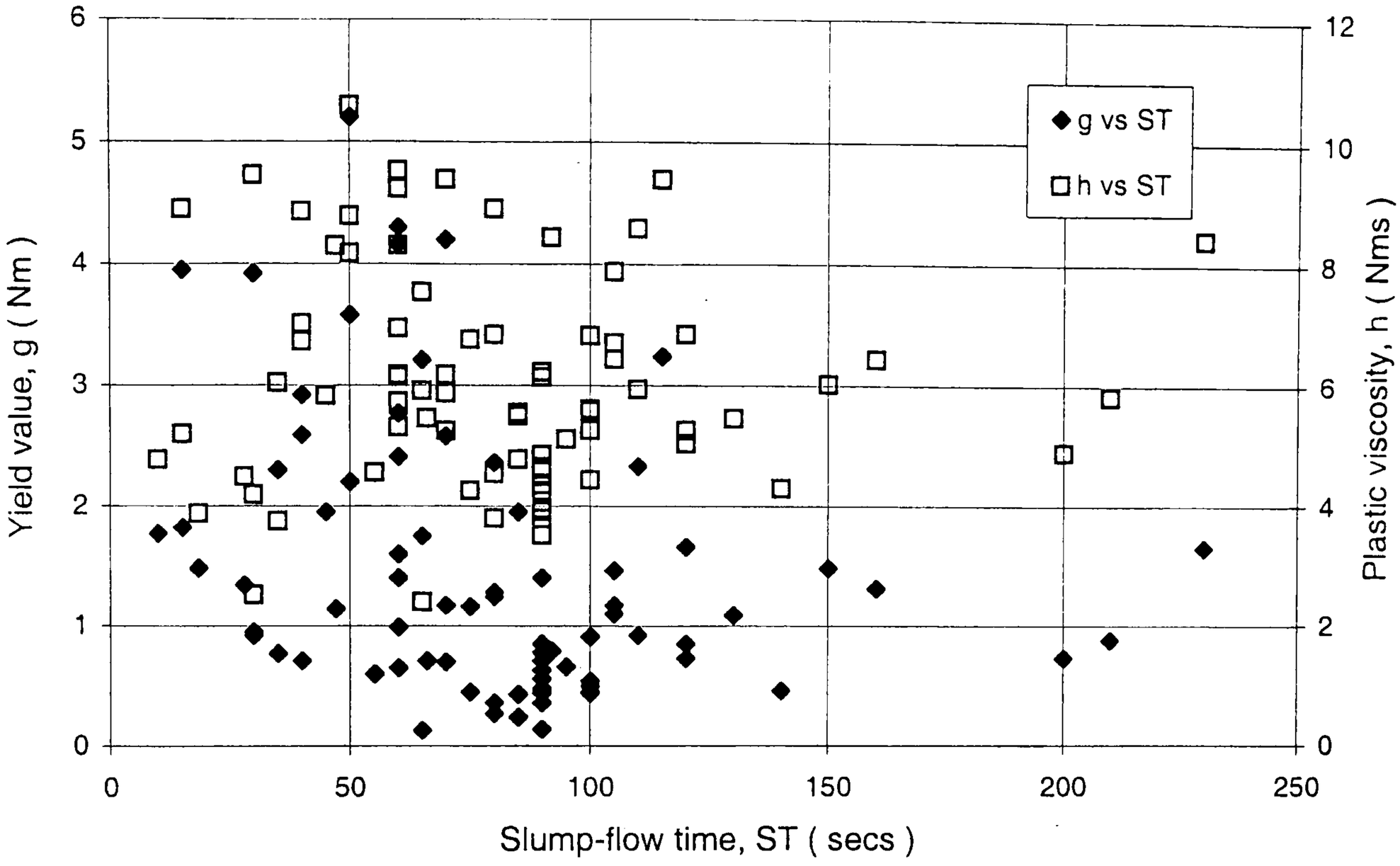

Figure 6.13 : Relationship between the Bingham parameters and slump-flow time (at slumps greater than or equal to 150 mm).

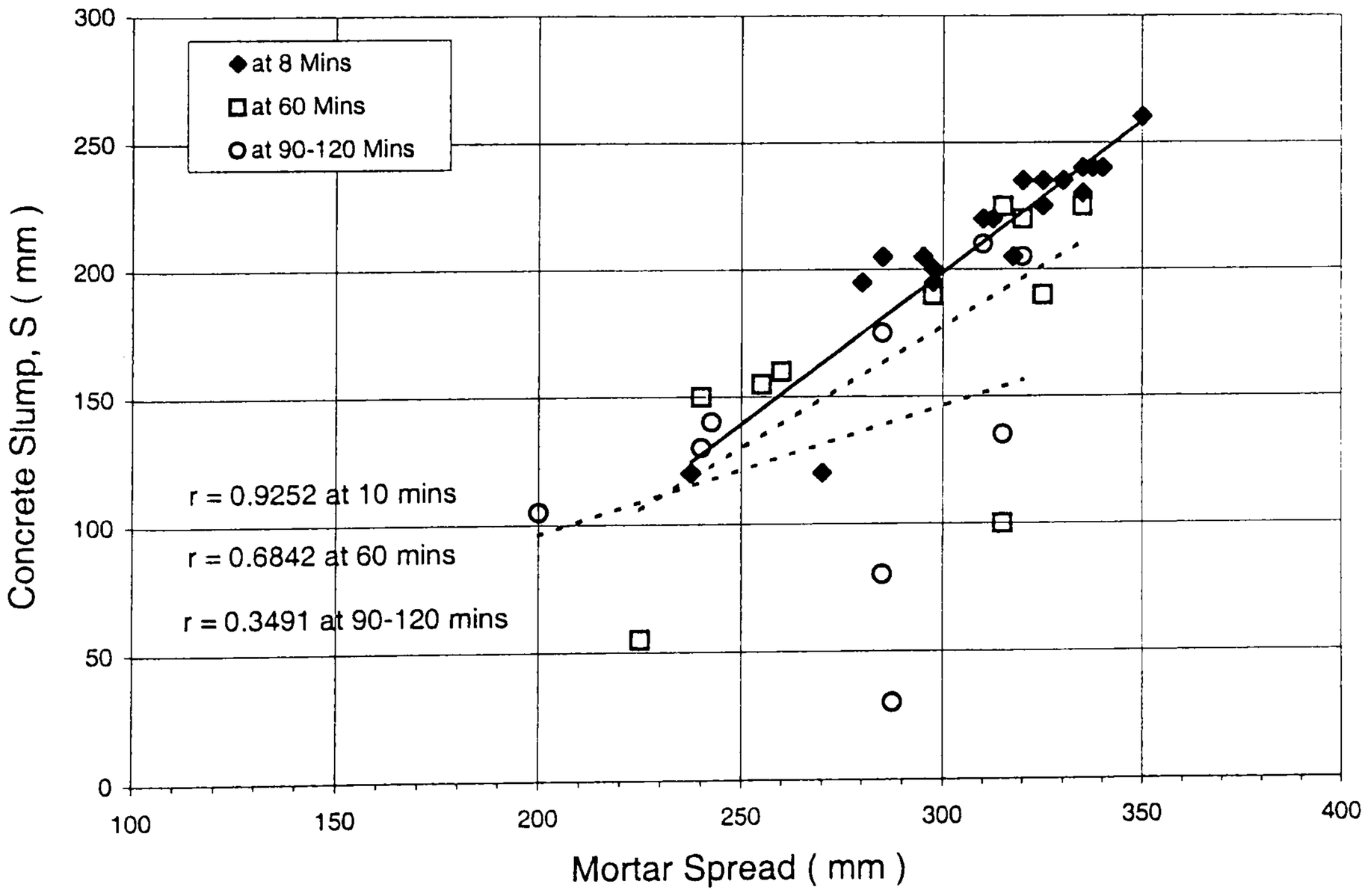

Figure 6.14 : Time-dependent relationships between the variations in mortar spread and concrete slump (for clarity the results at 30 mins of mixing are omitted).

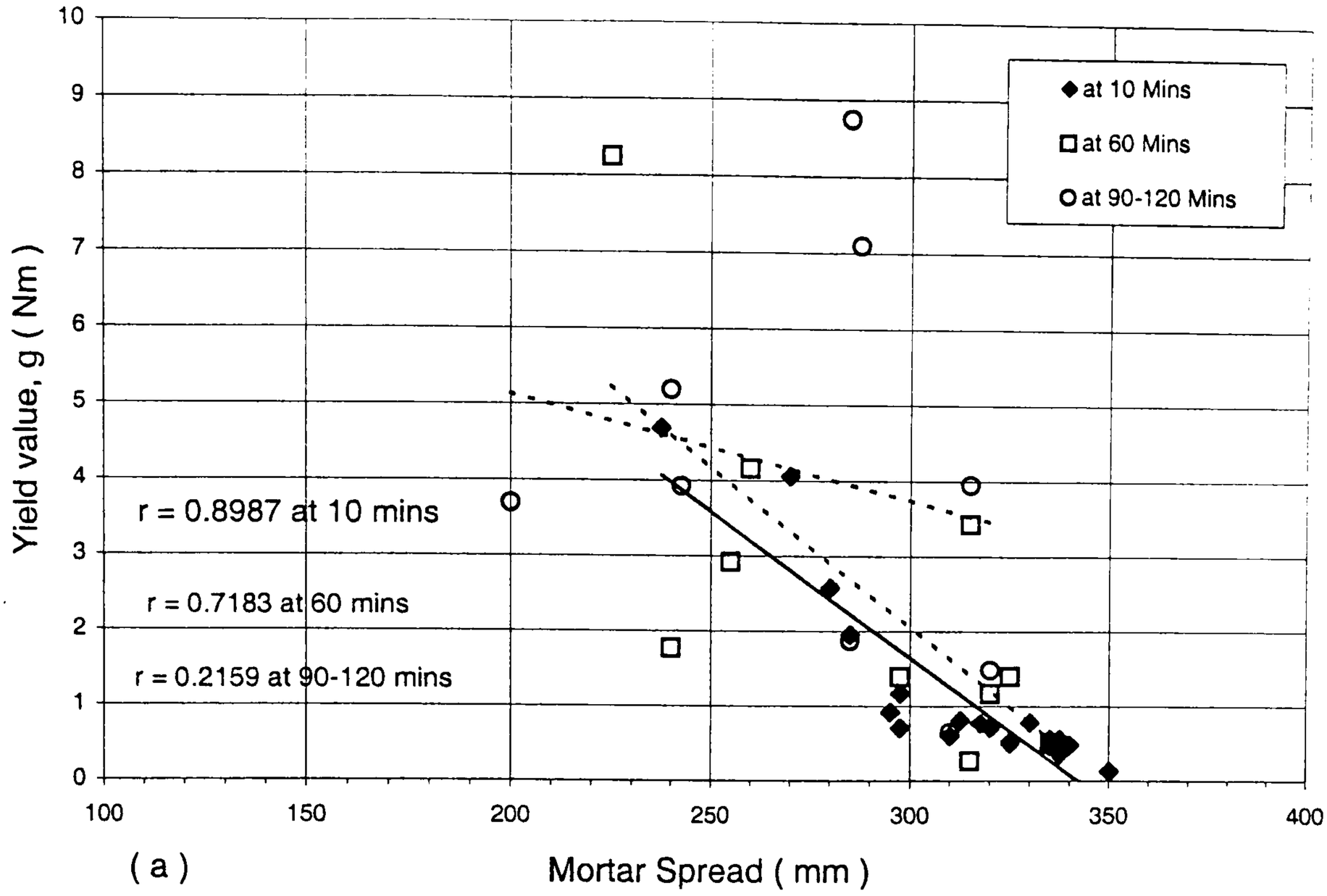

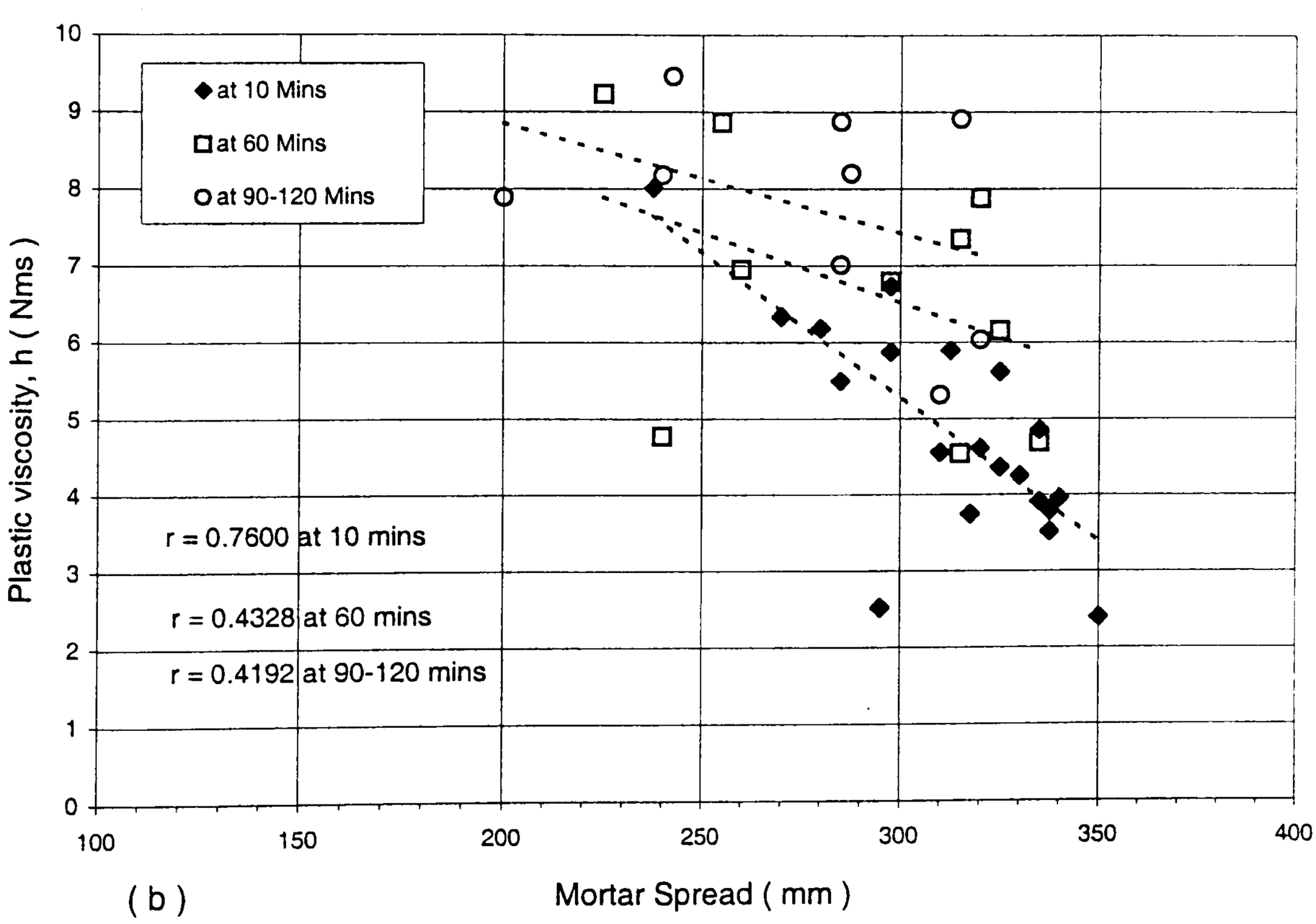

Figure 6.15 : Time-dependent relationships between mortar spread with (a) yield value and (b) Plastic viscosity (for clarity the results at 30 mins of mixing are omitted).

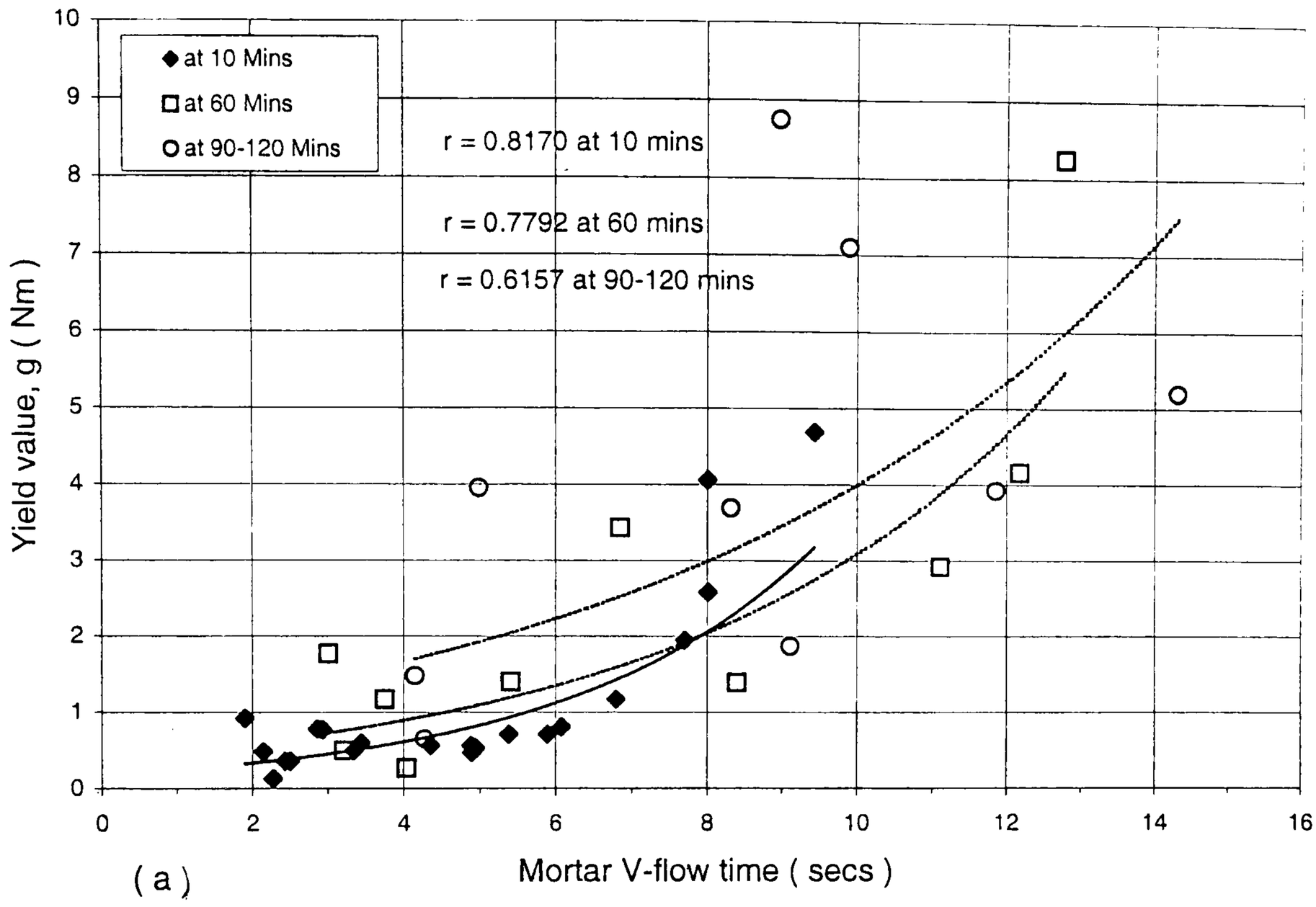

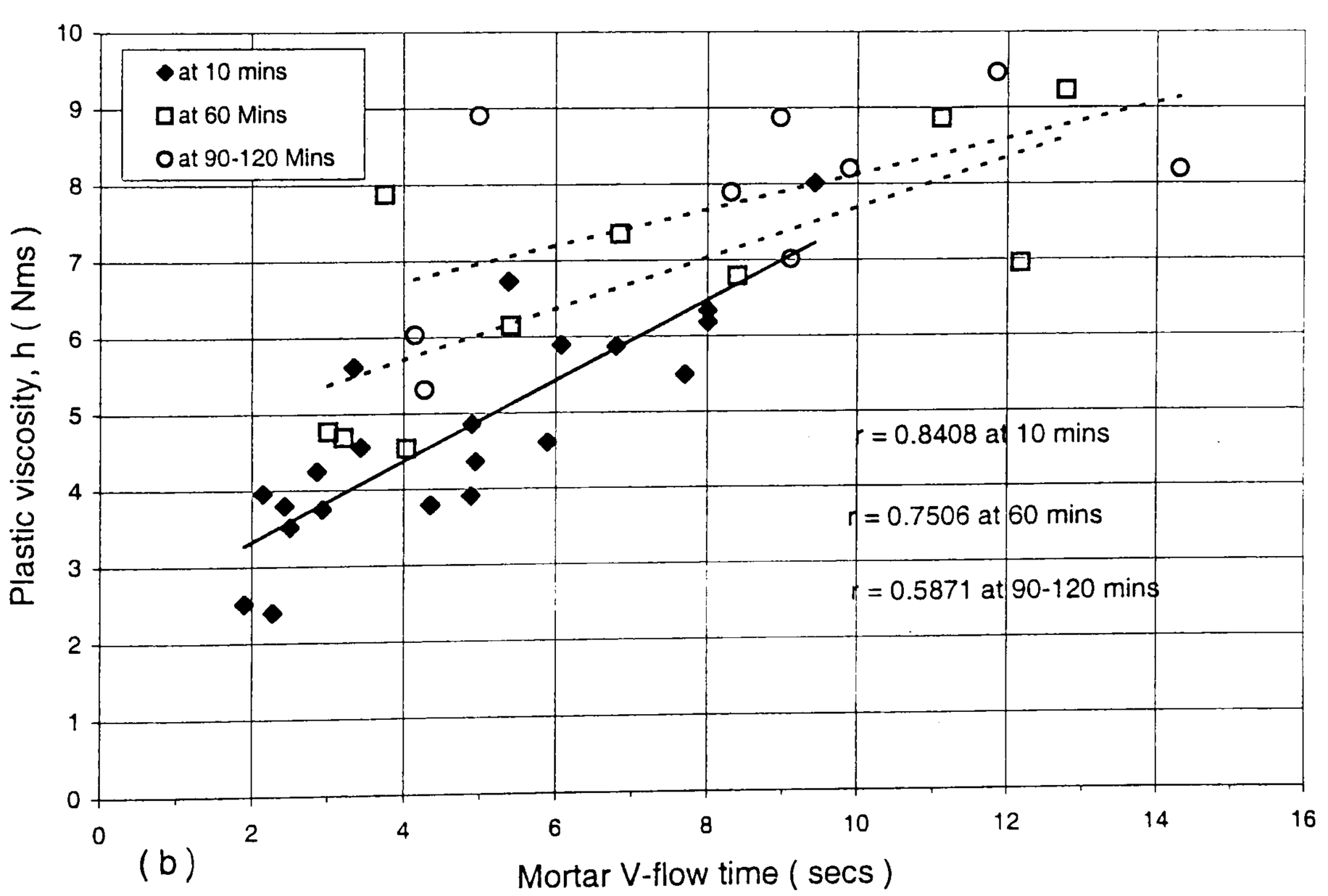

Figure 6.16 : Time-dependent relationships between mortar V-flow time with (a) yield value and (b) plastic viscosity (for clarity the results at 30 mins of mixing are omitted).

2. Tests on the mortar fractions are:
    - suitable for predicting the initial workabilities and fixing the saturation dosages of HSCs, but
    - less suitable for assessing their loss of workability.

One possible explanation for the longer workability retention in mortar compared to concrete may be related to the larger amounts of bleed water observed in the mortar fractions. These could replenish the cement particles with active superplasticizer molecules, and thus provide longer dispersion stability of the cement-water-superplasticizer system. A second possibility is that the cement agglomerates and/or hydration products may be more readily broken-down by the sand particles in mortar than by the coarse aggregates in concrete, and therefore exhibit a lower tendency to cluster with time. Further work involving studies of the workability, adsorption, Zeta potential and hydration characteristics of cement paste, mortar, and concrete may clarify the observed differences in workability retention.

6.8 Conclusions

- At a constant dosage of 2.00% s/w/b, a SNF (Conplast SP 435) **superplasticizer type** exhibits:
    - a lower initial workability (of 0.36 Nm (or 80%) and 1.45 Nms (or 33%)) compared to an Acrylate-based (D 2001) NG superplasticizer, but
    - longer workability retention than the Acrylate-based superplasticizer, and other superplasticizers based on SMF, MLS and Vinyl polymers.

- The initial workability properties and losses of workability of SMF, SNF, MLS, Vinyl and Acrylate-based **superplasticizer**s are principally **dosage** dependent.
    - The saturation dosage produces the highest initial workability and longest workability retention.
    - Lower SNF dosages give relatively larger time-dependent increases in yield value; whereas higher dosages mainly increase the rate of development of

plastic viscosity.

- The **optimum** delayed **addition time** of SMF, SNF, MLS, Vinyl and Acrylate-based superplasticizers occurs 4 mins after the cement first comes in contact with the mixing water. When compared to a shorter delayed addition time of, for example, 2 mins, the optimum addition time reduces the saturation dosage (by more than 10%), reduces the initial g and h values (by up to 43% and 19% respectively), and increases the workability retention (by 0.1 Nm (8%) and 0.67 Nms (or 21%)) in the first 120 mins.
  - A 0/4 mins split addition of SNF superplasticizer increases the initial yield value (by up to 0.56 Nm (or 156%)), reduces the initial plastic viscosity (by 1.00 Nms (or 28%)), but increases the rate of loss of workability (by as much as 1.65 Nm (or 147%) and 2.86 Nms (or 114%)) in the first 120 mins.
  - **Retarded** SNF and Acrylate-based **superplasticizer blends** reduce the initial workability (by up to 0.24 Nm (or 67%) and 1.65 Nms (or 42%)), but increase the workability retention in the first 120 mins by up to 4.82 Nm (or 96%) and 1.76 Nms (or 70%).

- The **compatibility** of cement types I, III and V with SMF, SNF, MLS, Vinyl and Acrylate-based superplasticizers shows no distinct (or unusual) performance differences.
  - With each of the five superplasticizers, cement types V and III respectively produce reduced and increased dosage demands, but higher and lower initial workabilities compared to Type I cements.
  - With cement Types I, III and V, the initial workability of the SNF is slightly lower than the Acrylate-based superplasticizer, but higher than SMF, MLS, and Vinyl-based polymers. The SNF superplasticizer produces longer workability retention than the SMF superplasticizer when used with cement Types I and V.

The SNF (Conplast SP 435) superplasticizer is used to assess the performance of CRMs in the next chapter.

Chapter 7
Assessment of Cement Replacement Materials

7.1 Introduction

Cement replacement materials (CRMs), such as PFA and GGBS, are widely used for reducing cost, reducing heat of hydration temperature rise, modifying the strength development characteristics and enhancing the durability of concrete. The use of both PFA and GGBS, unlike CSF, has also been widely reported to be beneficial in reducing the water demand (and hence superplasticizer dosage) by increasing the workability. The performance of these materials, like those of superplasticizers, have however not been adequately investigated (c.f. section 2.6).

This chapter reports tests used to assess the effects of different levels of cement replacements (at 0.26 w/b) on the SNF superplasticizer dosage demands and losses of workability in :

1. **binary blends** of
   - CSF (at 2.5, 5, 10, and 15%)
   - PFA (at 10, 20, 40 and 60%)
   - GGBS (at 20, 40, 60 and 80%), and
2. **ternary blends** of
   - PFA/CSF (at 20/10, 40/10 and 60/10%)
   - GGBS/CSF (at 20/10, 40/10, 60/10 and 80/10%).

The chapter also compares the SNF superplasticizer dosage demands and losses of workability in OPC, 10% CSF and two ternary PFA/CSF and GGBS/CSF mixes at **w/b ratios** of 0.30 and 0.22. In each case, mortar dosage-response tests were initially performed to fix the saturation dosages for the mixes; and were followed by selected tests on concrete to assess loss of workability with the slump test and LM system. The chapter begins with an assessment of the dispersion characteristics due to different delayed additions of the CSF slurry; and ends by summarizing the effects of CRMs on the superplasticizer **dosage demands**, **workability**, **mix stability** and **compactability**. The mixes tested were all produced with cement PC-8 (Table 4.1), using the proportions given in Table 3.6 (mixes 5, 6 and 7).

7.2 Partial cement replacement by CSF

7.2.1 Dispersion characteristics of CSF

The literature review in section 2.6.4 showed no overall agreement regarding the role of CSF on superplasticizer dosage demand and/or workability. Contrary to several researchers[18, 30, 39 197-198], many other researchers[14, 19, 148, 160, 192-196] have reported that the use of CSF in HPCs reduces workability and, therefore, requires a compensating addition of superplasticizer (pages 91-92).

The previous tests in section 6.2.3 had however indicated that the performance of mixes containing CSF is highly sensitive to mixing procedure (c.f. Table 6.1, mix R8). **Figure 7.1** summarizes the results of mortar tests in which the CSF slurry was added at 0, 15, 30, 45 and 60 secs from the start of the initial mixing sequence. The results show systematic increases in mortar spread and lower V-flow times with delayed additions of the slurry from 0 to 30 secs, but no further improvements in workability at 45 and 60 secs. As can be seen, the direct addition of the CSF slurry to the dry cement reduces the initial spread by as much as 40 mm (or 12%) and increases the V-flow time by 2.4 secs (or about 80%) compared to the 30 secs addition time.

These results are comparable to those obtained with the delayed additions of superplasticizers in figure 6.5, and therefore provide direct support of the superplasticizing and/or repulsive action of CSF particles as suggested by Yonezawa[30] (page 92).

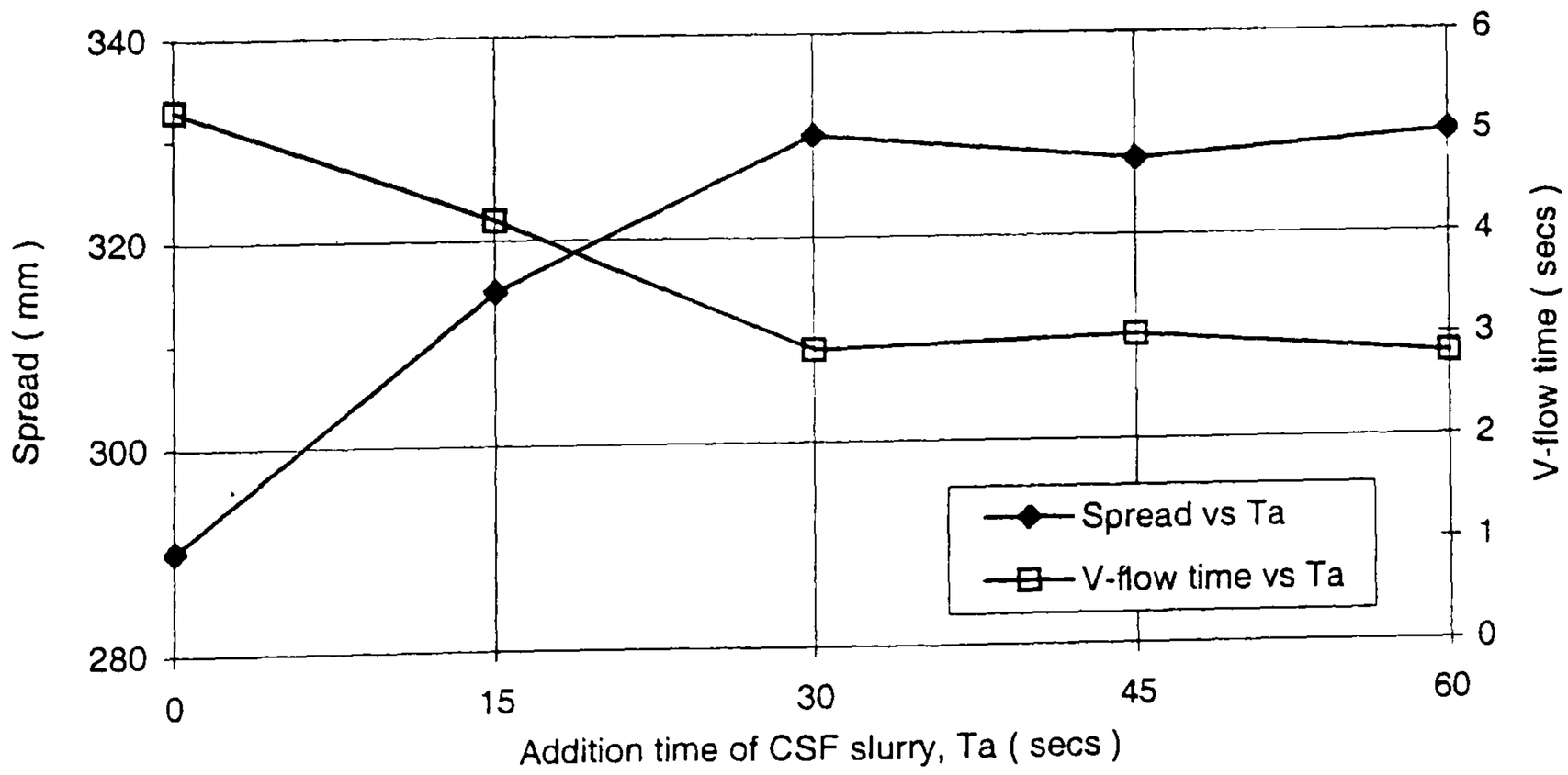

Figure 7.1 : Effects of CSF slurry addition time on mortar spread and V-flow time (using 10% CSF, at 0.26 w/b, and 2.00% s/w/b SNF).

7.2.2 Mortar dosage-response tests

Figure 7.2 shows the mortar dosage-response of the superplasticizer as a function of increasing CSF contents of 2.5, 5, 10 and 15%. As can be seen, there are systematic reductions in the saturation dosage demand (from 3.25 to 2.00% s/w/b) and improvements in workability with increasing CSF content up to an optimum replacement level of 10%. The 15% CSF replacement level gives an equal saturation dosage (2.00% s/w/b) but slightly lower workabilities compared to the 10% CSF replacement level.

These observations contradict those by de larrard[160, 195] and Agullo et al[148] (figure 2.56, page 92), showing increased dosage demand and higher saturation dosages with increasing CSF content. As mentioned previously (page 91), de larrard[195] and others[160, 196] attributed the increased dosage demand and reduced workability in CSF mixes primarily to the very fine size, and high specific surface area of the CSF particles. In their studies the CSF mixing procedure was however not reported, giving the impression that the slurry was added directly to the dry cement at the beginning of the mixing sequence.

The present results in figure 7.1 show that a direct addition of the CSF slurry to dry cement can produce significant reductions in workability and, hence, higher dosage demands. This may therefore be the main reason for the differences between the present results and those reported by de larrard[195] and others[14, 19, 148, 160, 192-194, 196].

7.2.3 Loss of workability in concrete

The slump and two-point test results for the 2.5, 5, 10 and 15% CSF replacement levels, at their respective saturation dosages (as found in mortar), are shown in figure 7.3(a-b). As can be seen, there are gradual increases in initial slump, but no significant differences in slump loss with increasing CSF content up to 10% (**figure 7.3(a)**). These results therefore contradict Punkki et al's findings[17] (c.f. figure 2.60).

in which the CSF was added directly to the dry cement (figure 2.40, procedure B), giving lower initial slumps and higher slump losses with increasing CSF content.

The two-point test results in **figure 7.3(b)** show continuous improvements in initial workability (i.e. lower g and h values), and longer workability retention with increasing CSF content up to an optimum of 10%. The 15% CSF mix gives slightly lower yield values, but larger time-dependent increases in plastic viscosity compared to the 10% CSF mix. The erratic variations in the Bingham parameters of the control OPC mix after the first 60 mins, appear to be related to considerable reductions in workability which are outside the measurable range of the two-point test apparatus (also c.f. page 244).

In this respect, it should be noted that the maximum initial slump of 195 mm obtained with the control OPC mix (using cement PC-8) is lower than the initial slumps produced by, for example, cements PC-4 to PC-6 in Table 5.1. The results however show that even a 2.5% cement replacement by CSF can increase the slump ceiling, and significantly improve the workability of the cement.

Soutsos 's initial workability measurements[53] with the MH system and a constant slump of 150 mm (c.f. figure 2.59), showed systematic improvements in workability with increasing CSF content, but no optimum replacement level. In contrast, Punkki et al's measurements[17] with the BML viscometer (c.f. figure 2.60), like those by Wallevik and Gjorv[50] with the MH system (figure 2.58), showed that an increasing content of up to 10% CSF slightly increases the initial yield value but reduces the plastic viscosity. With regards to loss of workability, Punkki et al[17] concluded that the presence of CSF reduces the development of plastic viscosity but increases the development in yield value. Their measured increases in initial plastic viscosity with increasing slump (figure 2.60), as discussed in sections 5.5.5, 6.3 and 6.4.1.2, are however indicative of the occurrence of up-lift effects in the BML viscometer.

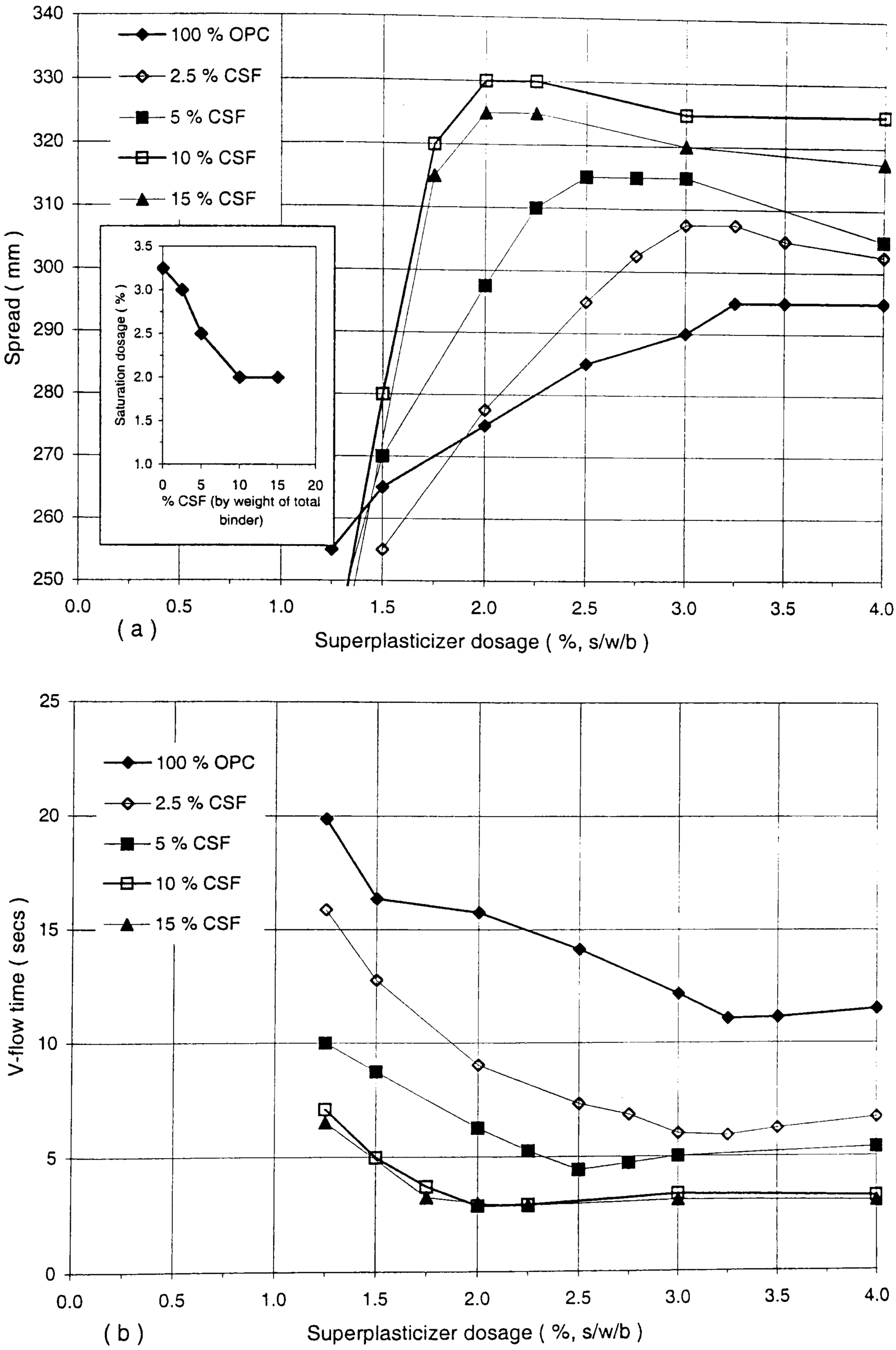

Figure 7.2 : Mortar dosage-response tests for the effects of increasing CSF content on (a) spread and (b) V-flow time at 0.26 w/b. (4 mins delayed add. of SNF).

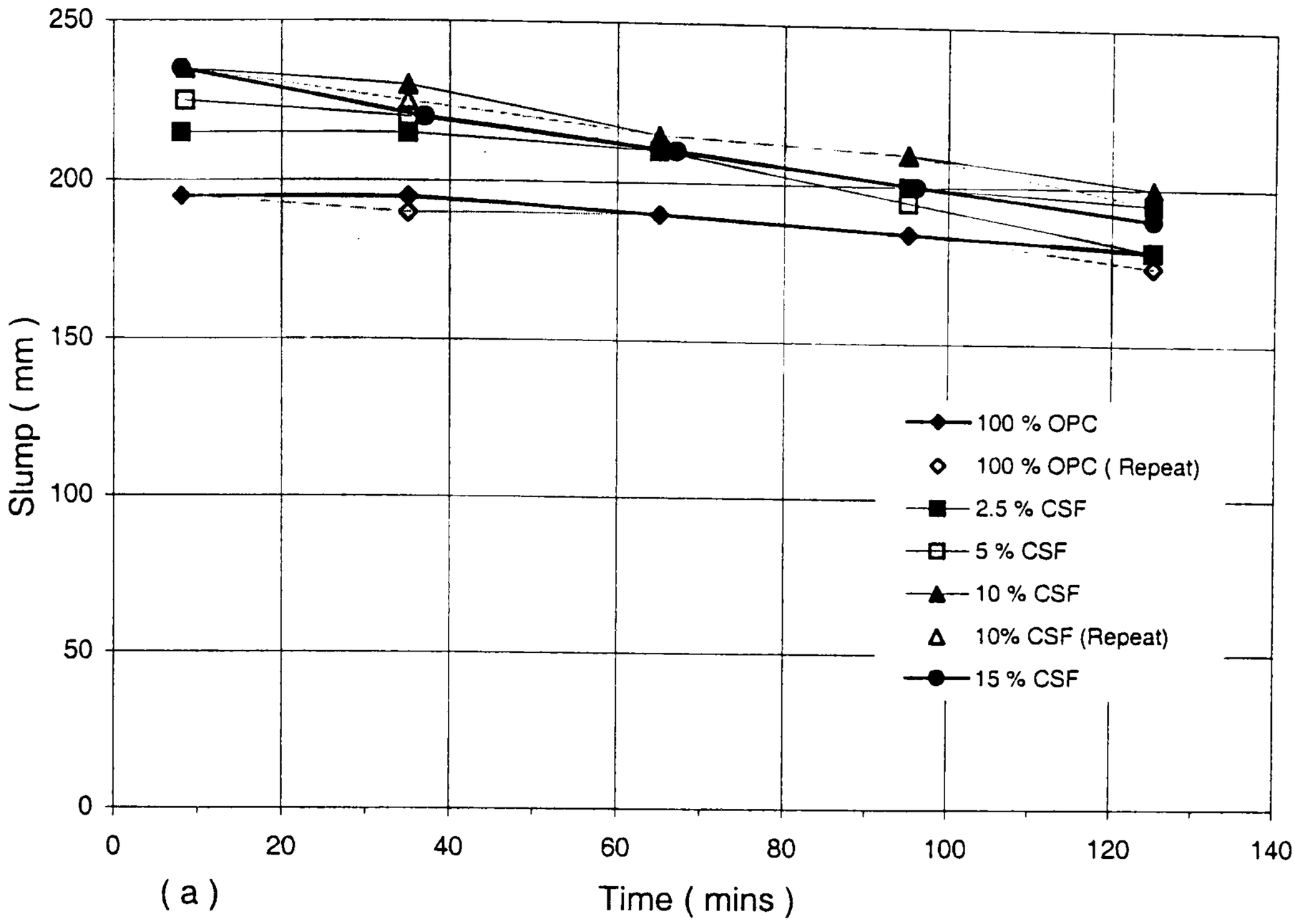

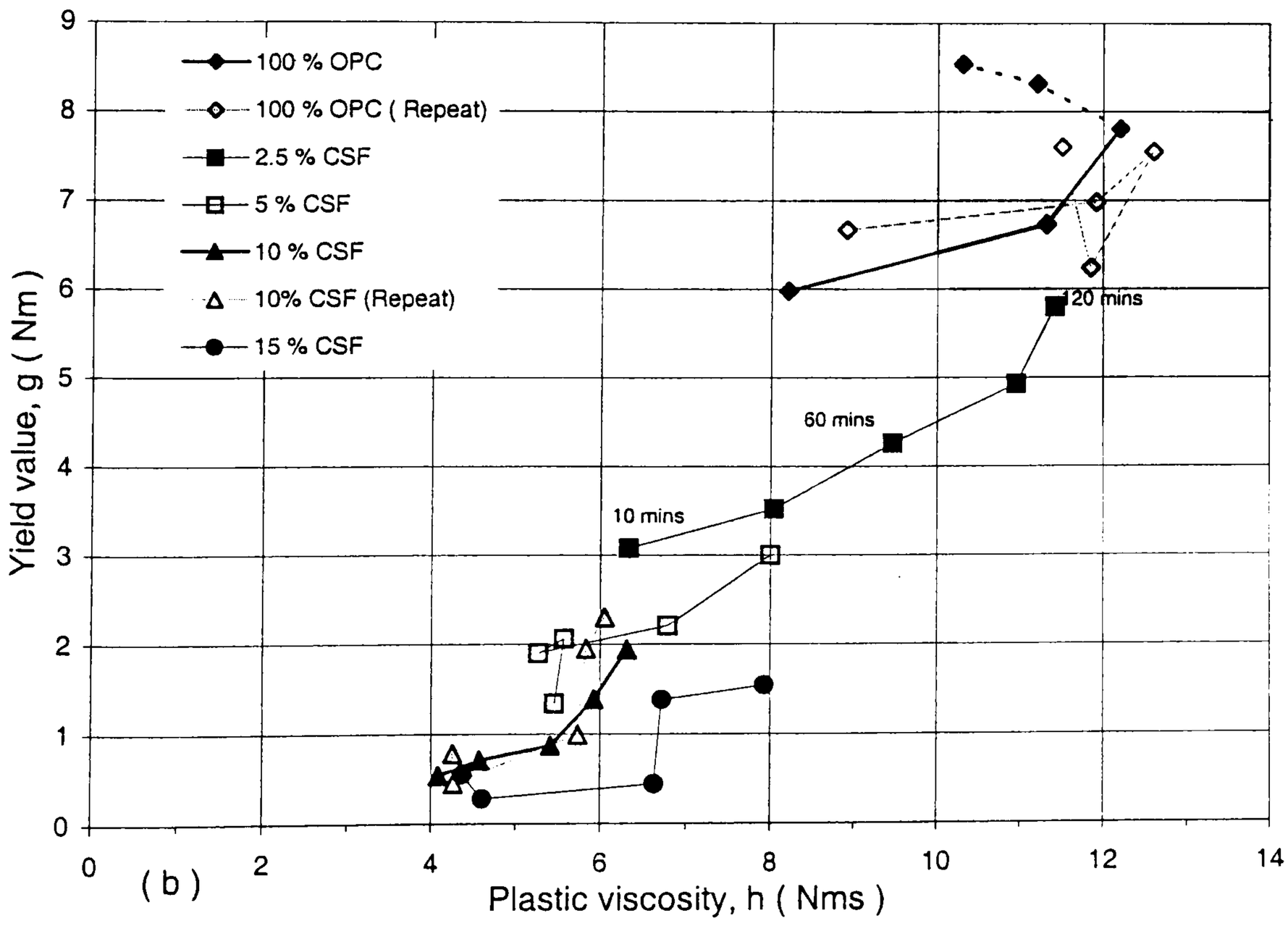

Figure 7.3 : Effects of increasing CSF content on (a) slump loss and (b) loss of workability at 0.26 w/b ratio. (All mixes tested at their respective sat. dosages, using 4 mins delayed add of SNF).

7.3 Partial cement replacement by PFA

7.3.1 Mortar dosage-response tests

The mortar dosage-response tests of the superplasticizer in **figure 7.4(a-b)** show continual improvements in workability and lower saturation dosages with increasing PFA content up to an optimum replacement level of 40%. The inclusion of 60% PFA in the binder produces a similar dosage-response to the 40% PFA mix. The results are in broad agreement with those reported by Soutsos[53] as shown in figure 2.50.

The review in section 2.6.2 revealed that several factors may be responsible for the effects of PFA on water demand and workability. Nagataki 's observations[175] (c.f. figure 2.49) indicated that the beneficial effects of PFA in reducing the water demand are directly related to the percentage of its spherical particles. In contrast, Owens[176] reported that the main factor influencing the water demand and workability properties of PFA mixes is the proportion of coarse particles greater than 45 μm. However, Besari et al[178] considered the improvements in workability to be due to the combined effects of an increased paste volume, and a ball-bearing action resulting from the spherical shape of the PFA particles.

Hansen[180] and Helmuth[181] have, on the other hand, reported that the reductions in water demands and improvements in workability are both the result of super-plasticizing and/or electrostatic effects associated with the PFA particles (page 83).

7.3.2 Loss of workability in concrete

The effects of the 10, 20 and 40% PFA contents on slump loss and loss of workability are shown in figure 7.5(a-b). **Figure 7.5(a)** shows higher initial slumps but, in agreement with Ryan and Munn 's observations[185] (page 84), no noticeable differences in slump loss due to partial cement replacements by PFA.

The two-point test results in **figure 7.5(b)** also show systematic improvements in

initial workability, but no conclusive effects on workability retention with increasing PFA content. When compared to the control OPC mix, the initial workability improvements occurring at the optimum 40% PFA replacement level (as found in mortar) are represented by as much as a fifteen-fold reduction in yield value (from about 6 to 0.4 Nm), and a 38% reduction in plastic viscosity (from 8.2 to 5.1 Nms).

Ellis 's initial workability measurements[182] with the LM system (figure 2.51) similarly showed reductions in both the Bingham parameters with increasing PFA content, but the confidence limits for his results are much larger than those obtained in section 6.2.3 (c.f. Table 6.1(a)). In contrast, Soutsos 's measurements[53] with the MH system and a constant slump of 150 mm (c.f. figure 2.52), showed continuous reductions in initial yield value, but consistently higher initial plastic viscosities with increasing cement replacement by up to 40% PFA. Several other researchers[85, 184] have also reported that PFA increases the initial plastic viscosity, but they have provided no explanation for this.

The present time-dependent measurements in figure 7.5(b) however show that even at a constant slump the concrete can experience significant losses in workability, represented by much larger increases in plastic viscosity than in yield value, particularly during the first 30 mins of mixing. That is, a constant slump is a deceptive indicator of constant workability. With regards to slump/workability retention, Ravina[186] suggested that during prolonged mixing the PFA agglomerates may break down, create repulsive forces between the cement particles, and prevent the build up of a skeleton structure which would otherwise stiffen the mix (page 84). In contrast, Baoju et al[99] attributed reduced slump losses occurring in utra-fine PFA mixes (page 84) to extended setting times, and the high specific surface area of the PFA particles, which they believe allows better interaction with the superplasticizer.

The fact that the control OPC and the 10-20% PFA mixes in figure 7.5 all show erratic variations in the Bingham parameters at plastic viscosities $\geq$ 12 Nms, suggests this to be a limiting range for the LM system under normal shearing conditions.

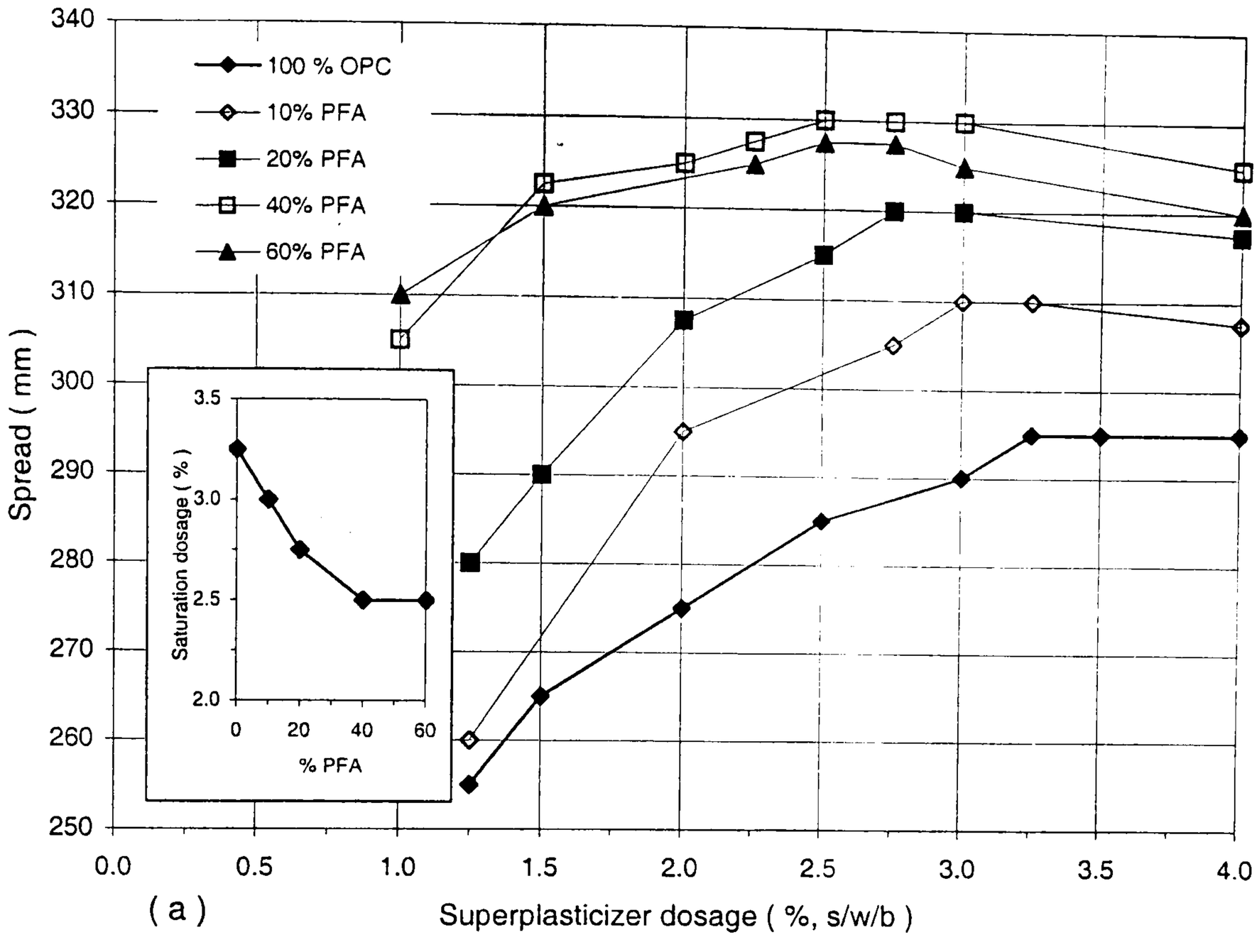

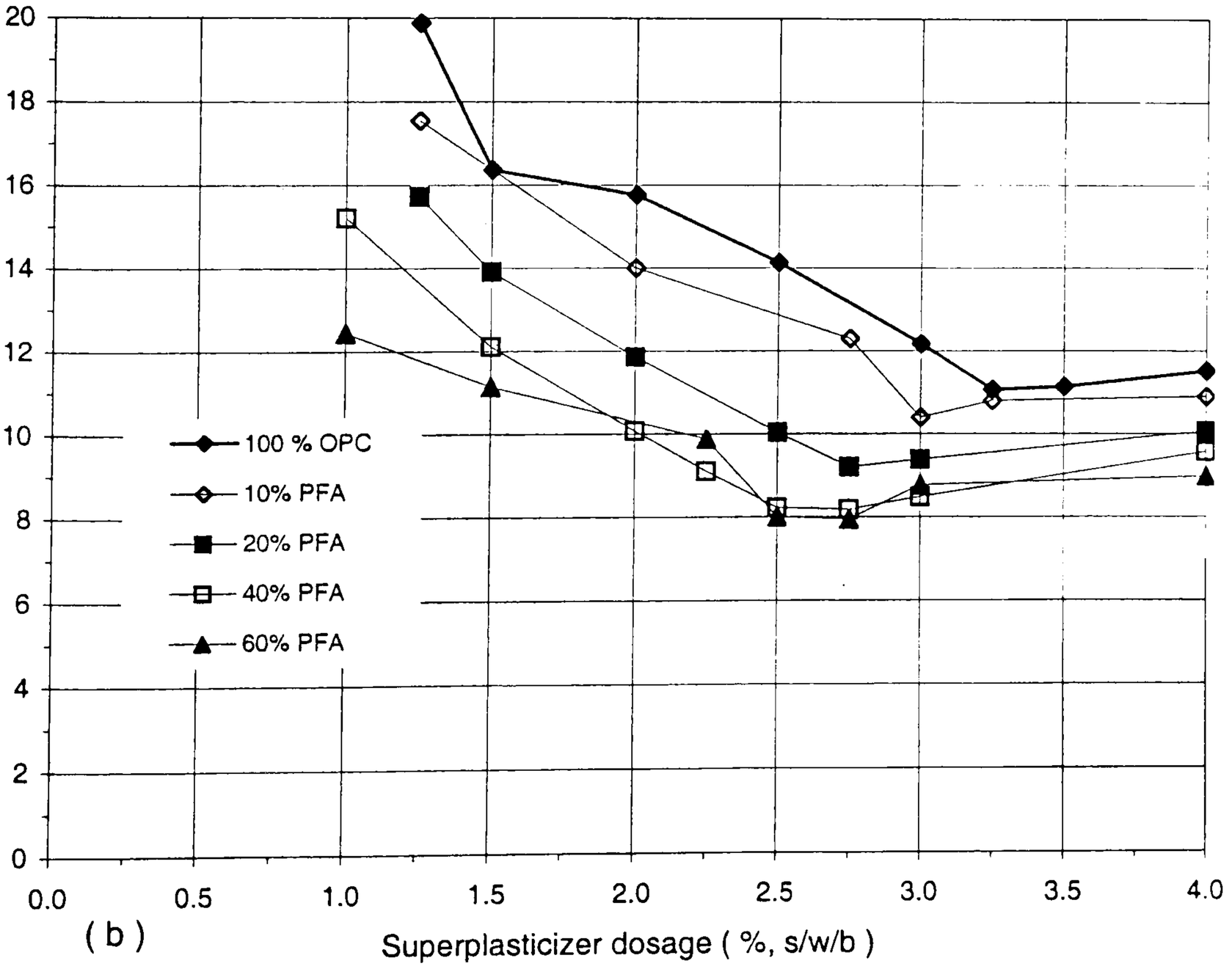

Figure 7.4 : Mortar dosage-response tests for the effects of increasing PFA content on (a) spread and (b) V-flow time at 0.26 w/b . (4 mins delayed add. of SNF).

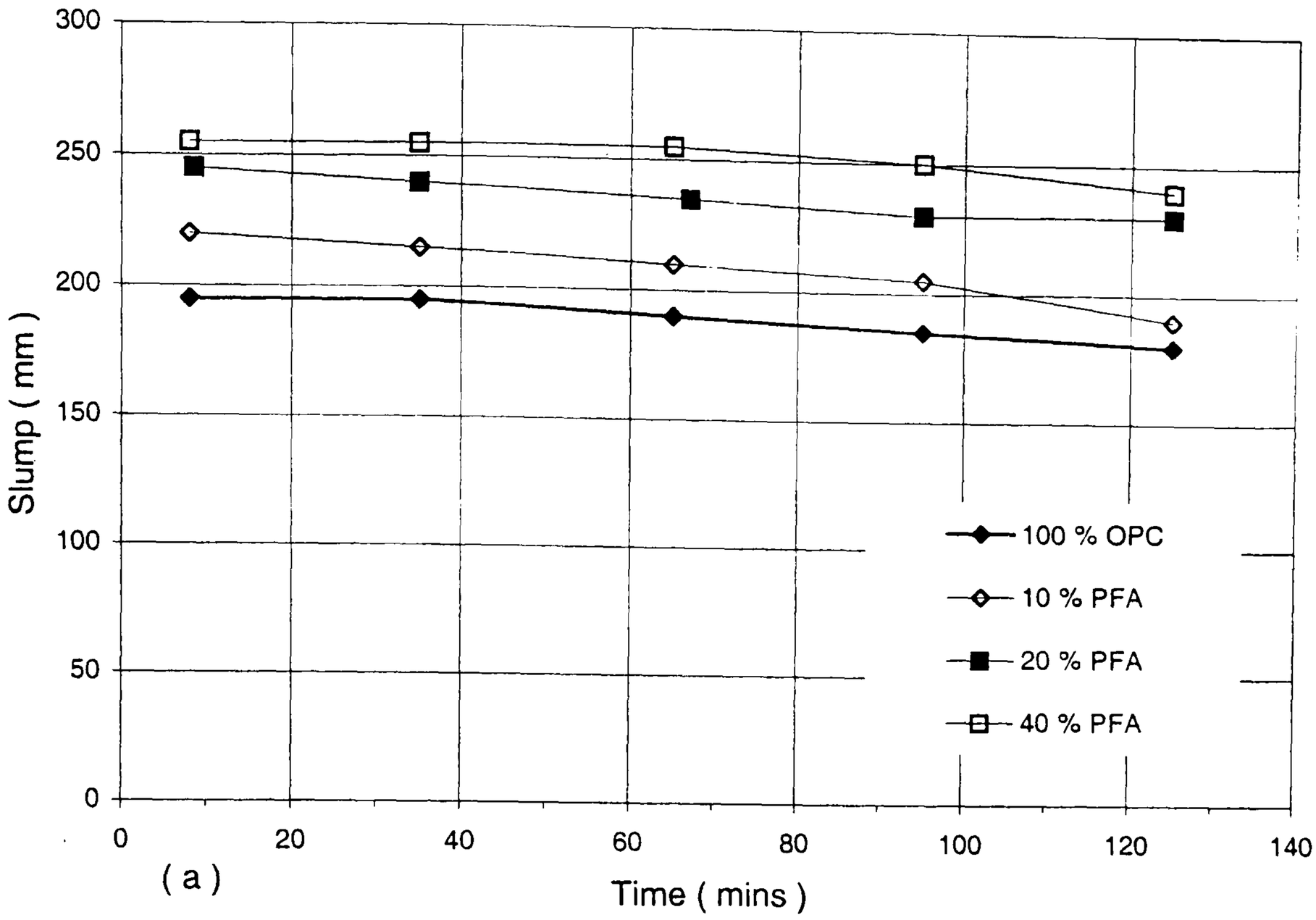

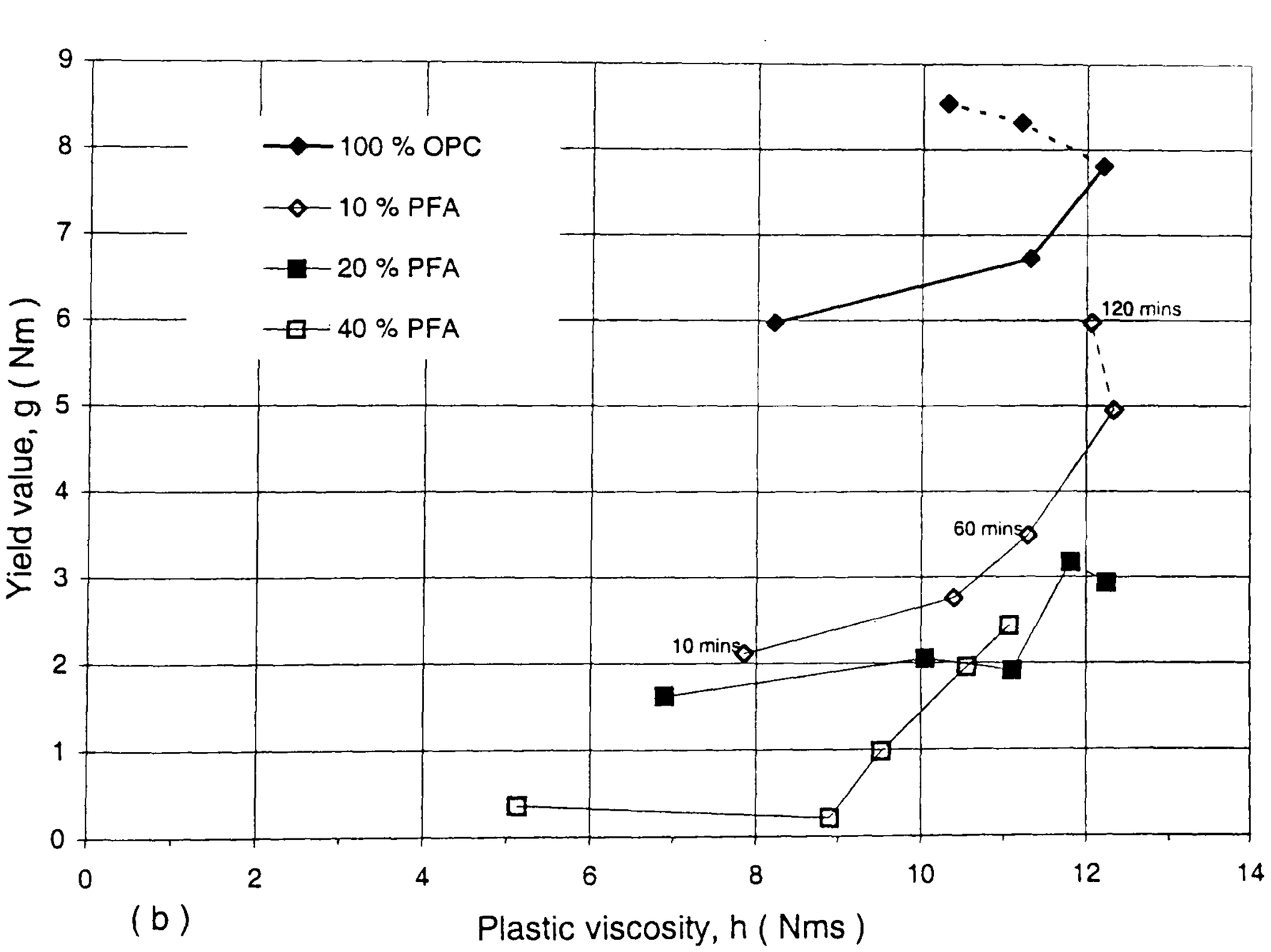

Figure 7.5 : Effects of increasing PFA content on (a) slump loss and (b) loss of workability at 0.26 w/b ratio. (All mixes tested at their respective sat. dosages, using 4 mins delayed add. of SNF).

7.4 Partial cement replacement by GGBS

7.4.1 Mortar dosage-response tests

The mortar dosage-response test results in **figure 7.6(a-b)** show increases in spread ceiling, but higher V-flow times with increasing cement replacement by up to 60% GGBS. The inclusion of 80% GGBS in the binder produced no flow through the V-funnel and a lower spread ceiling than the 60% replacement level. In contrast with the CSF and PFA mortar mixes (in sections 7.2-7.3), the saturation dosages from the spread and V-flow time measurements do not coincide, and vary in opposite directions with increasing GGBS content. When compared with the control OPC mix, the saturation dosage at the 60% GGBS replacement level is more than three times lower with respect to spread ceiling, but about 15% higher in terms of minimum V-flow time.

These results suggest that the inclusion of GGBS in the binder may have distinct effects on the adsorption and/or zeta potential properties of the superplasticizer. The 0/4 mins split addition of the superplasticizer at the 60% GGBS replacement level produces a similar saturation dosage, but reduces both the mortar spread ceiling and minimum V-flow time compared to its single introduction at 4 mins.

The contrasting effects of GGBS on the spread and V-flow time properties, may be one source of confusion regarding its influence on water demand and workability as reported by Nishibayashi et al[187] and others[18, 53, 189-190] (section 2.6.3). In agreement with the mortar-spread data in figure 7.6(a), Soutsos 's slump measurements[53] (c.f. figure 2.53) showed lower superplasticizer dosage requirements with increasing GGBS content. The fact that the dosage requirements from the spread and V-flow time measurements vary in opposite directions, and give different maximum workabilities, does however demonstrate the importance of full characterization of the workability properties when assessing binder performance.

Since the saturation dosages corresponding to minimum V-flow time show relatively higher maximum workabilities than those corresponding to spread ceiling, they were used to assess the loss of workability in concrete.

7.4.2 Loss of workability in concrete

The slump and two-point test results for the 20, 40 and 60% GGBS replacements are shown in figure 7.7(a-b). The results in **figure 7.7(a)** show higher initial slumps but, in agreement with Tazawa et al's[134] and Nishibayashi et al's[187] observations (page 89), negligible differences in slump loss with increasing GGBS content up to the 40% replacement level. These therefore contradict Dejellouli et al's suggestion[39] that partial cement replacement by GGBS, which is less reactive and reduces the amount of ettringite formed during early hydration, reduces the rate of slump loss in HSC (page 88-89).

The two-point test results in **figure 7.7(b)** show comparable initial yield values, but higher plastic viscosities with increasing GGBS content of up to 40%. In terms of loss of workability, both the 20 and 40% GGBS replacement levels show erratic variations in workability following the first 30-60 mins. These mixes were difficult to handle/sample after the first 10-30 seconds from re-mixing, and the initial two-point testing speed had to be progressively reduced from setting 6 (as used in the previous tests) to setting 4 (at 10 mins) and setting 2 (after 30 mins). With the 40% GGBS mix, considerable reductions in workability were experienced after the first 60 mins, which meant that no further two-point test measurements were possible.

In contrast, Soutsos[53] did not report any workability problems from his measurements with up to 60% GGBS, and concluded that GGBS has only a small effect on the workability properties of HSC (c.f. figure 2.54). The GGBS used in his investigation was supplied by Frodingham Cement Ltd., whereas that used in the

present research was supplied by Civil and Marine ltd. The main differences in the two sources of GGBS being in the CaO and SiO_2 contents (37.92% and 35.95% respectively compared to 41.3% and 33.7% as shown in Table 4.2). (Information regarding differences in the particle sizes of the two GGBS sources is not available).

Despite the high mortar-spread of the 60% GGBS mix (in figure 7.6(a)), the equivalent concrete mix at its saturation dosage corresponding to the minimum V-flow time of 35 secs (as shown in figure 7.6(b)) could not be produced. The concrete mixture after the initial mixing sequence consisted of discrete aggregate clusters cohesively coated with semi-dry paste, and was difficult to remove from the mixer. The results shown for the 60% GGBS mix in figure 7.7 represent the effect of a 2.00% s/w/b redose with the SNF superplasticizer, which increased the w/b ratio from 0.26 to 0.29. As can be seen, the rate of loss of workability of the mix during the first 30 mins is much higher than that obtained with the control OPC mix, and/or the 20 and 40% GGBS mixes.

Based on these results, it can therefore be concluded that partial cement replacements by GGBS :

- reduce the initial workability, and
- increase the rate of loss of workability in HSC.

These conclusions contradict those reached by Read et al[190] and Tachibana et al[18] (page 88), that the use of GGBS in HSC enhances workability, or gives longer workability retention as suggested by Dejellouli et al[39] (page 89). One possible reason for the differences in results may be linked to the exclusive use of the slump test in their studies. Another reason may be due to differences in the physical/chemical compositions of the GGBS used. In this respect, Wimpenny et al[191] attributed the significant performance differences of their two types/sources of GGBS in figure 2.55 to variations in particle size (ranging from 13-90 microns), and not chemical composition which was reported to be similar.

Moreover, compared to CSF and PFA, the GGBS particles are more angular[203], and their increased superplasticizer dosage demands as shown by the V-flow time measurements (in figure 7.6(b)) suggest that they form agglomerates which trap substantial amounts of water during the initial mixing sequence. The increased rate of loss of workability of the mixes, on the other hand, suggests that the rate of growth (or coagulation) of the cement-GGBS agglomerates with time plays a greater role in their loss of workability than the chemical bonds formed between neat cement particles through hydration.

Since the V-flow time appears to be the main factor influencing the ease of production of the mixes, further work should examine the effects of the 0/4 mins split addition method of superplasticizers (figure 6.6(b)) in improving the early workability properties of GGBS mixes. Further work should also examine how the workability properties are influenced by GGBS composition and gradation, at both high and low w/b ratios.

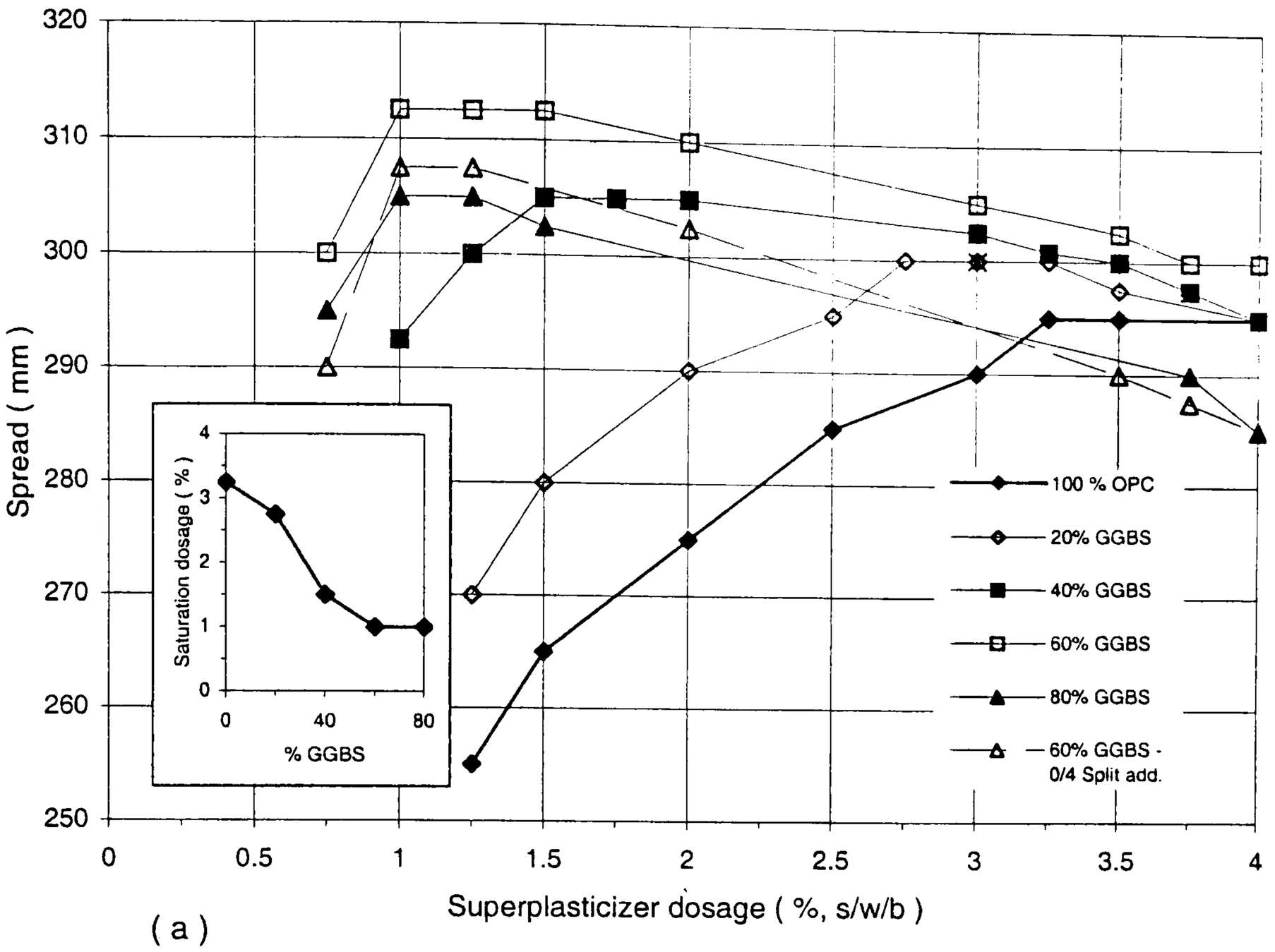

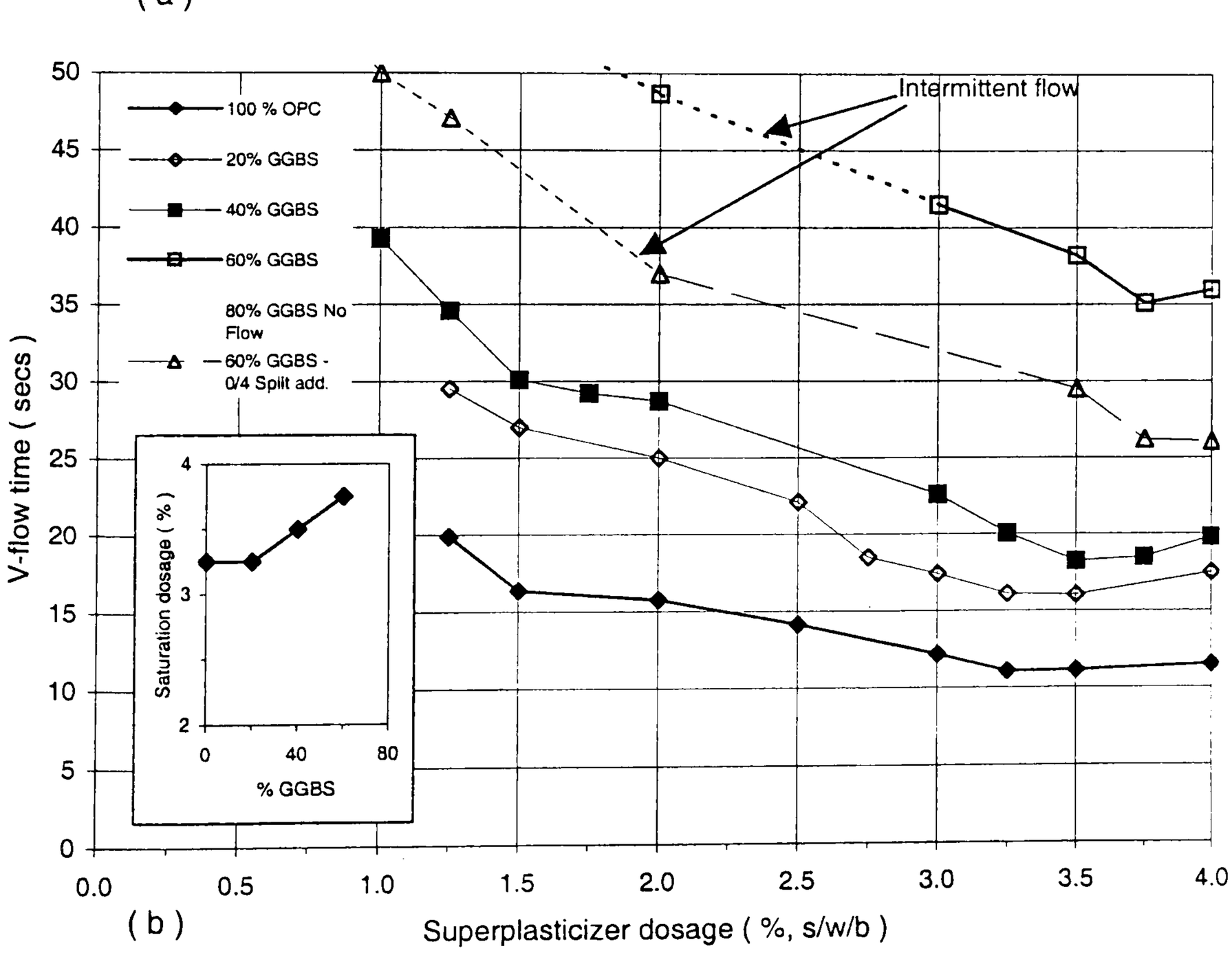

Figure 7.6 : Mortar dosage-response tests for the effects of increasing GGBS content on (a) spread and (b) V-flow time at 0.26 w/b . (4 mins delayed add. (including 0/4 mins split add.) of SNF at 60% GGBS)

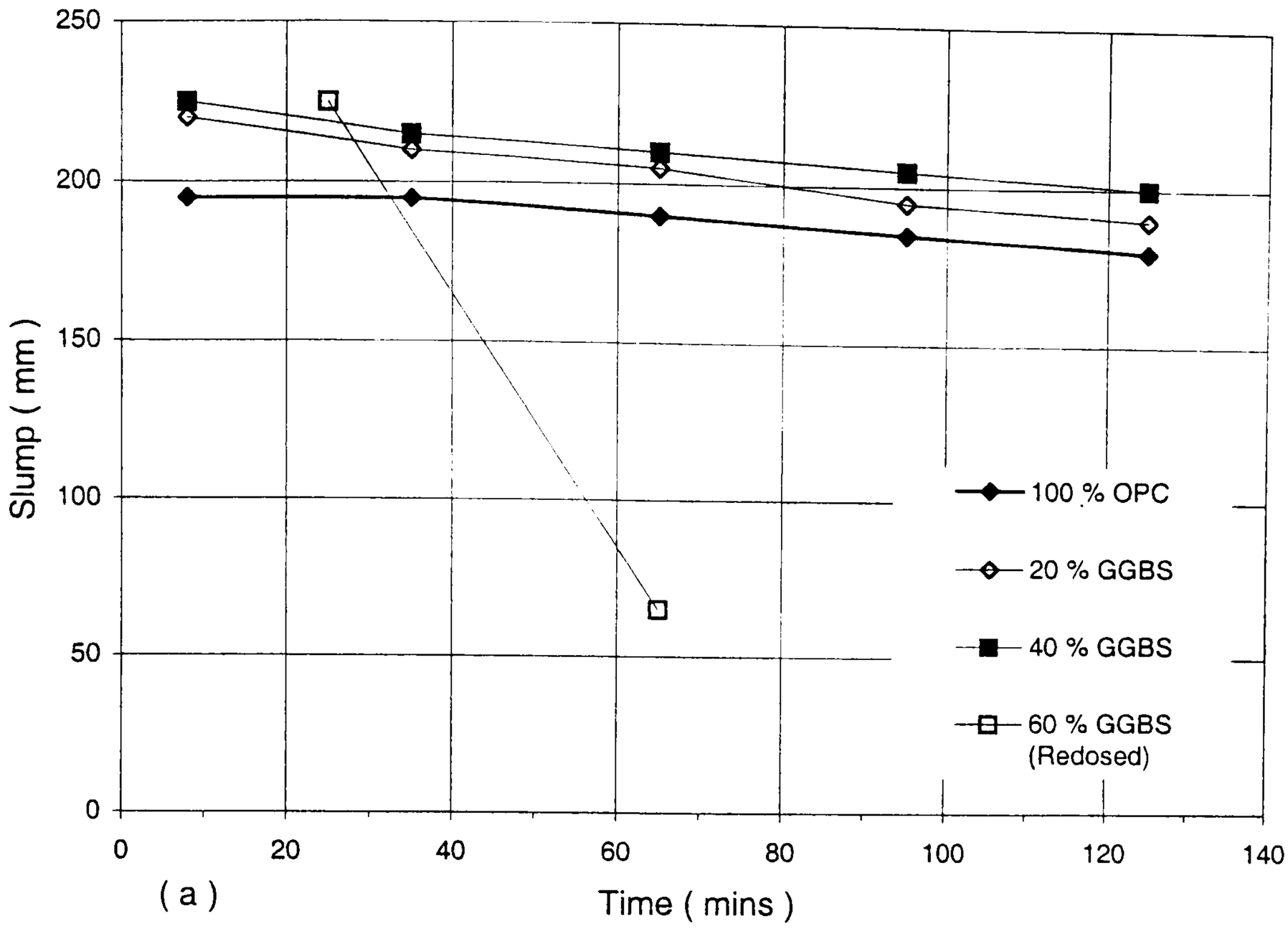

(a)

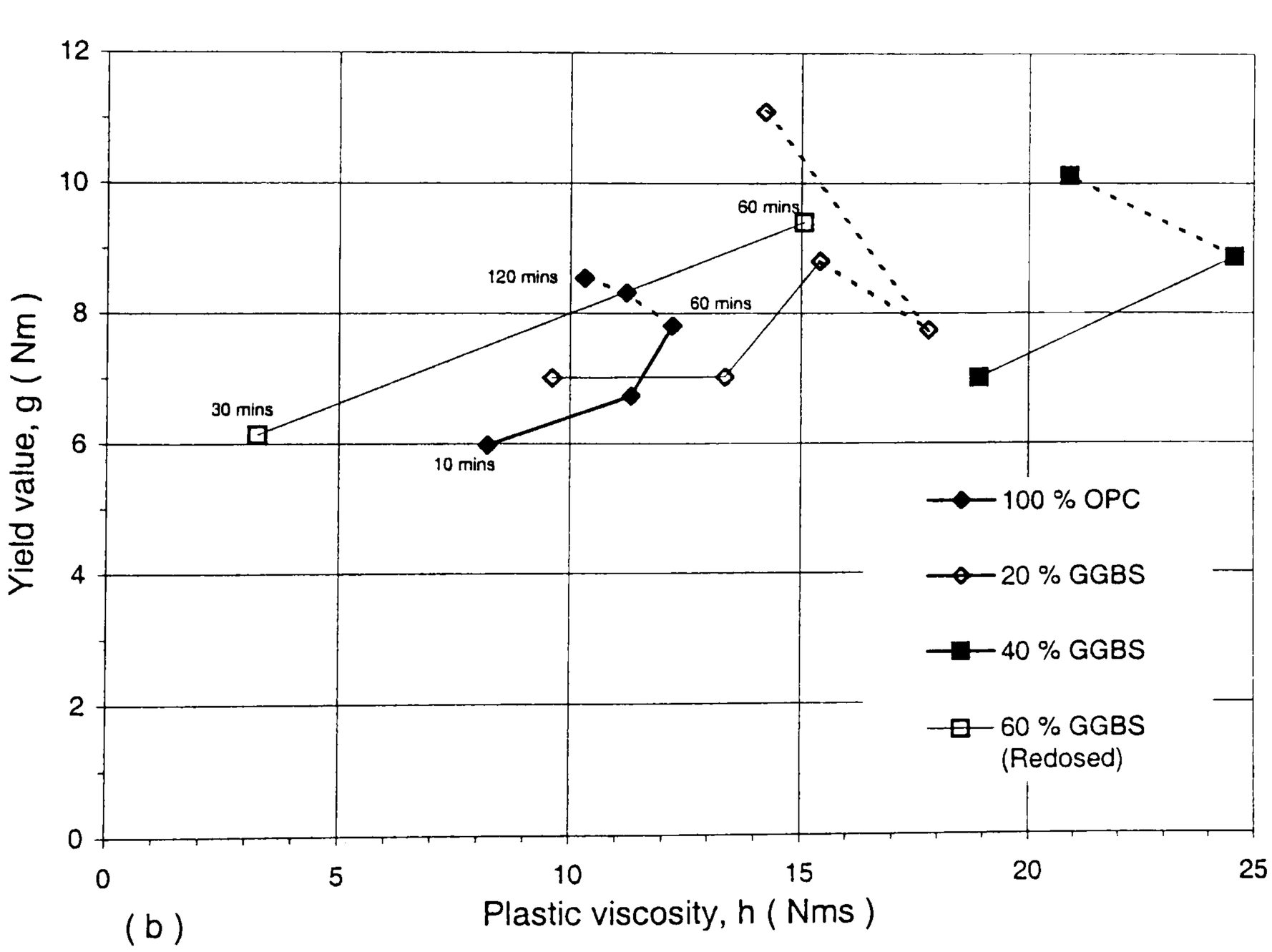

(b)

Figure 7.7 : Effects of increasing GGBS content on (a) slump loss and (b) loss of workability at 0.26 w/b ratio. (All mixes tested at their respective sat. dosages, using 4 mins delayed add. of SNF).

7.5 Ternary blends (of OPC and 10% CSF with PFA or GGBS)

7.5.1 Mortar dosage-response tests

The effects of ternary blended cements of PFA/CSF (at 20/10, 40/10, 60/10%) and GGBS/CSF (at 40/10, 60/10, 80/10) on the mortar dosage-response of the superplasticizer are shown in figures 7.8 and 7.9 respectively.

The ternary PFA/CSF blends in **figure 7.8** show systematic reductions in the saturation dosage demand, and slightly higher workabilities with increasing PFA content up to an optimum level of 40%. The 60% PFA + 10% CSF blend gives a similar saturation dosage, but slightly lower maximum workability than the 40% PFA + 10% CSF blend. When compared with the equivalent binary mixes in figure 7.4, the ternary blended PFA/CSF mixes give 1.00% s/w/b lower saturation dosages, up to 15 mm higher spread ceilings and 6.5 secs improvements in minimum V-flow times.

The ternary GGBS/CSF blends in **figure 7.9** show comparable maximum workabilities, but continuous reductions in the saturation dosage demand with increasing GGBS content up to an optimum level of 60%. The 80% GGBS + 10% CSF blend has a slightly higher saturation dosage, a lower spread ceiling and higher minimum V-flow time than the 60% GGBS + 10% CSF blend. When compared with the equivalent binary mixes (in figure 7.6), the ternary blended GGBS/CSF mixes give 15-25 mm higher spread ceilings, more than 15 secs lower V-flow times, and identical saturation points from the spread and V-funnel tests. Their maximum workabilities are however slightly lower than those obtained with the ternary PFA/CSF blends.

The fact that both the PFA/CSF and GGBS/CSF ternary blends exhibit significantly lower saturation dosages than their equivalent binary mixes, suggests that the CSF slurry plays an active role in releasing significant amounts of water trapped in

cement-PFA and cement-GGBS agglomerates. The dispersion characteristics of the slurry (as shown in figure 7.1), appear to be particularly pronounced with respect to improvements in the V-flow time, which is reduced by at least 5.6 secs (or 70%) in the ternary PFA/CSF blends, and 15 secs (or 85%) in the GGBS/CSF blends.

As mentioned previously in sections 2.6.5, there is very little information in the literature on ternary blends. Soutsos's work[53] with 50% GGBS + 10% CSF mixes showed that the superplasticizer dosage requirement to obtain a 150 mm slump is reduced by 0.20-1.0% s/w/b compared to binary 10% CSF mixes (c.f. figure 2.61). Similar findings with the slump test were also reported by Bayasi[177], Read et al[190] and Dejellouli et al[39] for ternary combinations of CSF with PFA or GGBS (page 97). Dejellouli et al[39] attributed the enhanced dosage performance in CSF blended mixes to a reduction in the quantity of C_3A and lower ettringite formation compared to the OPC mix. They have however not commented on how these are influenced by other CRMs, and/or how they differ in binary and ternary blends.

From their work on binary blended CSF mixes, Austin and Robins[197] have in contrast suggested that the small particle size and spherical shape of CSF produces more efficient filling of the void space between the much larger cement particles, which would otherwise trap free mixing water and reduce workability (page 92). The fact that all CSF particles are spherical and very small in size would, however, negate the filling effects as the main cause for the high dosage demands reported by, for example, de larrard[195] and others[14, 19, 148, 160, 192-194, 196] (pages 91-92). The present observations in figure 7.1 have instead shown that the performance of CSF blended mixes is highly sensitive to the time at which the slurry is added during the initial mixing sequence. That is, the CSF particles appear to generate similar electrostatic/steric effects as those produced by superplasticizers.

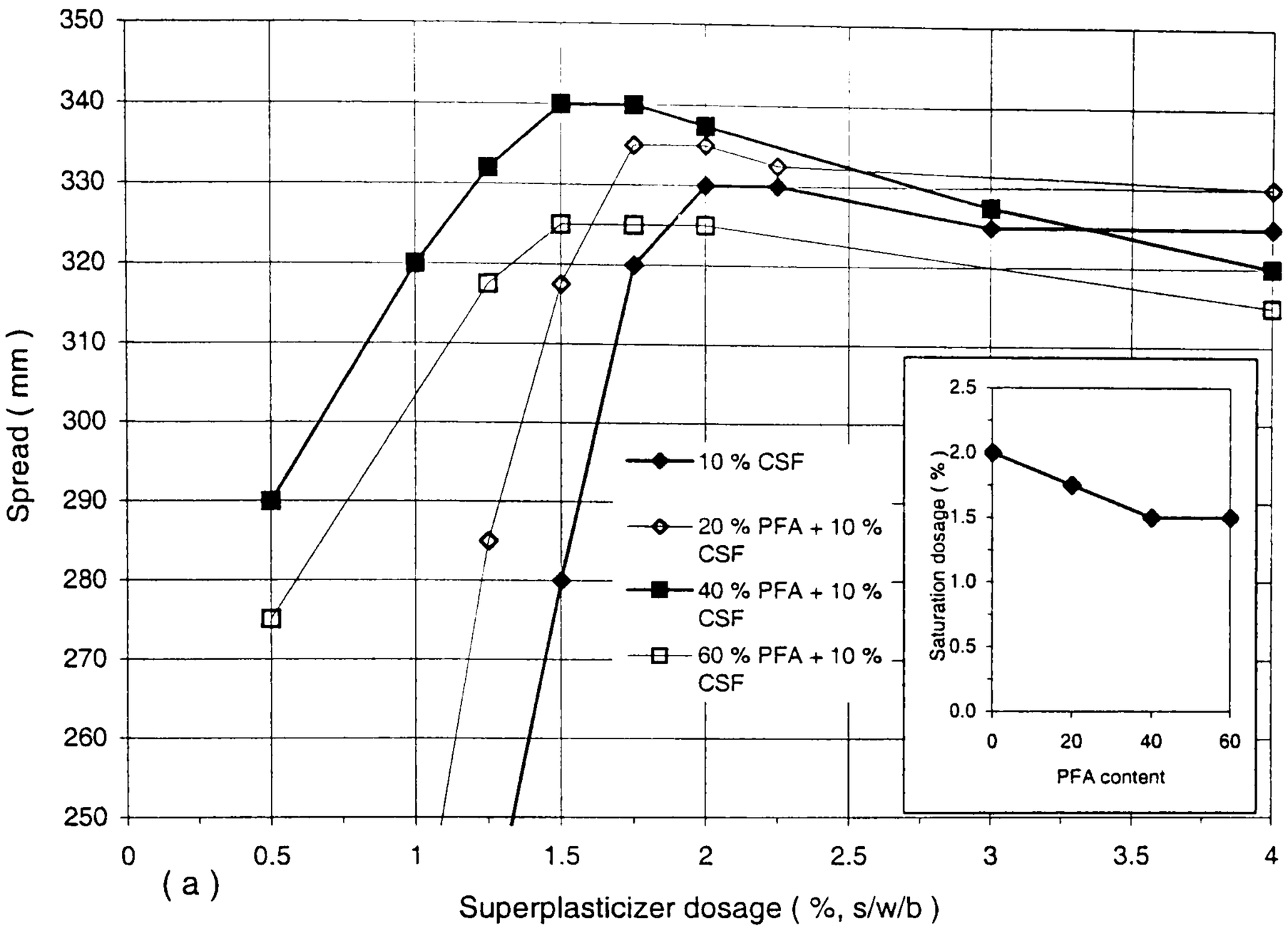

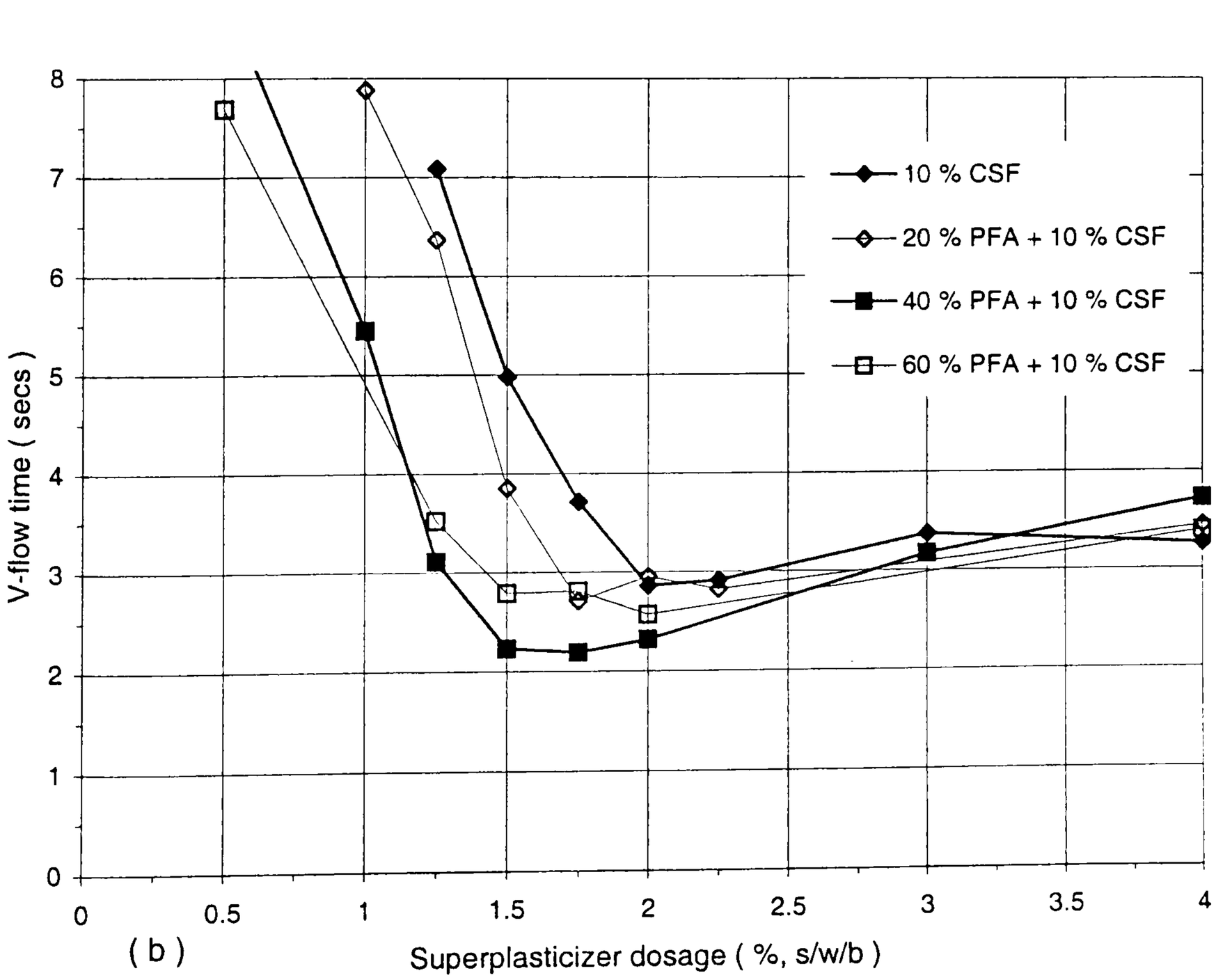

Figure 7.8 : Mortar dosage-response tests for the effects of ternary blends of PFA/CSF on (a) spread and (b) V-flow time at 0.26 w/b (4 mins delayed add. of SNF).

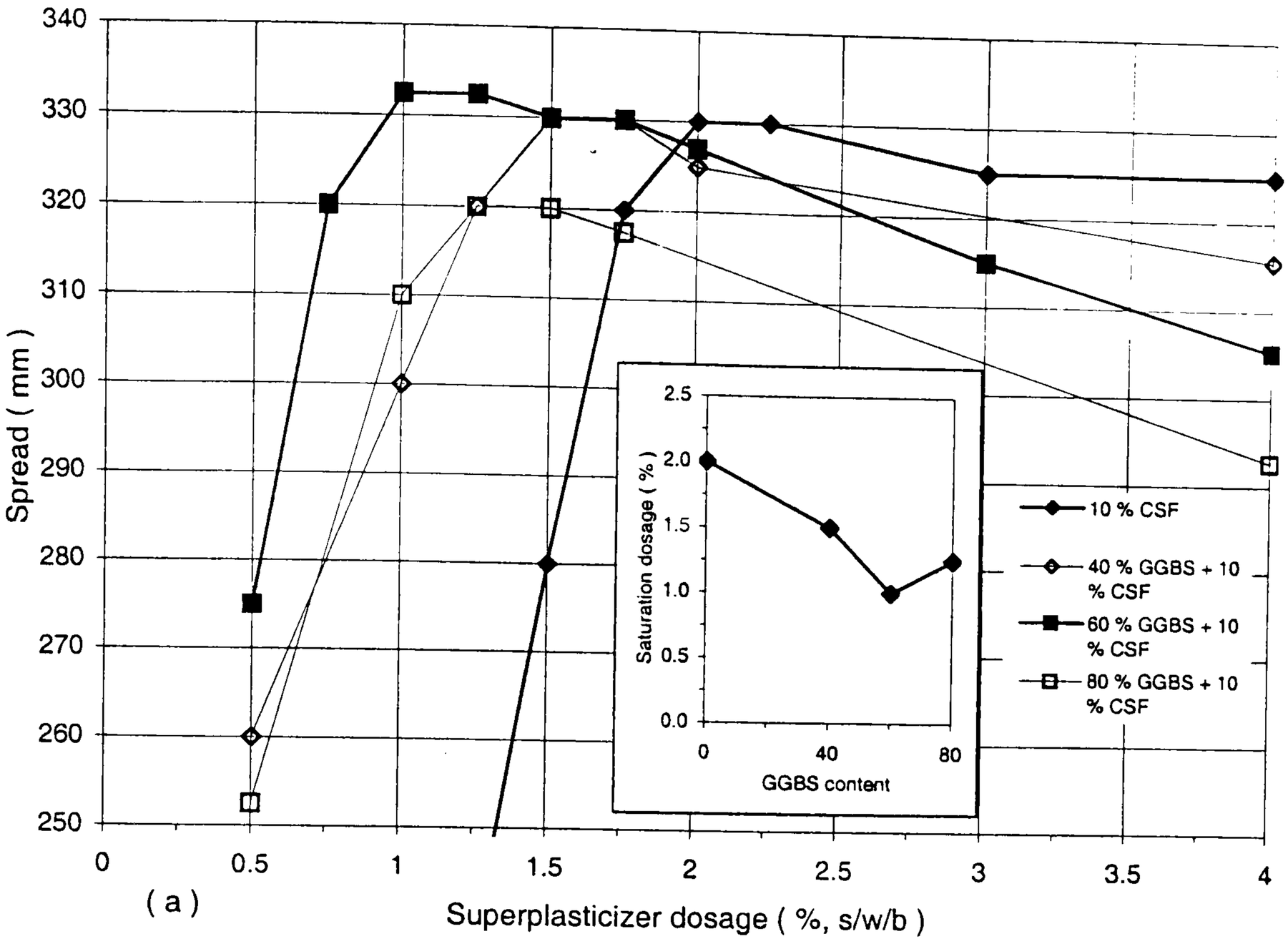

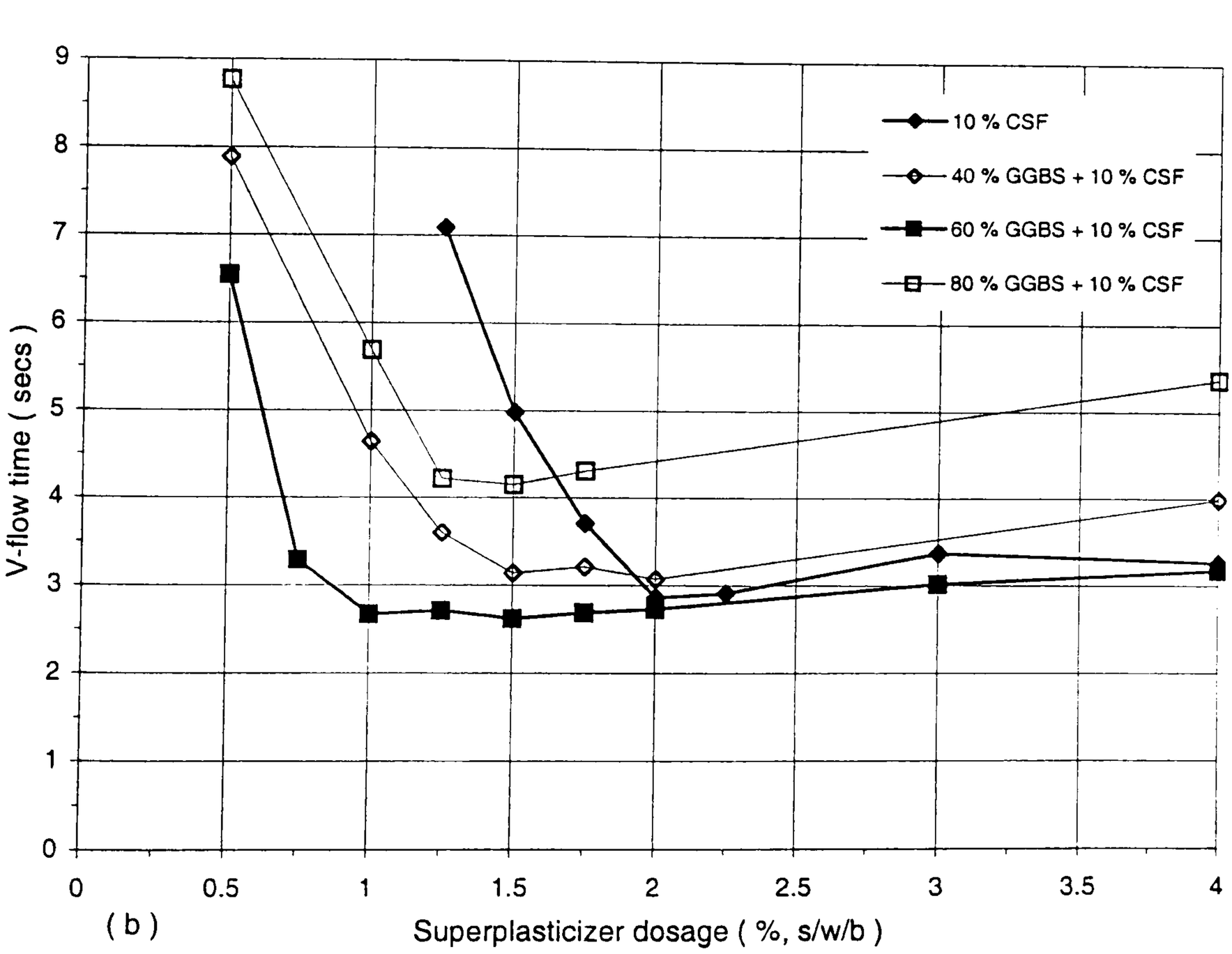

Figure 7.9 : Mortar dosage-response tests for the effects of ternary blends of GGBS/CSF on (a) spread and (b) V-flow time at 0.26 w/b . (4 mins delayed add. of SNF).

7.5.2 Loss of workability in concrete

Figure 7.10(a-b) compares the slump loss and workability retention of the ternary blends of PFA/CSF (at 20/10, 40/10%) and GGBS/CSF (at 40/10, 60/10%) with the control 10% CSF binary mix. In agreement with the mortar-spread values in figures 7.8-7.9(a), the results in **figure 7.10(a)** show slightly higher initial slumps with the ternary 40/10% PFA/CSF and 60/10% GGBS/CSF blends, but negligible differences in slump loss compared to the other mixes.

The two-point test results for the ternary PFA/CSF blends in **figure 7.10(b)** show higher initial workabilities, lower time-dependent increases in yield value, but similar developments in plastic viscosity with increasing PFA content. As can be seen, the initial workabilities and workability retentions of the ternary PFA/CSF blends are significantly higher than those obtained with the equivalent binary PFA mixes in figure 7.5(b). These are represented by up to 1.6 Nm and 3.1 Nms reductions in the initial Bingham parameters of the 20-40% PFA binary mixes, and by 0.5-1.7 Nm and 3.0-3.5 Nms smaller increases in their rate of growth during the first two hours.

The two-point test results for the ternary GGBS/CSF blends in **figure 7.10(b)** show similar initial workabilities and, like the PFA/CSF blends, lower increases in yield value, but slightly larger increases in plastic viscosity with time compared to the control 10% CSF mix. As can be seen, the workability properties produced by the 60/10% GGBS/CSF blend are noticeably higher than those with the 40/10% GGBS/CSF blend. When compared with, for example, the 40% GGBS binary mix in figure 7.7(b), the 40% GGBS + 10% CSF ternary blend considerably reduces the initial Bingham parameters (by nearly 7 Nm and 15 Nms) and decreases their growth during the first 30 mins (by about 2 Nm and 4 Nms).

In contrast with the equivalent binary GGBS mixes, the ternary GGBS/CSF blends also did not exhibit any noticeable stiffening after re-mixing, and their considerable

improvements in workability eliminated the difficulties previously experienced during two-point testing. The advantages of the ternary GGBS/CSF and PFA/CSF blends over their equivalent binary mixes are highlighted in figure 7.11 with regards to their effects on the initial workability properties.

From his initial workability measurements with the MH system at 0.26 w/b ratio, Soutsos[53] similarly found no significant differences between his 50/10% GGBS/CSF ternary and 10% CSF binary mixes (c.f. figure 2.62). He has however not evaluated the effects of binary and ternary blended cements on loss of workability.

Similar initial workability measurements have also been recently reported by Sheikh[265]. Although Sheikh's work involved ternary blended cements of both GGBS/CSF and PFA/CSF, it was limited to two-point workability test measurements with Tattersall's MH system at a constant slump of 200±20 mm.

The longer workability retentions of the ternary blends in figure 7.10(b), when compared with the equivalent binary mixes (in figures 7.5, 7.7(b)), suggest that the inclusion of CSF in the binder does not only disperse the cement-PFA and GGBS agglomerates, but it also slows down their formation with time. As can be seen the effect is more pronounced with PFA than with GGBS.

Based on the present findings it can therefore be concluded that the use of ternary blends of PFA/CSF and GGBS/CSF produces:

- significant reductions in the superplasticizer dosage demand, and
- much higher workabilities compared to the equivalent binary PFA and GGBS mixes.

These can in practice imply significant economic and technical advantages in the production of HS and other HPCs.

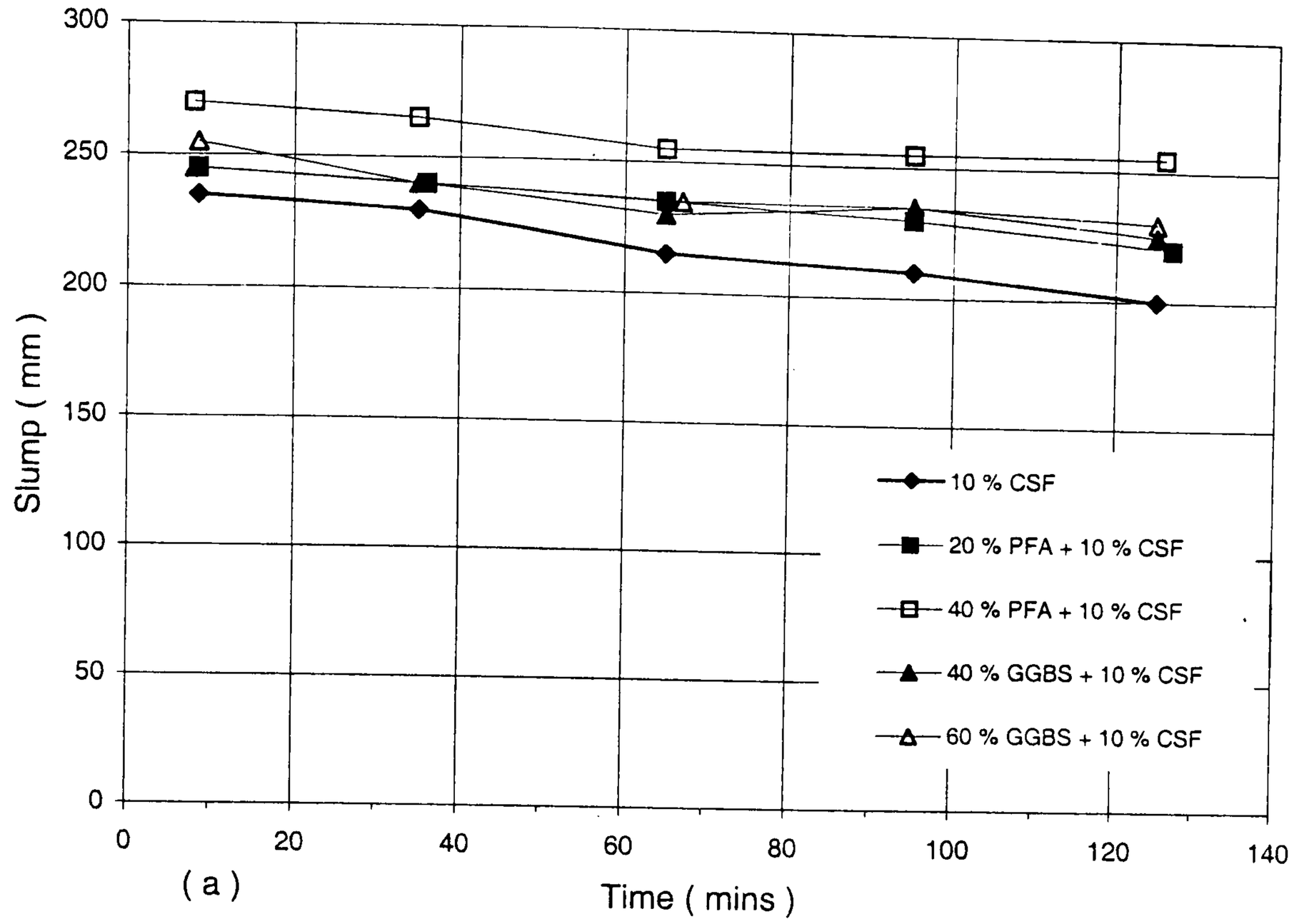

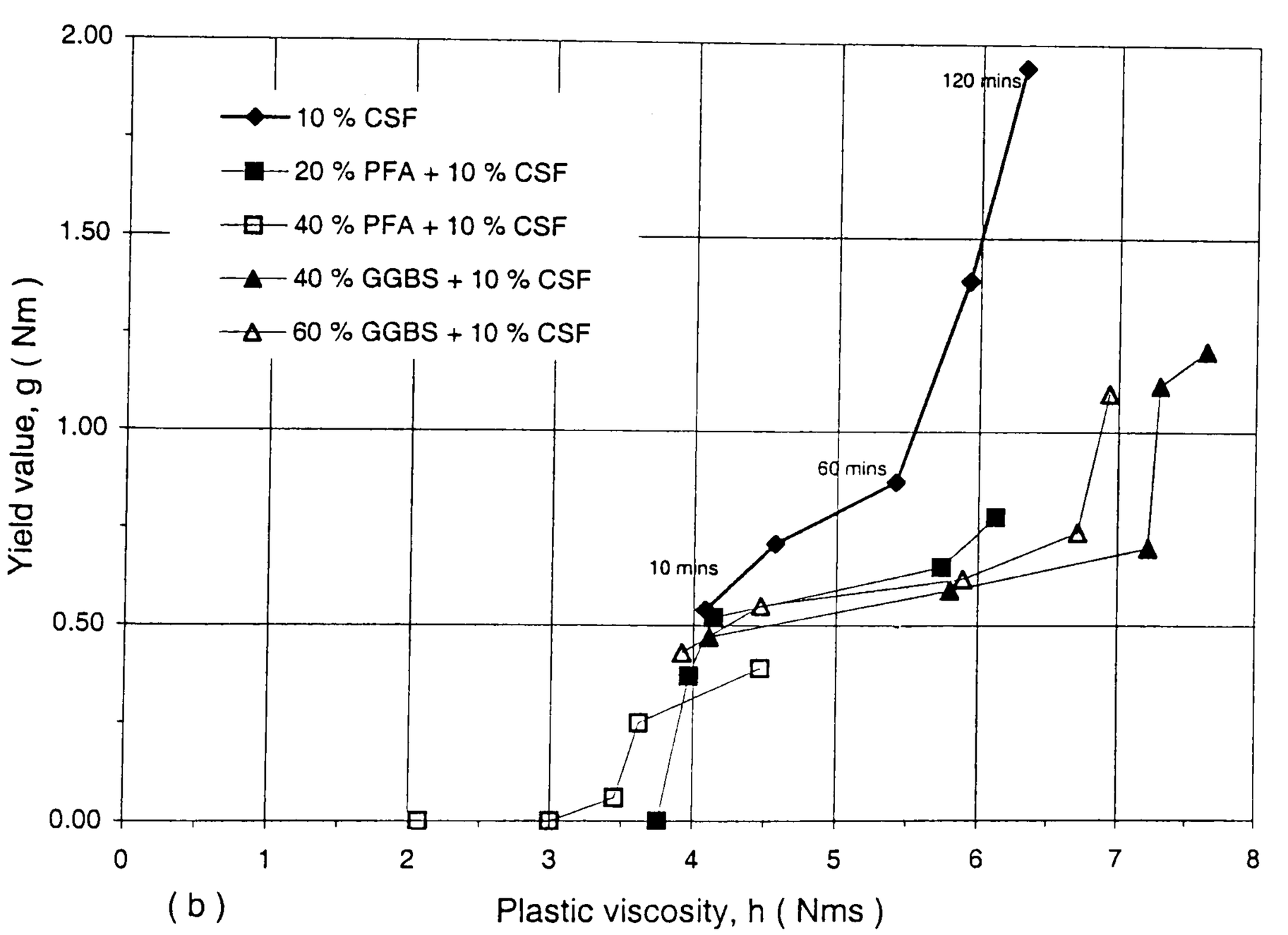

Figure 7.10 : Effects of Ternary Blends of 10% CSF with 20-40% PFA and 40-60% GGBS on (a) slump loss and (b) loss of workability at 0.26 w/b. (All mixes tested at their respective sat. dosages, using 4 mins delayed add. of SNF).

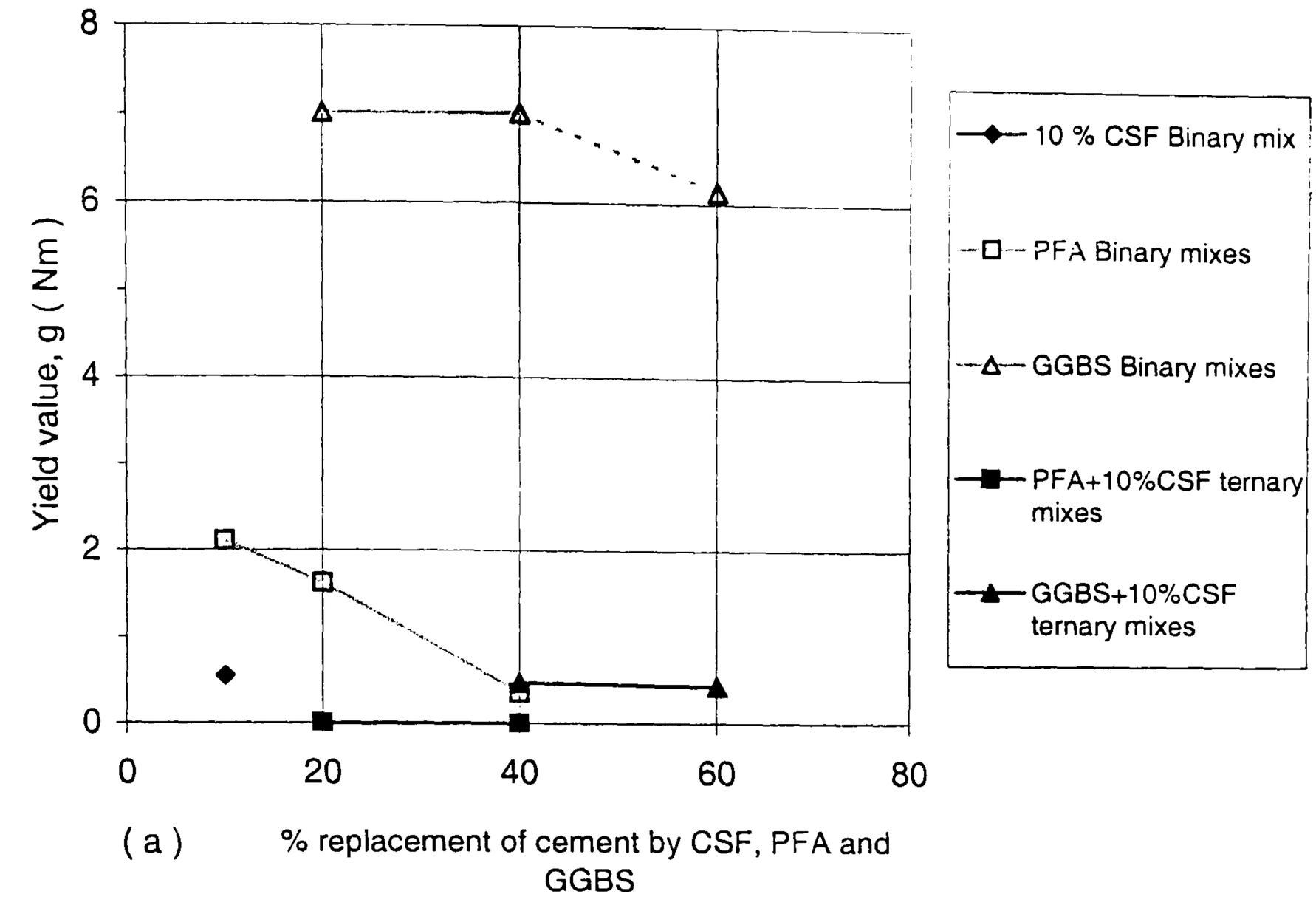

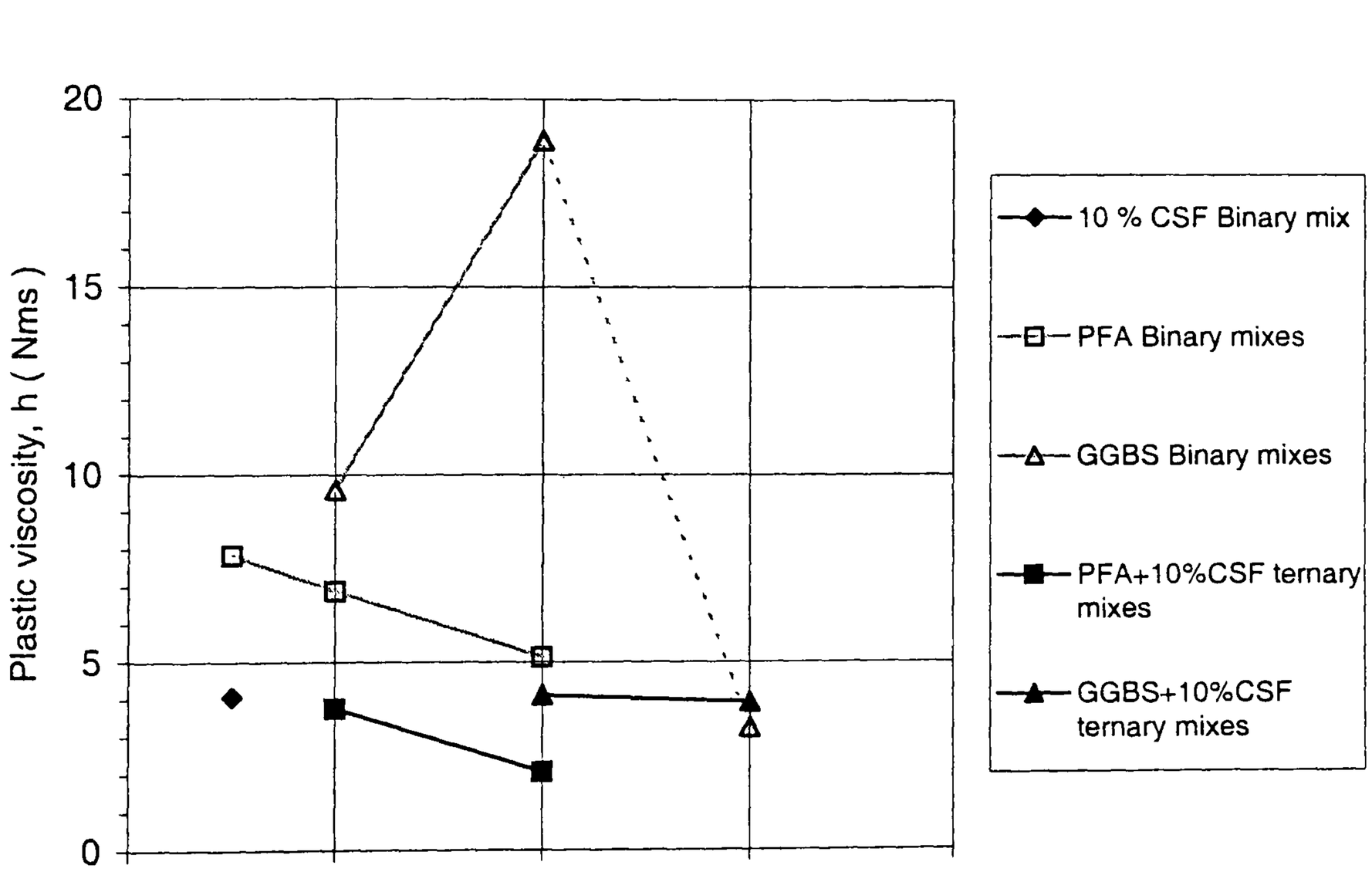

Figure 7.11 : Effects of Ternary blends (of PFA/CSF and GGBS/CSF) and their equivalent binary mixes on (a) initial yield value and (b) plastic viscosity (at 0.26 w/b ratio).

7.6 Influence of w/b ratio

As mentioned previously in section 2.3, there is a lack of quantitative information in the literature on the effects that different w/b ratios have on the rate of loss of workability as expressed by the Bingham model. This section compares the mortar dosage-response properties and losses of workability of the 10% CSF binary and two ternary (40% PFA + 10% CSF, 60% GGBS + 10% CSF) blends with the reference OPC mix at w/b ratios of 0.30 and 0.22.

The replacement levels for the CSF blended mixes represent the optimum values obtained at the 0.26 w/b ratio in sections 7.2 and 7.5. The 0.30 and 0.22 w/b ratios were previously found in section 5.3 to represent critical limits with regards to sharp increases in the Bingham parameters and, hence, ease of production of HSCs. The results at these two w/b ratios are separately discussed below, and then summarized with those at the 0.26 w/b ratio in section 7.6.3.

7.6.1 At 0.30 w/b ratio

(I) Mortar dosage-response tests

The mortar dosage-response tests in **figure 7.12(a-b)** show that the increase in w/b ratio from 0.26 to 0.30 reduces the saturation dosages, increases the spread ceilings and improves the minimum V-flow times of all four mix compositions. The OPC mix gives the highest: reduction in saturation dosage (from 3.25% to 1.75% s/w/b), increase in spread ceiling (from 295 to 315 mm) and improvement in minimum V-flow time (from about 11 to 4 secs) when compared to the equivalent mix at 0.26 w/b.

In contrast, the 10% CSF mix gives a 0.50% s/w/b reduction in saturation dosage, a 10 mm increase in spread ceiling, and a 1.1 secs (or about 40%) reduction in minimum V-flow time with the increase in w/b ratio. The ternary PFA/CSF blend, in

agreement with the results at 0.26 w/b ratio, shows a slightly higher saturation dosage but better workabilities compared to the GGBS/CSF blend.

(II) Loss of workability in concrete

As can be seen from **figure 7.13(a)** the ternary PFA/CSF blend gives a slightly higher initial slump, but no significant difference in slump loss compared to the OPC, CSF binary and ternary GGBS/CSF mixes. The slump curves are similar to those obtained with the equivalent mixes at the 0.26 w/b ratio.

The two-point test results in **figure 7.13(b)** however show that the increase in w/b ratio significantly improves the initial workabilities, and reduces the rate of loss of workability of the mixes compared to the 0.26 w/b ratio. The improvements in initial workability are greatest with the OPC mix, and are represented by considerable reductions in the Bingham parameters from 5.98 Nm and 8.20 Nms (at 0.26 w/b) to 0.77 Nm and 3.51 Nms (at 0.30 w/b). The longer workability retentions at the 0.30 w/b ratio are mainly represented by consistently lower yield values accompanied by, similar or, slightly lower time-dependent increases in plastic viscosity than at the 0.26 w/b ratio.

As before, the highest and lowest initial workabilities and workability retentions are respectively obtained with the ternary PFA/CSF blend and the reference OPC mix. The differences in the workabilities of the mixes are however less pronounced than those obtained at the 0.26 w/b ratio.

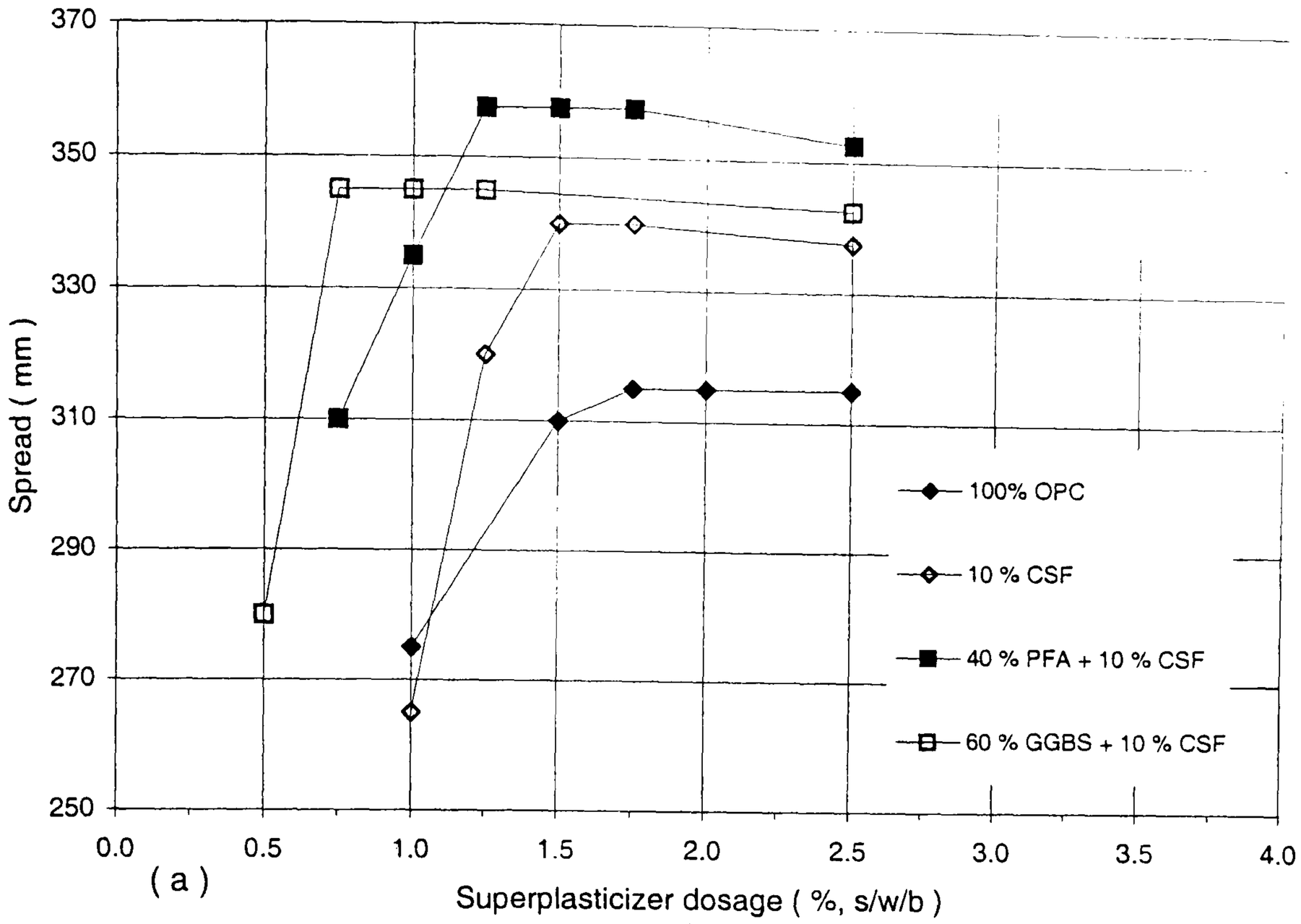

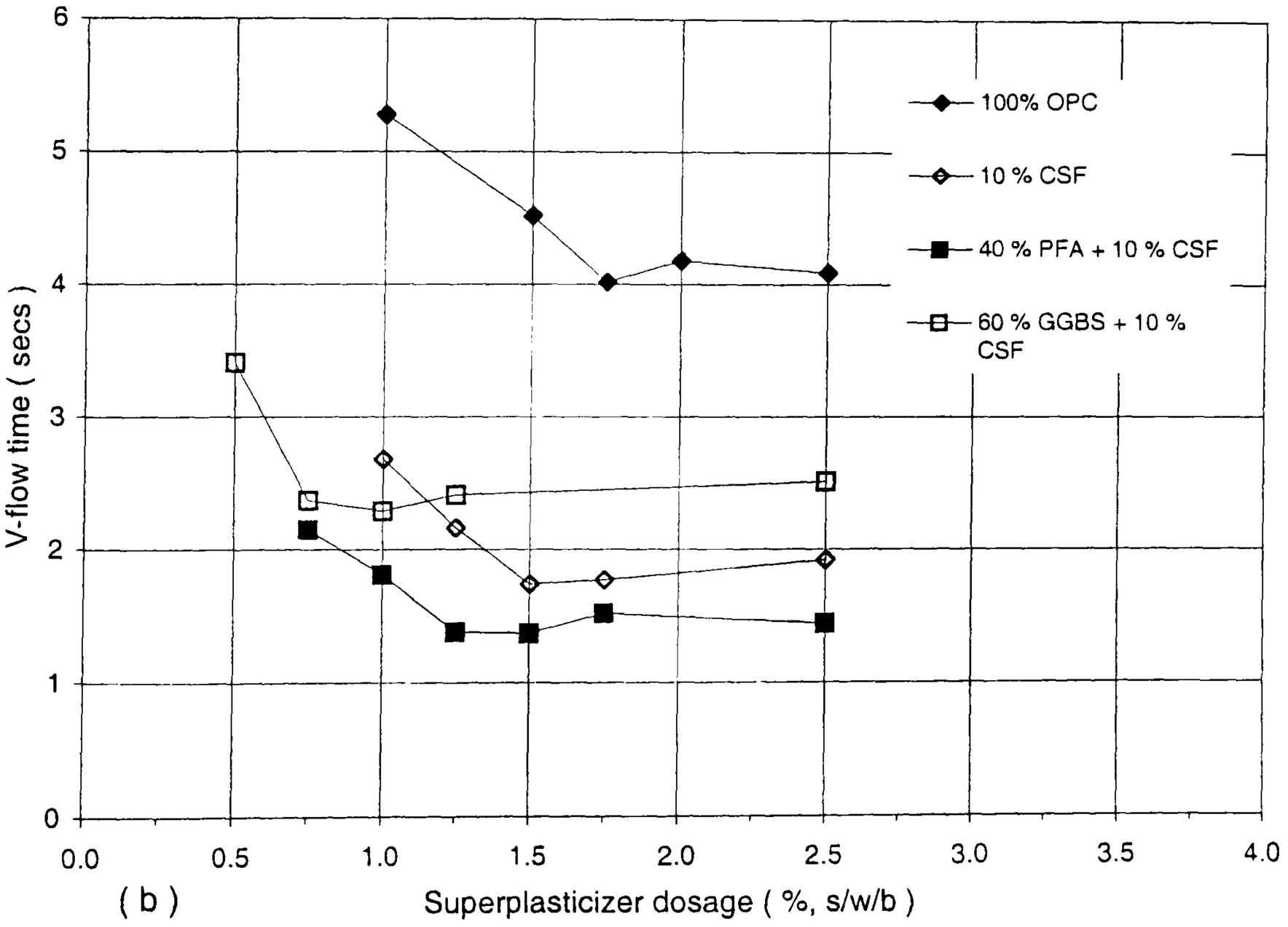

Figure 7.12 : Mortar dosage-response tests for the effects of OPC, 10% CSF, and ternary mixes of 40%PFA + 10%CSF and 60%GGBS+ 10% CSF on (a) spread and (b) V-flow time at 0.30 w/b.

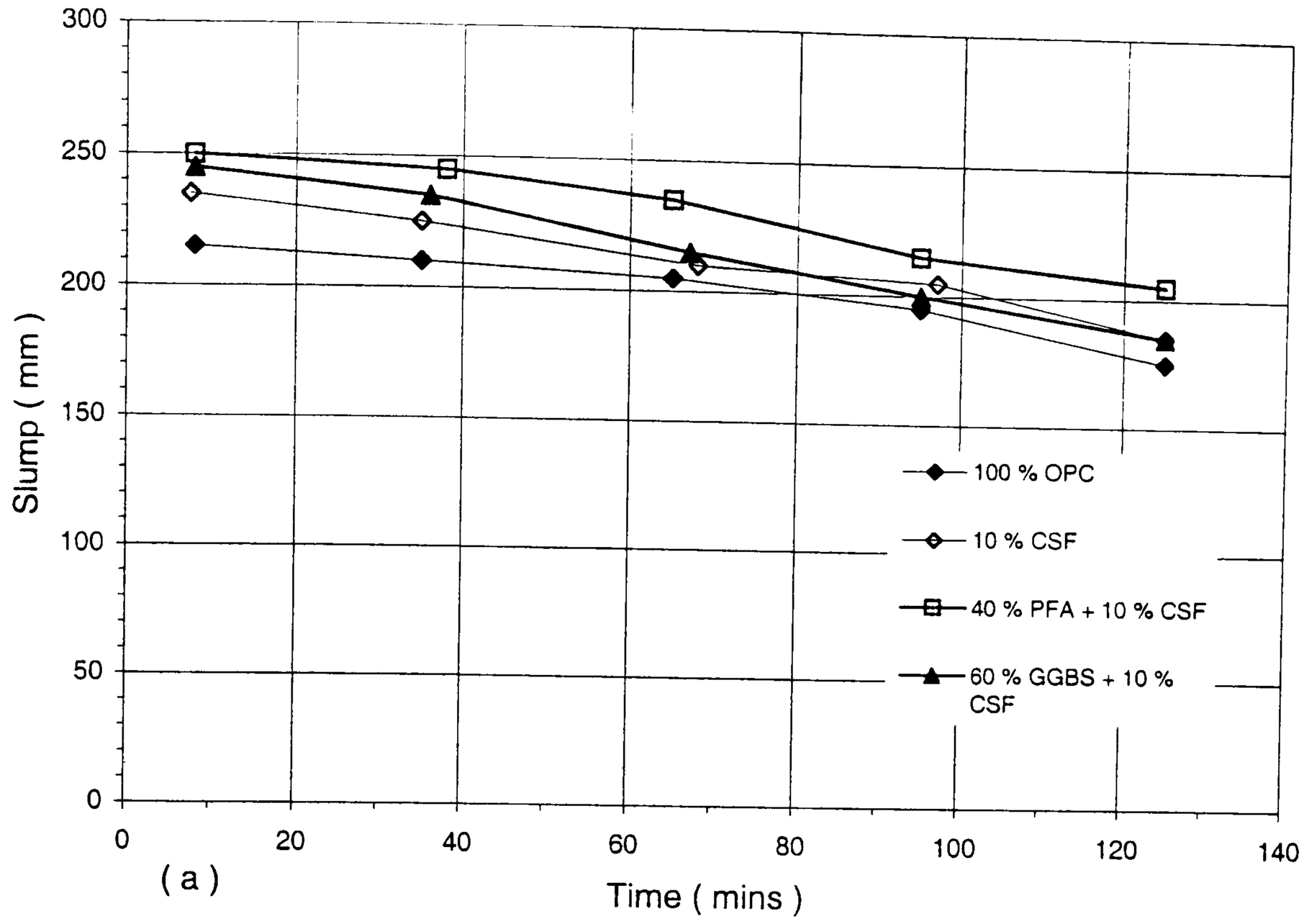

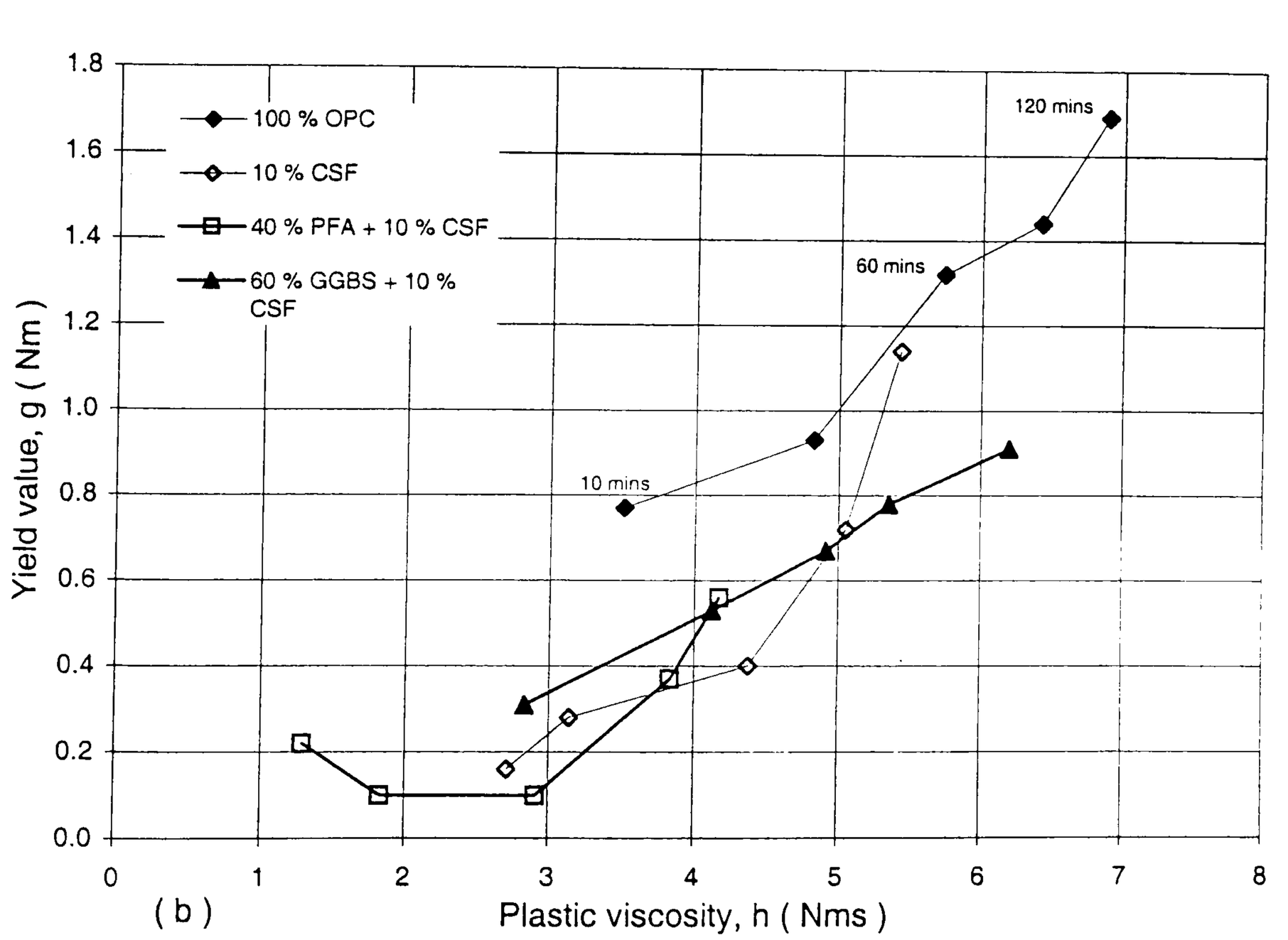

Figure 7.13 : Effects of OPC, 10%CSF, and Ternary blends of 40%PFA + 10%CSF and 60%GGBS+ 10% CSF on (a) slump loss and (b) loss of workability at 0.30 w/b ratio. (All mixes tested at their respective sat. dosages, using 4 mins delayed add. of SNF).

7.6.2 At 0.22 w/b ratio

(I) Mortar dosage-response tests

The mortar dosage response tests in **figure 7.14** show that the reduction of the w/b ratio to 0.22 significantly increases the saturation dosages, reduces the spread ceilings and gives considerably higher V-flow times than the 0.26 w/b. The GGBS/CSF ternary blend, in agreement with the results at the 0.30 and 0.26 w/b ratios, gives a lower saturation dosage but a reduced maximum workability compared to the PFA/CSF ternary blend.

Mortar tests with the OPC mix, using superplasticizer dosages of up to 5.00% s/w/b, produced a very low spread of 190 mm and no-flow through the V-funnel. Soutsos 's results[53] showed that the dosage requirement to obtain a constant slump of 150 mm (c.f. figure 2.61) was higher with OPC than with 10% CSF mixes at w/b ratios of 0.29-0.24, but he did not comment on the viability of the OPC mixes at lower w/b ratios. According to Aitcin and Neville[11], the workability constraints occurring in HPCs result from a closer proximity and greater tendency of the cement particles to flocculate at very low w/b ratios.

(II) Loss of workability in concrete

The slump curves in **figure 7.15(a)**, like those at the 0.30 and 0.26 w/b ratios, show a higher initial slump with the PFA/CSF ternary blend, but negligible differences in the rate of slump loss compared to the GGBS/CSF and 10% CSF blends. The similarities of the slump curves at the three w/b ratios can, in practice, imply that there is no significant effect of w/b ratio on loss of workability.

The two-point test results in **figure 7.15(b)** however show that the reduction in w/b ratio to 0.22 considerably reduces the initial workabilities. and gives much larger losses of workability than the equivalent mixes at the 0.30 and 0.26 w/b ratios. When

compared to the equivalent mixes at the 0.26 w/b ratio, the rate of loss of workability for the mixes at the 0.22 w/b ratio is approximately two times higher with respect to plastic viscosity, but about three-seven times larger with respect to yield value during the first two hours.

As before, the PFA/CSF ternary blend gives a higher initial workability and much longer workability retention than the GGBS/CSF and 10% CSF blends. The lower workability properties of the GGBS/CSF mix suggest that its 10% CSF content may be inadequate to efficiently disperse and slow down the formation of cement-GGBS agglomerates with time.

An attempt to produce the OPC mix at the 0.22 w/b ratio, with the 5.00% superplasticizer dosage used in mortar (page 265), was unsuccessful. The resulting concrete mixture consisted of individual aggregates coated with semi-dry cement paste and, even with a further redose of up to 2.00% s/w/b of the superplasticizer (which increased the w/b ratio to 0.25), the mix did not provide sufficient workability for two-point testing. This, and the problems experienced in producing the 60% GGBS binary mix (in page 249), suggests that:

- The V-flow time in mortar can serve as an invaluable index for assessing the ease of production of HSCs.
- A lack of flow of mortar in the V-funnel, and/or a very high V-flow time (of 35 secs or more), is indicative of non-viable concrete mixes.

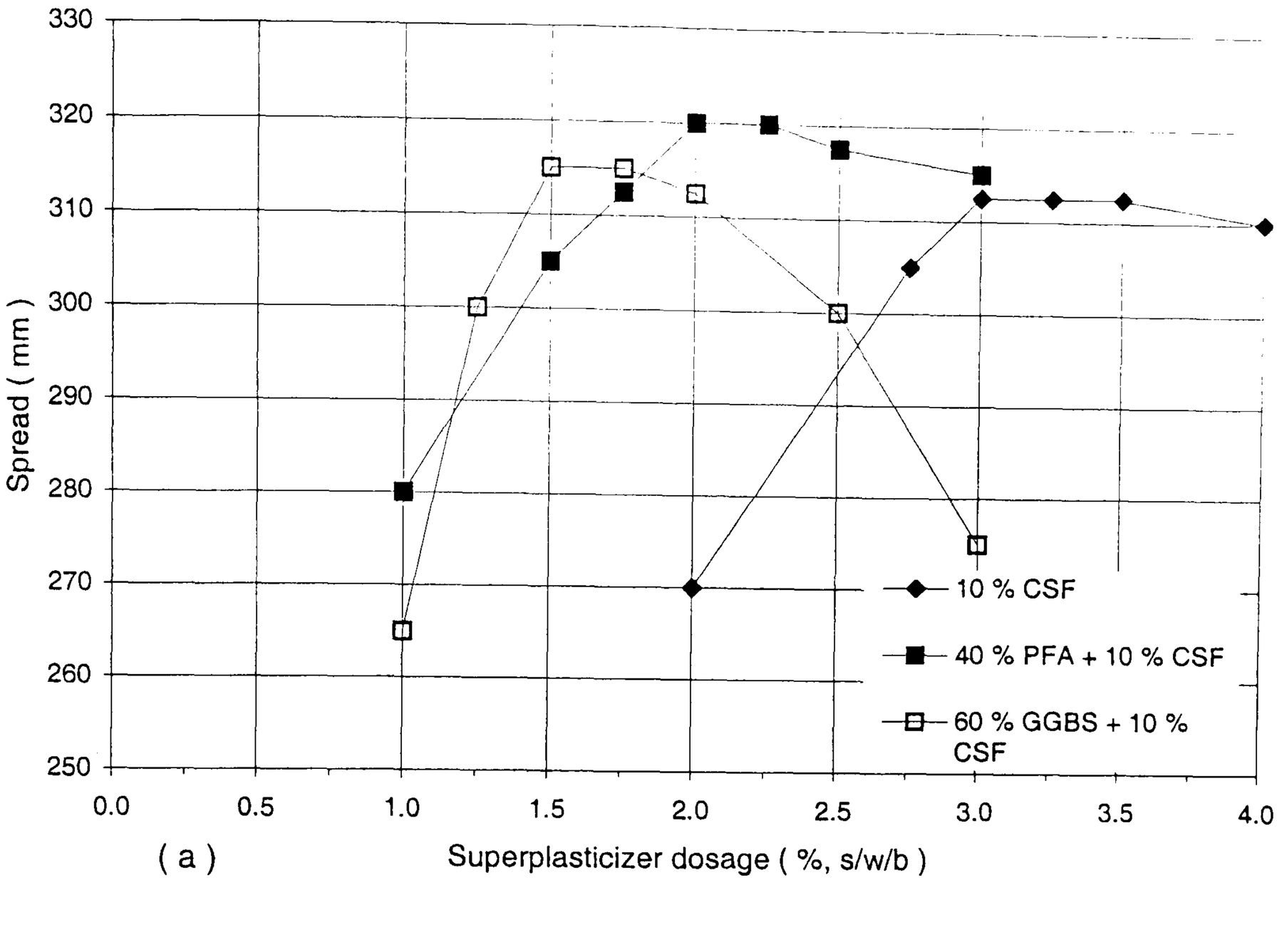

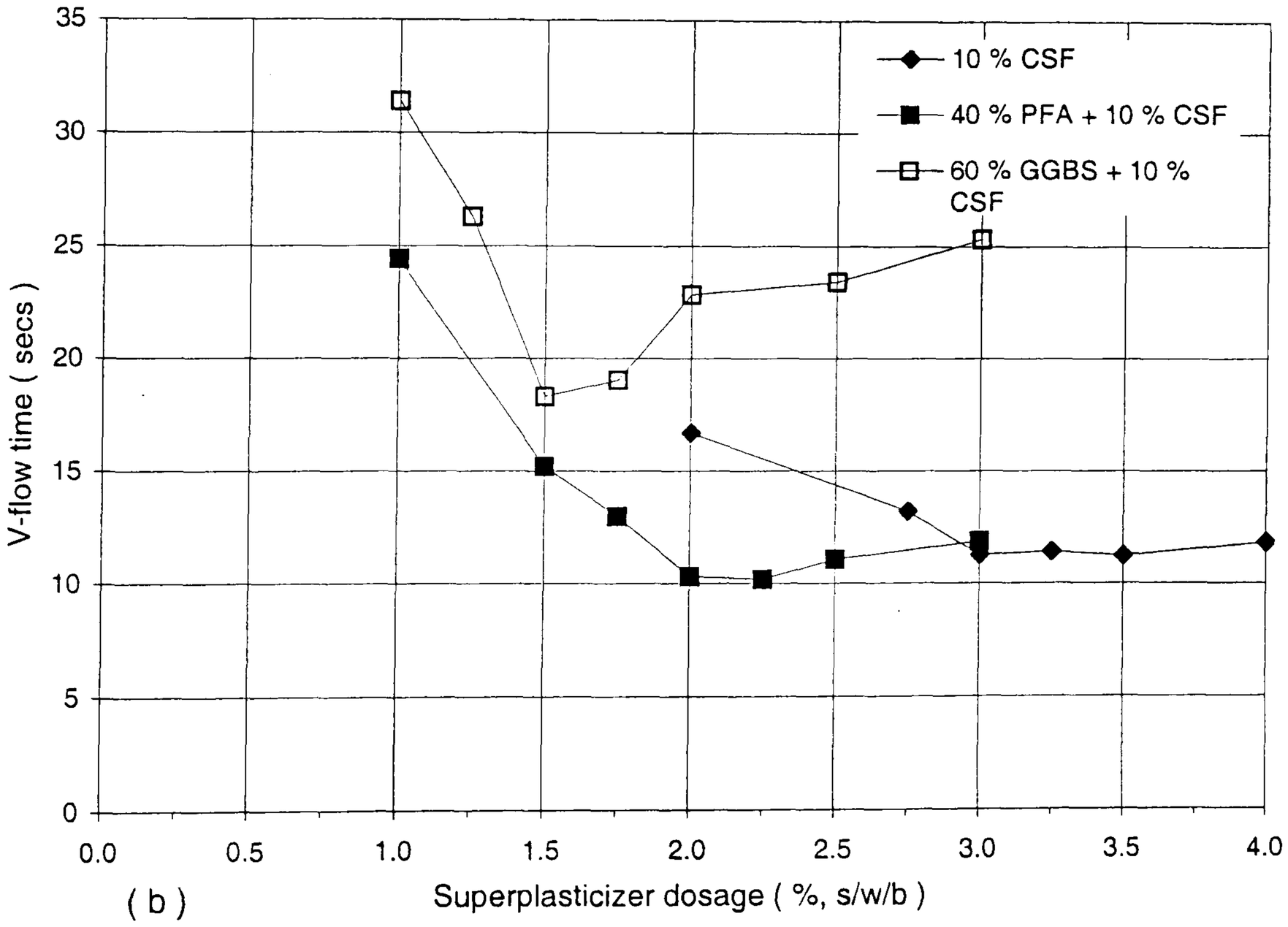

Figure 7.14 : Mortar dosage-response tests for the effects of 10% CSF, and trenary mixes of 40%PFA + 10%CSF and 60%GGBS + 10% CSF on (a) spread and (b) V-flow time at 0.22 w/b.

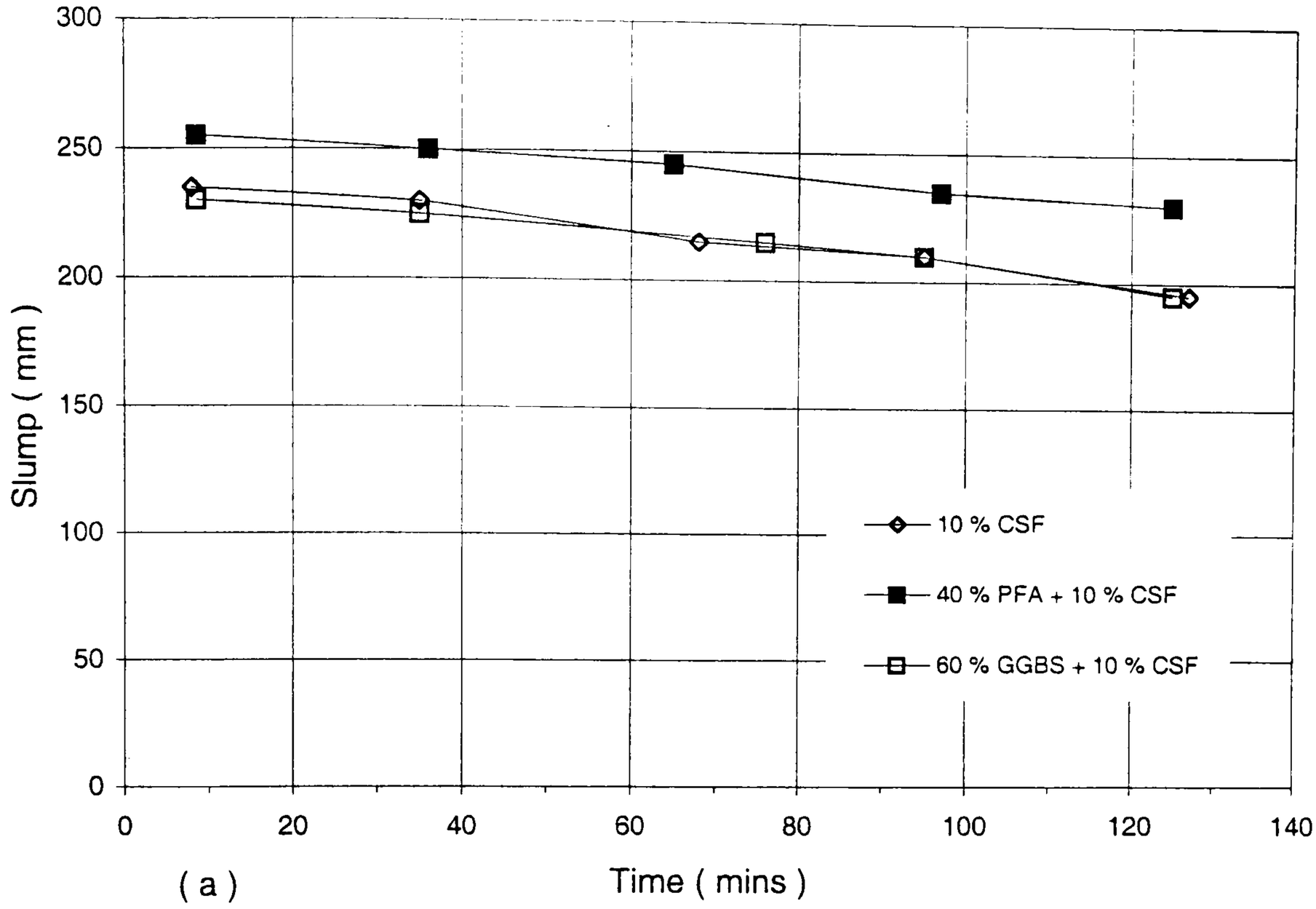

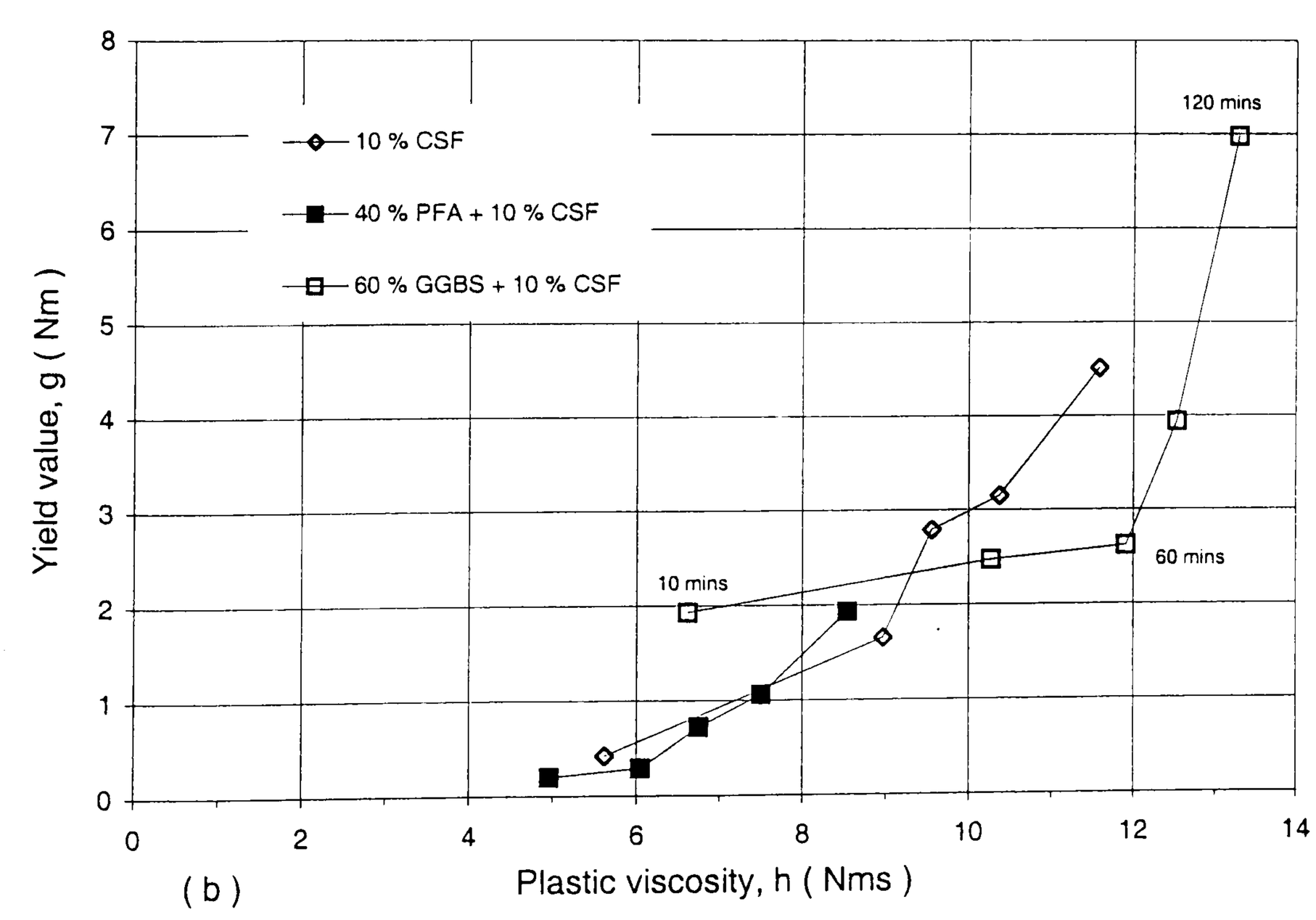

Figure 7.15 : Effects of 10% CSF, and Ternary mixes of 40%PFA + 10%CSF and 60%GGBS+ 10% CSF on (a) slump loss and (b) loss of workability at 0.22 w/b ratio. (All mixes tested at their respective sat. dosages, using 4 mins delayed add. of SNF).

7.6.3 Summary and further discussion

The effects of the 0.30-0.22 w/b ratios on the saturation dosages and losses of workability of the OPC, 10% CSF, and two ternary mixes are summarized in figures 7.16 and 7.17 respectively. These, and the effects of CRMs on mix stability and compactability, are separately discussed below.

(I) Effects of CRMs on superplasticizer dosage demand

As can be seen from **figure 7.16**, the saturation dosages of the superplasticizer increase with decreasing w/b ratio, and are greatest with the OPC mixes. The lowest saturation dosages at all three w/b ratios are obtained with the ternary GGBS/CSF blend, and are 0.50% s/w/b less than those with the PFA/CSF blend.

The consistently lower dosage demands shown by the 10% CSF mixes compared to the OPC mixes conflict with de Larrard 's[(195)] and Soutsos 's[(53)] findings (figures 2.56, 2.57), which showed higher dosage demands for the 10% CSF mixes at w/b ratios greater than 0.29. In agreement with the present results, Duval and Kadiri[(198)] showed that at the 10% CSF replacement level there are continual reductions in superplasticizer dosage demand at w/b ratios higher and lower than 0.29. In this respect, the results in figure 7.1 indicated that the contrasting effects of CSF on the superplasticizer dosage demands can be attributed to variations in the addition time of the CSF slurry.

Higher workabilities and, therefore, reduced superplasticizer dosages are obtained when the slurry is added 15-30 secs after the cement comes in contact with the mixing water.

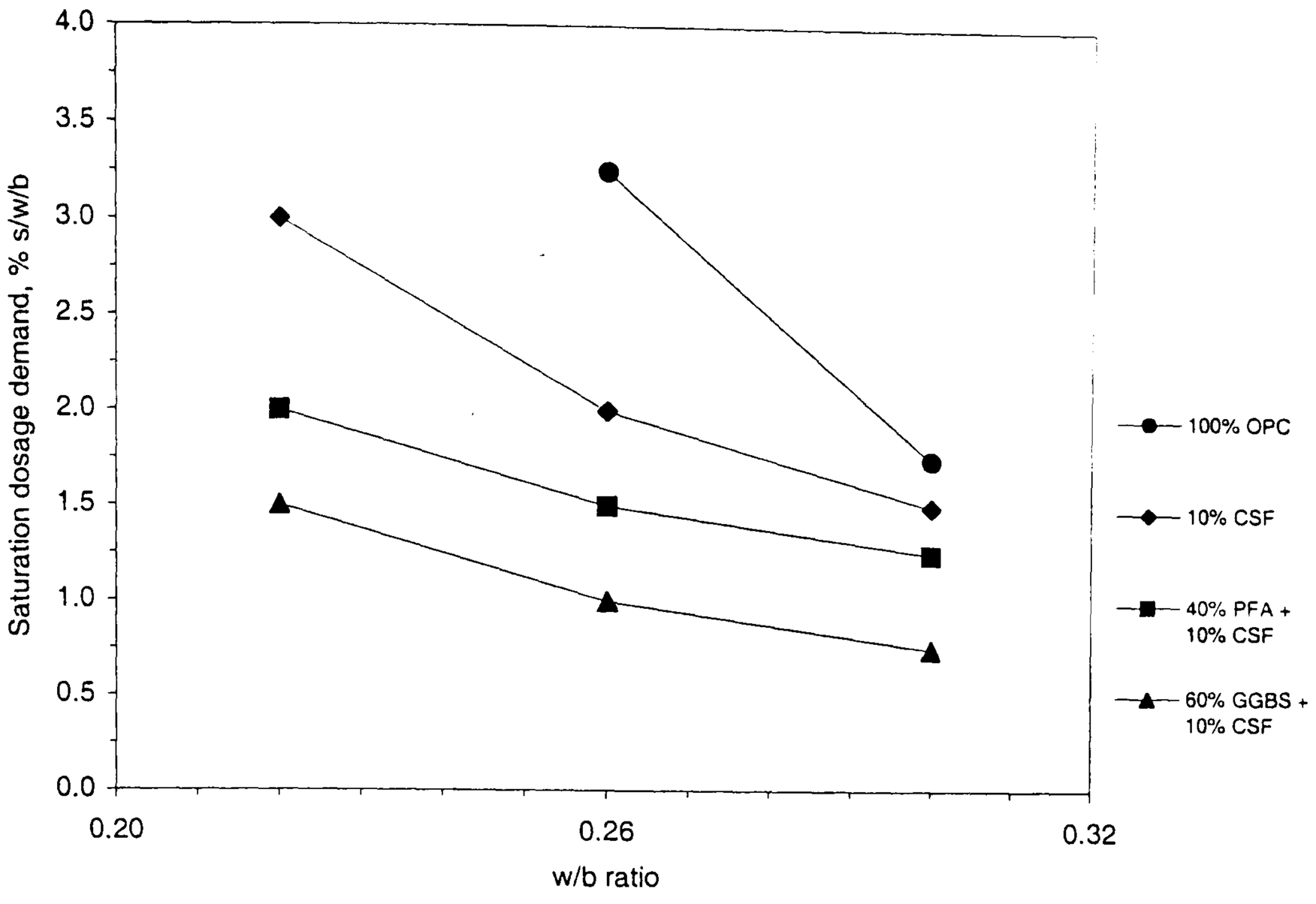

Figure 7.16 : Effects of decreasing w/b ratios of 0.30, 0.26 and 0.22 on the saturation dosage demands of OPC, 10% CSF, 40%PFA+10%CSF and 60%GGBS+10%CSF mixes.

(II) Effects of CRMs on workability

The results with the OPC and CSF blended mixes in **figure 7.17(a-b)** confirm the widely accepted view that the rate of loss of workability (when expressed in terms of the Bingham model) is higher with decreasing w/b ratio, and gives larger time-dependent increases in both the yield value and plastic viscosity. The results contrast with those obtained with the MH system (in figure 5.2(c)), showing continuous and more pronounced reductions in plastic viscosity with time and reduced w/b ratio.

As can be seen, the highest and lowest initial workabilities and workability retentions at all three w/b ratios are respectively produced by the 40% PFA + 10% CSF ternary and reference OPC mixes. The relatively larger losses of workability obtained with the GGBS/CSF blends in figure 7.17(b), suggest that the 10% CSF content is less effective in reducing the rate of growth (or flocculation) of cement-GGBS agglomerates with time than when used with ternary blends of PFA/CSF. Further

work is therefore needed to examine the effectiveness of higher CSF contents with ternary blends of GGBS at very low w/b ratios.

(III) Effects of CRMs on mix stability and compactability

In agreement with the results obtained with superplasticizers in figure 6.12, relationships drawn between the Bingham parameters and the segregation indices of the concrete mixes tested in sections 7.2.3-7.6.2 (c.f. Appendix C (figure C1)), showed that:

- at low-medium workabilities the segregation resistance is highly influenced by both the yield value and plastic viscosity, whilst
- at high workabilities (having zero or very low g values), the resistance to segregation is mainly governed by changes in the plastic viscosity.

The bleeding tendencies of the mixes and their compactabilities (as assessed by the cylinder-vibration method) were also found (as in sections 5.3.2 and 6.6) to vary with slump level, and were not necessarily influenced by the inclusion of CRMs (c.f. Appendix C (Table C15)). In contrast, Dodson[122] and others[128, 169] stated that the small particle size and dense particle packing of CRMs enhances both mix stability and compactability (page 99), but they did not comment on how these are influenced by slump/workability level. The results obtained in the present investigation indicate that the effects of CRMs on both the mix stability and compactability are primarily governed by the workabilities/slumps they impart and, hence, the dosages of superplasticizer used.

The effects of CRMs and superplasticizers on the compactability of HSCs are examined in the next chapter using the novel vibration method (outlined in section 4.3.3.3). The chapter includes a brief comparison with the results from the cylinder-vibration method.

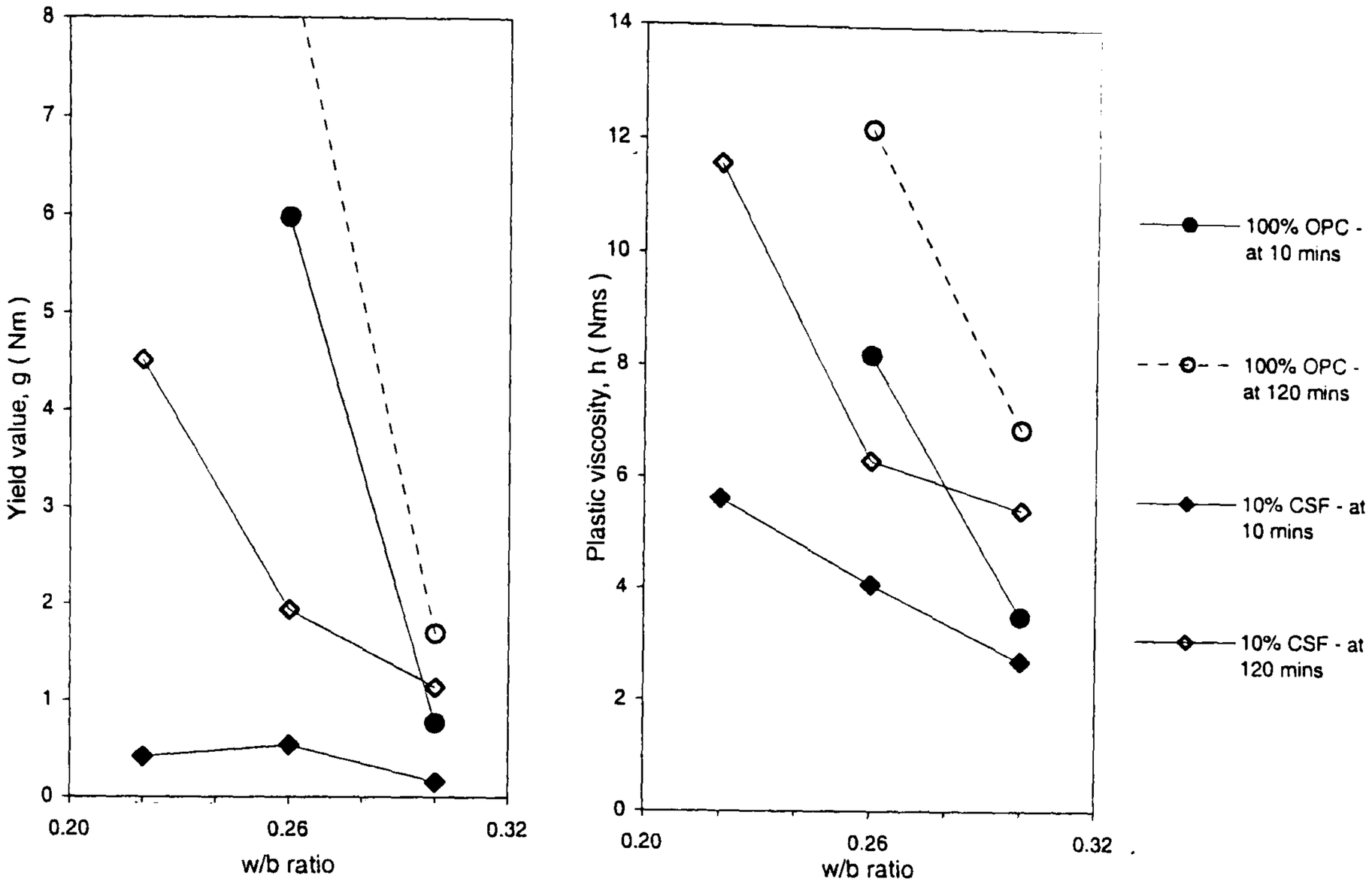

(a) OPC and 10%CSF mixes.

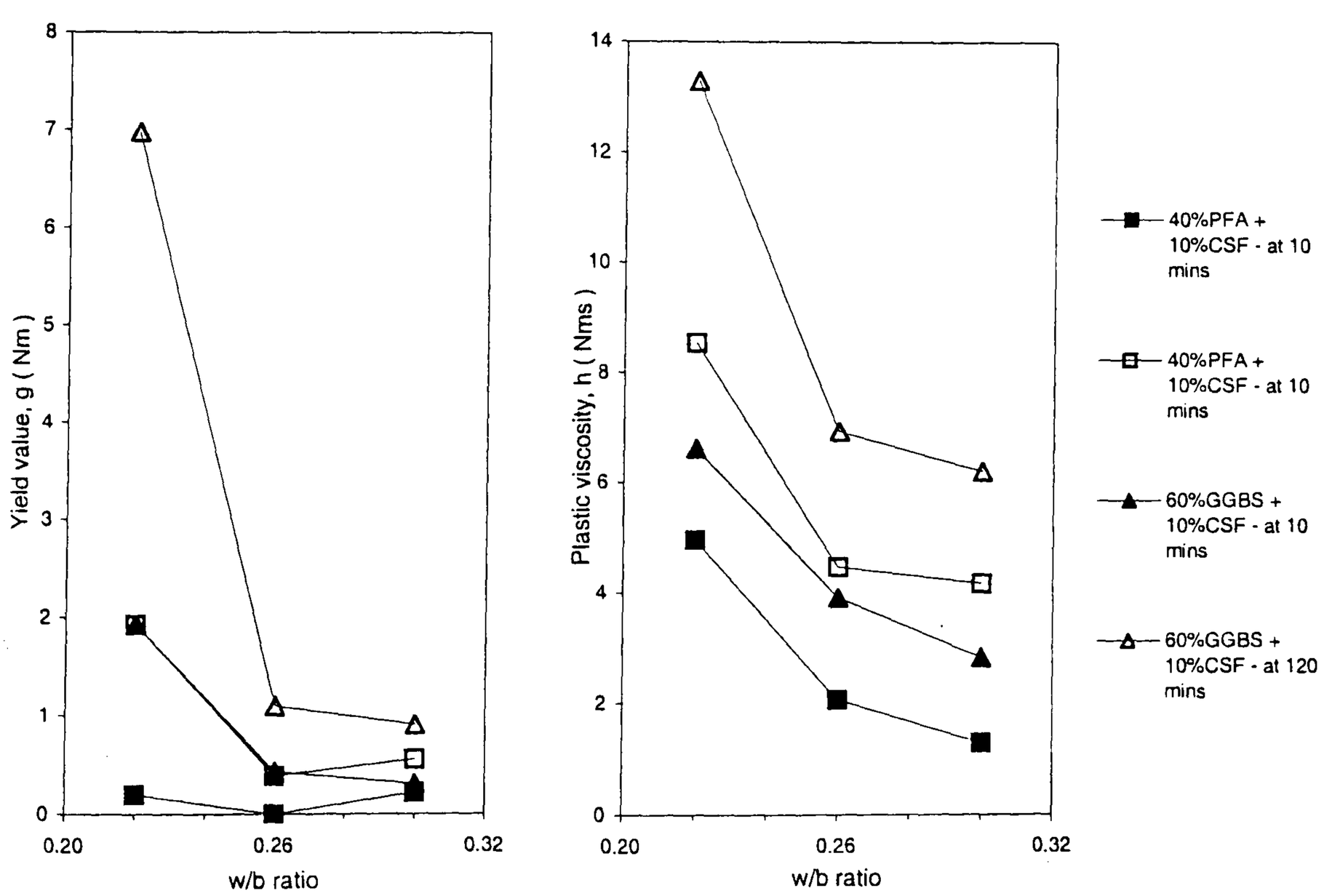

(b) Ternary PFA/CSF and GGBS/CSF blends.

Figure 7.17 : Effects of decreasing w/b ratios of 0.30, 0.26 and 0.22 on the developments in yield value and plastic viscosity of (a) OPC and 10% CSF mixes, and (b) ternary combinations of 40%PFA+10%CSF and 60%GGBS+10%CSF.

7.7 Conclusions

- The use of binary blended cements containing CSF or PFA reduces the saturation dosage demand (by as much as 38% and 23% respectively), and improves the initial workability properties (by 2.9-5.6 Nm and 0.4-4.1 Nms) compared to the equivalent OPC mix at 0.26 w/b ratio. The use of CSF at an optimum replacement level of 10% reduces the rate of loss of workability (by up to 1.5 Nm and 2.7 Nms in the first 60 mins), whereas PFA appears to have negligible effects on workability retention when it replaces up to 40% of the cement.

- In contrast, the use of GGBS in binary blended cements increases the saturation dosage demand (by as much as 15%), reduces the initial workability (by up to 1.0 Nm and 10.7 Nms), and increases the rate of loss of workability in the first 60 mins (by up to 2.2 Nm and 10.9 Nms) compared to the reference OPC mix.

- The use of ternary blends containing 10% CSF with 20-40% PFA or 40-60% GGBS at 0.26 w/b ratio reduces the superplasticizer dosage demand (by 36-40% and 57-73%), increases the initial workability (by 0.4-6.5 Nm and 3.1-14.8 Nms), and reduces the rate of loss of workability during the first 30 mins (by 0.1-3.2 Nm and 2.8-10.4 Nms) compared to the equivalent binary mixes. The optimum replacement levels for ternary blends of PFA/CSF and GGBS/CSF (at 0.26 w/b ratio) are 40%PFA+10%CSF and 60%GGBS+10%CSF.

- The inclusion of CSF in the binder imparts similar dispersion characteristics to those obtained with delayed additions of superplasticizers. These appear to release water trapped in cement, PFA and GGBS agglomerates, and slow down their formation with time.

- A reduction in the w/b ratio from 0.30 to 0.22 (in CSF blended mixes) increases the saturation dosage demand (by 60-100%), reduces the initial workability (by 0.2-1.6 Nm and 2.9-3.8 Nms), and increases the rate of loss of workability (by 1.4-4.5 Nm and 0.7-3.3 Nms) during the first two hours.

Chapter 8
Flow properties, Placing characteristics and Vibration response of HSC

8.1 Introduction

The previous three chapters highlighted the main problems associated with the various two-point test devices, and the influence of material selection on the workability of HSCs during mixing and transportation. Once the concrete is delivered to the works (usually by dumper or mixer trucks), it is placed and compacted. Placing is usually achieved by tremie, skip, conveyor belt, pumping and/or pouring the concrete directly into the forms. The compaction of the concrete, to expel as much entrapped air as possible and overcome its internal resistance to flow, is normally achieved by external or internal vibration techniques.

The evaluation of the Bingham parameters during the placing and compaction stages is not only vital in, for example, assessing the suitability of different construction equipment and rationalizing concrete production, but ultimately in optimising the strength development and durability characteristics of the hardened concrete. The review in sections 2.7 and 2.8 however indicated insufficient information in the literature on each of these key areas.

This chapter examines the variations in the Bingham parameters during the placing and compaction stages of HSC. The main areas considered are :

- Relationships between the Bingham parameters with the static and dynamic **slump-flow properties** under self-weight.
- Reductions in workability due to **stiffening effects** resulting from 5 mins delays between re-mixing and placing.
- The **vibration response** of fresh concretes **at different** :
  - **amplitudes** (of 0.1-0.7 mm) and a fixed frequency of 50 Hz,
  - **mix compositions** (involving CRMs, superplasticizers (at 0.26 w/b) and NSC (at 0.50 w/b ratio)).

8.2 Static and dynamic slump-flow properties under self-weight

Despite the wide criticisms of the slump test as an inadequate measure of workability[2, 30, 40, 201], it is still the most widely used field test to assess the flow properties of fresh concretes. In practice the slump measure is made on a stationary cone of concrete, and it is assumed that the shear rate associated with the test is zero[7, 40, 54], or, in other words, that the slump test assesses the yield value of the concrete but takes no account of its plastic viscosity.

These inferences have been experimentally supported by Tattersall[7] and others[49, 91, 246], showing that the slump in NSC varies almost linearly with yield value, but has no direct relationship with plastic viscosity. The inferences have also been supported by theoretical studies by, for example, Kurokawa et al[244], who carried out computer simulations of the slump test using expressions relating the two Bingham parameters (τ_y and η (or μ)) with the final slump (SL) and slump-flow spread (Sf) :

$$\tau_y = \frac{\rho.\,g.\,V}{25\times10^{-8}\sqrt{3}.\,\pi.\,Sf^2}, \qquad \eta = \frac{7\,\rho.\,g.\,D^2.\,H.\,SL.\,(Sf^2 - sf^2).\,t.sf}{7200\,Sf^2.\{sf^2.\,H - Sf^2.\,(H\text{-}SL)\}}$$

where ρ is the density of concrete (in kgm^{-3}), g is the acceleration due to gravity (9.81 ms^{-2}), V = volume of slump cone (in m^3), D is its base diameter (200 mm), H = initial height of material (300 mm), and sf = slump-flow spread value at a given time, t (in secs). From their model studies, Kurokawa et al[244] concluded that the effect on slump or slump-spread of a change in yield value is much greater than that of a comparable change in plastic viscosity (η). They suggested that it is only when the yield value is low that the plastic viscosity has some importance on the slump or slump-spread, but did not comment on how the progressive collapse of the concrete under self-weight relates to the Bingham parameters. In this respect, Kuroiwa et al[245] reported that the slump-flow time for the collapse spread to reach a value of 500 mm can be used as an index to estimate the plastic viscosity of HP-SCC mixes, but they did not provide any experimental or theoretical justification for this.

In contrast, Ferraris[48] and Ferraris and de Larrard[246] reported that the time taken for the concrete in the standard slump test to collapse/subside by a distance of 100 mm provides a measure of the plastic viscosity. They stated that this could be used in conjunction with the final slump (which they believe provides a reasonable measure of the yield value) to evaluate both the Bingham parameters. According to Ferraris and de Larrard[246] the yield stress (τ_o) and plastic viscosity (μ) can respectively be calculated from the final slump (S) and 100 mm slump-time (T) using the following semi-empirical equations :

$$\tau_o = \frac{\rho}{347}(300 - S) + 212$$

$$\mu = 1.08 \times 10^{-3}.\rho.T.(S - 175) \qquad \text{for } 200\text{mm} < S < 260\text{mm},$$

or

$$\mu = 25 \times 10^{-3}.\rho.T \qquad \text{for } S < 200\text{mm}.$$

where ρ is the density of the concrete (in kgm^{-3}), the final slump (S) and slump-time (T) are measured in mm and seconds. They stated that these equations were derived from finite element analysis of the slump test and measurements with the BT rheometer. According to them the equations assume that the final slump (S) is a function of $\mu/(\rho.g.T)$, and that differences in the slump-time (T) of concretes with the same slump and density (ρ) are due to differences in plastic viscosity. No justification was however given for these, and/or an appreciation of how their Bingham parameter measurements are influenced by the volume expansions exerted on the concrete by the BT rheometer (c.f. section 5.5.5).

This section examines possible relationships between the Bingham parameters from the LM system with slump test measurements under both static and dynamic conditions.

8.2.1 Slump and slump-spread - Bingham parameter relationships under static conditions

The relationships between the final slump (S) and slump-spread (SFS) measurements with the Bingham parameters are shown in figure 8.1(a-b). Relationships between the final slump and slump-flow time (ST) with the final slump-spread measurements are presented in figure 8.2. These relationships correspond to the concrete mixes shown in figures 6.10 and 7.3-7.15. The results of mixes which exhibited erratic variations in the Bingham parameters at plastic viscosities ≥ 12 Nms have been excluded, as these appeared to represent measurements exceeding the operating limits of the LM system (c.f. page 244).

Contrary to the observations by Tattersall[7] and others[49, 91] in NSC, the relationships in **figure 8.1(a-b)** show :

- fairly poor correlations between the final slump measurements with both the yield value (r= 0.6111) and plastic viscosity (r= 0.5101), but
- slightly better correlations between the final slump-spread measurements with the Bingham parameters (r = 0.6544, 0.5620) in HSC.

The relationships in **figure 8.2** show that at collapse slumps greater than or equal to 200 mm, the final slump-spread measurements also provide a better index of the flow properties under self-weight than the final slump value. In this range, the final slump-spread varies by nearly 300 mm (from about 400-700 mm) compared to a 50-70 mm variation in slump value. The results also show that there is no definitive relationship between the final slump-spread and the flow time (ST) taken for complete collapse under self-weight. (Non-flowing HSCs having slumps < 150 mm (or spreads < 300 mm), like the NSC mixes in section 5.2, generally collapsed instantaneously, i.e. had zero slump-flow time).

Although the previous observations in section 6.7.1 had also shown no direct relationship between the final slump-flow time (ST) with either the yield value or

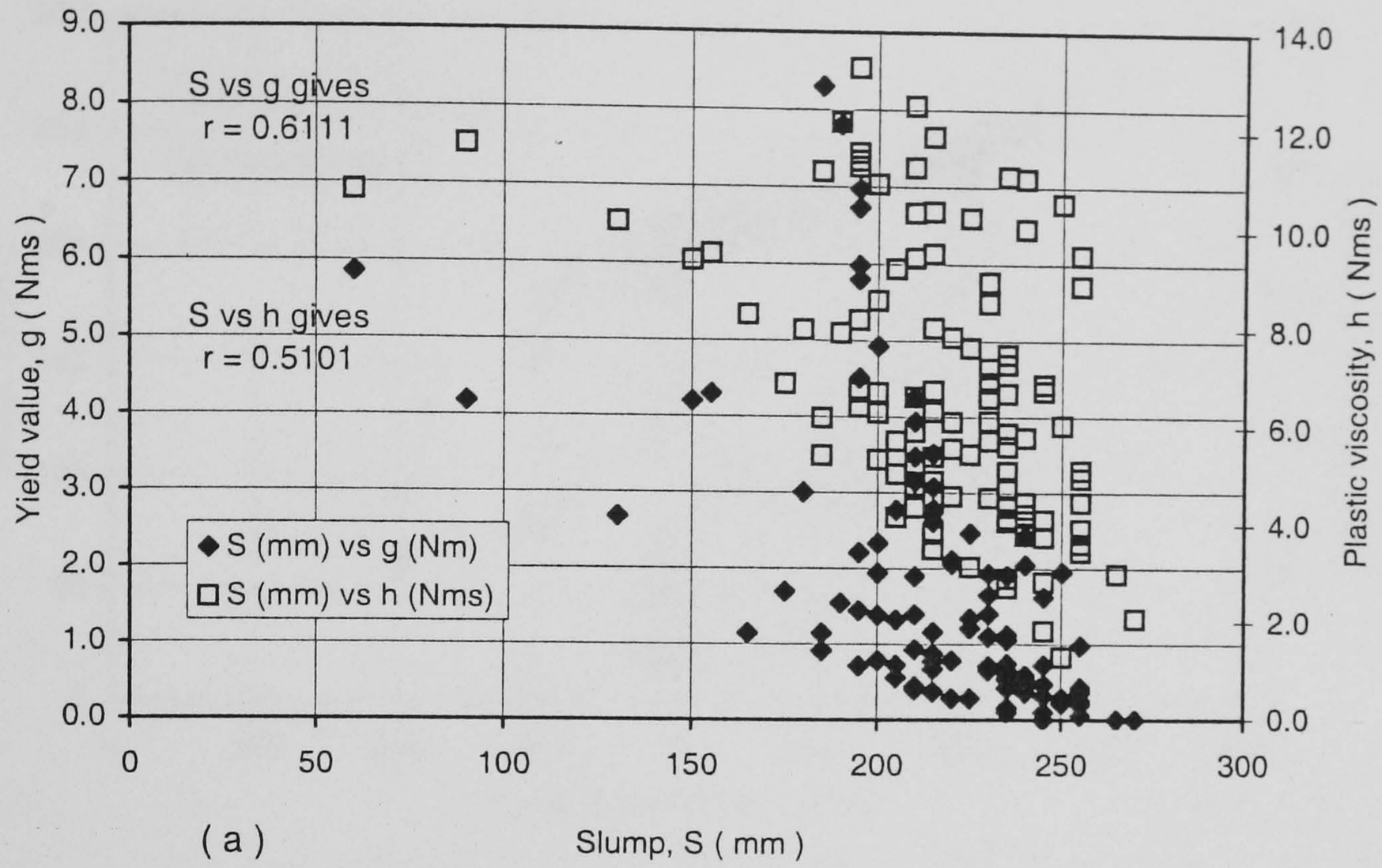

(a)

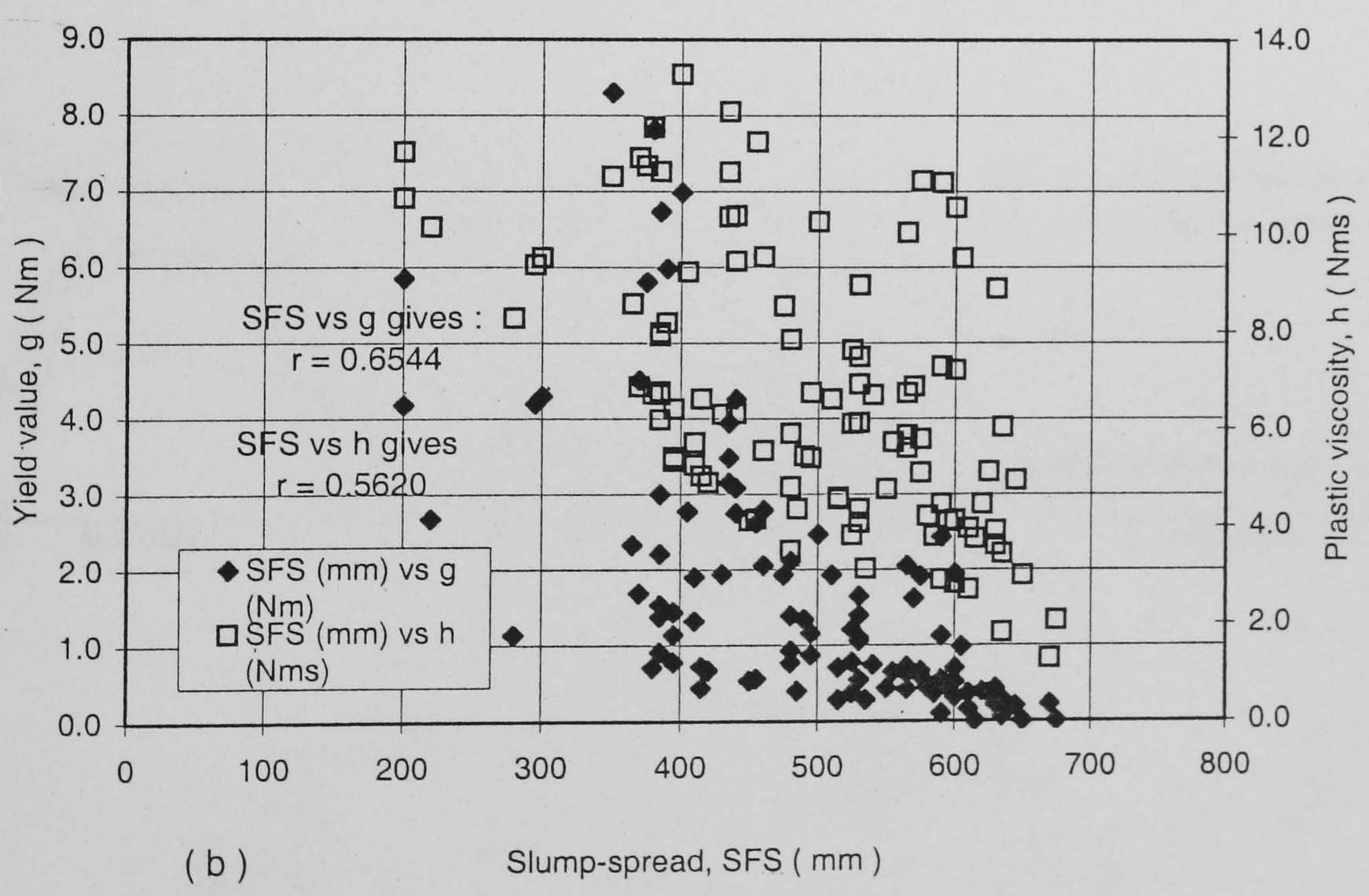

(b) Slump-spread, SFS (mm)

Figure 8.1 : Relationships between the Bingham parameters and (a) final slump and (b) slump-spread under static conditions (details of mixes given in Tables B10 and C3, 5, 7, 10, 12 and 14 of Appendices B and C).

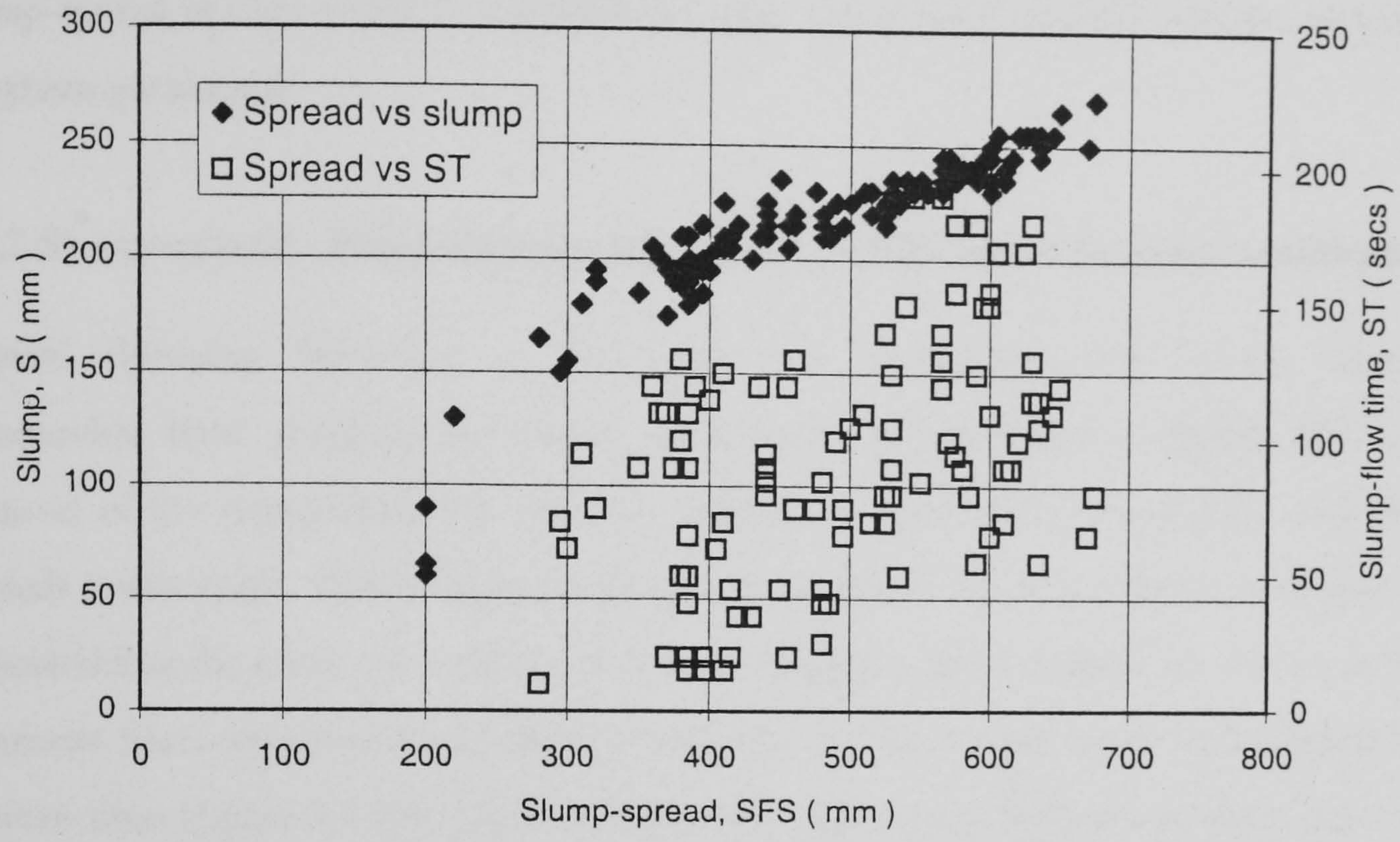

Figure 8.2 : Relationships between the final slump and slump-flow time with the final slump-spread

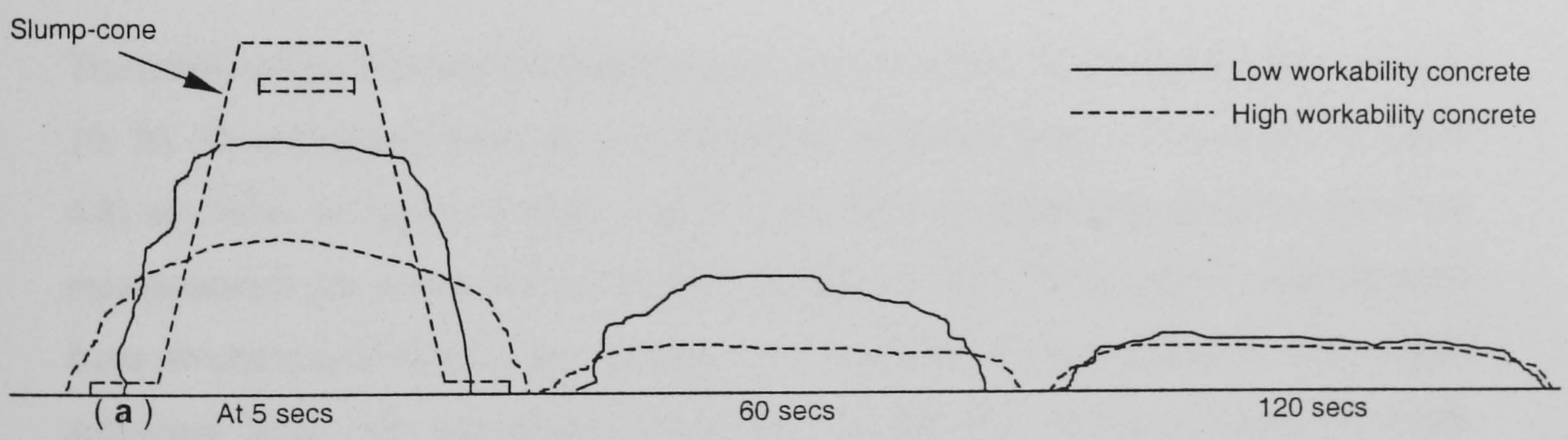

Figure 8.3 : Schematic illustration of typical slumping behaviour of low and high workability HSC mixes having comparable final slump/spread. (a) Progressive collapse, (b) graphical variations in slump and slump-spread, under dynamic conditions.

plastic viscosity, they indicated that there are significant differences in the rates of slump-spread at high and low workabilities and, hence, possible relationships with the Bingham parameters.

8.2.2 Slump-spread - Bingham parameter relationships under dynamic conditions

Typical slumping behaviour of high and low workability HSC mixes having comparable final slump/spread under self-weight are illustrated in **figure 8.3**. On removal of the slump-cone, the concrete starts to collapse/subside vertically, and then spreads horizontally. Observations of the slumping behaviour of the mixes in chapter 7 indicated that the lower the workability (i.e. the higher g and h values), the slower is the transition from vertical to horizontal deformation, and the smaller is the slump-spread at a given time (figure 8.3(b)). High workability mixes having high slump-flow times of up to 120 secs typically exhibited as much as 90-95% of their final slump-spread in the first 60 secs, compared to about 60-80% with low workability mixes having similar flow-times and/or spreads.

The relationships between the Bingham parameters and the slump-spread measured at 5, 10, 20, 30 and 60 secs from the time the slump-cone was lifted (as illustrated in figure 4.8) are show in figures 8.4(a-c) and 8.5(a-b). The corresponding final slump-spread measurements are shown for comparison in figure 8.5(c). These results were obtained from several spread-time measurements on the concrete mixes in chapter 7, and include additional tests with cement PC-9 and the two HP-SCC mixes presented in Table 3.7(b). (Details of the spread measurements are given in appendix D).

In contrast with the final slump-spread measurements in figures 8.1(b) and 8.5(c), the results in **figures 8.4(a-c)** and **8.5(a-b)** show highly significant relationships between the slump-spread at a given time with both the yield value and plastic viscosity, represented by high correlation coefficients of 0.93-0.88. These results therefore mean that the dynamic properties of flowing concretes under self-weight are directly related to the Bingham parameters - the lower the Bingham parameters, the faster the slump-

spread.

As can be seen, the slump-spread measurements at each flow time show quadratic relationships with the Bingham parameters, which appear to become increasingly more linear as the deformation of the concrete slows down and eventually stops (figure 8.5(a-c)). There are systematic reductions in the coefficients of the "SR^2 and SR" terms, and the in intercepts of the plastic viscosity - spread-time relations. The corresponding relationships between the slump-spread and yield value are more complex, exhibiting greater non-linearity, larger scatter at low spreads, and no conclusive trend with respect to intercept.

The existence of these relationships suggests that flowing HS and other HPCs experience similar variations in shear rates under their self-weight, as those occurring during two-point testing. This characteristic appears to have been overlooked by previous researchers[48, 244-246], and contrasts with the widely accepted view that the shear rate associated with the slump test is zero[7, 40, 54]. The systematic reductions in the correlation coefficients shown in figure 8.5(a-c), clearly demonstrate that the validity of the spread-time - Bingham parameter relationships only apply whilst the concrete is in a state of deformation.

The fact that the results of the two HP-SCC mixes fit the trends in figures 8.4-8.5 implies that the spread-time - Bingham parameter relationships represent intrinsic properties of flowing concretes, and are not necessarily dependent on mix proportions. SCC mixes are typically characterized by high paste contents of 37-45%[224], and very low yield values (down to zero Nm) to facilitate compactability under self-weight. The SCC mixes used in this study were tested with colleagues at UCL, and their mix proportions were given in Table 3.7(b).

The empirical equations obtained between the Bingham parameters and slump-spread (*SR*) at 5, 10, 20, 30 and 60 secs of deformation are summarized below:

$$\mathbf{g} = 7\text{x}10^{-5}\ SR_5^{\,2} - 0.0649\ SR_5 + 15.252; \quad \mathbf{h} = 5\text{x}10^{-5}\ SR_5^{\,2} - 0.0616\ SR_5 + 22.064 \qquad (\mathbf{8.1})$$

$$\mathbf{g} = 5\text{x}10^{-5}\ SR_{10}^{\,2} - 0.0573\ SR_{10} + 15.121; \quad \mathbf{h} = 3\text{x}10^{-5}\ SR_{10} - 0.0483\ SR_{10} + 20.722 \qquad (\mathbf{8.2})$$

$$\mathbf{g} = 4\text{x}10^{-5}\ SR_{20}^{\,2} - 0.0501\ SR_{20} + 14.824; \quad \mathbf{h} = 2\text{x}10^{-5}\ SR_{20} - 0.0394\ SR_{20} + 19.949 \qquad (\mathbf{8.3})$$

$$\mathbf{g} = 4\text{x}10^{-5}\ SR_{30}^{\,2} - 0.0494\ SR_{30} + 15.441; \quad \mathbf{h} = 1\text{x}10^{-5}\ SR_{30} - 0.0326\ SR_{30} + 19.236 \qquad (\mathbf{8.4})$$

$$\mathbf{g} = 3\text{x}10^{-5}\ SR_{60}^{\,2} - 0.0435\ SR_{60} + 15.236; \quad \mathbf{h} = -2\text{x}10^{-6}\ SR_{60} - 0.0215\ SR_{60} + 17.846 \qquad (\mathbf{8.5})$$

$$\text{i.e.} \qquad \mathbf{g} \text{ or } \mathbf{h} = A, B\ (SR_i)^2 - C, D\ (SR_i) + E$$

where SR_i is the slump-spread at time i = 5-60 secs after removal of the slump cone. A, B, C, D and E are constants depending on, for example, the variations in shear rate under self-weight, inter-particle forces within the concrete, and surface friction from the slump board.

These relationships contrast with the semi-empirical equations reported by Ferraris and de Larrard[246] with the BT rheometer (page 276), and the theoretical expressions reported by Kurokawa et al[244] (page 275), who in their model studies took no account of the dynamic behaviour of fresh concretes under self-weight, or the influences of internal and external frictional forces. A more representative theoretical assessment of the slumping behaviour of flowing concretes would need to include these factors, and may give a simplified expression for workability (f (**g**, **h**)) and/or spread rate ($\boldsymbol{SR}$) of the form:

$$f\ (\mathbf{g}, \mathbf{h}) \text{ or } \boldsymbol{SR} = f\left(\frac{dw}{dt} - \lambda\right) = f\left(d\left(\frac{\rho.\ g.\ \delta V, \xi_I}{dt}\right) - \lambda\right) \qquad (\mathbf{8.6})$$

where " dw " represents the changes in self-weight (as illustrated in **figure 8.6**) and inter-particle friction of the concrete in time interval " dt ". " λ " represents the surface

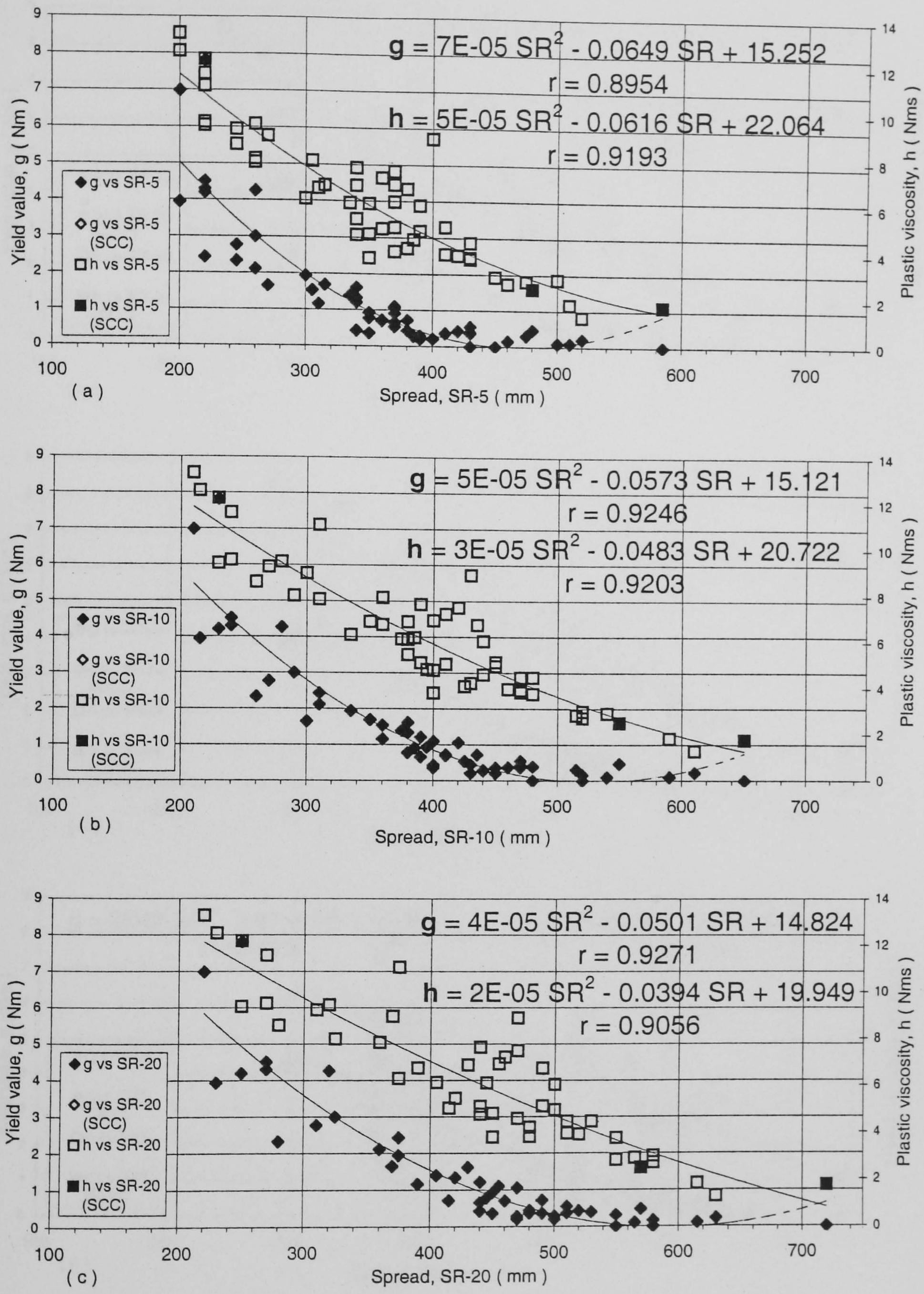

Figure 8.4 : Relationships between the Bingham parameters and slump-spread measured at (a) 5, (b) 10, and (c) 20 secs of deformation.

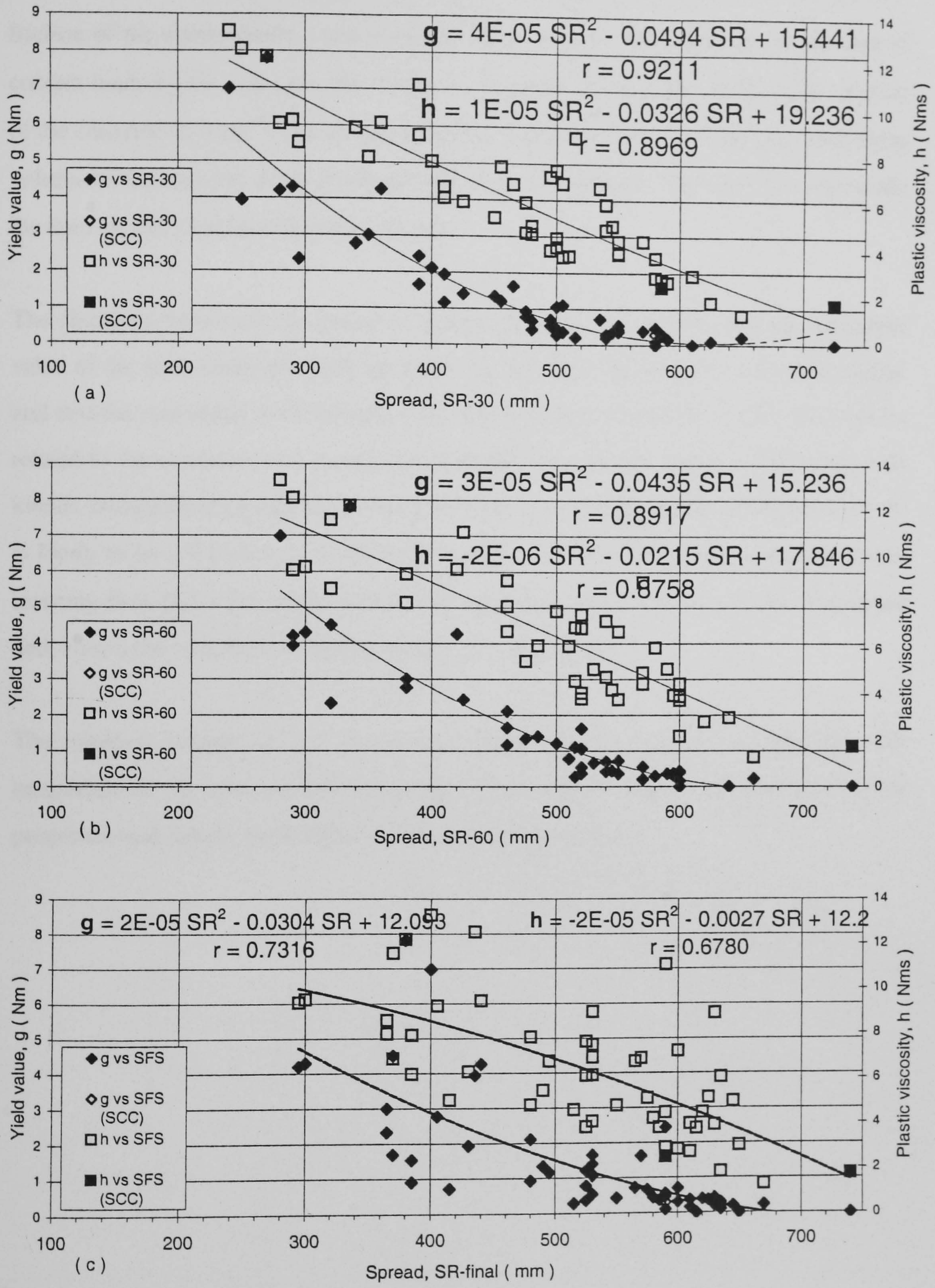

Figure 8.5 : Relationships between the Bingham parameters and slump-spread measured at (a) 30 and (b) 60 secs of deformation, and (c) under static conditions. (Note: mixes which stopped flowing between e.g. 20-30 secs, appear only in figs. 8.4(a-c) and 8.5(c)).

friction of the slump-board – which is also likely to vary, depending on the amount of contact made by the concrete. The terms ρ, g and δV respectively represent the density of the concrete (in kgm^{-3}), the acceleration due to gravity (9.81 ms^{-2}), and the decreasing volume of the concrete above the base-area of the slump-cone. The term "ξ_I" represents the inter-particle forces within the concrete.

The slumping behaviour illustrated in figures 8.3 and 8.6 suggests that the numerical value of the term *dw/dt* gradually decreases as the concrete deforms under self-weight, and that the maximum workability/spread would occur when *dw/dt* is zero. This can be related to the conversion of energy stored within the concrete before deformation, into kinetic energy during progressive slump collapse. The energy stored within the concrete is likely to be a function of its potential energy (ρ. g. δV) and its inter-particle forces resisting flow (ξ_I), whereas the kinetic energy is obviously a function of the flow speed and, hence, the variations in spread rate under self-weight.

The constant volume of the slump-cone means that at a given slump/spread, the magnitude of the inter-particle forces (ξ_I) is the main parameter influencing the flow properties and, hence, the Bingham values of fresh concretes.

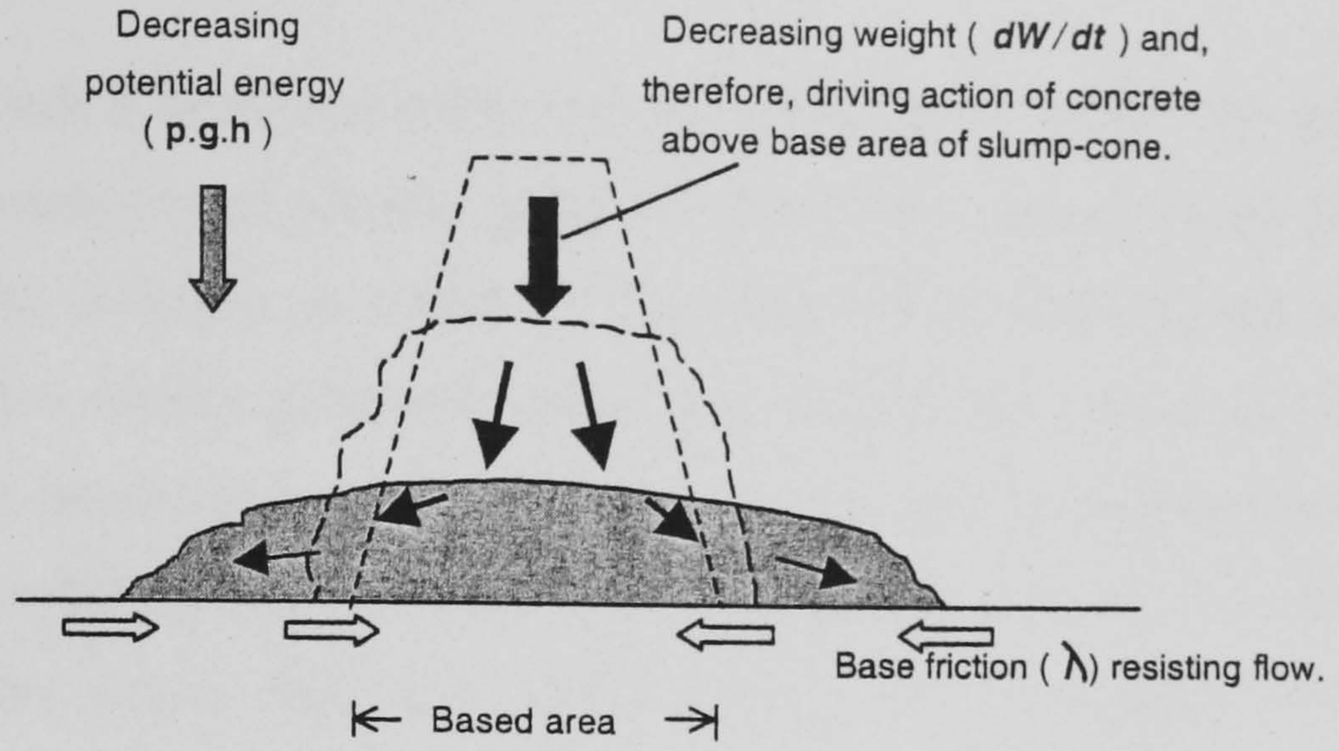

Figure 8.6 : Illustration of slumping behaviour and changes in self-weight of concrete over the base area of the slump-cone. (These, and the accompanying variations in inter-particle forces with time, appear to be responsible for the observed differences in flow properties of HPCs).

8.2.3 Potential applications of spread-time method

The existence of the empirical relationships between the Bingham parameters and slump-spread at a given time, as shown in equations 8.1 to 8.5, offer several interesting applications with regards to :

1. **Measuring workability** of flowing concretes without the use of two-point test devices.
2. **Assessing** the **stiffening properties** of HPCs during placing.
3. **Evaluating** the **vibration response** of fresh concretes during compaction.

The use of the spread-time - Bingham parameter relationships with regards to the last two applications is discussed in sections 8.3 and 8.4. The mixes used in the investigation were all produced with cement PC-9, which was previously found to give similar initial workability properties but more rapid losses of workability compared to the other Type I cements (c.f. figure 6.10).

8.3 Stiffening properties during placing

There is a general lack of quantitative information in the literature on how the Bingham parameters vary during typical placing operations. Based on a review of several field applications of HPC in France, de Larrard[90] stated that HPCs exhibit thixotropic (i.e. stiffening) properties, which significantly reduce their workability when allowed to rest for several minutes before placing. These are believed to result from agglomeration of the fine particles in HPC mixes while at rest[92], induce high pressures/low pumping rates, and therefore render the mixes difficult to pump, particularly over long distances[67].

From their measurements with the BT rheometer (c.f. figure 2.68), de Larrard and his co-workers[49, 67, 92] have however merely stated that the yield stress at rest (τ_0^R) is much higher than that during shearing (τ_0) and, therefore, has obvious links with the ease of re-working and placing fresh concrete. Although they suggested that the plastic viscosity is in practice the main parameter controlling the pumping rate and finishing characteristics, they did not comment on how these are, for example, influenced by the varying plastic viscosity shown by their non-linear flow curve at low shear rates (figure 2.68). They have also not commented on how the thixotropic properties (which they state are responsible for the workability reductions) differ from irreversible breakdown of structure, which is believed to cause non-linearity of flow-curves during two-point testing[154] (page 168).

This section compares the two-point test results after re-mixing with the stiffening properties (or workability reductions) due to 5 mins resting/standing of OPC and 10% CSF mixes at three placing times (of 35, 65 and 125 mins (and 0.26 w/b ratio)). The stiffening properties were in each case determined by measuring the slump-spread at 5, 10, 20, 30 and 60 secs, and using equations 8.1-8.5 to calculate the Bingham parameters and corresponding reductions in workability following the 5 mins resting of the mixes. The results obtained are shown in **Table 8.1**.

The close agreement between the calculated Bingham parameters at each of the three placing times demonstrates the validity of the spread-time – Bingham parameter relationships (equations 8.1-8.5) in evaluating the workability properties and, thus, in rationalizing placing operations. As can be seen, the thixotropic effects are more pronounced with the OPC mix than with the 10% CSF binary mix, particularly with regards to increases in plastic viscosity. After 5 mins resting, the Bingham values are typically increased by 0.3-1.6 Nm and 0.8-2.8 Nms with the OPC mix, compared to 0.2-0.5 Nm and 1.2-1.3 Nms with the CSF mix. In each case, the increases in the plastic viscosity after 5 mins resting of the mixes appear to be appreciably higher than those due to equivalent losses in workability as measured with the LM system after re-mixing.

These results suggest that the stiffening properties of HSC mixes are directly related to the type of binder used, and do not appear to significantly vary with time and/or loss of workability. The main practical outcome of these findings is in restricting placing durations to avoid pump blockages and/or reduce handling difficulties – particularly with OPC mixes. In order to determine suitable mix proportions, pumps and pumping pressures for successful and economic application of HSCs under field conditions, further work should for example examine :

- the stiffening properties due to binary GGBS mixes which were previously found to be considerable in the first 10-30 secs after re-mixing (section 7.4),

- how the spread-time properties, and therefore the Bingham parameters of HSCs, vary before and after being pumped at different pressures and distances, with and without resting of the mixes.

Table 8.1 : Stiffening properties of OPC and 10% CSF mixes after 5 mins resting (at 0.26 w/b ratio).

Mix	After re-mixing			Spread-time measurements after 5mins resting												
	Time	Two-point test		SR measurements							Calculated		Average		Increase * in	
		g	h	Time		SR	% of	Slump	SFS	ST	g	h	g	h		
	(mins)	(Nm)	(Nms)	(mins)	(s)	(mm)	SFS	mm	mm	secs	(Nm)	(Nms)	(Nm)	(Nms)	g	h
100% OPC	30	2.03	6.98	35	5	230	51	215	450	100	4.0	10.3	3.6	9.8	1.6	2.8
					10	260	58				3.9	10.1				
					20	295	66				3.7	9.9				
					30	340	76				3.2	9.3				
					60	375	83				3.2	9.5				
	60	3.87	8.75	65	5	200	48	200	415	95	5.0	11.6	4.9	11.2	1.0	2.4
					10	225	54				5.0	11.3				
					20	250	60				4.9	11.2				
					30	280	67				4.7	10.9				
					60	310	75				4.7	11.0				
	120	5.75	11.50	125	5	200	73	145	275	90	5.0	11.6	6.0	12.3	0.3	0.8
					10	200	73				5.8	12.2				
					20	205	75				6.3	12.6				
					30	220	80				6.5	12.5				
					60	240	87				6.6	12.6				
10% CSF	30	0.66	5.11	35	5	350	69	225	510	90	1.0	6.1	1.1	6.4	0.5	1.3
					10	385	75				1.1	6.3				
					20	425	83				1.2	6.4				
					30	455	89				1.2	6.5				
					60	495	97				1.2	6.6				
	60	1.40	6.14	65	5	320	68	210	470	80	1.5	7.0	1.7	7.3	0.3	1.2
					10	355	76				1.6	7.1				
					20	380	81				1.9	7.5				
					30	415	88				1.8	7.4				
					60	460	98				1.7	7.5				
	120	4.30	9.53	125	5	225	70	150	320	70	4.1	10.5	4.5	10.7	0.2	1.2
					10	245	77				4.3	10.6				
					20	265	83				4.5	10.8				
					30	280	88				4.7	10.9				
					60	315	98				4.6	10.8				

. SFS and ST represent the final slump-spread and corresponding flow time.

* represents differences between the 2-pt. test results and the average of the calculated g and h values.

. For more precise calculations of the Bingham parameters, equations 8.1-8.5 are used with up to 8 dpcs as shown in Appendix D.

8.4 Vibration response of HSC

As mentioned previously in section 5.3.3, the total work done during compaction is in practice composed of three main components, namely that done by: the concrete as it flows under its self-weight, the application of an external energy input, and that lost as friction around the reinforcement and formwork. The total work done during compaction/vibration of fresh concrete ($\mathbf{W_V}$) may therefore be expressed as:

$$\mathbf{W_V} = \frac{dw}{dt} + P_V - \lambda\varphi \qquad (\mathbf{8.7})$$

where *dw/dt* represents the work done by the concrete under its own self-weight, P_V is the externally applied work, and $\lambda\varphi$ is a function of the frictional resistance due to the contact surfaces (formwork, reinforcement etc). Of these, it is only the work lost against internal friction during collapse under self-weight that is an intrinsic property of the concrete alone.

As mentioned in section 2.7.2, the compactability or vibration response of fresh concrete has been subject to several investigations in the last 10-15 years[49, 89-92, 210-216], but none of these have managed to sufficiently characterise the changes in the Bingham parameters during the vibration process, and/or relate these to the hardened properties. The review indicated surprisingly little published data with the BT rheometer, which was developed with the added facility of directly measuring the variations in the Bingham parameters during vibration.

From their investigations with the BT rheometer, de Larrard[49] and his co-workers[89-92] merely concluded that the application of vibration significantly affects the flow properties of fresh concrete and reduces the yield value, but did not comment on how the plastic viscosity is affected. Similarly narrow conclusions were reached by other researchers[212-216], who also failed to provide sufficient information on how the plastic viscosity is influenced by vibration.

In this section the spread-time - Bingham parameter relationships (in equations 8.1-8.5) are compared with the vibration response of fresh concretes at a casting time of 120-130 mins and, three amplitudes of vibration (corresponding to 0.1, 0.4, and 0.7 mm). The work also includes tests to assess the effects of six mix compositions, involving five HSCs (at 0.26 w/b) and one superplasticized NSC (at 0.50 w/b, Table 3.7(b)). The HSC mixes comprised: OPC, 10% CSF, 40/10 PFA/CSF, 60/10 GGBS/CSF, and one mix in which the control SNF (Conplast SP 435) superplasticizer was replaced by the Acrylate-based (D2001) superplasticizer at the 10% CSF level. The two binary 10% CSF mixes included additional tests at a casting time of 60-70 mins to assess the effects of loss of workability. The basic mix proportions used for the HSC mixes correspond to those of mix 6 as shown in Table 3.6.

A schematic illustration of the test set-up used to assess the vibration response of the mixes is shown in **figure 8.7**. The test, as outlined in section 4.3 (figure 4.8), involved carrying out the slump test on a vibrating table, measuring the slump-spread at 5, 10, .. 60 secs, and then calculating the corresponding g and h values from equations 8.1-8.5.

8.4.1 Spread-time response curves

Typical spread-time response curves for the vibrated and non-vibrated 10% CSF mix are shown in **figure 8.8**. As can be seen, the application of vibration fluidises the concrete, causing it to slump at a faster rate, and reach higher slump-spreads compared to the non-vibrated concrete. The initial deformation during the vibration process is usually slow, taking about 2-3 secs to build-up, and is followed by accelerated subsidence before it slows down as the concrete approaches its maximum spread.

The differences in the areas under the spread-time curves for the vibrated and non-vibrated concrete provide an indication of the total mechanical work done on the concrete during vibration. These can in theory, therefore, be used in evaluating the external energy input (P_V) needed to achieve full compaction of a given concrete mixture, and/or in assessing the suitability of different compaction equipment.

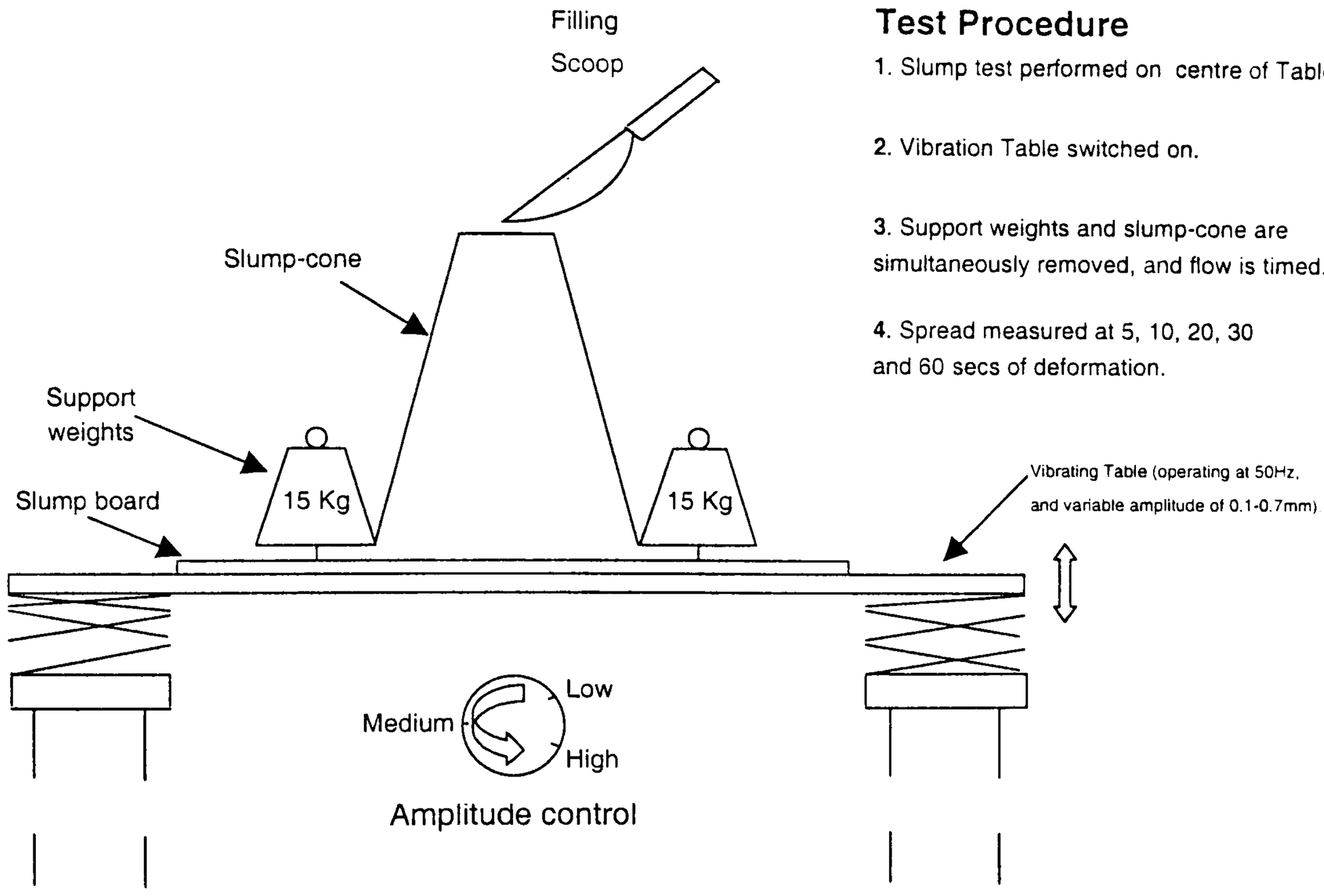

Test Procedure

1. Slump test performed on centre of Table.

2. Vibration Table switched on.

3. Support weights and slump-cone are simultaneously removed, and flow is timed.

4. Spread measured at 5, 10, 20, 30 and 60 secs of deformation.

Figure 8.7 : Schematic illustration of test set-up used to assess the vibration response of fresh concretes.

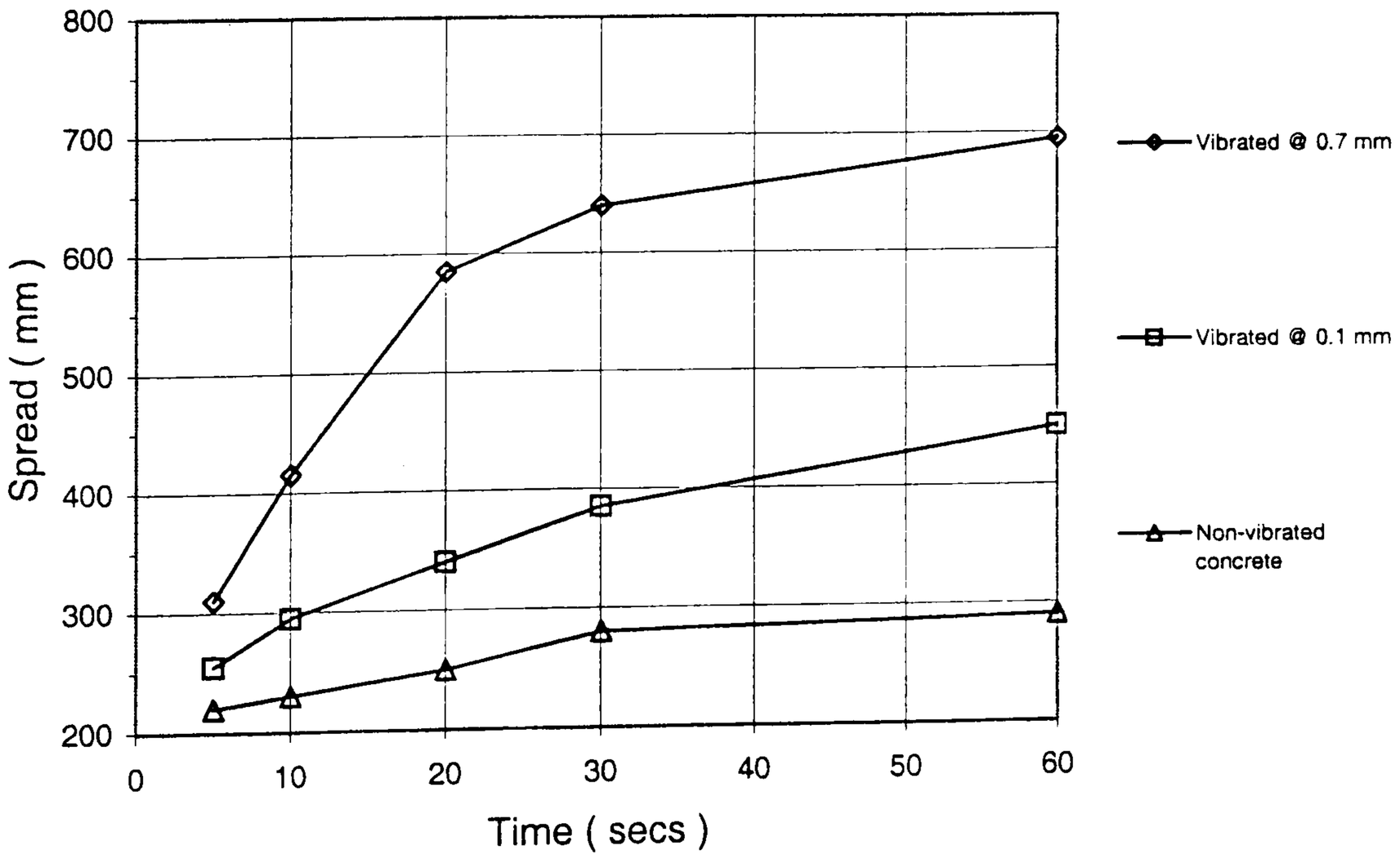

Figure 8.8 : Spread-time response curves for vibrated and non-vibrated 10% CSF mix at casting times of 120-130 mins (0.26 w/b ratio, SNF superplasticizer).

8.4.2 Effects of amplitude of vibration and mix composition

The Bingham parameters calculated from the vibration response measurements of the six mixes tested are shown in figures 8.9-8.11 and discussed below.

8.4.2.1 Effects of amplitude of vibration

The results in **figures 8.9-8.11** clearly show that the amplitude of vibration and its duration have significant and contrasting effects on the evolution of the Bingham parameters of the mixes during compaction by vibration. For each of the HSCs, it can be seen that both the Bingham parameters after the first 5 secs of vibration are significantly lower than those of the non-vibrated concrete, and they decrease at a faster rate with increasing amplitude of vibration. That is, the results, for the first time demonstrate that the plastic viscosity (like the yield value) does not increase or remain constant during vibration, but it actually decreases with increasing vibration input.

The results therefore contrast with the narrow conclusions reached by de Larrard et al[49] and others[90, 212-216] (section 2.7.2), that vibration appears to reduce and/or eliminate the yield value, but has little or no effect on the plastic viscosity compared to the non-vibrated concrete. A comparison of de Larrard et al's results[49] for their vibrated and non-vibrated concrete (c.f. figure 2.68), in fact shows noticeable increases in plastic viscosity during vibration as measured with the BT rheometer, particularly at low shear rates. These may be due to up-lift effects and consequent volume expansions of the concrete in the BT rheometer as discussed in previous chapters.

Although it has been reported that the BT rheometer is capable of generating vibration frequencies of 35-55 Hz[93], it is not clear what its amplitude of vibration range is, and whether the results shown in figure 2.68 represent the maximum vibration capacity of the device. Apart from showing similar increases in plastic viscosity during vibration, a major criticism of the non-linear flow curves reported by Tattersall and Baker[210] and by Kakuta and Kojima[212], as mentioned in section 2.7.2, is that they do not allow

numerical determination of the plastic viscosity during vibration.

8.4.2.2 Effects of mix composition

(I) With OPC mix

The results of the OPC mix in **figure 8.9(a)** show that at the highest vibration amplitude of 0.7 mm, the yield value is completely eliminated (reduced from about 6Nm to zero) in the first 30 secs, whilst the plastic viscosity continues to decrease at a decreasing rate with vibration duration. That is, the concrete during the vibration process behaves as a Newtonian fluid – possessing no yield value, but a non-zero plastic viscosity. The effect is therefore similar to the fluidising action produced by successive redoses/additions of superplasticizer as shown in figure 5.11.

As can be seen, the medium amplitude of 0.4 mm appears to mainly increase the vibration duration needed to obtain equivalent compactabilities and/or reach zero yield value. The results however show that the use of the lowest vibration amplitude of 0.1 mm is ineffective in sufficiently fluidising the mix, and eliminating the yield value.

In the first 60 secs of vibration, the 0.1mm amplitude reduces the yield value of the non-vibrated concrete by only 32% (from 5.7 to 3.9 Nm) and decreases its plastic viscosity by about 12% (from 11.5 to 10.1 Nms). This contrasts with a minimum vibratory amplitude of 0.04 mm recommended by Kolek[208] for compacting NSCs having 0.40-0.60 w/b ratios. According to L'Hermite and Tournon[207] the most important factor preventing full-compaction of fresh concretes is inter-particle friction, and it can be reduced by about 95% (from 0.02 to 0.001 MPa) during vibration of NSCs.

(II) With CSF blended mixes

In contrast to the OPC mix, the results of the 10% CSF binary and two ternary blended mixes in **figures 8.9(b)** and **8.10(a-b)** show that the inclusion of CSF in the binder is more effective in reducing the vibration duration and overcoming the high internal resistance of HSCs to flow. The best vibration response of the three CSF blended mixes

is obtained with the 40/10 PFA ternary blend in **figures 8.10(a)**, which is in agreement with the two-point test measurements in chapter 7. The yield value of the mix is completely eliminated during vibration at each of the three amplitudes, and the plastic viscosity is reduced by as much as 4.0-5.5 Nms (i.e. by about 65-90 %). The results of the PFA/CSF mix however suggest that, even in high workability concretes (having slumps ≥ 225 mm (c.f. figure 7.10)), some consolidation is still required to eliminate the yield value and/or ensure full-compaction.

The lower vibration response characteristics of the 10% CSF and GGBS/CSF mixes (in **figures 8.9(b)-8.10(b)**) are consistent with their lower workabilities before vibration, and are reflected by longer vibration durations to reach zero yield value at the 0.4 and 0.7 mm amplitudes. At the lowest vibration amplitude of 0.1 mm, the yield value in both of these mixes is not eliminated.

The results with the 10% CSF binary mix in figure 8.9(b) also demonstrate the importance of casting time during compaction. The longer the casting time (i.e. the lower the workability of the non-vibrated concrete), the lower are the reductions in the Bingham parameters during vibration, and the higher is the potential for incomplete compaction of the concrete.

Despite their contrasting vibration response properties, several tests with the cylinder-vibration method (used in chapters 5 and 6), indicated negligible differences in the compactability of the CSF blended mixes. As in the previous tests with the 2.50% and 4.00% dosed mixes (Table 6.5), the values from the cylinder-vibration tests with the CSF mixes typically fluctuated between 5-15 mm in the first two hours (c.f. Table C15). These suggest that the results from the cylinder-vibration method depend mainly on the slump properties of fresh concretes under self-weight, and not necessarily on their internal resistance to flow during vibration. As mentioned previously in section 5.3.3, most of the deformation in the cylinder-vibration tests occurs during the first 5 secs of compaction, and appears to be independent of vibration amplitude.

(III) Influence of superplasticizer type

A comparison of the vibration response curves of the 10% CSF mixes with the SNF and Acrylate-based superplasticizers in **figures 8.9(b) and 8.11(a)** shows no distinct effects of superplasticizer type on compactability during the first 60-70 mins. The lower vibration response of the Acrylate-based superplasticizer at the 120-130 mins casting time may, therefore, be attributed to its weaker dispersion retaining characteristics and faster losses in workability before vibration.

The consistent ranking order observed previously with the Acrylate and SNF superplasticizers in chapter 6 suggested that they exhibit similar mode(s) of action, but different dispersion retention capabilities. Further work should examine the vibration response characteristics of, for example, acrylic-based superplasticizers, which have been reported to operate primarily through steric hindrance, and are believed to influence workability and mix stability in different ways[34] (page 99).

(IV) With NSC

In agreement with the HSC mixes, the results in **figure 8.11(b)** show that when NSC is subjected to vibration both its Bingham parameters are reduced, and the rate of decay is larger with increasing vibration amplitude. As can be seen, the high workability of the NSC mix before vibration produces similar reductions in the Bingham parameters as those obtained with the ternary PFA/CSF mix at the 0.4-0.7 mm vibration amplitudes (figure 8.10(a)).

However, although the spread-time method gives consistently lower yield values than the non-vibrated NSC mix, it appears to grossly overestimate the plastic viscosity at the 0.1 mm amplitude by as much as 6.4 Nms (or 296 %) compared to that measured before vibration. At the higher vibration amplitudes of 0.4-0.7 mm, the plastic viscosities appear to be overestimated by up to 2.5 Nms compared to the non-vibrated NSC mix during the first 5 to 10 seconds, but are lower thereafter. Although many

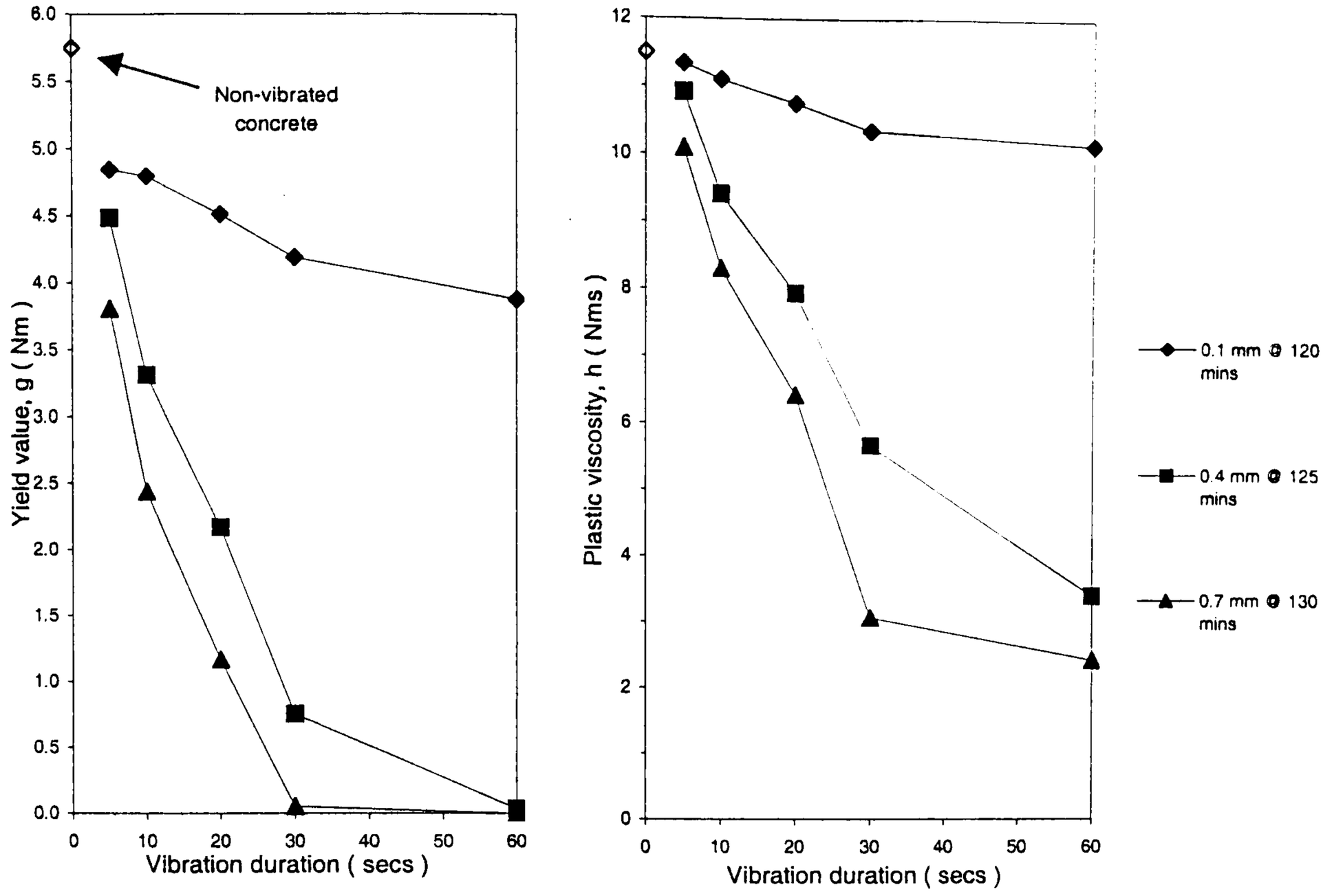

(a) OPC mix

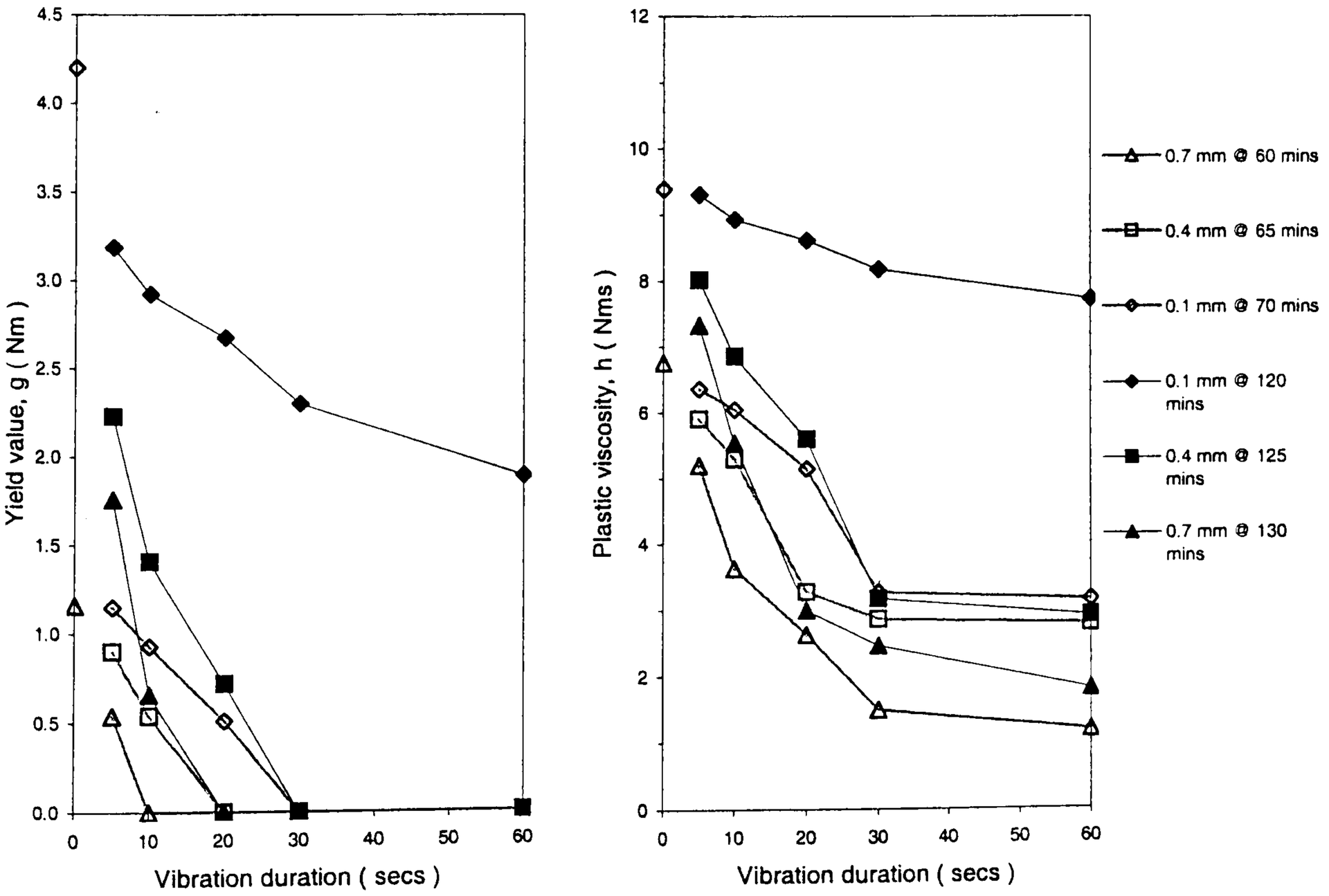

(b) 10% CSF mix

Figure 8.9 : Vibration response tests with (a) OPC and (b) 10% CSF mixes, at amplitudes of 0.1-0.7 mm and casting times of 60-130 mins (0.26 w/b ratio).

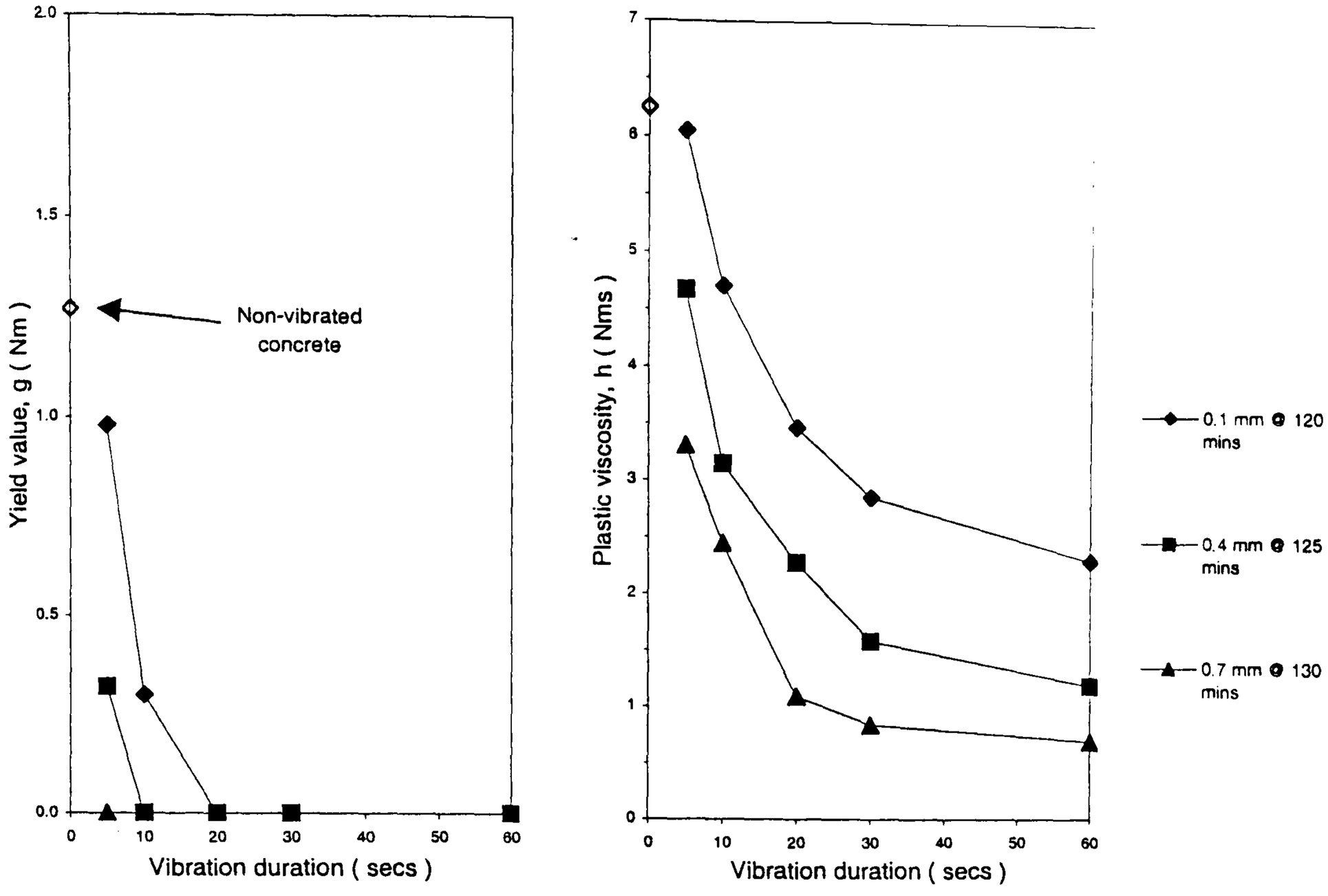

(a) 40/10 PFA/CSF mix

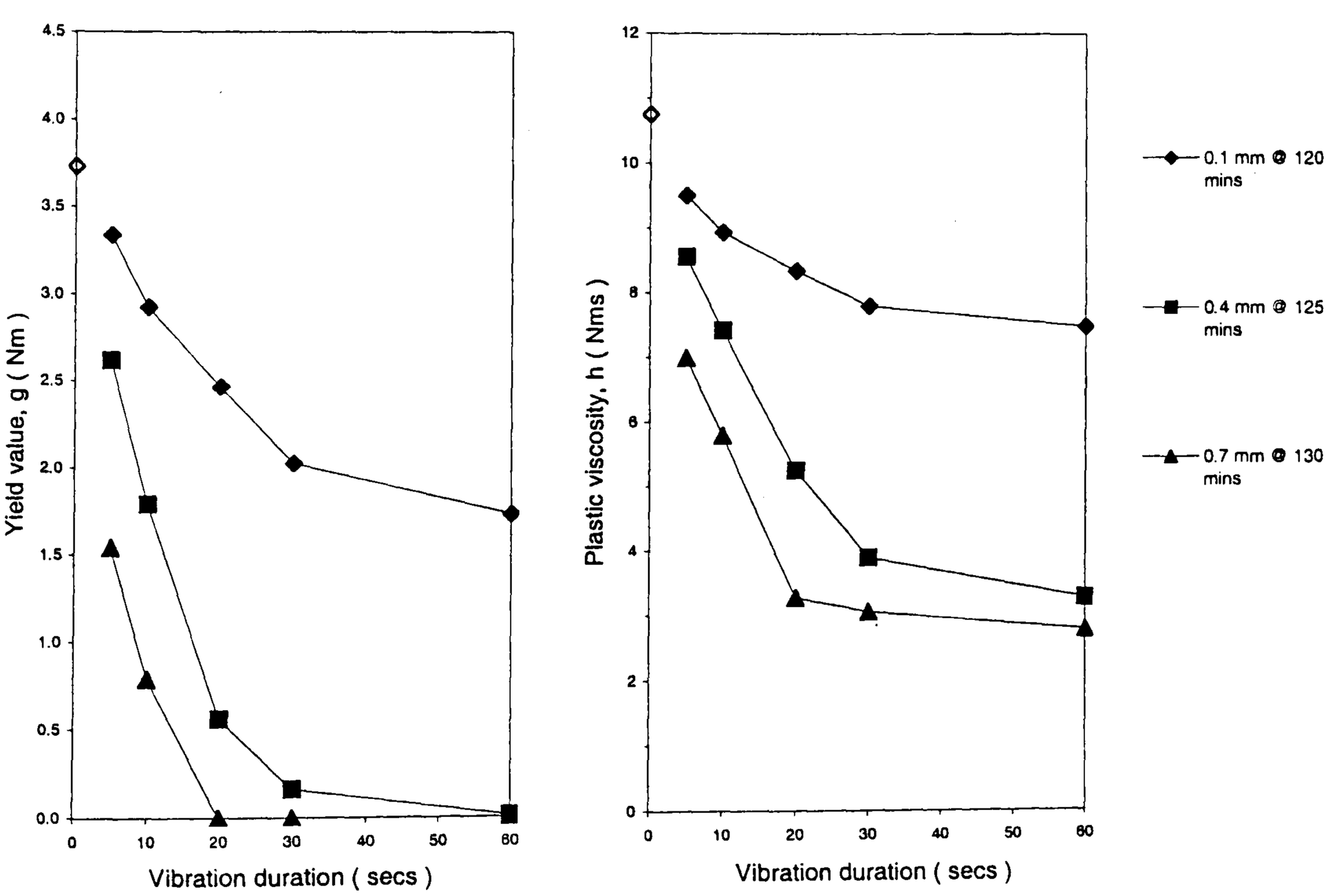

(b) 60/10 GGBS/CSF mix

Figure 8.10 : Vibration response tests with ternary mixes of (a) 40/10 PFA/CSF and (b) 60/10 GGBS/CSF, at amplitudes of 0.1-0.7 mm and a casting time of 60-130 mins (0.26 w/b ratio).

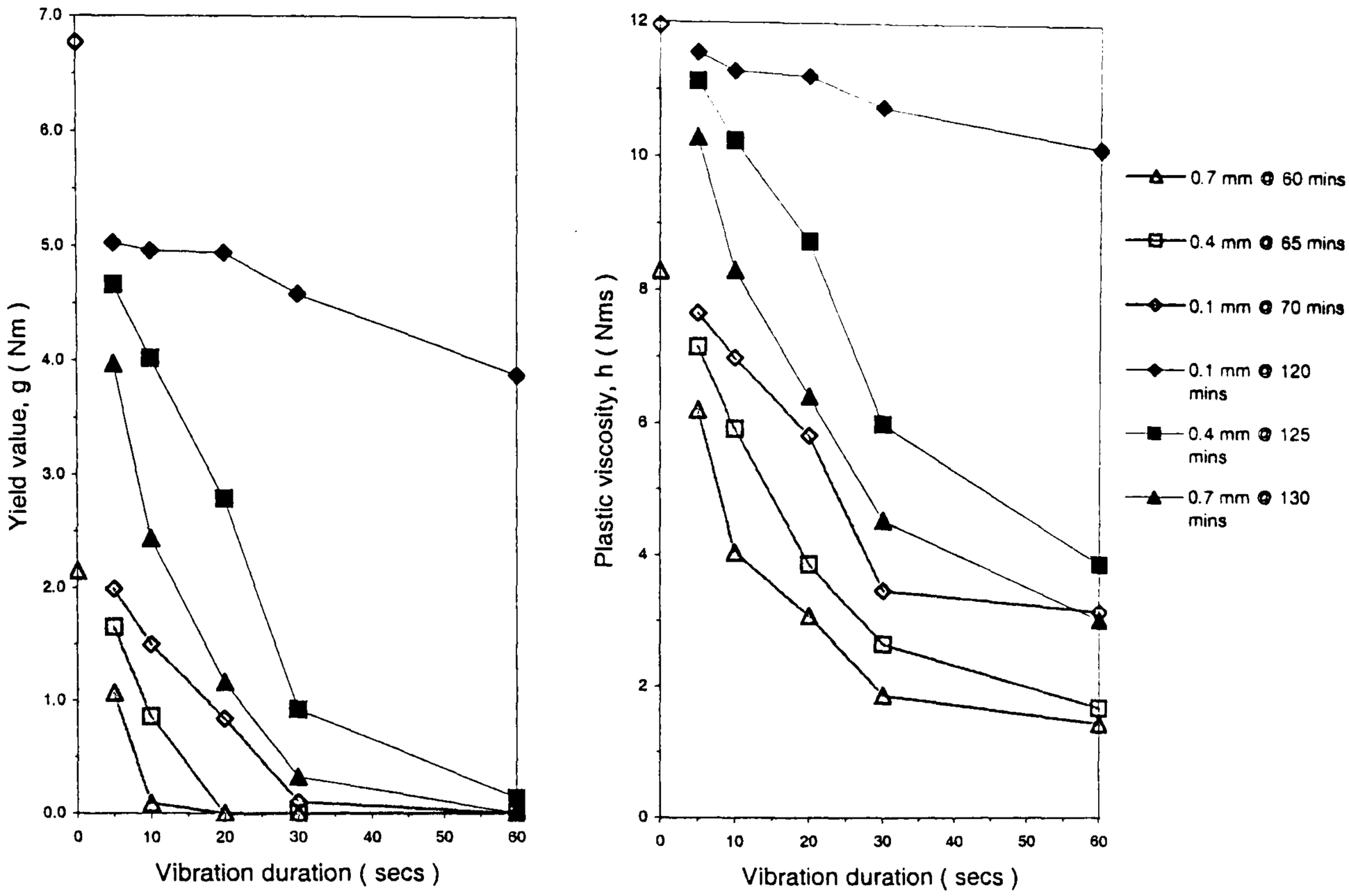

(a) 10% CSF mix with Acrylate superplasticizer (0.26 w/b)

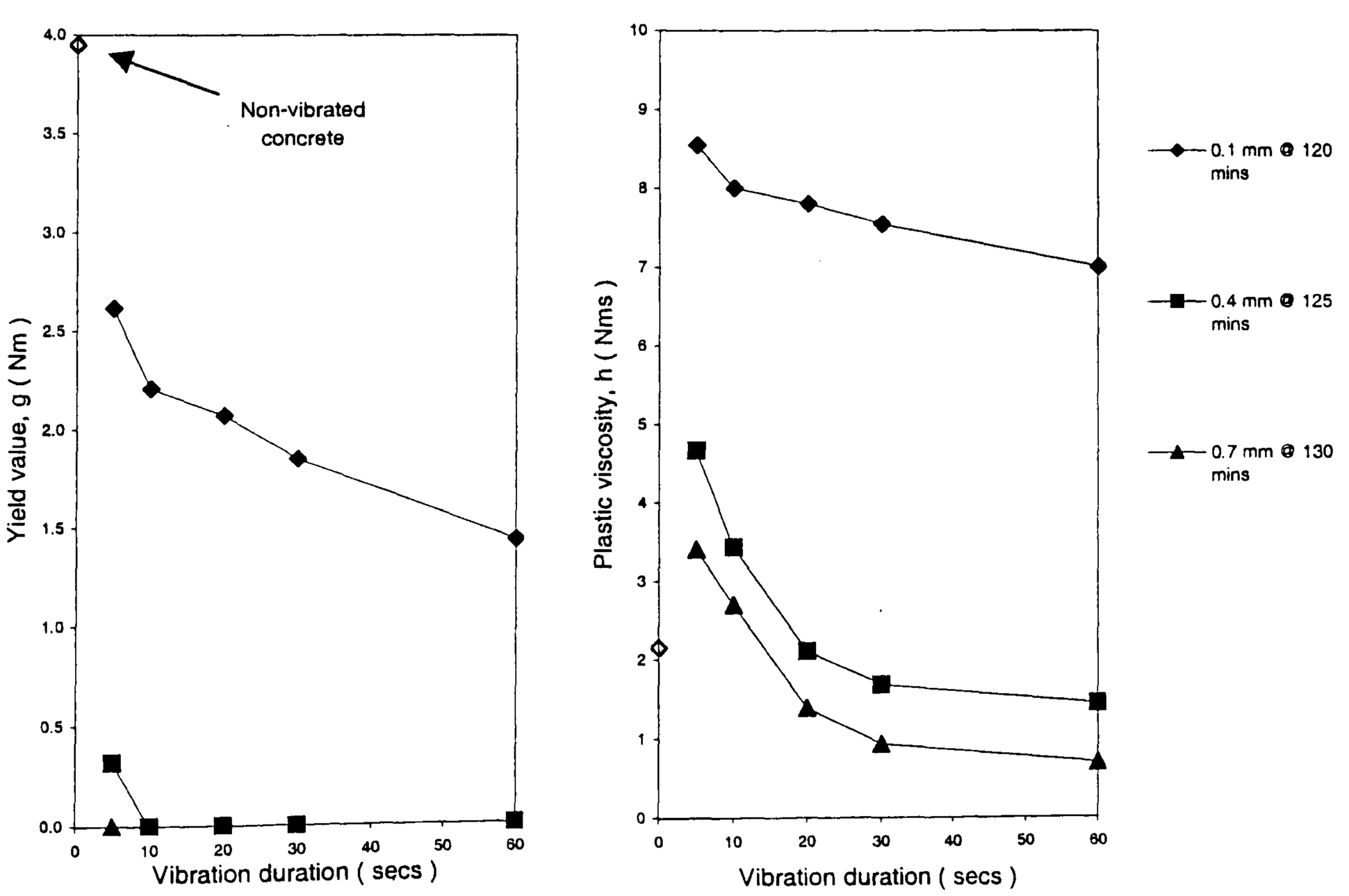

(b) NSC mix (0.50 w/b)

Figure 8.11 : Vibration response tests with (a) Acrylate superplasticizer and (b) superplasticized NSC, at amplitudes of 0.1-0.7 mm .

researchers[3, 5, 17, 30, 38] have stated that neither the static nor the dynamic properties of NSCs resemble those of HSCs, they did not comment on how they differ.

In section 5.3.1 it was found that the main features differentiating the flow properties of NSCs from HSCs are their instantaneous collapse under self-weight, and the fact that their plastic viscosities vary over a narrow range of 1-2 Nms. (Their yield values can be as high as 8 Nm, and are therefore comparable to those in HSCs). These characteristics suggest that the low plastic viscosity of NSC is the main parameter influencing its spread rate during vibration. The instantaneous collapse of NSCs under self-weight also suggests that they possess less inter-particle energy than HSCs, and that the work done on NSCs during vibration is primarily provided by the external energy input (Pv, in equation 8.7).

8.4.3 Summary and further discussion

The spread-time method developed in this research provides a simple and effective way of measuring the variations in the Bingham parameters during the placing and compaction stages of HSCs. The method has for the first time demonstrated that both the yield value and plastic viscosity decrease progressively during the vibration process.

Whether the yield value is reduced to zero depends primarily on the workability of the non-vibrated concrete, and the amplitude of vibration used. When these are high, fresh concrete behaves as a Newtonian fluid - i.e. possesses no yield value and a decreasing plastic viscosity. The fact that the plastic viscosity decreases to non-zero values during vibration, suggests that the yield value may be the main parameter influencing full-compaction of fresh concretes. These findings are in contrast with the narrow view presented by de Larrard et al[49] and others[90, 212-216], that the application of vibration mainly reduces the yield value, but has little or no effect on the plastic viscosity.

In practice the placing and compaction characteristics may depend critically on the size of pour, surface roughness of the formwork, the amount and orientation of reinforcement, and whether the concrete is, for example, pumped or poured directly into the forms. These factors cannot be simulated for by any of the existing two-point testing devices.

The accuracy of the spread-time measurements to evaluate the workability properties under typical field conditions, may be greatly improved by using electronic or visual recording techniques to continuously monitor the slump-spread during collapse. The present spread-time measurements were manually recorded to the nearest ±20 mm and ±1 second. One limitation of the method is its inability to characterise the workability of concretes exhibiting instantaneous collapse slumps under self-weight.

It is hoped that the spread-time method will contribute to rationalizing concrete placement operations, and in the conservation of energy resources by determining the optimum/minimum energy requirements for achieving full compaction. These may be evaluated from the areas under the spread-time curves, and/or the minimum Bingham values obtained during vibration. One major difficulty in using the theoretical expression postulated by Kirkham[209] (page 101) to quantify the energy requirements during compaction, concerns knowledge of the stiffness/damping effects (C_1) of the concrete. These would be expected to increase continuously with time and decreasing workability.

It is hoped that further work with the spread-time method would compare :

- the effectiveness of external and internal vibration techniques, as well as
- the influence of other vibration parameters, such as variable frequency, acceleration and waveform.

The effects of the vibration response properties of the six mixes tested in section 8.4.2 on the strength development, density and homogeneity of hardened concretes are discussed in the next chapter.

8.5 Conclusions

- The rate at which a fresh concrete mixture collapses/spreads during the slump test provides a measure of both its yield value and plastic viscosity. Athough the conclusions reached are based on correlations between spread-time and the Bingham parameters which may be (a) subject to errors and (b) specific to the range of mixes tested, they have been successfully used in assessing the placing and compaction characteristics of HSCs.

- During placing, HSCs exhibit significant thixotropic effects which reduce their workability after 5 mins from re-mixing. The effects are more pronounced in the OPC-mix than the equivalent binary 10% CSF mix, and are represented by increases in the g and h values of as much as 78% and 40% respectively.

- Both the yield value and plastic viscosity decrease progressively during compaction by vibration. Whether the yield value disappears, depends on the workability of the non-vibrated concrete, its mix composition and the amplitude of vibration applied.
  - At high workabilities and/or amplitudes of vibration, fresh concretes behave as Newtonian fluids – possessing no yield value, and progressive reductions in plastic viscosity (of up to 90% of the non-vibrated value).
  - The non-zero plastic viscosities during vibration suggest that the yield value is the main parameter influencing full-compaction of fresh concretes.
  - A 40%PFA+10%CSF ternary blended mix exhibits better vibration response properties (i.e. requires lower vibration durations and amplitudes) than a 60%GGBS+10%CSF ternary combination and, the reference OPC and 10%CSF mixes at 0.26 w/b ratio.

The effects of different vibrations durations (corresponding to 0, ½, 1, and 2 times those needed to reach zero yield value) and amplitudes (of 0.1, 0.4, and 0.7 mm) on the strength development characteristics, density and homogeneity of hardened concretes are discussed in the next chapter.

Chapter 9
28-day Strength Development (at different degrees of compaction by vibration)

9.1 Introduction

The compressive strength of a given concrete mixture depends on its composition, age, and the degree of compaction applied. Full compaction of a fresh concrete mixture requires satisfactory workability during casting in order to overcome its internal resistance to flow, allow it to fill all corners of the mould/formwork, form good bond to the reinforcement, and achieve its maximum strength and durability. Although it is widely accepted that the fresh concrete properties during compaction significantly influence the hardened properties[7-8, 214, 218, 223, 242], the literature review in section 2.8 indicated a lack of quantitative information showing how these relate at different vibration inputs.

This chapter presents the results of tests used to examine how the 28-day :

- **cube strength**,
- **density**, and
- **homogeneity** of short columns in the hardened state

are influenced by the Bingham parameter variations in the fresh state and different :

- **vibration durations** (corresponding to 0, ½, 1 and 2 times those needed to obtain zero yield value),
- **vibration amplitudes** (of 0, 0.1, 0.4 and 0.7 mm), and
- **mix compositions** (involving six mixes at 0.26 and 0.50 w/b ratios).

The cube strengths and densities of the mixes tested were evaluated using 100 mm^3 specimens, whilst the homogeneity was assessed using 500x100x100 mm prisms. The cube tests also included an assessment to determine how the 28-day strength development characteristics (at 0.26 w/b ratio) are influenced by two casting times of 60-70 mins and 120-130 mins.

9.2 Effects of vibration duration and amplitude on cube strength

As mentioned previously in section 2.8, Welton[218] reported that the application of vibration has five main roles in concrete, by: eliminating (1) mechanical and (2) unintentional **air voids**, (3) removing unnecessary **water**, (4) shaking the particles into their **closest nesting**, and (5) attacking the **micro-pores** and **micro-capillaries**. In contrast, several researchers[208, 216] have suggested that compaction by vibration is essentially a **two-stage process**: the first comprising rapid subsidence or **slumping** of the concrete, followed by **de-aeration** (i.e. removal of entrapped air bubbles).

Despite the importance of full-compaction on the mechanical properties of hardened concretes, the guidelines in both BS 1881: part 108[219] and ASTM C192-98[220] for compacting fresh concretes provide no direct provisions for relating the workability properties of non-vibrated concretes with, for example, the minimum energy requirements needed for full compaction. They merely recommend that the concrete should be "compacted to release as many entrapped air bubbles as possible", and suggest that "full-compaction is achieved when the surface of the concrete becomes relatively smooth".

These characteristics are however largely subjective, usually pronounced only during the initial slumping stage (i.e. in the first 5-10 secs) of vibration, and are not easily distinguishable. In contrast, the vibration response tests in chapter 8 showed that the workability/Bingham properties of non-vibrated concretes, and their potential to achieve full-compaction, are significantly influenced by mix composition, vibration duration and amplitude.

Tables 9.1-9.3 summarize the fresh properties of the mixes tested in chapter 8 (figures 8.9-8.11), together with their cube strengths and densities measured in the hardened state. The hardened properties in Table 9.1 correspond to 100mm cubes compacted at different vibration durations (equivalent to 0, ½, 1 and 2 times those

needed to obtain zero yield value). Those in Tables 9.2 and 9.3 respectively correspond to 100mm cubes compacted at different amplitudes (of 0-0.7 mm) and casting times (of 120-130 or 60-70 mins). The cube densities (as described in section 4.4.3) were evaluated by weighing the specimens in air and water, and are discussed in section 9.3.

As mentioned in chapter 4, the strength and density measurements were determined from duplicate mixes produced after completion of the fresh property tests in chapter 8. To reduce damping effects and enable optimization of the hardened properties, two cubes (each weighing approx. 2.5 kgs) were in each case cast using two steel moulds (weighing 7.5 kg each). Their combined weight (20kg) is comparable to that of the slump board and concrete-slump-cone (8 and 14 kg) used to assess the vibration response of the fresh concretes in chapter 8 (figure 8.7).

9.2.1 Effects of vibration duration

The results in **Table 9.1** and **figure 9.1** show that the cube strengths of the OPC and 10% CSF mixes increase with increasing vibration duration, up to the optimum duration needed to obtain zero yield value. The fact that the plastic viscosity of the mixes continues to decrease at higher vibration durations than those needed to obtain maximum cube strengths, clearly demonstrates that the yield value is the main parameter influencing the degree of compaction.

That is the results show that :

- The maximum compressive strength (or **full compaction**) of 100mm cubes occurs at vibration durations corresponding to zero yield value.
- Shorter vibration durations giving non-zero yield values produce lower cube strengths representing different degrees of **under-compaction**, whereas
- longer durations (corresponding to **over-compaction**) produce similar strengths as the fully compacted cubes.

In agreement with the results by Forssblad and Sallstrom[221] (c.f. figure 2.71), the present results with the 100 mm cube specimens indicate that the dangers of over-compaction are less significant than those resulting from under-compaction. The over-compacted cube strengths however contrast with Al-khalaf and Yousif 's findings[217] using 150 mm cube specimens. These showed that there are significant reductions in cube strength following full-compaction to maximum strength (c.f. figure 2.70). The effects that different vibration durations have on the strength development characteristics in deep concrete pours are discussed in section 9.5.

9.2.2 Effects of amplitude of vibration and mix composition

9.2.2.1 Effects of amplitude of vibration

As can be seen from **Table 9.2**, the cube strengths of the six mixes tested increase with increasing amplitude of vibration (from 0.1-0.4 mm), but are comparable at the medium and highest amplitudes of 0.4 and 0.7 mm. The results therefore confirm that the compressive strength increases with decreasing yield value, down to the lowest value (zero Nm) corresponding to full-compaction. The effect is illustrated with the results of the OPC and 10% CSF reference mixes in **figure 9.2**. The lower cube strengths at the 0-0.1 mm amplitudes can be attributed to, for example, less particle nesting and poorer pore refinement than at the higher amplitudes.

When compared to the non-compacted cubes, the results in Table 9.2 show that the relative improvements in cube strengths during vibration depend significantly on the slump-spread values (or self-levelling characteristics) of the mixes before vibration. The largest strength improvements obtained between the compacted and non-compacted cubes are shown by the 200 mm spread NSC mix, whilst the lowest are shown by the ternary PFA/CSF mix. The average cube strengths of the compacted NSC mix are as much as 30.5 Nmm^{-2} (or three times) higher than those cast without vibration, whereas the corresponding improvements in cube strength with the ultra-high spread PFA/CSF mix are only 5.7-7.2 Nmm^{-2} (or 6.5-8.1 %) higher.

The minor improvements in the vibrated PFA/CSF cube strengths nevertheless confirm the need for some compaction in high slump/workability mixes as shown in figure 8.10(a) – possibly to improve particle nesting and/or attack the micro-pores and capillaries as suggested by Welton[218] (page 106). Similar results have been reported by Chai[224], who found that the cube strengths of high workability SCC mixes, having slump-spreads between 600-700 mm after complete collapse under self-weight, are typically 3-5% lower than those fully-compacted by vibration.

Inspection of the non-compacted PFA/CSF cubes after de-moulding, indicated that the mix fills all corners of the mould and gives a smooth surface with no visible air voids. Welton 's[218] first two criteria (involving the elimination of mechanical and unintentional air voids) can therefore be sufficiently satisfied without vibration in high slump/spread mixes. The third criterion (the removal of unnecessary water) may in practice be better fulfilled by careful selection of materials and mix proportions, as large amounts of bleed water can produce layers of scum on concrete surfaces after vibration and, hence, consequent loss of durability.

9.2.2.2 Effects of mix composition

(I) With OPC and 10% CSF mixes

The 5-13 Nmm^{-2} higher 28-day cube strengths of the control 10% CSF mix when compared to the OPC reference mix in Table 9.2 are consistent with observations by, for example, Read et al[190] and Soutsos[53], using cubes and cylinders compacted in accordance with the BS 1881[219] and ASTM[220] guidelines. Read et al[190] found that the inclusion of 12% CSF at 0.27 w/b ratio increases the early age compressive strength development in the first 1-7 days by 5-10 Nmm^{-2}, and gives up to 20 Nmm^{-2} higher 28-day strengths. From his work at 0.26 w/b ratio, Soutsos[53] found little or no early age strength gains with the inclusion of 10% CSF in the binder, but similarly observed significant increases in strength of the order of 5-20 Nmm^{-2} at 28-days and beyond.

Improvements in the strength development characteristics of mixes containing CSF have generally been attributed to both physical and chemical effects resulting from :

- a **higher reactivity** of the utrafine CSF particles,
- their **filler effect** between the larger cement grains at early ages, and
- **enhancement of** the **transition zone** between the aggregates and hcp[168, 222, 247-9].

Apart from reducing the thickness of the transition zone, the presence of CSF is also believed to enhance its quality by converting larger amounts of the calcium hydroxide ($Ca(OH)_2$) produced by the hydrating cement into strength contributing calcium silicate hydrate (C-S-H) gels[168, 248].

(II) Ternary blended mixes

There is very little information in the literature on the strength development characteristics of ternary blended mixes incorporating OPC and CSF with PFA or GGBS, particularly at low w/b ratios of 0.30 or less. The cube strengths in Table 9.2 for the PFA/CSF and GGBS/CSF ternary mixes at each of the three vibration amplitudes show similar 28-day strengths, ranging from 94-96 and 92-99 Nmm^{-2}, which are approximately 18-27 Nmm^{-2} lower than those of the control 10% CSF mix.

From a study at 0.24 w/b ratio, Wei et al[248] found that a ternary mixture containing 7.5% PFA and 7.5% CSF produces similar 3-day strengths, but 3-15 Nmm^{-2} higher 28-day strengths compared to a binary 15% CSF mix. They attributed the strength increase to improved filling effects, higher pozzolanic reactivity, and enhancement of the interfacial bonds between the cement matrix and aggregates. In comparison to a 10% CSF control mix at 0.26 w/b ratio, Soutsos[53] found that his 50%GGBS+10%CSF mixture (c.f. figure 2.61) produces about 35 and 20 Nmm^{-2} lower strengths at 7 and 28 days, and increasingly similar strengths beyond 90 days.

According to Aitcin and Neville[11], the various binders in ternary blended cements

participate in different ways and at different rates in the hydration process. and in creating the bonds that govern the final strength of the concrete. In this respect it should be noted that both PFA and CSF are pozzolanic materials[249-250]. That is, they contain active silica and are in themselves not cementitious but, will in finely divided form and in the presence of water, chemically react with the calcium hydroxide ($Ca(OH)_2$) liberated by the hydrating cement to form cementitious compounds. In contrast, GGBS is a latent hydraulic material containing sufficient lime (CaO) and silica (SiO_2) to enable it to self-hydrate and form cementing C-S-H products. This is the main reason why GGBS can in practice be used at high cement replacement levels of up to 80%[187], compared to about 50% with PFA[251] and 20-25% with CSF[198].

(III) Influence of superplasticizer type

The effects of superplasticizers on the strength development characteristics are generally believed to be commensurate with reductions in the w/b ratio[8, 252-253]. According to Sharobim[254] a reduction in water content of 30% or more in superplasticized concrete can increase the compressive strength by about 50% compared to the control non-superplasticized concrete. Although the increased strengths have in some cases been associated with: greater exposure of the cement surface to hydration (due to increased dispersion of the particles)[8, 122, 255], stronger paste-aggregate bonding and reduced quantities of $Ca(OH)_2$[203], the w/b ratios in these investigations have often been lower than those of the control non-superplasticized mixes[34, 162, 254]. There is a lack of information in the literature as to the ultimate fate of superplasticizers in hardened concretes[58], and whether they fundamentally influence the nature of the final hydration products[122, 252].

The 10-15 Nmm^{-2} higher 28-day cube strengths produced by the control SNF superplasticizer when compared to the Acrylate-based (D2001) superplasticizer in Table 9.2, do however suggest that these polymers influence the long-term hydration behaviour and/or the nature of the hydration products formed. According to Aitcin and

Baalbaki[13] low molecular weight polymers induce more pronounced retardation (i.e. extend the setting processes and, hence, reduce the early-age strengths), primarily by adsorption on C_3S sites of the cement. The effects of superplasticizer molecular weights, chain lengths and/or chemical structures on the 28-day and long-term strengths are however not known and, therefore, need to be investigated. As mentioned in section 4.2.2, these superplasticizer details were not provided by the admixture suppliers.

(IV) NSC (influence of w/b ratio)

The compressive strength of a given concrete mixture as shown in figure 2.69 is inversely related to its w/b ratio[1, 8, 22, 52], and it is well known that during hydration portland cement combines chemically with about 17-22% water by mass of the unhydrated cement[11, 95]. In NSC, the excess unhydrated water is believed to create an open network of pores, a weaker cement paste-matrix and transition zone which reduce its strength and durability[11, 256].

As can be seen from Table 9.2, the variations in the cube strengths of the NSC mix are consistent with those for the HSC mixes, both show systematic improvements in compressive strength with increasing amplitude of vibration and decreasing yield value. The continuous reductions in the plastic viscosity of the mix, as found with the HSC mixes, do not appear to influence the maximum cube strengths obtained by vibration. These results therefore mean that although the spread-time method used in section 8.4 over-estimates the plastic viscosity of NSCs (figure 8.11(b)), it can nevertheless be successfully used to optimise their hardened properties.

Table 9.1 : Summary of fresh and hardened concrete properties for increasing vibration durations (at 0.7 mm amplitude, 120-130 mins casting time)

Mix	Vibration details		Fresh properties			Hardened concrete properties (at 28-days)					
						Density (kgm^{-3})			Comp. **strength** (Nmm^{-2})		
	Duration (secs)	T_{go}	Spread value (mm)	g value (Nm)	h value (Nms)	Cube 1	Cube 2	**Average**	Cube 1	Cube 2	**Average**
OPC	0	0	285	5.75	11.5	2482	2457	2469.5	71	57	64
	15	1/2	370+	1.8	7.4	2492.1	2487.1	2489.6	104.3	98.7	101.5
	30*	1	610	0	3.1	2509.4	2514.5	2512.0	109.5	111.5	110.5
	60	2	670	0	2.4	2512	2510	2511.0	106	112	109
10% CSF	0	0	295	4.20	9.39	2470	2479	2474.5	74	85	79.5
	10	1/2	415	0.66	5.5	2501	2493	2497.0	111.2	114.8	113
	20*	1	585	0	3.0	2517	2512	2514.5	118.7	121.3	120
	40	2	670+	0	2.2	2520	2511	2515.5	119.5	117.3	118.4

* represents the optimum/minimum vibration duration to obtain zero g value.

Tgo represents the vib. duration relative that required to obtain zero g value.

\+ represents fresh properties inferred/interpolated from vib.-response data (Appendix D).

Table 9.2 : Summary of fresh and hardened concrete properties of mixes compacted at increasing vibration amplitudes (120-130 mins casting time).

Mix	Vibration details		Fresh properties			Hardened concrete properties (at 28-days)					
						Density (kgm^{-3})			Comp. **strength** (Nmm^{-2})		
	Duration (secs)	**Amp-litude** (mm)	Spread value (mm)	g value (Nm)	h value (Nms)	Cube 1	Cube 2	**Average**	Cube 1	Cube 2	**Average**
OPC	0	0	285	5.75	11.5	2471	2483	2477	72.3	83.5	77.9
	60	0.1	345	3.89	10.2	2489	2482	2485.5	94.7	99.1	96.9
	60	0.4	630	0	3.4	2506	2506	2506	108.3	110.1	109.2
	30	0.7	610	0	3.1	2509	2505	2507	110.8	108.6	109.7
10% **CSF** (SNF)	0	0	295	4.20	9.39	2481	2495	2488	78.4	86.9	82.7
	60	0.1	450	1.89	7.71	2500	2499	2499.5	108.1	111.4	109.8
	30	0.4	605	0	3.2	2516	2520	2518	120.3	122.5	121.4
	20	0.7	585	0	3.0	2518	2519	2518.5	120.7	123.5	122.1
40 /10 **PFA/ CSF**	0	0	600	1.27	6.25	2486	2479	2482.5	86.3	91.1	88.7
	20	0.1	560	0	3.5	2503	2501	2502	92.2	96.7	94.5
	10	0.4	525	0	3.1	2496	2504	2500	94.8	97.0	95.9
	5	0.7	460	0	3.3	2507	2498	2502.5	93.7	96.4	95.1
60 /10 **GGBS/ CSF**	0	0	340	3.73	10.75	2477	2485	2481	72.9	80.7	76.8
	60	0.1	460	1.73	7.5	2493	2489	2491	89.8	93.4	91.6
	60	0.4	635	0	3.3	2511	2507	2509	100.7	97.3	99.0
	20	0.7	570	0	3.3	2505	2509	2507	99.2	96.3	97.8
10% CSF (**D2001** polymer)	0	0	200	6.77	11.95	2445	2470	2457.5	56	78	67.0
	60	0.1	345	3.89	10.2	2483	2487	2485	95.8	100.2	98.0
	60	0.4	610	0.14	3.88	2501	2496	2498.5	114	108	111.0
	60	0.7	645	0	3.0	2503	2506	2504.5	109	111	110.0
NSC (0.50 w/b)	0	0	200	3.95	2.16	2295	2327	2311	11.1	19.4	15.3
	60	0.1	480	1.44	7.0	2355	2357	2356	29.5	30.9	30.2
	10	0.4	510	0	3.4	2372	2367	2369.5	45.2	41.8	43.5
	5	0.7	455	0	3.41	2371	2385	2378	45.2	46.4	45.8

Table 9.3 : Influence of 60-70 mins casting time on the strength development characteristics of 10% CSF binary mixes (incorporating SNF and D2001 superplasticizers)

10% CSF (SNF)	0	0	495	1.16	6.76	2476	2471	2473.5	79.3	88.1	83.7
	30	0.1	600	0	3.3	2481	2485	2483	101.2	105.8	103.5
	20	0.4	570	0	3.3	2489	2493	2491	104.1	106.3	105.2
	10	0.7	500	0	3.6	2485	2489	2487	103.5	107.2	105.4
10% CSF (**D2001** polymer)	0	0	480	2.15	8.29	2467	2471	2469	67.0	73.0	70.0
	30	0.1	590	0	3.5	2479	2484	2481.5	89.0	95.0	92.0
	20	0.4	540	0	3.9	2483	2489	2486	93.7	98.3	96.0
	10	0.7	480	0	4.1	2485	2488	2486.5	94.5	99.5	97.0

. All mixes, except the NSC, have a 0.26 w/b ratio. All mixes were produced with the **SNF** superplasticizer, except the 5th and 2nd mixes in Tables 9.2 and 9.3 which used the Acrylate-based (**D2001**) superplasticizer.

. The **spread values** for the non-vibrated mixes represent the final collapse spreads (under self-weight), whereas those for the vibrated mixes represent slump-spreads measured at the specified vibration durations. (After vibration, the mixes continued to deform/flow at a decreasing rate, and their final slump-spread values were typically 50-150 mm larger than those in Tables 9.1-9.3).

. The non-vibrated cube densities represent the bulk values determined from the mass and dimensions of the cubes.

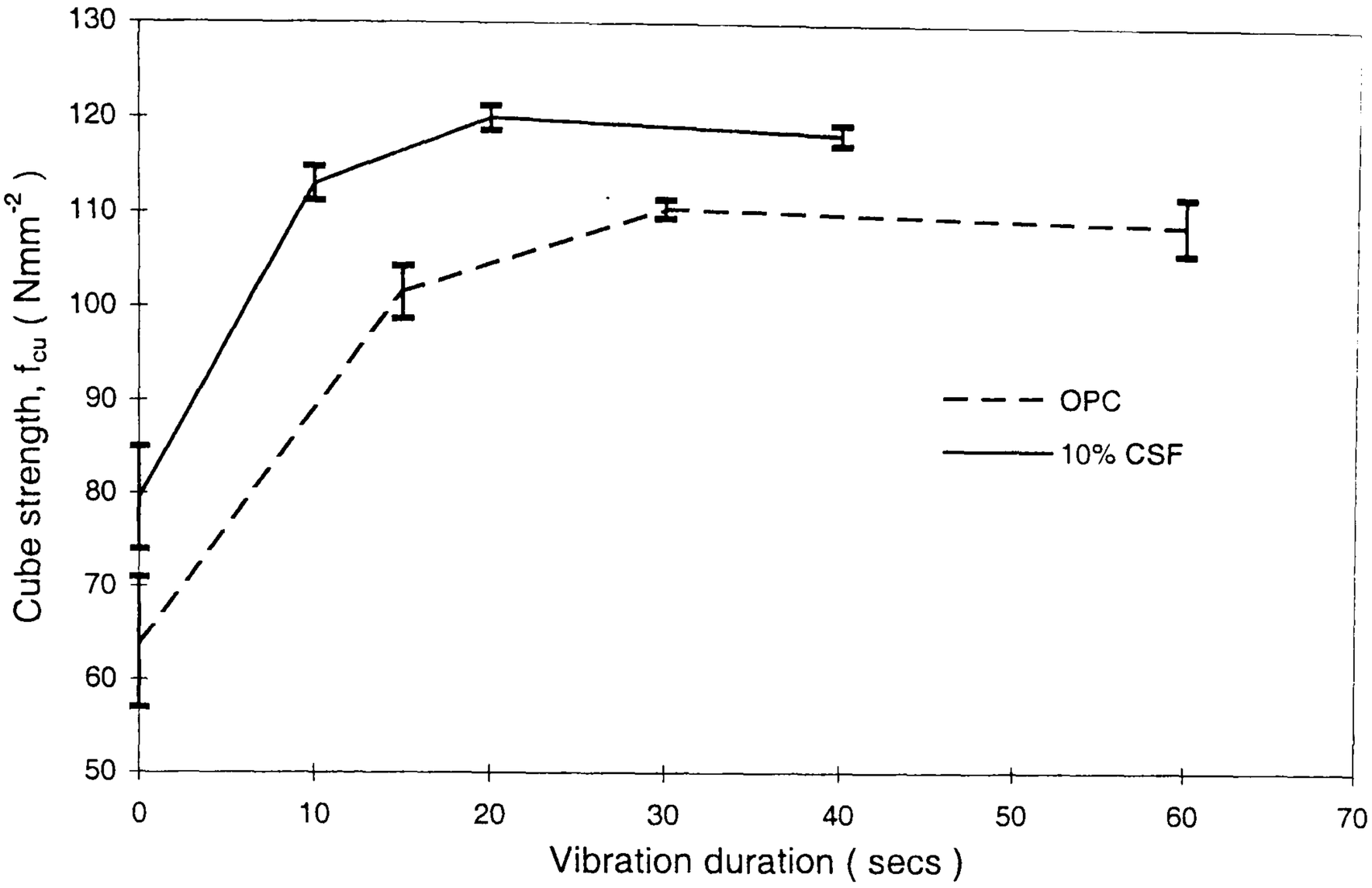

Figure 9.1 : Effects of increasing vibration duration on 28-day compressive strength development of OPC and 10% CSF mixes (100 mm cubes, 0.26 w/b ratio, 0.70 mm vibration amplitude).

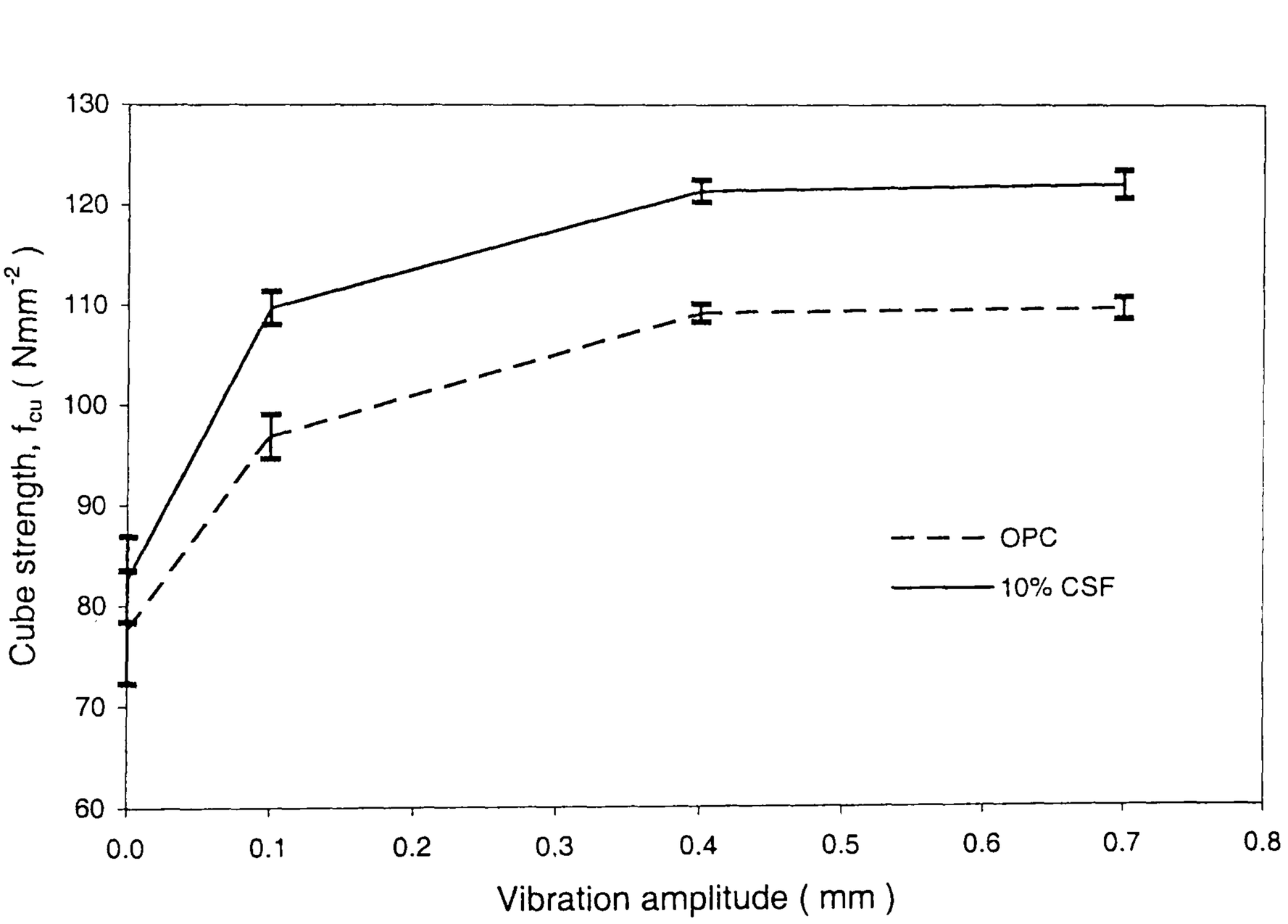

Figure 9.2 : Effects of increasing amplitude of vibration on 28-day compressive strength development of OPC and 10% CSF mixes (100 mm cubes, 0.26 w/b ratio, and varying vib. duration).

9.2.3 Effects of casting time

A comparison of the results in **Tables 9.2 and 9.3** shows that the vibrated cube strengths of the two binary 10% CSF mixes at the 60-70 mins casting time, and three amplitudes, are consistently lower (by as much as 6-16.7 Nmm^{-2}) than those compacted between 120-130 mins. The slightly lower non-vibrated cube strengths at the 120-130 mins casting time can be attributed to the reduced workability (or self-levelling properties) of the mixes with time.

As mentioned previously in section 2.8, Al-khalaf and Yousif[217] attributed their 3-4 Nmm^{-2} improvements in compressive strength with casting time in NSC to effects of revibration (c.f. figure 2.70(a)), which they suggest eliminate plastic shrinkage, settlement cracks and internal defects due to bleeding. They believe that the strength reductions occurring beyond the 3 hrs casting time (as shown in figure 2.70(b)) can be attributed to disturbance of the setting processes by vibration, which damages the bonds formed by the hydration products. Another possible cause for the increased strengths with casting time is loss of part of the mixing water (i.e. a reduction in the w/b ratio of the mixes) by evaporation.

It should be noted that both BS1881: part 108[219] and ASTM C 192M-98[220], like most concrete users/researchers, place no emphasis on the effects of casting time on strength development. The present results indicate that adequate provisions for casting time are important in HSC production, particularly with regards to quality control and settling construction disputes.

9.3 Effects of vibration duration and amplitude on cube density

The results in **Tables 9.1-9.3** clearly show that the cube densities of the mixes tested are closely related to cube strength, both increase systematically with increasing vibration duration and amplitude. That is, full-compaction of the concrete to maximum density (as with strength) occurs when the yield value is eliminated during vibration, and that

the continuous reductions in plastic viscosity with prolonged vibration (Table 9.1) have negligible effects on the densification of the cubes. (A graphical relationship between the measured cube strengths and densities is presented in section 9.4).

The hardened properties in Table 9.1 agree with those by Forssblad and Sallstrom[221], showing that prolonged vibration has insignificant effects on density and compressive strength (c.f. figure 2.71). Their results in figure 2.72 suggest that the gradual improvements in mechanical properties up to full-compaction are largely due to reduced total pore volume. In practice, the fewer and more discontinuous the pore spaces are in the hcp matrix, the greater is the densification of the concrete, and the lower is the susceptibility of the concrete to deterioration from ingress of chlorides, sulfates, or other aggressive agents[33, 94, 168, 221].

A possible reason for the consistently higher densities of the control 10% CSF cubes in Tables 9.1-9.3 is self-desiccation. As mentioned previously in section 1.3.2, HSCs containing CSF are believed to be more susceptible to self-desiccation during hardening[11-12, 44] (i.e. to loss of non-bound mixing water by evaporation). In this respect the interior of the control 10%CSF cubes (after removal from the curing water and compression testing) was found to be much drier than that of the other mixes.

9.4 Summary of results, and hardened property–Bingham parameter relationships

The results of the six mix compositions tested in Tables 9.1-9.3 have for the first time shown how the variations in the Bingham parameters during compaction influence the mechanical properties in the hardened state. As found, the 100 mm cube strengths and densities increase with increasing vibration durations and amplitudes.

- The maximum cube strengths and densities coincide with the optimum vibration durations/amplitudes needed to obtain zero yield value.
- Lower vibration durations/amplitudes giving non-zero yield values produce reduced cube strengths and densities, whereas higher vibration durations/amplitudes produce similar strengths and densities as the fully compacted cubes.

The mechanical properties of the cubes however appear to be unaffected by continuous reductions in plastic viscosity following full compaction at higher vibration durations/amplitudes.

Figure 9.3 shows the relationship between the cube strengths and densities of the mixes tested in Tables 9.1-9.3. Relationships between the measured cube strengths and the Bingham parameters (in Table 9.1-9.3), and between the improvements in cube strengths and reductions in Bingham parameters (up to full-compaction) are presented in figure 9.4(a) and 9.4(b). The results in **figure 9.3**, as mentioned earlier on page 313, clearly show that the cube strengths and densities are closely related, giving a high correlation coefficient of 0.9278. Similar results have been cited by Neville[8] for NSC mixes.

Although the results in Tables 9.1-9.3 indicated that the cube strengths and densities of the mixes tested increase with reductions in their Bingham parameters (up to full compaction), **figure 9.4(a)** shows that there are no overall relationships between the measured cube strengths with either the yield value ($r = 0.4610$) or plastic viscosity (0.2977). That is, the compressive strengths of the various mixes tested are ultimately governed by variations in their mix compositions (viz. the different CRMs, superplasticizers and w/b ratios used).

The results in **figure 9.4(b)** do however confirm that the observed improvements in cube strengths (up to full-compaction) are significantly influenced by the reductions in the Bingham parameters during vibration, giving fairly high correlation coefficients of 0.8158 (with yield value) and 0.7659 (with plastic viscosity). (Similar relationships were obtained between the cube densities and the Bingham parameters (c.f. Appendix E, figure E1)). The next section examines the effects of vibration duration and amplitude on the homogeneity of short concrete columns.

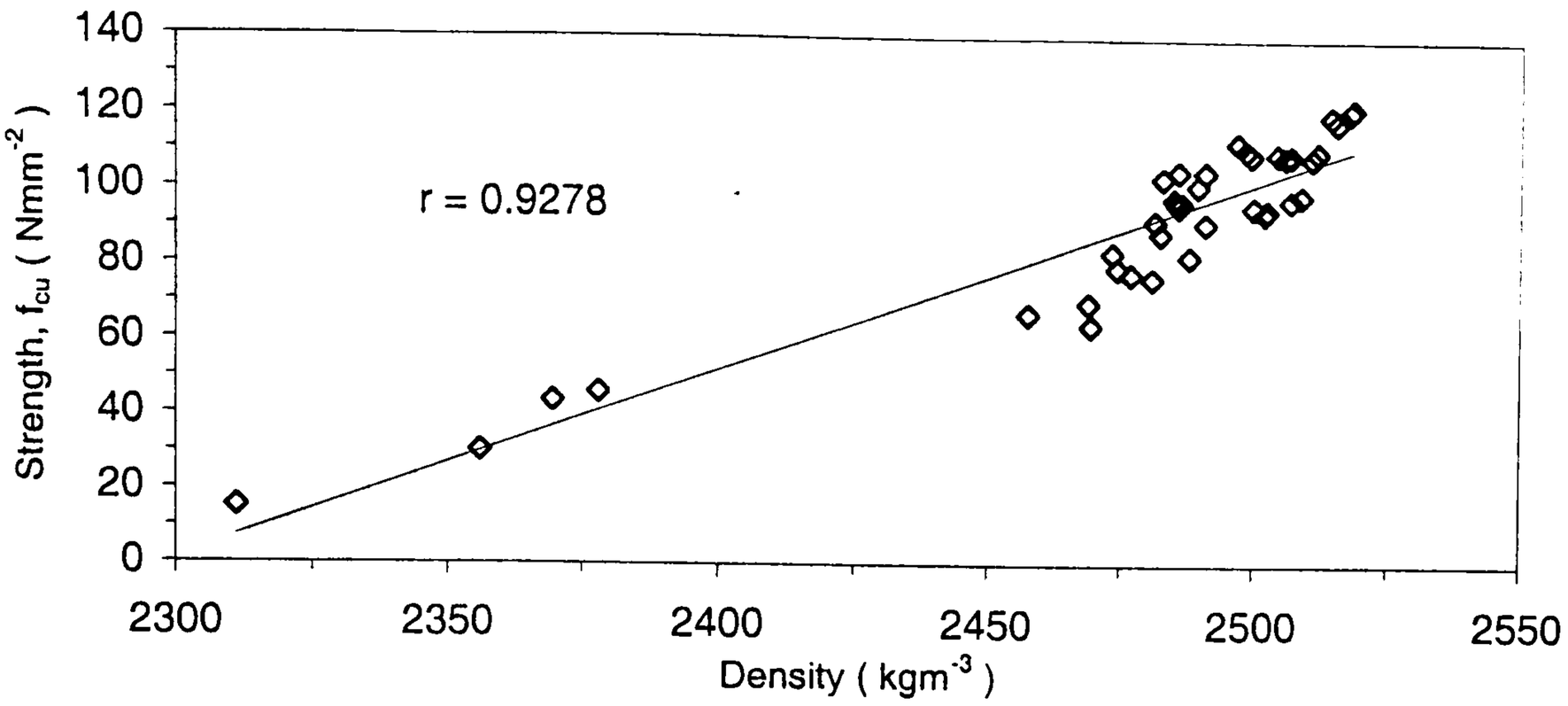

Figure 9.3 : Cube strength - density relationship for mixes in Tables 9.1-9.3.

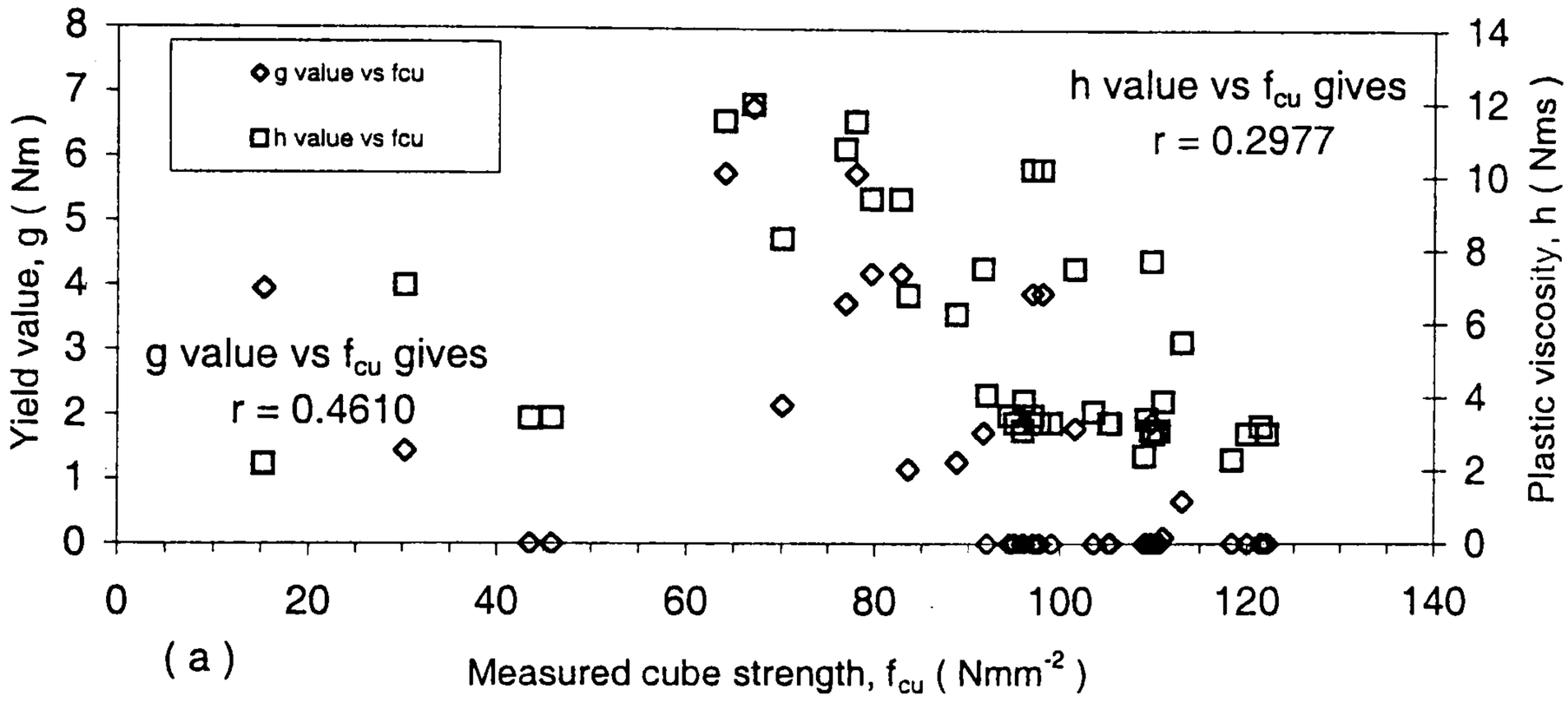

Figure 9.4 : Cube strength - Bingham parameter relationships in terms of their (a) magnitudes (as shown in Tables 9.1-9.3) and (b) differences in magnitude (up to full-compaction).

9.5 Effects of vibration duration and amplitude on the homogeneity of short concrete columns

Although both BS 1881: part 108[219] and ASTM C 192M-98[220] stress the need of avoiding excessive segregation caused by over-compaction of fresh concretes, they provide no guidelines for determining the minimum vibration durations and/or inputs required for effective compaction.

This section reports the results of tests on nine short columns (500x100x100 mm), which were cast to assess the effects of vibration duration and amplitude on the changes in strength and density produced by segregation of the OPC and 10% CSF reference mixes. Specimens cut from the columns for evaluation of the hardened properties, unfortunately, did not give perfectly dimensioned cubes. Their heights varied between 97-103 mm and, therefore, could not be used for direct determination of compressive strength as described in section 4.4.1.

Evaluation of the column strengths was instead based on non-destructive ultrasonic pulse velocity (UPV) measurements, and their relationship with the compressive strengths of standard 100 mm cubes. This involved measurements on the cubes tested in Table 9.1, and included data reported by Price and Hynes[257] showing a good linear relationship between UPV and cube strength (in moderate-high grade concretes produced with granite aggregate).

Although UPV measurements are known to be sensitive to, for example, surface moisture variations and aggregate type[8, 257], the two sets of results gave a highly significant empirical relation (strength, **fcu = 75.189 UPV + 256.54**) with a correlation coefficient of 0.9478 (as shown in **figure 9.5**). This was used to predict the strengths of the columns at 100 mm vertical intervals as described in section 4.4.2.

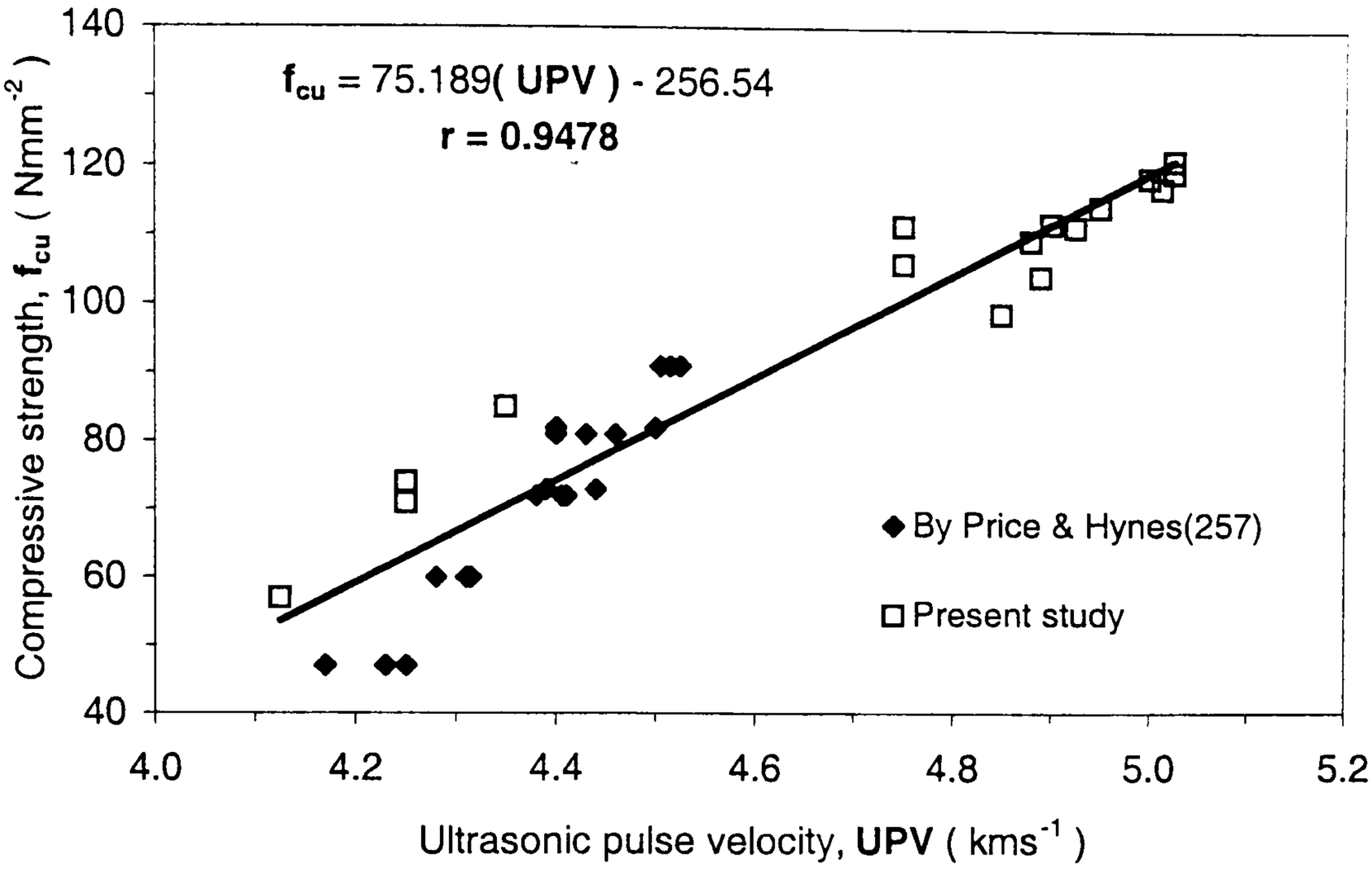

Figure 9.5 : Relationship between cube strength and UPV (for granite based mixes)

The results obtained with the mixes in **Tables 9.4-9.5** and **figures 9.6-9.7** confirm the observations by Tachibana et al[18] that the application of vibration invariably causes segregation of fresh concretes (c.f. figure 2.63), and accordingly reduces the homogeneity of hardened concretes. This is represented by progressive reductions in both column strength and density with height, and by wider variations in the mechanical properties between the upper and lower parts of the columns with increasing vibration durations and amplitudes.

9.5.1 Effects of vibration duration

The results in **Table 9.4** and **figure 9.6** show that full-compaction of the concrete, as defined by the elimination of the yield (g) value, decreases rather than increases the overall homogeneity (or uniformity) of the hardened concrete compared to lower degrees of compaction. The much higher mechanical properties of the fully-compacted concretes, do however confirm that the use of low vibration durations (producing non-zero g values) are, for example, less effective in: eliminating mechanical voids,

achieving the closest possible nesting and pore refinement of the concrete - as suggested by Welton[218].

The lower strengths and densities at the top of the over-vibrated columns (Nos. 3 and 6). on the other hand, indicate that the continuous reductions in plastic viscosity with prolonged vibration, can adversely influence the quality of the concrete in the upper parts of thick structural elements (or deep pours). The results are in disagreement with the cube measurements in Table 9.1, which revealed no clear relationship between the mechanical properties in the hardened state and the continuous reductions in plastic viscosity following full-compaction.

It is worth noting that, the narrower differences in upper-lower column strengths and densities of the OPC mix (7.7-18.7 Nmm^{-2}, 11-22 kgm^{-3}) when compared to the 10% CSF mix (10.8-22 Nmm^{-2}, 15-26 kgm^{-3}) in Table 9.4, are consistent with the segregation indices of the mixes before vibration (5 and 8% respectively). That is, the results suggest that there is good agreement between the segregation resistance of fresh concretes during two-point testing and the homogeneity of hardened concretes. Similar inferences were reached by Ellis and Wimpenny[258], who compared the torque changes (T_C) of NSC mixes during two-point testing, with UPV measurements on concrete columns vibrated for a fixed duration of 2 minutes.

9.5.2 Effects of vibration amplitude, and further discussion

The results in **Table 9.5** and **figure 9.7**, in agreement with the cube measurements in Table 9.2, show that the column strengths and densities increase with increasing amplitude of vibration from 0-0.4 mm, and are comparable at the medium and highest amplitudes of 0.4 and 0.7 mm. That is, the results confirm that the mechanical properties in the hardened state increase with decreasing yield value, down to the lowest value (zero Nm) corresponding to full-compaction of the fresh concrete as found in Table 9.2.

Observations during compaction of the mixes in Tables 9.4-9.5 indicated that the concrete in the columns undergoes some re-circulation of flow, similar to that reported by Kakuta and Kojima[212] from their vibration tests with the LM system (page 103). The effect was accompanied by intense bubbling on the top column surface, and was more pronounced at higher degrees of compaction.

Visual inspection of the upper and lower cube specimens in Tables 9.4-9.5, indicated that the reduced homogeneity during vibration results from : higher coarse aggregate concentrations (i.e. sedimentation) on the bottom of the columns, and an accumulation of bleed water (producing thicker deposits of scum) on the top. The occurrence of bleed water channels and aggregate concentrations in concrete are in practice associated with fissures in the hcp matrix, weak bonding with reinforcement, porosity and consequent loss of durability[156, 259].

In contrast to the present observations with the table vibrator, Forssblad and Sallstrom[221] reported that the use of internal poker vibrators for durations of 15 secs or more, can cause localised segregation (or dislodgement) of moderate-strength concretes in areas close to the vibrator insertions, and adversely affect their air-void system (or durability) in the hardened state. The present results however show that depending on mix composition, workability before vibration and vibration input, vibration durations of up to 60 secs or more may be required for effective compaction with external (or table) vibrators, and that these cause segregation of the whole concrete mass. Although ACI committee 309[65] reported that the radius of action of internal poker vibrators is as much as 50% lower in reinforced concrete than in plain concrete, it has not stated how this compares to the use of external vibration.

Further work should therefore compare the effectiveness of both external and internal vibration techniques, assess the minimum energy requirements to achieve full-compaction in reinforced concrete, and examine the confining effects of the reinforcement in reducing segregation in typical structural elements.

Table 9.4 : Summary of fresh properties and hardened concrete column measurements corresponding to increasing vibration durations (at 0.7 mm amplitude, and 120-130 mins casting time).

Mix	Column No. (& amp-litude)	Vibration details: Duration (secs)	Vibration details: T_{go}	Fresh properties: Spread value (mm)	Fresh properties: g value (Nm)	Fresh properties: h value (Nms)	Hardened concrete properties (at 28-days): Column height (mm)	UPV (kms^{-1})	Predicted strength (Nmm^{-2})	Cube No.	Density (kgm^{-3})	Range in column Strength (& density)
OPC	1 (0.7 mm)	15	1/2	370	1.8	7.5	450	4.71	97.3	5	2479	7.7 (11)
							350	4.74	99.8	4	2484	
							250	4.76	101.5	3	2483	
							150	4.80	104.1	2	2488	
							50	4.81	104.9	1	2490	
	2 (0.7 mm)	30*	1	610	0	3.1	450	4.77	102.4	5	2497	13.3 (17)
							350	4.81	104.9	4	2503	
							250	4.87	109.3	3	2509	
							150	4.93	113.8	2	2513	
							50	4.95	115.7	1	2514	
	3 (0.7 mm)	60	2	670	0	2.4	450	4.74	99.8	5	2495	18.7 (22)
							350	4.78	103.2	4	2504	
							250	4.84	107.6	3	2511	
							150	4.94	114.8	2	2515	
							50	4.99	118.5	1	2517	
10% CSF	4 (0.7 mm)	10	1/2	415	0.66	5.5	450	4.83	106.7	5	2497	10.8 (15)
							350	4.84	107.6	4	2501	
							250	4.90	112.0	3	2507	
							150	4.95	115.7	2	2510	
							50	4.98	117.5	1	2512	
	5 (0.7 mm)	20*	1	585	0	3.0	450	4.89	111.1	5	2504	15.9 (20)
							350	4.94	114.8	4	2507	
							250	5.01	120.3	3	2514	
							150	5.06	124.2	2	2519	
							50	5.10	127.1	1	2524	
	6 (0.7 mm)	40+	2	670	0	2.3	450	4.80	104.1	5	2500	22.0 (26)
							350	4.87	109.3	4	2506	
							250	4.96	116.6	3	2517	
							150	5.05	123.2	2	2520	
							50	5.09	126.1	1	2526	

Table 9.5 : Summary of fresh properties and hardened concrete column measurements corresponding tc increasing amplitudes of vibration (at 120-130 mins casting time).

Mix												
10% CSF	7 (0 mm) Ref. column	0	0	295	4.20	9.39	450	4.63	91.6	5	2491	5.7 (7)
							350	4.65	93.2	4	2494	
							250	4.68	95.6	3	2495	
							150	4.67	94.8	2	2499	
							50	4.71	97.3	1	2498	
	8 (0.1 mm)	60	1	450	1.89	7.71	450	4.81	104.9	5	2497	10.7 (12)
							350	4.85	108.5	4	2499	
							250	4.88	110.2	3	2505	
							150	4.93	113.8	2	2506	
							50	4.95	115.7	1	2509	
	9 (0.4 mm)	30	1	605	0	3.2	450	4.90	112.0	5	2500	14.1 (22)
							350	4.93	113.8	4	2508	
							250	4.98	117.5	3	2511	
							150	5.05	123.2	2	2520	
							50	5.09	126.1	1	2522	
	5 (0.7 mm)	20*	1	585	0	3.0	450	4.89	111.1	5	2504	15.9 (20).
							350	4.94	114.8	4	2507	
							250	5.01	120.3	3	2514	
							150	5.06	124.2	2	2519	
							50	5.10	127.1	1	2524	

* represents the optimum vibration duration and, + represents fresh properties infered from vibration-response data (c.f. figure 8.9).

The UPV measurements represent average values determined on cube centres in two mutually perpendicular directions.

In each case, the combined weight of concrete cast and column-mould was approximately 26.5 kg.

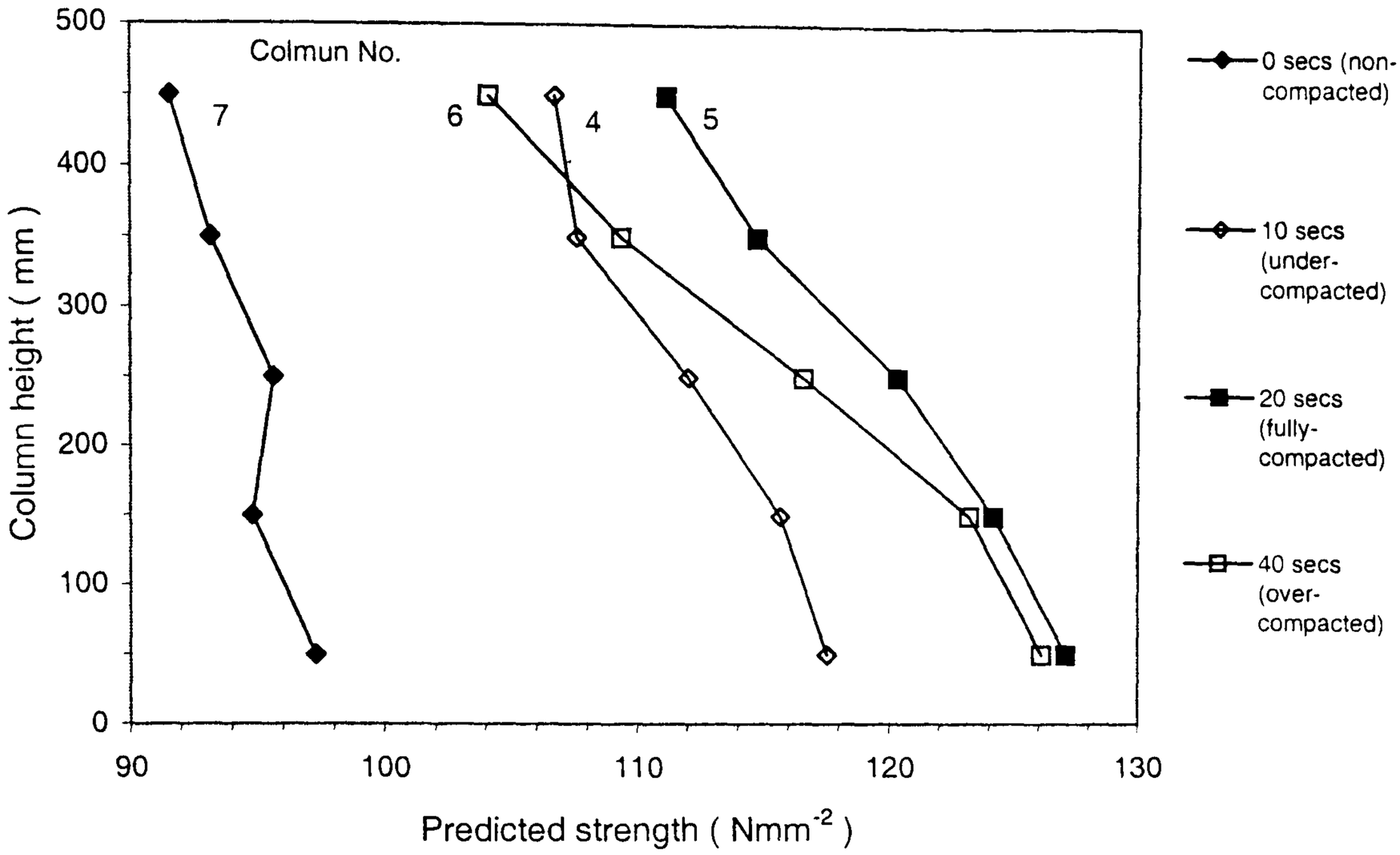

Figure 9.6 : Variations in 28-day column strength with increasing vibration duration (10% CSF mix, 0.26 w/b, 0.70 mm vib. amplitude).

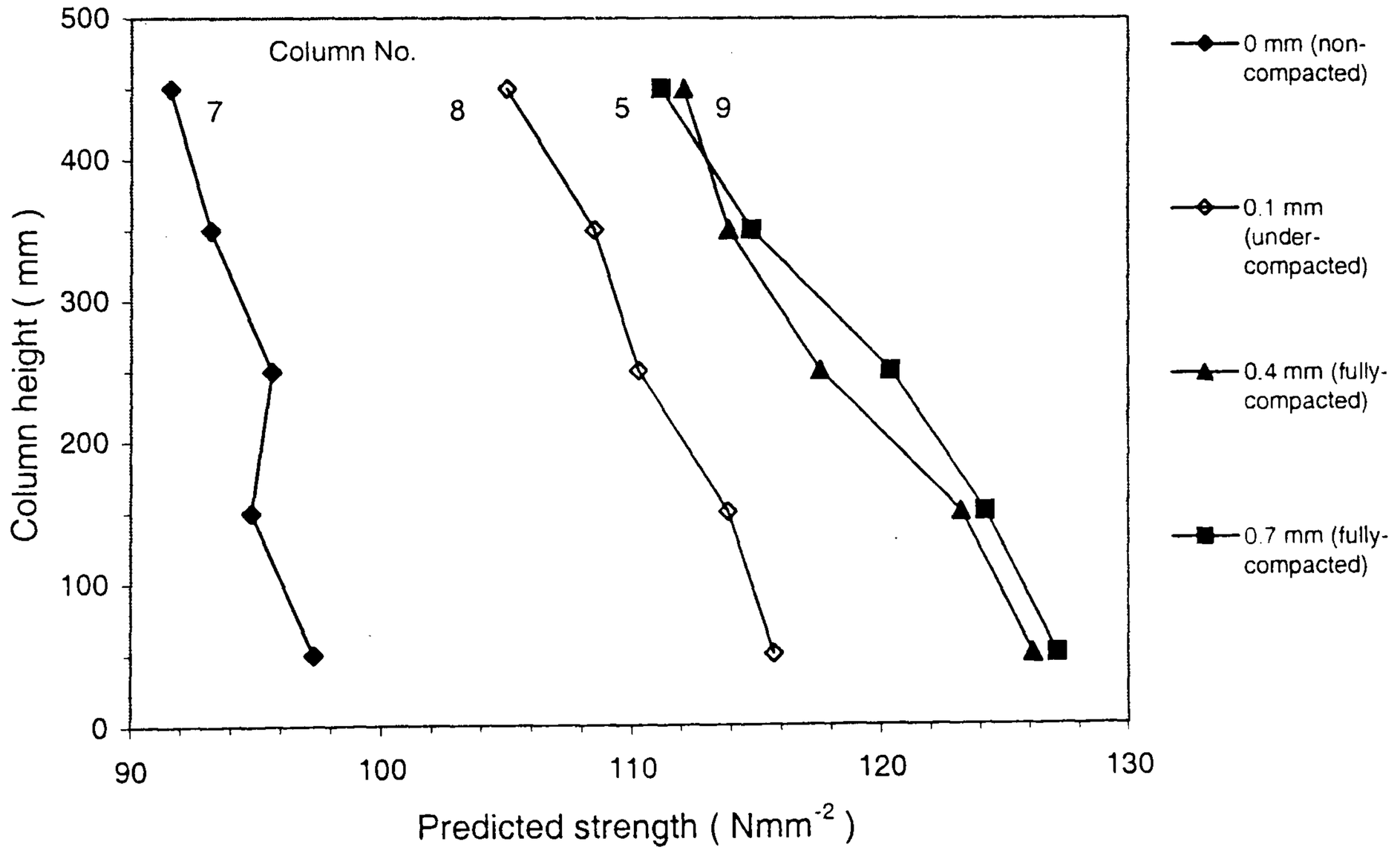

Figure 9.7 : Variations in 28-day column strength with increasing amplitude of vibration (10% CSF mix, 0.26 w/b, varying vib. duration).

9.5 Conclusions

- The 28-day compressive strengths, densities and homogeneities of hardened concretes are significantly influenced by reductions in the Bingham parameters during compaction by vibration.

- The yield value is the main parameter influencing the improvements in compressive strength and densification of hardened concretes, whilst the plastic viscosity appears to mainly influence the homogeneity (or structural integrity) at high degrees of compaction, particularly in deep/large pours.

- The compressive strengths and densities of 100 mm cubes and short columns (500x100x100 mm) increase by up to 46.5 Nmm^{-2} and 58.5 kgm^{-3} with increasing vibration durations/amplitudes compared to the non-compacted specimens. The maximum strengths and densities coincide with the attainment of the lowest yield value (of zero Nm) corresponding to full-compaction of fresh concretes.

- Continuous reductions in plastic viscosity following full-compaction at high vibration durations/amplitudes, produce local defects represented by up to 22 Nmm^{-2} and 26 kgm^{-3} reductions in column strengths and densities with increasing column height. The lower the plastic viscosity during vibration, the larger is the difference in the homogeneity between the upper and lower parts of concrete columns.

- The 28-day cube strengths and densities produced by a 10% CSF binary mix, at 0.26 w/b ratio and varying vibration durations/amplitudes, are 9-13 Nmm^{-2} and 2.5-14 kgm^{-3} higher than those of the reference OPC mix, and 18-27 Nmm^{-2} and 8.5-18 kgm^{-3} higher than those due to ternary blended mixes of 40%PFA+10%CSF and 60%GGBS+10%CSF. The 28-day cube strengths and densities produced by an OPC mix at 0.26 w/b ratio and varying vibration durations/amplitudes are as much as 67 Nmm^{-2} and 137 kgm^{-3} higher than those at 0.50 w/b ratio.

Chapter 10
Conclusions and Recommendations for Further Work

10.1 Introduction

This chapter presents the main conclusions from the experimental work carried out in chapters 5-9, their practical implications for HSC users, and then recommendations for further work. The main areas covered were:

1. Preliminary **rheological measurements** (focusing on the effects of decreasing w/b ratio, rheological relationships, and the suitability of test methods).
2. Assessment of **superplasticizers**.
3. Assessment of **cement replacement materials** (**CRMs**).
4. **Flow properties**, **placing** characteristics, and **vibration response** of HSC.
5. 28-day **strength development** (at different degrees of compaction by vibration).

10.2 Conclusions

(I) Preliminary Rheological Measurements

1. A reduction in the w/b ratio from 0.42 to 0.26 reduces the initial workability (i.e. increases both the yield value and plastic viscosity), but gives no conclusive trend with respect to loss of workability when assessed by the MH system at a constant initial slump of 220±5 mm (c.f. figure 5.2, and also page 327 (point 4)).

2. Two-point workability measurements with the MH system indicate that:
   - the yield value has a greater influence on the mix stability of HSCs than the plastic viscosity (c.f. figure 5.6(b), page 163); whereas
   - the plastic viscosity has a greater influence on the compactability under self-weight than the yield value (c.f. figure 5.6(a)). (In contrast, measurements with the LM system indicate that the segregation resistance of high workability HSCs is mainly governed by the plastic viscosity (c.f. figure 6.12). The effects

of vibration on the Bingham parameters are given in section 10.2 (IV)).

3. Tattersall's assertions that the MH and LM versions of his two-point test apparatus respectively measure medium-to-high and medium-to-low workabilities are misleading and incorrect (c.f. figure 5.10-5.11 and Tables 5.1-5.2).
   - The MH system suffers from significant up-lift effects exerted by the helical shape of its impeller. These increase the volume of the concrete during testing by much as 30%, reduce its shearing resistance with decreasing slump, and lead to continuous reductions in plastic viscosity with time.
   - In contrast, the LM system does not cause any noticeable volume expansions of the concrete and, is capable of measuring representative variations of workability in the high-medium slump range.

4. Mortar spread and V-funnel flow time measurements respectively show slightly greater dependencies on the yield value and plastic viscosity, but can not be explicitly related to either of the Bingham parameters (sections 5.6 and 6.7.2). The mortar fractions of HSCs are:
   - suitable for predicting the initial workability properties and fixing the saturation dosages, but
   - less suitable for assessing loss of workability (c.f. figures 6.14-6.16).

(II) Assessment of Superplasticizers

1. A comparison of conventional and new-generation superplasticizers (based on SMF, SNF, MLS, Vinyl and Acrylate polymers), at a constant dosage of 2.00% s/w/b and 0.26 w/b ratio, shows:
   - higher initial workability with the Acrylate-based NG superplasticizer, but
   - longer workability retention with the SNF superplasticizer (c.f. figure 6.2).

2. The initial workability properties and losses of workability of SMF, SNF, MLS, Vinyl and Acrylate-based superplasticizers are principally dosage dependent (c.f. figure 6.3, page 201).

- The saturation dosage produces the highest initial workability and longest workability retention.
- Lower SNF dosages give relatively larger time-dependent increases in yield value; whereas higher dosages mainly increase the rate of development of plastic viscosity (c.f. figure 6.4).

3. The optimum addition time of SMF, SNF, MLS, Vinyl and Acrylate-based superplasticizers is 4 mins after the cement first comes in contact with the mixing water. Shorter addition times increase the dosage demand, reduce the initial workability, and give faster losses in workability (c.f. figures 6.5-6.6, and Table 6.3).
   - A 0/4 mins split addition of SNF superplasticizer increases the initial yield value, reduces the initial plastic viscosity, but increases the rate of loss of workability in the first 120 mins (c.f. figure 6.7).
   - Retarded SNF and Acrylate-based superplasticizer blends reduce the initial workability, but give longer workability retention in the first 120 mins compared to the non-retarded mixes (c.f. figure 6.7).

4. The compatibility of cement types I, III and V with SMF, SNF, MLS, Vinyl and Acrylate-based superplasticizers shows no distinct performance differences.
   - With each of the five superplasticizers, cement types V and III respectively produce reduced and increased dosage demands, but higher and lower initial workabilities compared to Type I cements (c.f. figure 6.8-6.9).
   - With cement Types I, III and V, the initial workability of the SNF is slightly lower than the Acrylate-based superplasticizer, but higher than the SMF, MLS, and Vinyl-based polymers. The SNF superplasticizer produces longer workability retention than the SMF superplasticizer when used with cement Types I and V (c.f. figures 6.2, 6.10).

(III) Assessment of Cement Replacement Materials (CRMs)

1. The use of binary blended cements containing CSF or PFA reduces the saturation dosage demand of the SNF superplasticizer (c.f. figures 7.2. 7.4), and improves the initial workability properties compared to the equivalent OPC mix at 0.26 w/b ratio. The use of CSF at an optimum replacement level of 10% reduces the rate of loss of workability (c.f. figure 7.3(b)), whereas PFA appears to have negligible effects on workability retention when it replaces up to 40% of the cement (c.f. figure 7.5).

   In contrast, the use of GGBS in binary blended cements increases the saturation dosage demand (c.f. figure 7.6(b)), reduces the initial workability, and increases the rate of loss of workability compared to the reference OPC mix (c.f. figure 7.7(b)).

2. The use of ternary blended cements containing 10% CSF with 20-40% PFA or 40-60% GGBS at 0.26 w/b ratio significantly reduces the superplasticizer dosage demand (c.f. figures 7.8-7.9), increases the initial workability, and reduces the rate of loss of workability compared to the equivalent binary mixes (c.f. figures 7.10(b), 7.5(b) and 7.7(b)). The optimum replacement levels for ternary blends of PFA/CSF and GGBS/CSF (at 0.26 w/b ratio) are 40%PFA+10%CSF and 60%GGBS+10%CSF.

3. The inclusion of CSF in the binder imparts similar dispersion characteristics to those obtained with delayed additions of superplasticizers (c.f. figure 7.1). These appear to release water trapped in the cement, PFA and GGBS agglomerates, and slow down their formation with time.

4. A reduction in the w/b ratio from 0.30 to 0.22 (in CSF blended mixes) increases the saturation dosage demand (c.f. figure 7.16), reduces the initial workability, and increases the rate of loss of workability during the first two hours (c.f. page 270, figure 7.17).

(IV) Flow properties, Placing characteristics and Vibration Response

1. The rate at which fresh concrete spreads during the slump test provides a measure of both its yield value and plastic viscosity (c.f. figures 8.4-8.5). Spread-time - Bingham parameter relationships can be successfully used in assessing the placing and compaction characteristics of HSCs.

2. During placing, HSCs exhibit significant Stiffening effects which reduce their workability after 5 mins from re-mixing. The effects are more pronounced in the OPC mix than the equivalent binary 10% CSF mix (c.f. Table 8.1).

3. Both the yield value and plastic viscosity decrease progressively during compaction by vibration (c.f. figures 8.9-8.11). Whether the yield value disappears, depends on the workability of the non-vibrated concrete, its mix composition and the amplitude of vibration applied.
   - At high workabilities and/or amplitudes of vibration, fresh concretes behave as Newtonian fluids – possessing no yield value, and reduced plastic viscosity.
   - The non-zero plastic viscosities during vibration suggest that the yield value is the main parameter influencing full compaction of fresh concretes.
   - A 40%PFA+10%CSF ternary blended cement mix exhibits better vibration response properties (i.e. requires lower vibration durations and amplitudes) than a 60%GGBS+10%CSF ternary combination and, the reference OPC and 10%CSF mixes at 0.26 w/b ratio.

(V) 28-day Strength Development (at different degrees of vibration)

1. The 28-day compressive strengths and densities of hardened concretes are significantly influenced by the reductions in the Bingham parameters during compaction by vibration.

2. The yield value is the main rheological parameter influencing the improvements in compressive strengths and densities of hardened concretes after vibration (c.f. Tables 9.1-9.3), whilst the plastic viscosity appears to mainly influence the homogeneity (or structural integrity) at high degrees of compaction (c.f. Tables 9.4-9.5).

3. The compressive strengths and densities of 100 mm cubes and short columns (500x100x100 mm) increase by up to 46.5 Nmm^{-2} and 58.5 kgm^{-3} with decreasing yield value resulting from increasing vibration durations/amplitudes (c.f. Tables 9.1-9.5, figures 9.1-9.2 and 9.6-9.7). The maximum strengths and densities of the specimens coincide with the attainment of the lowest yield value (of zero Nm) corresponding to full compaction of fresh concretes.

   - In 100mm cubes, lower vibration durations/amplitudes giving non-zero yield values produce reduced strengths and densities, whereas higher vibration durations/amplitudes produce similar strengths and densities as the fully compacted cubes.
   - In 500x100x100mm columns, continuous reductions in plastic viscosity following full compaction at higher vibration durations/amplitudes, produce local defects represented by up to 22 Nmm^{-2} and 26 kgm^{-3} reductions in column strengths and densities (c.f. Tables 9.4-9.5, figures 9.6-9.7). The lower the plastic viscosity during vibration, the larger is the difference in the homogeneity between the upper and lower parts of concrete columns.

4. The 28-day cube strengths produced by a 10% CSF binary mix, at 0.26 w/b ratio and varying vibration durations/amplitudes, are 9-13 Nmm^{-2} higher than those of the reference OPC mix, and 18-27 Nmm^{-2} higher than those produced by ternary blended cement mixes containing 40%PFA+10%CSF and 60%GGBS+10%CSF. The 28-day cube strengths produced by an OPC mix at 0.26 w/b ratio and varying vibration durations/amplitudes are as much as 67 Nmm^{-2} higher than those at 0.50 w/b ratio (c.f. Table 9.2).

10.3 Practical implications of the results for users of HSC

The results and conclusions reached in this thesis can help HSC users overcome the uncertainties associated with the assessment of its workability/rheological properties, material selection, and rationalization in construction operations.

The results indicate that the initial workability properties and rate of loss of workability of HSCs can be successfully assessed by Tattersall's LM system, or alternatively by the spread-time method developed in this research (chapters 5 and 8). Although the latter is only applicable for flowing concretes (i.e. those having slumps $\geq$ about 150 mm), it demonstrates how the placing and compaction characteristics of the material could be simply and effectively evaluated and rationalized (as outlined in page 331).

The rheological measurements in chapters 5 and 8 indicate that the stability and compactability properties of HSC mixes are not distinct and independent, but can in fact be adequately described by variations in workability (i.e. the two Bingham parameters). The results show that :

- Mix stability is negatively correlated to workability - the lower the g and h values (i.e. the higher the workability), the lower the mix stability (i.e. increased bleeding and segregation tendencies), whereas the
- Compactability is positively correlated to workability, i.e. it increases with reductions in the g and h values (higher workabilities) up to full compaction, where the plastic viscosity then governs the subsequent consolidation properties of the concrete.

With regards to material selection, the results in chapters 6 and 7 demonstrate how the initial workability and loss of workability properties of HSCs can be optimized through the use of superplasticizers and CRMs. In particular the results show that :

- The optimum performance of superplasticizers based on SMF, SNF, MLS, Vinyl and Acrylate polymers occurs when they are dosed at their respective saturation dosages and, added 4 mins after the cement first comes in contact with the mixing water.
- The inclusion of CSF in both binary and ternary blended cements significantly reduces the superplasticizer dosage demand, and enhances the workability properties of HSCs at w/b ratios of 0.30-0.22.

The spread-time method, in chapter 8, allows HSC users to :

- identify suitable mixes which reduce, for example, handling and pumping difficulties during placing, and
- ascertain the changes in the Bingham parameters due to the application of different vibration durations/amplitudes during compaction.

The method also shows (in chapter 9) how the vibration response (or Bingham) properties during compaction can be effectively used to optimise the mechanical properties in the hardened state. By minimizing the damping/mass differences during testing and casting, the method enables concrete users to :

- identify the optimum/minimum vibration duration and amplitude needed to achieve maximum strengths and densities (i.e. full compaction),
- avoid the problems associated with over-compaction, and hence conserve energy resources from the vibration response properties in the fresh state.

More work is however needed to ascertain the validity and effectiveness of the spread-time method under typical field conditions involving, for example, different pumps or compaction equipment, pour sizes and reinforcement configurations.

10.4 Recommendations for Further Work

1. Comparisons of measurements obtained with the LM system and those reported for the BML viscometer and BT rheometer indicated that these two instruments produce significant up-lift effects (i.e. volume expansions) of the concrete during testing, similar to those obtained with the MH system. An evaluation of concrete volume expansions in the BML viscometer and BT rheometer is therefore needed to confirm these indications.

2. A comparative study should be undertaken to determine how molecular weight, chain length, and the inclusion of different side-chains in conventional and new-generation superplasticizers influences the Bingham parameters and their evolution with time.

A study is also required to determine the effects of soluble alkalis, calcium sulfates, and steric hinderance on the Bingham properties of HSCs having different cements, CRMs, and w/b ratios.

Measurements of the workability, adsorption, Zeta potential and hydration characteristics of cement paste, mortar, and concrete should be performed to clarify the differences in workability retention observed between mortar and concrete.

Analysis of the liquid-phases in superplasticized concretes and/or mortars is also required to determine how the Bingham parameters are influenced by the electrostatic and/or steric effects in real mixes. Previous researchers have traditionally assessed these effects using suspensions or dilute pastes having w/b ratios outside the practical range (i.e. > 1.0).

3. Adsorption and Zeta-potential measurements should also be performed to establish how the addition time of the CSF slurry influences the electrostatic and/or steric effects generated during the initial mixing sequence.

An investigation should be carried out to determine whether the rapid losses of workability observed in binary GGBS mixes are due to the immobilisation of increasing quantities of mixing water by cement-GGBS agglomerates with time.

The effects of CSF contents (exceeding 10%) in reducing the rate of loss of workability in ternary blended cements containing GGBS, or other CRMs such as metakaolin (page 76), should also be explored in mixes having low w/b ratios.

4. An identification of the factors influencing the inter-particle forces during slump collapse, and how they differ in NS and HSCs, is needed in developing representative mathematical models of the slumping process, and how this relates to the Bingham parameters.

The vibration-response measurements in chapter 8 were carried out at a fixed frequency of 50 Hz and without clamping the slump board to the vibrating table. It would therefore be interesting to compare the vibration response properties of NS and HSCs at different vibration frequencies and amplitudes, under both clamped and unclamped conditions.

The merits of the spread-time – Bingham parameter relationships in assessing the efficiencies of different pumping and compaction equipment and, in defining suitable g and h values for typical construction operations needs to be ascertained. An evaluation of the minimum energy requirements to produce full compaction from differences in the areas under the spread-time curves (figure 8.7) also needs to be undertaken.

5. A micro-structural analysis of the hardened cement paste (hcp) matrices produced by SNF and Acrylate-based superplasticizers is needed to determine whether the differences in their 28-day compressive strengths (Tables 9.2-9.3) are due to fundamental changes in the hydration products. This could be extended to assess

their effects on both the early and long-term strength development characteristics, and could include a wider range of superplasticizers.

An investigation should be carried out to determine how the continuous reductions in plastic viscosity following full compaction influence the presence of micro-pores/capillaries, and hence the durability of hardened concretes.

Further work should also compare the effectiveness of external and internal vibration techniques in both plain and reinforced concrete, and examine the confining effects of the reinforcement in reducing segregation in typical structural elements.

REFERENCES

1. ACI Committee 363. *State-of-the-art Report on High Strength Concrete*. ACI Journal, proceedings Vol. 81, No. 4, July-August 1984, pp. 364-411.

2. Domone, P. L. J. and Soutsos, M. N. *An Approach to the Proportioning of High-Strength Concrete mixes*. Concrete International, October 1994, pp. 26-31.

3. Gjorv, O. E. *High Strength Concrete*. Advances in concrete technology, CANMET, 1994, pp. 19-82.

4. Ryan, W. G.; and Potter, R. J. *Application of High-Performance Concrete in Australia*. High Performance Concrete Proceedings, ACI International Conference, Supplementary papers, Singapore, 1994, pp. 1-15.

5. Lew, H. S.; and Frohnsdorff, G. J. *U.S. Program on High-performance concrete*. High Performance Concrete Proceedings, ACI International Conference, Supplementary papers, Singapore, 1994, pp. 67-74

6. Hsu, K.C., Chiu, J.J., Chen S.D., and Tseng, Y.C. *Effect of addition time of a superplasticizer on cement adsorption and on concrete workability*. Cement and Concrete Composites, 21, 1999, pp. 425-430.

7. Tattersall, G. H. *Workability and quality control of fresh concrete*. Chapman and Hall, 1991.

8. Neville, A. M. *Properties of Fresh Concrete*. Longman Scientific and Technical, 4th edition, 1995.

9. Yoshida, T. *Making concrete with the highest strength*. Journal of the Japan society of Civil Engineers, Vol. 26, No. 11, 1930, pp. 997-1016.

10. Menzel, C. A. *Strength and volume change of steam cured cement mortar and concrete*. ACI proceedings, Vol. 31, Nov. - Dec. 1934.

11. Aitcin, P. C. and Neville, A. *High-performance Concrete Demystified*. Concrete International, January 1993, pp 21-26.

12. Malier, Y. *Introduction. High Performance Concrete from Material to Structure*. Edited by Yves Malier, E & FN SPON, 1992, pp. xiii-xxiv.

13. Aitcin, P.-C. and Baalbaki, M. *Concrete Admixtures - Key Components of Modern Concrete*. Concrete Technology; New Trends, Industrial Applications.

proceedings of the International RILEM Workshop, Edited by A. Aguado et al. Barcelona, November 1994, pp. 33-47.

14. Chan, S. Y. N., Feng N. Q., and Tsang K. C. *HSC Incorporating Carrier Fluidifying Agent*. Radical Concrete Technology, Proc. of the international conference held at the University of Dundee, Scotland, 1996, pp. 113-122.

15. Nawy, E. G. *Fundamentals of High Strength High Performance Concrete*. Longman Group Limited, 1996, 365 pp.

16. Penttala, V. *Possibilities of Increasing the Workability Time of High-strength Concretes*. RILEM proceedings, University of Hanover, Hanover, October 1990, pp 93-102.

17. Punkki J., Golaszewski, J., and Gjorv, O. E. *Workability Loss of High-Strength Concrete*. ACI Materials Journal, Sep.-Oct. 1996, pp. 427-431.

18. Tachibana, D.; Imai, M.; Yamazaki, N.; Kawai, T.; and Inada, Y. *High-Strength Concrete Incorporating Several Admixtures*. High-Strength Concrete : Second International Symposium, ACI, SP 121-16, 1990, pp. 309-330.

19. Detwiler, G. *High-Strength Silica Fume Concrete - Chicago Style*. Concrete International, October 1992, pp. 32-36.

20. Foster, S. W. *High-Performance Concrete - Stretching the Paradigm*. Concrete International, October 1994, pp. 33-34.

21. Helland, S. *Norwegian Experience with High Strength Concrete*. RILEM Proceedings, Special Concretes: Workability and Mixing, Edited by P. J. M. Bartos, Paisley, Scotland, March 1993, pp. 131-143.

22. Bresson, J. *Mixing and Compacting Techniques for the Production of Very High Performance Precast Concrete Products*. 4th International Symposium on Utilization of High-strength/High-performance concrete, Paris 1996, pp. 269-272.

23. Aitcin, P. C.; Laplante, P.; and Bedard, C. *Development and Experimental Use of 90-MPa (13,000 psi) Field Concrete*. High-Strength Concrete, SP-87, ACI, Detroit, 1986, pp. 14-17.

24. Randall, V. and Foot, K. *High-strength concrete for Pacific First Centre*. Concrete International, Vol. 10, No. 4, 1989, pp. 14-16.

25. Burnett, I. *High-strength Concrete in Melbourne, Australia*. Concrete International, Vol. 10, No. 4, 1989, pp. 17-21.

26. Ryell, J. and Bickley, J.A. *Scotia Plaza : High-Strength Concrete for Tall Buildings*. Proceedings on the Utilization of High-strength Concrete, Stavanger, Norway, 1987, pp. 641-653.

27. Yonezawa, T.; Tsurumaki, H.; Ando, S.; Nakashima, T.; and Kinoshita, M. *Design and Construction of a PC bridge with depth-span ratio of 1/40, using 100 N/mm^2 ultra-high-strength concrete*. Journal of Prestressed Concrete, Japan, Vol. 36, No. 3, 1994, pp. 11-23.

28. Mitsui, K.; Yonezawa, T.; Kinoshita, M.; and Shimono, T. *Application of a New Superplasticizer for Ultra High-strength Concrete*. Fourth CANMET / ACI conference on Superplasticizers and other Chemical Admixtures in concrete, SP 148-2, 1994, pp. 27-45.

29. Price, W.F. *Two Examples of High Performance Concrete in Practice, Part 2*. Quality Concrete, May 1995, pp. 127-130.

30. Yonezawa, T. *The Contribution of Fluidity Improving Technology to the Widespread use of High-strength Concrete*. Radical Concrete Technology, Proceedings of International Conference held at the University of Dundee, Scotland, June 1996, pp. 525-542.

31. Sandvik, M., Hang, A.K., Hunsbedt, O.S., and Moksnes, J. *Condensed silica fume in high-strength concrete for offshore structures*. ACI Publication, SP-114, 1989, pp. 1117-1129.

32. Haug, A. K. *Concrete Technology, the Key to Current Concrete Platform Concepts*. ACI, SP 149-4, 1995, pp. 63-80.

33. Penttala, V. *Compatibility of binder and superplasticizer in high-strength concrete*. Nordic Concrete Research, 5, 1986, pp. 117-128.

34. Collepardi, M. *Admixtures Used to Enhance Placing Characteristics of Concrete*. Cement & Concrete Composites, 20, 1998, pp. 103-112.

35. Maximilien, S., Ambroise, J., and Pera, J. *Influence of Acrylic Polymers on the Rheology of Mortars*. Fourth CANMET/ACI International Conference on Superplasticizers and Other Chemical Admixtures in Concrete, Edited by V. M. Malhotra, SP 148-5, October 1994, pp. 89-*104*.

36. Bernhardt, C.; and Fynboe, C. *High Strength Concrete Beams*. Nordic Concrete Research, No. 5, Oslo, 1986, pp. 19-26.

37. Schmidt, W.; and Hoffman, E. J. *" 9000 psi Concrete – Why ? Why Not ? "* Civil

Engineering – ASCE, Vol. 45, No. 5, May 1975, pp. 52-55.

38. Yen, T., Tang, C.W., Chang, C.S., and Chen, K.H. *Flow behaviour of high strength high-performance concrete*. Cement and Concrete Composites, 21, 1999, pp. 413-424.

39. Dejellouli, J.; Aitcin, P.C and Chaallal, O. *Use of Ground Granulated Slag in High-Performance Concrete*. High-Strength Concrete : Second International Symposium, ACI, SP 121-18, 1990, pp 351-368.

40. Hu C., Larrard F, and Gjorv O. E. *Rheological testing and modelling of fresh high performance concrete*. Materials and Structures, No. 28, 1995, pp. 1-7.

41. Aitcin, P. C. *The Use of Superplasticizers in high performance concrete*. High Performance Concrete : From Material to Structure, Edited by Yves Malier, E and FN SPON, 1992, pp. 14-33.

42. Scanlon, J. M. *Chemical Admixtures: Are ASTM Standards Appropriate To the Need of the User ?* Concrete International, September 1994, pp. 61-64.

43. Price, W.F. *High Strength Concrete*. Current practice, Sheet No. 118, Concrete Magazine, June 1999.

44. Larrard, F. Ithurralde, G.; Acker, P.; and Chauvel, D. *High – Performance Concrete for a Nuclear Containment*. High-Strength Concrete : Second International Symposium, ACI, SP 121-27, 1990, 549-565.

45. Muguruma, H. and Watanabe, F. *Ductility Improvement of High-Strength Concrete Columns with lateral Confinement*. High-Strength Concrete : Second International Symposium, ACI, SP 121-4, 1990, pp. 47-60.

46. Jansen, J. J. *Structural Aspects of High Strength Concrete*. Concrete Technology; New Trends, Industrial Applications, proceedings of the International RILEM Workshop, Edited by A. Aguado et al, Barcelona, November 1994, pp. 187-212.

47. Ali, F.A., O'Connor, D. and Abu-Tair, A. *Explosive spalling of high-strength concrete columns in fire*. Magazine of Concrete Research, Vol. 53, No. 3, June 2001, pp. 197-204.

48. Ferraris, C.F. *Measurement of the Rheological Properties of High Performance Concrete: State of the Art Report*. Journal of Research of the National Institute of Standards and Technology, Vol. 104, No. 5, Sep.-Oct. 1999, pp. 461-478.

49. de Larrard, F., Sedran, T., Hu, C., Szitkar, J.C., Joly, M., and Derkx, F. *Evolution of the Workability of Superplasticized Concretes : Assessment with the BTRHEOM*

Rheometer. RILEM proceedings, Paisley, Scotland, June 1996, pp. 377-387.

50. Wallevik, O. H. and Gjorv, O. E. *Practical Description of the Rheology of Fresh Concrete*. BML Division of Building Materials, University of Trondheim, the Norwegian Institute of Technology, December 1990, 12 pp.

51. FIP/CEB *High-Strength Concrete, State-of-the-art Report*. CEB Bullitin d' information, No. 197, August 1990.

52. Parrott, L. *The Production and Properties of High-Strength Concrete*. Concrete. November 1969, pp. 443-448.

53. Soutsos, M. N. *Mix Design, Workability, Adiabatic Temperature, and Strength Development of High Strength Concrete*. University College London, Dep. of Civil and Environmental Engineering. Ph.D. thesis, 1992.

54. Helland, S. *Slip Forming of Concrete with Low Water content*. Concrete, Dec. 1984, pp. 19-21.

55. Taylor, H. F. W. *Cement Chemistry*. Academic Press Limited, 1990, 455 pp.

56. Hobbs, D.W. *Workability and Water Demand*. RILEM Proceedings on: Special Concretes: Workability and Mixing, Published by Bartos P. J. M., Paisley, Scotland, March 1993, pp. 55-65.

57. Mehta, P.K. and Monteiro, P.J.M. *CONCRETE: Structure, Properties, and Materials*. Second Edition, Prentice Hall, 1993, 548 pp.

58. Aitcin, P. C., Jolicoeur, C., Macgregor, J. G. *Superplasticizers: How They Work and Why They Occasionally Don't*. Concrete International, May 1994, pp. 45-52.

59. ASTM C 125-93. *Standard terminology relating to concrete and concrete aggregates*.

60. Glanville, W. H., Collins, A. R. and Mathews, D. D. *The grading of aggregate and the workability of concrete*. Road Research Technical paper No. 5, Her Majesty's Stationary Office (MHSO), 2nd edition, London, 1963.

61. Ritchie, A. G. B. *The Rheology of Fresh Concrete*. Journal of the Construction Division, proceedings of the ASCE, January 1968, pp. 55-74.

62. Newman, k. *Properties of concrete*. Structural Concrete. Reinforced Concrete Association, Vo. 2, N0. 11, 1965.

63. Uzomaka, O. J. *Plastic Concrete*. Concrete Vol. 4, No. 4, April 1970, pp. 155-

157.

64. Tassios, T. P. *Plasticity and cohesiveness of fresh concrete*. RILEM Leeds 1973, pp. 1.3-1 to 1.3-36.

65. ACI Committee 309. *Behaviour of Fresh Concrete During Vibration*. ACI Journal, January-February 1981, pp. 36-53.

66. Tattersall, G. H. and Banfill, P. F. G. *Rheology of Fresh Concrete*. London, Pitman, 1983.

67. de Larrard, F. *Why Rheology Matters*. Concrete International, August 1999, pp. 79-81.

68. Tattersall, G. H. *The Principles of Measurement of Workability of Fresh Concrete and a Proposed Simple Two-point Test*. RILEM Proceedings, Leeds, England, Vol. 1, March 1973, pp. 2.2-1 to 2.2-33.

69. Johnston, C. D. *Influence of Aggregate Void Condition and Particle Size on the Workability and Water Requirement of Single-sized Aggregate-paste Mixtures*. RILEM Proceedings Edited by Wierig, 1990, pp. 67-76.

70. Neville, A. M. *Summary*. RILEM Proceedings, Leeds 1973, pp. ix-xvii.

71. Powers, T. C. *Properties of fresh concrete*. John Wiley, 1968 (Chapter 10: Rheology of freshly mixed concrete).

72. Abrams, D. A. *Design of Concrete Mixes*. Structural Materials Research Laboratory, Levis Institute, May 1925, 99. 1-20, Reprints from Minutes of the Annual Meeting of the Portland Cement Association, New York, December, 1918.

73. BS EN 12350-2: 2000. *Testing fresh concrete : Slump test*. January, 2000.
(Formally described by - British Standards Institution BS 1881 : part 102. *Testing Concrete: Method for determination of slump*. British Standards Institution, London, 1983).

74. British Standards Institution BS 1881 : part 103. *Testing Concrete: Method for determination of compacting factor*. British Standards Institution , London, 1993.

75. British Standards Institution BS 1881 : part 104. *Testing Concrete: Method for determination of Vebe time*. British Standards Institution , London, 1983.

76. British Standards Institution BS 1881 : part 105. *Testing Concrete: Method for determination of flow*. British Standards Institution , London, 1984.

77. Scullion, T. *The measurement of the workability of concrete*. Thesis submitted to the university of Sheffield for the degree of M. A., 1975, 182 pp.

78. Tattersall, G. H. and Bloomer, S. J. *Further development of the two-point test for workability and extension of its range*. Magazine of Concrete Research, Vol. 31. No. 109: December 1979, pp. 202-210.

79. Tattersall, G. H. and Bloomer, S. J. Contribution by Eze-Uzomaka, O. J. Discussion paper. *Further development of the two-point test for workability and extension of its range*. Magazine of Concrete Research, Vol. 31. No. 109: December 1979, pp. 242-245.

80. Bloomer, S. J. *Further development of the two-point test for the measurement of the workability of concrete*. Ph.D. Thesis, University of Sheffield, 1979.

81. Tattersall, G.H. *Progress in the measurement of workability by the two-point test*. Properties of fresh concrete, RILEM Proceedings, edited by H.-J. Wierig, Hanover, October 1990, pp. 203-211.

82. Cabrera, J. G. and Hopkins, C. J. *A modification of the Tattersall two-point test apparatus for measuring concrete workability*. Magazine of Concrete research, Vol. 36, No. 129, 1984, pp. 237-240.

83. Wimpenny, D. E. and Ellis, C. *Oil-pressure measurement in the two-point workability apparatus*. Magazine of Concrete Research, Vol. 39, No. 140, 1987, pp. 169-174.

84. Wallevik, O. H. and Gjorv, O. E. *Modification of the two-point workability apparatus*. Magazine of Concrete Research, Vol. 42, No. 152, 1990, pp. 135-142.

85. Domone, P. L. J., Xu, Y. and Banfill, P. F. G. *Development of the two-point workability test for high-performance concrete*. Magazine of Concrete Research, V. 15, No. 3, June 1999, pp. 171-179.

86. Wallevik, O. H. and Gjorv, O. E. *Development of a Coaxial Cylinders Viscometer forFresh Concrete*. RILEM proceedings, Hanover, 1990, pp. 213-224.

87. Gjorv, O. E. *Concrete Workability: A More Basic Approach Needed*. Selected Research Studies from Scandanevia - Report TVBM 3078, Lund Institute of Technology, Lund, 1997, pp. 45-56.

88. Mork, J. H. *A Presentation of the BML Viscometer*. RILEM Proceedings, Edited by P. Bartos, Paisley, Scotland, June 1996, pp. 369-375.

89. de Larrard, F., Szitkar, J. C. , Hu, C. and Joly, M. *Design of a Rheometer for Fluid Concrete*. RILEM Proceedings, Edited by P. Bartos, Paisley, Scotland, June 1993, pp. 201-208.

90. de Larrard, F. *High-performance Concrete from the Laboratory to Practical Utilization*. RILEM Proceedings, Barcelona, 1994, pp. 177-196.

91. Hu, C., de Larrard, F., Sedran, T., Boulay, C., Bosc, F. and Deflorenne, F. *Validation of BT RHEOM, the new rheometer for soft-to-fluid concrete*. Materials and Structures, Vol. 29, December 1996, pp. 620-631.

92. de Larrard, F., Hu, C., Sedran, T., Szitkar, J.C., Joly, M., Claux, F., and Derkx, F. *A New Rheometer for Soft-to-Fluid Fresh Concrete*. ACI Materials Journal, May-June 1997, pp. 234-243.

93. Banfill, P.F.G., and Tattersall, G.H. Discussion of reference 92 (*A New Rheometer for Soft-to-Fluid Fresh Concrete*. ACI Materials Journal, May-June 1997, pp. 234-243). ACI Materials Journal, January-February 1999, pp. 126-133.

94. Malier, Y. *The French Approach to Using HPC*. Concrete International, July 1991, pp. 28-32.

95. Owens, P. L. *Water and its Role in Concrete*. Concrete International, November 1989, pp. 68-74.

96. Tattersall, G. H. *The rationale of a two-point workability test*. Magazine of Concrete Research, Vol. 25, No. 84: September 1973, pp. 169-172.

97. Ellis, C. *The Rheological and Mechanical Properties of Water Reduced Superplasticized High Strength Concretes*. 4th International Symposium on Utilization of High-strength/High-performance Concrete, Paris, 1996, pp. 273-280.

98. Dewar, J. D. The workability of fresh concrete. RILEM, Leeds university, 1973, pp 7.6-1 to 7.6-30.

99. Baoju, L., Youjun, X., Shiqiong, Z., and Qianlian, X. *Influence of ultra-fine fly ash composite on the fluidity and compressive strength of concrete*. Cement and Concrete Research, 130, 2000, pp. 1489-1493.

100. Pollet, B., Lavaud, R., and Baron, J. *Slump Loss: A Single Rule for Ordinary Concrete*. Proceedings Sixth CANMET/ACI International Conference: Fly Ash, Silica Fume, Slag and Natural Pozzolans in Concrete, Editor V.M. Malhotra, Bangkok, Thailand, SP 178-23, 1998, pp. 411-416.

101. Mehta, P.K., and Aitcin, P.C. *Microstructural Basis for Selection of Materials and Mix Proportions for High-Strength Concrete*. High-Strength Concrete, ACI Special Publication, No. 121, Detroit, 1990, pp. 265-286.

102. Saeed, A. *Workability measurement with particular reference to the control of concrete production*. Ph.D. Thesis, University of Sheffield, 1982.

103. Pillar, A.G., and Manuel, F.C. *High-Performance Concrete: Requirements for Constituent Materials and Mix Proportioning*. ACI Materials Journal, May-June 1996, pp. 233-241.

104. Neville, A.M. *Properties of concrete*. Pitman, 1977.

105. Murdock, L. J. and Blackledge, G. F. *Concrete Materials and Practice*. Fourth Edition, Edward Arnold, 1968. (Cited by Ref. 7).

106. Tuthill, L. H. *Slump Loss*. Concrete International, Jan. 1979, pp 31-35.

107. Davis, R. E.; Mielenz, R. C.; and Polivka, M. *Importance of Petrographic Analysis and Special Tests not Usually Required in Judging Concrete*. Journal of Materials, Vol. 2, No. 3, September 1967, pp 461-486.

108. Tucker, G. R., U.S. Patent 2 141 569, *Concrete and Hydraulic Cement*. 1938, 5 pp.

109. Agarwal, S.K., Masood, I., and Malhotra, S.K. *Compatibility of superplasticizers with different cements*. Construction and Building Materials, 14, 2000, pp. 253-259.

110. ASTM C-494. *Specification for Chemical Admixtures for Concrete*. American Society for Testing Materials.

111. Kreijger, P. C. *Plasticizers and dispersing admixtures*. Concrete International (Ci80), Admixtures - The Concrete Society, The Construction Press, April 1980, pp. 1-16.

112. BS 5075 : Part 3 : 1985. *Specification for superplasticizing admixtures*. Specification for air-entraining admixtures. British Standards Institution, 2 Park Street, London W1A 2BS.

113. Rixom, M. R., and Mailvaganam, N. P. *Chemical Admixtures for Concretes*. E and F. N. SPON, Ltd, 1986, 300 pp.

114. Ramachandran, V. S. *Recent Progress in the Development of Chemical*

Admixtures. CANMET, 1994, pp. 785-838.

115. Bache, H. H. *Densified cement / ultrafine particle based materials*. Second International Conference on Superplasticizers in Concrete. Ottawa, Canada, 1981, pp. 1-39.

116. Meyer, L. M., Perenchio, W. F. *Theory of Concrete Slump Loss as Related to the Use of Chemical Admixtures*. Concrete International, Vol. 1, No.1, January 1979, pp. 36-43.

117. Mollah, M.Y.A., Adams, W.J., Schennach, R., and Cocke, D.L. *A review of cement-superplasticizer interactions and their models*. Advances in Cement Research, Vol. 12, No. 4, October, 2000, pp. 153-161.

118. Billberg, P., Pertersson, O., and Norberg, J. *New Generation of Superplasticizers*. RILEM proceedings, Paisley, Scotland, June 1996, pp. 295-306.

119. Jeknavorian, A. A., Roberts L. R., Jardine L., Koyata H. and Darwin D. C. *Condensed Polyacrylic Acid-Aminated Polyether Polymers as Superplasticizers for Concrete*. Fifth CANMET/ACI, Superplasticizers and Other Chemical Admixtures in Concrete, SP 173-4, 1997, pp. 55-81.

120. Ramachandran, V. E. *Concrete Admixture Handbook*. Noyes Publication, New Jersey, 1984.

121. Ferrari, G., Basile, F., Dal Bo, A., and Mantoni, A. *The Influence of Molecular Weight of Beta Naphthalene Sulfonate-Based Polymers on the Rheological Properties of Cement Mixes*. Il Cemento, Vol. 83, 1986, pp. 445-454.

122. Dodson, V. H. *Concrete Admixtures*. Published by Van Nostrand Reinhold, New York, 1990, 205 pp.

123. Singh, N. B., Sarvahi, R., and Singh, N. P. *Effect of Superplasticizers on he Hydration of Cement*. Cement and Concrete Research, Vol. 22, 1992, pp. 725-735.

124. Banfill, P. F. G. *Workability of Flowing Concrete*. Magazine of Concrete Research, Vol. 32, No. 110, March 1980, pp. 17-27.

125. Wallevik, O. and Simmerman, T. *Effect of Some Plasticizers on the Rheological Behaviour of Fresh Cement Paste*. Production Methods and Workability of Concrete, RILEM Proceedings, Edited by Bartos P. J. M., Mars D. L. and Cleland D. J., Paisley Scotland, June 1996, pp. 307-318.

126. Malhotra, V. M. *Superplasticizers: Their effects on Fresh and Hardened Concrete*. Concrete International, May 1981, pp. 66-81.

127. Perenchio W. F. and Whiting, D. A, and Kantro, D. L. *Water Reduction: Slump Loss, and Entrained Air-void Systems as influenced by Superplasticizers.* Superplasticizers in Concrete, ACI Publication, Detroit, SP 62, 1979. pp. 137-155.

128. Mailvaganam N. P. *Factors influencing Slump Loss in Flowing Concrete.* Superplasticizers in Concrete, SP 62-19, ACI, Detroit, 1979, pp. 389-403.

129. Jolicoeur, C., and Simard, M.A. *Chemical Admixtures-Cement Interactions: Phenomenology and Physico-Chemical Concepts*. Cement and Concrete Composites, 20, 1998, pp. 87-101.

130. Fujiu, A., Tanaka, H., and Iizuka, M. *Slump Control by Reactive Polymer Dispersant*. Review of the 39th General Meeting, Cement Association, Japan, 1985, p. 72.

131. Mitsui, K., Kasami, H., Yoshita, Y. and Kinoshita, M. *Properties of High Strength Concrete with Silica Fume using High Range Water Reducer of the Slump Retaining Type*. Proceedings of the Conference Superplasticizers and Other Chemical Admixtures, Edited by V. M. Malhotra, ACI, SP-119, 1989, pp. 79-97.

132. Fukuda, M., Mizunuma, T., Izumi, T., Iizuka, M., and Hisaka, M. *Slump Control and Properties of Concrete with a New superplasticizer. I: Laboratory Studies and Test methods*. RILEM Proceedings on Admixtures for Concrete, Important Properties, Barcelona, May 1990, pp. 10-19.

133. Collepardi, M., Coppola, L., Cerulli, L., Ferrari, G., Pistolesi, C., Zaffaroni, P. and Quek, F. *Zero Slump Loss Superplasticizer Concrete*. Proceedings of the Congress our World in Concrete and Structures. Singapore, 1993, pp. 73-80.

134. Tazawa, E. I., Yonekura, A., Takahashi, M., Miyazawa, S., and kawai, K. *Plasticizing characteristics of Sulfonic Acid Polymer Containing Methacrylic Acid Derivatives*. Fourth CANMET/ACI International Conference on Superplasticizers and Other Chemical Admixtures in Concrete, Edited by V. M. Malhotra, SP 148-21, 1994, pp. 353-*366*.

135. Kinoshita, M., Suzuki, T., Yonezawa, T., Mitsui, K. *Properties of Acrylic Graft Copolymer-Based New Superplasticizer for Ultra High-Strength Concrete.* Fourth CANMET/ACI International Conference on Superplasticizers and Other Chemical Admixtures in Concrete, Edited by V. M. Malhotra, SP 148-16, 1994,

pp. 281-299.

136. Daimon, M. and Roy, D. M. *Rheological Properties of Cement Mixes: I Methods, Preliminary Experiments, and Adsorption Studies*. Cement and Concrete Research, 8, 6, 1978, pp. 753-764.

137. Uchikawa, H., Hanehara S. and Sawaki, D. *The Role of Steric Repulsive Force in the Dispersion of Cement Particles in Fresh Paste Prepared with Organic Admixture*. Cement and Concrete Research, Vol. 27, No. 1, 1997, pp. 37-50.

138. Ernsberger, F. M. and France, W. G. *Some physical and chemical properties of weight-fractionated lignosulphonic acid, including the dissociation of lignosulphonates*. Journal of Physics and Colloid Chemistry, Vol. 52, 1936, pp. 267-276.

139. Ernsberger, F. M. and France, W. G. Ind. Eng. Chem. 37, 1945, pp. 598-600.

140. Daimon, M. and Roy, D. M. *Rheological Properties of Cement Mixes: II Zeta Potential and Preliminary Viscosity Studies*. Cement and Concrete Research, Vol. 9, 1979, pp. 103-110.

141. Hattori, and Kenichi. *Experiences with Mighty Superplasticizer in Japan*. Superplasticizers in Concrete, ACI, Detroit, SP-62, 1979, pp. 37-66.

142. Penttala, V. E. *Effects of Delayed dosage of Superplasticizer on High Performance Concrete*. Utilization of High Strength Concrete, Proceedings, Volume 2, Symposium in Lillehammer, Edited by Holand I. and Sellevold E., Norway, June, 1993, pp. 874-881.

143. Collepardi, M. *Concrete Admixtures Handbook*, Editor: V. S. Ramachandran, Noyes Publications, 1984, pp. 116-210.

144. Banfill, P. F. G. A Discussion of the Papers *Rheological Properties of Cement Mixes*, by Diamon, M. and Roy, D. M. Cement and Concrete Research, Vol. 9, 1979, pp. 795-796.

145. Tanaka, Y. O., Matsuo, S., Ohta, A. and Ueda, M. *A New Admixture for High Performance Concrete*. Proceedings of the Concrete in the Service of Mankind, editors R. K. Dhir and M. J. McCarthy, Dundee, Scotland, 1996, pp. 291-300.

146. Kinoshita, M., Yamaguchi, S., Yamamoto, T. and Tomosawa, F. *Chemical Structure and Performance of New type of high range water reducing A. E. Agent*. Cement Association of Japan, Proceedings of Cement and Concrete, No.

44, 1990, pp. 222-227.

147. Anderson, P. J., and Roy, D. M. *The Effects of Adsorption of Superplasticizers on the Surface of Cement*. Cement and Concrete Research, Vol. 17, 1987, pp. 805-813.

148. Agullo, L., Toralles-Carbonari, B., Gettu, R., and Aguado, A. *Fluidity of cement pastes with mineral admixtures and superplasticizer – A study based on the Marsh cone test*. Materials and Structures, Vol. 32, August-September 1999, pp. 479-485.

149. Coleman, E. and Diamond, S. *Studies of Low-Porosity Concretes Designed for Bridge Deck Applications: 1. Introductory Remarks, Mix Designs, Strength Development, and Rheological Properties*. Cement and Concrete Research, Vol. 14, 1984, pp. 670-678.

150. de Larrard, F., Bosc, F., Catherine, C., and Deflorenne, F. *The AFREM Method for the Mix-Design of high performance concrete*. Materials and Structures, Vol. 30, August- September 1997, pp. 439-446.

151. Ozawa, K., Sakata, N., Okamura, H. *Evaluation of self-Compactability of Fresh Concrete Using the funnel Test*. Concrete Library of JSCE, No. 25, June 1995, pp. 59-75.

152. Chiocchio, G. and Paolini, A. E. *Optimum time for adding superplasticizers to Portland cement pastes*. Cement and Concrete Research, Vol. 15, No. 5, 1985, pp. 901-908.

153. Kim, B.G., Jiang, S.P., and Aitcin, P.C. *Slump improvement mechanism of alkalies in PNS superplasticized cement pastes*. Materials and Structures, Vol. 33, July, 2000, pp. 363-369.

154. Banfill, P. F. G. *The rheology of fresh mortar*. Magazine of Concrete Research, V. 43, No. 154, March 1991, pp. 13-21.

155. Ravina, D. and Mor, A. *Consistency of Concrete Mixes: Effects of Superplasticizers*. Concrete International, July 1986, pp. 53-55.

156. Mindess, S. and Young, J.F. *Concrete*. Prentice-Hall, Inc., 1981, 657 pp.

157. Previte, R.W., *Concrete Slump Loss*. Journal of the American Concrete Institute, proceedings, Vol. 74, No. 8, August 1977, pp. 361-367.

158. West, R. P. *Concrete retempering without strength loss*. Properties of fresh

concrete, RILEM Proceedings, edited by H.-J. Wierig, Hanover. October 1990, pp. 134-142.

159. Edmeades, R. M. and Hewlett, P. C. *Superplasticized Concrete - High Workability Retention*. Concrete International (Ci80), Admixtures - The Concrete Society, The Construction Press, April 1980, pp 49-72.

160. de Larrard, F. *A mix Performance Method for High Performance Concrete*. High Performance Concrete: From Material to Structure, Edited Y. Malier. E and FN Spon, 1992, pp. 48-62.

161. Blick, R. L. *Some factors influencing high-strength concrete*. Modern Concrete, Vol. 36, No. 12, April 1973, pp. 38-47.

162. Collepardi, M. *Superplasticizers and Air Entraining Agents: State of the Art and Future Needs*. Proceedings of V. M. Malhotra Symposium, Concrete Technology: Past, Present, and Future, edited by P.K. Mehta and S. Francisco, SP 144-20, 1994, pp. 399-416.

163. Edmeades, R. M., Hewlett, P. C. and Thomas, R. E. R. *An explanation of some anomalous admixture behaviour*. Paper Presented at Discussion on Research Aspects of Admixtures for Cement, Mortars and Concrete, BRE, Garston, June 1984, and also at Concrete Materials Research Seminar, July 1984.

164. Johnston, C. D. *Admixture-Cement Incompatibility: A Case History*. Concrete International, April 1987, pp. 51-60.

165. Dodson, V. H. and Hayden, T. D. *Another Look at the Portland Cement / Chemical Admixture Incompatibility Problem*. American Society for Testing and Materials, Cement, Concrete and Aggregates, 1989, pp. 52-56.

166. Jiang, S., Kim, B.-G. and Aitcin, P.-C. *Importance of Adequate Soluble Alkali Content to Ensure Cement / Superplasticizer Compatibility*. Cement and Concrete Research, 29, 1999, pp. 71-78.

167. Hanna et al. *Rheological behaviour of Portland cement in the presence of a superplasticizer*. Proceedings Third Int. Conf., Ottawa, Canada, ACI, SP 119-9, 1989, pp. 171-188.

168. Neville, A. and Aitcin, P.C. *High performance concrete – An overview*. Materials and Structures, Vol. 31, March 1998, pp. 111-117.

169. Mehta, P. K. *Pozzolanic and Cementitious By-Products in Concrete - Another Look*. Proceedings of Third International Conference on Fly Ash, Silica Fume,

Slag, and Natural Pozzolans in Concrete, Edited by V.M. Malhotra, Trondheim. Norway, SP 114-1, 1989, pp. 1-43.

170. ASTM C 150-94. *Standard specification for Portland cement.*

171. ACI Committee 212. *Guide for the Use of High-Range Water-Reducing Admixtures (Superplasticizers) in Concrete*. Concrete international, April 1993, pp. 40-47.

172. Khalil, S. M. and Ward, M. A. *Effect of sulphate content upon heat evolution and slump loss of concretes containing high-range water reducers (superplasticizers)*. Magazine of Concrete Research, March 1980, pp. 28–38.

173. Ahmad, S. H. *Short Term Mechanical Properties*. High Performance Concrete: Properties and Applications. Edited by Shah S. P. and Ahmad S. H., McGraw-Hill Inc., 1994, pp. 27-64.

174. Mork, J. H. and Gjorv, O. E. *Effect of Gypsum-Hemihydrate Ratio in Cement on Rheological Properties of Fresh Concrete*. ACI Materials Journal, March-April 1997, pp. 142-146.

175. Nagataki, S. *Mineral Admixtures in Concrete: State of the Art and Trends*. Proceedings of V. M. Malhotra Symposium, Concrete Technology: Past, Present, and Future, edited by P.K. Mehta and S. Francisco, SP 144-22, 1994, pp. 447-482.

176. Owens, P. L. *Fly ash and its usage in concrete*. Journal of the Concrete Society (England), Vol. 13, No. 7, 1979, pp. 21-26.

177. Bayasi, Z. *Effects of Fly Ash on the Properties of Silica-Fume Concrete*. Concrete International, April 1992, pp. 52-54.

178. Besari, M. S., Munaf, D. R., Hanafiah and Iqbal M. M. *Stability of Mechanical Properties and Interface Density of High Performance Fly Ash Concrete*. Proceedings of the International Conference Edited by Dhir R. K. and Hewlett P. C., Dundee, Scotland, June 1996, pp. 47-56.

179. Malhotra, V. M. *Superplasticizers: A Global Review with Emphasis on Durability and Innovative Concretes*. Proceedings of the Third International Conference on Superplasticizers and Other Chemical Admixtures in Concrete, edited by Malhotra V.M., Ottowa, Canada, SP 119-1, 1989, pp. 1-17.

180. Hansen, T. C. *Modified DOE Mix Design for high volume fly ash concretes and controlled low strength concretes*. Magazine of Concrete Research, V. 44, No.

158, March 1992, pp. 39- 45.

181. Helmuth, R. A. *Water-reducing Properties of Fly Ash in Cement Pastes, Mortars, and Concretes: Causes and Test Methods*. ACI Proceedings, SP-91, 1986, pp. 723-740.

182. Ellis, C. *The application of the Two-Point Workability Test and British Standard Tests to OPC/PFA Concretes*. Proceedings of the International Symposium on: The Use of PFA in Concrete, Editors: Cabrera J. G. and Cusens A. R., April 1982, pp. 121-132.

183. Banfill, P. F. G. *An Experimental Study of the Effect of PFA on the Rheology of Fresh Concrete and Cement Paste*. Proceedings of the International Symposium on: The Use of PFA in Concrete, Edited by Cabrera J. G. and Cusens A. R., April 1982, pp. 160-171.

184. Ivanhov, Y. and Zacharieva, S. *Influence of Fly Ash on the Rheology of Fresh Concrete*. Proceedings of the International Symposium on: The Use of PFA in Concrete, Editors: Cabrera J. G. and Cusens A. R., April 1982, pp. 133-140.

185. Ryan, W. G. and Munn, R. L. *Some Recent experiences in Australia with Superplasticizing Admixtures*. Superplasticizers in Concrete, ACI, Detroit, SP-62, 1979, pp. 123-136.

186. Ravina, D. *Slump Retention of Fly Ash Concrete With and Without Chemical Admixtures*. Concrete International, April 1995, pp 25-29.

187. Nishibayashi, S., Yoshino, A., Hideshima, S., Takada, M. and Chikada, T. *A Study on Superplasticized Concrete Containing High Volumes of Blast-Furnace Slag*. Proceedings of the Third International Conference on Superplasticizers and Other Chemical Admixtures in Concrete, edited by Malhotra V.M., Ottowa, Canada, SP 119-23, 1989, pp. 445-455.

188. Meusel, J. W. and Rose, J. H. *Production of blast furnace slag at Sparrows Point, and the workability and strength potential of concrete incorporating the slag*. Special publication, ACI, Detroit, SP-79, 1979, pp. 867-890.

189. Swamy, R. N., Sakai, M. and Nakamura, N. *Role of Superplasticizers and Slag for Producing High Performance Concrete*. Fourth CANMET/ACI International Conference on Superplasticizers and Other Chemical Admixtures in Concrete, Edited by V. M. Malhotra, SP 148-1, 1994, pp. 1-25.

190. Read P., Carette G. G., and Malhotra V. M. *Strength Development Characteristics of High-strength Concrete Incorporating Supplementary Cementing Materials.*

High-Strength Concrete, ACI, Special Publication, SP 121-26, Detroit, 1990, pp. 527-547.

191. Wimpenny, D. E. and Sir William Halcrow & Partners. *Rheology and Hydration Characteristics of Blended cement concretes*. Conference of Cement and Concrete Science, Oxford University, Sep. 1994, pp. 1-11.

192. ACI Committee 226. *Silica Fume in Concrete*. ACI Materials Journal, March-April 1987, pp. 158-166.

193. Yogendran, V., Langan, B. W., Haque, M. N., and Ward, M. A. *Silica Fume in High-Strength Concrete*. ACI Materials Journal, March-April 1987, pp. 124-129.

194. Sellevold, E. J. and Radjy, F. F. *Condensed Silica Fume (Microsilica) in Concrete: Water Demand and Strength Development*. Fly Ash, Silica Fume, Slag and Other Mineral By-Products in Concrete, ACI, Detroit, SP-79, 1983, pp. 677-694.

195. de Larrard, F. *Ultrafine Particles for Making Very High Performance Concretes*. High Performance Concrete: From Material to Structure, Edited Y. Malier, E and FN SPON, Paper No. 3, 1992, pp. 34-47.

196. Malhotra, V. M. *Fly Ash, Slag, Silica Fume, and Rice-Husk Ash in Concrete: A Review*. Concrete International, April 1993, pp. 23-28.

197. Austin, S. A. and Robins P. J. *The Influence of Superplasticizer on Mixture Proportioning and the Strength and Durability of Silica Fume Concrete*. Fourth CANMET/ACI International Conference on Superplasticizers and Other Chemical Admixtures in Concrete, Edited by V. M. Malhotra, SP 148-15, 1994, pp. 259-279.

198. Duval, R. and Kadri, E. H. *Influence of Silica Fume on the Workability and the Compressive Strength of High-Performance Concrete*. Cement and Concrete Research; Vol. 28, No. 4, 1998, pp. 533-547.

199. Beaupre, D., Mindess, S. and Pigeon, M. *Rheology of Fresh Shortcrete*. RILEM Proceedings, Special Concretes: Workability and Mixing, Edited by P. J. M. Bartos, Paisley, Scotland, March 1993, pp. 225-236.

200. Juvas, K. J. *Experiences in measuring rheological properties of concrete having workability from high-slump to no-slump*. Properties of fresh concrete, RILEM Proceedings, edited by H.-J. Wierig, Hanover, October 1990, pp. 179-185.

201. Smeplass, S. *Applicability of the Bingham model to high strength concrete*. RILEM Proceedings, Special Concretes: Workability and Mixing, Edited by P. J.

M. Bartos, Paisley, Scotland, March 1993, pp. 145-152.

202. Osterberg, T. *Measurement of Properties of Fresh High Performance Concrete and Effects on the Mixing Process*. RILEM Proceedings, Special Concretes: Workability and Mixing, Edited by P. J. M. Bartos, Paisley. Scotland, March 1993, pp. 17-30.

203. Sone, T., Sarkar, S.L., and Uchikawa, H. *The Influence of Cross-Linked and NSF Superplasticizer on the Flow Properties of Blended Cements*. Fourth CANMET/ACI International Conference on Superplasticizers and Other Chemical Admixtures in Concrete, Edited by V. M. Malhotra, SP 148-9, 1994, pp. 153-175.

204. Shilstone, J. M. (Sr.) and Shilstone, J. M. (Jr.). *Concrete Mixtures and Construction Needs*. Concrete International, December 1989, pp. 53-57.

205. Almeida, I. R. and Goncalves, A. F. *Properties of freshly mixed concretes*. Properties of Fresh Concrete, Proceedings RILEM, edited by H. J. Wierig, University of Hanover, Hanover, October 1990, pp 227-235.

206. Miura, N., Takeda, N., Chikamatsu, R. and Sogo, S. *Application of Super Workable Concrete to Reinforced Concrete Structures with Difficult Construction Conditions*. ACI Proceedings, SP 140-8, 1994, pp. 163-186.

207. L'Hermite, R. and Tournon, G. *Vibration of Fresh Concrete (La vibration du beton frais)*. Annales, Institute Technique du Batiment et des Travaux Publics, Paris, 1948. (Cited by Ref. 65).

208. Kolek J. *Research on the Vibration of Fresh Concrete*. Reports, Conference on Vibrations–Compaction Techniques, Julius Hoban, Budapest, 1963. (Cited by Ref. 65).

209. Kirkham, R.H.H. *The Compaction of Concrete by Surface Vibration*. Reports, Conference on Vibrations-Compaction Techniques, Budapest, 1963. (Cited by Ref. 65).

210. Tattersall, G.H. and Baker, P.H. *The effect of vibration on the rheological properties of fresh concrete*. Magazine of Concrete Research, Vol. 40, No. 143, June 1988, pp. 79-89.

211. Tattersall, G.H. and Baker, P.H. *An investigation on the effect of vibration on the workability of fresh concrete*. Magazine of Concrete Research, Vol. 41, No. 146, March 1989, pp. 3-9.

212. Kakuta, S. and Kojima, T. *Effect of Chemical Admixtures on the Rheology of*

Fresh Concrete During Vibration. Proceedings of the Third International Conference on Superplasticizers and Other Chemical Admixtures in Concrete, edited by Malhotra V.M., Ottowa, Canada, SP 119-10, 1989, pp. 189-208.

213. Mori, H. and Tanigawa, Y. *Flow Simulation of Fresh Concrete Subjected to Vibration*. Magazine of Concrete Research, Vol. 42., No. 153, December 1990, pp. 223-232.

214. Banfill, P. F. G. *Vibration and Rheology of Fresh Concrete – A Further Look*. RILEM proceedings, Paisley, Scotland, 1996, pp. 319-325.

215. Banfill, P. F. G., Yongmo, X., and Domone, P. L. J. *Relationship between the rheology of unvibrated fresh concrete and its flow under vibration in a vertical pipe apparatus*. Magazine of Concrete Research, Vol. 51, No. 3, June 1999, pp. 181-190.

216. Soutsos, M. N., Bungey, J. H. and Brizell, M. J. *Vibration of Fresh Concrete: Experimental Set-up and Preliminary Results*. Radical Design and Concrete Practices, Edited by Dhir R. H. and Paine K. A., Proceedings of the International Seminar held at the University of Dundee, Scotland, U.K., September 1999, pp. 91-101.

217. Al-Khalaf, M.N. and Yousif, H.A. *Effect of Revibration on the Stability and Compactability of Concrete*. Cement and Concrete Research, Vol. 15, No. 5, 1985, pp. 842-848.

218. Welton, H. A. *Why Vibrate?* Consolidation of concrete, ACI, SP 96-8, 1987, pp. 119-124.

219. BS 1881 : Part 108 : 1983. *Testing concrete : Method for making test cubes from fresh concrete*. British Standards Institution, 2 Park Street, London W1A 2BS.

220. ASTM C 192/C 192M - 98. *Standard Practice for Making and Curing Concrete Test Specimens in the Laboratory*. American Society for Testing Materials (ASTM), 100 Barr Harbor Drive, West Conshohocken, PA 19428-2959, USA.

221. Forssblad, L. and Sallstrom, S. *Concrete Vibration – What's Adequate?* Concrete International, September 1995, pp. 42-48.

222. Wild, S., Sabir, B.B., and Khatib, J.M. *Factors Influencing Strength Development of Concrete Containing Silica Fume*. Cement and Concrete Research, Vol. 25, No. 7, 1995, pp. 1567-1580.

223. Kwan, A.K.H. *Use of condensed silica fume for making high strength, self-*

consolidating concrete. Canadian Journal of Civil Engineering, Vol. 27, 2000, pp. 620-627.

224. Chai, H-W. *Design and Testing of Self-Compacting Concrete*. University College London, Dep. of Civil and Environmental Engineering, Ph.D. thesis, April 1998.

225. BS EN 197-1. *Cement: composition, specifications and conformity criteria for common cements*. 2000.

226. BS 3892 : part 1 : 1993. *Specification for pulverised-fuel ash for use with Portland cement*. British Standards Institution, 2 Park Street, London W1A 2BS.

227. BS 6699 : 1992. *Specification for ground granulated blastfurnace slag for use with Portland cement*. British Standards Institution, 2 Park Street, London W1A 2BS.

228. BS 812 : Part 3 : 1975. *Method for sampling and testing of mineral aggregates, sands and fillers : Mechanical Properties*. British Standards Institution, 2 Park Street, London W1A 2BS.

229. Japanese Industrial Standard 9.1. *Physical testing methods for cements: 5. Flow table*. JIS 5021,1992.

230. Okamura, H., Maekawa, K., and Ozawa, K. *High performance concrete*. (in Japanese) Gihoudou Pub., Tokyo, 1993, 323 pp.

231. *Operating Instructions for the Two-point Workability Test Apparatus*. Metrix Construction equipment division, CCL plant limited.

232. Khayat, K.H., Sonebi, M. and Yahia, A. *Statistical Models to Predict Flowability, Washout Resistance and Strength of Underwater Concrete*. Production Methods and Workability of Concrete, Proceedings of International RILEM Conference, Paisley, Scotland, June, 1996, pp. 463-481.

233. BS EN 12350-4: 2000. *Testing fresh concrete : Degree of compactability*. January, 2000.

234. BS 1881 : Part 116 : 1983. *Method for the determination of compressive strength of concrete cubes*. British Standards Institution, 2 Park Street, London W1A 2BS.

235. BS 1881 : Part 4 : 1970. *Methods of testing concrete for strength*. British Standards Institution, 2 Park Street, London W1A 2BS.

236. BS 1881: Part 203: 1986. *Testing concrete: Recommendations for measurement of velocity of ultrasonic pulses in concrete*. British Standards Institution, 2 Park Street, London W1A 2BS.

237. Teychenne, D.C., Franklin, R.E., and Entroy, H.C. *Design of Normal Concrete Mixes*. Building Research Establishment Report, 1988.

238. Cusens, A. R. *The Measurement of Workability of Dry Concrete Mixes*. Magazine of Concrete Research, 8, (22), 1956, pp. 23-30.

239. Banfill, P.F.G. and Saunders, D.C. *On the Viscometric Examination of Cement Pastes*. Cement and Concrete Research, Vol. 11, 1981, pp. 363-370.

240. Uzomaka, O. J. A *Concrete Rheometer and its Application to a Rheological Study of Concrete Mixes*. Proceedings of the 6th International Congress of Rheology, Lyons, Vol. 4, September 1972, pp. 233-235.

241. Murata, J. and Kikukawa, H. *Studies on Rheological Analysis of Fresh Concrete*. Fresh Concrete: Important Properties and their Measurement. Proceedings of RILEM Seminar, Leeds University, Leeds, Vol. 1, March 1973, pp. 1.2-1 to 1.2-33.

242. Ferraris, C.F., Brower, L.E., Banfill, P., Beaupre, D., Chardelaine, F., de Larrard, F., Domone, P., Nachbaur, L., Sedran, T., Wallevik, O., and Wallevik, J.E. *Comparison of concrete rheometers : International tests at LCPC (Nantes, France, in October, 2000)*. National Institute of Standards & Technology, NISTIR 6819, September 2001, pp. 1-65.

243. BS 5497 : Part 1: 1987. *Precision of test methods. Guide for the determination of repeatability and reproducibility for a standard test method*. British Standards Institution, 2 Park Street, London W1A 2BS.

244. Kurokawa, Y., Tanigawa, Y., Mori, H. and Komura, R. *A Study on the Slump Rest and Slump-flow Test of Fresh Concrete*. Transactions of the Japanese Concrete Institute, Vol. 16, 1994, pp. 25-32.

245. Kuroiwa, S., Matsuoka, Y., Hayakawa, M. and Shindoh, T. *Application of Super Workable Concrete to Construction of a 20-Storey Building*. ACI Proceedings,

SP 140-7, 1994, pp. 147-161.

246. Ferraris, C.F. and de Larrard, F. *Modified Slump Test to Measure the Rheological Parameters of fresh Concrete*. Cement, Concrete and Aggregates. ASTM, CCGDP, Vol. 20, No. 2, December 1998, pp. 241-247.

247. Rao, P. and Olek, J. *Comparison of the Effect of Blended Cementitious Materials on Selected Properties of High-Performance Pastes and Concretes*. Fourth International Symposium on Utilization of High-Strength/High-Performance Concrete, Paris, 1996, pp. 143-152.

248. Wei, S., Ganghua, P. and Dajun, D. *Effect of the Combined Use of Ultra-fine Fly Ash and Silica Fume on Strength of HPC*. Proceedings: ACI International Conference on High-Performance Concrete, Edited by V.M. Malhotra, SP 172-16, Malaysia, 1997, pp. 299-312.

249. Zain, M.F.M, Safiuddin, Md., Mahmud, H. *Development of high performance concrete using silica fume at relatively high water-binder ratios*. Cement and Concrete Research, Vol. 30, 2000, pp. 1501-1505.

250. Duchesne, J. and Berube, M.-A. *Long-term effectiveness of supplementary cementing materials against alkali-silica reaction*. Cement and Concrete Research, Vol. 31, 2001, pp. 1057-1063.

251. Sivasundaram, V., Carretta, G.G. and Malhotra, V.M. *Properties of concrete incorporating low quantity of cement and High Volumes of Low-Calcium Fly Ash*. Proceedings of Third International Conference on Fly Ash, Silica Fume, Slag, and Natural Pozzolans in Concrete, Edited by V.M. Malhotra, Trondheim, Norway, SP 114-2, 1989, pp. 45-55.

252. Yilmaz, V.T. and Glasser, F.P. *Influence of Sulphonated melamine formaldehyde superplasticizer on cement hydration and microstructure*. Advances in Cement Research, Vol. 2, No. 7, July 1989, pp. 111-119.

253. Lahalih, S.M. *Effect of Polymerization Conditions of Sulfonated melamine formaldehyde superplasticizers on concrete*. Cement and Concrete Research, Vol. 18, No. 4, July 1988, pp. 513-531.

254. Sharobim, K.G. *High-Performance Concrete Placed Under Water*. Proceedings: ACI International Conference on High-Performance Concrete, Edited by V.M. Malhotra, SP 172-24, Malaysia, 1997, pp. 445-463.

255. Hewlett, P.C. *Cement Admixtures: Use and Applications*. Longman, Essex (2nd

Edition), 1988.

256. Prokopski, G. and Langier, B. *Effect of water/cement ratio and silica fume addition on the fracture toughness and morphology of fractured surfaces of gravel concretes*. Cement and Concrete Research, 30, June, 2000, pp. 1427-1433.

257. Price, W.F. and Hynes, J.P. *In-situ strength testing of high strength concrete*. Magazine of Concrete Research, Vol. 48, No. 176, September 1996, pp. 189-197.

258. Ellis, C and Wimpenny, D.E. *The assessment of mix stability using the two-point test*. Proceedings by Banfill, March 1990, pp. 281-291.

259. Soshiroda, T. *Effects of Bleeding and Segregation on the Internal Structure of Hardened Concrete*. Properties of fresh concrete, RILEM Proceedings, edited by H.-J. Wierig, Hanover, October 1990, pp. 253-260.

260. Kostuch, J.A. Walters, G.V. and Jones, T.R. *High performance concrete incorporating metakaolin – a review*. Concrete 2000, Vol. 2, 1993, pp. 1799-1811.

261. Wild, S. Khatib, J. and Jones, A. *Relative strength, pozzolanic activity and cement hydration in superplasticized metakaolin concrete*. Cement and Concrete Research, Vol. 26, No. 10, 1996, pp. 1537-1544.

262. Bai, J. Wild, S., Sabir, B.B. and Kinuthia, J.M. *Workability of Concrete Containing pulverized fuel ash and metakaolin*. Magazine of Concrete Research, Vol. 51, No. 3, June 1999, pp. 207-216.

263. Illuston, J.M. *Construction Materials : Their Nature and Behaviour*. E & FN SPON – Chapman & Hall, Second edition, 1994, 518 pp.

264. BS 1881 : part 114 : 1983. *Testing Concrete : Methods of Determination of Density of Hardened Concrete*.

265. Sheikh, V. *Fresh properties, Temperature rise, and Strength Development of High Strength Concrete with Binary and Ternary Blended cements*. University College London, Dep. of Civil and Environmental Engineering, Ph.D. thesis, 2001. (This research was carried out concurrently with the present research, which was completed in the summer of 1998).

Appendix A

. Two-point test Calibration results

. FORTRAN Programs used to analyse two-point test data

. Test results for Preliminary Rheological Measurements
(in Chapter 5)

. Additional Relationships for section 5.4.

Table A1: Torque/Pressure calibration data

Speed Setting	**Idling** Pressure (psi)	**Total** Pressure (psi)	**Net** Pressure (psi)	Spring Balance (N)	Lever Arm (m)	**Torque** (Nm)
0.5	130	136	6	0.55	0.2	0.11
		216	86	9.35	0.2	1.87
		329	199	20.75	0.2	4.15
		360	230	27.80	0.2	5.56
		375	245	26.34	0.2	5.27
		431	301	32.04	0.2	6.41
		459	329	36.01	0.2	7.20
		437	307	33.43	0.2	6.69
1	137.5	155	17	1.60	0.2	0.32
		165	27	2.26	0.2	0.45
		233	95	10.00	0.2	2.00
		245	107	11.72	0.2	2.34
		319	181	18.71	0.2	3.74
		338	200	18.71	0.2	3.74
		345	207	21.61	0.2	4.32
		495	357	38.38	0.2	7.68
		507	369	39.67	0.2	7.93
2	143	154	11	1.18	0.2	0.24
		152	9	0.97	0.2	0.19
		198	55	8.06	0.2	1.61
		192	49	5.38	0.2	1.08
		284	141	16.23	0.2	3.25
		353	210	22.58	0.2	4.52
		470	327	35.15	0.2	7.03
3	150	155	5	0.54	0.2	0.11
		227	77	9.03	0.2	1.81
		333	183	19.89	0.2	3.98
		307	157	16.56	0.2	3.31
		520	370	39.78	0.2	7.96
		453	303	33.33	0.2	6.67
4	162	285	123	13.44	0.2	2.69
		279	117	10.86	0.2	2.17
		432	270	27.50	0.2	5.50
		473	311	34.72	0.2	6.94
		487	325	34.94	0.2	6.99
		517	355	38.16	0.2	7.63
		493	331	37.09	0.2	7.42
5	175	177	2	0.30	0.2	0.06
		182	7	0.75	0.2	0.15
		216	41	3.98	0.2	0.80
		452	277	29.35	0.2	5.87
		527	352	37.63	0.2	7.53
		542	367	38.81	0.2	7.76

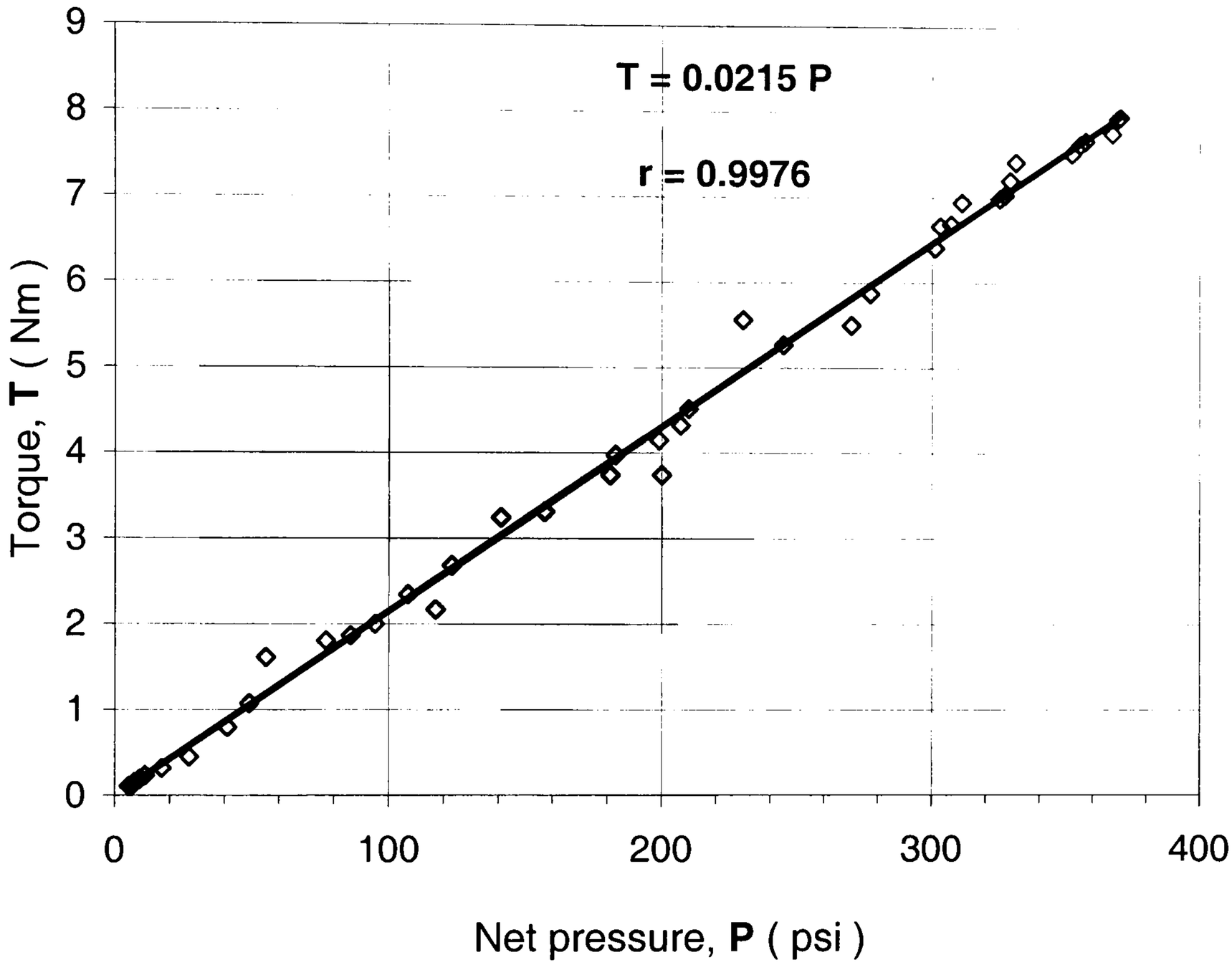

Figure A1 : Torque-Pressure calibration of two-point test apparatus

Table A2: Pressure/Voltage data (obtained from idling and mortar tests)

From idling data		Using Mortar	
Pressure (psi)	Voltage (volts)	Pressure (psi)	Voltage (volts)
200	2.05	388	3.11
192	1.99	370	3.02
185	1.96	358	2.94
178	1.92	345	2.86
172	1.88	330	2.78
165	1.84	315	2.71
158	1.80	298	2.59
150	1.75	275	2.50
143	1.71	262	2.40
138	1.68	245	2.30
130	1.64	225	2.20
123	1.60	-	-

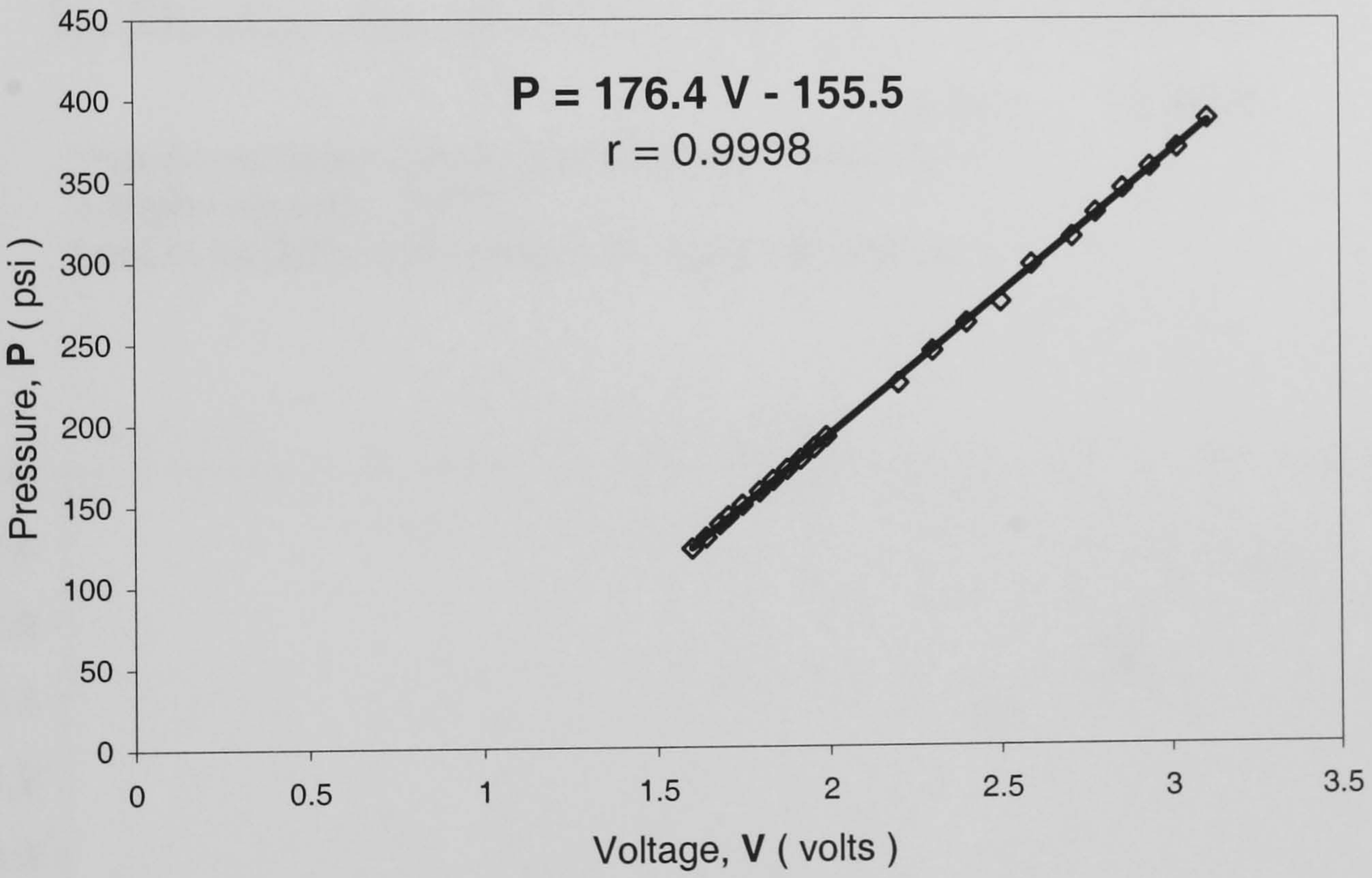

Figure A2: Pressure/Voltage Calibration of two-point test apparatus

Table A3 : Shaft speed / speed setting data for determination of gear ratio.

Speed Setting	Shaft speed		Flywheel		Gear ratio
	Tachometer* (rpm)	/60 (rps)	DVM+ (volts)	Speed (rps)	
0.5	8	0.13	0.32	0.64	4.800
1.0	18	0.30	0.74	1.49	4.953
1.5	28	0.47	1.17	2.34	5.006
2.0	39	0.65	1.60	3.20	4.917
2.5	52	0.87	2.03	4.07	4.694
3.0	64	1.07	2.49	4.98	4.669
3.5	78	1.30	2.92	5.84	4.492
4.0	89	1.48	3.35	6.71	4.521
4.5	103	1.72	3.79	7.58	4.414
4.0	91	1.52	3.38	6.75	4.451
4.5	103	1.72	3.81	7.62	4.439
4.0	87	1.45	3.38	6.75	4.655
3.5	80	1.33	2.94	5.88	4.410
3.0	64	1.07	2.51	5.01	4.697
2.5	52	0.87	2.04	4.07	4.696
2.0	40	0.67	1.61	3.22	4.833
1.5	29	0.48	1.17	2.34	4.850
1.0	19	0.32	0.75	1.49	4.705
0.5	8	0.13	0.31	0.63	4.695

Average = **4.6815**

* Hand-held tacheometer used to measure shaft speed
+ Digital volmeter (DVM)
1 volt of the DVM is equivalent to 2 rps of the flywheel

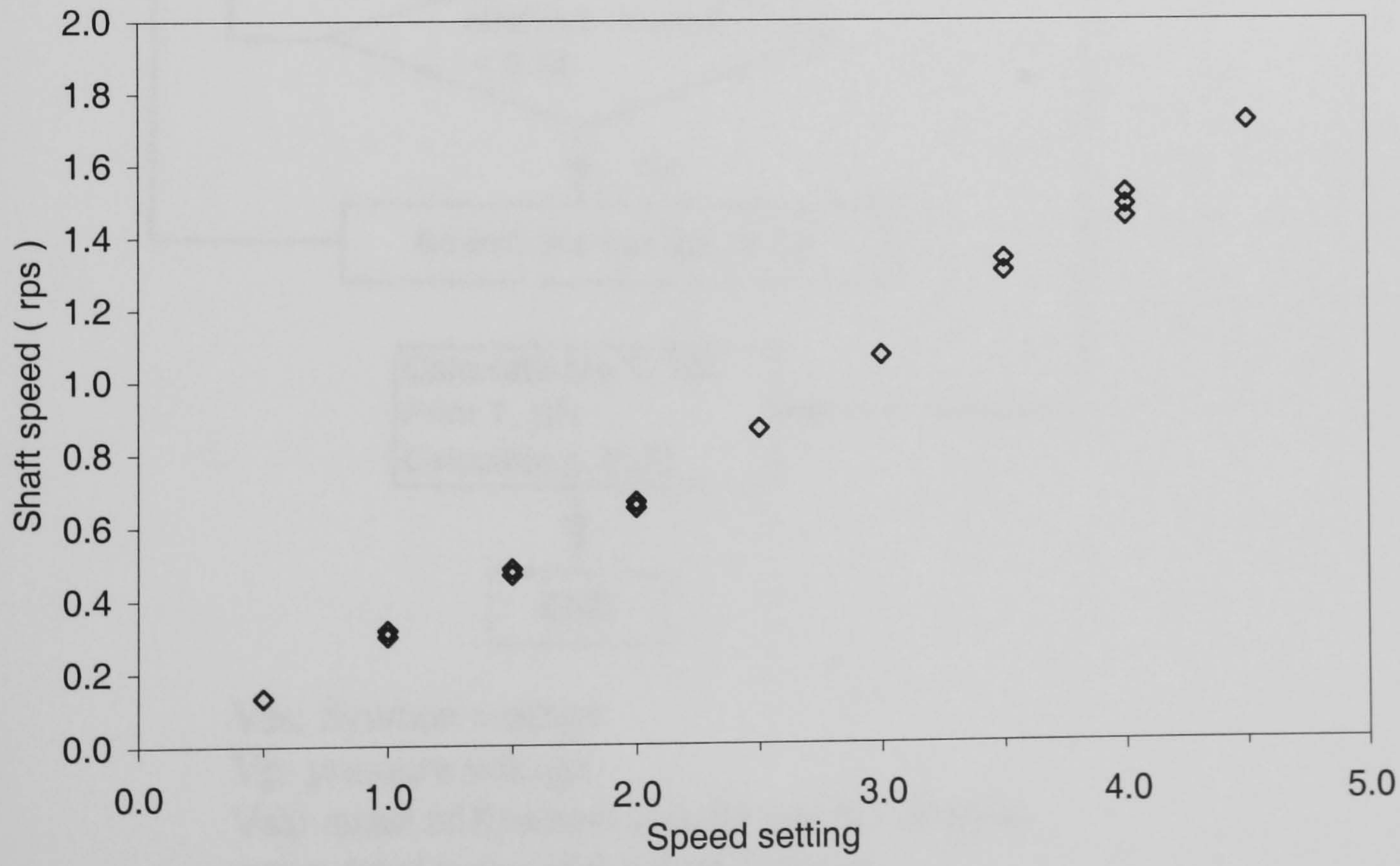

Figure A3: Calibration of shaft speed / speed setting

Program mc.exe

Flow Chart of MC.EXE

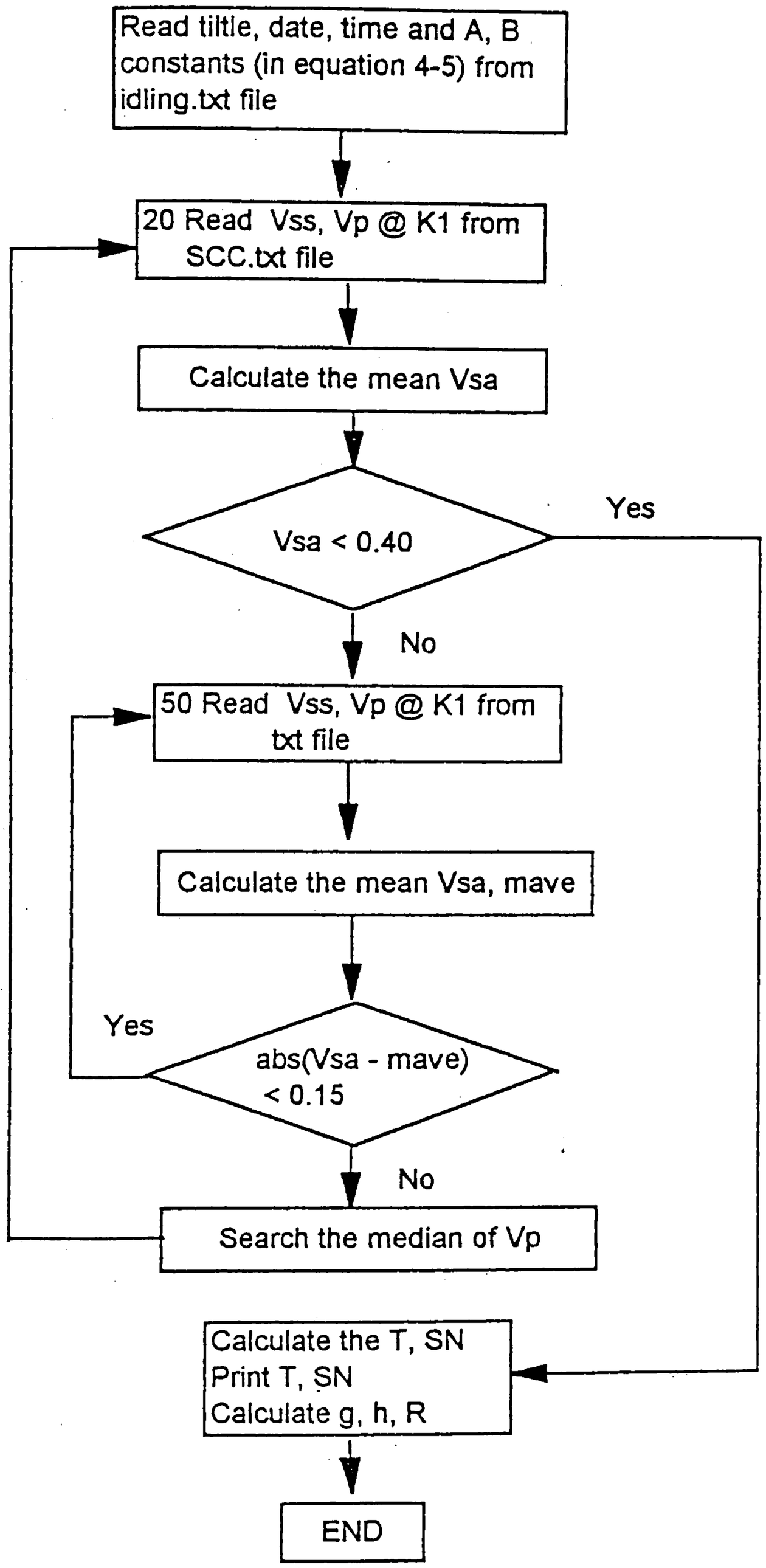

Vss: flywheel voltage
Vp: pressure voltage
Vsa: mean of flywheel voltage per K1 samples
mave: total mean of flywheel voltage
T: torque
SN: impeller shaft speed
g and h: rheological constants
R: correlation coefficient

```
      integer n,i,j,k,nm,jp,tjp(30),tnm(30),inp,ib,np
      real vp(30000), vss(30000), vsa(100), vsd(100),mave,tmave,mean
      real sigma,sn(300),sp(300),mp,tmp,vpa(100),vpd(100),psum,t(30)
      real a,b,r,ip(30),fsv(30),ipv(30),med
      character*20 f1,f2,title
      character*31 date
      character*22 time
      character*72 ititle,inr
      parameter (k1=100)
      write(*,*) 'By Paul Hsi-Wen Chai, Civil Eng. of UCL, Nov. 1995'
      write(*,*)
      print *, 'Enter the name of the data file'
      read '(a)', f1
      print *, 'Enter the name of the out file'
      read '(a)', f2
      open(1,file=f1,status='old')
      open(2,file=f2,status='unknown')
      open(3,file='iab.dat',status='old')
      read(3,17) ititle
      read(3,17) inr
   17 format(1x,a71)
      read(3,*)ai,bi


      read (1,6) title
    6 format(a17)
      do 10 i=1,7
      read(1,*)
   10 continue
      read (1,7) date
    7 format(a31)
      read (1,9) time
    9 format(t10,a22)
      do 15 i=1,8
      read(1,*)
   15 continue

      write(2,*) 'Run mc.exe under DOS system(<0.15,k1=100,<0.40 out
     + T=0.0215P,use median,19/Sept/96)'
   25 write(2,8) title,date,time
      write(2,17) ititle
      write(2,17) inr
      write(2,23) 'Idling pressure ai bi==>',ai,bi
   23 format(1x,a24,8x,f7.5,8x,f7.5)
    8 format(1x,a17,t20,a31,a22)
      write(2,*) ' n    flywheel speed voltage  pressure voltage
     +idling pressure voltage'
      write(*,*) ' n    flywheel speed voltage  pressure voltage
     +idling pressure voltage'

      j=1

   20 read(1,*)(vss(n),vp(n), n=1,k1)
      i=1
      nm=1
      vsa(i)=mean(vss,1,k1)
      if (vsa(i) .lt. 0.40) then
      go to 200
      endif
      mave=vsa(i)
```

```
      tmave=mave
   50 i=i+1
      do 100 n=1+(i-1)*k1,i*k1
      read(1,*) vss(n),vp(n)
  100 continue
      vsa(i)=mean(vss,1+(i-1)*k1,k1)

      if (abs(vsa(i)-mave) .le. 0.15) then
      tmave=tmave+vsa(i)
      nm=nm+1
      mave=tmave/nm
      write(*,150) vsa(i),mave,i
  150 format(1x,t7,f8.3,t21,f8.3,t35,i3)
      else
      write(*,*) '*****************************************'
      write(*,*) vsa(i),mave, abs(vsa(i)-mave),j
      write(*,*) '*****************************************'
      call median(n-1,vp,med)
      sn(j)=mave
      sp(j)=med
      tnm(j)=n-1
      mave=vsa(i)
      j=j+1
      go to 20
      endif

      go to 50
  200 do 300 n=1,j-i
      write(2,310) tnm(n), sn(n),sp(n),sn(n)*bi+ai
      write(*,310) tnm(n), sn(n),sp(n),sn(n)*bi+ai
  300 continue
  310 format(1x,i4,t15,f8.3,7x,t38,f8.3,15x,f8.3)
      write(2,*) '-----------------------------------------'
      write(*,*) '-----------------------------------------'
      write(*,*) '                Torque(Nm)      Shaft speed(rps)'
      write(2,*) '                Torque(Nm)      Shaft speed(rps)'
      do 400 i=1,j-1
      p=(176.44*sp(i)-155.5)-(176.44*(sn(i)*bi+ai)-155.5)
      t(i)=0.0215*p
      sn(i)=sn(i)/0.5/4.681486
      write(2,290) t(i),sn(i)
      write(*,290) t(i),sn(i)
  400 continue
  290 format(1x,t15,f8.3,t38,f8.3)
      call rab(j-1,sn,t,a,b,r)
c     call gra(j-1,sn,t,title)
      close(1)
      close(2)
      close(3)
      end
```

```
function mean(x,j,n)
real mean, x(30000), sum
```

```
      integer n,i,j
      sum=0
      do 1000 i=1,n
      sum=sum+x(j)
      j=j+1
1000  continue
      mean=sum/n
      end


      function sigma(x,k,n)
      real sigma, x(30000), sumr,r,av1,mean
      integer n,i,k
      sumr=0
      av1=mean(x,k,n)
      k=k-n
      do 1010 i=1,n
      r=x(k)-av1
      sumr=sumr+r*r
      k=k+1
1010  continue
      sigma=sqrt(sumr/(n-1))
      end

      function irun(x)
      real x
      integer irun
      if( mod(x*10,10) .gt. 4 ) then
      irun=x+1
      else
      irun=x
      endif
      end

      subroutine median(n,x,med)

      real x(6000),tmax,med
      integer n,i,j,m

      do 1012 i=1,n
      do 1014 j=i+1,n
      if (x(j) .gt. x(i)) then
      tmax=x(j)
      x(j)=x(i)
      x(i)=tmax
      endif
1014  continue
1012  continue
      if (mod(n,2) .eq. 0) then
      m=n/2
      med=(x(m)+x(m+1))/2
      else
      m=(n+1)/2
      med=x(m)
      endif
      return
      end

      subroutine rab(n,x,y,a,b,r)
```

```
      real x(300),y(300),a,b,r,tx,ty,txy,ty2,tx2,tz(350),hcl
      integer n,nn,k

c tz:The t distribution 90% confidence limit    tz(n)    d.f=n-2

      do 1020 i=1,350
      tz(i)=0
 1020 continue
      nn=n

      tz(4)=2.920
      tz(5)=2.353
      tz(6)=2.132
      tz(7)=2.015
      tz(8)=1.943
      tz(9)=1.895
      tz(10)=1.860
      tz(11)=1.833
      tz(12)=1.812
      tz(13)=1.796
      tz(14)=1.782
      tz(15)=1.771
      tz(16)=1.761
      tz(17)=1.753
      tz(18)=1.746
      tz(19)=1.740
      tz(20)=1.734
      tz(21)=1.729
      tz(22)=1.725
      tz(23)=1.721
      tz(24)=1.717
      tz(25)=1.714
      tz(26)=1.711
      tz(27)=1.708
      tz(28)=1.706
      tz(29)=1.703
      tz(30)=1.701
      tz(31)=1.699
      tz(32)=1.697
      tz(34)=1.6942
      tz(37)=1.690
      tz(40)=1.6864
      tz(42)=1.684
      tz(45)=1.681
      tz(47)=1.679
      tz(50)=1.6772
      tz(52)=1.676
      tz(57)=1.6735
      tz(62)=1.671
      tz(67)=1.669
      tz(72)=1.667
      tz(77)=1.6655
      tz(82)=1.664
      tz(87)=1.663
      tz(92)=1.662
      tz(97)=1.661
      tz(102)=1.660
      tz(112)=1.659
      tz(122)=1.658
      tz(132)=1.657
```

```
      tz(142)=1.656
      tz(152)=1.655
      tz(162)=1.654
      tz(182)=1.653
      tz(202)=1.653

1030  if (tz(nn) .eq. 0) then
      nn=nn-1
      go to 1030
      endif

      tz(n)=tz(nn)
      tx=0
      ty=0
      txy=0
      tx2=0
      ty2=0
      k=0

      do 1100 i=1,n

      if (x(i) .eq. 0) then
      k=k+1
      endif

      tx=tx+x(i)
      ty=ty+y(i)
      txy=txy+x(i)*y(i)
      tx2=tx2+x(i)*x(i)
      ty2=ty2+y(i)*y(i)
1100  continue

      n=n-k
      b=(n*txy-tx*ty)/(n*tx2-tx*tx)
      a=(ty-b*tx)/n
      r=(n*txy-tx*ty)/sqrt((n*tx2-tx*tx)*(n*ty2-ty*ty))
      write(2,*) '-------------------------------------------------'
      write(*,*) '-------------------------------------------------'
      write(2,76) 'n=',n
      write(*,76) 'n=',n
      write(2,77) 'Two point test constant g(Nm)=',a
      write(*,77) 'Two point test constant g(Nm)=',a
      write(2,78) 'Two point test constant h(Nm s)=',b
      write(*,78) 'Two point test constant h(Nm s)=',b
      write(2,79) 'Linear regression correlation coefficient r=',r
      write(*,79) 'Linear regression correlation coefficient r=',r
      hcl=tz(n)*sqrt((1-r*r)/r/r/(n-2))*100
      write(2,80) '90% confidence limits on g(%)=',sqrt(tx2/n)*b/abs(a)*
     +hcl
      write(*,80) '90% confidence limits on g(%)=',sqrt(tx2/n)*b/abs(a)*
     +hcl
      write(2,80) '90% confidence limits on h(%)=',hcl
      write(*,80) '90% confidence limits on h(%)=',hcl
      write(*,*)
76    format(1x,a2,i2)
77    format(1x,a30,f5.2)
78    format(1x,a32,f5.2)
79    format(1x,a44,f6.4)
80    format(1x,a30,f6.2)
      return
```

Program mct20.exe

```
      integer n,i,j,k,nm,jp,tjp(30),tnm(30),inp,ib,np
      real vp(30000), vss(30000), vsa(100), vsd(100),mave,tmave,mean
      real sigma,sn(300),sp(300),mp,tmp,vpa(100),vpd(100),psum,t(30)
      real a,b,r,ip(30),fsv(30),ipv(30),med
      character*20 f1,f2,title
      character*31 date
      character*22 time
      character*72 ititle,inr
      parameter (k1=100)
      write(*,*) 'By Paul Hsi-Wen Chai, Civil Eng. of UCL, Nov. 1995'
      write(*,*)
      print *, 'Enter the name of the data file'
      read '(a)', f1
      print *, 'Enter the name of the out file'
      read '(a)', f2
      open(1,file=f1,status='old')
      open(2,file=f2,status='unknown')
      open(3,file='iab.dat',status='old')
      read(3,17) ititle
      read(3,17) inr
   17 format(1x,a71)
      read(3,*)ai,bi


      read (1,6) title
    6 format(a17)
      do 10 i=1,7
      read(1,*)
   10 continue
      read (1,7) date
    7 format(a31)
      read (1,9) time
    9 format(t10,a22)
      do 15 i=1,8
      read(1,*)
   15 continue

      write(2,*) 'Run mct20.exe under DOS system(<0.15,k1=100,<0.40 out
     + T=0.0215P,use median,13/May/97, gear 20, 2.25 LM)'
   25 write(2,8) title,date,time
      write(2,17) ititle
      write(2,17) inr
      write(2,23) 'Idling pressure ai bi==>',ai,bi
   23 format(1x,a24,8x,f7.5,8x,f7.5)
    8 format(1x,a17,t20,a31,a22)
      write(2,*) ' n    flywheel speed voltage  pressure voltage
     +idling pressure voltage'
      write(*,*) ' n    flywheel speed voltage  pressure voltage
     +idling pressure voltage'

      j=1

   20 read(1,*)(vss(n),vp(n), n=1,k1)
      i=1
      nm=1
      vsa(i)=mean(vss,1,k1)
      if (vsa(i) .lt. 0.40) then
      go to 200
      endif
      mave=vsa(i)
```

```
      tmave=mave
   50 i=i+1
      do 100 n=1+(i-1)*k1,i*k1
      read(1,*) vss(n),vp(n)
  100 continue
      vsa(i)=mean(vss,1+(i-1)*k1,k1)

      if (abs(vsa(i)-mave) .le. 0.15) then
      tmave=tmave+vsa(i)
      nm=nm+1
      mave=tmave/nm
      write(*,150) vsa(i),mave,i
  150 format(1x,t7,f8.3,t21,f8.3,t35,i3)

      if (vsa(i) .lt. 0.40) then
      go to 200
      endif

      else

      write(*,*) '*****************************************'
      write(*,*) vsa(i),mave, abs(vsa(i)-mave),j
      write(*,*) '*****************************************'
      call median(n-1,vp,med)
      sn(j)=mave
      sp(j)=med
      tnm(j)=n-1
      mave=vsa(i)
      j=j+1
      go to 20
      endif

      go to 50

  200 do 300 n=1,j-1
      write(2,310) tnm(n), sn(n),sp(n),sn(n)*bi+ai
      write(*,310) tnm(n), sn(n),sp(n),sn(n)*bi+ai
  300 continue
  310 format(1x,i4,t15,f8.3,7x,t38,f8.3,15x,f8.3)
      write(2,*) '-----------------------------------------'
      write(*,*) '-----------------------------------------'
      write(*,*) '                Torque(Nm)       Shaft speed(rps)'
      write(2,*) '                Torque(Nm)       Shaft speed(rps)'
      do 400 i=1,j-1
      p=(176.44*sp(i)-155.5)-(176.44*(sn(i)*bi+ai)-155.5)
      t(i)=0.0215*p
      sn(i)=sn(i)/0.5/20.00*2.25
      write(2,290) t(i),sn(i)
      write(*,290) t(i),sn(i)
  400 continue
  290 format(1x,t15,f8.3,t38,f8.3)
      call rab(j-1,sn,t,a,b,r)
      call gra(j-1,sn,t,title)
      close(1)
      close(2)
      close(3)
      end
```

```
      function mean(x,j,n)
      real mean, x(30000), sum
      integer n,i,j
      sum=0
      do 1000 i=1,n
      sum=sum+x(j)
      j=j+1
1000  continue
      mean=sum/n
      end


      function sigma(x,k,n)
      real sigma, x(30000), sumr,r,av1,mean
      integer n,i,k
      sumr=0
      av1=mean(x,k,n)
      k=k-n
      do 1010 i=1,n
      r=x(k)-av1
      sumr=sumr+r*r
      k=k+1
1010  continue
      sigma=sqrt(sumr/(n-1))
      end

      function irun(x)
      real x
      integer irun
      if( mod(x*10,10) .gt. 4 ) then
      irun=x+1
      else
      irun=x
      endif
      end

      subroutine median(n,x,med)

      real x(6000),tmax,med
      integer n,i,j,m

      do 1012 i=1,n
      do 1014 j=i+1,n
      if (x(j) .gt. x(i)) then
      tmax=x(j)
      x(j)=x(i)
      x(i)=tmax
      endif
1014  continue
1012  continue
      if (mod(n,2) .eq. 0) then
      m=n/2
      med=(x(m)+x(m+1))/2
      else
      m=(n+1)/2
```

```
      med=x(m)
      endif
      return
      end

      subroutine rab(n,x,y,a,b,r)

      real x(300),y(300),a,b,r,tx,ty,txy,ty2,tx2,tz(350),hcl
      integer n,nn,k

c tz:The t distribution 90% confidence limit    tz(n)    d.f=n-2

      do 1020 i=1,350
      tz(i)=0
 1020 continue
      nn=n

      tz(4)=2.920
      tz(5)=2.353
      tz(6)=2.132
      tz(7)=2.015
      tz(8)=1.943
      tz(9)=1.895
      tz(10)=1.860
      tz(11)=1.833
      tz(12)=1.812
      tz(13)=1.796
      tz(14)=1.782
      tz(15)=1.771
      tz(16)=1.761
      tz(17)=1.753
      tz(18)=1.746
      tz(19)=1.740
      tz(20)=1.734
      tz(21)=1.729
      tz(22)=1.725
      tz(23)=1.721
      tz(24)=1.717
      tz(25)=1.714
      tz(26)=1.711
      tz(27)=1.708
      tz(28)=1.706
      tz(29)=1.703
      tz(30)=1.701
      tz(31)=1.699
      tz(32)=1.697
      tz(34)=1.6942
      tz(37)=1.690
      tz(40)=1.6864
      tz(42)=1.684
      tz(45)=1.681
      tz(47)=1.679
      tz(50)=1.6772
      tz(52)=1.676
      tz(57)=1.6735
      tz(62)=1.671
      tz(67)=1.669
      tz(72)=1.667
      tz(77)=1.6655
      tz(82)=1.664
```

```
      tz(87)=1.663
      tz(92)=1.662
      tz(97)=1.661
      tz(102)=1.660
      tz(112)=1.659
      tz(122)=1.658
      tz(132)=1.657
      tz(142)=1.656
      tz(152)=1.655
      tz(162)=1.654
      tz(182)=1.653
      tz(202)=1.653

1030  if (tz(nn) .eq. 0) then
      nn=nn-1
      go to 1030
      endif

      tz(n)=tz(nn)
      tx=0
      ty=0
      txy=0
      tx2=0
      ty2=0
      k=0

      do 1100 i=1,n

      if (x(i) .eq. 0) then
      k=k+1
      endif

      tx=tx+x(i)
      ty=ty+y(i)
      txy=txy+x(i)*y(i)
      tx2=tx2+x(i)*x(i)
      ty2=ty2+y(i)*y(i)
1100  continue

      n=n-k
      b=(n*txy-tx*ty)/(n*tx2-tx*tx)
      a=(ty-b*tx)/n
      r=(n*txy-tx*ty)/sqrt((n*tx2-tx*tx)*(n*ty2-ty*ty))
      write(2,*) '-------------------------------------------------'
      write(*,*) '-------------------------------------------------'
      write(2,76) 'n=',n
      write(*,76) 'n=',n
      write(2,77) 'Two point test constant g(Nm)=',a
      write(*,77) 'Two point test constant g(Nm)=',a
      write(2,78) 'Two point test constant h(Nm s)=',b
      write(*,78) 'Two point test constant h(Nm s)=',b
      write(2,79) 'Linear regression correlation coefficient r=',r
      write(*,79) 'Linear regression correlation coefficient r=',r
      hcl=tz(n)*sqrt((1-r*r)/r/r/(n-2))*100
      write(2,80) '90% confidence limits on g(%)=',sqrt(tx2/n)*b/abs(a)*
     +hcl
      write(*,80) '90% confidence limits on g(%)=',sqrt(tx2/n)*b/abs(a)*
     +hcl
      write(2,80) '90% confidence limits on h(%)=',hcl
      write(*,80) '90% confidence limits on h(%)=',hcl
```

```
      write(*,*)
   76 format(1x,a2,i2)
   77 format(1x,a30,f5.2)
   78 format(1x,a32,f5.2)
   79 format(1x,a44,f6.4)
   80 format(1x,a30,f6.2)
      return
      end



      subroutine gra(n,x,y,ch)

      real x(300),y(300)
      integer Isn(300),it(300),n,m
      character*20 ch
      character line(60),iast
      data line /60*1H /, iast /1H*/

      do 1200 I=1,n
      isn(i)=irun(x(i)*1000/25)
      it(i)=irun(y(i)*10/2)
 1200 continue

      write(2,93) '   r.p.s                ',ch
      write(*,93) '   r.p.s                ',ch
   93 format(1x,a22,a17)
      do 1205 i=1,60
      j=61-i
      do 1204 k=1,n
      if (isn(k) .eq. j)  then
      m=it(k)
      line(m)=iast
      endif
 1204 continue
      if (mod(j,5) .eq. 0) then
      write(2,89)j*0.025,line
      write(*,89)j*0.025,line
      else
      write(2,88)line
      write(*,88)line
      endif
   88 format(7x,1HI, 60A1)
   89 format(1x,f5.3,2H +, 60A1)
      line(m)=' '
 1205 continue

  x-axis
      write(2,91)2,4,6,8,10,12
      write(*,91)2,4,6,8,10,12
   91 format(7x,2H+-,12(5H---+-),2H--/ 8x,6i10)
      write(2,*)'                                        Torque(Nm)'
      write(*,*)'                                        Torque(Nm)'
      return
```

Table A4 : Slump and two-point test results for NSC mixes in figure 5.1

Mix	Slump measurements		Two-point test measurements			
	Time (mins)	Slump (mm)	Time (mins)	Yield value g (Nm)	Plastic viscosity h (Nms)	r
1 (dry aggs, 100% OPC)	8	180	12	2.22	1.73	0.9872
	26	150	31	3.07	1.59	0.9804
	50	100	55	4.60	1.09	0.9769
	66	80	69	4.61	1.79	0.9752
	81	60	85	6.52	1.18	0.9713
	100	35	-	-	-	-
2 (pre-saturated aggs)	7	170	10	2.22	1.74	0.9786
	24	170	29	2.69	1.32	0.9769
	42	170	47	2.86	1.27	0.9744
	66	135	72	3.81	1.14	0.9723
	85	100	89	4.58	1.20	0.9709
	103	80	107	5.58	1.22	0.9683
3 (dry aggs, 100% PFA)	8	245	11	0.97	1.13	0.9907
	35	220	30	1.77	1.20	0.9878
	65	180	60	2.43	1.14	0.9819
	95	125	90	3.76	0.86	0.9794
	125	65	120	6.49	0.44	0.9699
4 (pre-saturated aggs., 100%PFA)	10	240	15	1.12	1.28	0.9943
	30	240	36	1.22	1.29	0.9927
	56	240	61	1.31	1.39	0.9931
	89	230	97	1.66	1.31	0.9868
	135	210	139	1.79	1.67	0.9853
	153+	205	158	1.99	1.81	0.9851
5 (plain)	11	100	14	4.28	1.43	0.9791
	26	80	29	5.30	1.70	0.9788
	48	55	53	6.88	0.51	0.9601
	66	35	-	-	-	-
6 (superplasticized)	6	170	10	2.96	1.83	0.9877
	25	120	29	4.78	1.47	0.9814
	42	80	47	6.57	0.52	0.9722
	61	40	-	-	-	-

+ represents results not shown in figure 5.1

Table A5 : Slump and two-point test results for HSC mixes in figure 5.2

Mix	Slump measurements				Two-point test measurements			
	Time (mins)	Slump (mm)	Spread SFS (mm)	ST (secs)	Time (mins)	Yield value g (Nm)	Plastic viscosity h (Nms)	r
1 (0.42 w/b)	6.5 15 32 45 62 75 90	225 220 200 165 120 75 40	495 490 435 370 220 200 200	~ 10	10 30 60	0.45 1.75 3.21	4.78 4.64 4.4	0.9887 0.9856 0.9807
2 (0.40 w/b)	7 15 32 45 62 75 90	220 210 190 155 95 60 35	480 450 410 300 200 200 200	~ 10	10 30 60	0.99 1.72 3.41	5.03 4.71 4.46	0.9902 0.9867 0.9811
3 (0.38 w/b)	6 17 35 45 65 90 -	220 200 145 115 80 50 -	490 405 300 200 200 200 -	~ 15	10 30 60	0.8 1.83 3.71	5.4 5.13 4.52	0.9878 0.9836 0.9789
4 (0.34 w/b)	7 17 35 45 62 75 90	230 215 195 170 110 70 40	505 490 400 350 200 200 200	~ 20	10 30 60	1.5 2.28 3.88	5.97 5.29 4.67	0.9799 0.9803 0.9704
5 (0.30 w/b)	8 15 27 52 77 -	225 210 170 110 45 -	485 420 340 200 200	~ 30	10 30 60	3.06 3.78 6.83	10.11 8.8 5.92	0.9876 0.985 0.9793
6 (0.26 w/b)	8 35 45 65 75 90	225 200 170 110 70 50	500 395 345 210 200 200	~ 90	10 30 60	10.11 8.89 10.73	8.84 10.19 6.45	0.9811 0.9764 0.9751
7 (0.22 w/b)	8 35 -	150 50 -	310 200 -	> 120	10 30 -	14.7 16.1 -	15.4 10.7 -	0.9343 0.9201 -

Table A6 : Mix stability and compactability test results for HSC mixes in figure 5.4-5.5.

Mix	Mix stability measuremensts					Compactability measurements				
	Time (mins)	**Bm**	**Tc** (Nm)	**SI** (%)	Time (mins)	**SC** (kg/m^3)	Time (mins)	**CF**	Time (mins)	**dH** (mm)
1 (0.42 w/b)	10	8	1.65	19	12	2300	10	0.958	12	2
					32	2215	30	0.891	32	10
	30	6	1.58		62	2140	60	0.952	62	30
					90	1945	75	0.940	75	40
	60	1	1.06	14			90	0.910	90	55
2 (0.40 w/b)	10	8	1.57	-	10	-	10	-	12	3
					30	-	30	-	32	8
	30	7	1.57		60	-	60	-	62	19
					75	-	75	-	75	35
	60	1	1.06	-	90	-	90	-	90	55
3 (0.38 w/b)	10	7	1.42	15.1	12	2285	10	0.992	12	9
					32	2187	30	0.967	32	20
	30	5	1.48		62	2105	60	0.951	62	24
					75	-	75	0.961	75	39
	60	1	0.95	10	90	-	90	0.920	90	55
4 (0.34 w/b)	10	8	1.14	12.0	12	2365	10	0.981	12	3
					32	2275	30	0.967	32	5
	30	7	0.76		62	2190	60	0.977	62	15
					90	1950	75	0.964	75	39
	60	1	0.76	9			90	0.930	90	60
5 (0.30 w/b)	10	7	0.95	9						
					12	2398	10	0.978	12	7
	30	4	0.57		32	2348	30	0.941	32	20
					62	2205	60	0.926	62	60
	60	0	0.7	8.7	75	1975	75	0.824	75	80
										-
6 (0.26 w/b)	10	8	0.57	7	12	2405	10	-	12	7
					32	2315	30	-	32	15
	30	7	0.38		62	2267	60	-	62	35
					75	2195	75	-	75	50
	60	2	0.57	6.1	90	2005	90	-	90	75
7 (0.22 w/b)	10	2	-	3.5	-	-	-	-	12	40
	30	0	-	-	-	-	-	-	-	-
					-	-	-	-	-	-

. **Bm** = Subjective bleeding mark, **Tc** = Torque change, **SI** = Segregation index.

. SC = Self-compacting properties (cube method), CF = compacting factor test value, **dH** drop in height (cylinder-vibration method).

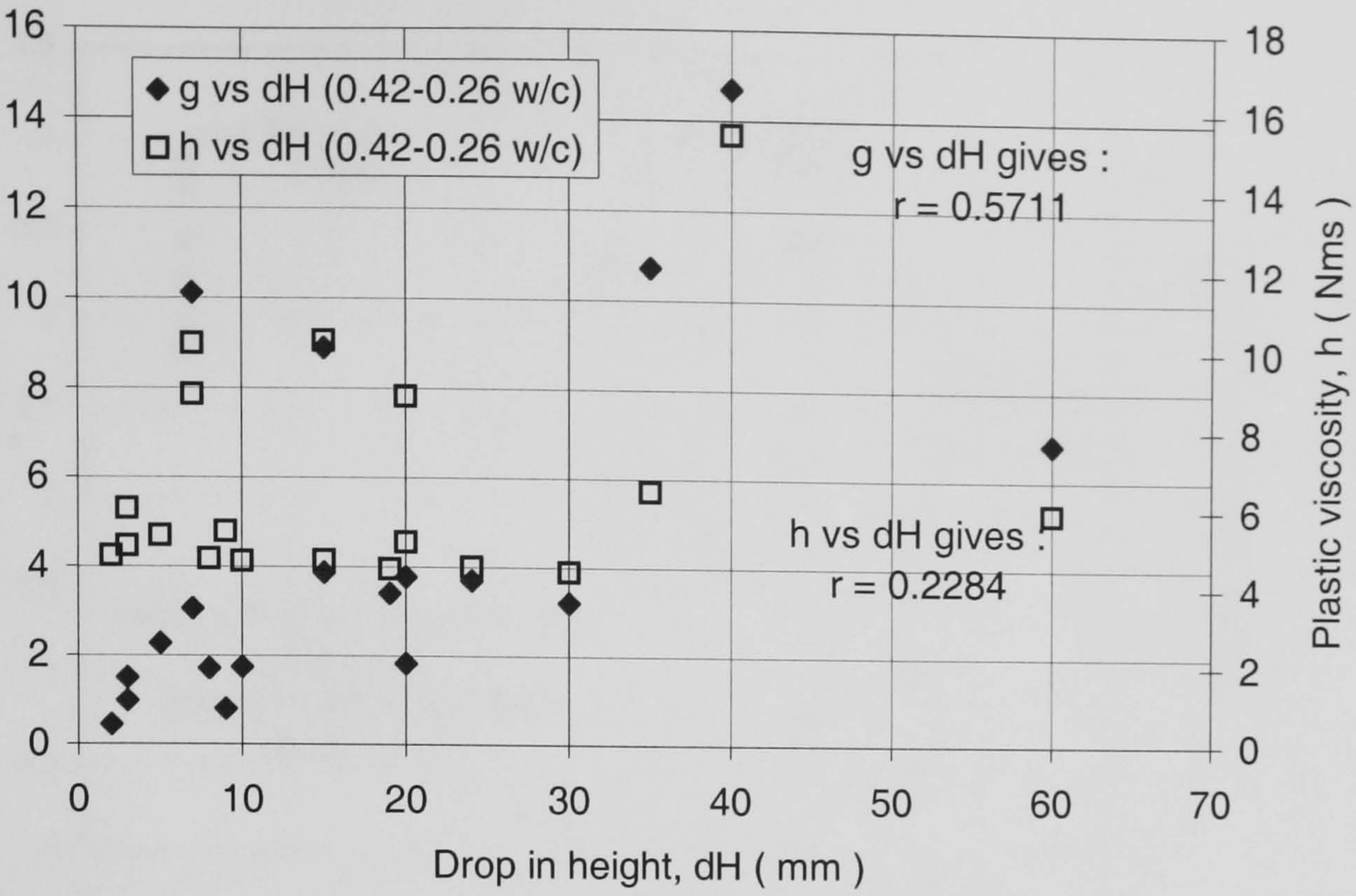

Figure A4 : Relationship between cylinder-vibration measurements and the Bingham parameters (at 0.42-0.22 w/b ratios)

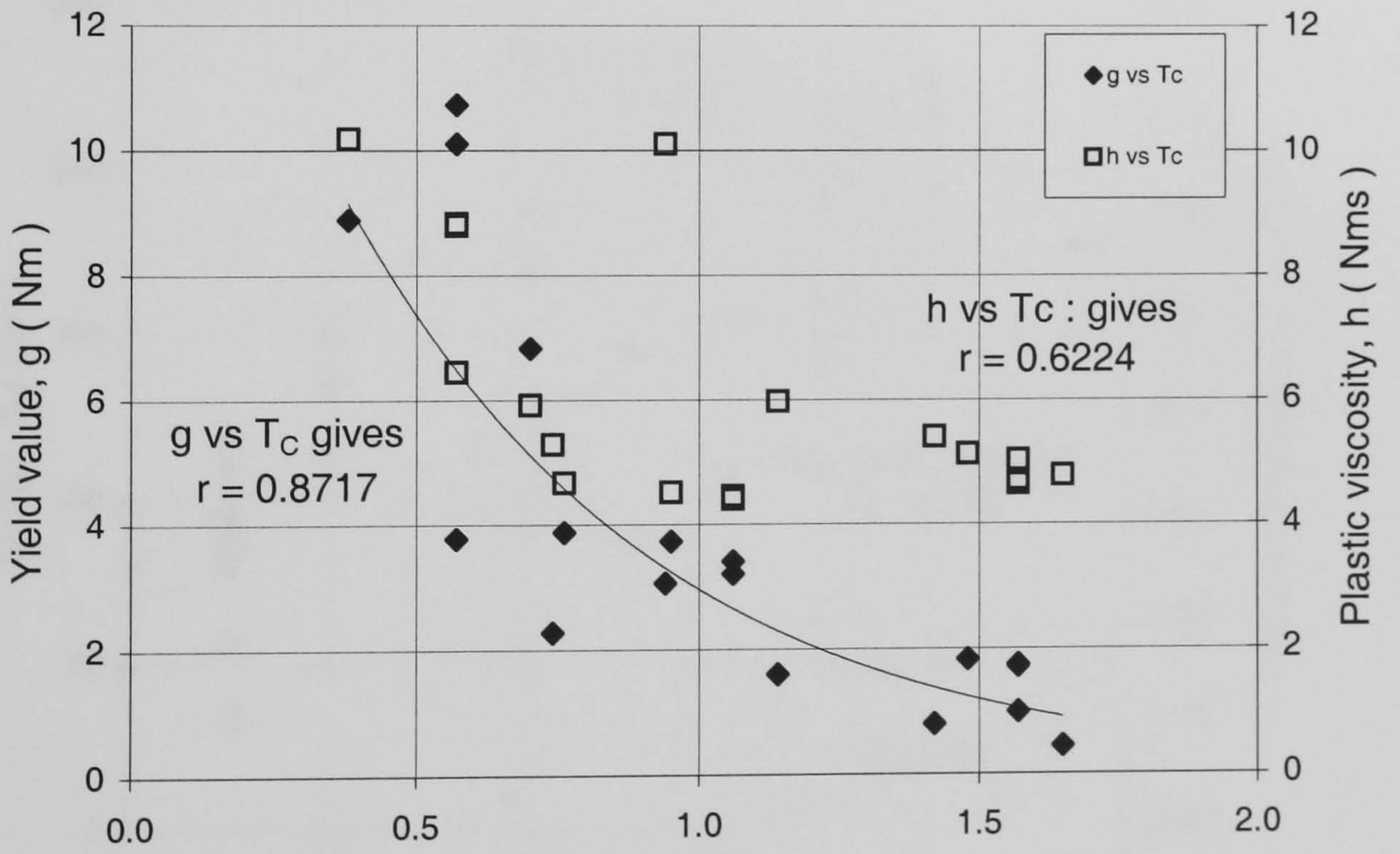

Figure A5 : Relationships between the two-point test parameters and segregation resistance (as assessed by Tc)

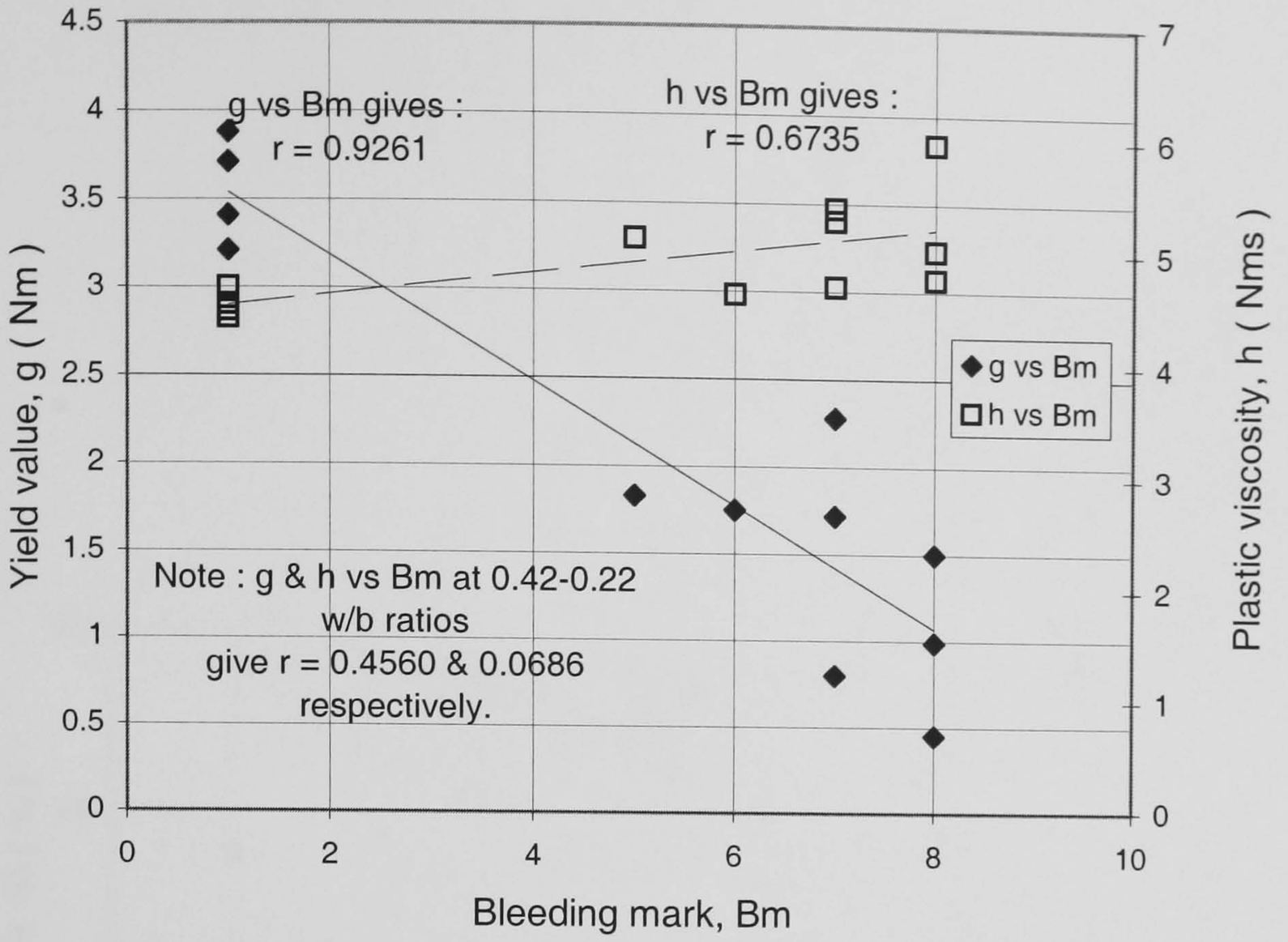

Figure A6 : Relationships between the Bingham parameters and Bleeding mark (at 0.42-0.34 w/b ratios)

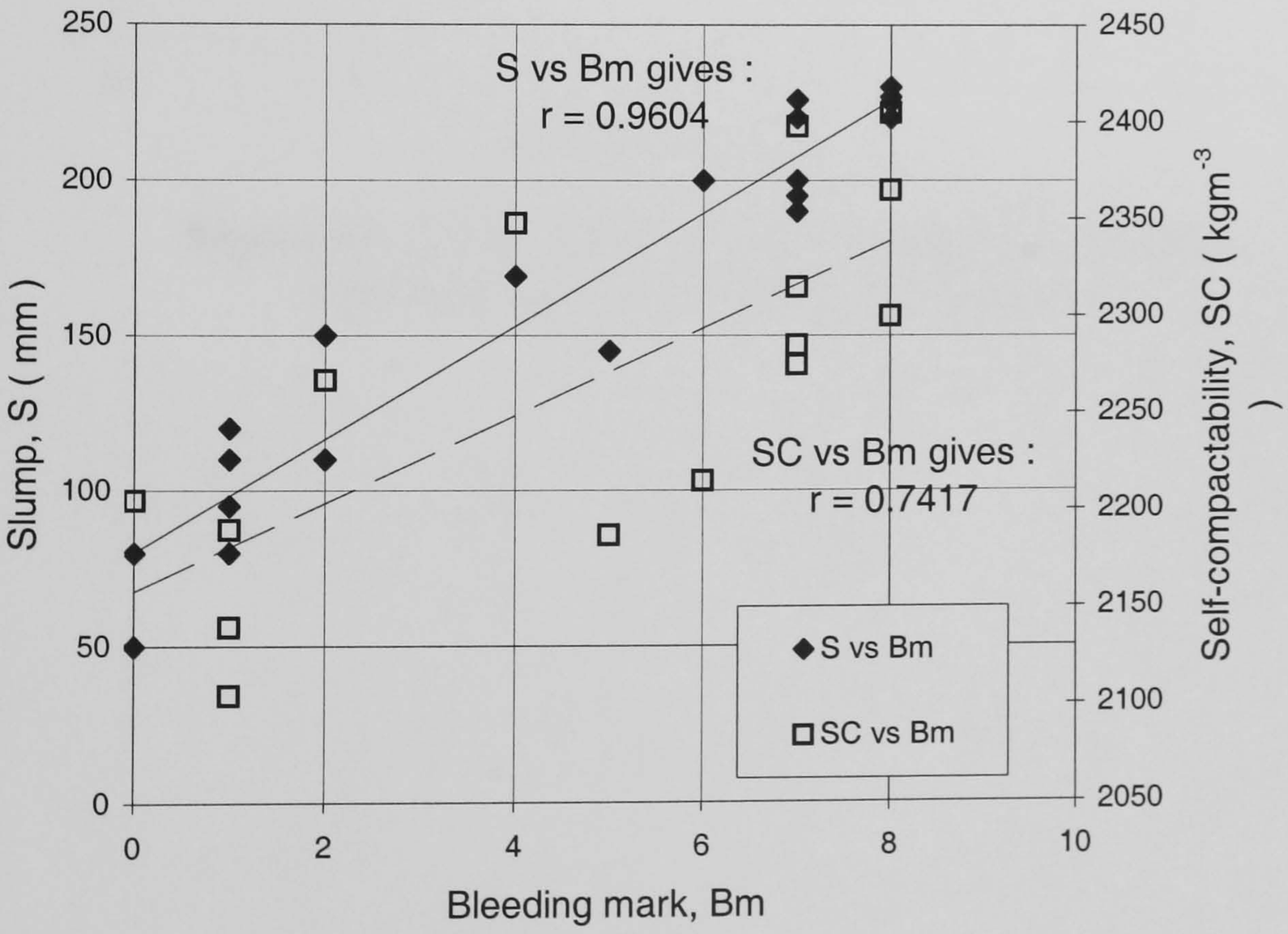

Figure A7 : Relationships between Bleeding mark with slump and self-compactability (at 0.42-0.22 w/b ratios).

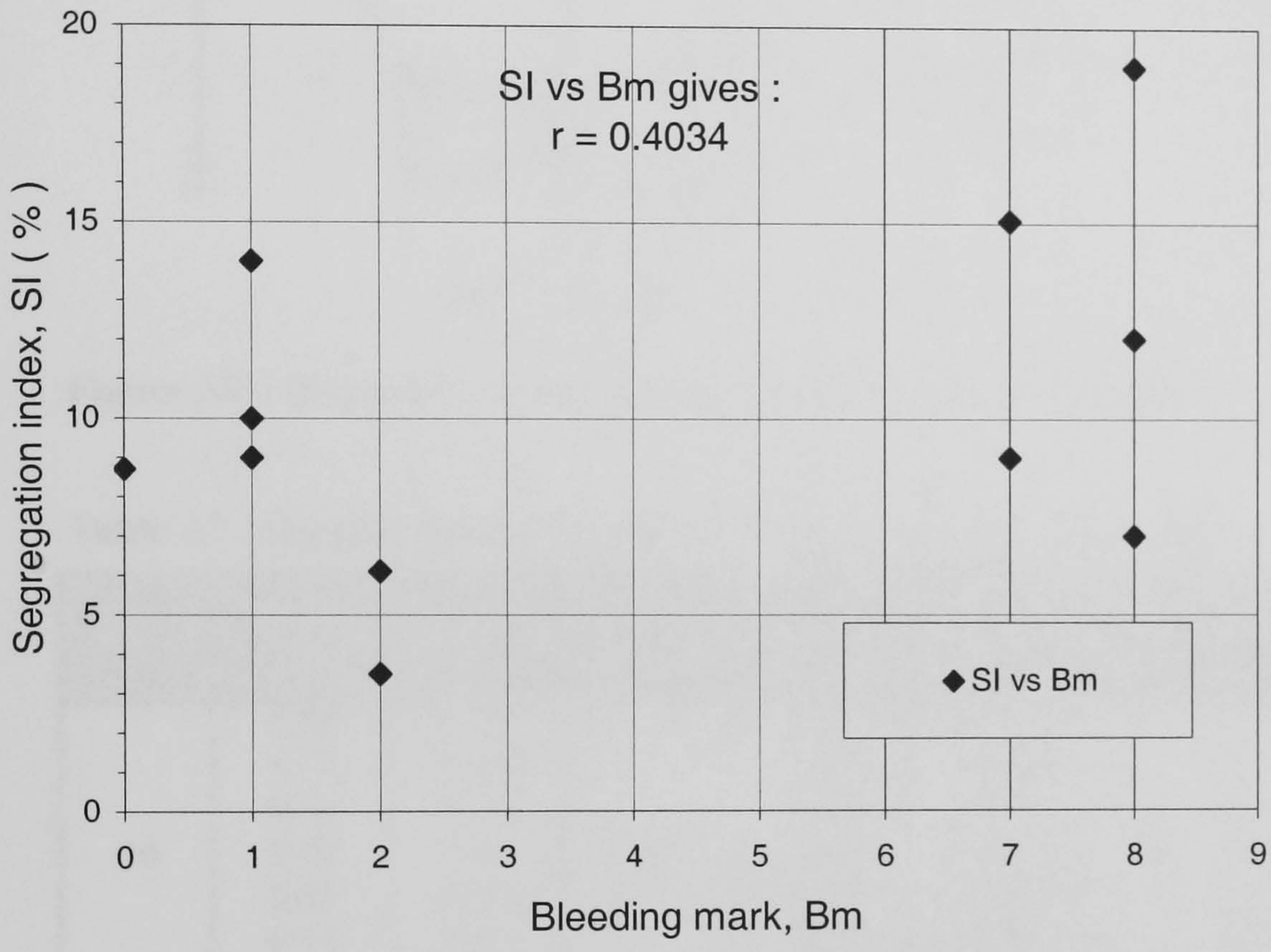

Figure A8 : Relationship between segregation resistance and Bleeding mark (at 0.42-0.22 w/b ratios)

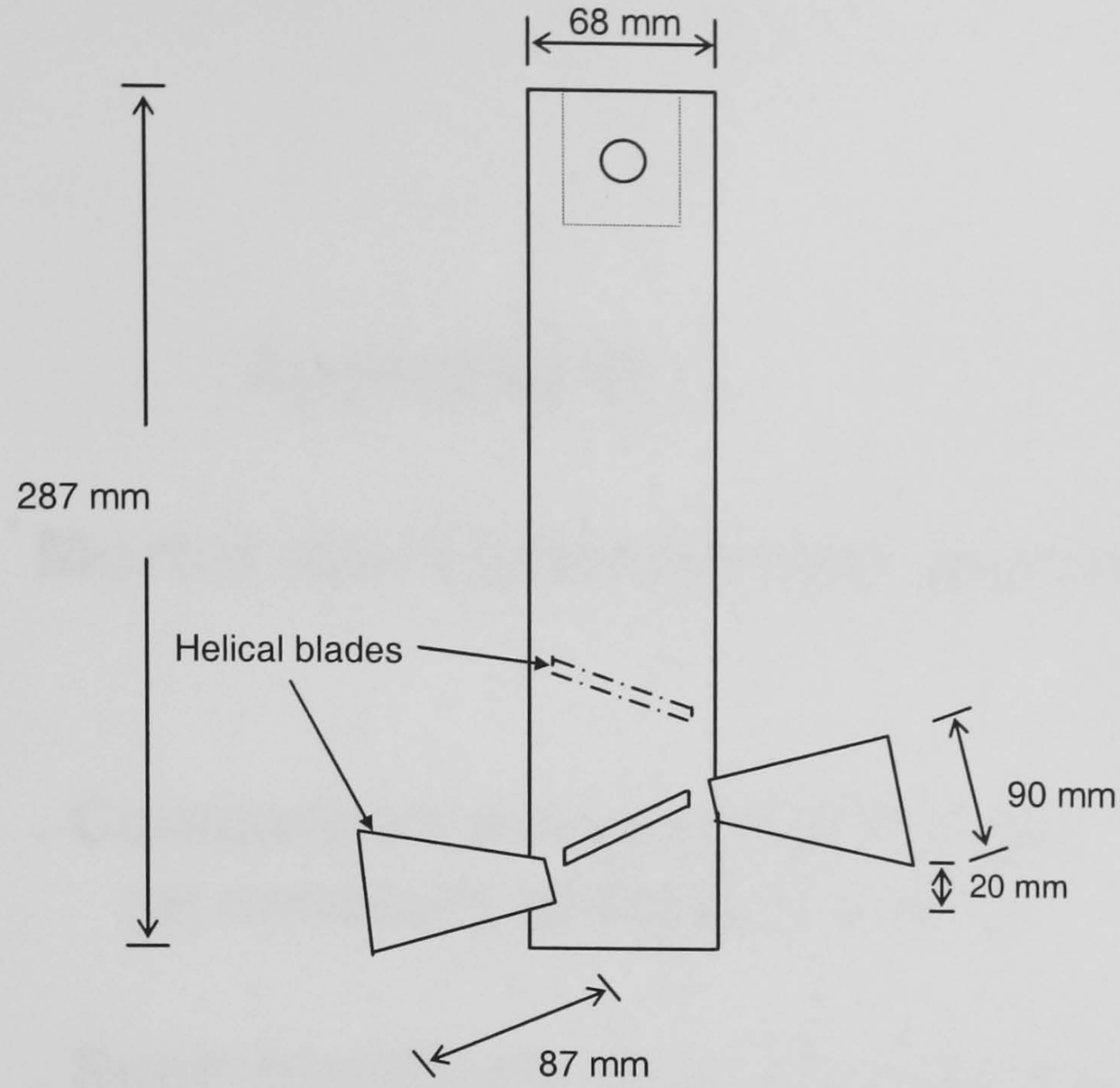

Figure A9 : Dimensions of large helical impeller used in section 5.5.2.

Table A7 : Impeller Speed / Torque test results for up-curves in figure 5.7.

Time (mins)	Speed (rps)	Torque (Nm)	Time (mins)	Speed (rps)	Torque (Nm)	Time (mins)	Speed (rps)	Torque (Nm)
	1.28	20.69		1.28	19.00		1.28	17.86
	1.11	20.44		1.11	18.89		1.11	17.81
	0.95	19.73		0.95	18.71		0.95	17.80
10	0.79	19.1	30	0.79	18.42	60	0.79	17.22
	0.63	17.75		0.63	17.78		0.63	16.89
	0.46	15.41		0.46	16.31		0.46	15.97
	0.30	12.91		0.30	13.84		0.30	13.74
	0.14	10.51		0.14	11.22		0.14	11.46

Table A8 : Mortar spread and V-funnel test results in figure 5.12

w/b ratio	Time (mins)	Spread (mm)	Time (mins)	V-flow time (secs)
0.42	8	320	10	3.5
0.38	8	320	10	5.4
0.3	9	330	11	14
0.26	8	325	10	17.06
0.22	10	280	12	> 30[+]
0.22[*]	15	325*	17	32

* Redosed. [+] Intermittent flow.

All mixes prepared with moist sand

Appendix B

Mortar and Concrete test results for

. Comparison of superplasticizers
(at constant dosage of 2.00%)

. Superplasticizer dosage performance

. Superplasticizer mixing procedure

. Cement-superplasticizer compatibility

Table B1 : Mortar spread and V-funnel test results in figure 6.1

Admixture Type/brand	Time (mins)	Spread (mm)	Time (mins)	V-flow time (secs)
SMF (Conplast M1)	8 30 60	185 175 152.5	9 34 65	9.48 11.9 20.79
SMF (Sika FF)	7.5 30 60 91	237.5 235 225 202.5	10 34 64 94	9.43 9.89 12.78 18.77
SNF (Conplast SP 435)	8.5 30 61 90	312.5 307.5 297.5 285	9 35 65 94	6.07 7.18 8.4 9.11
SNF (Sika N)	8 30 60 91	310 305 292.5 280	9 35 64 94	6.15 6.5 7.45 9.8
MLS (Conplast SP4)	8 30 60 90	280 270 255 242.5	9 34 64 93	8.01 10.41 11.11 11.85
Pre-blended (Conplast SP 450)	8 30 60 90	250 240 225 210	10 35 64 95	18.49 24.89 32 44
Pre-blended (Darcem SP6)	7.5 31 60 90	315 305 292.5 282.5	10 35 62 95	5.77 7.5 8.7 9.39
Vinyl (Sika 10)	8 31 60 90	285 275 260 240	9 35 64 95	7.7 10.49 12.17 14.31
Acrylate (Darcem, D 2001)	7.5 30 60 90	335 330 315 287.5	9 35 63 95	4.89 5.84 6.84 9.89
Retarder (Conplast R)	8 30 60 90	145 145 140 137.5	No flow	
Air-entrainer (Conplast PA21)	8 30 60 90	190 187.5 175 165	10 35 65 93	4.16 4.9 5.8 7.2

Table B2(a) : Slump and two-point test results for HSC mixes in figure 6.2

Superplasticizer Type (& brand)	Slump measurements				Two-point test measurements				SI
	Time (mins)	Slump (mm)	Spread SFS (mm)	ST (secs)	Time (mins)	Yield value g (Nm)	Plastic viscosity h (Nms)	r	(%)
SMF (Sika FF)	7	120	215	0	10	4.69	8.01	0.9929	4.5
	35	80	180	-	30	6.33	11.15	0.9765	
	65	50	-	-	60	8.25	9.23	0.9530	3.2
SNF (SP 435)	7.5	220	475	75	10	0.81	5.89	0.9913	11.8
	35	210	410	70	30	1.17	6.21	0.9886	
	65	190	365	60	60	1.39	6.79	0.9944	
	95	170	310	50	90	1.87	7.01	0.9884	
	125	150	245	-	120	3.04	8.14	0.9948	4.9
MLS (D SP 4)	7.5	195	375	70	10	2.58	6.18	0.9827	10.3
	35	170	300	60	30	2.41	8.31	0.9941	
	65	155	260	40	60	2.92	8.86	0.9899	
	95	140	235	30	90	3.92	9.46	0.9805	7.62
	125	120	210	-	120	5.21	10.81	0.9798	
Vinyl (Sika 10)	7	205	-	85	10	1.95	5.49	0.9934	10.3
	35	185	-	65	30	3.21	5.91		
	65	160	-	60	60	4.16	6.95	0.9827	
	95	130	-	50	90	5.20	8.18	0.9681	
	125	110	-	-	120	7.20	9.33	0.936	5.03
Acrylate (D 2001)	7.5	240	560	100	10	0.45	4.44	0.9979	15.0
	35	215	425	70	30	0.70	5.25	0.9937	
	65	100	200	0	60	3.43	7.35	0.9804	
	95	30	200	-	90	7.10	8.20	0.9754	5.0
	125	-	-	-	120	-	-	-	

Table B2(b) : Slump and two-point test results for repeat mixes in Table 6.2

Superplasticizer Type (& brand)	Slump measurements				Two-point test measurements				SI
	Time (mins)	Slump (mm)	Spread SFS (mm)	ST (secs)	Time (mins)	Yield value g (Nm)	Plastic viscosity h (Nms)	r	(%)
SMF (Sika FF)	7	90	205	-	10	5.06	7.66	0.9712	3.75
	35	75	200	-	30	6.28	9.45	0.9633	
	65	55	200	-	60	7.13	8.30	0.9601	-
Acrylate (D 2001)	8	240	555	90	10	0.47	4.85	0.9873	12.0
	35	190	-	-	30	0.69	5.95	0.9811	
	65	95	200	-	60	4.07	8.21	0.9752	
	95	20	200	-	90	8.38	8.89	0.9733	2.5

Table B3(a) : Mortar-dosage response test results in figure 6.3

Superplasticizer type	**Dosage** (%, s/w/b)	Spread (mm)	V-flow time (secs)
SMF (Sika FF)	1.25	120	No flow
	1.50	195	17.14
	1.75	**240**	**9.29**
	2.00	237.5	9.43
	2.25	240	9.84
	2.50	237.5	9.71
	3.00	237.5	12.21
	4.00	215	14.66
SNF (SP 435)	1.25	225	11.42
	1.50	270	8.0
	1.75	295	7.3
	2.00	312.5	6.07
	2.25	327.5	5.2
	2.50	**337.5**	**4.35**
	2.75	337.5	4.51
	3.00	335	4.88
	3.50	*325*	5.53
	4.00	320	5.89
MLS (SP 4)	1.25	205	17.49
	1.50	250	11.32
	1.75	**282.5**	**7.78**
	2.00	280	8.01
	2.25	282.5	7.9
	2.5	280	8.1
	3.00	270	9.7
	4.00	270	12.08
Vinyl (Sika 10)	1.50	230	10.44
	1.75	270	8.68
	2.00	285	7.7
	2.25	**295**	**6.88**
	2.50	290	7.05
	3.00	295	7.31
	4.00	285	8.12
Acrylate (D 2001)	1.00	215	10.36
	1.50	305	6.1
	1.75	320	5.67
	2.00	335	4.98
	2.25	**340**	**4.53**
	2.50	340	4.81
	3.00	332.5	4.9
	4.00	330	5.36

All measurements were taken immediately after the initial mixing sequence (i.e. at 8-10 mins).
Values in **BOLD** represent saturation values

Table B3(b) : Mortar loss of workability measurements with SMF, SNF, MLS, Vinyl and Acrylate-based superplasticizers at their respective saturation dosages (in Table B3(a)) and 0.5% over-doses.

Superplasticizer type	**Dosage** (%, s/w/b)	Time (mins)	Spread (mm)	Time (mins)	V-flow time (secs)
SMF (Sika FF)	* 1.75 (Sat. dosage)	8	240	10	9.83
		60	230	62	10.75
		120	215	124	12.78
	2.25 (Over-dosed)	8	240	10	10.2
		60	230	62	11.83
		120	205	124	14.17
SNF (SP 435)	2.50 (Sat. dosage)	8	337.5	10	4.35
		60	335	62	5.27
		120	325	124	7.06
	3.00 (Over-dosed)	8	335	10	4.88
		60	330	62	5.72
		120	310	124	7.33
MLS (SP 4)	* 1.75 (Sat. dosage)	8	285	10	7.95
		60	277.5	62	9.88
		120	265	124	11.36
	2.25 (Over-dosed)	8	282.5	10	7.82
		60	270	62	10.13
		120	255	124	13.25
Vinyl (Sika 10)	2.25 (Sat. dosage)	8	295	10	6.88
		60	282.5	62	8.79
		120	265	124	12.41
	2.75 (Over-dosed)	8	295	10	7.21
		60	280	62	8.68
		120	255	124	13.75
Acrylate (D 2001)	* 2.25 (Sat. dosage)	8	342.5	10	4.37
		60	335	62	6.03
		120	310	124	8.49
	2.75 (Over-dosed)	8	335	10	4.69
		60	330	62	6.33
		120	295	124	9.57

* represents repeat mixes

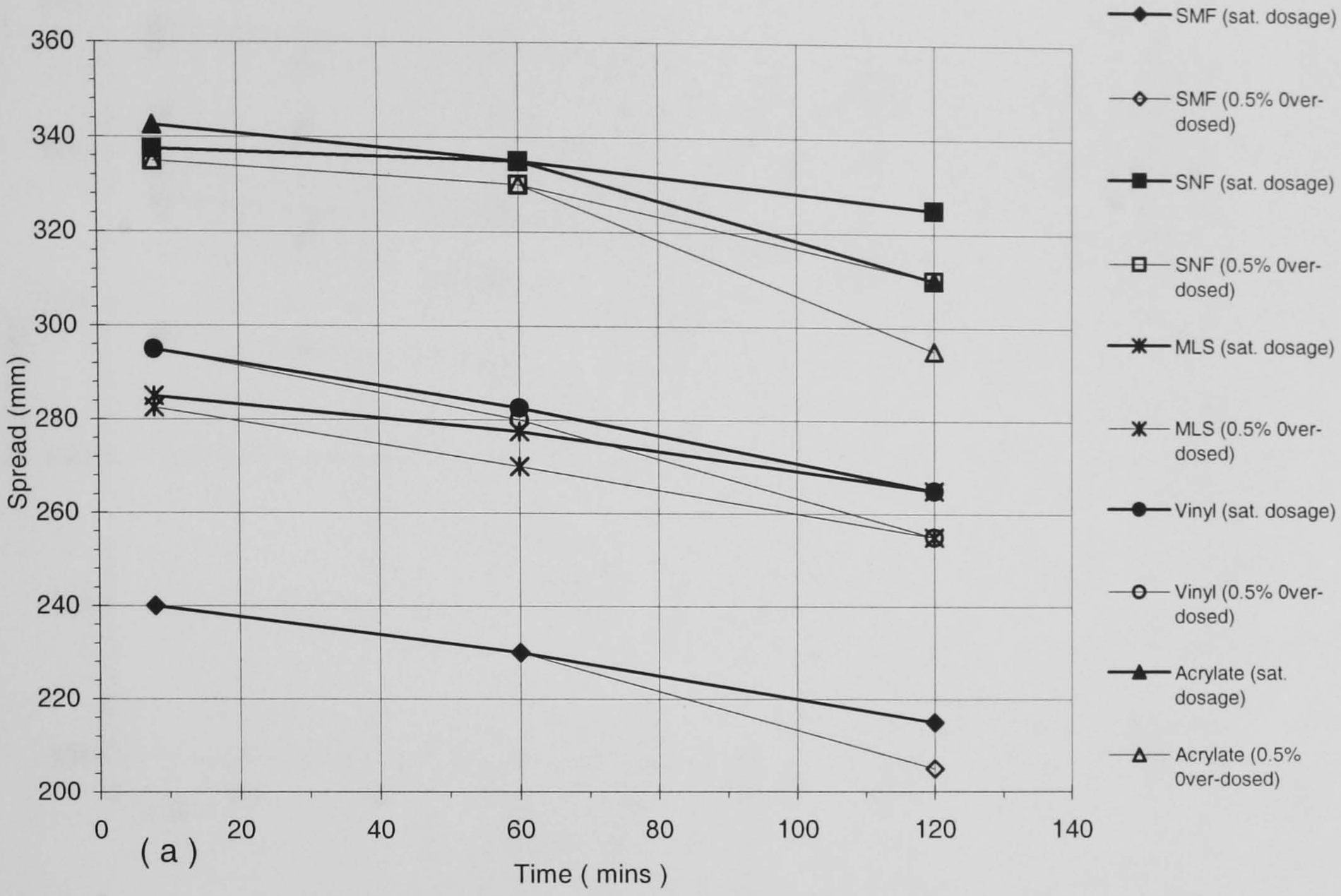

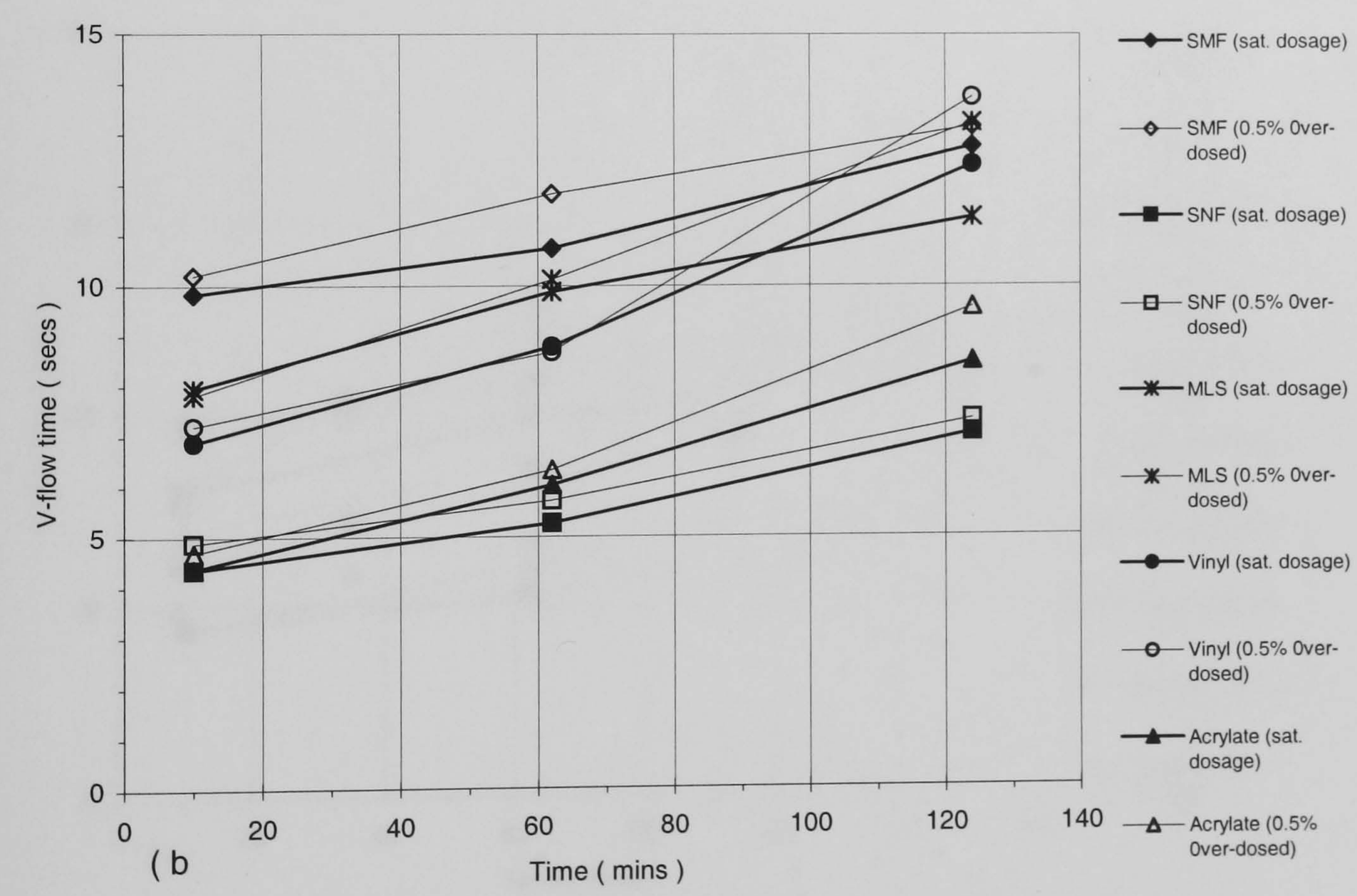

Figure B1 : Comparison of SMF, SNF, MLS, Vinyl and Acrylate superplasticizers at their saturation dosages, and for 0.5% over-doses. In terms of (a) mortar spread and (b) V-flow time (using 1 min delayed Addition, 10 % CSF, 0.26 w/b).

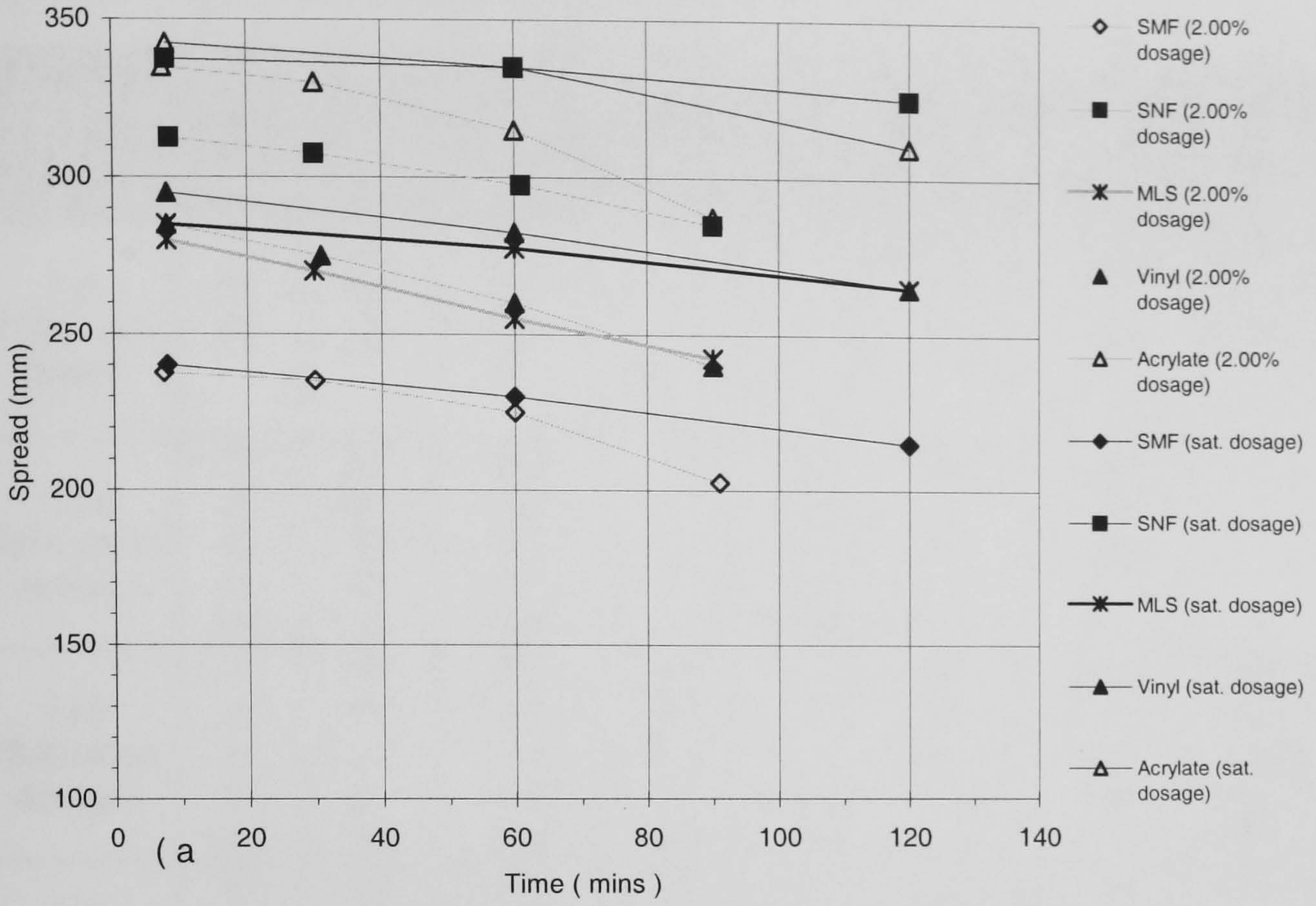

(a

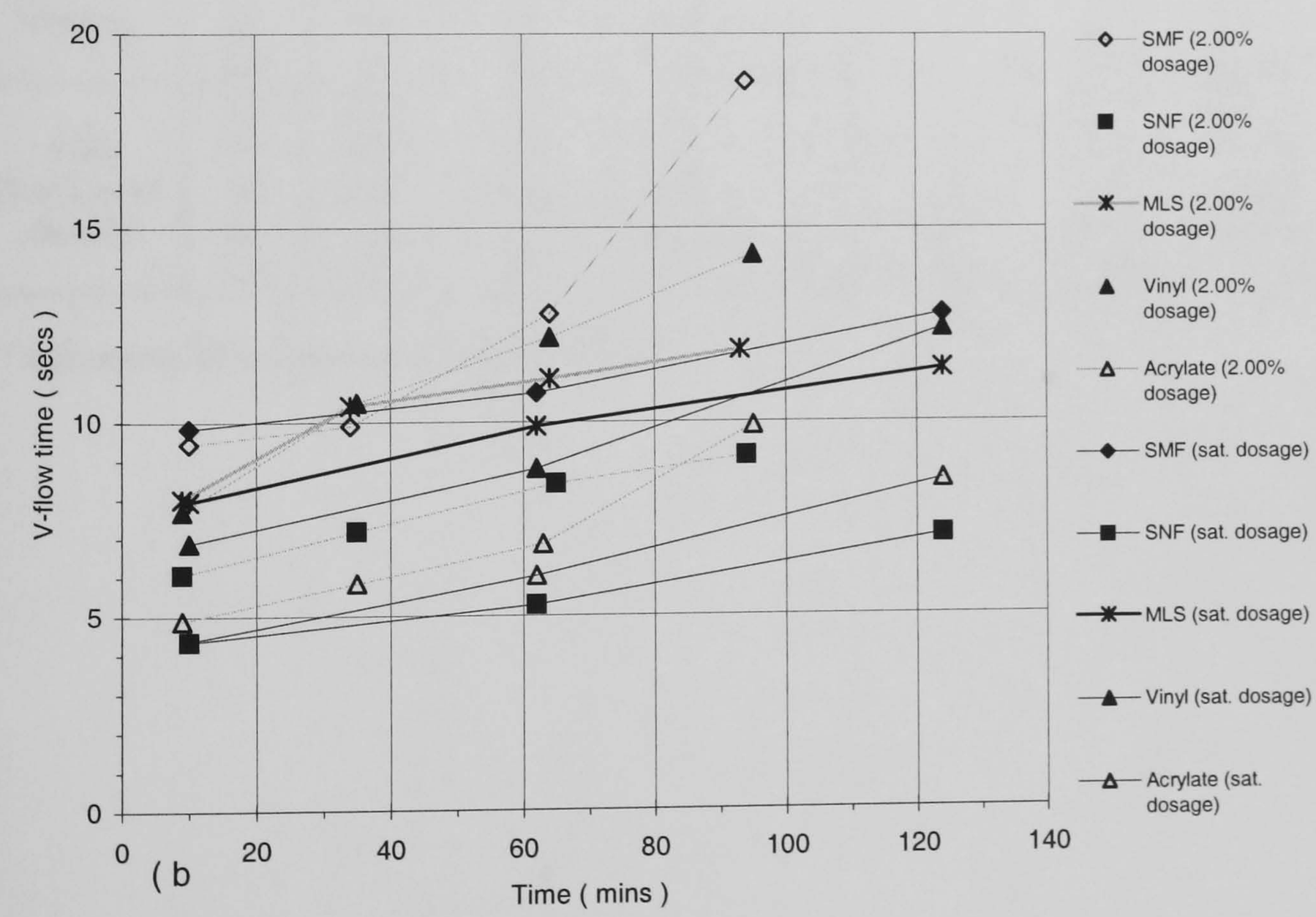

(b

Figure B2 : Comparison of SMF, SNF, MLS, Vinyl and Acrylate superplasticizers at their saturation dosages, and at a constant dosage of 2.00% in terms of (a) mortar spread and (b) V-flow time (using 1 min delayed Addition, 10 % CSF, 0.26 w/b).

Table B4 : Slump and two-point test results for HSC mixes in figure 6.4

Dosage	Slump measurements				Two-point test measurements				SI
(%)	Time (mins)	Slump (mm)	Spread SFS (mm)	ST (secs)	Time (mins)	Yield value g (Nm)	Plastic viscosity h (Nms)	r	(%)
1.5 (1.0% uder-dosed)	7	120	200	-	10	4.06	6.33	0.9844	5.66
	35	80	200	-	30	5.44	6.73	0.9707	
	65	50	200	-	60	7.68	6.29	0.9671	4.68
* 2.00 (0.5% under-dosed)	7.5	221	474	-	10	0.82	5.58	-	11.29
	35	209	397	-	30	1.19	6.03	-	
	65	190	353	-	60	1.50	6.55	-	
	95	174	307	-	90	2.10	7.04	-	
	125	154	259	-	120	3.09	7.73	-	5.80
2.50 (Saturation dosage)	8	240	570	90	10	0.56	3.79	0.9912	15.07
	35	235	540	120	30	0.73	5.04	0.9926	
	65	225	480	110	60	0.92	5.94	0.9946	
	95	215	400	105	90	1.10	6.44	0.9910	
	125	200	360	105	120	1.46	6.71	0.9805	8.41
3.00 (0.5% over-dosed)	8.5	235	570	90	10	0.56	3.91	0.9873	14.15
	35	230	525	210	30	0.88	5.82	0.9936	
	65	220	450	160	60	1.31	6.44	0.9919	
	95	210	410	230	90	1.65	8.43	0.9943	
	125	195	390	115	120	3.24	9.39	0.9875	7.57
4.00 (1.5% over-dosed)	8.5	230	525	90	10	0.71	4.61	0.9876	14.37
	35	225	500	130	30	1.09	5.46	0.9922	
	65	210	410	120	60	1.66	6.85	0.995	
	95	195	340	80	90	2.36	8.91	0.9895	
	125	170	285	50	120	3.58	10.59	0.9834	5.7

* represents statistical average from Table 6.1

Table B5 : Mortar-dosage response test results in figure 6.5

Addition time Ta (mins)	SNF dosage (%, s/w/b)	Spread (mm)	V-flow time (secs)
0	1.50	245	8.79
	1.75	280	7.98
	2.00	297.5	6.79
	2.25	310	7.17
	2.50	320	6.43
	3.00	330	6.25
	3.50	**335**	**5.85**
	4.00	322.5	6.09
1	1.50	270	8
	1.75	295	7.3
	2.00	312.5	6.07
	2.25	327.5	5.2
	2.50	**337.5**	**4.35**
	3.00	335	4.88
	3.50	325	5.53
	4.00	320	5.89
2	1.75	317.5	5.41
	2.00	325	4.94
	2.25	**335**	**4.04**
	2.5	330	4.32
3	2.00	335	3.49
4	1.50	310	3.09
	1.75	330	2.73
	2.00	**337.5**	**2.5**
	2.25	337.5	2.71
	2.50	335	2.48
	3.00	327.5	2.61
	4.00	322.5	2.67
6	2.00	330	2.69
8	1.50	317.5	2.75
	1.75	325	2.35
	2.00	**325**	**2.45**
	4.00	310	2.71

All measurements were taken immediately after the initial mixing sequence (i.e. at 8-10 mins).
Values in **BOLD** represent saturation values.

Table B6 : Slump and two-point test results for HSC mixes in figure 6.6

Addition time (mins)	Slump measurements				Two-point test measurements				SI
	Time (mins)	Slump (mm)	Spread SFS (mm)	ST (secs)	Time (mins)	Yield value g (Nm)	Plastic viscosity h (Nms)	r	(%)
0	7	200	360	70	10	1.17	5.87	0.9886	10.4
	35	165	295	60	30	1.60	6.18	0.9876	
	65	130	237.5	40	60	2.59	7.02	0.9856	
	95	95	210	-	90	3.04	7.26	0.9897	
	125	75	205	-	120	4.54	7.90	0.9826	6.2
1 (Statistical average)	7.5	221	474	-	10	0.82	5.58	-	11.3
	35	209	397	-	30	1.19	6.03	-	
	65	190	353	-	60	1.50	6.55	-	
	95	174	307	-	90	2.10	7.04	-	
	125	154	259	-	120	3.09	7.73	-	5.8
2	8	225	485	90	10	0.63	4.36	0.9914	15.7
	35	220	460	100	30	0.44	5.58	0.9930	
	65	205	390	90	60	0.85	6.23	0.9944	
	95	195	375	80	90	1.24	6.84	0.9896	
	125	185	360	65	120	1.85	7.54	0.9925	7.8
4	8	240	585	90	10	0.36	3.52	0.9924	18.4
	35	230	545	140	30	0.46	4.30	0.9967	
	65	225	510	-	60	0.50	4.69	0.9908	
	95	215	460	120	90	0.85	5.26	0.9909	
	125	205	445	150	120	1.48	6.03	0.9843	11.7

Table B7 : Slump and two-point test results for HSC mixes in figure 6.7

Variable	Slump measurements				Two-point test measurements				SI
	Time (mins)	Slump (mm)	Spread SFS (mm)	ST (secs)	Time (mins)	Yield value g (Nm)	Plastic viscosity h (Nms)	r	(%)
50/50% 0/4 mins Split add.	8	205	360	30	10	0.92	2.52	0.9812	9.36
	35	180	295	18	30	1.48	3.88	0.9869	
	65	150	255	10	60	1.77	4.77	0.9807	
	95	120	210	-	90	2.19	6.91	0.9902	
	125	105	220	-	120	3.69	7.89	0.9842	6.49
90 / 10 % SNF/ R blend (4 mins)	7.5	220	450	55	10	0.6	4.56	0.9907	14.57
	35	225	510	85	30	0.24	5.55	0.9873	
	65	225	465	80	60	0.27	4.54	0.9842	
	95	215	440	66	90	0.71	5.46	0.9857	
	125	210	395	60	120	0.65	5.31	0.9822	14.11
90 / 10 % D 2001/R blend (4 mins)	8	235	520	100	10	0.50	5.61	0.9932	12.56
	35	235	535	100	30	0.91	6.83	0.9806	
	65	220	525	105	60	1.17	7.88	0.9956	
	95	190	400	50	90	2.20	8.79	0.9726	
	125	135	260	15	120	3.95	8.91	1.0	7.15
D 2001 4 mins delayed	8.5	240	555	90	10	0.48	3.96	0.9855	18.58
	35	225	480	100	30	0.73	4.89	0.989	
	65	190	365	60	60	1.4	6.15	0.9815	
	95	100	205	-	90	5.42	9.83	0.9635	
	130	20	200	-	120	8.75	8.87	0.9502	5.79

Table B8 : Mortar-dosage response test results in figure 6.8

Cement	SNF dosage (%, s/w/b)	Spread (mm)	V-flow time (secs)
Type I (PC-7)	1.50	310	3.09
	1.75	330	2.73
	2.00	**337.5**	**2.50**
	2.25	337.5	2.63
	2.50	335	2.48
	3.00	327.5	2.61
	4.00	322.5	2.67
Type I (PC-8)	1.50	280	4.98
	1.75	320	3.71
	2.00	**330**	**2.86**
	2.25	330	2.91
	3.00	325	3.37
	4.00	325	3.26
Type I (PC-9)	1.00	250	3.73
	1.25	310	2.99
	1.50	322.5	2.92
	1.75	330	2.55
	2.00	**337.5**	**2.43**
	2.25	335	2.72
	4.00	325	2.67
Type III (RH)	1.50	205	4.04
	2.00	278.5	3.14
	2.25	305	3.09
	2.50	**317.5**	**2.93**
	2.75	315	3.29
	3.00	317.5	3.14
	4.00	307.5	3.34
Type V (SR)	1.00	300	3.01
	1.25	325	2.73
	1.50	340	2.53
	1.75	**350**	**2.27**
	2.00	350	2.14
	2.50	347.5	2.39
	4.00	342.5	2.47

All measurements were taken immediately after the initial mixing sequence (i.e. at 8-10 mins).
Values in **BOLD** represent saturation values

Table B9 : Mortar-dosage response test results in figure 6.9

Superplasticizer type	Cement	Dosage (%, s/w/b)	Spread (mm)	V-flow time (secs)
SMF (Sika FF)	**Type I** (PC-7)	1.25	170	9.78
		1.50	**242.5**	**6.71**
		1.75	240	7.04
		2.00	240	7.45
	Type III (RH)	2.25	105	No flow
		2.50	**117.5**	
		3.00	115	
		3.50	115	No flow
	Type V (SR)	1.25	225	6.64
		1.50	**297.5**	**5.38**
		1.75	295	5.54
		2.00	297.5	5.49
		2.50	292.5	5.94
MLS (SP 4)	**Type I** (PC-7)	1.25	260	9.01
		1.50	**285**	**7.04**
		1.75	285	7.44
		2.00	277.5	7.71
	Type III (RH)	1.75	225	9.91
		2.00	255	8.09
		2.25	**255**	**7.91**
		2.50	255	8.39
		3.00	250	8.94
	Type V (SR)	1.00	230	8.93
		1.25	300	6.03
		1.50	**320**	**4.53**
		1.75	320	5.16
		2.00	320	5.64
		2.50	317.5	5.69
Vinyl (Sika 10)	**Type I** (PC-7)	1.25	255	8.47
		1.50	290	5.58
		1.75	**305**	**5.36**
		2.00	305	5.32
	Type III (RH)	1.50	257.5	7.83
		1.75	280	6.41
		2.00	**280**	**6.22**
		2.25	280	6.49
		3.00	272.5	6.75
	Type V (SR)	1.00	275	5.44
		1.25	320	3.70
		1.50	**335**	**2.93**
		1.75	335	3.20
		2.00	330	3.40
		2.50	330	3.48
Acrylate (D 2001)	**Type I** (PC-7)	1.25	307.5	4.00
		1.50	325	3.17
		1.75	**342.5**	**2.14**
		2.00	340	2.39
	Type III (RH)	1.50	235	4.79
		1.75	290	3.41
		2.00	**335**	**2.52**
		2.25	335	2.47
		2.50	332.5	2.51
	Type V (SR)	0.75	300	4.20
		1.00	360	3.01
		1.25	**370**	**2.50**
		1.50	367.5	2.45
		2.00	370	2.79

Table B10 : Slump and two-point test results for HSC mixes in figure 6.10.

Addition time (mins)	Slump measurements				Two-point test measurements				SI
	Time (mins)	Slump (mm)	Spread SFS (mm)	ST (secs)	Time (mins)	Yield value g (Nm)	Plastic viscosity h (Nms)	r	(%)
SNF+ Type V (SR)	8	260	640	65	10	0.13	2.40	0.9901	25.0
	35	245	580	90	30	0.14	4.65	0.9902	
	65	225	525	100	60	0.54	5.26	0.9889	
	95	205	430	92	90	0.79	8.44	0.9893	8.8
	125	165	362.5	80	120	1.28	8.91	0.9816	6.8
SNF+ Type III (RH)	7	205	392.5	35	10	0.77	3.75	0.9921	13.7
	35	195	380	30	30	0.95	4.19	0.9943	
	65	175	315	28	60	1.34	4.49	0.9887	
	95	155	260	15	90	1.82	5.20	0.9863	
	125	125	235	-	120	2.87	6.98	0.9918	7.1
SNF+ Type I (PC-7)	8	240	-	-	10	0.36	3.52	0.9924	16.1
	35	230	-	-	30	0.46	4.30	0.9967	
	65	225	-	-	60	0.50	4.69	0.9908	
	95	215	-	-	90	0.85	5.26	0.9909	
	125	205	-	-	120	1.48	6.03	0.9843	11.7
SNF+ Type I (PC-8)	8.5	235	515	90	10	0.78	4.25	0.9862	14.7
	35	225	500	75	30	0.45	4.26	0.9880	
	65	215	415	60	60	0.99	5.73	0.9773	
	95	210	385	45	90	1.95	5.83	0.9823	
	125	195	315	35	120	2.30	6.05	0.9848	8.7
SNF+ Type I (PC-9)	8	240	585	80	10	0.36	3.80	0.9951	22.0
	35	235	575	95	30	0.66	5.11	0.9897	
	65	230	530	90	60	1.40	6.14	0.9905	
	95	200	365	110	90	2.33	8.59	0.9867	
	125	155	300	60	120	4.30	9.53	0.9713	7.4
SNF+ Type I (PC-9) (repeat)	8	240	580	90	10	0.44	4.22	0.9885	16.1
	35	235	550	85	30	0.43	4.78	0.9867	
	65	215	495	75	60	1.16	6.76	0.9822	
	95	205	405	60	90	2.77	9.24	0.9781	
	125	150	295	70	120	4.20	9.39	0.9709	8.2
SMF+ Type V	7.5	195	355	40	10	0.71	6.73	0.9943	11.0
	35	165	300	47	30	1.14	8.30	0.9856	
	65	130	215	-	60	2.68	10.16	0.9888	
	95	90	210	-	90	4.18	11.70	0.9849	
	125	60	200	-	120	5.85	10.75	0.9778	3.9

Appendix C

Mortar & Concrete test results for:

(Chapter 7)

. Binary mixes of
  - . CSF
  - . PFA
  - . GGBS

. Ternary mixes of
  - . PFA/CSF
  - . GGBS/CSF

. Effects of W/B ratios of
  - . 0.30
  - . 0.20

. Effects of CRMs on segregation resistance and compactability

Table C1 : Mortar spread and V-funnel test results in figure 7.1

CSF addition time (secs)	Spread (mm)	V-flow time (secs)
0	290	5.3
15	315	4.2
30	330	2.9
45	327.5	3.02
60	330	2.81

Table C2 : Mortar-dosage response test results in figure 7.2

Mix	Dosage (%)	Spread (mm)	V-flow time (secs)
100% OPC	1.25	255	19.88
	1.50	265	16.36
	2.00	275	15.76
	2.50	285	14.13
	3.00	290	12.17
	3.25	295	11.07
	3.50	295	11.14
	4.00	295	11.52
2.5% CSF	1.25	-	15.88
	1.50	255	12.77
	2.00	277.5	9.04
	2.50	295	7.32
	2.75	302.5	6.85
	3.00	307.5	6.01
	3.25	307.5	5.92
	3.50	305	6.23
	4.00	302.5	6.71
5% CSF	1.25	240	10
	1.50	270	8.74
	2.00	297.5	6.27
	2.25	310	5.26
	2.50	315	4.43
	2.75	315	4.72
	3.00	315	5.01
	4.00	305	5.39
10% CSF	1.25	235	7.09
	1.50	280	4.98
	1.75	320	3.71
	2.00	330	2.86
	2.25	330	2.91
	3.00	325	3.37
	4.00	325	3.26
15% CSF	1.25	230	6.52
	1.75	315	3.25
	2.00	325	2.98
	2.25	325	2.87
	3.00	320	3.11
	4.00	317.5	3.05

All measurements taken immediately after the initial mixing sequence

Table C3 : Slump and two-point test results for HSC mixes in figure 7.3

Mix	Slump measurements				Two-point test measurements				SI
	Time (mins)	Slump (mm)	Spread SFS (mm)	ST (secs)	Time (mins)	Yield value g (Nm)	Plastic viscosity h (Nms)	r	(%)
100% OPC	8	195	390	120	10	5.98	8.20	0.9744	6.77
	35	195	385	110	30	6.73	11.31	0.9667	
	65	190	380	130	60	7.81	12.2	0.9677	
	95	185	350	90	90	8.32	11.2	0.9553	
	125	180	310	95	120	8.54	10.3	0.9402	5.16
100% OPC (repeat)	8	195	-	-	10	6.67	8.9	0.9571	8.71
	35	190	-	-	30	6.98	11.91	0.9601	
	65	190	-	-	60	7.55	12.6	0.9525	
	95	185	-	-	90	6.24	11.85	0.9441	
	125	175	-	-	120	7.60	11.5	0.9322	7.19
2.5% CSF	8	215	440	90	10	3.08	6.33	0.9893	12.0
	35	215	-	-	30	3.52	8.04	0.9888	
	65	210	440	80	60	4.26	9.46	0.9834	
	95	200	-	-	90	4.93	10.95	0.9643	
	125	195	375	-	120	5.80	11.42	0.9593	4.5
5% CSF	8.5	225	490	100	10	1.34	5.46	0.9847	9.22
	35	220	460	75	30	2.06	5.57	0.9819	
	65	210	410	70	60	1.90	5.27	0.9811	
	95	195	385	50	90	2.21	6.79	0.9852	
	125	180	385	65	120	3.02	8.01	0.9786	7.5
10% CSF	8.5	235	530	90	10	0.54	4.08	0.9903	16.5
	35	230	515	-	30	0.71	4.57	0.9873	
	65	215	495	65	60	0.87	5.41	0.9869	
	95	210	480	45	90	1.39	5.92	0.9851	
	125	200	430	35	120	1.94	6.31	0.9779	8.1
10% CSF (repeat)	8.5	235	-	-	10	0.78	4.25	0.9862	12.5
	35	225	-	-	30	0.45	4.26	0.988	
	65	215	-	-	60	0.99	5.73	0.9773	
	95	210	-	-	90	1.95	5.83	0.9823	
	125	195	-	-	120	2.30	6.05	0.9848	10.2
15% CSF	8	235	530	80	10	0.55	4.37	0.9923	17.1
	37	220	515	70	30	0.28	4.60	0.9937	
	67	210	415	45	60	0.44	6.63	0.9885	
	96	200	385	40	90	1.38	6.72	0.9813	
	125	190	385	20	120	1.54	7.93	0.9932	7.0

Table C4 : Mortar-dosage response test results in figure 7.4

Mix	Dosage (%)	Spread (mm)	V-flow time (secs)
100% OPC	1.25	255	19.88
	1.50	265	16.36
	2.00	275	15.76
	2.50	285	14.13
	3.00	290	12.17
	3.25	295	11.07
	3.50	295	11.14
	4.00	295	11.52
10% PFA	1.25	260	17.54
	2.00	295	14
	2.75	305	12.3
	3.00	310	10.4
	3.25	310	10.8
	4.00	307.5	10.9
20% PFA	1.25	280	15.72
	1.50	290	13.91
	2.00	307.5	11.86
	2.50	315	10.04
	2.75	320	9.21
	3.00	320	9.39
	4.00	317.5	10.07
40% PFA	1.00	305	15.21
	1.50	322.5	12.11
	2.00	325	10.08
	2.25	327.5	9.11
	2.50	330	8.23
	2.75	330	8.19
	3.00	330	8.48
	4.00	325	9.57
60% PFA	1.00	310	12.45
	1.50	320	11.15
	2.25	325	9.88
	2.50	327.5	8.01
	2.75	327.5	7.95
	3.00	325	8.77
	4.00	320	8.98

Table C5 : Slump and two-point test results for HSC mixes in figure 7.5

Mix	Slump measurements				Two-point test measurements				SI
	Time (mins)	Slump (mm)	Spread SFS (mm)	ST (secs)	Time (mins)	Yield value g (Nm)	Plastic viscosity h (Nms)	r	(%)
	8	195	390	120	10	5.98	8.20	0.9744	6.77
100%	35	195	385	110	30	6.73	11.31	0.9667	
OPC	65	190	380	130	60	7.81	12.2	0.9677	
	95	185	350	90	90	8.32	11.2	0.9553	
	125	180	310	95	120	8.54	10.3	0.9402	5.16
	8	220	480	85	10	2.11	7.85	0.9919	8.5
10%	35	215	440	-	30	2.75	10.40	0.9923	
PFA	65	210	435	-	60	3.48	11.29	0.9804	
	95	205	410	-	90	4.95	12.33	0.9732	
	125	190	375	90	120	5.98	12.06	0.9704	3.5
	8.5	245	570	100	10	1.62	6.89	0.9925	6.5
20%	35	240	565	130	30	2.05	10.05	0.9956	
PFA	67	235	575	180	60	1.91	11.11	0.9871	
	95	230	545	190	90	3.17	11.81	0.9812	
	125	230	565	190	120	2.93	12.25	0.9886	7.5
	8	255	625	170	10	0.36	5.13	0.9900	11.1
40%	35	255	630	180	30	0.21	8.90	0.9927	
PFA	65	255	605	170	60	0.98	9.52	0.9911	
	95	250	600	155	90	1.95	10.56	0.9836	
	125	240	590	180	120	2.43	11.07	0.9921	6.5

Table C6 : Mortar-dosage response test results in figure 7.6

Mix	Dosage (%)	Spread (mm)	V-flow time (secs)
100% OPC	1.25	255	19.88
	1.50	265	16.36
	2.00	275	15.76
	2.50	285	14.13
	3.00	290	12.17
	3.25	295	11.07
	3.50	295	11.14
	4.00	295	11.52
20% GGBS	1.25	270	29.5
	1.50	280	27
	2.00	290	25
	2.50	295	22.1
	2.75	300	18.5
	3.00	300	17.42
	3.25	300	16.11
	3.50	297.5	16.04
	4.00	295	17.5
40% GGBS	1.00	292.5	39.3
	1.25	300	34.6
	1.50	305	30.1
	1.75	305	29.2
	2.00	305	28.7
	3.00	302.5	22.6
	3.25	301	20.07
	3.50	300	18.23
	3.75	297.5	18.51
	4.00	295	19.8
60% GGBS	0.75	300	-
	1.00	312.5	60
	1.25	312.5	55
	1.50	312.5	53
	2.00	310	48.7
	3.00	305	41.5
	3.50	302.5	38.2
	3.75	300	35.1
	4.00	300	36
80% GGBS	0.75	295	NO FLOW
	1.00	305	
	1.25	305	
	1.50	302.5	
	3.75	290	
	4.00	285	
60% GGBS (Split add.)	0.75	290	55
	1.00	307.5	50
	1.25	307.5	47.1
	2.00	302.5	37
	3.50	290	29.5
	3.75	287.5	26.2
	4.00	285	26.07

Table C7 : Slump and two-point test results for HSC mixes in figure 7.7

Mix	Slump measurements				Two-point test measurements				SI
	Time (mins)	Slump (mm)	Spread SFS (mm)	ST (secs)	Time (mins)	Yield value g (Nm)	Plastic viscosity h (Nms)	r	(%)
100% OPC	8	195	390	120	10	5.98	8.20	0.9744	6.77
	35	195	385	110	30	6.73	11.31	0.9667	
	65	190	380	130	60	7.81	12.2	0.9677	
	95	185	350	90	90	8.32	11.2	0.9553	
	125	180	310	95	120	8.54	10.3	0.9402	5.16
20% GGBS	8	220	440	95	10	7.01	9.6	0.9750	4.44
	35	210	385	90	30	7.02	13.35	0.9647	
	65	205	360	120	60	8.8	15.41	0.9667	
	95	195	320	-	90	7.74	17.79	0.9712	
	125	190	320	75	120	11.1	14.2	0.9136	2.0
40% GGBS	8	225	410	125	10	7.01	18.91	0.9472	1.5
	35	215	395	-	30	8.87	24.58	0.9707	
	65	210	380	100	60	10.12	20.9	0.9514	
	95	205	320	-	90	-	-	-	-
	125	200	300	-	120	-	-	-	-
60% GGBS (redosed)	8	No slump	-	-	-	-	-	-	-
	25	225	440	85	30	6.14	3.25	0.9893	
	65	65	200	-	60	9.4	15.06	0.9102	
	-	-	-	-	-	-	-	-	-
	-	-	-	-	-	-	-	-	-

Table C8 : Mortar-dosage response test results in figure 7.8

Mix	Dosage (%)	Spread (mm)	V-flow time (secs)
10% CSF	1.25	235	7.09
	1.50	280	4.98
	1.75	320	3.71
	2.00	330	2.86
	2.25	330	2.91
	3.00	325	3.37
	4.00	325	3.26
20/ 10% PFA/CSF	1.00	230	7.88
	1.25	285	6.37
	1.50	317.5	3.85
	1.75	335	2.71
	2.00	335	2.95
	2.25	332.5	2.82
	4.00	330	3.44
40/ 10% PFA/CSF	0.50	290	8.83
	1.00	320	5.45
	1.25	332	3.11
	1.50	340	2.23
	1.75	340	2.19
	2.00	337.5	2.32
	3.00	327.5	3.17
	4.00	320	3.72
60/ 10% PFA/CSF	0.50	275	7.69
	1.25	317.5	3.52
	1.50	325	2.79
	1.75	325	2.81
	2.00	325	2.57
	4.00	315	3.39

Table C9 : Mortar-dosage response test results in figure 7.9

Mix	Dosage (%)	Spread (mm)	V-flow time (secs)
10% CSF	1.25	235	7.09
	1.50	280	4.98
	1.75	320	3.71
	2.00	330	2.86
	2.25	330	2.91
	3.00	325	3.37
	4.00	325	3.26
40/ 10% GGBS/CSF	0.50	260	7.89
	1.00	300	4.64
	1.25	320	3.6
	1.50	330	3.14
	1.75	330	3.21
	2.00	325	3.07
	4.00	315.5	3.99
60/ 10% GGBS/CSF	0.50	275	6.55
	0.75	320	3.29
	1.00	332.5	2.67
	1.25	332.5	2.71
	1.50	330	2.62
	1.75	330	2.69
	2.00	327	2.73
	3.00	315	3.02
	4.00	305	3.17
80/ 10% GGBS/CSF	0.50	252.5	8.77
	1.00	310	5.69
	1.25	320	4.22
	1.50	320	4.15
	1.75	317.5	4.31
	4.00	292.5	5.37

Table C10 : Slump and two-point test results for HSC mixes in figure 7.10

Mix	Slump measurements				Two-point test measurements				SI
	Time (mins)	Slump (mm)	Spread SFS (mm)	ST (secs)	Time (mins)	Yield value g (Nm)	Plastic viscosity h (Nms)	r	(%)
10% CSF	8.5	235	530	90	10	0.54	4.08	0.9903	16.5
	35	230	515		30	0.71	4.57	0.9873	
	65	215	495	65	60	0.87	5.41	0.9869	
	95	210	480	45	90	1.39	5.92	0.9851	
	125	200	430	35	120	1.94	6.31	0.9779	8.1
20/10% PFA/CSF	8.5	245	615	90	10	**-0.01**	3.76	0.9937	17.2
	36	240	610	90	30	0.37	3.97	0.9914	
	65	235	600	110	60	0.52	4.14	0.991	
	95	230	555		90	0.65	5.74	0.9899	
	127	220	525	80	120	0.78	6.12	0.9948	11.0
40/10% PFA/CSF	8	270	675	80	10	**-0.07**	2.07	0.9897	23.4
	35	265	650	120	30	**-0.11**	3.00	0.9956	
	65	255	635	115	60	0.06	3.45	0.9966	
	95	255	630	115	90	0.25	3.62	0.9930	
	126	255	620	100	120	0.39	4.47	0.9913	14.5
40/10% GGBS/CSF	8	245	595	150	10	0.47	4.11	0.9974	15.3
	35	240	575	155	30	0.59	5.8	0.9951	
	65	230	600	150	60	0.70	7.22	0.9873	
	95	235	590		90	1.12	7.3	0.9815	
	125	225	525	140	120	1.21	7.64	0.9875	11.0
60/10% GGBS/CSF	8.5	255	630	130	10	0.43	3.92	0.9900	17.8
	35	240	590	125	30	0.55	4.47	0.9904	
	67	235	565	140	60	0.62	5.89	0.9917	
	95	235	540	150	90	0.74	6.71	0.9870	
	125	230	530	105	120	1.10	6.93	0.9906	10.5

Note : Values in **BOLD** were taken as zero (since yield value cannot be negative).

Table C11 : Mortar-dosage response test results in figure 7.12

Mix	Dosage (%)	Spread (mm)	V-flow time (secs)
100% OPC	1.00	275	5.28
	1.50	310	4.52
	1.75	315	4.02
	2.00	315	4.18
	2.50	315	4.09
10% CSF	1.00	265	2.68
	1.25	320	2.16
	1.50	340	1.74
	1.75	340	1.77
	2.50	337.5	1.92
40/ 10% PFA/CSF	0.75	310	2.15
	1.00	335	1.81
	1.25	357.5	1.38
	1.50	357.5	1.37
	1.75	357.5	1.52
	2.50	352.5	1.44
60/ 10% GGBS/CSF	0.50	280	3.41
	0.75	345	2.37
	1.00	345	2.29
	1.25	345	2.41
	2.50	342.5	2.51

Table C12 : Slump and two-point test results for HSC mixes in figure 7.13

Mix	Slump measurements				Two-point test measurements				SI
	Time (mins)	Slump (mm)	Spread SFS (mm)	ST (secs)	Time (mins)	Yield value g (Nm)	Plastic viscosity h (Nms)	r	(%)
100% OPC	8	215	480	25	10	0.77	3.51	0.9891	17.5
	35	210	480	40	30	0.93	4.82	0.9953	
	65	205	410	15	60	1.32	5.73	0.9901	
	95	195	395	-	90	1.44	6.42	0.9873	
	125	175	370	20	120	1.69	6.89	0.9825	10.2
10% CSF	7.5	235	610	70	10	0.16	2.71	0.9904	23
	35	225	535	50	30	0.28	3.14	0.9924	
	68	210	485	40	60	0.40	4.37	0.9944	
	97	205	415	20	90	0.72	5.05	0.9872	
	125	185	395	15	120	1.14	5.43	0.9858	11.9
40/10% PFA/CSF	8	250	670	65	10	0.22	1.29	0.9469	29.2
	38	245	635	55	30	0.10	1.83	0.9851	
	65	235	590	55	60	0.10	2.91	0.9954	
	95	215	525	70	90	0.37	3.83	0.9930	14.1
	125	205	455	20	120	0.56	4.17	0.9891	-
60/10% GGBS/CSF	8	245	600	65	10	0.31	2.83	0.9907	18.1
	36	235	450	45	30	0.53	4.12	0.9894	
	67	215	420	35	60	0.67	4.91	0.9873	
	95	200	395	20	90	0.78	5.35	0.9863	
	125	185	385	15	120	0.91	6.20	0.9777	11.1

Table C13 : Mortar-dosage response test results in figure 7.14

Mix	Dosage (%)	Spread (mm)	V-flow time (secs)
10% CSF	2.00	270	16.7
	2.75	305	13.2
	3.00	312.5	11.27
	3.25	312.5	11.41
	3.50	312.5	11.22
	4.00	310	11.81
40/ 10% PFA/CSF	1.00	280	24.4
	1.50	305	15.2
	1.75	312.5	12.98
	2.00	320	10.32
	2.25	320	10.19
	2.50	317.5	11.06
	3.00	315	11.86
60/ 10% GGBS/CSF	1.00	265	31.41
	1.25	300	26.3
	1.50	315	18.3
	1.75	315	19.04
	2.00	312.5	22.84
	2.50	300	23.41
	3.00	275	25.33

Table C14 : Slump and two-point test results for HSC mixes in figure 7.15

Mix	Slump measurements				Two-point test measurements				SI
	Time (mins)	Slump (mm)	Spread SFS (mm)	ST (secs)	Time (mins)	Yield value g (Nm)	Plastic viscosity h (Nms)	r	(%)
10% CSF	8	235	565	130	10	0.42	5.62	0.9947	12.2
	35	230	530	125	30	1.65	8.97	0.9852	
	68	215	460	130	60	2.79	9.55	0.9822	
	95	210	435	120	90	3.15	10.37	0.9914	
	127	195	370	110	120	4.51	11.58	0.9770	5.7
40/10% PFA/CSF	8.5	255	645	110	10	0.20	4.96	0.9926	10.4
	36	250	635	105	30	0.29	6.05	0.9854	
	65	245	565	120	60	0.72	6.75	0.9878	
	97	235	530	90	90	1.06	7.50	0.9821	
	125	230	475	75	120	1.93	8.54	0.9895	8.6
60/10% GGBS/CSF	8.5	230	510	110	10	1.93	6.62	0.959	8.1
	35	225	500	105	30	2.47	10.27	0.9752	
	76	215	455	120	60	2.62	11.91	0.9693	
	95	210	435	120	90	3.94	12.53	0.9515	
	125	195	400	115	120	6.98	13.29	0.9323	3.25

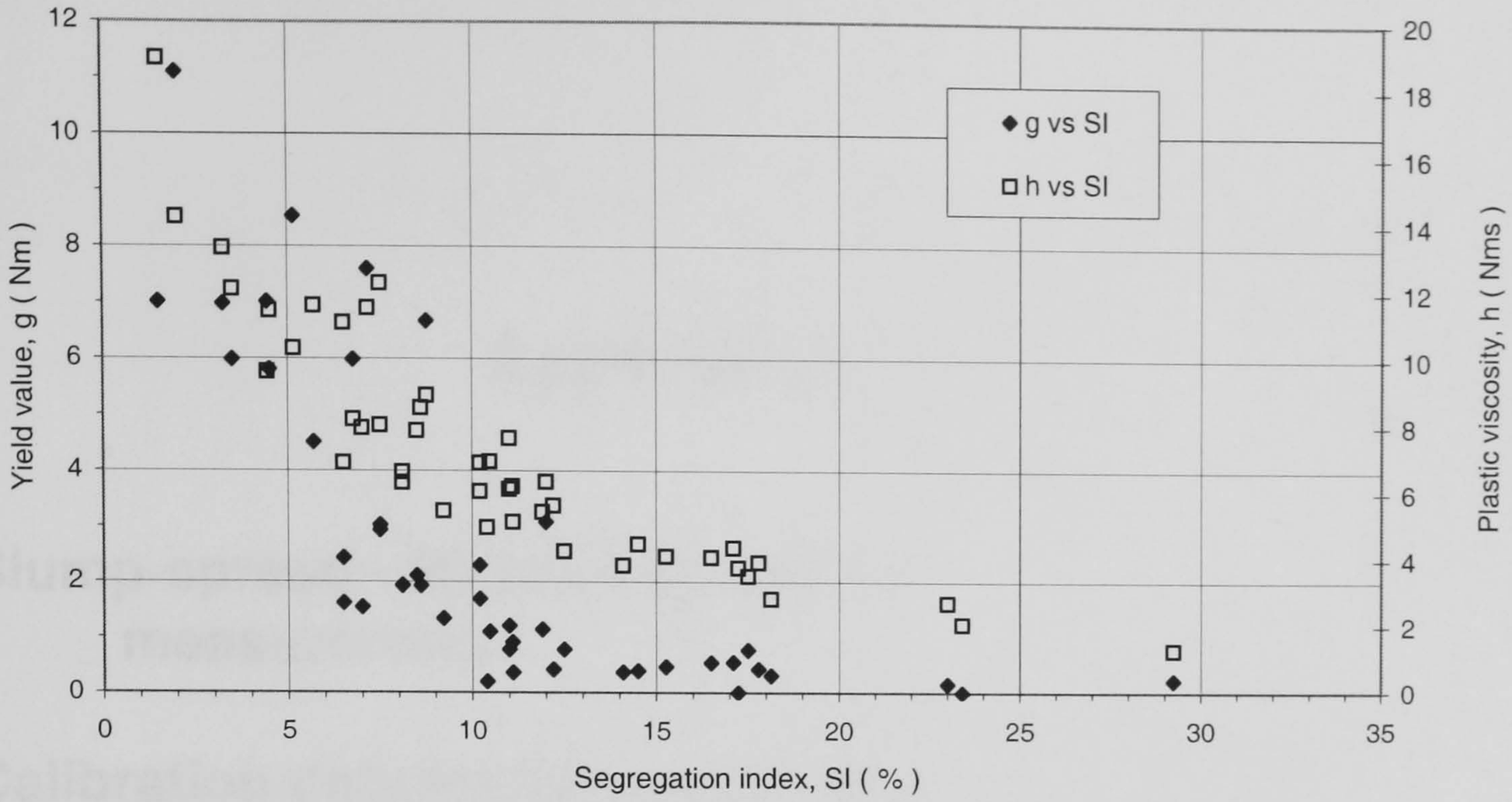

Figure C1: Relationship between the Bingham parameters and the segregation resistance of mixes in Chapter 7.

Table C15 : Some compactability measurements with the cylinder-vibration method for selected mixes in chapter 7.

Mix (w/b)	Time (secs)	Slump (mm)	Bleeding Tendency B_M	Time (mins)	Yield value g (Nm)	Plastic viscosity h (Nms)	Time (secs)	**Compactability dH** (mm)
OPC (0.26)	8	195	7	10	5.98	8.20	12	10
	65	190	6	60	7.81	12.2	62	20
	125	180	5	120	8.54	10.3	128	25
10% CSF (0.26)	8.5	235	8	10	0.54	4.08	11	5
	65	215	8	60	0.87	5.41	63	10
	125	200	7	120	1.94	6.31	127	10
40/10% PFA/CSF (0.26)	8	270	10	10	0	2.07	12	5
	65	255	9	60	0.06	3.45	69	5
	126	255	9	120	0.39	4.47	130	10
60/10% GGBS/CSF (0.26)	8	255	9	10	0.43	3.92	12	5
	67	235	8	60	0.62	5.89	70	10
	125	230	8	120	1.10	6.93	130	15
OPC (0.30)	8	215	9	10	0.77	3.51	12	10
	65	205	8	60	1.32	5.73	67	5
	125	175	8	120	1.69	6.89	130	15
10% CSF (0.30)	8	235	9	10	0.16	2.71	12	5
	65	210	9	60	0.40	4.37	68	5
	125	185	8	120	1.14	5.43	127	10

Appendix D

. Slump-spread - Bingham parameter
measurements.

. Calibration data for Vibrating Table
(under both damped and undamped conditions).

. Spread-time - Bingham parameter relationships
(equations 8.1-8.5).

. Vibration-response measurements for

. OPC and 10% CSF mixes

. Ternary PFA/CSF and GGBS/CSF mixes

. Acrylate-based superplasticized mix
(at 0.26 w/b) and NSC mix (at 0.50 w/b).

Table D1.1 : Spread-time measurements for OPC and Binary CSF mixes in figure 7.3

Mix	Two-point test measurements			Slump-spread-time measurements							
				Time	Static			Dynamic			
	Time (mins)	g (Nm)	h (Nms)	(mins)	Slump (mm)	SFS (mm)	ST (secs)	Time (secs)	SR (mm)	Rate (mm/s)	% of SFS
100% OPC	60	7.81	12.20	65	190	380	130	5	220	44	58
								10	230	23	61
								20	250	13	66
								30	270	9	71
								60	335	6	88
	120+	8.54	10.30	125	180	310	95	5	200	40	65
								10	210	21	68
								20	220	11	71
								30	230	8	74
								60	255	4	82
2.5% CSF	60	4.26	9.46	65	210	440	80	5	260	52	59
								10	280	28	64
								20	320	16	73
								30	360	12	82
								60	420	7	95
5% CSF	10	1.34	5.46	8.5	225	490	100	5	340	68	6
								10	380	38	78
								20	420	21	86
								30	450	15	92
								60	475	8	97
	120	3.02	8.01	125	180	385	65	5	260	52	68
								10	290	29	75
								20	325	16	84
								30	350	12	91
								60	380	6	99
10% CSF	10	0.54	4.08	8.5	235	530	90	5	370	74	70
								10	425	43	80
								20	-	-	-
								30	495	17	93
								60	520	9	98
	120	1.94	6.31	125	200	430	35	5	300	60	70
								10	335	34	78
								20	375	19	87
								30	410	14	95
								60	-	-	-
15% CSF	30	0.28	4.60	37	220	515	70	5	385	77	75
								10	440	44	85
								20	470	-	-
								30	500	17	97
								60	515	9	100
	120	1.54	7.93	125	190	385	20	5	305	61	79
								10	360	36	94
								20	-	-	-
								30	-	-	-
								60	-	-	-

Note

SFS and **ST** represent the final slump-spread and slump-flow time.

SR is the slump-spread measured at 5, 10, 20, 30 and 60 secs of deformation.

+ represents measurements outside the range of the 2-pt. Test apparatus (c.f. secs. 7.2.3 & 7.3.2).

Table D1.2 : Spread-time measurements for binary PFA mixes in figure 7.5.

Mix	Two-point test measurements			Slump-spread-time measurements							
				Time	Static			Dynamic			
	Time (mins)	g (Nm)	h (Nms)	(mins)	Slump (mm)	SFS (mm)	ST (secs)	Time (secs)	SR (mm)	Rate (mm/s)	% of SFS
10% PFA	10	2.11	7.85	8	220	480	85	5	260	52	54
								10	310	31	65
								20	360	18	75
								30	400	13	83
								60	460	8	96
	120+	5.98	12.06	125	190	375	90	5	220	44	59
								10	240	24	64
								20	260	13	69
								30	295	10	79
								60	340	6	91
20% PFA	10	1.62	6.89	8.5	245	570	100	5	340	68	60
								10	380	38	67
								20	430	22	75
								30	465	16	82
								60	520	9	91
	120+	2.93	12.25	125	230	565	190	5	225	45	40
								10	285	29	50
								20	330	17	58
								30	365	12	65
								60	450	8	80
40% PFA	10	0.36	5.13	8	255	625	170	5	410	82	66
								10	450	45	72
								20	490	25	78
								30	545	18	87
								60	590	10	94
	30	0.21	8.90	35	255	630	180	5	400	80	63
								10	430	43	68
								20	470	24	75
								30	515	17	82
								60	570	10	90
	120	2.43	11.07	125	240	590	180	5	220	44	37
								10	310	31	53
								20	375	19	64
								30	390	13	66
								60	425	7	72

Table D1.3 : Spread-time measurements for binary GGBS mixes in figure 7.7.

Mix	Two-point test measurements			Slump-spread-time measurements							
				Time	Static			Dynamic			
	Time (mins)	g (Nm)	h (Nms)	(mins)	Slump (mm)	SFS (mm)	ST (secs)	Time (secs)	SR (mm)	Rate (mm/s)	% of SFS
20% GGBS	10+	7.01	9.60	8	220	440	95	5	200	40	45
								10	200	20	45
								20	210	11	48
								30	220	7	50
								60	275	5	63
	120+	11.1	14.20	125	190	320	75	5	200	40	63
								10	200	20	63
								20	200	10	63
								30	215	7	67
								60	300	5	94
40% GGBS	10+	7.01	18.91	8	225	410	125	5	200	40	49
								10	200	20	49
								20	200	10	49
								30	230	8	56
								60	300	5	73
	60+	10.12	20.9	65	210	380	100	5	200	40	53
								10	200	20	53
								20	200	10	53
								30	210	7	55
								60	270	5	71
60% GGBS	30+	6.14	3.25	25	225	440	85	5	200	40	45
								10	230	23	52
								20	270	14	61
								30	300	10	68
								60	380	6	86

Note **SFS** and **ST** represent the final slump-spread and slump-flow time.

SR is the slump-spread measured at 5, 10, 20, 30 and 60 secs of deformation.

+ represents measurements outside the range of the 2-pt. Test apparatus (c.f. secs. 7.2.3 & 7.3.2).

Table D1.4 : Spread-time measurements for Ternary PFA/CSF mixes at 0.26 w/b ratio (in figure 7.10)

Mix	Two-point test measurements			Slump-spread-time measurements							
				Time	Static			Dynamic			
	Time (mins)	g (Nm)	h (Nms)	(mins)	Slump (mm)	SFS (mm)	ST (secs)	Time (secs)	SR (mm)	Rate (mm/s)	% of SFS
20/10 % PFA/CSF	10	0.00	3.76	8.5	245	615	90	5	430	86	70
								10	480	48	78
								20	550	28	89
								30	580	19	94
								60	600	10	98
	30	0.37	3.97	35	240	610	90	60	410	7	67
								5	460	92	75
								10	510	51	84
								20	550	28	90
								30	595	20	98
	120	0.78	6.12	127	220	525	80	60	350	6	67
								10	380	38	72
								20	445	22	85
								30	475	16	90
								60	510	9	97
40/10 % PFA/CSF	30	0.00	3.00	35	265	650	120	5	450	90	69
								10	520	52	80
								20	580	29	89
								30	610	20	94
								60	640	11	98
	120	0.39	4.47	126	255	620	100	5	430	86	69
								10	480	48	77
								20	530	27	85
								30	570	19	92
								60	600	10	97

Table D1.4 : Spread-time measurements for Ternary GGBS/CSF mixes at 0.26 w/b ratio (continued)

Mix	Two-point test measurements			Slump-spread-time measurements							
				Time	Static			Dynamic			
	Time (mins)	g (Nm)	h (Nms)	(mins)	Slump (mm)	SFS (mm)	ST (secs)	Time (secs)	SR (mm)	Rate (mm/s)	% of SFS
40/10 % GGBS/CSF	60	0.70	7.22	67	230	600	150	5	360	72	60
								10	410	41	68
								20	460	23	77
								30	495	17	83
								60	540	9	90
	120	1.21	7.64	125	225	525	140	5	340	68	65
								10	390	39	74
								20	440	22	84
								30	455	15	87
								60	500	8	95
60/10 % GGBS/CSF	10	0.43	3.92	8.5	255	630	130	5	420	84	67
								10	470	47	75
								20	520	26	83
								30	550	18	87
								60	600	10	95
	30	0.55	4.47	35	240	590	125	5	430	86	73
								10	470	47	80
								20	510	26	86
								30	550	18	93
								60	570	10	97
	120	1.10	6.93	125	230	530	105	5	370	74	70
								10	400	40	75
								20	455	23	86
								30	505	17	95
								60	515	9	97

Table D1.5 : Spread-time measurements for mixes at **0.30 w/b** ratio (in figure 7.13)

Mix	Two-point test measurements			Slump-spread-time measurements							
				Time	Static			Dynamic			
	Time (mins)	g (Nm)	h (Nms)	(mins)	Slump (mm)	SFS (mm)	ST (secs)	Time (secs)	SR (mm)	Rate (mm/s)	% of SFS
100% OPC	30	0.93	4.82	35	210	480	40	5	350	70	73
								10	395	40	82
								20	450	23	94
								30	475	16	99
								60	-	-	-
	120	1.69	6.89	125	175	370	20	5	315	63	85
								10	350	35	95
								-	-	-	-
								-	-	-	-
								-	-	-	-
10% CSF	10	0.16	2.71	7.5	235	610	70	5	460	92	75
								10	520	52	85
								20	580	29	95
								30	590	20	97
								60	600	10	98
	90	0.72	5.05	97	205	415	20	5	360	72	87
								10	410	41	99
								20	415	21	100
								-	-	-	-
								-	-	-	-

Table D1.5 : Spread-time measurements for mixes at **0.30 w/b** ratio (continued)

Mix	Two-point test measurements			Slump-spread-time measurements							
				Time	Static			Dynamic			
	Time (mins)	g (Nm)	h (Nms)	(mins)	Slump (mm)	SFS (mm)	ST (secs)	Time (secs)	SR (mm)	Rate (mm/s)	% of SFS
40/10 % PFA/CSF	10	0.22	1.29	8	250	670	65	5	520	104	78
								10	610	61	91
								20	630	32	94
								30	650	22	97
								60	660	11	99
	30	0.10	1.83	38	245	635	55	5	510	102	80
								10	590	59	93
								20	615	31	97
								30	625	21	98
								60	-	-	-
	60	0.10	2.91	65	235	590	55	5	500	100	85
								10	540	54	92
								20	565	28	96
								30	580	19	98
								60	-	-	-
	90	0.37	3.83	95	215	525	70	5	430	86	82
								10	470	47	90
								20	480	24	91
								30	500	17	95
								60	520	9	99
60/10 % GGBS/CSF	10	0.31	2.83	8	245	600	65	5	475	95	79
								10	515	52	86
								20	550	28	92
								30	585	20	98
								60	595	10	99
	120	0.91	6.20	125	185	385	15	5	370	74	96
								10	385	39	100
								-	-	-	-
								-	-	-	-
								-	-	-	-

Table D1.6 : Spread-time measurements for mixes at **0.22 w/b** ratio (in figure 7.15)

Mix	Two-point test measurements			Slump-spread-time measurements							
				Time	Static			Dynamic			
	Time (mins)	g (Nm)	h (Nms)	(mins)	Slump (mm)	SFS (mm)	ST (secs)	Time (secs)	SR (mm)	Rate (mm/s)	% of SFS
10% CSF	30	1.65	8.97	35	230	530	125	5	270	54	51
								10	300	30	57
								20	370	19	70
								30	390	13	74
								60	460	8	87
	120	4.51	11.58	127	195	370	110	5	220	44	59
								10	240	24	65
								20	270	14	73
								30	-	-	-
								60	320	5	86
40/10 % PFA/CSF	10	0.20	4.96	8.5	255	645	110	5	390	78	60
								10	450	45	70
								20	500	25	78
								30	540	18.0	84
								60	570	9.5	88
	30	0.29	6.05	36	250	635	105	5	390	78	61
								10	440	44	69
								20	500	25	79
								30	540	18	85
								60	580	9.7	91
	60	0.72	6.75	65	245	565	120	5	380	76	67
								10	435	44	77
								20	490	25	87
								30	535	18	95
								60	550	9.2	97
	90	1.06	7.50	97	235	530	90	5	370	74	70
								10	420	42	79
								20	470	24	89
								30	500	17	94
								60	520	9	98
60/10 % GGBS/CSF	90	3.94	12.53	95	210	435	120	5	200	40	46
								10	215	22	49
								20	230	12	53
								30	250	8	57
								60	290	4.8	67
	120	6.98	13.29	125	195	400	115	5	200	40	50
								10	210	21	53
								20	220	11	55
								30	240	8.0	60
								60	280	4.7	70

Table D1.7 : Additional measurements with cement PC-9, using 10% CSF at **0.26 w/b ratio** (from figure 6.10)

Mix	Two-point test measurements			Slump-spread-time measurements							
				Time	Static			Dynamic			
	Time (mins)	g (Nm)	h (Nms)	(mins)	Slump (mm)	SFS (mm)	ST (secs)	Time (secs)	SR (mm)	Rate (mm/s)	% of SFS
10 % CSF	10	0.36	3.80	8	240	585	80	5	350	70	60
								10	400	40	68
								20	450	22.5	77
								30	505	16.8	86
								60	550	9.2	94
	30	0.66	5.11	35	235	575	95	5	370	74	64
								10	390	39	68
								20	440	22	77
								30	480	16.0	83
								60	530	8.8	92
	60	1.40	6.14	65	230	530	90	5	335	67	63
								10	375	37.5	71
								20	405	20.25	76
								30	425	14.2	80
								60	485	8.1	92
	90	2.33	8.59	95	200	365	110	5	245	49	67
								10	260	26	71
								20	280	14	77
								30	295	9.8	81
								60	320	5.3	88
	120	4.30	9.53	125	155	300	60	5	220	44	73
								10	240	24	80
								20	270	13.5	90
								30	280	9.3	93
								60	300	5.0	100
10 % CSF (Repeat)	10	0.44	4.22	8	240	580	90	5	380	76	66
								10	430	43	74
								20	480	24	83
								30	500	16.7	86
								60	545	9.1	94
	30	0.43	4.78	35	235	550	85	5	340	68	62
								10	400	40	73
								20	440	22	80
								30	480	16.0	87
								60	540	9.0	98
	60	1.16	6.76	65	215	495	75	5	310	62	63
								10	360	36	73
								20	390	19.5	79
								30	410	13.7	83
								60	480	8.0	97
	90	2.77	9.24	95	205	405	60	5	245	49	60
								10	270	27	67
								20	310	15.5	77
								30	340	11.3	84
								60	380	6.3	94
	120	4.20	9.39	125	150	295	70	5	220	44	75
								10	230	23	78
								20	250	12.5	85
								30	280	9.3	95
								60	290	4.8	98

Table D1.8 : Additional measurements with SCC mixes in Table 3.7(b).

Mix	Two-point test measurements			Slump-spread-time measurements							
				Time	Static			Dynamic			
	Time (mins)	g (Nm)	h (Nms)	(mins)	Slump (mm)	SFS (mm)	ST (secs)	Time (secs)	SR (mm)	Rate (mm/s)	% of SFS
SCC1	25	0.47	2.50	20	255	590	35	5	480	96	81
								10	550	55	93
								20	570	28.5	97
								30	580	19.3	98
								60	-	-	-
SCC2	40	0.00	1.75	35	280	740	65	5	585	117	79
								10	650	65	88
								20	720	36	97
								30	725	24.2	98
								60	740	12.3	100

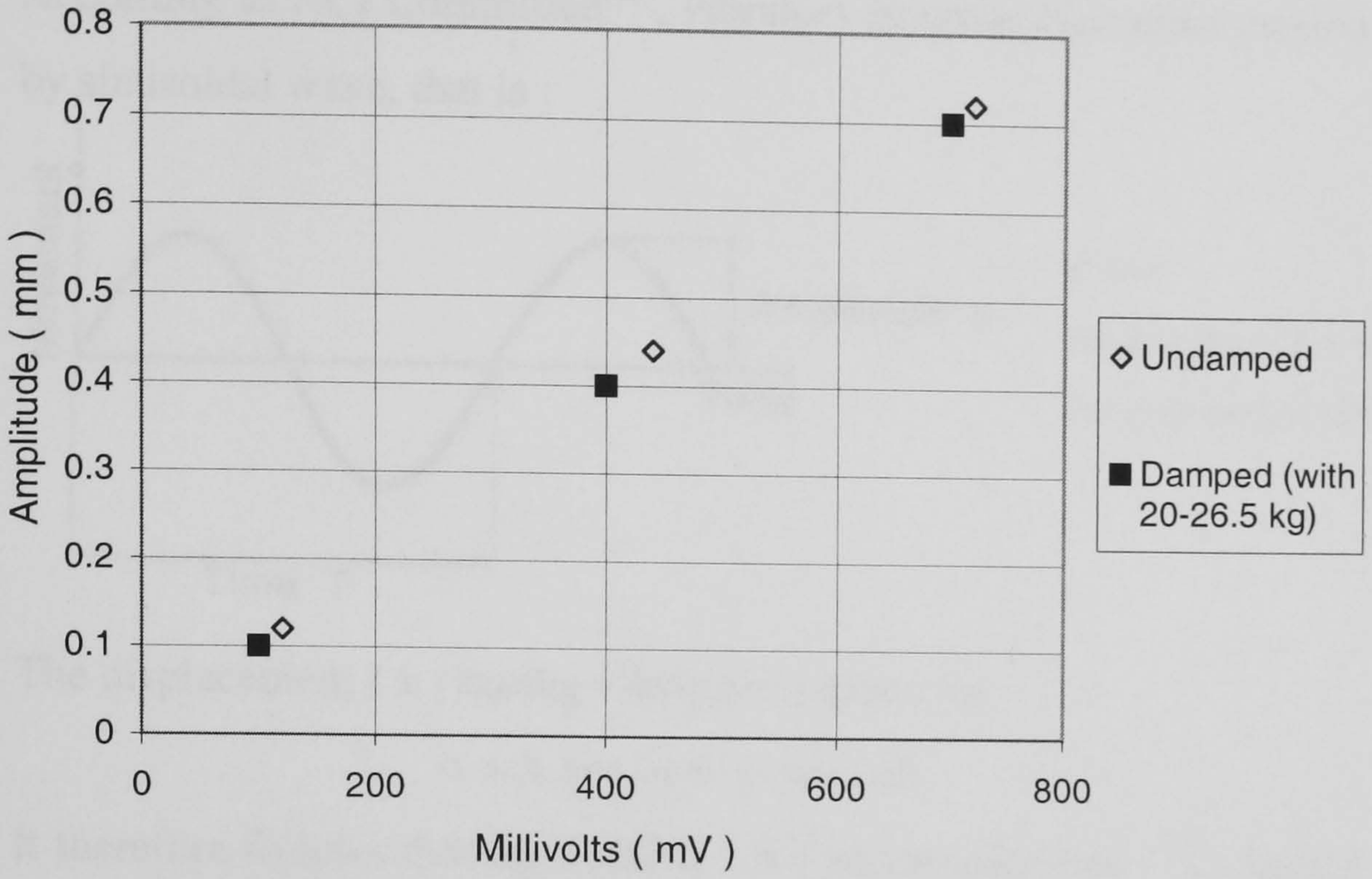

Figure D1: Calibration data for vibration table (under both damped and undamped conditions).

Calibration data corresponding to damped and undamped conditions.

Table Setting	Undamped		Damped (using 2 moulds + 2 cubes)		Damped (using 1 Prism + 5 cubes)	
	mV	mm	mV	mm	mV	mm
Low	120	0.12	100	0.10	99	0.09
Medium	440	0.44	400	0.40	400	0.40
High	720	0.72	700	0.70	700	0.70

Note : A Linear Variable Displacement Transducer (LVDT) was placed 100mm from the edge of the table, and a Leader Oscilloscope used to record the amplitude in mV.
The period was 20 milliseconds, which implies a frequency of 50 Hz.

The 0.10, 0.40 and 0.70 mm vibrational amplitudes correspond to vibrational accelerations of 1, 4 and 7g respectively.

Vibration Theory

According to ACI Committee[65], vibrators generate Harmonic motion characterized by sinusoidal wave, that is :

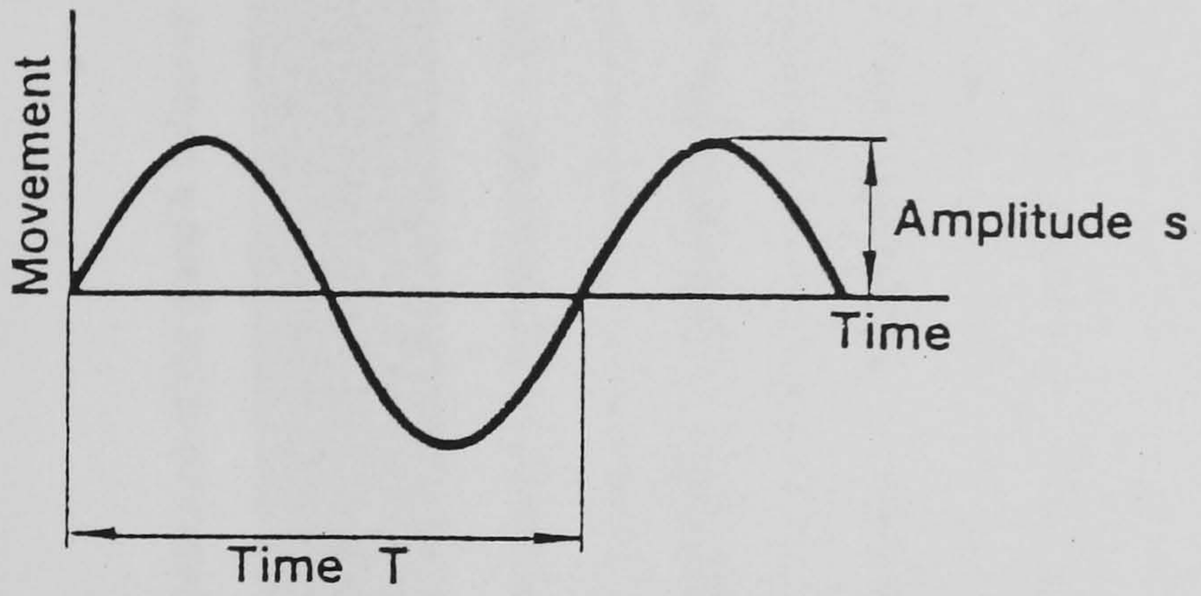

where

the frequency, $f = 1/T$, is in Hz

the amplitude, s, is in mm.

The displacement (**x**) during vibration is given by

$$x = s.\ \sin \omega t = s.\ \sin 2\pi ft$$

It therefore follows that the velocity ($\dot{x}$) and acceleration ($\ddot{x}$) during the vibration process are respectively given by :

$$\dot{x} = (2\pi\ .\ f)\ s.\ \cos 2\pi ft$$

$$\ddot{x} = (4\pi^2\ .\ f^2)\ s.\ \sin 2\pi ft$$

That is the max. vibrational acceleration (which occurs when " $\sin 2\pi ft$" is equal to 1) is given by:

$$\ddot{x}_{max.} = (4\pi^2\ .\ f^2)\ s$$

Sample calculation

For the 0.70 mm amplitude, the max. acceleration during vibration of the table vibrator (having a fixed frequency of 50 Hz) is

$$\ddot{x}_{max.} = (4\pi^2\ .\ f^2)\ s$$

$$= 4\ (\ 3.14159\ )^2\ (\ 50\ )^2\ (\ 0.7\ )$$

$$= 4\ (\ 9.8696\ )\ (\ 2500\ )\ (0.7\ )$$

$$= 69087\ mms^{-2}$$

$$= 69.087\ ms^{-2}$$

$$= 7.04\ g \qquad (\text{where } g = 9.81\ ms^{-2})$$

Table D2 : Spread-time - Bingham parameter relations (up to 8 decimal places) used to provide more precise calculations of the g and h values in chapter 8.

Equation	Spread-time - **yield value** relationships	Spread-time - **plastic viscosity** relationships
(8.1)	**g** = 0.00006890 SR_5^2 - 0.06488747 SR_5 + 15.25178623	**h** = 0.00004519 SR_5^2 - 0.06155827SR + 22.06427338
(8.2)	**g** = 0.00005422 SR_{10}^2 - 0.05734455 SR_{10} + 15.12120810	**h** = 0.00002825 SR_{10}^2 - 0.04830375 SR_{10} + 20.72203677
(8.3)	**g** = 0.00004223 SR_{20}^2 - 0.05008777 SR_{20} + 14.82400728	**h** = 0.00001782 SR_{20}^2 - 0.03941081 SR_{20} + 19.94949056
(8.4)	**g** = 0.00003957 SR_{30}^2 - 0.04936332 SR_{30} + 15.44107920	**h** = 0.00000995 SR_{30}^2 - 0.03258415 SR_{30} + 19.23638192
(8.5)	**g** = 0.00003077 SR_{60}^2 - 0.04351557 SR_{60} + 15.23631747	**h** = -0.00000224 SR_{60}^2 - 0.02152055 SR_{60} + 17.84593066

SR_i represents the spread measured at 5, 10, 20, 30, and 60 secs.

Table D3 : Fresh property measurements of non-vibrated concrete mixes (produced with cement PC-9)

Mix	Slump measurements				Two-point test measurements				SI
	Time (mins)	Slump (mm)	SFS (mm)	ST (s)	Time (mins)	g (Nm)	h (Nms)	r	(%)
OPC	8	235	500	125	10	0.91	5.79	0.9755	12
	35	220	470	110	30	2.03	6.98	0.9833	
	65	210	425	100	60	3.87	8.75	0.9612	
	125	150	280	90	120	5.75	11.50	0.9522	5.1
10% CSF	8	240	580	90	10	0.44	4.22	0.9885	16.1
	65	215	495	75	60	1.16	6.76	0.9822	
	125	150	295	70	120	4.20	9.39	0.9709	8.2
PFA/CSF	8	260	670	110	10	0	1.95	0.9905	32
	65	255	650	100	60	0.62	2.81	0.9887	
	125	240	600	100	120	1.21	6.25	0.9869	12.5
GGBS/CSF	8	255	640	95	10	0.33	3.93	0.9892	18.5
	65	220	535	85	60	1.35	7.41	0.9850	
	125	180	370	70	120	3.73	10.75	0.9803	-
Acrylate (D2001) superplasticizer	8	245	620	80	10	0.11	3.87	0.9919	20.5
	65	200	480	80	60	2.15	8.29	0.9827	
	125	70	200	0	120	6.77	11.95	0.9613	3.75
NSC (at 0.50 w/b)	8	220	360	< 5	10	1.36	1.41	0.9694	15.2
	65	190	320	0	60	2.34	1.80	0.9254	
	125	85	200	0	120	3.95	2.16	0.9817	11.8

The shorter ST values for NSC may be associated with reduced bleeding tendency and inter-particle forces.

Table D4.1 : Vibration response data for OPC and 10% CSF mixes (in figure 8.9)

Mix	Non-vibrated concrete measurements							Vibration response measurements					Calculated	
	Slump test				Two-point test			Amp-	SR measurements				g	h
	Time (mins)	Slump (mm)	SFS (mm)	ST (s)	Time (mins)	g (Nm)	h (Nms)	litude (mm)	Time (s)	SR (mm)	Rate mm/s	% of SFS	value (Nm)	value (Nms)
OPC	125	150	280	90	120	5.75	11.5	0.10	5	205	41	73	4.85	11.34
									10	230	23	82	4.80	11.11
									20	265	13	95	4.52	10.76
									30	300	10	107	4.19	10.36
									60	345	6	123	3.89	10.15
								0.40	5	215	43	77	4.49	10.92
									10	280	28	100	3.32	9.41
									20	365	18	130	2.17	7.94
									30	490		175	0.75	5.66
									60	630	11	225	0.03	3.40
								0.70	5	235	47	84	3.81	10.09
									10	315	32	113	2.44	8.31
									20	425	21	152	1.16	6.42
									30	610		218	0.05	3.06
									60	670	11	239	0.00	2.42
10% CSF	65	215	495	75	60	1.16	6.76	0.70	5	380	76	77	0.54	5.20
									10	500	50	101	0.00	3.63
									20	605	30	122	0.00	2.63
									30	690	23	139	0.00	1.49
									60	720	12	145	0.00	1.19
								0.40	5	355	71	72	0.90	5.91
									10	425	43	86	0.54	5.30
									20	570	29	115	0.00	3.28
									30	620	21	125	0.00	2.86
									60	655	11	132	0.00	2.79
								0.10	5	340	68	69	1.15	6.36
									10	395	40	80	0.93	6.05
									20	480	24	97	0.51	5.14
									30	600	20	121	0.07	3.27
									60	640	11	129	0.00	3.16
	125	150	295	70	120	4.20	9.39	0.10	5	255	51	86	3.19	9.31
									10	295	30	100	2.92	8.93
									20	340	17	115	2.68	8.61
									30	385	13	131	2.30	8.17
									60	450	8	153	1.89	7.71
								0.40	5	290	58	98	2.23	8.01
									10	365	37	124	1.41	6.85
									20	460	23	156	0.72	5.59
									30	605	20	205	0.06	3.16
									60	650	11	220	0.00	2.91
								0.70	5	310	62	105	1.76	7.32
									10	415	42	141	0.66	5.54
									20	585	29	198	0.00	2.99
									30	640	21	217	0.00	2.46
									60	695	12	236	0.00	1.81

Calculated g values at high spreads (SR's), which can be -ve or show increases as determined from equs. 8.1-8.5, are taken as zero.

Table D4.2 : Vibration response data for Ternary PFA/CSF and GGBS/CSF mixes (in figure 8.10)

Mix	Non-vibrated concrete measurements							Vibration response measurements					Calculated	
	Slump test				Two-point test			Amp-	SR measurements				**g**	**h**
	Time (mins)	Slump (mm)	SFS (mm)	ST (s)	Time (mins)	**g** (Nm)	**h** (Nms)	litude (mm)	Time (s)	**SR** (mm)	Rate mm/s	% of SFS	value (Nm)	value (Nms)
PFA/CSF	125	240	600	100	120	1.21	6.25	0.10	5	350	70	58	0.98	6.05
									10	450	45	75	0.30	4.71
									20	560	28	93	0.02	3.47
									30	620	21	103	0.00	2.86
									60	675	11	113	0.00	2.30
								0.40	5	400	80	67	0.32	4.67
									10	525	53	88	0.00	3.15
									20	625	31	104	0.00	2.28
									30	685	23	114	0.00	1.59
									60	720	12	120	0.00	1.19
								0.70	5	460	92	77	0.00	3.31
									10	565	57	94	0.00	2.45
									20	700	35	117	0.00	1.09
									30	725	24	121	0.00	0.84
									60	740	12	123	0.00	0.69
GGBS/CSF	125	180	370	70	120	3.73	10.75	0.10	5	250	50	68	3.34	9.50
									10	295	30	80	2.92	8.93
									20	350	18	95	2.47	8.34
									30	400	13	108	2.03	7.79
									60	460	8	124	1.73	7.47
								0.40	5	275	55	74	2.62	8.55
									10	345	35	93	1.79	7.42
									20	475	24	128	0.56	5.25
									30	570	19	154	0.16	3.90
									60	635	11	172	0.01	3.28
								0.70	5	320	64	86	1.54	6.99
									10	405	41	109	0.79	5.79
									20	570	29	154	0.00	3.28
									30	610	20	165	0.00	3.06
									60	655	11	177	0.00	2.79

Table D4.3 : Vibration response data for Acrylate (D2001) and NSC mixes (in figure 8.11)

Mix	Non-vibrated concrete measurements							Vibration response measurements					Calculated	
	Slump test				Two-point test			Amp-	SR measurements				g	h
	Time (mins)	Slump (mm)	SFS (mm)	ST (s)	Time (mins)	g (Nm)	h (Nms)	litude (mm)	Time (s)	SR (mm)	Rate mm/s	% of SFS	value (Nm)	value (Nms)
D 2001	65	200	480	80	60	2.15	8.29	0.70	5	345	69	72	1.07	6.21
									10	480	48	100	0.09	4.05
									20	580	29	121	0.00	3.09
									30	670	22	140	0.00	1.87
									60	710	12	148	0.00	1.44
								0.40	5	315	63	66	1.65	7.16
									10	400	40	83	0.86	5.92
									20	540	27	113	0.09	3.86
									30	630	21	131	0.00	2.66
									60	700	12	146	0.00	1.68
								0.10	5	300	60	63	1.99	7.66
									10	360	36	75	1.50	6.99
									20	450	23	94	0.84	5.82
									30	590	20	123	0.09	3.48
									60	640	11	133	0.00	3.16
	125	70	200	0	120	6.77	11.95	0.10	5	200	40	100	5.03	11.56
									10	225	23	113	4.96	11.28
									20	250	13	125	4.94	11.21
									30	285	10	143	4.59	10.76
									60	345	6	173	3.89	10.15
								0.40	5	210	42	105	4.66	11.13
									10	255	26	128	4.02	10.24
									20	335	17	168	2.78	8.75
									30	475	16	238	0.92	6.00
									60	610	10	305	0.14	3.88
								0.70	5	230	46	115	3.97	10.30
									10	315	32	158	2.44	8.31
									20	425	21	213	1.16	6.42
									30	540	18	270	0.32	4.54
									60	645	11	323	0.00	3.03
NSC (0.50 w/b)	125	85	200	0	120	3.95	2.16	0.10	5	275	55	138	2.62	8.55
									10	325	33	163	2.21	8.01
									20	370	19	185	2.07	7.81
									30	410	14	205	1.85	7.55
									60	480	8	240	1.44	7.00
								0.40	5	400	80	200	0.32	4.67
									10	510	51	255	0.00	3.43
									20	635	32	318	0.00	2.11
									30	680	23	340	0.00	1.68
									60	710	12	355	0.00	1.44
								0.70	5	455	91	228	0.00	3.41
									10	550	55	275	0.00	2.70
									20	680	34	340	0.00	1.39
									30	720	24	360	0.00	0.93
									60	740	12	370	0.00	0.69

Appendix E

Additional data for:
(Chapter 9)

. UPV-cube strength data

. Cube density - Bingham parameter relationships

. Column strength and density relationships

Table E1 : 100 mm cube strength and UPV data (in figure 9.5)

Present study		By Price & Hynes[257)]	
Comp. Strength (Nmm^{-2})	UPV (Kms^{-1})	Comp. Strength (Nmm^{-2})	UPV (Kms^{-1})
71	4.25	47	4.17
57	4.13	47	4.23
104.25	4.89	47	4.25
98.75	4.85	60	4.28
		60	4.31
109.5	4.88	60	4.32
111.5	4.75	72	4.38
106	4.75	73	4.39
112	4.90	72	4.41
		72	4.41
74	4.25	73	4.44
85	4.35	81	4.40
111.5	4.93	82	4.40
114.5	4.95	81	4.43
118.75	5.00	81	4.46
121.25	5.03	82	4.50
119.5	5.03	91	4.51
117.25	5.01	91	4.52
		91	4.53

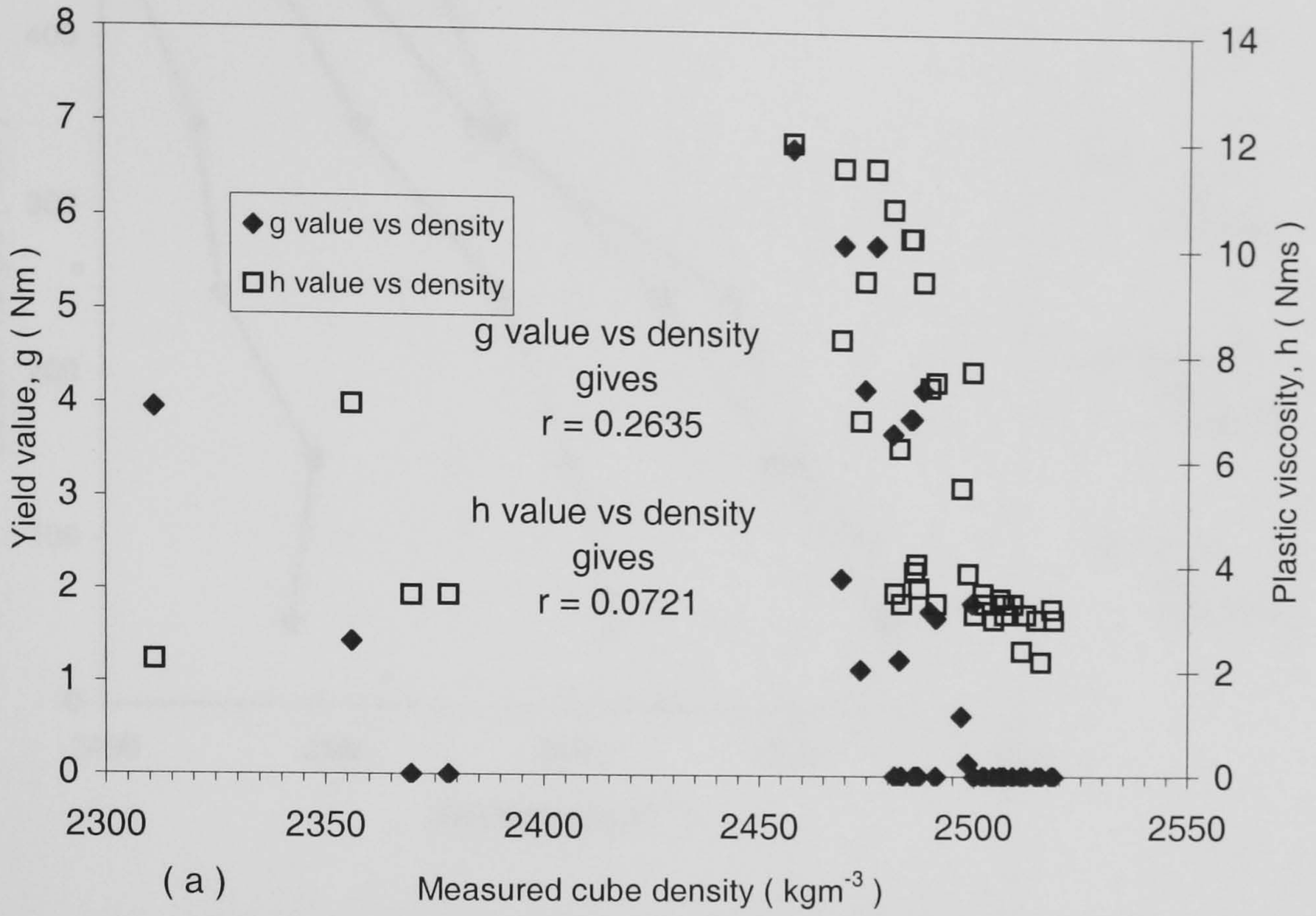

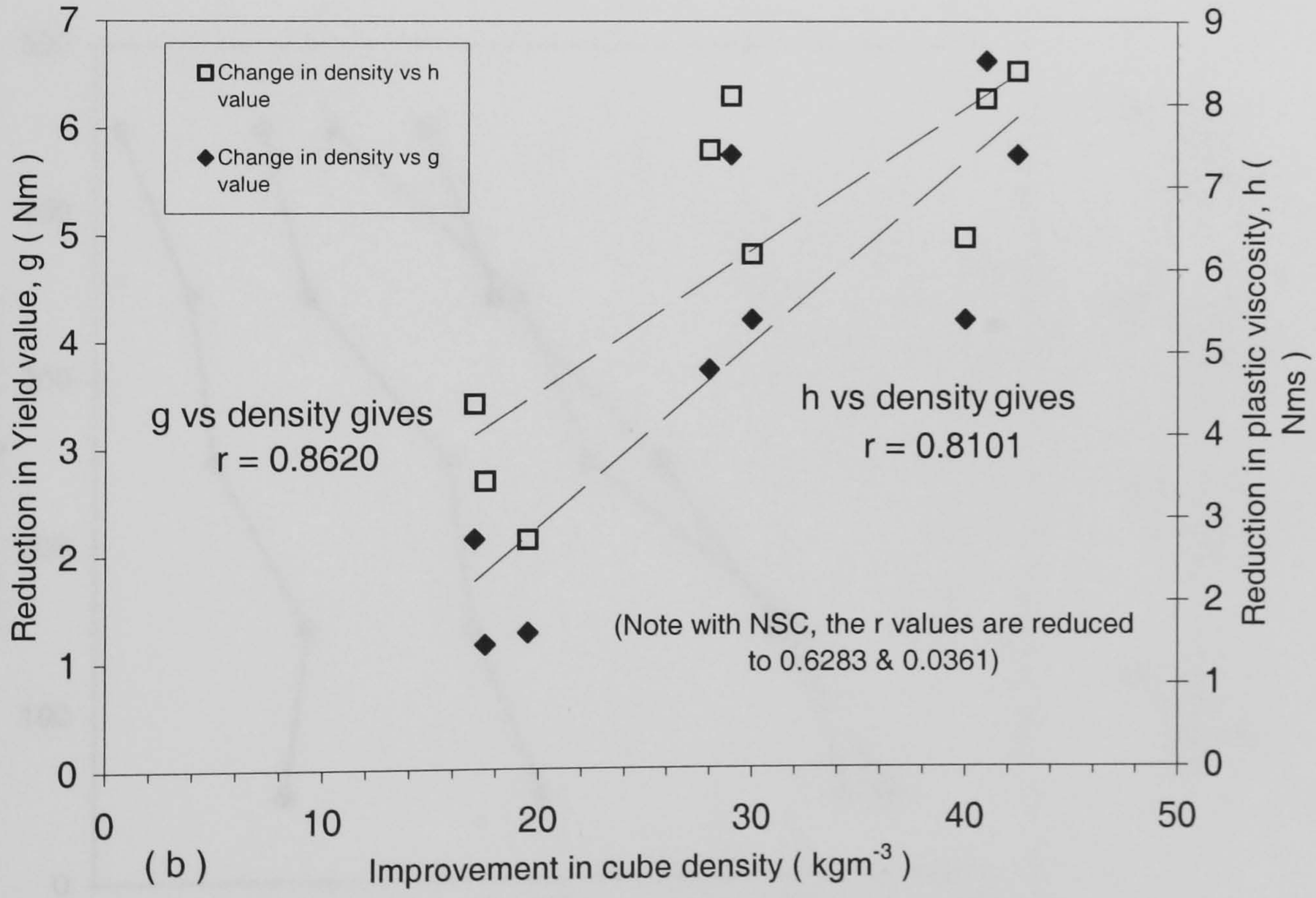

Figure E1 : Cube density - Bingham parameter relationships in terms of their (a) magnitudes (as shown in Tables 9.1-9.3) and (b) differences in magnitude (up to full-compaction, and excluding results for NSC).

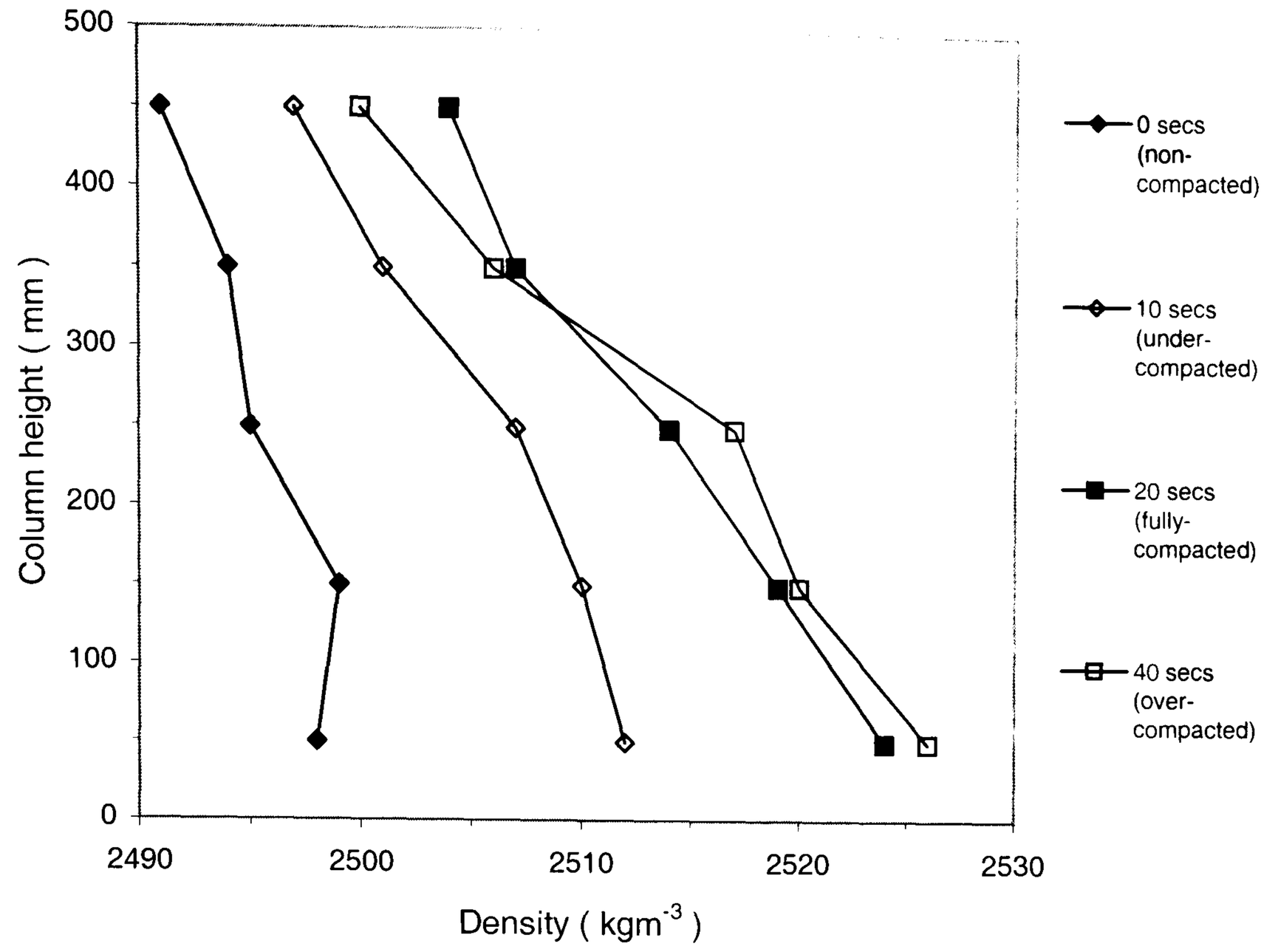

Figure E2 : Variations in 28-day column **density** with increasing **vibration duration** (10% CSF mix, 0.26 w/b).

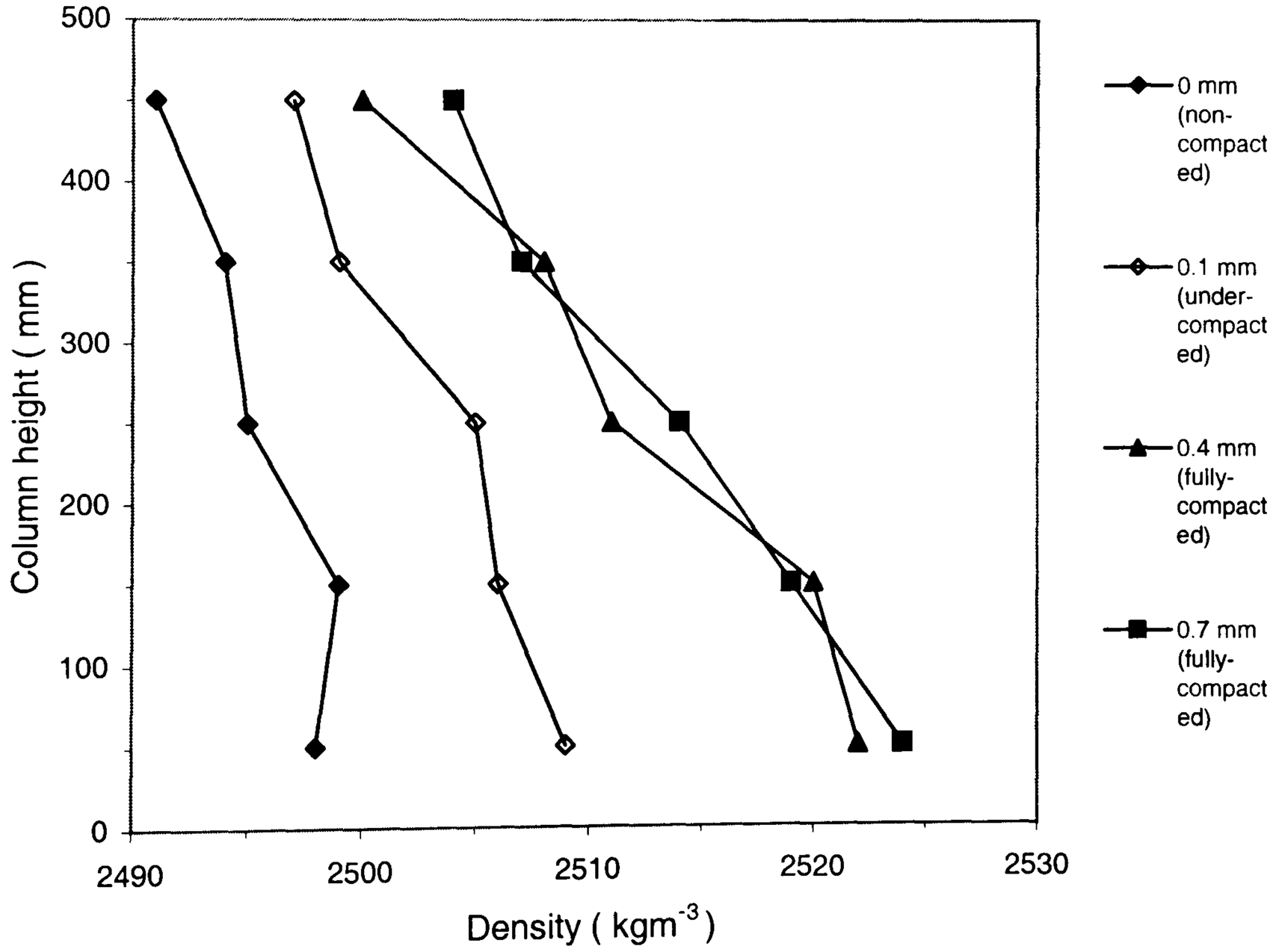

Figure E3 : Variations in 28-day column **density** with increasing **amplitude of vibration** (10% CSF mix, 0.26 w/b).

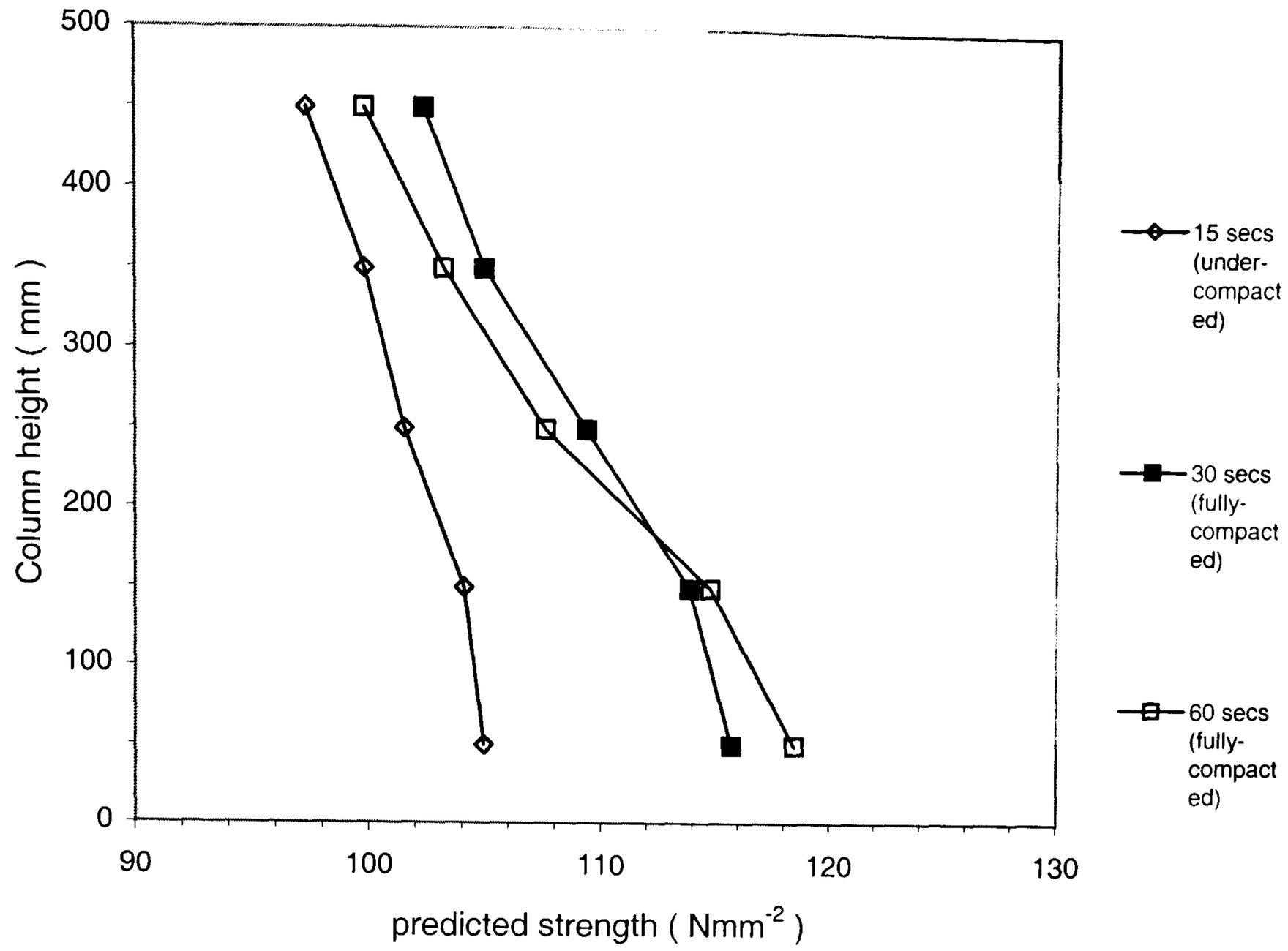

Figure E4 : Variations in column **strength** with increasing **vibration duration** (100% **OPC** mix, 0.26 w/b).

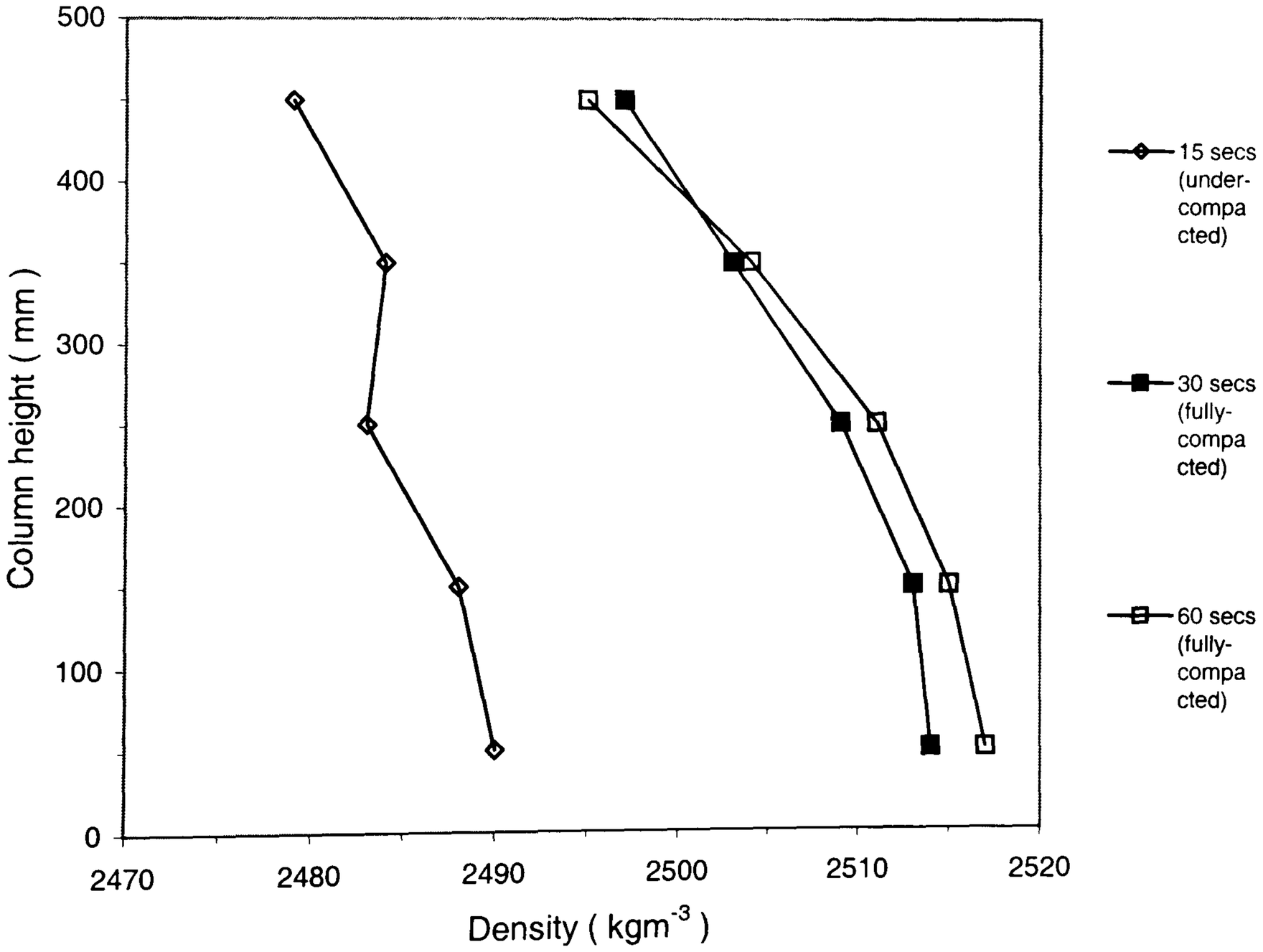

Figure E5 : Variations in column **density** with increasing **vibration duration** (100% **OPC** mix, 0.26 w/b).

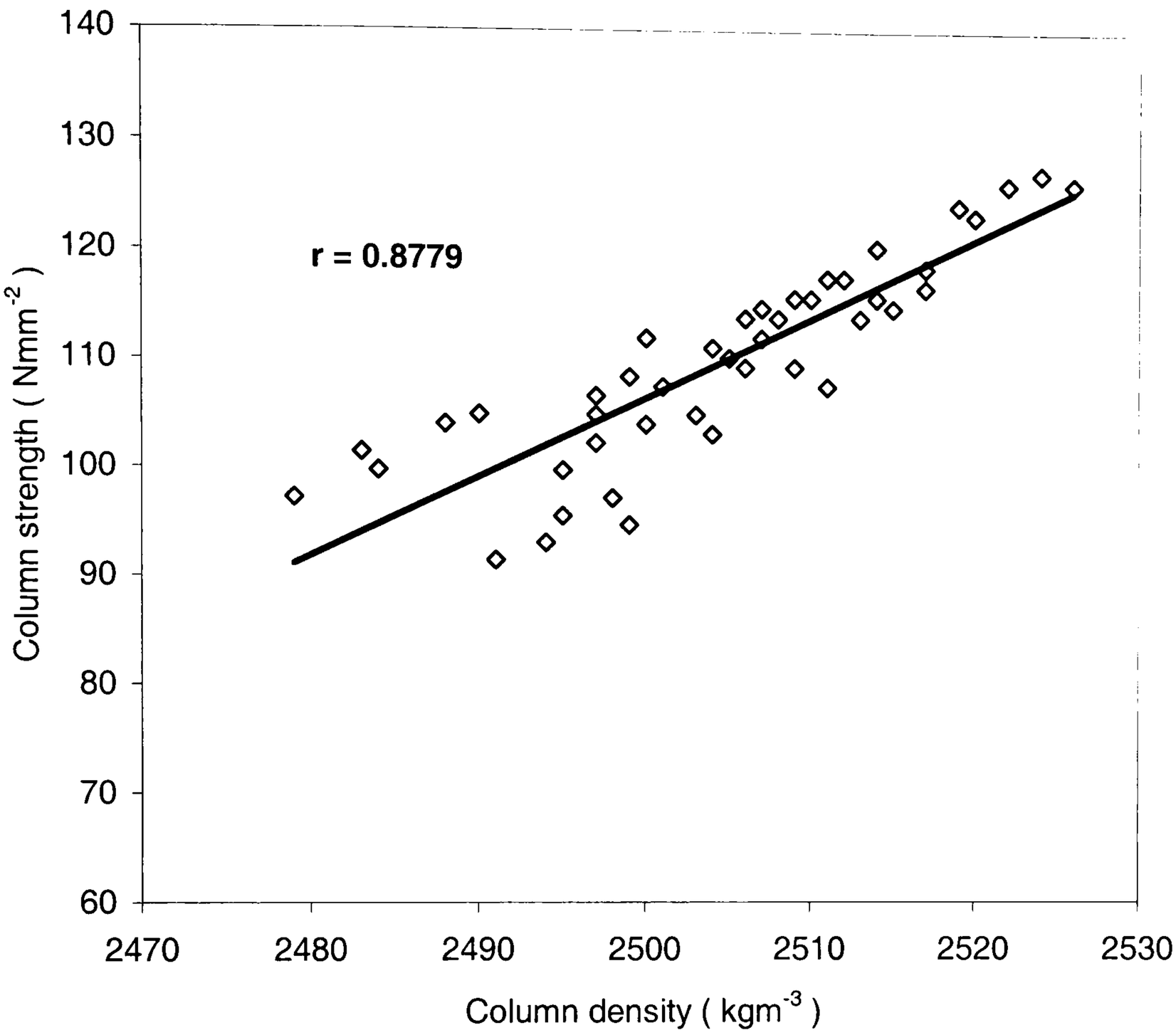

Figure E6 : Column strength vs density relationship for OPC and 10% CSF mixes in Tables 9.4 and 9.5.

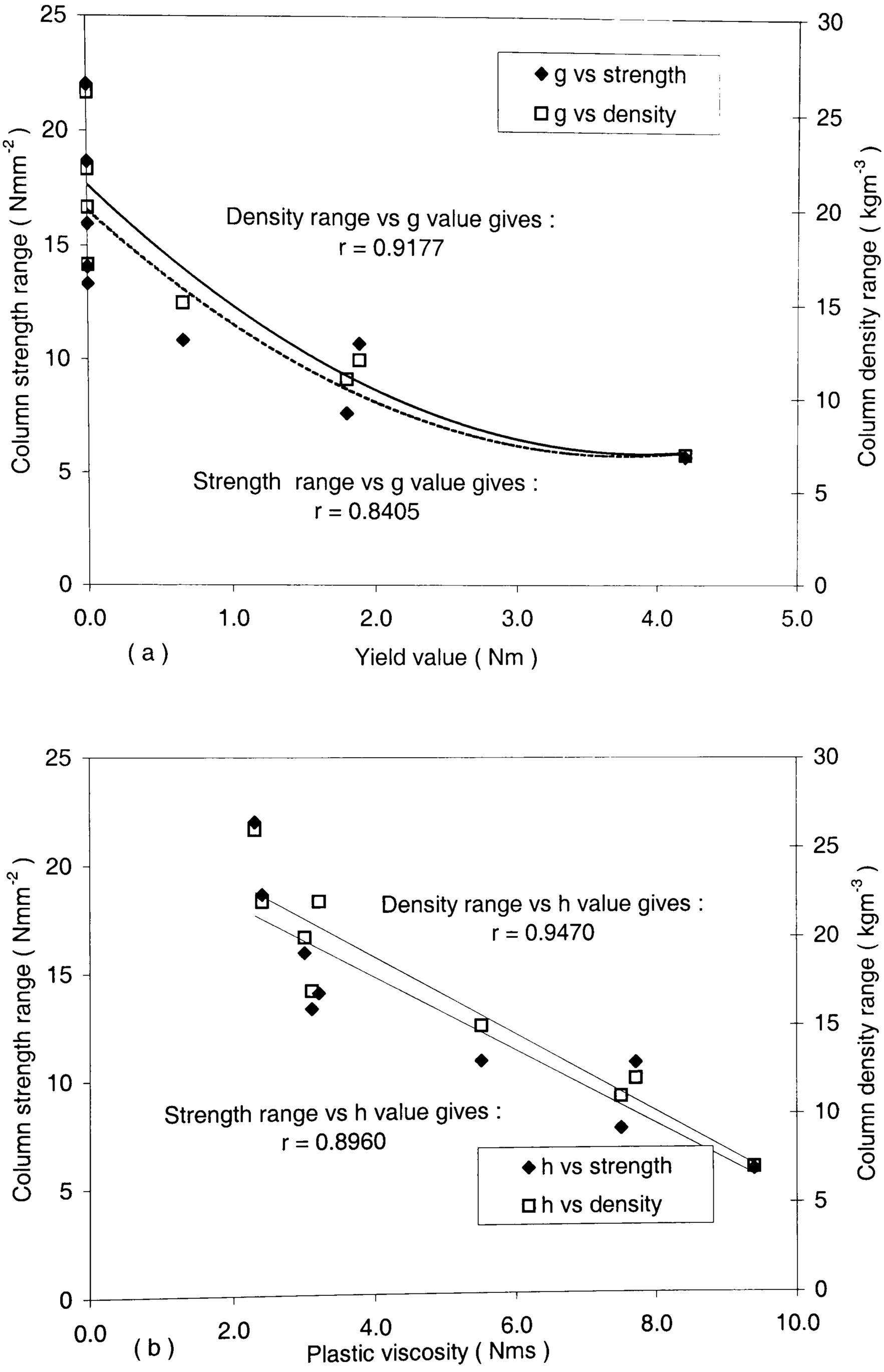

Figure E7 : Relationships between differences in upper-lower column strengths and densities with (a) yield value and (b) plastic viscosity.